ENHANCED MICROCOMPUTER OPERATION OF X-RAY DIFFRACTOMETERS AND SUBSEQUENT APPLICATIONS

A thesis submitted to the Council for National Academic Awards as part fulfilment of the requirements for the Degree of Doctor of Philosophy

by

NEIL SUTHERLAND STEWART

School of Applied Sciences

The Robert Gordon Institute of Technology

Aberdeen

in collaboration with

The Rutherford Appleton Laboratory

Didcot, Oxfordshire

May 1992

To Kathy

DECLARATION

All the experimental work described in this thesis was carried out by Neil S Stewart in the laboratories of The Robert Gordon Institute of Technology, The Rutherford Appleton Laboratory and as acknowledged.

It has not been accepted in substance or concurrently submitted in candidature for any other degree.

Neil Stewart
(Candidate)

Philip J Cox
(Director of Studies)

ACKNOWLEDGEMENTS

I would like to thank Dr.P.J.Cox for his expert advice, support and boundless enthusiasm which acted as a catalyst throughout the entire research programme. I would also like to extend my thanks to Dr.C.C.Wilson and to the staff at the Rutherford Appleton Laboratory, for the opportunity to utilise their extensive resources.

Much of the work involved the collaboration of Dr's R.A.Howie, A.B.Turner and J.L.Wardell from the Chemistry Department of Aberdeen University and I am indebted to them for their time and constructive input.

I am also grateful for the assistance provided by Dr's E.A.Addinal, J.Harper, I.T.Liddell and M.A.S.Sweet and also to the technical staff from the School of Applied Science at the Robert Gordon Institute of Technology. Special thanks is conveyed to Dr.S.M.V.S.Doidge-Harrison for her advice and friendship, both of which were greatly appreciated.

On a personal level, I would like to thank my parents for their backing, both emotionally and financially. And finally I cannot express sufficiently my gratitude to Kathleen Scott for her patience and support which have helped maintain the momentum required to complete the task of compiling this thesis. **Thank you**.

ABSTRACT

ENHANCED MICROCOMPUTER OPERATION OF X-RAY DIFFRACTOMETERS AND SUBSEQUENT APPLICATIONS

Neil Sutherland Stewart

The work described within this thesis is mainly concerned with the solution and refinement of the molecular structures of a variety of novel compounds. A number of X-ray and neutron diffractometers have been utilised for the analysis of specific compounds, depending on the nature of the investigation. Each of the instruments represented differing levels of computer automation and instrumentation. A powder diffractometer, representing old technology was interfaced to a microcomputer to enhance the instruments performance.

A brief overview is given of the numerical processes involved in the elucidation and refinement of molecular structures from X-ray and neutron diffraction data. Particular attention has been placed on the role of computers to perform these calculations.

The operation of the diffractometers employed in this study has been discussed comparing the benefits of each. A detailed report of the techniques used to enhance the low resolution diffractometer and of the experiments performed to highlight the increased performance has been included.

Single crystal and powder diffraction studies were made of a wide variety of crystalline materials ranging from steroids to organometallic compounds. The X-ray structures were solved using Direct and Patterson vector methods from experimental data collected on a four circle diffractometer at Aberdeen University.

Neutron diffraction experiments, performed at the Rutherford Appleton Laboratory, were commissioned to determine and refine the positions of the hydrogen atoms of two known structures, previously solved by X-ray studies.

Finally a critical evaluation of current computer automated diffractometers is presented, highlighting the new areas of instrument development.

CONTENTS

LIST OF FIGURES

LIST OF TABLES

The basic principles of X-ray Crystallography have been well established for more than half a century but the present level of interest in this field indicates that there is still a great deal of scope for more innovative work. This has been largely due to the combined effects of rapid digital computer development and to the advancements in instrumentation, thus allowing more sophisticated experiments to be undertaken.

The work described in this thesis has involved a variety of X-ray and neutron diffractometers, each of differing complexity. This chapter outlines the general theory relating to the procedures and mechanisms involved in the process of crystal structure determination and refinement.

1.1 Crystal diffraction

1.1.1 X-ray scattering by an atom

The intensity of second generation X-rays emitted by the electrons in an atom is dependent upon direction. Figure 1.1 shows a simplified two dimensional model of an atom with two electrons fixed in their orbits about the nucleus. The incident beam can be thought of as two parallel rays which are in phase at the wavefront X-Y. If these rays are examined after being scattered by the electrons, in the straight through position, they will still be in phase having travelled equal path lengths. However if the rays are observed at wavefront X-Z at an angle of θ° from the incident beam, they will have travelled different path lengths. Generally, the path difference will be a fraction of the X-ray wavelength and so the two rays will interfere with one another. The ability of an atom to scatter X-rays in this manner is called the Scattering factor.

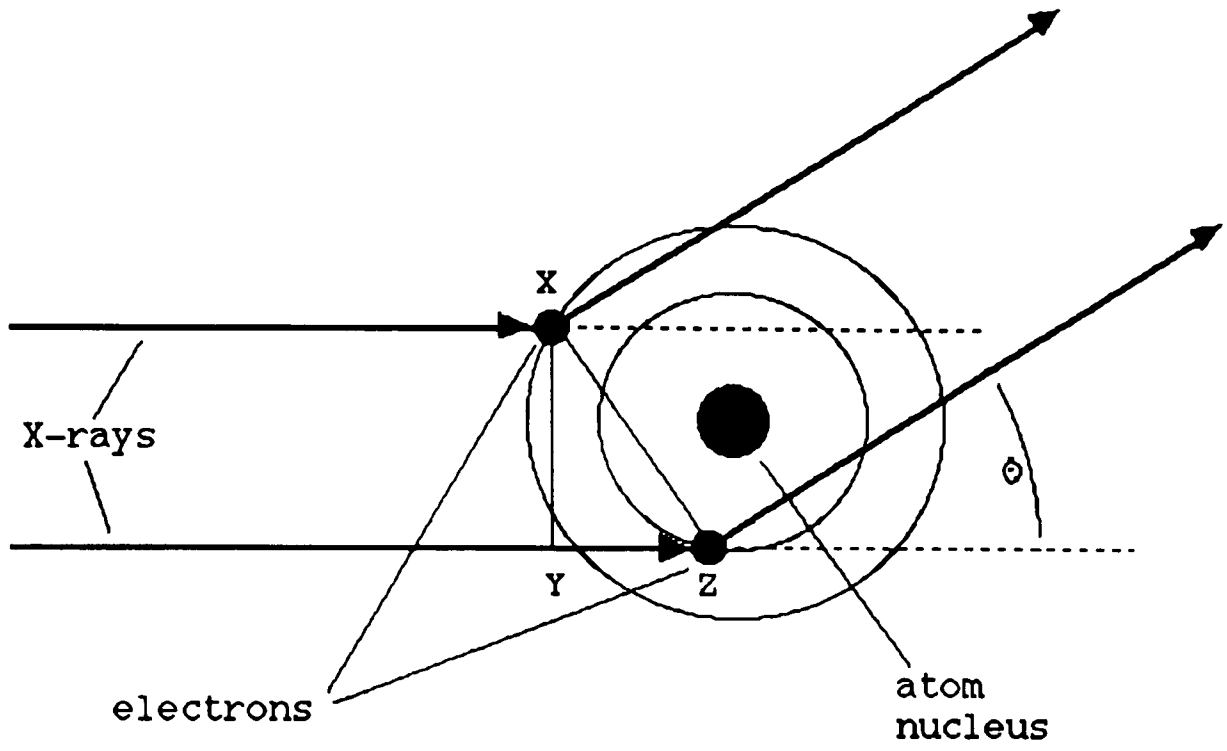

Figure 1.1 X-ray scattering by electron clouds.

1.1.2 X-ray scattering factor

The atomic scattering factor,**f** , increases with mass number and is proportional to Z, the number of electrons. The angular dependence of the scattering factor for fluorine[1] is shown in Figure 1.2. The model in Figure 1.1, is an ideal one and is valid if the atom is at rest. The model breaks down when the atom is allowed to vibrate due to thermal effects. With the atom and electrons vibrating, this has the effect of spreading the electron density out, thus reducing the scattering strength per $Å^3$. The decrease in scattering caused by temperature effects and the angular variation can be expressed mathematically as follows[2]:-

$$f = f_o.\exp(-B.\sin^2\Theta/\lambda^2) \qquad (1.1)$$

Where $B=8\pi^2u^2$ and u^2 is the mean square atomic vibration.

When an X-ray beam is reflected from a set of crystal planes, with Miller indices (**hkl**) and angle of incidence, Θ, the resultant beam amplitude is related to the individual scattering factors, evaluated

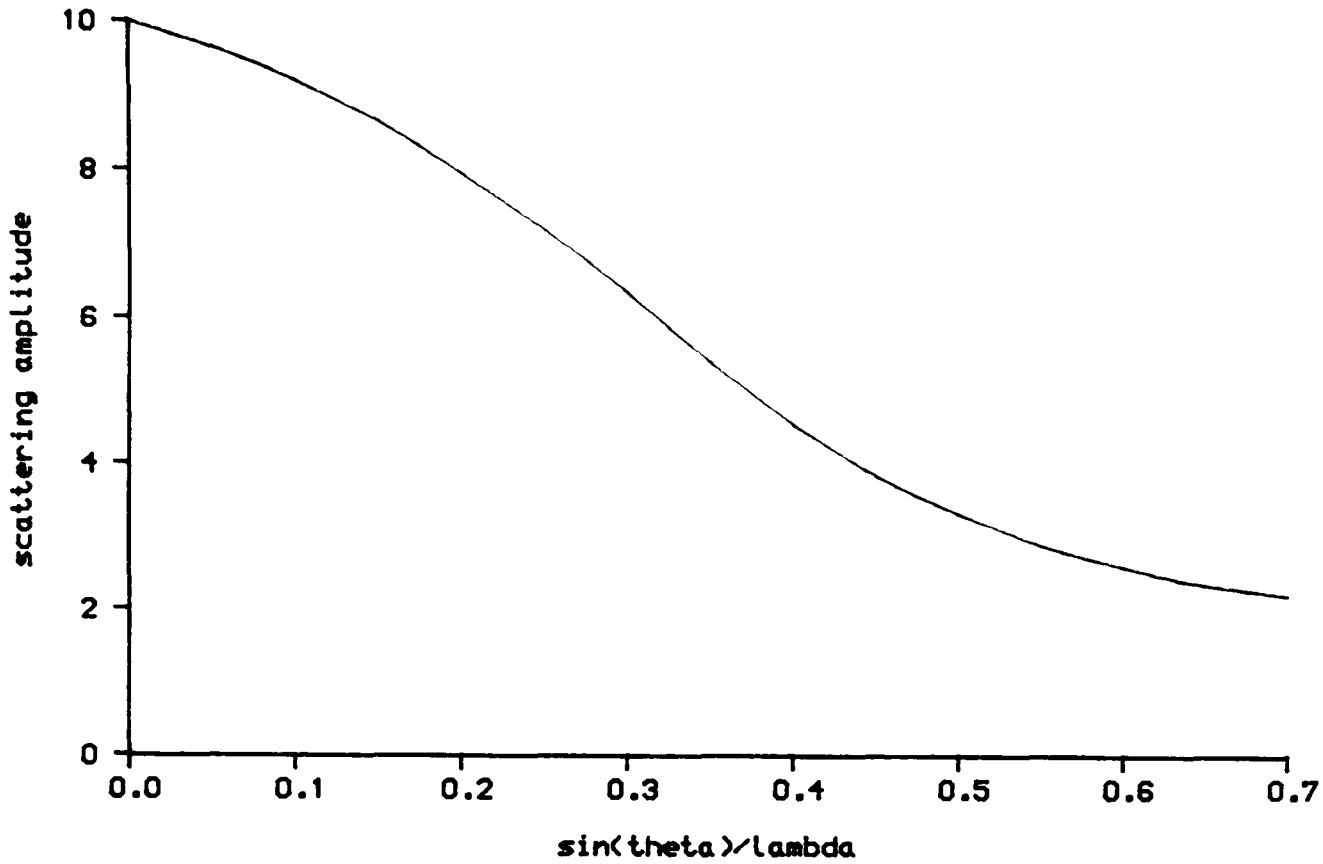

Figure 1.2 The angular dependence of the scattering factor for fluorine.

for the $\sin\theta/\lambda$ value, for all the atoms in the unit cell. For an undeviated beam, the resultant amplitude is simply the sum of all the scattering factors.

$$A_{000} = \sum_{j=1}^{N} f_{o_j}.\exp(-B.\sin^2\Theta/\lambda^2) = \sum_{j=1}^{N} f_{o_j} \qquad (1.2)$$

1.1.3 X-ray structure factor

For all other reflexions, the expression is not as elementary, since the individual X-ray beams from each atom have different path lengths. The phase of each atom is expressed relative to the chosen origin of the unit cell. For a (**hkl**) reflexion the phase for a atom with coordinates (x,y,z) is expressed as follows:-

$$\phi_j = 2\pi(\mathbf{h}x_j + \mathbf{k}y_j + \mathbf{l}z_j) \qquad (1.3)$$

The total scattering amplitude or structure factor can be expressed by either of the following equations.

$$F_{hkl} = \sum_{j=1}^{N} f_j.(\cos \phi_j + i.\sin \phi_j) \qquad (1.4)$$

$$F_{hkl} = \sum_{j=1}^{N} f_j.\exp(i\phi_j) \qquad (1.5)$$

1.1.4 Neutron diffraction

The process of neutron diffraction and subsequent data processing is, in general terms, very similar to X-ray scattering. The differences between the two methods, lies in the scattering mechanisms. With thermal neutrons, which are generally considered to behave as particles, a de Broglie wavelength can be associated. The de Broglie wavelength of a particle is determined by both its mass (m) and its velocity. Equation 1.6 gives the wavelength for a particle at temperature T Kelvin.

$$\lambda = \frac{h}{(5mkT)^{1/2}} \qquad (1.6)$$

Where **h** and **k** are the Planck and Boltzmann constants respectively.

Evaluating equation 1.6 for thermal neutrons predicts a wavelength of the order of Angstroms, which is comparable with X-radiation.

The scattering of the neutron occurs by a mechanism of capture. The neutron capture cross-section of an atom does not follow a linear relationship as does the X-ray scattering factor. This is one of the features which makes the very expensive process of neutron diffraction worthwhile. Figure 1.3 shows the relationship between atomic mass and scattering length of selected elements[3]. It should be noted that ^{1}H

has a large negative scattering length and so its presence in a neutron diffraction analysis is easily determined regardless of the size of its neighbouring atoms. Neutron diffraction is ideal for determination of the positions of H atoms, and for other light elements in the presence of heavy atoms, which are poorly defined by X-ray data. Also it is possible to distinguish between certain atoms of similar atomic mass, e.g., the two isotopes ^{1}H and ^{2}H are seen to be identical in X-ray studies but have very different neutron scattering lengths.

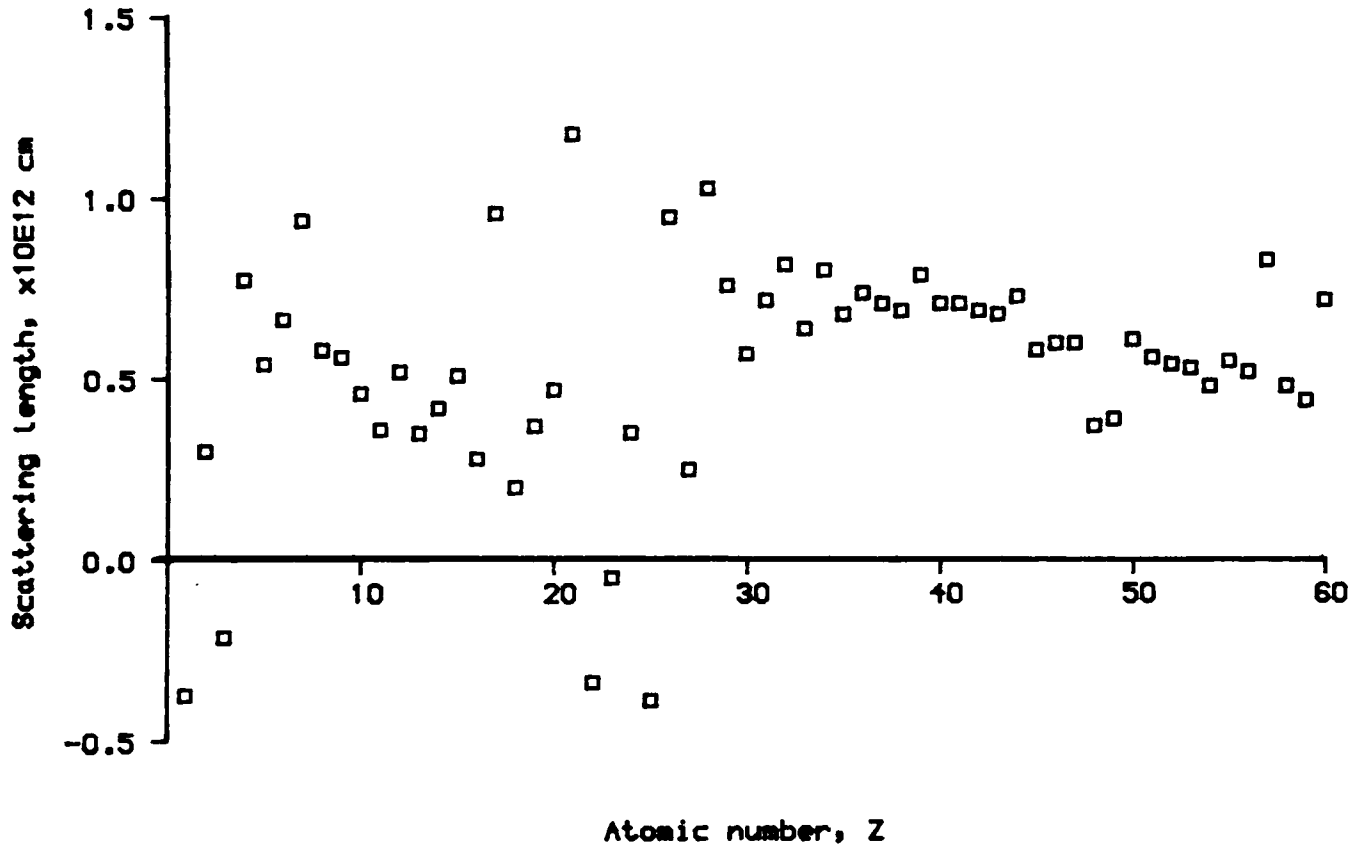

Figure 1.3 The neutron scattering lengths for selected elements.

The neutrons bound in an atom nucleus are concentrated in a small volume and so the differences in path lengths are so small relative to the neutron wavelength that destructive interference is not favoured in any direction. Therefore there is no variation in the scattering factor with $\sin\theta/\lambda$. This fact simplifies structure solution. The

general principles for neutron structure determination are therefore essentially the same as X-ray work, substituting scattering lengths, b_j, for scattering factors.

$$F_{hkl} = \sum_{j=1}^{N} b_j . \exp(i\phi_j) \qquad (1.7)$$

It is for this reason that the remaining discussion will be expressed in terms of X-ray diffraction.

1.2 Data reduction techniques[4]

In practice the scattered amplitudes are measured as beam intensities, I_{hkl}, where the following relationship holds:-

$$I_{hkl} \propto F_{hkl}^{2} \qquad (1.8)$$

There are several mechanisms which describe loss in intensities of diffracted X-rays. The most marked of these effects will be discussed below.

1.2.1 Lorentz factor

The Lorentz factor arises because the time taken for a reciprocal lattice point to pass through the sphere of reflection varies with its position in reciprocal space and the direction in which it approaches the sphere. As a result the predicted relative intensities of reflexions can differ significantly from measured values. The particular operating geometry of the instrument used for data collection will determine the nature of the correction to be applied. For an equi-inclination Weissenberg diffractometer the correction is formulated around the inclination angle, μ, and θ.

$$L = \frac{\sin \Theta}{\sin 2\Theta.(\sin^2\Theta - \sin^2\mu)^{1/2}} \qquad (1.9)$$

Equation 1.9 will take on different forms depending on the particular instrument used for the data collection.

1.2.2 Polarisation

The production of X-rays by striking a metallic target produces an unpolarised beam which can be resolved into two mutually perpendicular components. Since the electric vector, **E**, is continually changing direction and magnitude, the two components will vary. However on a time averaged scale, they can be assumed to be equal. As with optical reflection, a diffracted X-ray beam can become partially or completely polarised.

The intensity of the component vibrating parallel to the reflecting surface, $\mathbf{E}_x$, is governed purely by the electron density of the material. However the amplitude of the perpendicular component, $\mathbf{E}_y$, varies both with the electron density and cos 2θ.

The fraction of original intensity is described by equation 1.10.

$$p = \frac{1 + \cos^2 2\Theta}{2} \qquad (1.10)$$

It is clear from equation 1.10 that there can be a maximum reduction in X-ray intensity of 50%. Such a large variation cannot be left uncorrected if accurate intensities are required.

1.2.3 Absorption

Absorption can have a significant effect on diffracted intensities. It arises from the fact that different reflexions will travel through

different path lengths of crystal attenuating the diffracted beam by varying degrees.

The correction for absorption is often omitted from data reduction processes due to the complex calculations involved. The correction for each reflexion involves calculating the path distance travelled within the crystal by the beam, from each infinitesimal point within the crystal and then integrating these results for the entire crystal volume. If the crystal is irregular in shape then this can prove to be a very major task indeed.

The problem however, can be simplified by making an empirical correction based on the experimental data. By positioning the crystal such that an axial reflexion occurs and rotating the ω-axis, the variation in intensity can be noted (Chapter 4). An equation can be derived from the experimental data, expressing the intensity variation in terms ω.

It has also been noted that some crystalline materials will undergo decomposition whilst placed in the X-ray beam[5], thus gradually diminishing the total scattering strength. As a precaution a modern diffractometer can be instructed to periodically monitor the intensities of a few strong well defined reflexions. If there is significant variation, the scattering strengths of these reflexions are used to calculate scaling coefficients which are applied to the complete data set.

1.3 Unit cell contents from structure factors

1.3.1 Fourier transforms and electron density distribution[6]

The structure factor evaluated for any reflexion will depend on the contents of the unit cell. To make sense of the structure factor

amplitudes from a data set, a more direct expression linking the amplitudes with the electron density is required. A Fourier transform of expression 1.4 gives the following relationship:-

$$\rho(x,y,z) = \frac{1}{V} \sum_{h=-\infty}^{h=\infty} \sum_{k=-\infty}^{k=\infty} \sum_{l=-\infty}^{l=\infty} F_{hkl}.\exp(-2\pi i(\mathbf{h}x + \mathbf{k}y + \mathbf{l}z)) \qquad (1.11)$$

Evaluating the periodic expression in three dimensions, relative to the crystal axes, produces a map representing the electron density within the unit cell. By identifying the regions of high density, the atom positions can be determined.

However, the solution to the problem is not as elementary as the above description indicates. In order to evaluate the expression, the phases of each of the reflexions are required. At this stage nothing is known about the phases. To progress further, the phases of the reflexions must be evaluated from the experimental structure factor amplitudes alone. This is known as the Phase Problem.

1.3.2 The Phase Problem

There have been many methods devised to overcome the phase problem, each of which rely on the information contained within the structure factor amplitudes themselves.

There are currently two major ways in which phases can be calculated. These are known as Direct Methods and Patterson maps.

1.4 Structure solution by Direct Methods

There are three basic methods which can reveal the phases of reflexions directly. Of these, the least elegant is the method of trial and error.

1.4.1 Trial and error

This involves placing the atoms of the asymmetric unit in random positions and calculating theoretical structure factors for the proposed atomic arrangement. Comparison of the observed and calculated structure factors will indicate the suitability of the proposed model. Such a process only became feasible with the arrival of high-speed computers. Clearly, such an unsystematic approach can be very time consuming when there are numerous atoms. However, the number of trial model arrangements can be significantly reduced by placing constraints on the atom positions, rejecting certain improbable interatomic combinations. The intermolecular and intramolecular potentials for atom combinations would reveal whether atoms could be feasibly bonded. If the molecular structure is known, but its packing arrangement is uncertain, the whole molecule could be rotated within the asymmetric unit, maintaining bond lengths and angles[7,8]. Trial and error works best when the number of unknowns is small or a good deal of information is already available. With transputer development, new generation artificial intelligence routines may be able to solve structures more readily than is presently possible.

1.4.2 Isomorphous replacement

This technique is normally applied to crystal structures where there are heavy atoms present. The heavy atoms represent a large proportion of the scattering material in the unit cell and they therefore have a significant effect on the overall phases of the structure factors. If the heavy atom positions can be determined, the remaining atoms in the unit cell can be identified[9].

This method requires data sets to be collected on two or more

isomorphic crystals, differing only in structure by the type of heavy atoms present. The structure factors will have the same overall phase, but different magnitudes. By comparing the two data sets it is possible to ascertain approximate phases for the heavy atoms.

This technique is obviously restricted to a small number of structures where suitable derivatives can be synthesised with the same structure. It has little or no use in organic structure elucidation, but there has been some success with protein crystals where other common methods of solution fail.

1.4.3 Direct phasing

Direct phasing is a truly direct method, which uses the information held in the structure factor amplitudes to directly calculate the phases. In the case of a centrosymmetric structure the problem of phase reduces to a question of sign, where only two discrete values can be assumed. The structure factor for any permitted reflexion is thus defined as either $|\mathbf{F}_{hkl}|$ or $-|\mathbf{F}_{hkl}|$. In the case of the non-centrosymmetric structure, the problem is far more severe, since phases are capable of assuming any value between zero and 2π . The progression from phaseless structure factor amplitudes to phased reflexions is best described in terms of a centrosymmetric structure.

1.4.4 Inequality relationships

When measuring the (**hkl**) reflexions for a single crystal, the (**000**) reflexion is always strongest. This occurs for $2\Theta=0^{\circ}$, where all the atoms scatter in phase. It can be shown that for a centrosymmetric structure the following is true[10]

$$F_{hkl} < F_{000} \cdot \left[\frac{F_{000}}{2} + \frac{F_{2h2k2l}}{2} \right] \qquad (1.12)$$

By rearranging expression 1.12, a more convenient format can be produced. It can be seen that the left hand side of 1.13 will always be positive and can be evaluated without a knowledge of the phases. Substitution of the known values into 1.13, will produce the phase for reflexion (**2h 2k 21**).

$$\left[\frac{F_{hkl}}{F_{000}}\right]^2 < \frac{1}{2}\cdot\left[1 \pm \frac{|F_{2h2k21}|}{|F_{000}|}\right] \qquad (1.13)$$

However this method works on the premise that the reflexions chosen for the inequality relationships have large intensities. This theorem was later developed to take into account symmetry effects, thus improving the reliability of the expression[11].

1.4.5 Probabilities

When there are insufficient strong reflexions or the number of atoms in the asymmetric unit becomes too large for accurate phasing, the inequalities can be replaced by probabilities. These now state whether a phase is probable for a given reflexion.

If the phases of several reflexions can be determined by inequalities, then simple electron density graphs can be made[12]. From the graphs the probabilities of the phases being correct can be determined. This is best exemplified in a one dimensional case with the density function evaluated for the (**100**) reflexion in a centrosymmetric structure. Shown in Figure 1.4, the electron density along the x-axis is plotted for both +ve and -ve phases. The maximum turning points of the plots at x=0.0 and x=0.5 indicate the most probable atom sites if the (**100**) reflexion is strong. If the (**200**) reflexion is also significant the phase predictions can be made. Plotting the electron density for (**200**)

in Figure 1.5 shows two possible maximum electron density sites for each phase value. By combining the two plots for all phase combinations, it can be seen in Figures 1.6 and 1.7 that the minimum negative electron density occurs when (**200**) has positive phase, regardless of the (**100**) phase. Therefore it can be concluded that the phase of (**200**) is probably positive despite the phase of the (**100**). The principle of positivity of electron density can be expressed in a relationship for strong reflexions, based on the products of the signs of the reflexions[13]. The expression takes the form:-

$$S(\mathbf{H}).S(\mathbf{K}) \approx S(\mathbf{H}-\mathbf{K}) \qquad (1.14)$$

Where **H** represents the indices (**hkl**) for a reflexion, **K** represents (**h'k'l'**) and **H-K** represents (**h-h' k-k' l-l'**). S() means sign of reflexion and ≈ means probably true.

In the case of the (**100**) and (**200**) reflexions,

$$S(100).S(100) \approx S(200) \qquad (1.15)$$

In this expression the sign for (**200**) will always be +ve, even if (**100**) phase is -ve or +ve. This relationship holds for strong reflexions where the indices sum together.

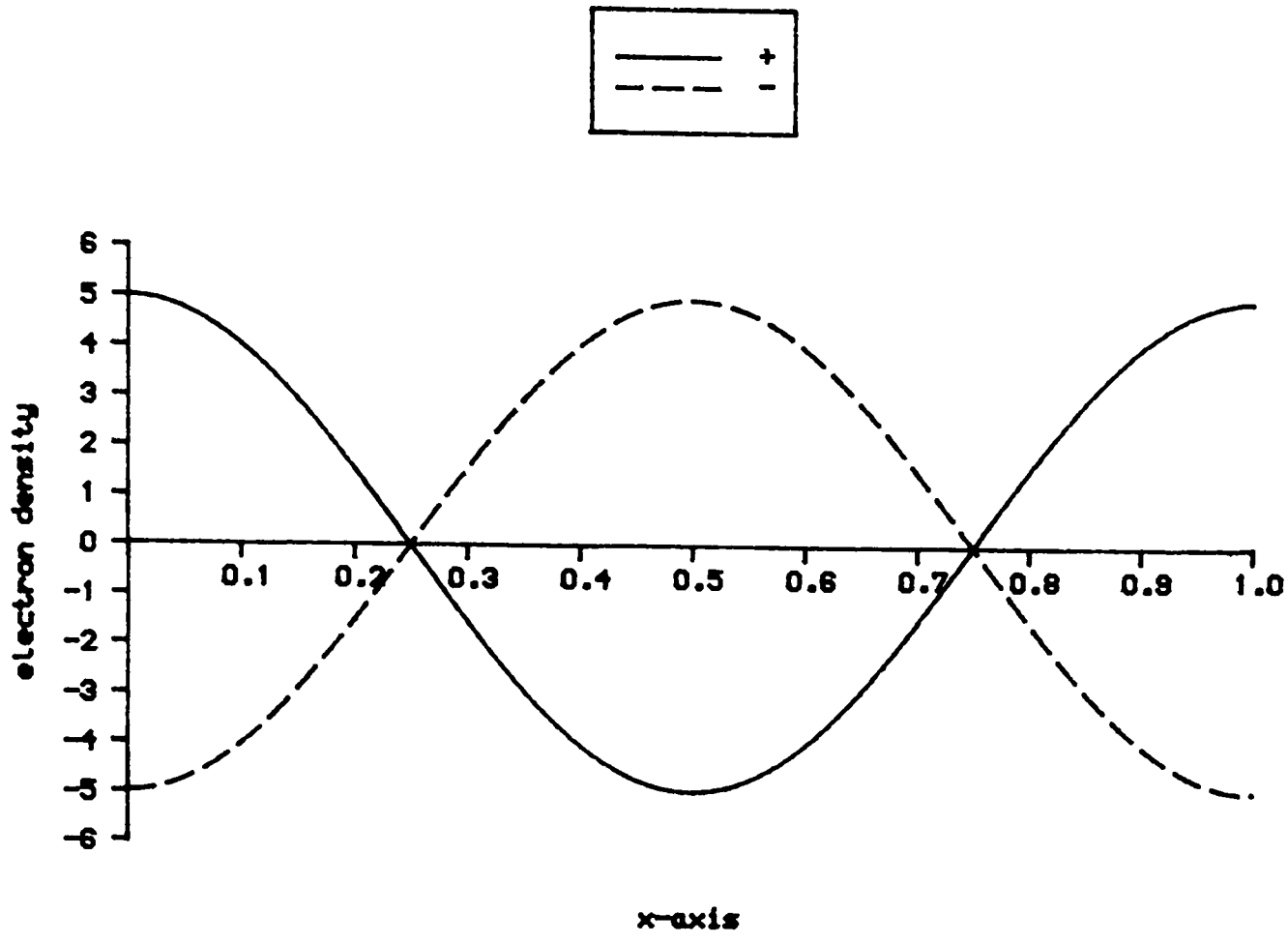

Figure 1.4 The one dimensional electron density function for the (100) reflexion for a centrosymmetric structure. Both possible phases are represented. For a +ve phase the maximum is found at x=0.0/1.0. With the -ve phase the maximum is found at x=0.5.

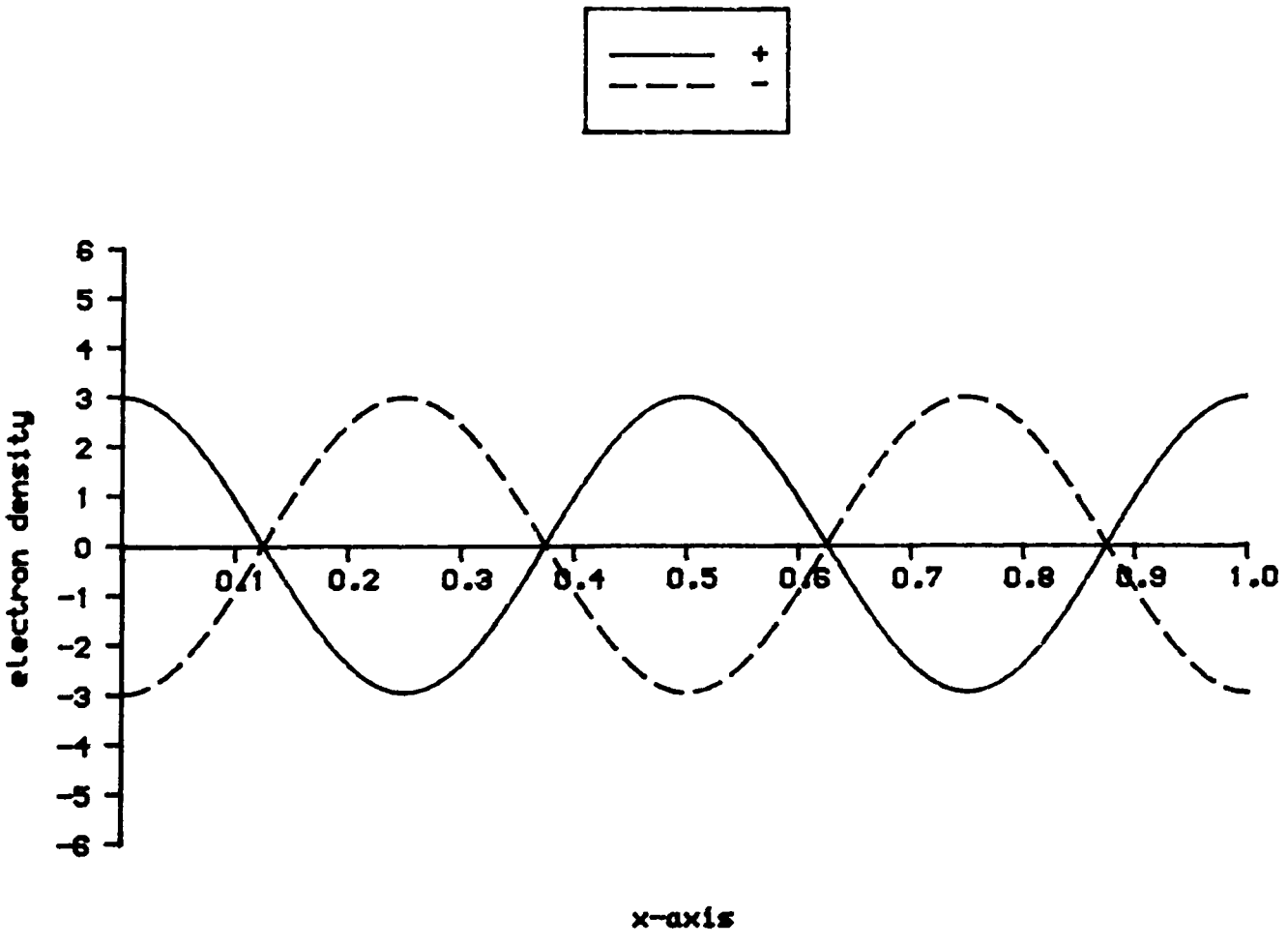

Figure 1.5 The one dimensional electron density function for the (200)reflexion for a centrosymmetric structure. Maxima are found at x=0.0, 0.5 & 1.0 for +ve phase and at x=0.75 for -ve.

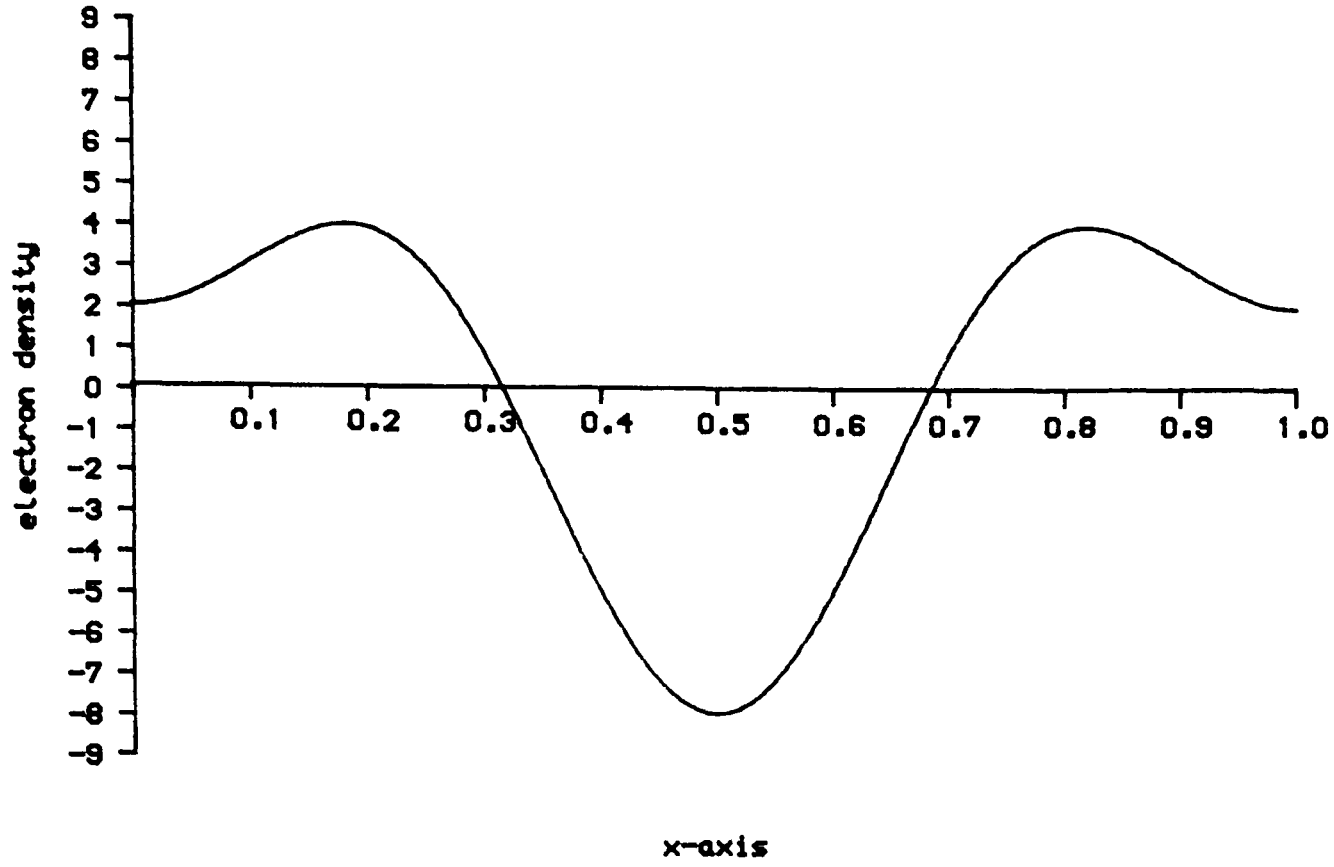

Figure 1.6(a) The electron density function evaluated for both the (100) and (200) reflexions. (100) +ve and (200) -ve.

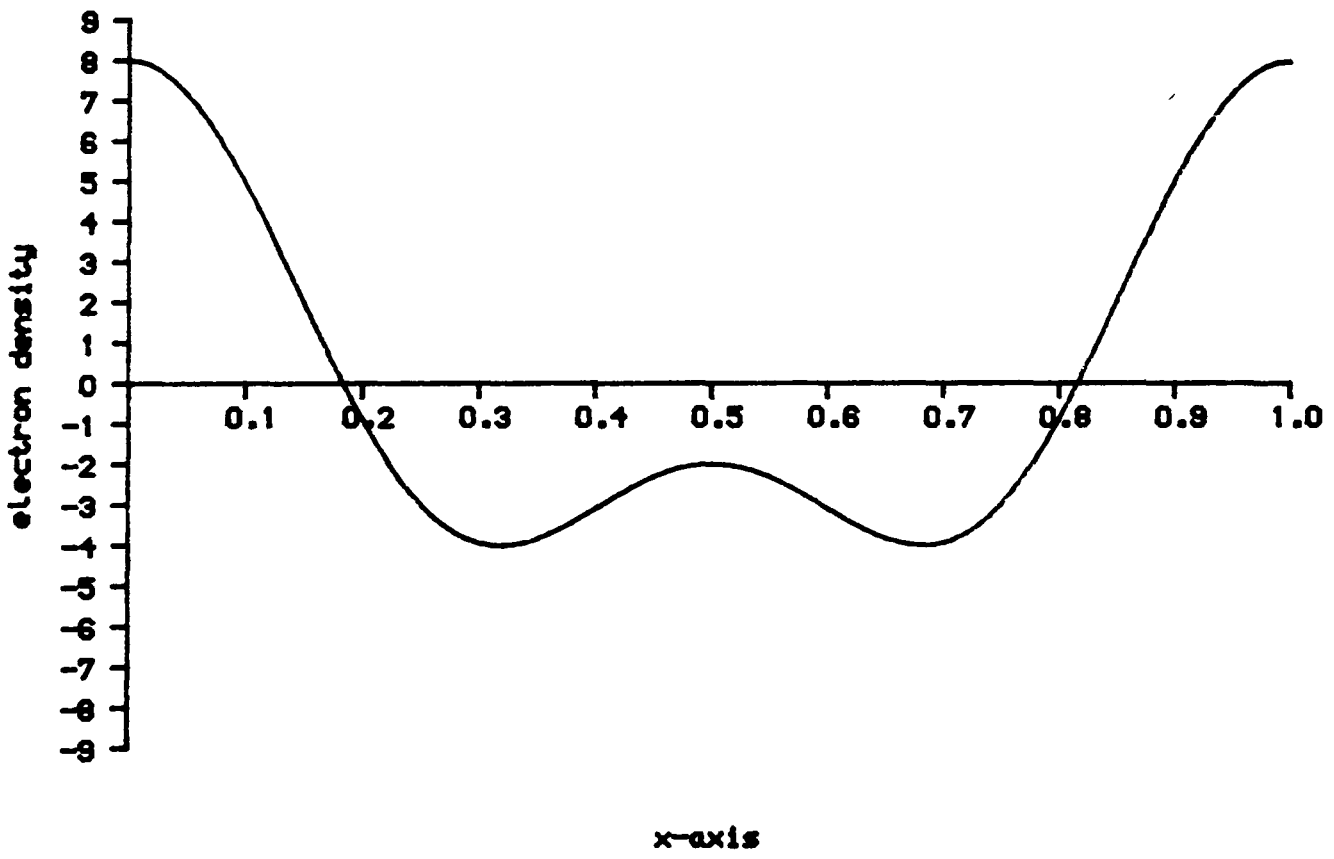

Figure 1.6(b) As 1.6(b), but with (100) +ve and (200) +ve.

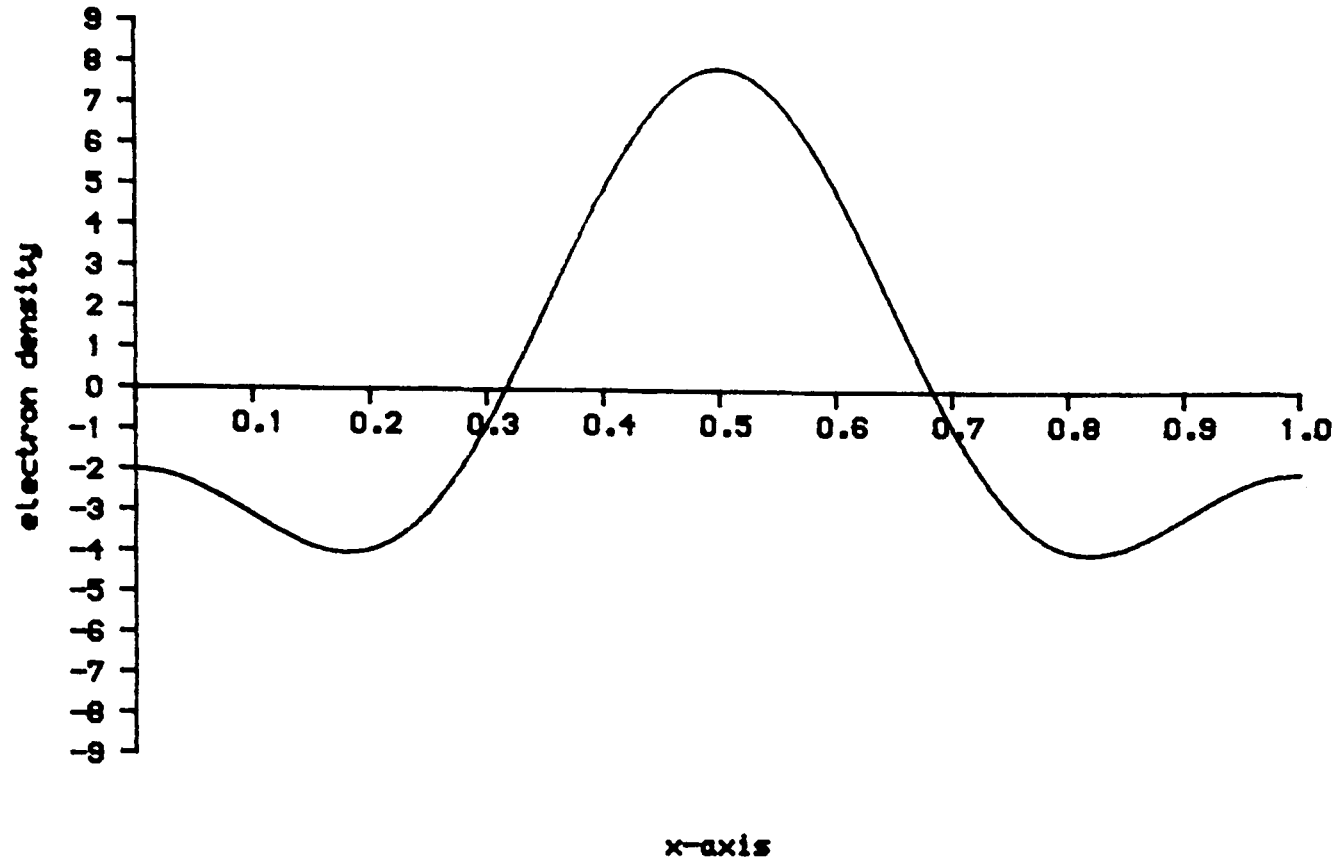

Figure 1.7(a) The electron density function evaluated for both the (100) and (200) reflexions. (100) -ve and (200) +ve.

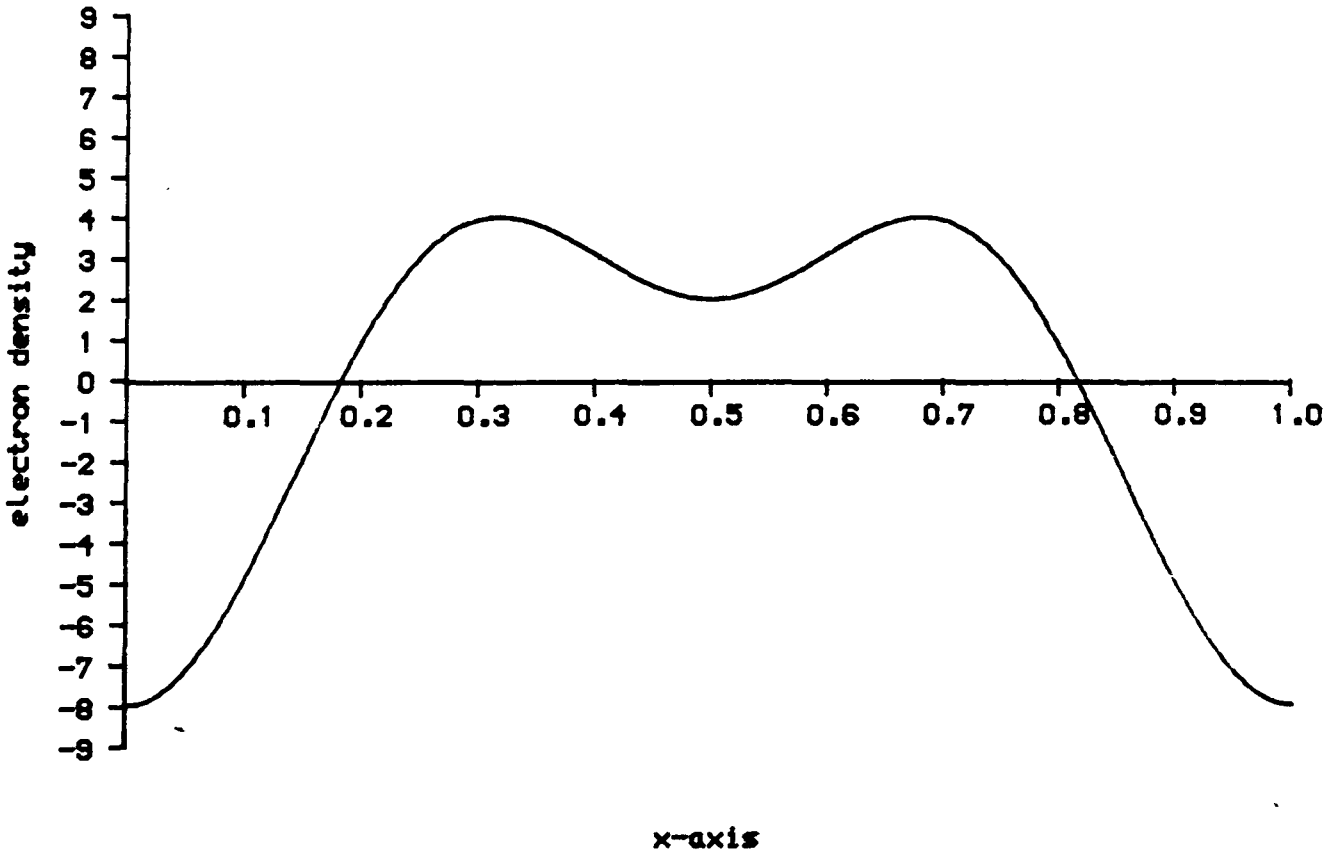

Figure 1.7(b) As 1.7(a), but with (100) -ve and (200) -ve.

This expression was further developed[14] and the likelihood of the expression being correct was found to be dependent on the magnitude of the Triple Product. (Equation 1.16)

$$\mathbf{E} = \mathbf{E}_H . \mathbf{E}_K . \mathbf{E}_{H-K} \qquad (1.16)$$

In this expression the structure factor amplitudes are replaced by normalised structure factors[15], $\mathbf{E}_{hkl}$. The calculation of $\mathbf{E}_{hkl}$ values using equation 1.17, represents the r.m.s. value of $\mathbf{F}_{hkl}$ evaluated for a random arrangement of atoms in the unit cell. This has the effect of producing sharper peaks than those shown in Figure 1.6.

$$E_{hkl} = \frac{F_{hkl}}{(\epsilon \sum f_j)^{1/2}} \qquad (1.17)$$

Where ϵ is an integer which is dependent upon the crystal space group.

If the Triple Product is large then the probability of the relationship being correct is high. The probability that $\mathbf{E}_{hkl}$ is positive can be expressed as follows[16]:-

$$P_+ = \frac{1}{2} + \frac{1}{2} \cdot \tanh \left[\frac{|\mathbf{E}_{hkl}| \sum \mathbf{E}_K \cdot \mathbf{E}_{H-K}}{N^{1/2}} \right] \qquad (1.18)$$

Once probable phases have been established for several reflexions, new Triplet relationships can be developed for other strong reflexions. Continued repetition of this process can produce a large number of phased reflexions, sufficient to calculate a reliable electron density map.

In the case of non-centrosymmetric structures these relationships become less trivial, since there are no restrictions on the phase

values. The introduction of the Tangent formula[17] enabled phase angles to be directly estimated from normalised structure factors. The reliability of the tangent formula has been found to diminish with increasing number of atoms per unit cell. This method has been used successfully to determine the structures of non-centrosymmetric crystal systems[18].

$$\tan(\phi_H) \approx \frac{\sum |\mathbf{E}_K||\mathbf{E}_{H-K}| \sin(\phi_K + \phi_{H-K})}{\sum |\mathbf{E}_K||\mathbf{E}_{H-K}| \cos(\phi_K + \phi_{H-K})} \qquad (1.19)$$

1.5 Structure solution by Patterson vector method[19]

Direct methods are now used to solve many structures, however there are occasions when it may fail. Often a structure has too many atoms for direct phasing to be effective. In cases where heavy atoms are present the Patterson function can be used to determine the heavy atom coordinates, thus allowing approximate phases to be calculated.

1.5.1 Patterson function

The Patterson function is a Fourier transform of the electron density equation 1.11, but it uses the phaseless quantity $|\mathbf{F}_{hkl}|$, thus avoiding the phase problem. Therefore the Patterson function can be evaluated directly from indexed structure factor amplitudes calculated from the experimental intensities. The function is given below:-

$$P(u,v,w) = \frac{1}{V} \sum_{h=-\infty}^{h=\infty} \sum_{k=-\infty}^{k=\infty} \sum_{l=-\infty}^{l=\infty} |F_{hkl}|^2 \cos(\phi_{u,v,w}) \qquad (1.20)$$

Where **V** is the volume of the unit cell and u, v and w refer to three dimensional coordinates in the Patterson map, based on the lattice parameters from the unit cell.

Instead of the synthesis leading directly to a distribution of electron density within the unit cell, it produces a similar map, where peaks correspond to interatomic vectors. The map is evaluated in three dimensions in finite steps for all reflexions. A peak with coordinates (u,v,w), relates to two atoms with coordinates in the unit cell, x_1, y_1, z_1 and x_2, y_2, z_2 , such that

$$u = x_1 - x_2 \tag{1.21}$$

$$v = y_1 - y_2 \tag{1.22}$$

$$w = z_1 - z_2 \tag{1.23}$$

P(u,v,w) is the peak height of the map at that point.

1.5.2 Vector map

In an ideal vector map describing a unit cell containing N atoms, there will be N^2-N unique interconnecting vectors representing every interatomic combination. There will be N zero length vectors positioned at the origin of the map, which correspond to vectors initiating and terminating on the same atom. These are called the Identity vectors.

In Figure 1.8(a), the idea of the vector map is presented graphically in two dimensions. For simplicity, the unit cell is square and has three identical atoms, A, B and C. Within the unit cell there are nine vector combinations; AA, AB, AC, BB, BA, BC, CC, CA and CB. These vectors are represented on the two dimensional Patterson Vector map in Figure 1.8(b). AA, BB and CC are the identity vectors superimposed upon one another at the origin producing strong peaks. It is evident from this diagram that the vector map has a centre of symmetry, which is a feature of all Patterson maps, regardless of the crystal space group.

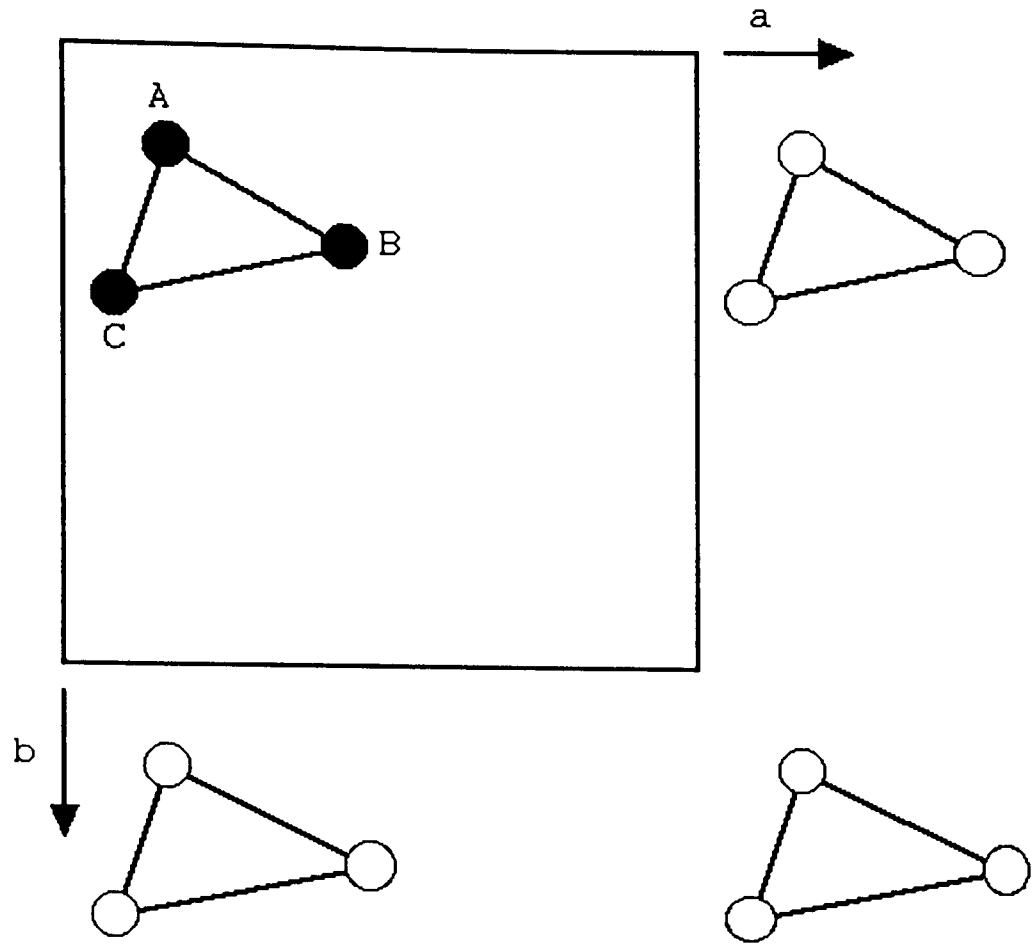

Figure 1.8(a) A two dimensional square lattice containing three atoms per asymmetric unit. The atoms in bold represent the asymmetric unit.

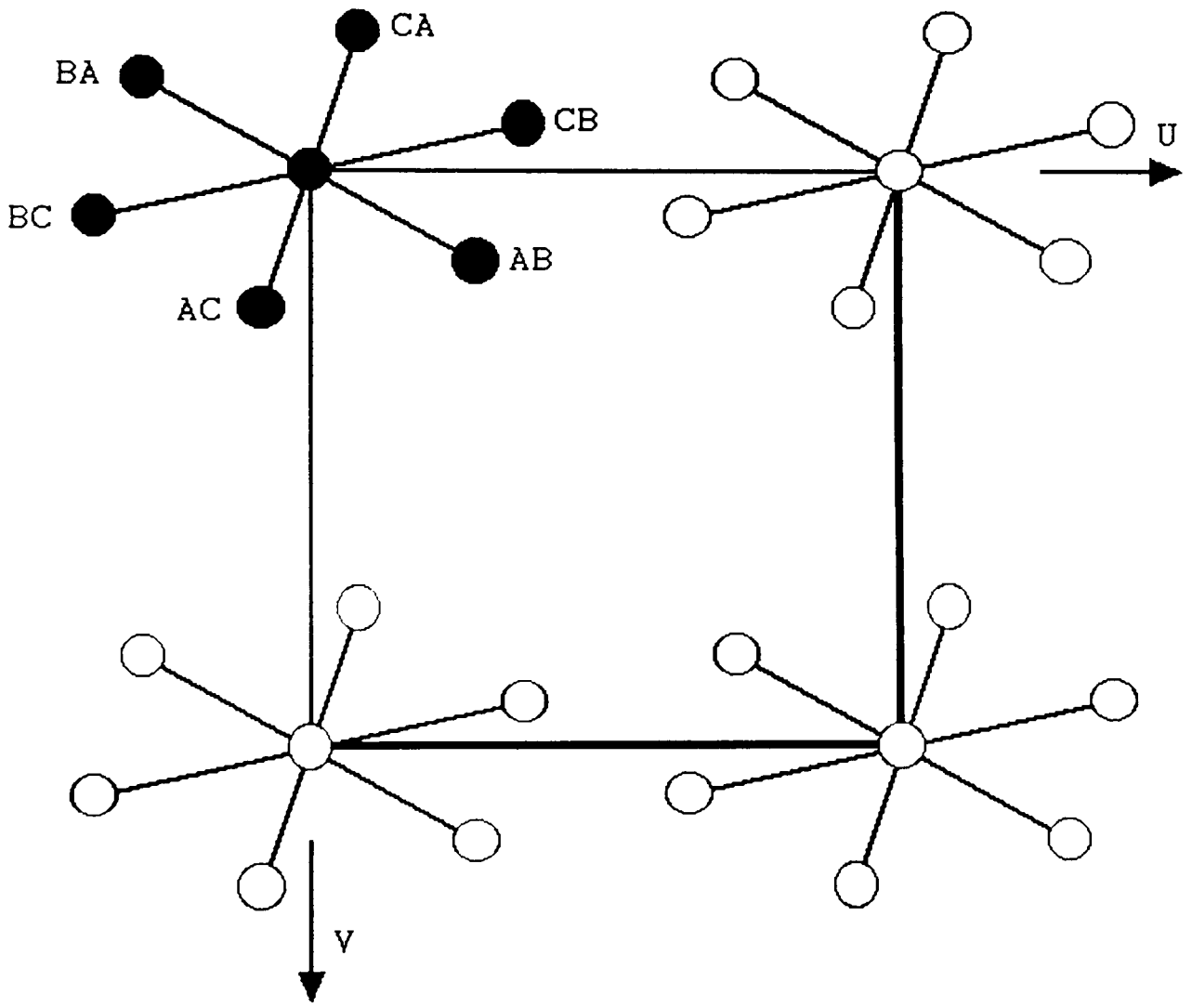

Figure 1.8(b) The corresponding theoretical Patterson vector map based on the simple three atom structure. In total there are nine vectors, with three identity vectors superimposed upon one another at the origin.

This ideal situation is based on the assumption that the electrons within the atom are concentrated about an infinitesimal point. In reality there extends a finite volume in space around the atom nucleus containing the electrons and so there will be a range of vectors reaching from any point within the approximate sphere of electrons of one atom to any point within the second atom's sphere. Therefore there are an infinite number of vectors ranging in length from the separation of the two closest electrons to the two farthest.

The result of the synthesis, is a rather blurred image of broad overlapping peaks. Since the probability of finding an electron further out from the nucleus diminishes according to a normal distribution, assuming isotropic vibrations, the majority of the scattering mass is close to the centre of the atom. The maximum height of the peak therefore occurs at the centre of the peak distribution.

1.5.3 Sharpened Patterson map

The overlapping of the peaks can make the interpretation of the map difficult, whether it is performed by human eye or by computer programs. The map may be clarified by using modified structure factors which describe atoms with the electrons concentrated about the nucleus.

Converting the structure factor amplitudes to point structure factor amplitudes, $\mathbf{F}_{point}$, removes the angular variation of the atomic scattering factor. The expression relating experimental $\mathbf{F}_{hkl}$ to $\mathbf{F}_{point}$, for a given (**hkl**) plane, is given by equation 1.24.

$$F_{point} = \frac{\sum Z_i}{\exp(-B.\sin^2\theta/\lambda^2).\sum f_{o_j}} \cdot F_{hkl} \qquad (1.24)$$

The Patterson synthesis is calculated using the $\mathbf{F}_{point}$ values instead of F_{hkl} values. With the electrons considered to be located at one point, the vector overlap is significantly reduced. The sharpened map may also be calculated using normalised structure factors, $\mathbf{E}_{hkl}$, producing the same effect.

The difference between the standard Patterson map and the sharpened map is highlighted in Figure 1.9. The maps are still incomplete since the synthesis is performed with only a finite number of structure factors.

A common problem with the Patterson method is that all the identity vectors all superimpose upon one another, creating one large peak at the origin which can mask any other less intense peaks close to the origin. This can be overcome by performing a subtraction of the average squared structure factor amplitude from each term in the summation.

$$|F_{hkl}|^2 = |F_{hkl}|^2 - \sum f_j^2 \qquad (1.25)$$

1.5.4 Calculation of heavy atom positions

The weight of a peak in a vector map is proportional to the product of the atomic numbers of the two atoms involved in the interatomic vector. The weight is determined by integrating the area under the peak distribution, as with powder diffraction traces, but in most cases it is simply approximated to the height of the peak, P(u,v,w). Atoms in one asymmetric unit are related to similar atoms in adjacent asymmetric units by the symmetry operators which are specific to the crystal space group. Some of the vectors will describe these translations or combinations of them. In the case of a heavy atom

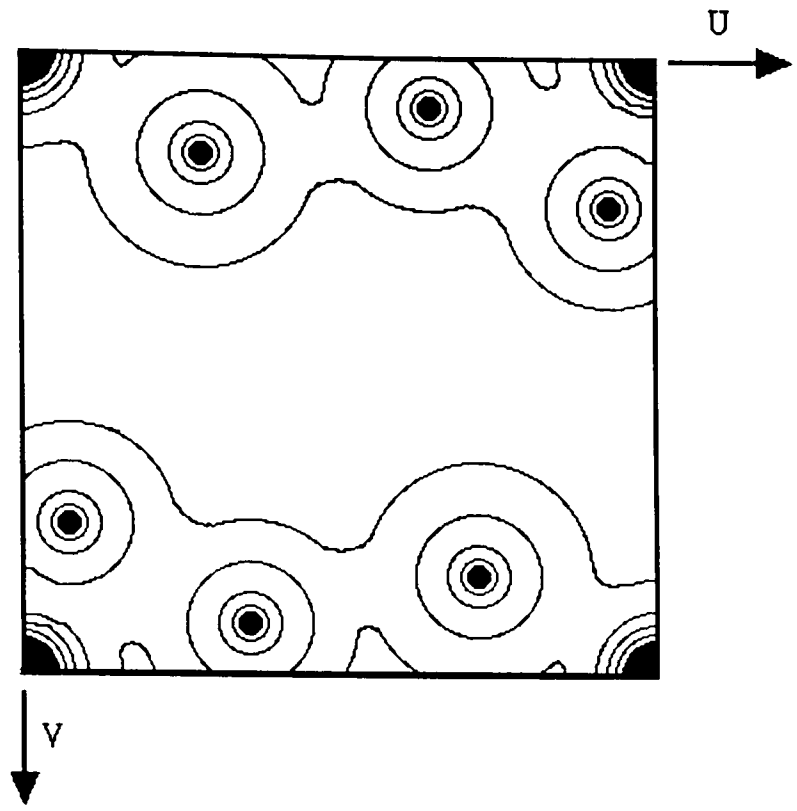

Figure 1.9(a) A simulated Patterson map based on the two dimensional structure featured in Figure 1.8(a). The contour lines represent the spread of interatomic vectors.

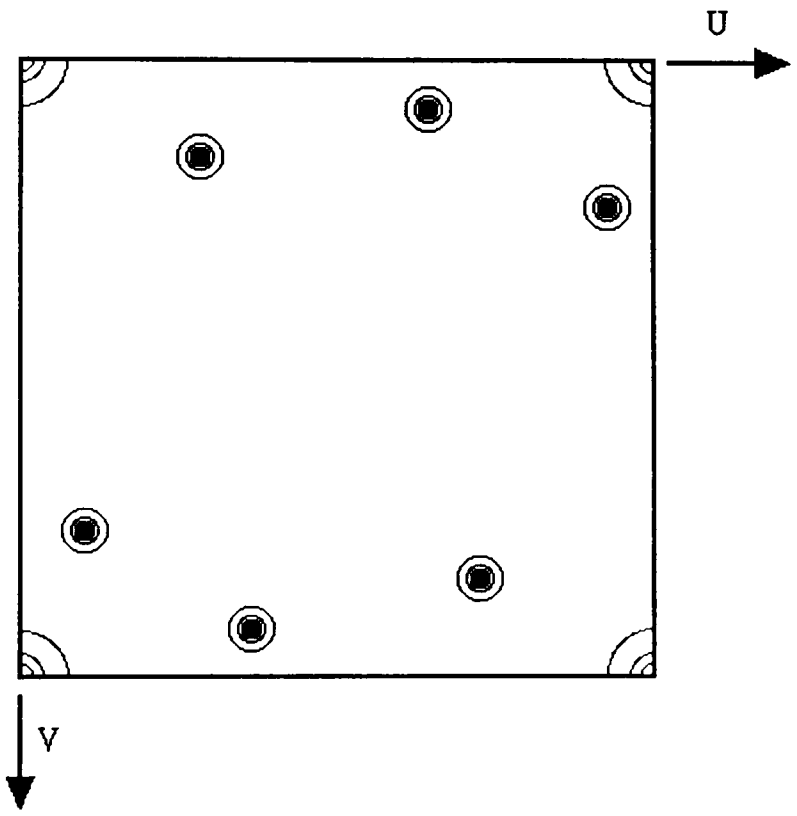

Figure 1.9(b) The above vector map after sharpening and origin subtraction.

structure the vector map will be dominated by the vectors linking the heavy atoms. By exploring the vector map, the most intense peaks can be extracted for coordinate solution. A series of simultaneous equations can be set up by combining the symmetry operators.

For the trigonal space group R3, the symmetry operators, based on a hexagonal axial system, are as follows:-

$$(X,Y,Z) \qquad (1.26)$$

$$(-Y,X-Y,Z) \qquad (1.27)$$

$$(Y-X,-X,Z) \qquad (1.28)$$

By subtracting operator (1.27) from (1.26), produces the vector (X+Y, 2Y-X, 0), which consists of X and Y terms only. If a strong vector from the Patterson vector list has Z=0, then it is likely that this vector corresponds to the interatomic separation described by the combination of (1.26) and (1.27). Substitution of the numerical coordinates of the vector into the new expression will yield values for X and Y. Combination of (1.26) and (1.28) will produce another vector which can be solved in a similar fashion. If there is agreement between the values, then the atomic coordinates can be assumed to be correct.

Since the heavy atom probably contributes most to the scattering it will have a profound effect on the phases for all reflexions. With the phase of the heavy atoms thus determined, approximate phases can be assigned to the observed structure factors. This permits crude electron density calculations to be made in an attempt to identify the other light atoms in the structure.

The dominance of scattering by the heavy atoms can however, make the

task of finding other light atoms difficult, if not impossible. Slight shifts of the positions of the light atoms during structure refinement, may occur without significantly effecting the overall quality of fit between observed and calculated structure factors. As a consequence atomic coordinates can have large uncertainties and bond lengths may refine to unacceptable values. For Patterson methods to be work most effectively, the sum of the atomic masses of all the light atoms in the structure should be of similar magnitude to the sum of the atomic masses of all the heavy atoms.

1.6 Structure refinement

Depending on the method used to phase the reflexions, a portion of the structure will be known. With Direct Methods, the structure can be close to complete, requiring only a small amount of fine tuning. With Patterson methods however, there may be only one or two atom positions known. However these heavy atoms will usually represent a considerable proportion of the total scattering matter.

The proposed structure needs to be verified, by comparing the trial model data with the observed data.

1.6.1 Fourier difference synthesis[20]

The Fourier electron density expression 1.11 relates the structure factor amplitudes and corresponding phases to the electron density distribution within the unit cell.

$$\rho_o(x,y,z) = \frac{1}{V} \sum_{h=-\infty}^{h=\infty} \sum_{k=-\infty}^{k=\infty} \sum_{l=-\infty}^{l=\infty} Fo_{hkl}.\exp(i\phi_{hkl}) \qquad (1.29)$$

With only a finite number of observed reflexions, the triple summation is incomplete. The expression can be rewritten as follows:-

$$\rho_o(x,y,z) = \frac{1}{V} \sum_h \sum_k \sum_l Fo_{hkl}.\exp(i\phi_{hkl}) + R \qquad (1.30)$$

Where R represents the omitted terms from the triple summation.

A crude electron density map can be generated from the calculated structure factor amplitudes and phases for the estimated atom positions of the trial structure.

$$\rho_c(x,y,z) = \frac{1}{V} \sum_h \sum_k \sum_l Fc_{hkl}.\exp(i\phi_{hkl}) + R' \qquad (1.31)$$

Again R′ represents the correction for the limited number of observations included in the synthesis.

Subtraction of the two maps, generated by equations 1.30 and 1.31, produces the difference map. Positive areas on the map will indicate regions of unaccounted electron density, whilst negative values represent incorrectly placed atoms.

The process of synthesising the maps and then subtracting them, can be combined in one overall operation, called a Difference Synthesis.

$$\rho_o-\rho_c = \frac{1}{V} \sum_h \sum_k \sum_l (Fo-Fc)_{hkl}.\exp(i\phi_{hkl}) \qquad (1.32)$$

The two terms R and R′ are virtually equal and so can be discarded from the equation. An approximate difference map, calculated from the limited number of reflexions, may be able to reveal new atom positions. If the new atom positions are included in the model, the synthesis can be repeated producing a more accurate map.

1.6.2 Least squares refinement[21]

The initial difference maps are relatively crude and so positional parameters will only be approximate. The positional and thermal parameters need to be adjusted to achieve the best agreement between the observed and calculated structure factors. Least Squares refinement represents a systematic approach of modifying each of the parameters to their optimum values.

The structural parameters are adjusted such that the evaluation of equation 1.33 produces a value approaching zero.

$$D = \sum_{i=1}^{N} \omega_{hkl} . (|F_o| - |kF_c|)^2 \qquad (1.33)$$

Where ω_{hkl} is the weight of an observation and k is the scaling factor. A weighting scheme is applied to all the reflexions, which takes into account the reliability of each reflexion. The weighting scheme is generally based around the reciprocal of the square of the estimated standard error of the structure factor amplitude. The relationship is given by equation 1.34. This ensures that well defined reflexions are given greater priority over weak ones in the process of least squares refinement.

$$\omega_{hkl} = \sigma_{hkl}^{-2} \qquad (1.34)$$

Where σ_{hkl} is the estimated experimental error of $|F_{hkl}|$.

The structure factor expression is non-linear and so the best fit positional and thermal parameters cannot be evaluated directly. Equation 1.33 can be arranged in a more useful form by differentiating it with respect to each of the individual parameters and equating the resulting n expressions to zero.

$$\sum \omega_{hkl} \cdot \left|Fo\right| - \left|kFc(a_1, a_2, .., a_n)\right| \cdot \frac{\partial \left|kFc(a_1, a_2, .., a_n)\right|}{\partial a_j} = 0 \qquad (1.35)$$

Where j=1,2,3....,n and a_j represents each of the parameters in the structure factor equation. For a data set consisting of n parameters, there will be n systems of equations.

The equations are not linear and so direct calculation of the optimum parameters is not possible. However, the calculated structure factor expression can be approximated by a Taylor series, omitting the terms with powers of two or more.

$$\left|kFo(p_1 . p_2 , .., p_n)\right| = \left|Fc\right| + \frac{\partial \left|kFc(a)\right|}{\partial p_1} \cdot \Delta p_1 + \ldots + \frac{\partial \left|kFc(a)\right|}{\partial p_n} \cdot \Delta p_n \qquad (1.36)$$

Where a_1, a_2,..., a_n are the initial parameter values and p_1, p_2,..., p_n are the refined values. $\Delta p_j = p_j - a_j$.

By rearranging the terms, the system of n equations take on the following forms.

$$\sum \omega_H \cdot \frac{\partial \left|kFc\right|}{\partial p_1} \cdot \frac{\partial \left|kFc\right|}{\partial p_1} \cdot \Delta p_1 + \ldots + \sum \omega_H \cdot \frac{\partial \left|kFc\right|}{\partial p_1} \cdot \frac{\partial \left|kFc\right|}{\partial p_n} \cdot \Delta p_n = \sum \omega_H \cdot \frac{\partial \left|kFc\right|}{\partial p_1} \cdot (Fo-Fc)_H \qquad (1.37)$$

$$\sum \omega_H \cdot \frac{\partial \left|kFc\right|}{\partial p_2} \cdot \frac{\partial \left|kFc\right|}{\partial p_1} \cdot \Delta p_1 + \ldots + \sum \omega_H \cdot \frac{\partial \left|kFc\right|}{\partial p_2} \cdot \frac{\partial \left|kFc\right|}{\partial p_n} \cdot \Delta p_n = \sum \omega_H \cdot \frac{\partial \left|kFc\right|}{\partial p_2} \cdot (Fo-Fc)_H \qquad (1.38)$$

$$\vdots$$

$$\sum \omega_H \cdot \frac{\partial \left|kFc\right|}{\partial p_n} \cdot \frac{\partial \left|kFc\right|}{\partial p_1} \cdot \Delta p_1 + \ldots + \sum \omega_H \cdot \frac{\partial \left|kFc\right|}{\partial p_n} \cdot \frac{\partial \left|kFc\right|}{\partial p_n} \cdot \Delta p_n = \sum \omega_H \cdot \frac{\partial \left|kFc\right|}{\partial p_n} \cdot (Fo-Fc)_H \qquad (1.39)$$

Evaluation of these n linear equations and solving for Δp_j yields new approximations for the parameters. These new values may be re-

substituted and the evaluation repeated. Each cycle of least squares effectively improves the quality of fit for each parameter, until further cycling will no longer produce a significant change. When this stabilisation occurs, the values have arrived at their optimum values. Depending on the starting values and the constraints placed upon the parameters, the refinement should produce sensible values if the presumed structure is correct.

The task of solving a series of n equations with n unknowns can be a vast undertaking when n becomes a sizable figure. Solution of the equations for p is best performed by a computer using matrix arithmetic, where the n equations are arranged as shown in Figure 1.10.

The normal conventions of solving simultaneous equations by matrix arithmetic are applied using all of the terms. When all the n terms in matrix A are used, the method of solution is called Full Matrix least squares.

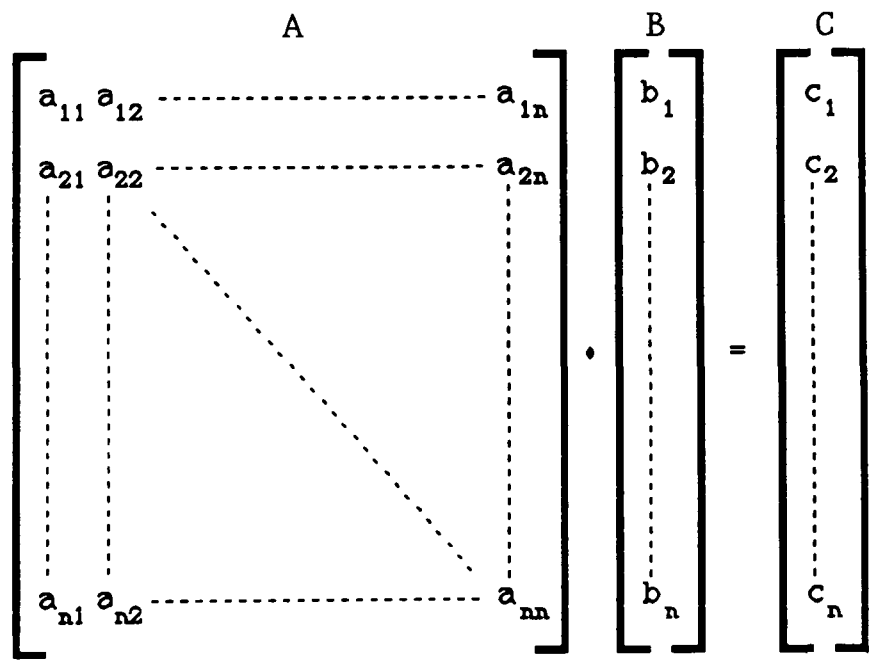

Figure 1.10 Schematic representation of matrix arithmetic.

Solution by this comprehensive method can involve vast numbers of calculations, even when modest crystal structures are refined. However

since the solution of equations does not actually derive the optimum values for the parameters in the first computation but rather by a converging series of calculations, there is scope for simplification of the calculation.

From equations 1.37 to 1.39, it can be seen that in each equation there is a sum of squares term following the diagonal of the matrix. These terms will always be positive and will have a tendency to be much larger than the other terms in the equations. The other terms can assume either +ve or -ve values and therefore the summations tend to cancel out. Thus the equations can be solved directly for p_j. This method significantly improves the time for computation and is called Diagonal Matrix least squares. This technique assumes that the n parameters in each equation can be refined independently. However, for one atom being refined isotropically, the three positional parameters and the temperature factor are correlated and so Diagonal Matrix refinement is unsuitable.

A variation of the diagonal matrix is blocked matrix least squares[22], where more parameters are included in each line in the matrix. For the refinement of an atom with isotropic thermal motion, the four parameters x, y, z and u, are closely correlated. To solve for all four parameters, giving improved parameter values, a system of four simultaneous equations is required. Thus blocks of terms, following the diagonal of the matrix, are involved in the refinement for each atom. This is shown schematically in Figure 1.11.

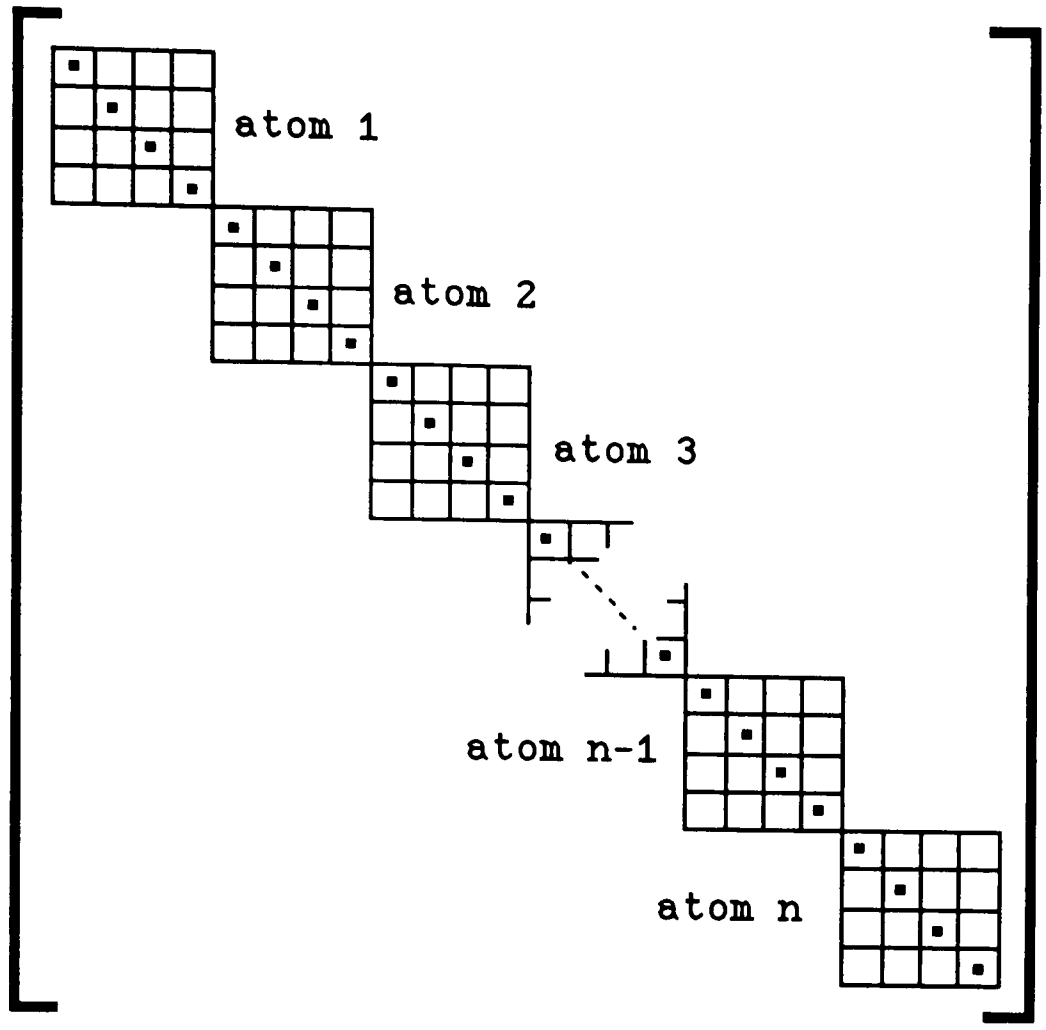

Figure 1.11 Blocked matrix.

This method is more powerful than Diagonal Matrix least squares, but since the number of computations is reduced, it is far quicker than Full Matrix. The choice between using Full or Blocked techniques will be dependent on the particular structure under investigation.

These processes can also be performed on a system of equations using intensities rather than amplitudes, with equal effect.

1.6.3 Figures of merit

During the structure refinement it is necessary to monitor the progress of the parameters by manually checking the revised parameter list. It is difficult to ascertain the significance of the shifts in the atomic parameters, but the thermal parameters will often reflect the suitability of the model. For convenience it is preferable to assign a numerical value representing the agreement between the crystal model and the crystal itself. This can be expressed by

comparing the sums of the differences of calculated and observed structure factors, known as the residual figure of merit, **R**.

$$R = \frac{\sum(F_o - F_c)}{\sum F_o} \qquad (1.40)$$

For all reflexions.

A value of less than 0.1 will normally indicate that the proposed structure is correct, requiring only subtle variations to be applied to the model[23]. A random structure[24] can have an R value of around 0.6 and it is possible to have R as low as 0.2-0.3, yet the assumed structure can still be erroneous[25]. Therefore the residual value should not be solely relied upon to determine the level of agreement between the crystal model and crystal structure.

There are other statistics which can express the reliability of the model. Examination of the difference map, after the refinement of the accepted structure has stabilised, will reveal if there are still regions of unaccounted electron density. The terms $\Delta\rho_{max}$ and $\Delta\rho_{min}$ refer to the maximum and minimum electron density regions in the difference map. In an ideal structure, the magnitude of both of these parameters will be zero, but in reality, due to a limited number of observations, values of 0.5 $e\text{Å}^{-3}$ are common.

CHAPTER 2. Diffractometer geometries and their operation.

In the course of the research, work has been carried out on several difractometers. These instruments vary in complexity and can offer differing levels of information from a crystalline sample. However, they all rely on the same basic principles for diffraction to occur. The geometries, sample preparation and operating principles of each of the instruments will be explained individually, highlighting the main differences.

2.1 Powder diffraction

The two powder diffractometers used in these studies have essentially the same operation but differ in the X-ray sources and the maximum interplanar spacing resolution.

2.1.1 Principle of random orientation[26]

The powder method requires that the crystalline sample is reduced to a fine powder such that for a given X-ray wavelength, some of the crystallites will be by coincidence in the correct position to satisfy Bragg's law,.i.e, $n\lambda=2d\sin\Theta_{hkl}$. For each d_{hkl}, there will be a cone of radiation produced, with a semi-vertical angle of 2Θ . Each cone is produced by the scattering of individual crystallite planes, with the same interplanar spacing, orientated parallel to both the incident beam and the semi-vertical axis of the cone. A schematic representation of the diffraction cones is shown in Figure 2.1.

In a finite sample with a finite number of crystallites, the diffraction cone can often be non-uniform in intensity. This is due to an effect called Preferred Orientation. This is manifest by an ordering of the crystalline particles, such that the overall orientation can no longer be described as random. This ordering is commonly caused by crystals with regular morphology aligning such that

dominant crystal axes are parallel, thus favouring diffraction in a common direction. The subject of preferred orientation will be discussed further in Chapter 3.

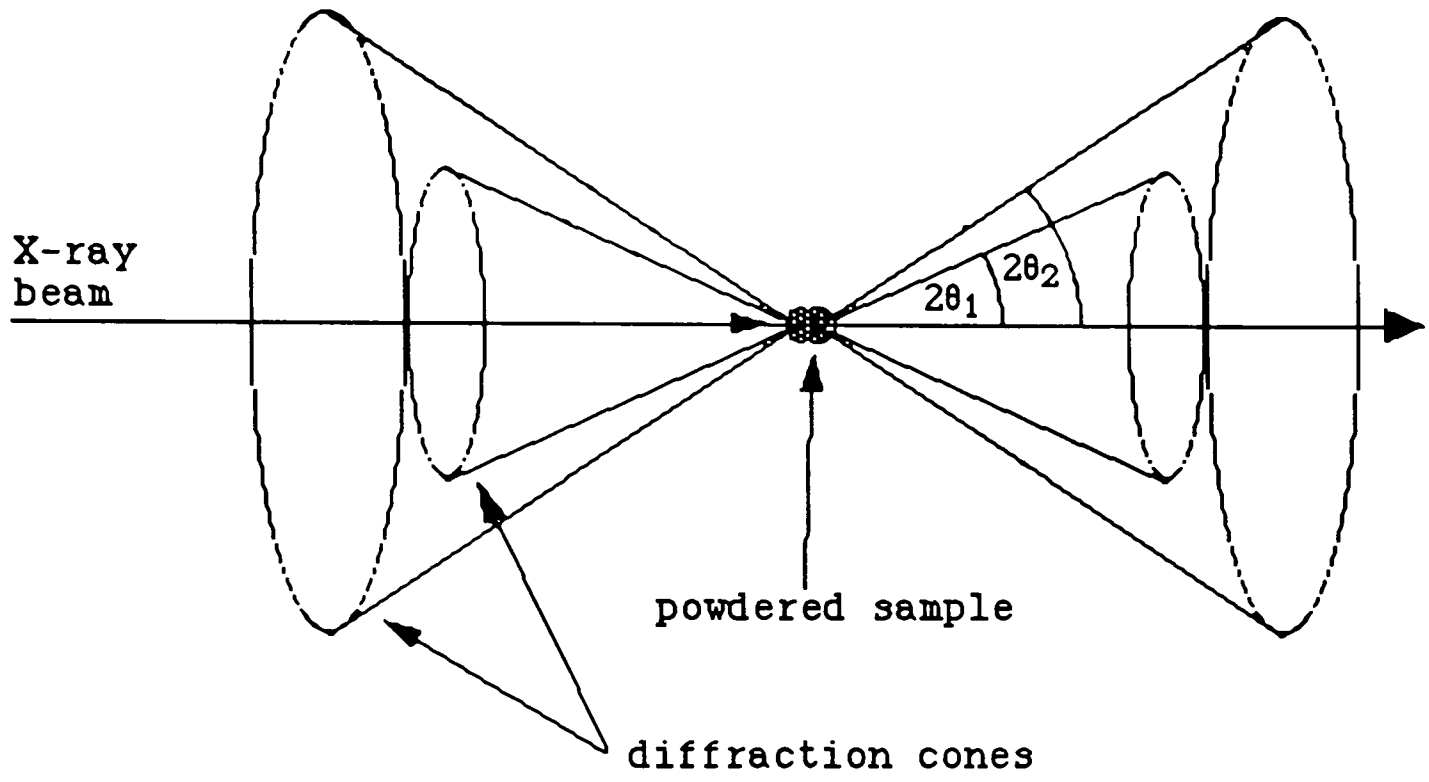

Figure 2.1 The diffraction cones produced by a powdered sample irradiated by monochromatic X-rays.

2.1.2 Focusing geometry[27]

Commercial powder diffractometers can vary in operating principles, but they all tend to be based around a focusing $\theta/2\theta$ design. The powder sample is placed in the centre of the diffractometer circle, with both the fixed X-ray source and detector mounted on the circumference. See Figure 2.2. The convergent monochromatic X-ray beam is focused on the centre of the sample at an angle of θ° relative to the beam. The detector is mounted on a rotating goniometer arm, which is positioned at $2\theta^\circ$ relative to the incident beam. Therefore as the sample is rotated through θ°, the detector is moved through $2\theta^\circ$. This ensures that the angle of incidence is equal to the angle of reflection at all times.

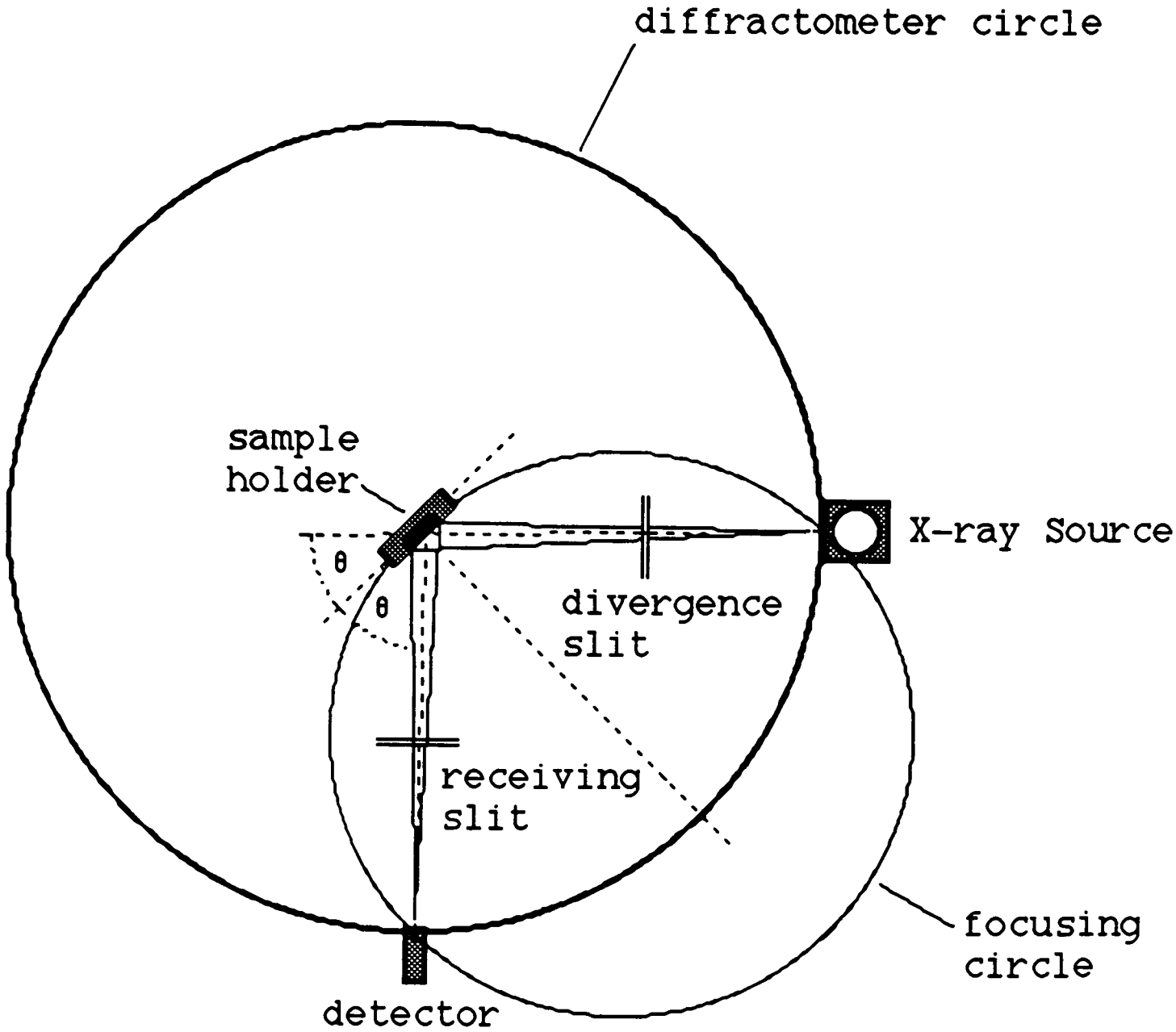

Figure 2.2 The basic geometry of a powder diffractometer using a focused beam.

The sample, X-ray source and detector also lie on the circumference of a smaller circle called the Focusing circle. The radius of the focusing circle is a function of 2θ and so changes as the detector and sample move. Ideally the sample surface should have the same curvature as the focusing circle to preserve the beam focus. However in a practical situation where a flat specimen is substituted, the loss of perfect focus can result in line broadening and peak shift.

2.1.3 One dimensional diffraction data

The process of collecting data using a powder diffractometer usually involves the continuous measurement of the diffracted intensities

through a predetermined range of 2θ°. As the goniometer rotates through the 2θ range, it cuts through only a few degrees of arc of the diffraction cones, which are considered to be uniform. The information is initially presented by means of a trace, as shown in Figure 2.3, displaying the relationship between 2θ and the diffraction intensity. The 2θ position of any of the diffraction cones is dependent only on d_{hkl}. thus there can be difficulty in distinguishing between peaks corresponding to separate crystal planes. In most crystal structures, it is common for two or more crystal planes to have identical or similar interplanar spacings and so on a powder diffraction trace the peaks can become superimposed. In the case of a cubic crystal, the six planes of the form [100], have identical interplanar spacings and so the Bragg peaks will appear superimposed upon one another. Thus six unique observations have been condensed into one. As a result, powder diffraction methods invariably means fewer observations than single crystal methods, therefore reducing the potential size of data sets.

2.1.4 Intensity calculation by peak fitting

The trace contains information of interest to the crystallographer, namely the integrated intensities, but more importantly the interplanar spacings. The extraction of the d_{hkl} values for each peak is a relatively simple process, however the calculation of the peak intensities is more complicated. Simple powder analysis can use the peak heights as approximations for the intensities, but in more exacting work, the integrated intensities are required.

Before peaks can be measured, it is necessary to correct the trace for Lorentz, polarisation and absorption effects. With computer controlled data acquisition, these processes can be carried out either as the

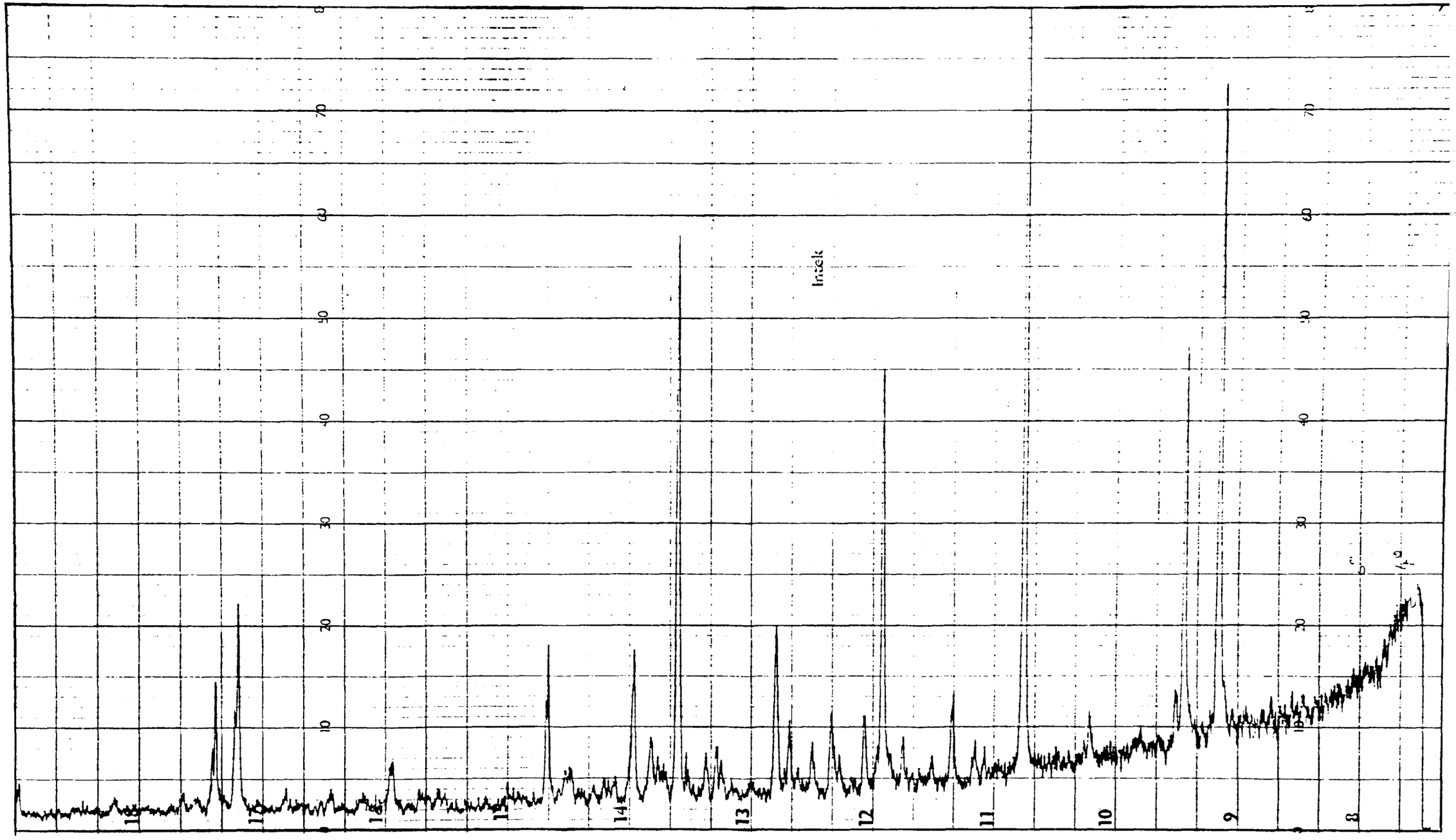

Figure 2.3 A typical powder diffraction trace of an organic compound produced by a Philips PW1050 diffractometer. λ=1.5418 Å. (Note the low 2θ values are to the right of the trace)

data is being collected or after the scan.

The calculation of the area beneath the peak is most effectively performed by finding a mathematical relationship which best describes the peak shape. This is achieved by fitting a curve of suitable geometry to the experimental data and refining the fit by least squares for optimum effect. A normal Gaussian distribution is common, but several hybrid functions have also been adopted to account for peak asymmetry[28-30]. The Rietveld method involves fitting one function, based on the theoretical trace produced from known cell parameters and atom positions of the crystal, to the experimental trace[31].

Figure 2.4 shows typical experimental data for a single peak with the presumed mathematical relationship superimposed. The quality of fit is indicated by the residual plot beneath the peak. The case of an overlapping peak represents a more complex problem.

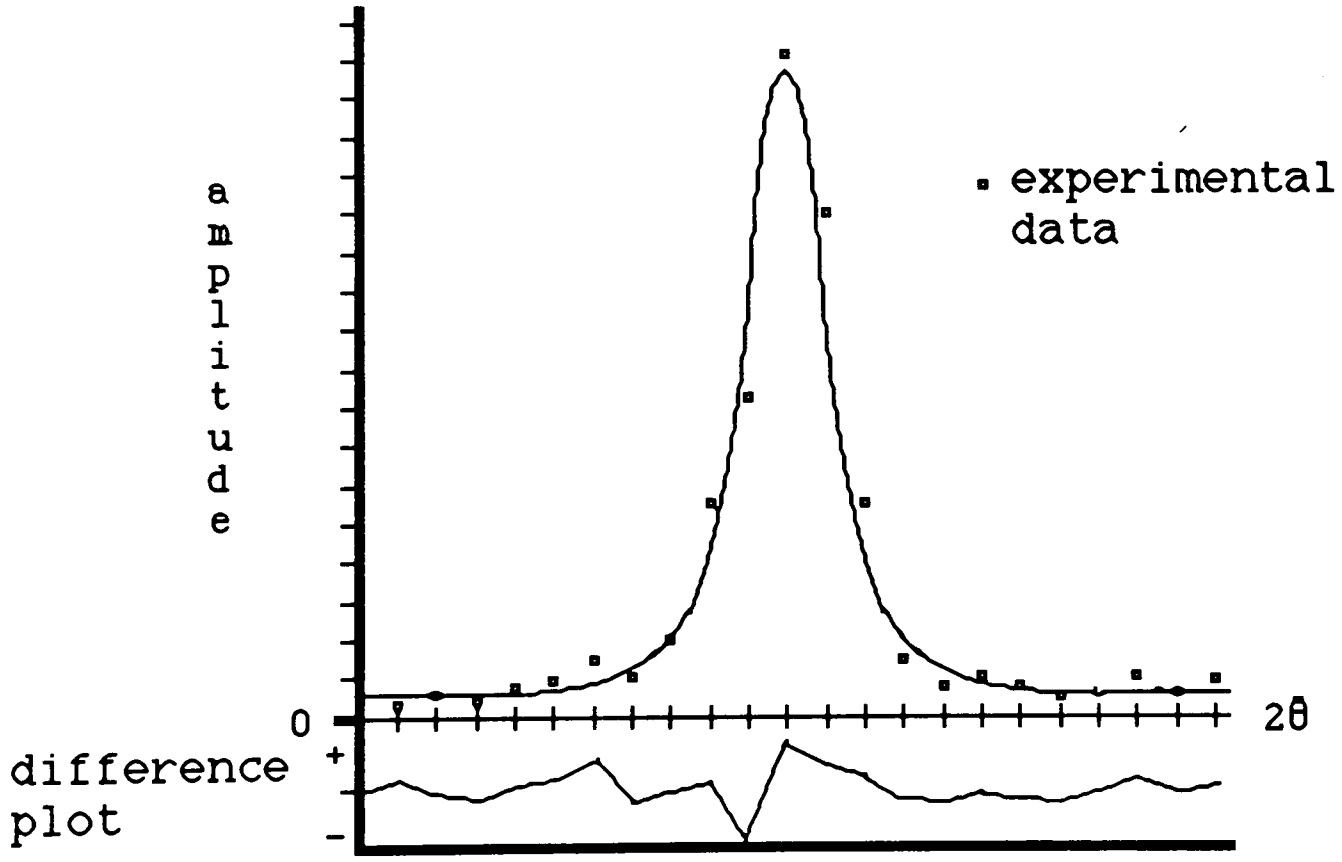

Figure 2.4 A theoretical demonstration of fitting experimental powder data to a symmetric Gaussian distribution. The goodness of fit is represented graphically below the trace by subtracting the theoretical value from the experimental value.

2.2 Low resolution powder diffractometer (LRPD)[32]

The Phillips PW1050 powder diffractometer was brought onto the market in the late 1950's. It was intended primarily for sample identification and phase analysis and so had a reasonably low resolution. A schematic diagram of the instrument is shown in Figure 2.5.

2.2.1 Instrument geometry

The LRPD is generally operated in a $\Theta/2\Theta$ continuous vertical scanning mode as discussed in 2.1.2. The beam focus is established by a series of interchangeable coaxial metal slits. The Ni filtered Cu X-ray beam is uniformly radial as it passes through the tube shutter. The Soller and divergence slits help to reduce the horizontal and vertical divergence producing a near parallel beam focused on the sample surface. Selection of a suitable divergence slit will dictate the surface area of the sample being irradiated.

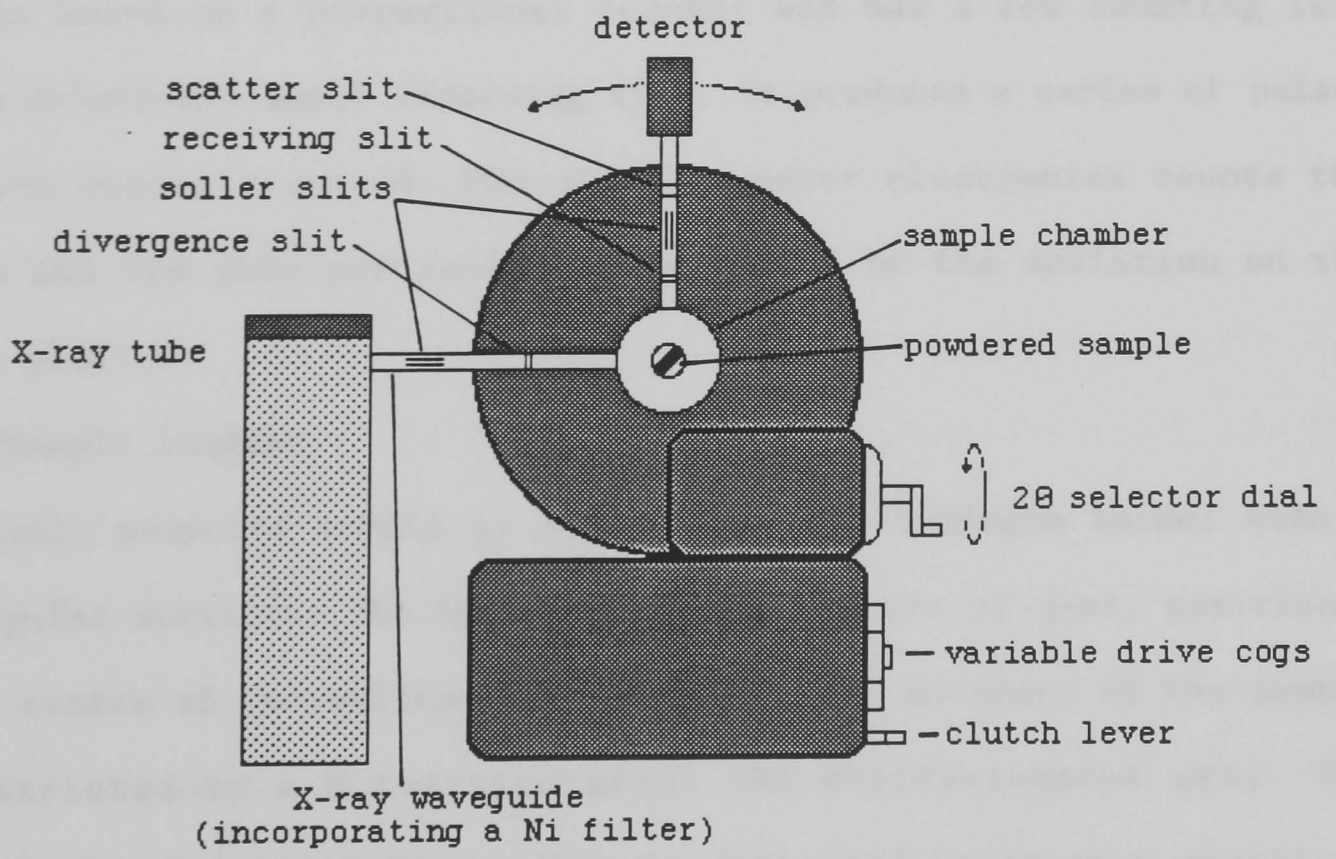

Figure 2.5 The Philips PW1050 powder diffractometer viewed from a direction perpendicular to the plane of the diffraction circle.

The diffracted beam is initially passed through the receiving slit positioned at the reflected beam focus. This restricts the received beam to a small solid angle. The additional Soller and scatter slits help to produce a near parallel beam incident upon the detector window. Generally the narrower the slits the sharper the diffraction peaks. This however, has the negative effect of reducing the scattering intensities.

2.2.2 X-ray source

A Nickel filtered Copper target tube , λ=1.5418 Å, is normally operated with a filament current of 20mA and accelerating potential of 40kV. The instrument at RGIT is not equipped with a monochromator and so the $K\alpha_2$ component of the characteristic spectrum is still evident in the beam. This is an obvious weakness of the system and so restricts the quality of the experimental data.

2.2.3 Detector

This is based on a proportional counter and has a low counting loss with a relatively small resolving time. It produces a series of pulses for each quanta received. The diffractometer electronics counts the pulses and the rate per second is reflected by the deviation on the scroll plotter.

2.2.4 Sample loading

The finely powdered sample is loaded into an aluminium holder with a rectangular aperture. The holder is fixed in a set of jaws, positioned at the centre of the diffractometer circle. The movement of the sample is restricted to a θ rotation about the diffractometer axis. The subject of optimum sample loading is discussed in greater detail in Chapter 3.

2.2.5 Data collection

The conventional operation of the diffractometer utilises a paper scroll plotter where the diffraction trace is plotted with intensity versus $2\theta^{\circ}$. The extraction of the crystallographic data from the trace is acquired by a manual operation. The 2θ values, and consequently the d_{hkl} values, are simply measured from the paper using the rough calibrations of the scroll. However the peak intensities are less straight-forward.

The peak intensities are either crudely estimated from the background subtracted peak height or approximated by fitting triangles to the peak. By assuming the peaks to be triangular, the area and the intensity, of the peaks can be calculated.

The operation of this instrument was enhanced by processing the diffraction data by microcomputer, allowing more complex methods of data analysis to be applied. Both the d_{hkl} values and integrated peak intensities are calculated by the software package CENPOD, using Gaussian peak fitting routines which permits a θ resolution of better than 0.01°. Details of the enhancement are discussed in Chapter 3.

2.3 Synchrotron high resolution powder diffractometer (SRS)[33]

Station 9.1 at the synchrotron radiation source (SRS) facility, Daresbury laboratories, Warrington, is a very high resolution powder diffractometer which has a basic geometry similar to that of LRPD, however the quality and quantity of information, capable of being extracted from a sample, is vastly superior. Its outstanding level of operation has been achieved by maintaining very high tolerances in the construction of the active mechanical components and by using a highly monochromatic X-ray beam.

2.3.1 Instrument geometry

The instrument can be used in several operational modes. The conventional $\theta/2\theta$ scan is carried as step scans. The detector and sample are rotated by direct feedback encoders giving positional accuracy of 0.0001° and 0.001° respectively. Using accurate stepper motors, the instrument is capable of being driven rapidly to predetermined positions. The instrument differs from the LRPD, by the addition of a set of long very fine collimators positioned in front of the detector. This has the effect of minimising the levels of secondary X-ray scattering being picked up at the detector and so reducing peak widths to 0.05°.

2.3.2 X-ray source

The X-rays are produced by accelerating electrons to energies of 2GeV in a synchrotron cyclic accelerator. As the electrons pass around the storage ring they are constantly accelerating and so they emit very intense bursts of white electromagnetic radiation. Each instrument positioned around the ring incorporates some form of beam filtering to select the range of wavelengths of interest. At station 9.1 the beam is monochromated with a channel cut silicon (**111**) monochromator mounted on a computer driven servo. This permits a range of wavelengths of 1 - 2.5 Å to be selected automatically, with a typical beam flux of 1.4×10^{10} photons/mm^2/second at 1.5 Å. Despite the very high flux, the spread of wavelengths, $\Delta\lambda/\lambda$, is less than 3×10^{-4}.

The automatic wavelength selection also permits the instrument to operate as an energy dispersive spectrometer. In this mode the detector is fixed in a constant 2θ position and the monochromator is stepped through its range slowly. At each monochromator position, the

silicon crystal will be in position to diffract a short range of wavelengths, $\lambda + \Delta\lambda$. It has been found that this operation is more accurate than using energy sensitive detectors and white radiation. Another advantage of the fixed detector/source arrangement, makes it suitable for high pressure or non-ambient temperature studies as the sample environment can often restrict movement. This allows reaction vessels to be designed with fixed entrance/exit windows, minimising potential interference from external influences.

2.3.3 Detector

A variety of detectors can be used on 9.1, depending on the individual experiment. Generally they fall into the two categories of scintillation or solid state detectors. Factors such as rise time, dead time and wavelength uniformity will dictate which assemblies are most suitable for specific studies.

2.3.4 Sample loading

The powdered sample is placed in a sample holder similar that used in the LRPD except that the loading aperture is circular which is capable of being rotated during data collection. In the step scan mode the detector and sample mount are stationary and so rotation of the sample is possible. This has the advantage of reducing preferred orientation effects and therefore samples need very little sample preparation. In the case of materials which react with the atmosphere or they are only available in small quantities, the samples are loaded into sealed glass capillaries.

2.3.5 Data collection

The method of data collection is fully automated and the trace is stored on computer as data pairs in the form of 2θ and intensity. The

method used to extract the experimental structure factors is dependent upon the type of investigation. Generally, the Rietveld profile fitting technique is applied for structure refinement.

Interplanar spacings are reproducible to 0.0004° or to one standard deviation of the average peak position determined by least squares fitting routines. This makes it suitable for very accurate unit cell refinement. The intensities are also very reliable and make the data suitable for *ab initio* structure determination. The excellent signal to noise ratio makes it possible to detect impurities in the sample.

Its number of applications is not just restricted to reflexion intensity extraction. Due to the very accurate theta positioning, small peak shifts can be monitored. In stress analysis of thin film deposits on amorphous substrates any physical stress can be picked up. Shifts of 0.04° to 0.001° have been noted.

2.4 Single crystal diffraction

The use of single crystals allows far more information to be extracted. The crystal is orientated in three dimensions, thus allowing all possible reflexions to be brought into the diffracting position relative to the beam. The three dimensional arrangement of the reflecting planes of the reciprocal lattice relates each crystal plane to a unique position in space. Since there is no significant peak overlap, all planes belonging to a form with the same interplanar spacing can now be individually measured. This increases the number of possible reflexions which can be collected, making it ideal for structure solution.

In the research programme, three different Single Crystal Diffractometers (SXD) were used. These instruments all have similar

features, but each represent innovations in design, dictated by new technologies. Each of the SXD have different data collection processes and so each one will be discussed in turn.

2.5 2-Circle SXD (2C-SXD)[34]

The 2C-SXD is a STOE Stadi-2 diffractometer based around a Weissenberg equi-inclination geometry. The name derives from the number of computer controlled rotation circles, which can alter the orientation of the crystal sample relative to the X-ray beam and the detector. A schematic diagram of the instrument is shown in Figure 2.6.

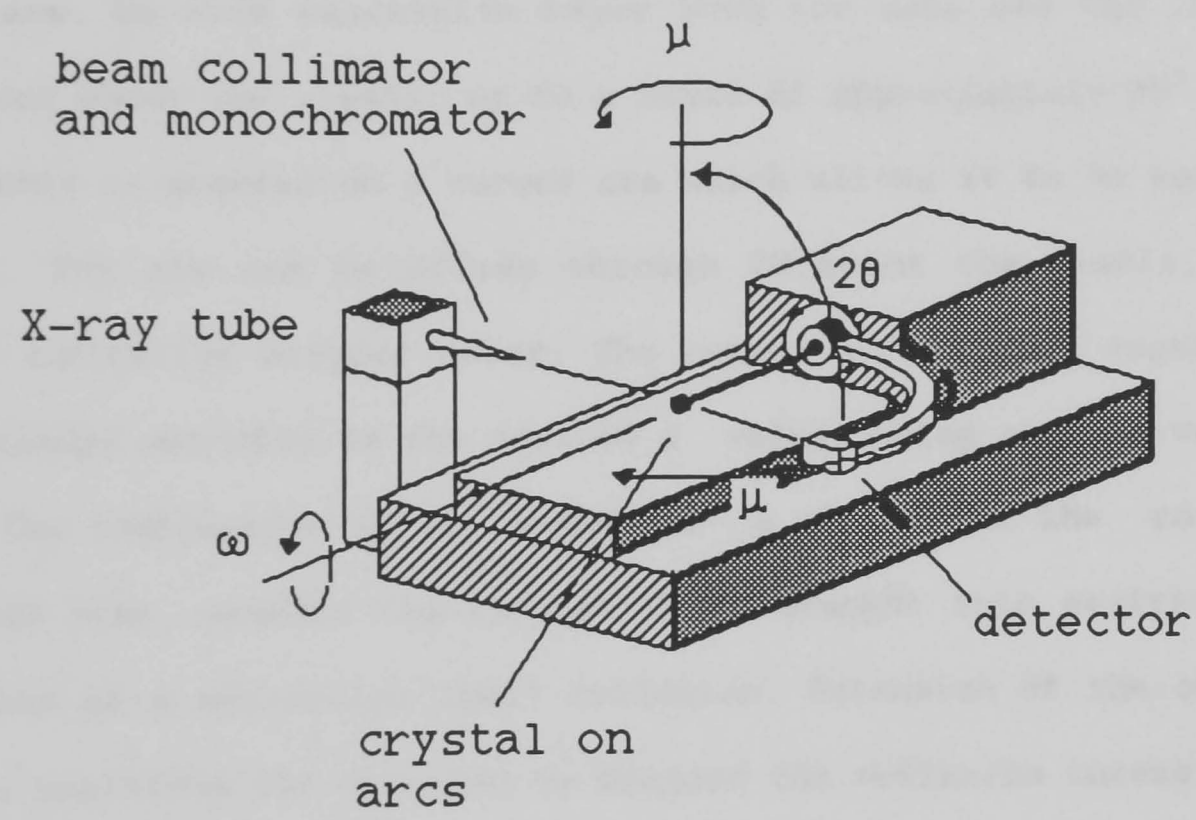

Figure 2.6 A schematic representation of the STOE Stadi-2 two circle single crystal diffractometer.

2.5.1 Equi-inclination geometry

A simple rotation photograph shows that for a single crystal system mounted with a crystal axis parallel to the rotation axis, the diffraction spots take on the form of parallel layer lines. Each layer

line represents a different layer of the reciprocal lattice. If the crystal is mounted about the b-axis, the different layers relate to orders of **k**.

The 2C-SXD makes use of this geometry so that each layer line can be examined, by rotating the crystal about the ω-axis and moving the detector into position. The semi-vertical axis of the zero layer diffraction cone has an angle of 0° and so the counter is positioned in line with the incoming beam and the crystal. For the upper layers both the crystal and counter are required to be rotated round by μ degrees, so that both the X-ray beam and counter lie along the surface of the cone. On each successive layer both the base and the counter are rotated about the μ-axis, up to a limit of approximately 30°.

The detector is mounted on a curved arm which allows it to be moved in two ways. The arm can be driven through 2θ about the ω-axis, by a computer controlled stepper motor. The curved arm is also capable of being extended manually to the desired μ value, using a crude vernier scale. The combination of the automated ω circle and the rotation of the SXD base, permits the crystal to be brought into position for diffraction of a particular (**hkl**) reflexion. Extension of the counter arm by μ, positions the detector to measure the reflexion intensity.

2.5.2 X-ray source

As with all diffractometers using monochromatic radiation, it is necessary to physically restrict the quality and direction of the beam. The beam is monochromated by a graphite crystal, removing the Kß component, leaving a narrow distribution of wavelengths. The beam is collimated, by passing it through a long narrow alloy cylinder, producing a parallel beam accurately focussed on the ω-axis. It is

important that the beam be wide enough to completely bathe the crystal through a complete ω rotation, otherwise some reflexion intensities will be subject to discrepancies. However, there is an optimum cross-sectional area for the beam, such that for low 2θ reflexions, particularly the zero layer ones, the beam does not mask the genuine diffracted beam.

2.5.3 Detector

The combination of a slightly divergent beam, background and amorphous scattering, can often result in broadening of the diffracted beam. These effects need to be minimised if peak intensities are to be reliably measured. To restrict the width of the detected beam, further collimating slits are incorporated. Two removable long narrow slits positioned perpendicular to one another create a small aperture in front of the detector window.

2.5.4 Crystal mounting and orientation

The single crystal is mounted on a fibreglass rod, using a small quantity of amorphous contact adhesive, which is known to be relatively inert. The rod is fixed to a set of arcs by means of modelling clay. A set of arcs are a device which allow the crystal to be manipulated about two orthogonal axes of rotation, thus permitting the crystal to be aligned before loading onto the 2C-SXD.

This process is usually carried out on a Weissenberg geometry rotation camera, using photographic films. By systematically readjusting the two arcs, the crystal can be centred and aligned parallel to the rotation axis, assuming that the original orientation of the crystal on the rod is approximately correct.

When the arcs are set on the ω-axis of the 2C-SXD, it is common to

find that the centring and even the alignment are subject to some change. Realignment is performed by observing the crystal with a travelling microscope through a complete ω scan. Final adjustments can be made to optimise the crystal position by monitoring the directions of some reflexions.

In the case of non-triclinic crystals, the procedure for fine adjustment is based around axial reflections. For non-zero layer axial crystal planes which are perpendicular to the ω-axis, they remain in the diffraction condition regardless of the ω position. This however, is dependent on whether the crystal is accurately mounted about the ω-axis. The basic steps to align a virtually correct crystal are outlined as follows

(i) Set the counter arm and diffractometer base to the equi-inclination angle, calculated from the accepted cell parameters, for a strong axial reflexion. The counter is positioned with $2\theta=0^{\circ}$, in the plane of the crystal and the X-ray beam.

(ii) At an arbitrary ω angle, maximise the diffraction intensity for the reflexion by adjusting the base. This is repeated for three other ω positions , $\omega+90^{\circ}$, $\omega+180^{\circ}$ and $\omega+270^{\circ}$, on each occasion noting the optimum μ value.

(iii) The four inclination values are averaged and the base is set to this value. The two arcs are adjusted to give maximum intensities, at two ω positions separated by 90°. The crystal may require to be recentred at this point.

(iv) Steps (i) to (iii) are repeated until the four inclination values are virtually identical.

In the case of a triclinic crystal, this process cannot be applied and

so a different approach, using strong reference reflexions from the zero order layer, is adopted.

2.5.5 Indexing reflexions

Once the crystal has been satisfactorily aligned, the process of indexing or assigning Miller indices to the reflexions can begin. Without a prior knowledge of the space group and relative strengths of the reflexions, the task would be very time consuming and impractical. Using the information available from the zero and first order Weissenberg films greatly simplifies matters. Careful examination of the films allows the intensities to be indexed and any systematic absences identified. Rough measurements of the film will also permit ω and 2θ values to be assigned to strong reflexions.

The detector, minus the collimating slits, is driven to the diffracting position of one of the strong reflexions. The crystal is rotated through ω, noting the relative strengths and positions of any detected peaks. In general the stronger reflexions are to be found at low 2θ values and so these are easiest to locate. However, there are often large errors associated with the positions of these reflexions. Comparison of the ω separations of the peaks measured on the ω scan and those on the Weissenberg films, will allow trial indices to be assigned to the reflexions. The suitability of the indices can be tested by attempting to locate the peaks with higher 2θ values. The high 2θ peaks are weaker but their positions will have less error associated with them.

Invariably this process will take several attempts before the correct indices are found. With satisfactory indexed peaks the process is repeated with the collimating slits in place, thus allowing more

accurate crystal positioning.

2.5.6 Data collection

For the data collection process, the slits are replaced in the detector to reduce peak broadening. With the 2C-SXD it is necessary to measure reflexions from one axial layer at a time. The diffractometer is instructed to systematically measure reflexions up to preset **hkl** limits or to a maximum 2Θ limit, $2\Theta_{max}$.

Rather than driving the crystal and detector to the calculated positions for a reflexion (**hkl**) and taking an individual intensity reading, it is far more accurate to step through the peak. The peaks can be scanned through ω, 2Θ or ω & 2Θ. In this case ω scans were carried out. As with powder diffraction, the peaks vary in width due to the Lorentz effect. In general, peak widths increase with decreasing 2Θ and increasing layer line number.

In the case of an ω scan, a static reading of the background level at a value $\Delta\omega$ from peak centre is taken. The crystal is step scanned through ω in predetermined increments, pausing and recording the intensity for a set time, and then finally repeating the background measurement on the other side of the peak. The value of $\Delta\omega$ is calculated for each peak, to ensure that all the diffracted energy associated with the (**hkl**) peak is measured.

As the layer number increases, reflexions with high Miller indices are found at increasingly higher 2Θ values. Thus fewer and fewer reflexions are measured with increasing layer number.

2.6 4-Circle SXD (4C-SXD)[35]

The Nicolet P3 4C-SXD is a natural progression of the 2C-SXD utilising more computer control. It has more positional flexibility, with 4

automated control circles; hence the name. Data collection is not only quicker, but requires little or no knowledge of crystal orientation. The improvement in accuracy of the results produced by a 4C-SXD over a 2C-SXD is debatable and will obviously vary from instrument to instrument.

2.6.1 Instrument geometry

The basic instrument shown in Figure 2.7 appears initially to have little in common with the 2C-SXD. The main feature of the instrument is the Eulerian cradle, which is used to manipulate the crystal bringing the desired planes into a diffracting position. The cradle has three independent rotation axes, ϕ, χ and ω.

The sample is mounted on a set of arcs which is fitted to a sledge inside the main cradle circle. The axis on which the sample is mounted can be rotated about the ϕ-axis, which is analogous to the ω rotation of the 2C-SXD. The sledge is also capable of being driven around the inside of the χ circle cradle. Finally the χ circle assembly can be driven around the vertical ω-axis. The combination of the three independent rotations allows the crystal to be orientated in virtually any position in three dimensional space relative to the X-ray beam. There are however, occasions when the cradle itself can obscure the path of the X-ray beam producing blind spots.

2.6.2 X-ray source

The X-rays are normally produced from a conventional X-ray tube with a Mo target. The beam is filtered and monochromated by a graphite monochromator producing a wavelength of 0.71069 Å. The beam is collimated into a near parallel beam before being made incident on the sample.

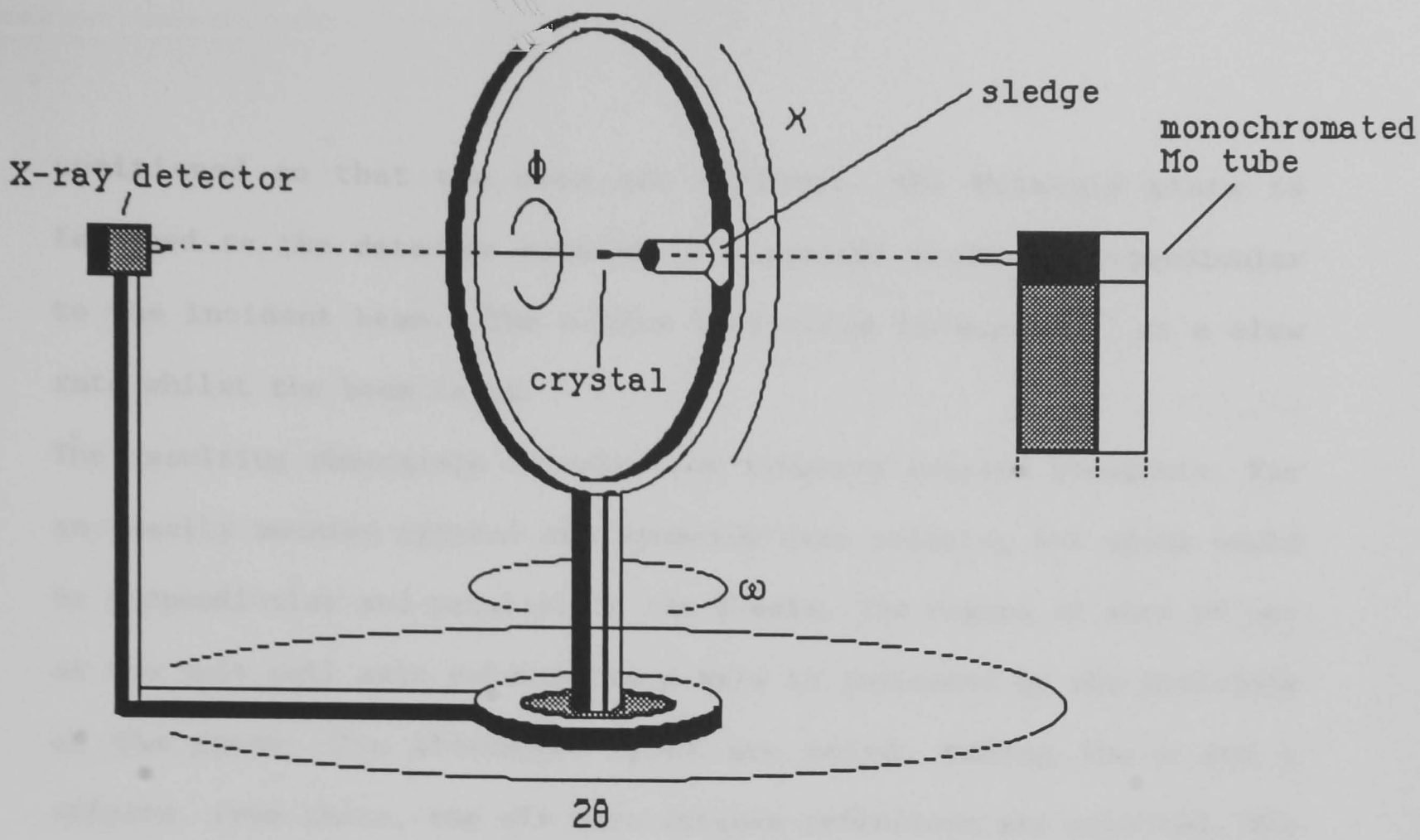

Figure 2.7 A schematic representation of the Nicolet P3 four circle single crystal diffractometer.

2.6.3 Detector

The detector is mounted on the fourth arc, 2Θ, with near complete rotational freedom. This is the only direction of detector movement which is possible, unlike the 2C-SXD. The detector has a fixed height, so that it lies in the same plane as the X-ray beam. This geometrical simplification is possible because of the positional flexibility of the sample on the cradle. The crystal is not only capable of being brought into a diffracting position, but it can be adjusted such that diffracted beam is in the same plane as the beam and the detector.

2.6.4 Crystal mounting and orientation

As with the 2C-SXD, it is necessary to take rotation photographs to ascertain the initial orientation of the crystal mounted on the arcs. Following an optical centring procedure by eye, the crystal is positioned for a photograph. All the circles are driven to zero. The χ circle is made perpendicular to the incident beam and the sledge is

positioned so that the arcs are vertical. The Polaroid plate is fastened to the detector mounted in a central position perpendicular to the incident beam. The ϕ-axis is rotated through 360° at a slow rate whilst the beam is on.

The resulting photograph reveals four symmetry related quadrants. For an ideally mounted crystal the symmetry axes relating the spots would be perpendicular and parallel to the ϕ-axis. The degree of skew of one of the unit cell axis relative to ϕ-axis is indicated by the positions of the spots. The strongest spots are noted, taking the x and y offsets. From these, the six most intense reflexions are selected. The x and y offsets are stored on the control computer.

The film cartridge is removed and for each of the selected spots from the film, the circles are driven to bring the individual reflexions in line with the detector. From the crude x and y positions, rough 2θ and χ estimates are made. The calculated values are driven to and a ϕ scan is carried out until a maximum intensity is found. The computer individually adjusts each of the circles to optimise the intensity of the reflexion. The optimum position is determined by taking half-width maximums of the peaks. With the crystal suitably centred, the process of identifying the unit cell and indexing the reflexions is carried out next.

2.6.5 Unit cell parameter determination

If the cell parameters are unknown, there is a program which will list possible solutions based on the initial data. The program outputs a list of axial parameters and the cosines of the proposed interaxial angles. The most plausible set of parameters are manually selected from the list using a combination of the rotation photographs, crystal

morphology and hands on experience. Generally, the smallest cell volume is selected. However, there are cases where a larger non-primitive cell is preferred, simplifying the structure solution. The suitability of the chosen axes can be determined from further photographic evidence.

2.6.6 Partial rotation axial photographs

As before, the Polaroid cartridge is fitted in front of the detector, with 2θ set to zero. One of the crystal axes is positioned to be vertical by rotation of the ϕ and χ circles. With the beam on, the ω circle is driven through approximately 20°, performing the same function as a Weissenberg rotation. From the Polaroid film, the interlayer lines can be measured, thus giving a value for the rotation axis length. The measurement is relatively crude, but it will give a good indication whether the selected cell is correct. If necessary this may be repeated for the other two axes. If the correlation is good then the next step is to index the reflexions

2.6.7 Auto-indexing

The indexing program is run again, producing the same list of possible cells. With the knowledge gained from the rotation photographs, the assumed cell is entered and the six or so reflexions are assigned Miller indices. With the approximate cell parameters the volume of the cell is calculated. If it is negative then this indicates that the cell chosen has a left hand set of axes. This is corrected by expressing the angles relative to a right handed axial system.

2.6.8 Least squares and orientation matrix

The cell parameters calculated in the auto-indexing program can be subject to significant errors resulting from the use of the low 2θ

reflexions. In the indexing program the initial Miller indices calculated for each reflexion will have had non-integer values indicating small errors in the measurements. These are converted to integer values and from these values and the angular positions of the reflexions, the cell parameters are recalculated by a least squares optimisation routine.

An orientation matrix is calculated, defining the position of the unit cell with respect to the angular coordinate system of the diffractometer. Once this matrix is accurately known, the crystal can be positioned for any reflexion within the limitations of the diffractometer.

The accuracy of both the cell parameters and the orientation matrix is dependent on the accuracy of the angular coordinates of the initial six reflexions. The initial centring and indexing of the reflexions is carried out on the intense low 2θ reflexions. The intense centres makes the process of finding half-width maximums relatively simple. However, as mentioned previously, the low 2θ reflexions can have large errors, due to their broadening. If higher 2θ reflexions are now used, the crystal positioning can be fine tuned.

2.6.9 Rapid data collection and cell refinement

The initial cell parameters determined from the Polaroid film are refined using the positions of strong reflexions, with 2θ around 20-25°, as observations. The scanning speed is high and so the intensities will tend to be associated with errors. When all reflexions lying within the 2θ limit have been measured, the list is sorted in order of maximum intensity and up to 14 reflexions are selected for the refinements. Fewer reflexions may be necessary,

depending on the symmetry of the unit cell. Symmetrically equivalent reflexions are included in the list effectively increasing the number of observations. For all space groups there will be **-h-k-l** for all **hkl** reflexions and in higher symmetry cases there will be related reflexions.

The least squares procedure is loaded again and the cell parameters and orientation matrix are refined further. Once these stabilise, the program calculates the ideal angular coordinates for each of the 14 reflexions. The least squares routine is used to further refine both the unit cell parameters and the orientation matrix. The crystal is finally recentred as before, producing improved angular coordinates for the 14 reflexions. The cell parameters and orientation matrix are refined again. The parameters must fall within preset standard deviations, otherwise the data can not be considered suitable for further data collection.

2.6.10 Data collection

At this stage, the crystal and the diffractometer are suitably aligned, therefore data collection can begin. The range of reflexions are restricted by the X-ray wavelength and so the Miller indices and $2\theta_{max}$ are set within practical limits. The scanning speed is significantly reduced to improve the error statistics. The reflexion peaks are measured by $\theta/2\theta$ step scans, ensuring that the detector and beam remain in the same plane at all times.

If from the preliminary Polaroid photographs or from some other source, the operator is aware of the space group and therefore the systematic absences, the diffractometer can be programmed to avoid wasting time by measuring them, and will only measure truly unique

reflexions. Significant reductions in beam time can be achieved in this manner. However, in general the full data set is collected since the systematic absences are required for atom phasing in Direct methods.

During the collection process it is possible that the crystal will decompose in the beam, thereby reducing the amount of scattering material and hence the intensities will no longer be scaled to one another. The diffracted intensities are checked every 50 reflexions or so by remeasuring two strong reflexions. The sequence of values are stored in a file as coefficients, expressing the ratio of the initial reflexion intensities to the intensities of the remeasured reflexions. If there are significant variations, the reflexions can be scaled by applying the correct coefficient to the group of reflexions.

Once the data collection is complete, an empirical absorption measurement can be performed if necessary. The circles are rotated so that an axial reflexion is in position to diffract. The ϕ circle is rotated through 360° in steps of around 10°, and the intensity of the reflexion is noted. If there is no significant variation in intensity the correction is not performed. However if there is, the intensity variation is used to scale the data. In most cases the absorption effect is minimal and it is therefore ignored.

2.7 Neutron SXD (SXD)

SXD is a newly commissioned instrument based at the ISIS neutron scattering facility at the Rutherford Appleton Laboratory, Oxfordshire. It is an extremely powerful instrument, which has been developed around *state-of-the-art* instrumentation, with a fundamentally simple diffraction geometry. However it is the use of a

pulsed source of polychromatic neutrons instead of X-rays which accounts for its impressive performance rating.

2.7.1 Instrument geometry

SXD is based on a simple Laue camera using a white radiation source, but employing a position sensitive detector (PSD) to record the diffraction events and using the time-of-flight technique to resolve diffraction orders, rather than a photographic film. Figures 2.8(a) and 2.8(b) show schematic diagrams of the instrument vessel, neutron beam and the PSD. The instrument was designed to use an Eulerian cradle to manipulate the crystal, but due to problems relating to reliability, the installation of the cradle has been delayed. Instead the crystal is mounted on a set of conventional crystal arcs, fixed to a computer controlled rotating shaft, with the ω-axis of rotation perpendicular to the neutron beam.

In this mode there is restricted orientation of the crystal relative to the arcs, but due to the Laue geometry and polychromatic beam this is not a major problem. The method of data collection will be discussed in 2.7.6.

2.7.2 Neutron source[36]

An essential difference between this instrument and all the others used, is that it utilises a neutron beam. The neutron facility at RAL is presently the most powerful source of pulsed neutrons for condensed matter research in the world.

The neutron flux is produced by a spallation process where energetic protons are used to bombard a heavy metal target. The spallation process can be explained by a series of accelerating procedures. Initially an ion source produces H^- ions which are accelerated in a

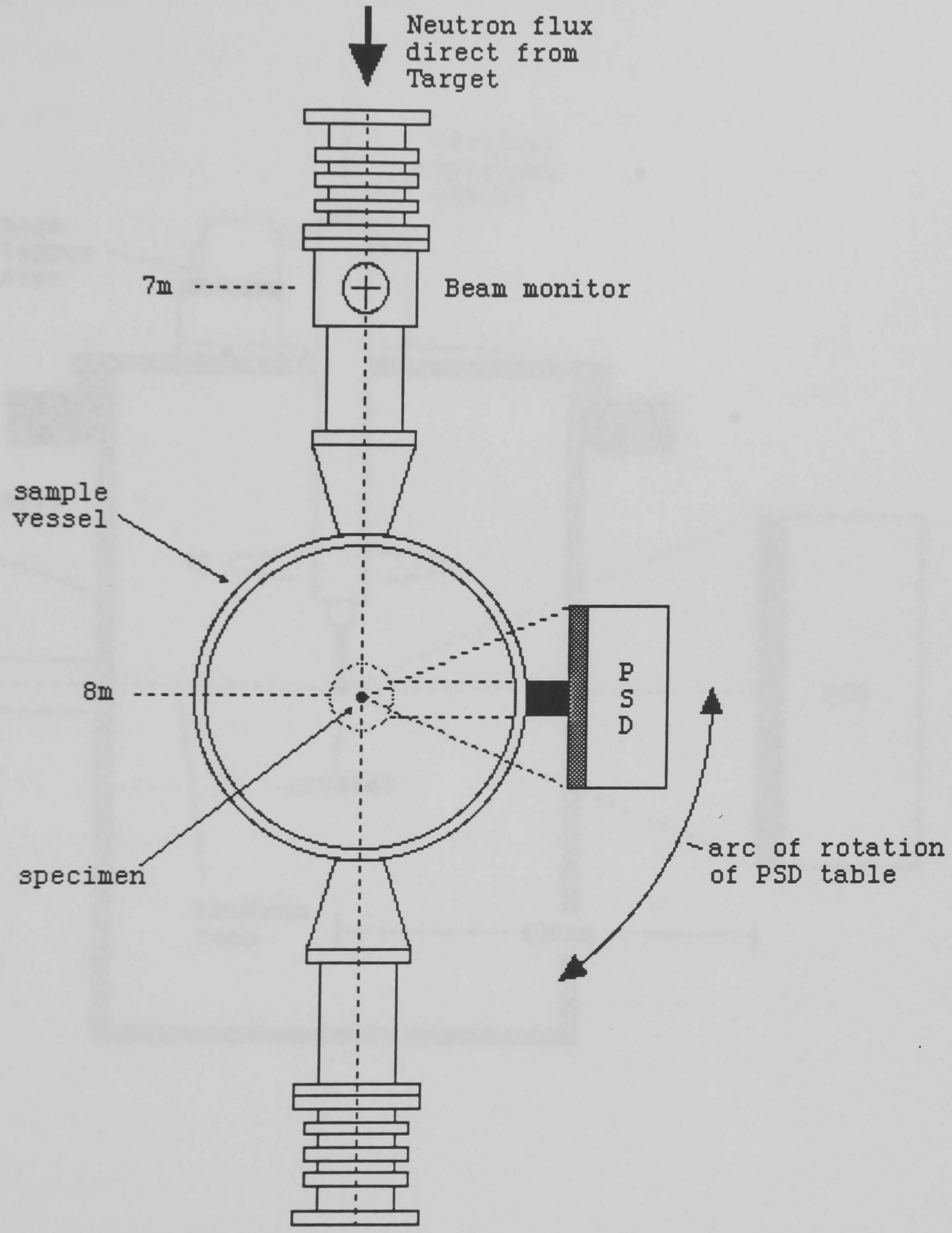

Figure 2.8(a) The neutron single crystal diffractometer viewed from above the instrument. The 7 and 8m markers indicate the distance from the target centre.

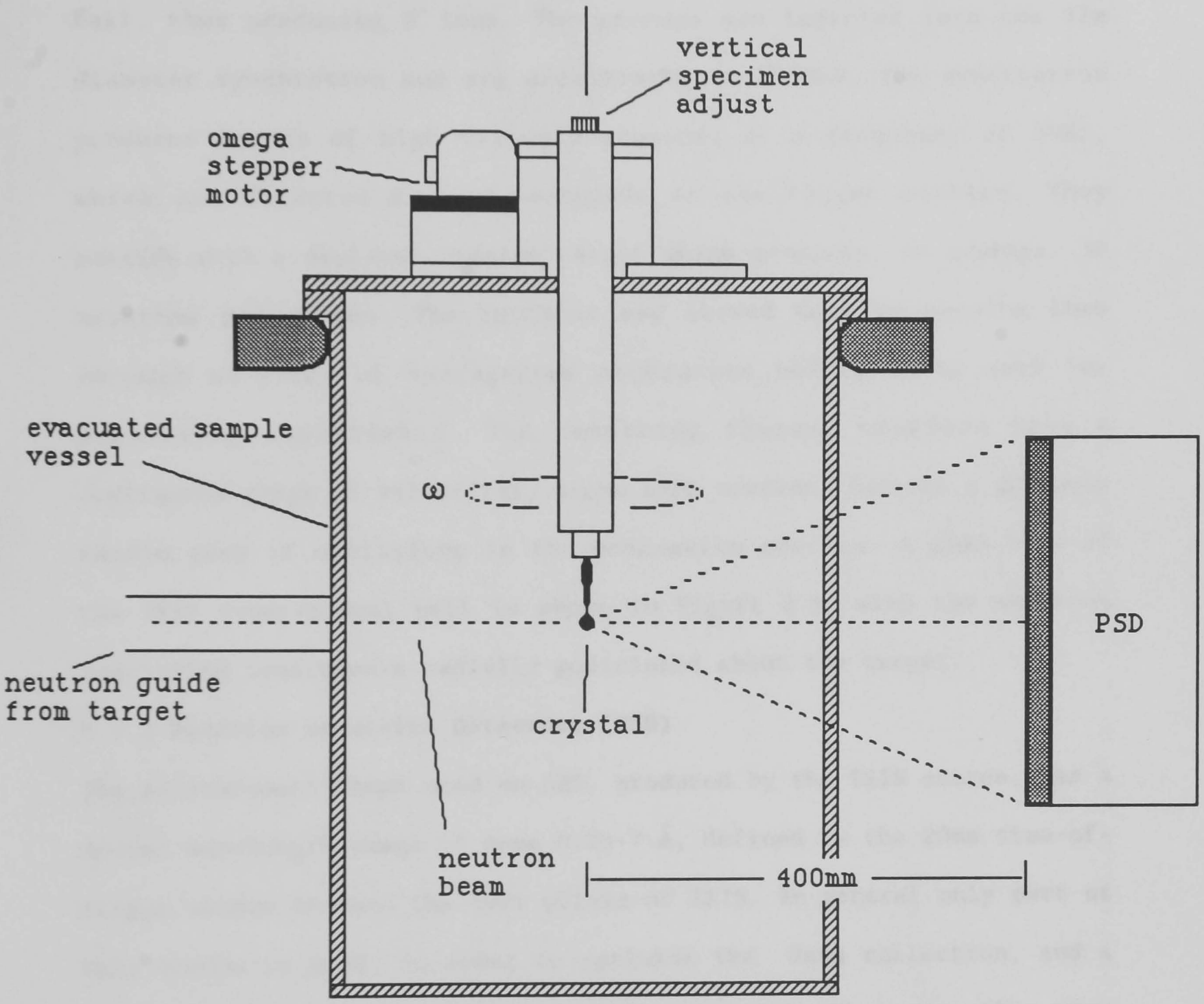

Figure 2.8(b) A cross section of the instrument vessel, viewed in the plane of the neutron beam.

preinjector column to 665 KeV. The ions are further accelerated in a linear accelerator, increasing their energy to 70MeV. The H^- ions are stripped of their electrons by passing them through a thin alumina foil, thus producing H^+ ions. The protons are injected into the 52m diameter synchrotron and are accelerated to 800MeV. The synchrotron produces bursts of high velocity protons, at a frequency of 50Hz, which are directed down a waveguide to the target station. They collide with a depleted Uranium target which produces, on average, 30 neutrons per proton. The neutrons are slowed down by passing them through an array of hydrogenous moderators before being used for scattering experiments. The resulting thermal neutrons have a continuous range of velocities, since each neutron follows a uniquely random path of collisions in the moderation process. A plan view of the ISIS experimental hall is shown in Figure 2.9, with the numerous scattering instruments radially positioned about the target.

2.7.3 Position sensitive detectors (PSD)

The polychromatic beam used on SXD, produced by the ISIS source, has a useful wavelength range of some 0.25-7 Å, defined by the 20ms time-of-flight window between the 50Hz pulses of ISIS. In general only part of this window is used, in order to optimise the data collection, and a useful wavelength range of 0.48-4.8 Å is typical. There are thus many reflexions which satisfy the diffraction condition in a single pulse for a fixed incident angle and the crystal thus diffracts many reflexions in a single setting, as in a Laue photograph. For a normal restricted aperture detector, as used with both the 2 and 4-Circle SXD, this would not be advantageous. However the employment of a PSD allows many Bragg reflexions to be observed "simultaneously" in a

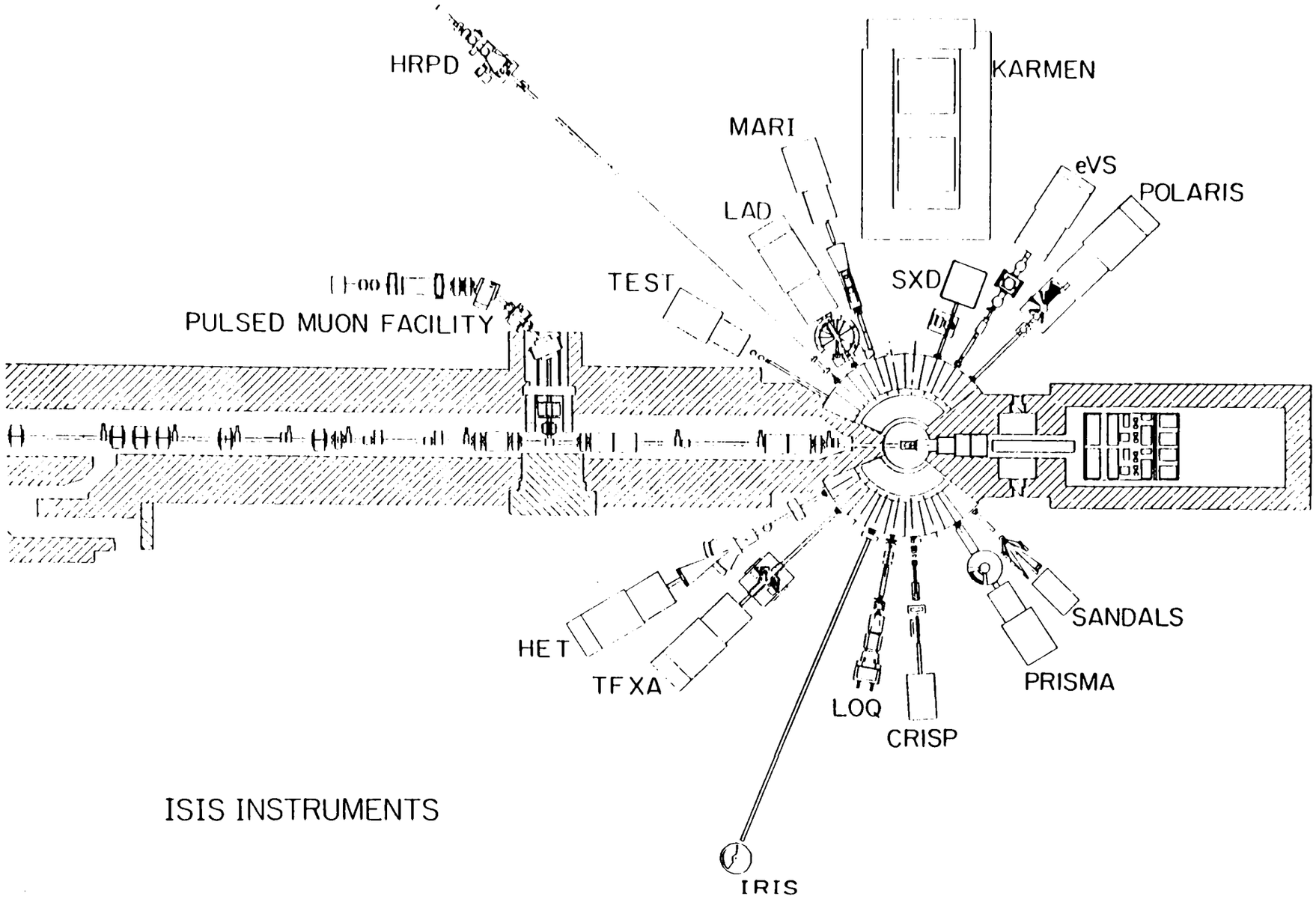

Figure 2.9 A plan view of the ISIS neutron facility at the Rutherford Appleton Laboratory.

single histogram. It is this surveying of substantial volumes of reciprocal space in a single scattering geometry which is the main power of a time-of-flight Laue diffractometer such as SXD.

There are currently two experimental PSD instruments being used on SXD, both with different operational characteristics.

2.7.3.1 The Anger camera[37,38]

The SXD Anger camera is composed of 45 hexagonal photomultiplier tubes arranged in a continuous matrix, as shown in Figure 2.10. The surface of the detector has a ^{6}Li doped glass plate doped with Ce, which acts as a scintillator producing light photons on the event of a neutron capture. The released photons are amplified by the matrix of photomultiplier tubes, producing a significant output voltage for each neutron capture. Each tube is connected to a digital bus enabling the electronic surge produced by the diffraction event to be measured.

At a given threshold voltage, the event is acknowledged and readings are taken from the surrounding 6 tubes, labelled sequentially in a clockwise fashion. The actual position of the event can be calculated from the radial distribution of the photon surges in the tubes about the central tube using equations 2.1, 2.2 and 2.3. The calculated position of the event has been shown to be accurate to within 2-3mm. Thus the 45 element matrix can be considered to behave as a 300 x 300 mm array of 4096 unique virtual detectors, covering a solid angle of 20 x 20°. Each of these detectors is assigned a time channel in the DAE memory and so the event history of each channel can be stored in computer memory.

$$X = \alpha(a_6 + a_7 - a_3 - a_4) \qquad (2.1)$$

$$Y = \frac{\alpha}{\sqrt{3}} \cdot (2a_2 + a_3 + a_7 - a_4 - a_6 - 2a_5) \qquad (2.2)$$

$$Z = a_1 + ß(a_2 + a_3 + a_4 + a_5 + a_6 + a_7) \qquad (2.3)$$

Where a_n is the photon flux of the nth photomultiplier tube in the cluster.
α and ß are constants which relate to the radial photon distribution function.
X/Z and Y/Z locate the position of the event on the detector.

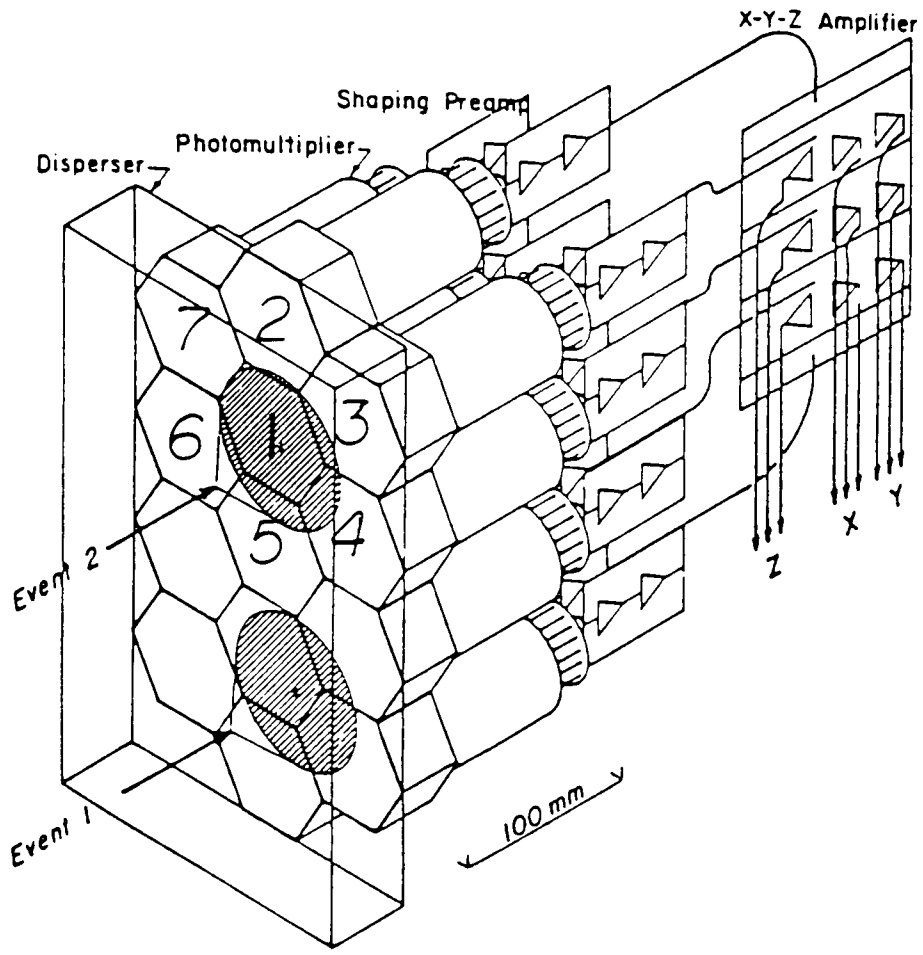

Figure 2.10 The Anger camera composed of an array of 45 hexagonal photomultiplier elements. The shaded areas represent the radial distribution of light emitted from the scintillator sheet on the capture of a neutron.

2.7.3.2 ZnS fibre optic detector[39]

The ZnS detector is a solid state device of smaller proportions, measuring 80 x 80 mm, but it essentially performs the same task as the larger Anger camera.

The detector consists of an square array of 16 x 16 ceramic elements

covered by a sheet of ^{6}Li doped ZnS. These elements take the form of hollow inverted pyramids, with the apex connected to fibre optic cables. The light pulses are transmitted to 32 photomultiplier tubes via the optical fibres. The square array of the inverted pyramids enables the position of the neutron event on the ZnS sheet to be determined to within 5 mm. The information is stored in time channels in the same way as the Anger camera.

2.7.3.3 PSD comparison

Both detectors essentially perform the same task. For any given crystal orientation, the position and the TOF of all detector events, relative to the ISIS cycle, can be monitored.

Both PSDs have been proven to produce excellent results, however the ZnS plate is smaller and so can only record smaller areas of reciprocal space. Figure 2.11 shows a histogram of the relative efficiencies of each of the ZnS detector pixels.

2.7.4 Time of flight analysis

As mentioned in the introductory theory, thermal neutrons obey Newtonian physics and can travel at varying velocities. The energy and therefore the wavelength of the neutron are dictated by de Broglies equation. Figure 2.12 represents the wavelength characteristic of the beam when monitored by the ZnS detector.

The moderated neutrons from the target station will have a continuous range of energies and velocities. Assuming all the neutrons produced on each successive cycle of the synchrotron are initially grouped together, they will arrive at the crystal sample at different times. For a given crystal orientation selected wavelengths will undergo diffraction and those which are directed toward the PSD will be

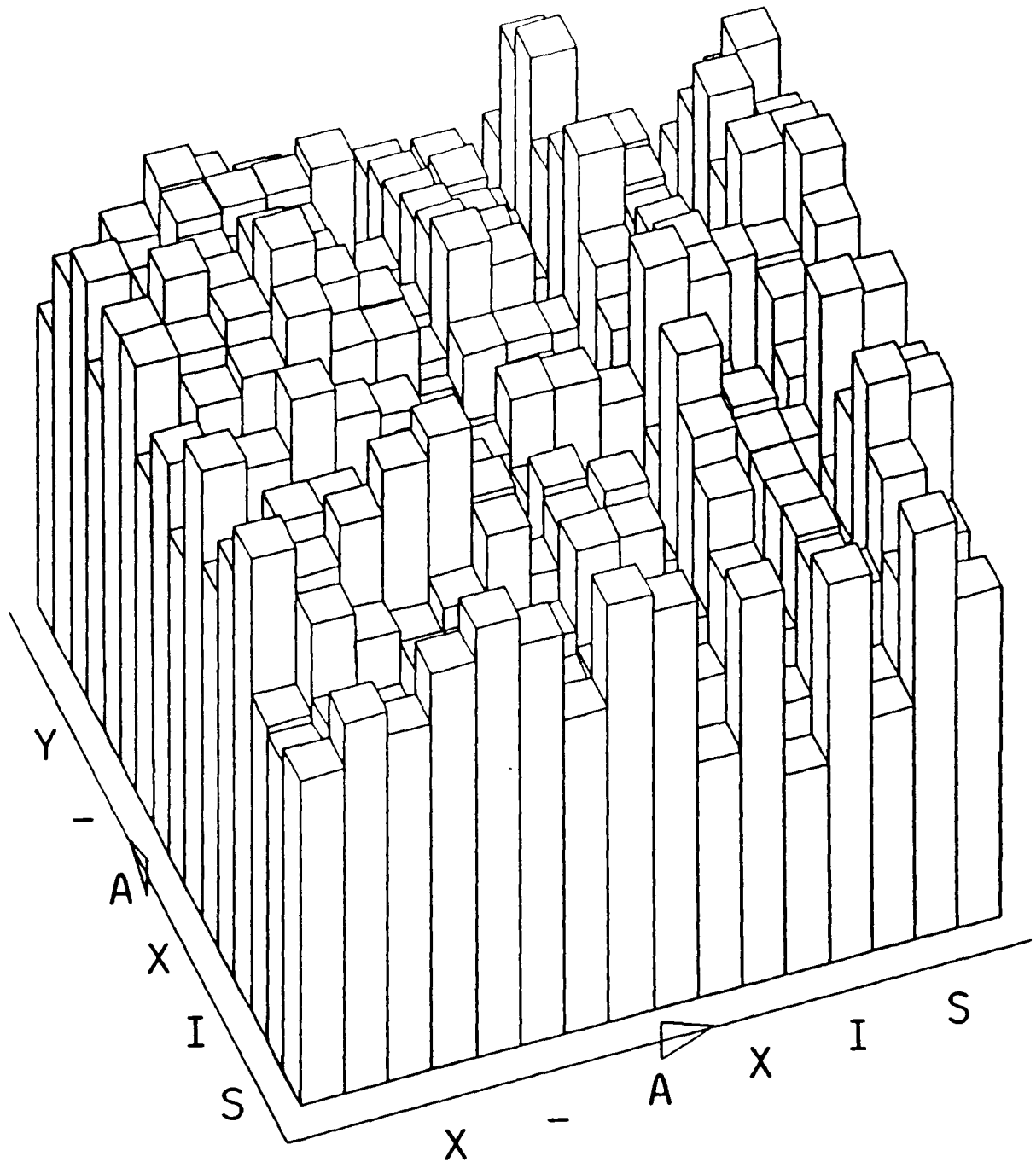

Figure 2.11 This histogram represents the relative efficiency of each of the pixel elements on the ZnS detector.

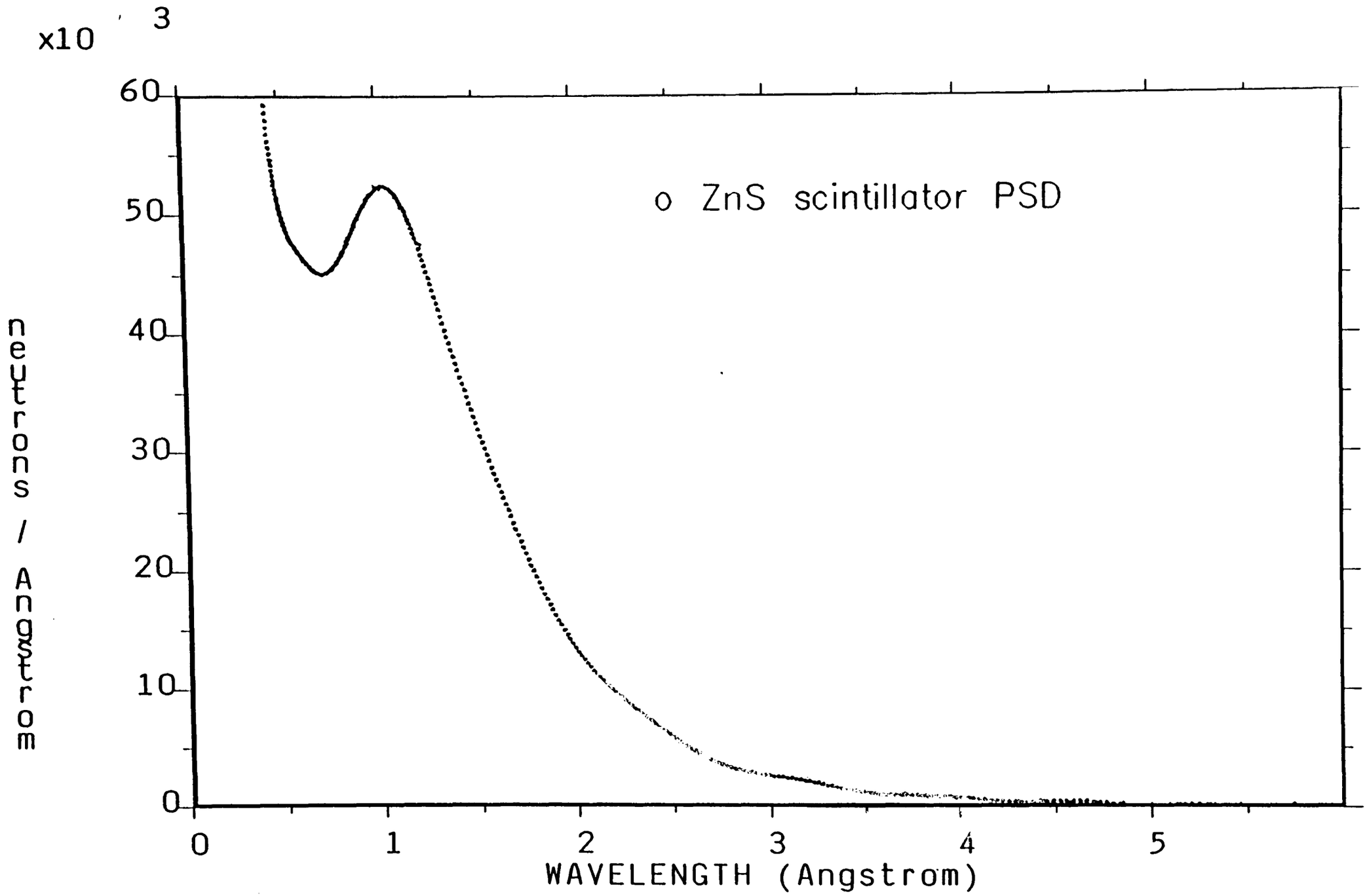

Figure 2.12 The averaged wavelength dependence of the pixels on the ZnS detector. (Note useful flux in the 0.4 - 4.8 Å range)

detected over a short period of time. The time-of-flight (TOF) is defined as the time lag between the instant of neutron production at the target and the detection at the PSD and is proportional to the wavelength of the diffracted beam. A TOF profile for SrF_2 over the range 0-10000 μsec is shown in Figure 2.13, which illustrates the (hhh) Laue row of reflexions. The profile has been corrected for the wavelength dependent flux profile shown in Figure 2.12.

2.7.5 Sample mounting and orientation

Due to the relatively weak beam flux compared to an X-ray beam, the crystal sample needs to be significantly larger in volume than conventional X-ray single crystals.

The crystal is generally mounted on an aluminium rod by a contact adhesive. The rod is shrouded with a coiled strip of Cd, which helps to reduce scattering from the rod. The exact positioning of the crystal is not as important as with the 2C-SXD, but if the experimenter can align one of the crystal axes with the rod, then the data collection is simplified.

The crystal is approximately aligned with an axis parallel to the ω-axis. Aligning the crystal is best performed by noting the angular displacement of a specific reflexion from the centre of the detector. The crystal is rotated through 180° and the displacement of the (-**h**-**k**-**l**) reflexion is noted. The two reflexions can be identified as being equivalent by calculating the interplanar spacing from the TOF values and detector coordinates. Once the two reflexions have been verified as being related, the arcs are adjusted until both reflexions can be detected at the same detector element. This is analogous to the process of aligning the interlayer lines of a rotation photograph.

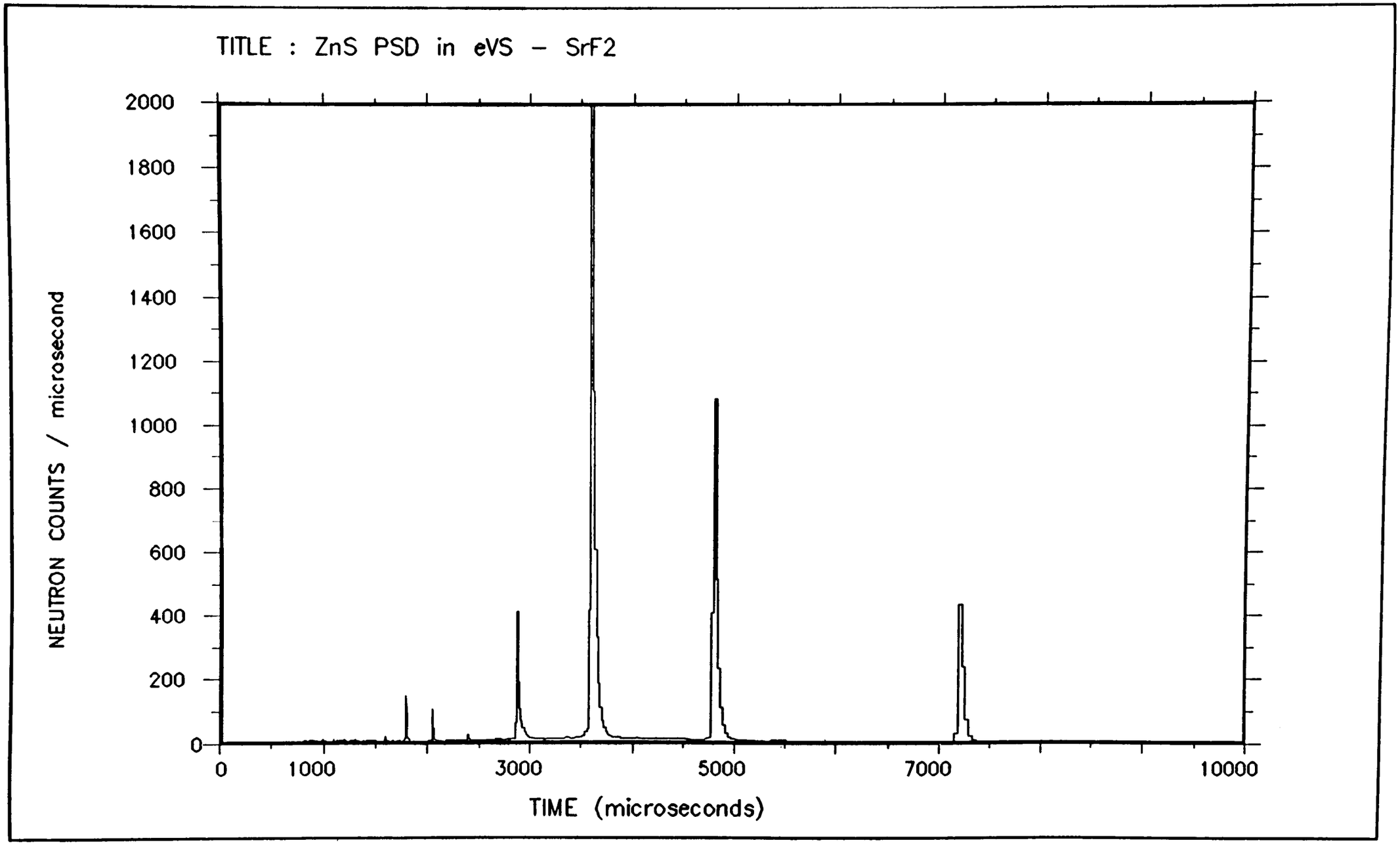

Figure 2.13 The time of flight profile of one pixel of the ZnS detector, showing a group of reflexions from SrF_2.

Unlike the 2C- and 4C-SXD's, the sample does not require further manipulation to collect data. More importantly, it does not require a knowledge of the cell parameters or the orientation matrix to collect data. This is a major benefit of TOF and PSD diffractometers.

2.7.6 Data collection of a hemisphere

The most systematic approach to data collection involves collecting a series of overlapping histograms for predetermined ω rotation. For example, in two dimensions, the ZnS PSD can measure reflexions over a solid angle of approximately 10 x 10°. If the crystal is rotated about ω by 8°, the following histogram would contain several reflexions from the previous one. The overlapping of the histograms therefore ensures that no reflexions in the accessible region are missed. This process is generally repeated for a ω rotation of 180°, collecting some 20 histograms. Further rotation about ω is not necessary since all the unique reflexions in this region are then located.

The repeated collection of histograms for a ω revolution represents a significant proportion of unique reciprocal space, however more reflexions can be measured if the crystal arcs are adjusted. Repeating the above process for other arc settings has the effect of bringing new regions of the reciprocal lattice into position for diffraction.

2.7.7 Cell parameters and UB matrix

In most cases SXD is used to investigate further structural features of crystals, which have been previously solved by X-ray methods. Thus the cell parameters are usually known prior to the data collection on SXD.

Using selected strong indexed reflexions and a knowledge of the unit cell parameters, the orientation of the crystal and therefore the

reciprocal lattice can be related to the ω-axis by calculating the UB matrix. The method of least squares refinement is employed to produce an improved matrix.

2.7.8 Peak search routines

An automatic peak search routine is employed to locate the positions of the Bragg peaks from the histograms. This results in a list of peak heights, coordinates and TOF's. The reflexions are indexed by relating each TOF to a d_{hkl} value. For structural work, peak heights are insufficient and so the peaks must be integrated. In the case of powder diffraction data the peaks are two dimensional and so the peak fitting is relatively simple. However, since the detector is two dimensional and the TOF histograms are in three dimensions, the integration process is less trivial. Using the peaks coordinates as the centre of the peak, ellipsoids are fitted around the peak. The ellipsoids give cross-sectional areas for each "slice", thus allowing a three dimensional function to be fitted to the peak. The list of intensities are scaled with the beam profile. The structure factor amplitudes are calculated for each using equation 2.4[40].

$$I_h = \frac{i_o(\lambda).V.N^2.|F_h|^2.\lambda_h^4.\epsilon(\lambda,\alpha).A_h(\lambda).E_h(\lambda)}{2.\sin^2\Theta_h} \qquad (2.4)$$

Where I_h is the measured intensity of reflexion hkl.
$i_o(\lambda)$ is the incident flux.
V is the crystal volume.
N is the number density of unit cells.
$|F_h|$ is the structure factor magnitude for reflexion hkl.
λ_h is the wavelength at which hkl is measured.
$\epsilon(\lambda,\alpha)$ is the detector efficiency. α relates to the x & z offsets of the PSD.
Θ_h is the Bragg angle.
$A_h(\lambda)$ and $E_h(\lambda)$ are the absorption and extinction corrections.

CHAPTER 3. Enhanced low resolution powder diffractometer and applications.

3.1 Introduction

The original electronics hardware of the PW1050 LRPD are now somewhat dated by modern instrument standards. With patience however, favourable results are possible, but this needs experience in powder diffraction techniques and a good working knowledge of the instrument itself. The instrument has been upgraded by incorporating a now dated 8-bit microcomputer for processing the experimental data. One of the main criteria proposed in the upgrade was to leave the instruments drive mechanism intact such that it was still capable of being operated by conventional means. This would allow the instrument, which is extensively used in the School of Applied Science, to be fully functional over the development period.

3.2 Hardware development

There were two main areas of development which were required. The system had to be capable of extracting a reliable diffraction trace and secondly the data collection had to be synchronised with the constant rotation of the goniometer arm. Both of these functions were successfully incorporated to the enhanced system by means of novel electronic interfaces.

3.2.1 Data acquisition

At any instant during the operation of the LRPD, the simultaneous diffracted intensity can be monitored by either the scroll plotter or by the asynchronous scaler counter mounted in the electronics rack. The rate at which the scaler counts is proportional to the number of events at the detector. The data which is displayed on the counter is also available from the back of the rack from a digital bus. It was from this port that the diffraction data were gathered.

The data bus carries the six figure number on 24 data lines represented in the binary coded decimal (BCD) format. Thus each digit in the datum is written on four adjacent lines. The BBC Master 128K microcomputer selected for the enhanced system is based around an 8-bit architecture and is therefore incompatible with the 24-bit bus. In order for the micro to be able to read the data words, a digital interface board was developed to split the 24-bit word into three separate 8-bit words.

The interface board was based around the popular 6522 Versatile Interface Adaptor (VIA)[41]. These integrated circuits (IC) are themselves incorporated on the motherboard of the BBC micro and are therefore fully compatible. A schematic diagram of the interface is shown in Figure 3.1.

The essential operation of the board can be best summarised by the following steps.

(i) At the instant the micro is instructed to read a data word from the board, the EN line from the VIA is sent high.

(ii) There are three tri-state latch ICs each connected to eight neighbouring data lines. All three latches simultaneously acknowledge the change of state of the EN line and as a result the data on all 24 lines are latched. The information held on each of the three groups of eight lines is stored in the corresponding ICs 8-bit internal register. If the information on the lines changes at any time after the latching, the contents in the internal registers will not change. This has the result of effectively 'freezing' the data line.

(iii) The latches are connected to a common data bus which terminates at the A port of the VIA. This bus is used to read the contents of the

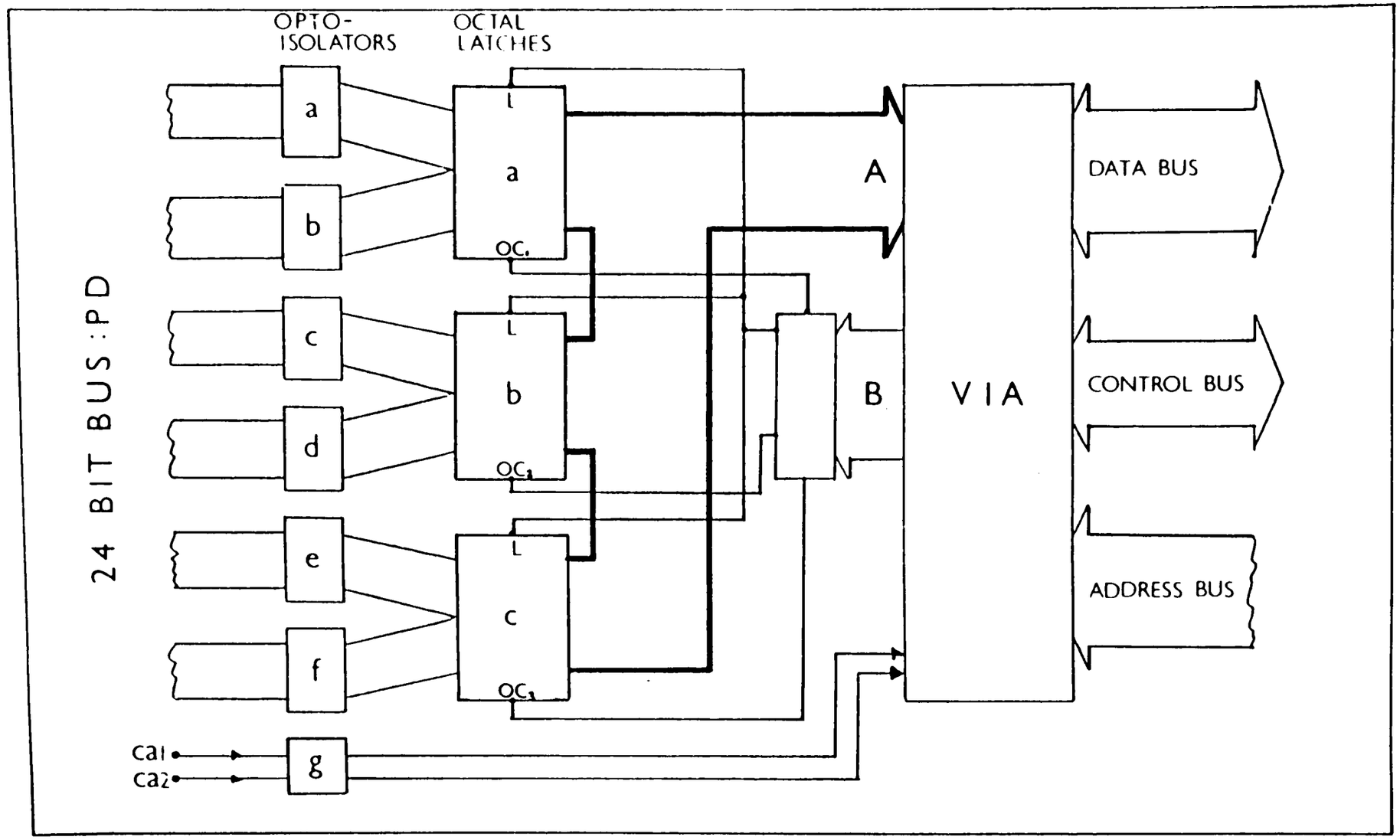

Figure 3.1 A schematic representation of the data logging interface built around a Versatile Interface Adaptor integrated circuit.

internal registers of the latches. The tri-state latches have the ability to effectively disconnect themselves from the data bus when they are disabled. In this state their output pins have a very high resistance and therefore cannot corrupt any data already on the bus.

(iv) One by one the latches are enabled using the oc1, oc2 and oc3 lines. The computer reads the three bytes of information at the A port and stores the data in three variable locations in computer memory. Due to limited online computer memory available, the three bytes of information are compressed to just two. The information is held as hexadecimal rather than BCD, which allows a maximum datum value of 65535 to be stored. This limit has been found to be more than adequate for normal tube operation.

A timing diagram in Figure 3.2 shows the sequence of events relative to the 1-MHz clock.

In addition to the four ICs mentioned already there are numerous other components essential to the boards operation. The row of three 10k ohms resistors have been included to prevent the other components from being overloaded from excessive currents. The output from the BCD data bus is not compatible with the transistor-transistor logic (TTL) components on the interface board. The BCD bus is capable of delivering currents greater than those which are suitable for TTL components. The opto-isolator ICs perform two functions. The first has the effect of electrically disconnecting the interface board and more importantly the operator from the electronics rack, where operating voltages can be as high as 50 kV. Secondly they convert the non TTL negative logic format (NLF) binary pulses into a TTL compatible signal. The output lines from the opto-isolators are tied to earth via

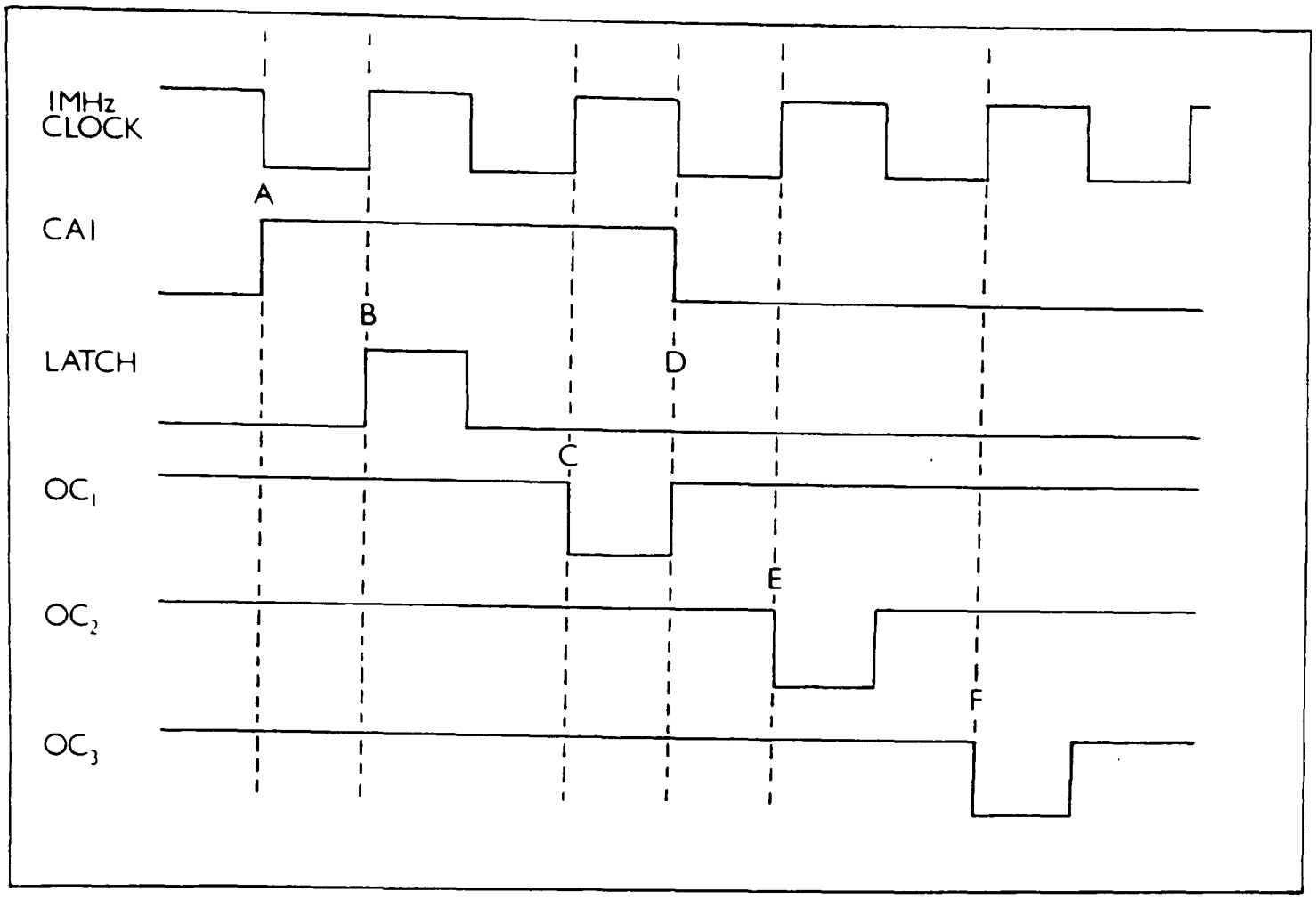

Figure 3.2 The timing diagram sequence for the data logging procedure.

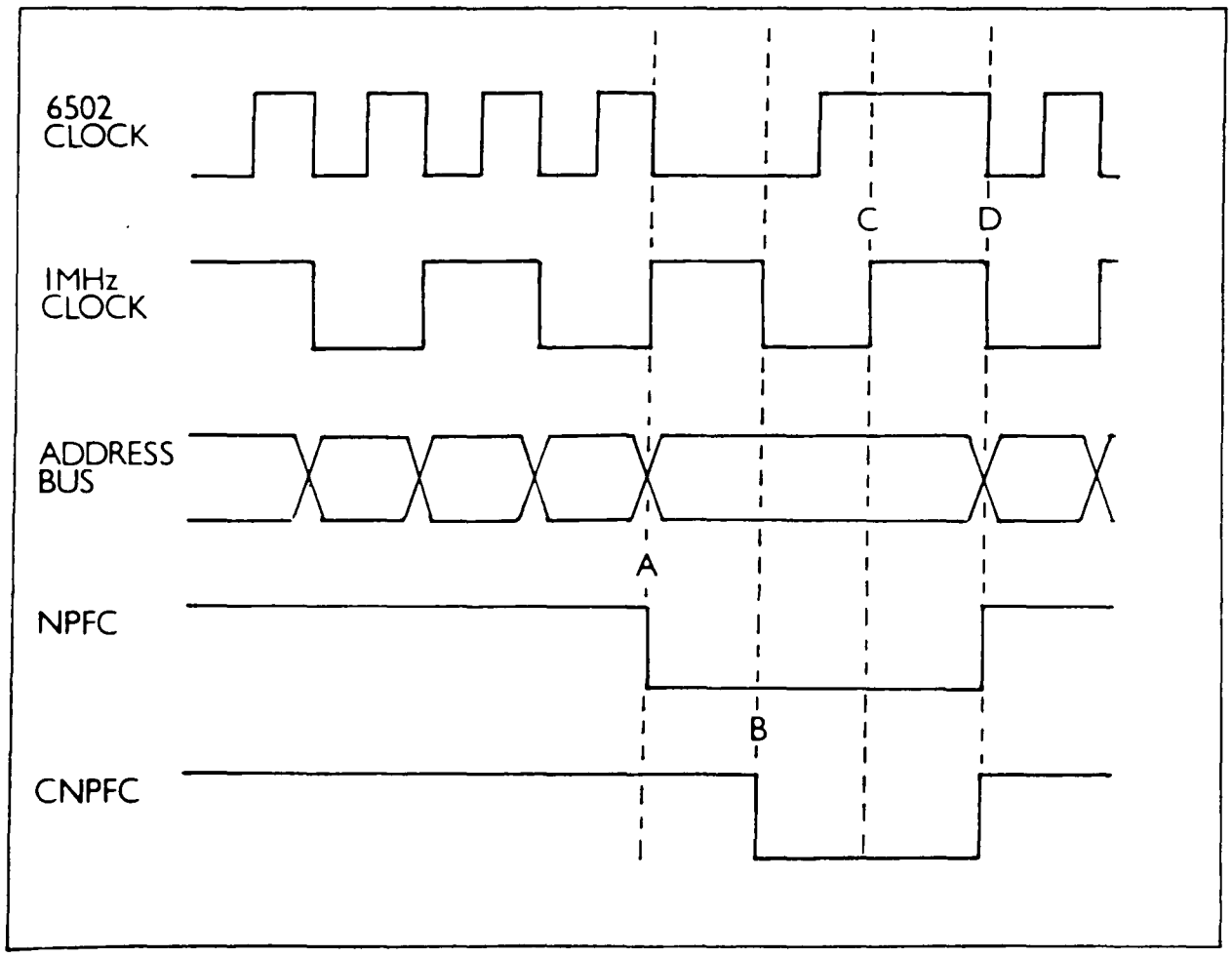

Figure 3.3 The timing diagram for accessing peripheral devices from a BBC master microcomputer.

separate 10k ohms resistors. These were found to be necessary to clearly define the two distinct logic levels.

The 1-MHz bus on the BBC micro is intended for peripheral devices and development boards. As the name suggests the bus operates from a clock frequency of 1-MHz, which is a frequency commonly used in many peripheral devices. The BBC's central processing unit (CPU), however operates at twice the frequency when accessing internal addresses and performing arithmetic operations. The apparent incompatibility of operating frequencies for the BBC and for peripherals on the 1-MHz bus, is remedied by the slowing down of the CPU clock when the 1-MHz bus is addressed. This is done by stretching the CPU clock as shown in Figure 3.3. The 1-MHz bus can only be addressed when the CPU clock changes from high to low. When the two clocks are coincident, at point D on Figure 3.3, the normal 2-MHz frequency is reestablished on the CPU. The stretching of the clock, however introduces a potentially undesirable effect, which can be explained by means of the diagram in Figure 3.3.

When the 1-MHz bus is addressed the NPFC control flag is sent low, as shown at point A. The NPFC signal is generated by the BBC and is intended for enabling peripheral devices when they are being addressed. The NPFC signal will remain low until the CPU clock makes the transition from high to low state, D. During the period of time between A and D, all the information on the address and data busses will remain unchanged. The VIA is enabled when both the 1-MHz clock is high and NPFC is low. This set of circumstances arises twice between A and D and as a result the register addressed on the VIA is accessed twice. Carrying out an operation twice may have the effect of

resetting a status flag which had just been cleared. This would cause the interface board to malfunction. To prevent the occurrence of this phenomenon, a 'clean up' circuit was incorporated into the circuit.[42] The clean up circuit is shown in Figure 3.4. Using two d-type flip-flop gates, the NPFC signal can only go low when the 1-MHz clock is also low. The 1-MHz signal is inverted by the flip-flop at A, which acts as the enable for the second flip-flop at B. The second flip-flop uses the inverted clock and the low NPFC signal to produce the CNPFC signal. Thus the VIA is enabled for as little time as is necessary. The CNPFC timing is shown if Figure 3.3. The CNPFC output signal is combined with the hi-nybble of the 8-bit address lines to produce the low level chip select signal (CS).

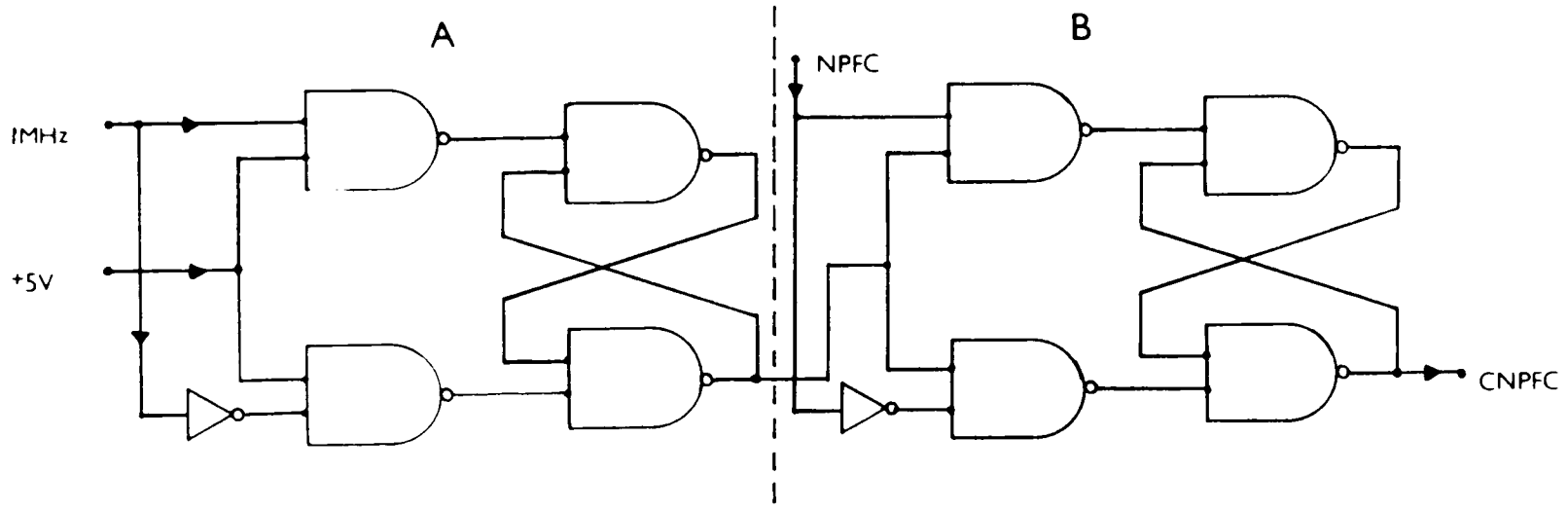

Figure 3.4 A simple 'clean-up' circuit preventing double access. (note the fundamental logic units are NAND gates)

3.2.2 Synchronisation

Due to the initial design criterion of not removing the original drive mechanism, the use of a stepper motor to control the goniometer arm was rejected. Instead, the microcomputer was employed to monitor the goniometer rather than to control it.

The powder diffractometer (PD) generates a square wave pulse every

half-degree of 2θ, by means of a micro-switch on the rotation shaft. The frequency of the pulses are dictated by the ratio of the motor and driven shaft cogs. This signal was initially used by the scroll plotter to produce a reference square wave along the bottom of the diffraction trace giving a rough guide to the 2θ value. This signal is now incorporated into the interface board via a line coded ca2.

The half-degree marker has been used by the enhanced system to update the current position of the goniometer. Obviously a resolution of better than 0.5° is required for even the most basic analysis on the PD and so a second control line was introduced. The rotation of the drive cog attached to the clutch mechanism was found to rotate once for every one degree of 2θ. A infrared fibre optic link was established across the teeth of the cog-wheel. As the cog-wheel rotates, the fibre optic beam is interrupted by the passing of the teeth. The electrical output of the infrared detector generates a rough sinusoidal wave. The signal is clipped to produce a square wave pulse and then amplified. The result is a train of square pulses with a fairly constant frequency which are transmitted along the line coded ca1. A schematic diagram of the fibre optic link is shown in Figure 3.5.

On reception of the pulse, the microcomputer is instructed to read the data on the 24-bit bus. The cog-wheel has 96 teeth and so a rotation of one degree 2θ can be sampled at 96 even intervals. The combination of the half degree interrupt, ca2, and the fibre optic line, ca1, gives the system a theoretical resolution of 2θ better than 0.02°.

Both of these signals are connected to the VIA with the same safety arrangement as the data lines. They are constantly monitored by the

Interrupt Flag Register (IFR) housed in the VIA, which can be polled at any time by the micro.

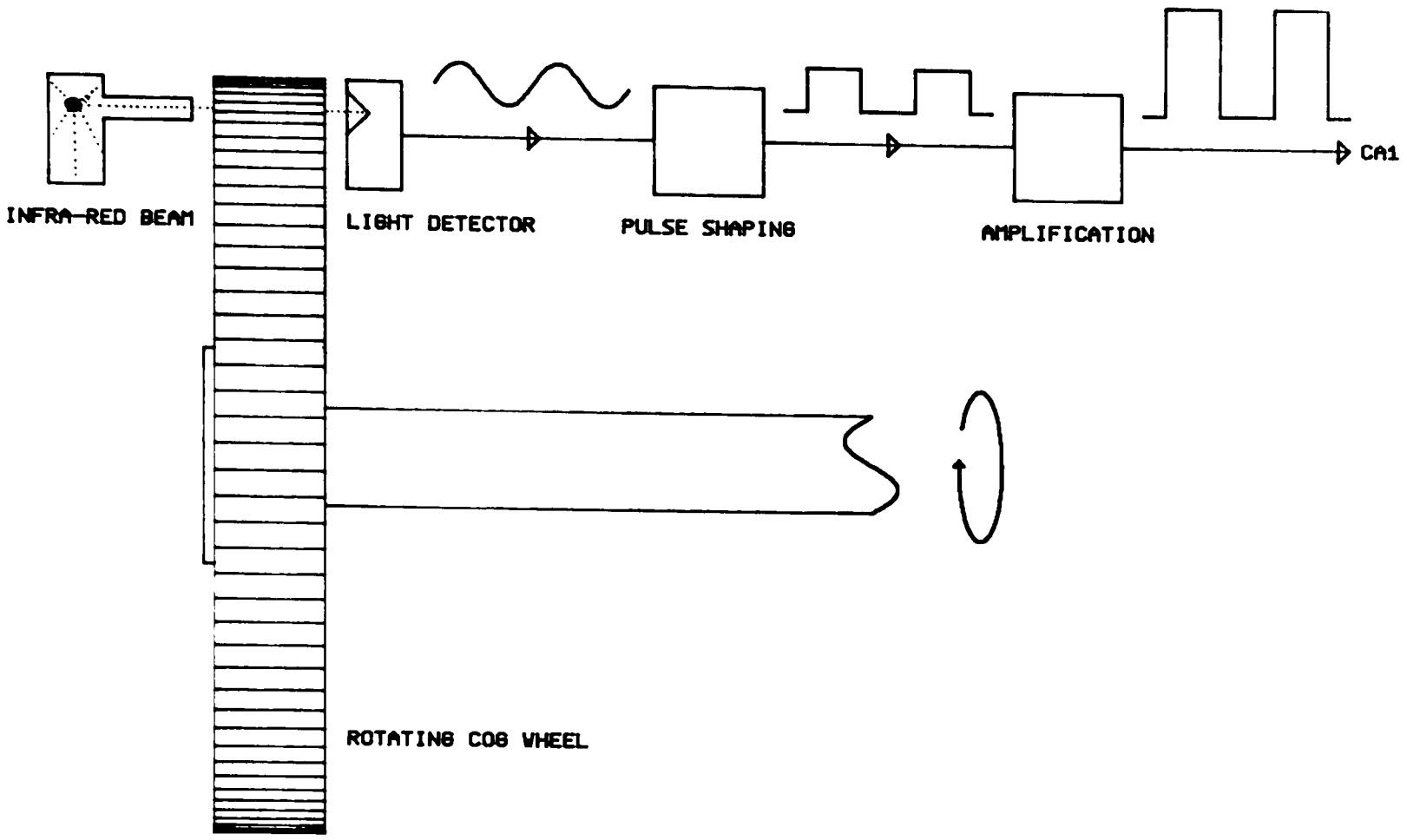

Figure 3.5 A schematic representation of the infrared fibre optic link, synchronising the data logging to the rotation of the diffractometer cog wheel.

3.3 Software development

A suite of computer programs written in BBC BASIC IV and 6502 machine code were developed to complement the hardware developments of the LRPD[43]. The programs are all menu driven from one control program CENPOD. (**C**omputer **EN**hanced **PO**wder **D**iffractometer). The basic functions and operating principles of CENPOD are described below in general terms. The CENPOD operator's manual is featured in appendix A, where the facilities are discussed in greater detail. Full documented listings of the BASIC and Assembler programs are included.

3.3.1 Data collection

Using the program SCAN, the micro can be programmed to scan a selected 2θ range up to a maximum of 160°. Although the BBC Master 128K is a powerful and flexible microcomputer, it does not have a continuous memory map. Instead the memory is broken down into discrete blocks. Thus it was not possible to store large amounts of data sequentially in memory. However it does have a bank of 64 Kbytes in Sideways Ram (SR) separate from the main memory map, comprising of 4 x 16 Kbyte memory blocks. The three bytes of data per sample are converted into 16-bit words and then stored in a small array capable of holding all the data for half a degree. After half a degree; on arrival of the ca2 interrupt; the contents of the array are transferred into the SR. Subsequent half degree packages are stored in the SR sequentially. On completion of the scan the diffraction trace data is transferred onto floppy disc where it is stored in three files. Two large files are available for the diffraction trace if necessary, and the third holds information regarding the scan limits and type of radiation used. These files hold all the relevant information for the subsequent data processing programs.

3.2.2 Data processing

It was initially proposed that routines be written to automatically search through the data-file, corresponding to the diffraction trace, looking for peaks. Once found, it would determine their associated interplanar spacings and calculate the intensities from the peak height. This is merely the same operation as would be performed by a person working from a paper scroll and is acceptable in theory.

The start and finish of a peak on a trace are easily detected by the

human eye, since any assumptions are made by comparisons with experience. However, in the case of a computer model, the rise and fall in data values corresponding to the trace height need to be compared with some preset value which relates to an authentic peak. Since the characteristics of each trace are different, then this tolerance would have to be set by considering the nature of each individual the trace. Some time was spent developing algorithms, based on statistical analysis of the whole trace, to detect significant variations in the trace height, representing real peaks. Early results proved to be encouraging, but as more complicated diffraction traces were analysed, the routines either failed to detect small peaks or interpreted the spurious background scattering as peaks. At high 2θ the Bragg peaks begin to overlap, which further confuses the routines. Given these problems, it was decided that to pursue this problem would be time consuming and a distraction from the immediate goals of the research programme. Instead a semi-automatic graphical program, PROFILE, was developed. PROFILE allows the operator to have an active role in the decision making.

By displaying the trace on a VDU, the user can identify to the computer the positions of the peaks of interest using on-screen cursors. In this fashion the search routines would only be executed over selected areas of the trace. A typical trace is shown in Figure 3.6.

The entire trace is displayed in a graphics window at the top of the screen, and by using the programmed function keys, any five degree section of the trace can be selected for viewing in the larger graphics window. This plot will reveal more information than the whole

condensed trace, making the positioning of the cursors more accurate. If a peak overlaps from one five degree window to the next, the graphics window can be moved up by increments of two degrees until the whole peak is visible.

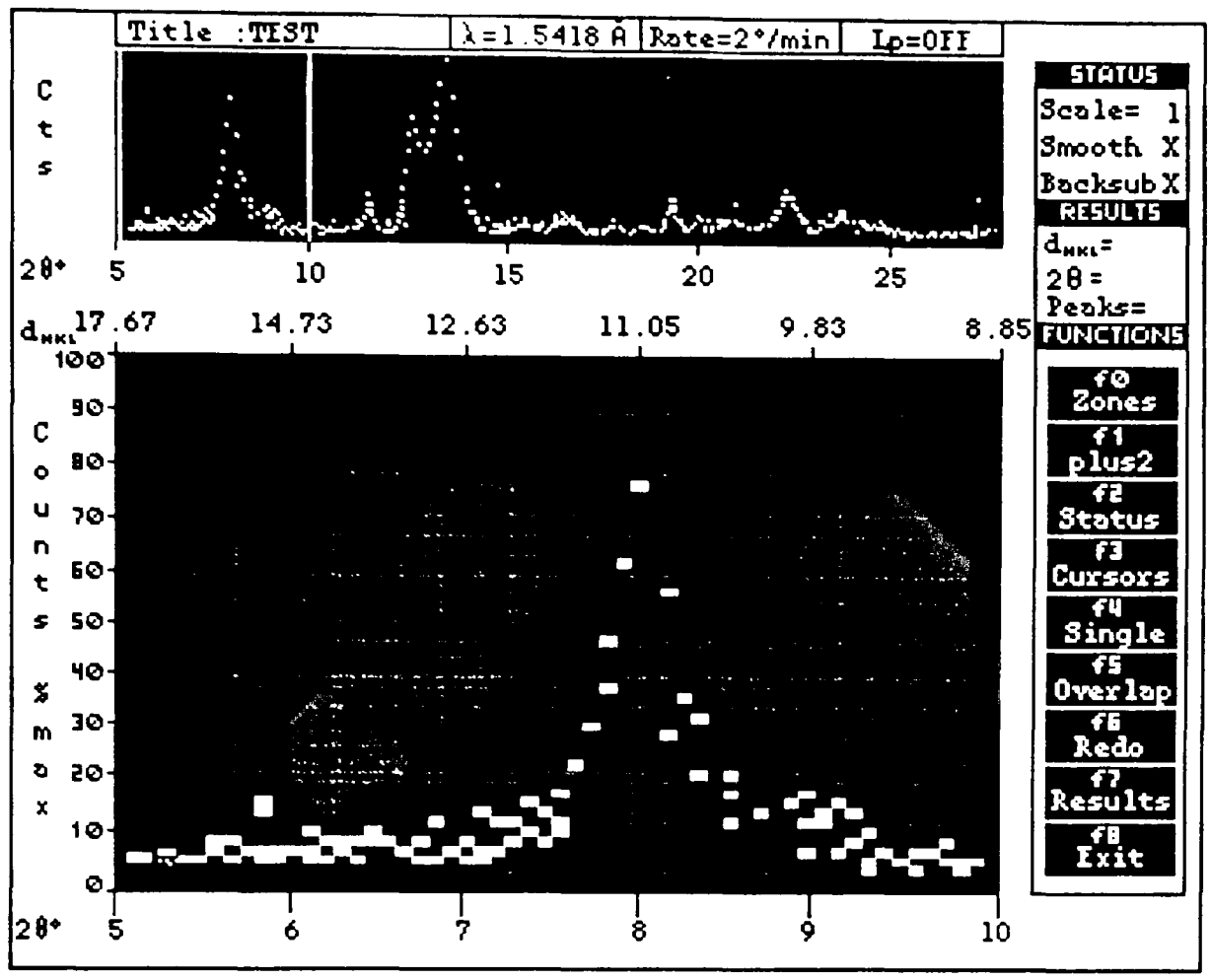

Figure 3.6 A representation of the PROFILE screen display of the powder trace. The entire trace is plotted in the upper graphics window and enlarged 5° sections are plotted below.

A common problem with many of the traces is that there will be a high degree of unwanted spurious noise. This makes the problem of positioning the cursors more difficult, and so it was necessary to incorporate a smoothing routine. This performs a moving average calculation on groups of adjacent data values within the current graphics window. This has the overall effect of removing any spurious noise generated by the interface and also reduces scatter, leaving a much improved trace. As a side effect the heights of the peaks become slightly diminished, however the relative intensities remain virtually

constant. The effects of the smoothing routine can be compared to the original untreated data in Figure 3.7.

To extract the integrated intensities and inter-planar spacings from the Bragg peaks, the system uses peak fitting routines. The basic Gaussian distribution in equation 3.1 was used to describe the characteristic of the experimental data.

$$I = I_o.\exp(-(2\theta-\mu)^2/\sigma^2) \qquad (3.1)$$

Where I_o is the maximum peak intensity.
μ represents the absolute 2θ position of the peak, determined by full width half maximums (FWHM).
σ is the variance of the function describing the broadness.

To measure a reflexion, the corresponding peak is first identified by placing cursors on either side of the peak's apex. From the positions of the cursors, the locations in memory where the peak data resides are calculated. The computer scans through these locations searching for the maximum turning point and hence calculates the full width half maximum (FWHM) points[44]. A vertical cursor is used to identify the estimated background for the peak. A Gaussian peak is fitted to the diffraction peak by sampling the peak at several points and calculating the peak parameters. At present, there are no least squares refinements performed on the fit.

The measurement of an overlapping peak is treated in a similar fashion. The apex of the peak is found and then with a third cursor, the apex of the second peak is determined. In this case the FWHM points may not be true and so it is necessary to sample intensities from the region between the two apexes. Rough estimates of the variance of the peaks can be ascertained using equation 3.2. This

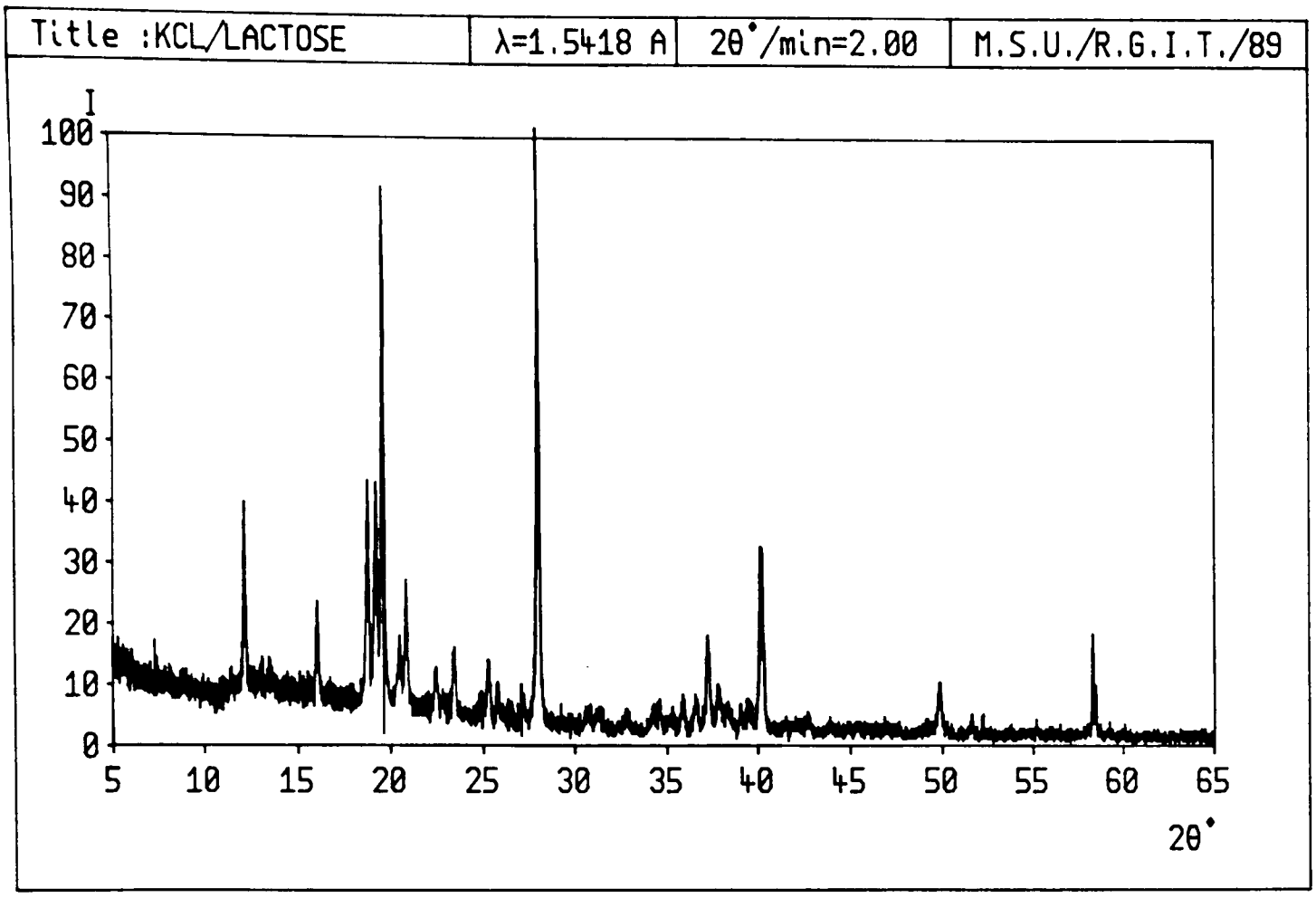

Figure 3.7(a) The powder diffraction trace for a mixture of potassium chloride and lactose, produced by CENPOD. The data is untreated and so the background noise levels are high.

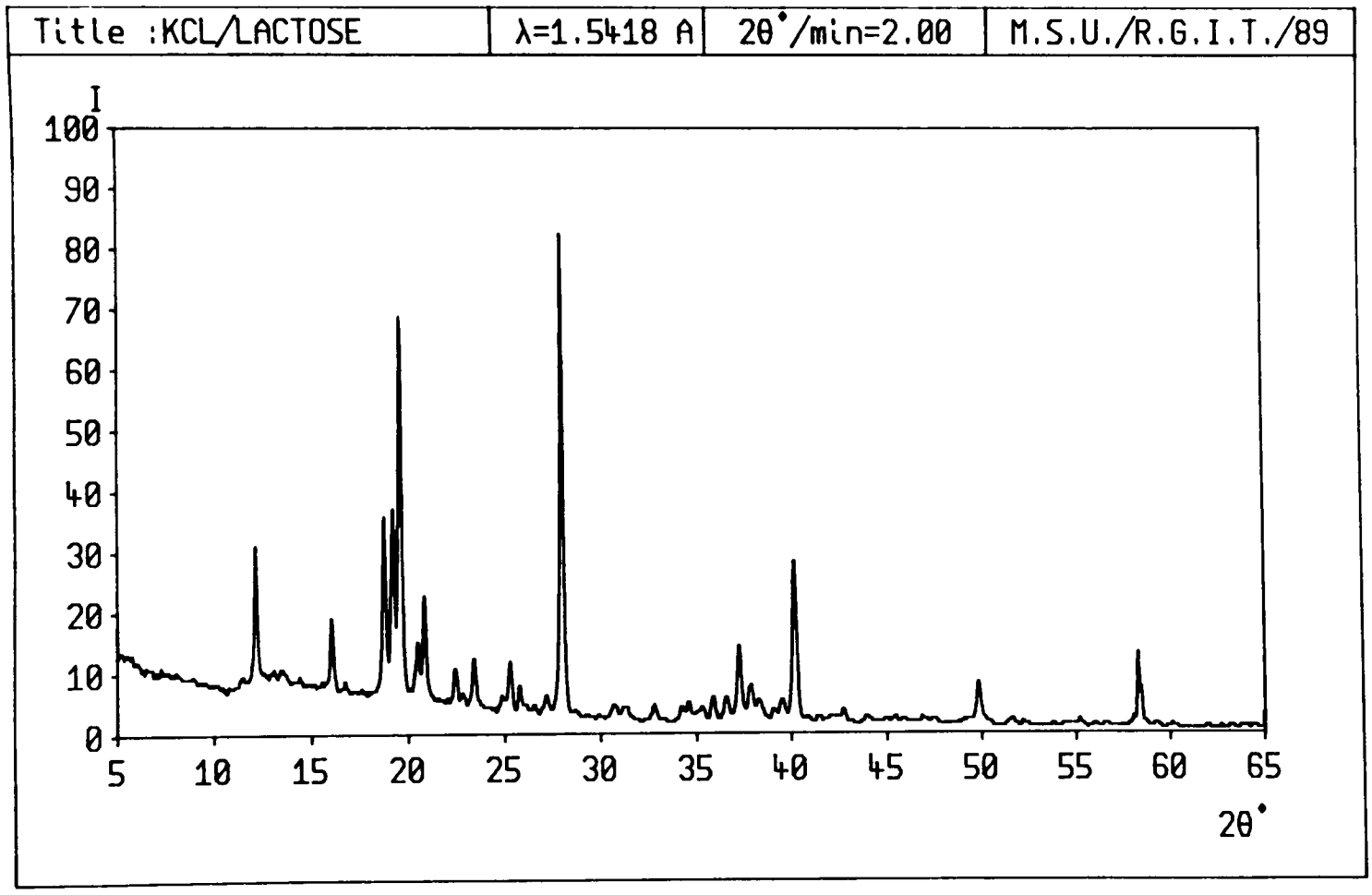

Figure 3.7(b) As 3.7(a), but the diffraction data has been subjected to the smoothing routine. Note the slight diminishing of the absolute intensities.

method for intensity calculation is only approximate, but it has proved to be reliable and an improvement over simple peak triangulation techniques. More elegant peak deconvolution methods have been investigated, but they required far greater computing power than the BBC Master could provide[45-48].

$$\sigma_1^2 = \frac{(2\Theta_2-\mu_1)^2(2\Theta_1-\mu_2)^2-(2\Theta_1-\mu_1)^2(2\Theta_2-\mu_2)^2}{(\ln(I_1)+\ln(I_2)-\ln(I_2))(2\Theta_1-\mu_2)^2-(\ln(I_1)+\ln(I_2)-\ln(I_1))(2\Theta_2-\mu_2)^2} \quad (3.2)$$

$2\Theta_1$ and $2\Theta_2$ represent the angular positions of the two sample points.
μ_1 and μ_2 are the assumed mean positions of the overlapping peaks.
I_1 and I_2 are the background subtracted peak heights.

3.2.3 Data analysis

The primary use for the LRPD at RGIT is for sample identification and phase analysis. The process of systematically comparing the experimental data with entries from the JCPDS[49] (Joint Committee on Powder Diffraction Standards) file, can be a time consuming and difficult exercise, especially when the unknown sample is of a multi-phase composition. As part of the system enhancement a crystallographic database search routine was developed to reduce the amount of human interaction.

The computer subroutine incorporated into PROFILE, works through the database file comparing the interplanar spacings, d_{hkl}, accepting those values which lie within a calculated tolerance. A rather pessimistic error in 2Θ of 0.1° was set. Since the relationship between 2Θ and d_{hkl} is not linear, a separate tolerance Δd_{hkl} is calculated for each reflexion. For each entry in the database which is compared, it receives a figure of merit. This is simply the average relative intensity of the reflexions which match the test data. The

entries are arranged in order of figure of merit, with the best three selected for display on the screen. A typical output is shown in Figure 3.8, where the highlighted data pairs indicate successful matches. This routine can help to identify the components of multiphase samples, but it is obviously limited to a small number of contributing compounds.

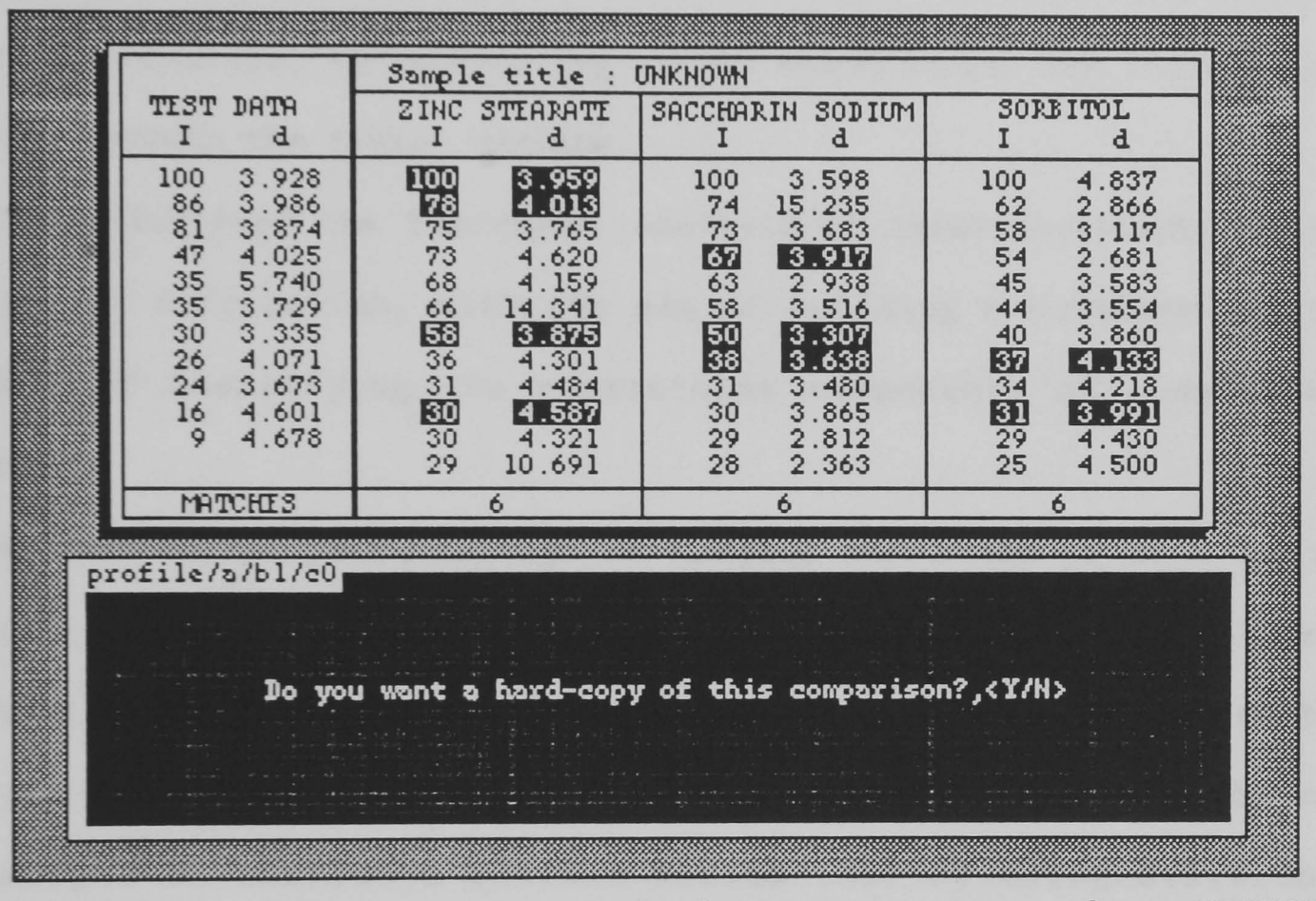

Figure 3.8 A representation of the screen output from CENPOD, displaying the results from a comparison of experimental reflexions with the powder diffraction database.

In a similar fashion, the experimental data may be input to the database, thus expanding it. The database is currently defined to hold up to 200 samples per magnetic disc.

Other facilities in PROFILE allow the trace of a sample to be plotted on an XY plotter in a similar fashion to the original scroll plot. This has the advantage that the 2θ scale and intensities are clearly marked and that subsequent plots may be superimposed. Superimposing the plots can help to make quantitative and qualitative predictions about sample composition relative to known samples.

3.4 Enhanced LRPD applications

3.4.1 Pharmaceutical database

The initial proposed application for the enhanced system was to examine commercially used tablet excipients. These excipients are largely the inactive ingredients used to make up the bulk of a tablet. These range from binding chemicals, used to help the tablets withstand external abrasions, to lubricating agents which assist the flow of the mixture through the tablet machine.

The study involved the individual analysis of these excipients by X-ray powder diffraction, with the aim of building a database system capable of identifying the constituent components of commercial tablets.

The method of recrystallisation of samples was found to be a major variable. Many chemical materials, such as cimetidene, have been found to exist in several crystalline states, which are often dictated by the processes involved during recrystallisation[50,51]. A study of polymorphs of cortisone acetate showed that by using different combinations of organic solvents and water, different crystal structures resulted. From this it was apparent that for the database to have accurate and useful data, the methods of recrystallisation of samples were to be noted.

3.4.2 Sample preparation

Samples recrystallised with the same polymorphic form, were still found to exhibit inconsistencies in their diffraction traces. The positioning of the peaks were correct, but the relative intensities were found to vary significantly. This effect was due to preferred orientation, brought about by the method of sample preparation. To

minimise the preferred orientation, a sample preparation technique had to be adopted, capable of reproducing traces from the same bulk sample with a variation of intensities below +/-15%.

Preferred orientation can be minimised by reducing the mean particle size of the powder sample[52]. This was achieved by grinding the sample with a ball mill or a mortar and pestle. In the case of a ball mill, the grinding action can often be so vigorous as to raise the temperature of the powder thus causing it to undergo a phase change. Clearly this effect is undesirable and so in cases of materials which were thought to be sensitive to temperature variation, the mortar and pestle was used. As a final precaution the powdered samples are passed through a fine sieve. The effects of grinding and sieving are demonstrated in a sequence of plots in Figure 3.9.

The plots show superimposed powder diffraction traces of sucrose scanned over the same range using the same operating conditions but with varying degrees of sample preparation. Figure 3.9(a) shows the traces of sucrose after gentle grinding in the mortar. Figure 3.9(b) shows sucrose after grinding in the ball mill. There is a slight improvement in consistency, but it is not conclusive. Figure 3.9(c) shows traces of the same used powder in 3.9(b), but after being passed through a 63 micron sieve. The peaks are sharper and well matched and the background exhibits less random scatter. Finally in Figure 3.9(d), the samples are ground in the ball mill and then passed through the 45 micron sieve. Again the traces are improved. By decreasing the aperture further would result in still better traces. The variations exhibited in Figure 3.9(d) are minimal and within the acceptable tolerances. The effects of preferred orientation can still be

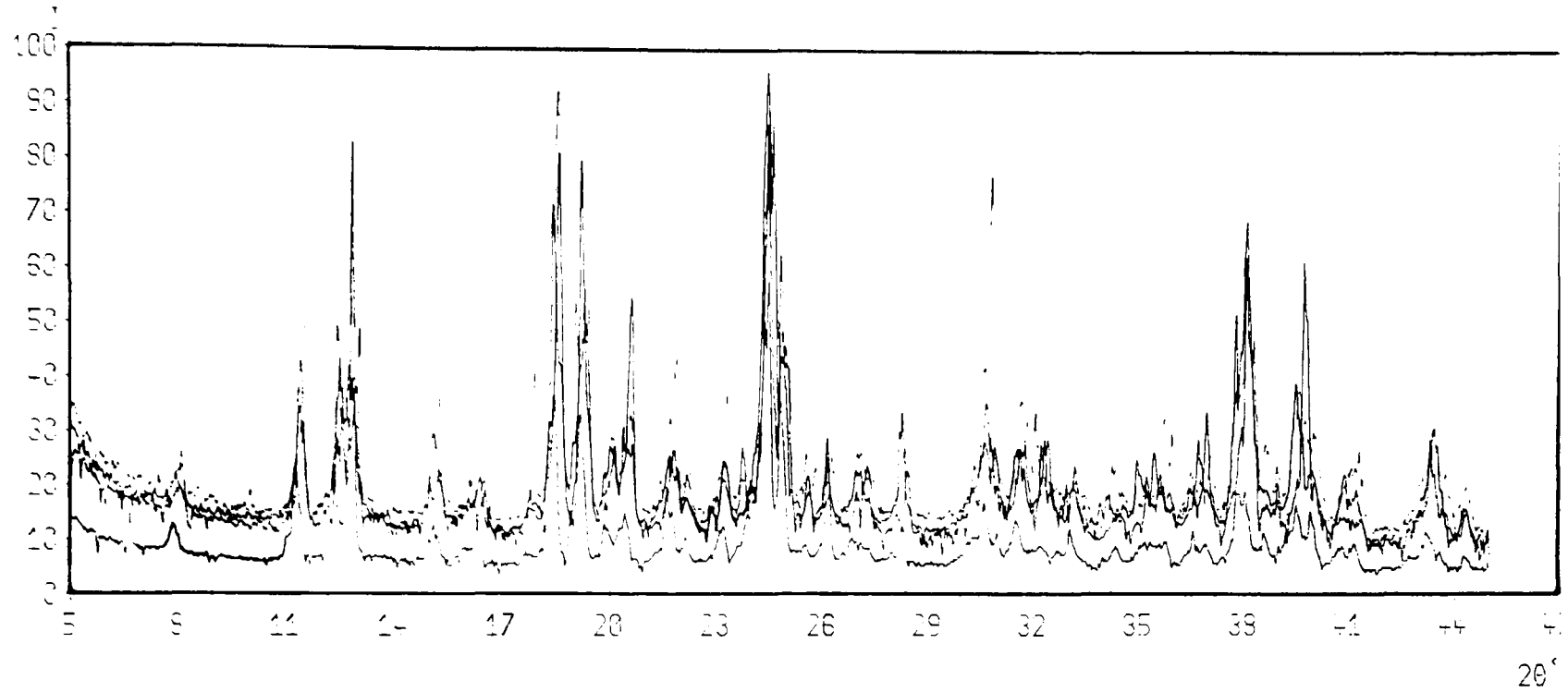

Figure 3.9(a) Four superimposed plots of sucrose scanned over a 2θ range of 5-45°.The sucrose was left in the basic granulated form, thus resulting in a wide range of intensities.

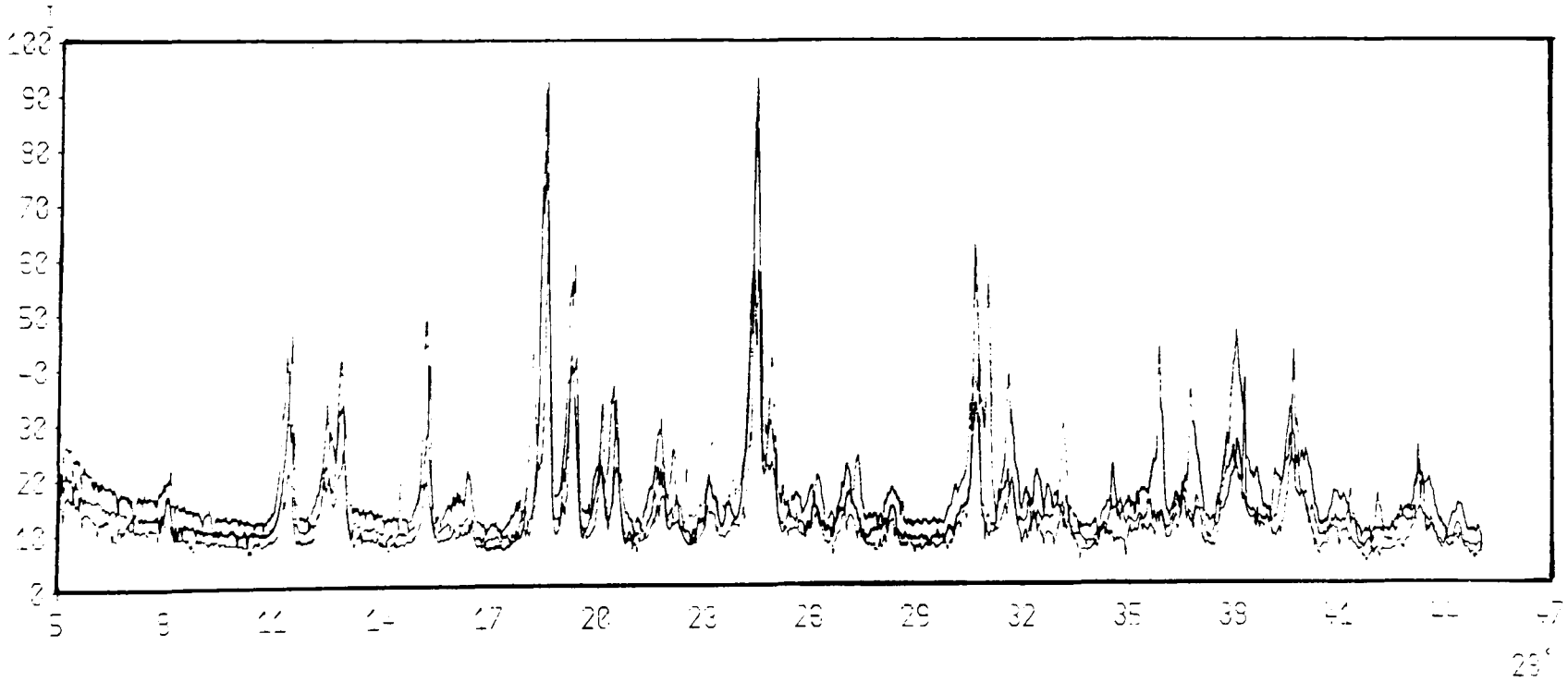

Figure 3.9(b) The sucrose was ground in a ball mill reducing the granules to a fine powder. The three superimposed plots show a marked improvement in the intensity reproducibility.

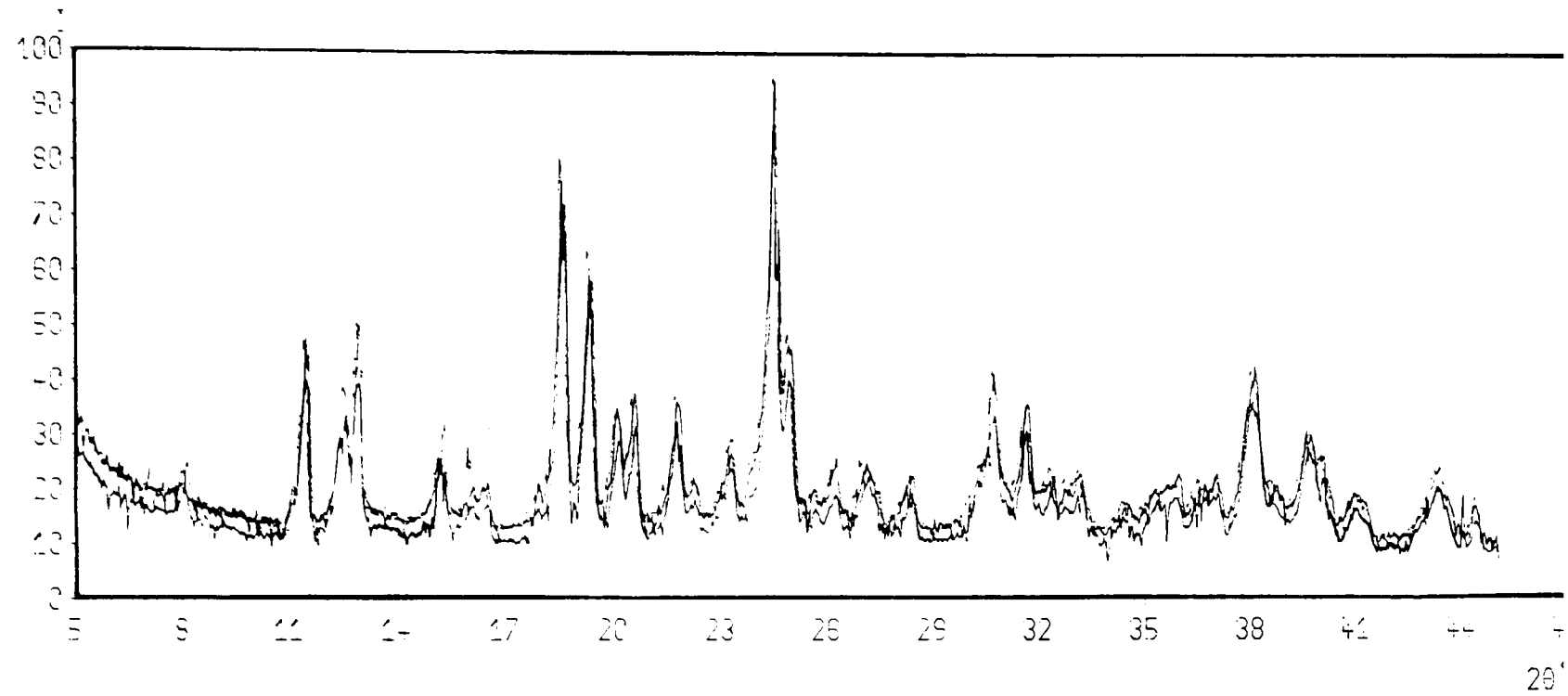

Figure 3.9(c) The ground sucrose was passed through a 63μm sieve ensuring a maximum particle size.

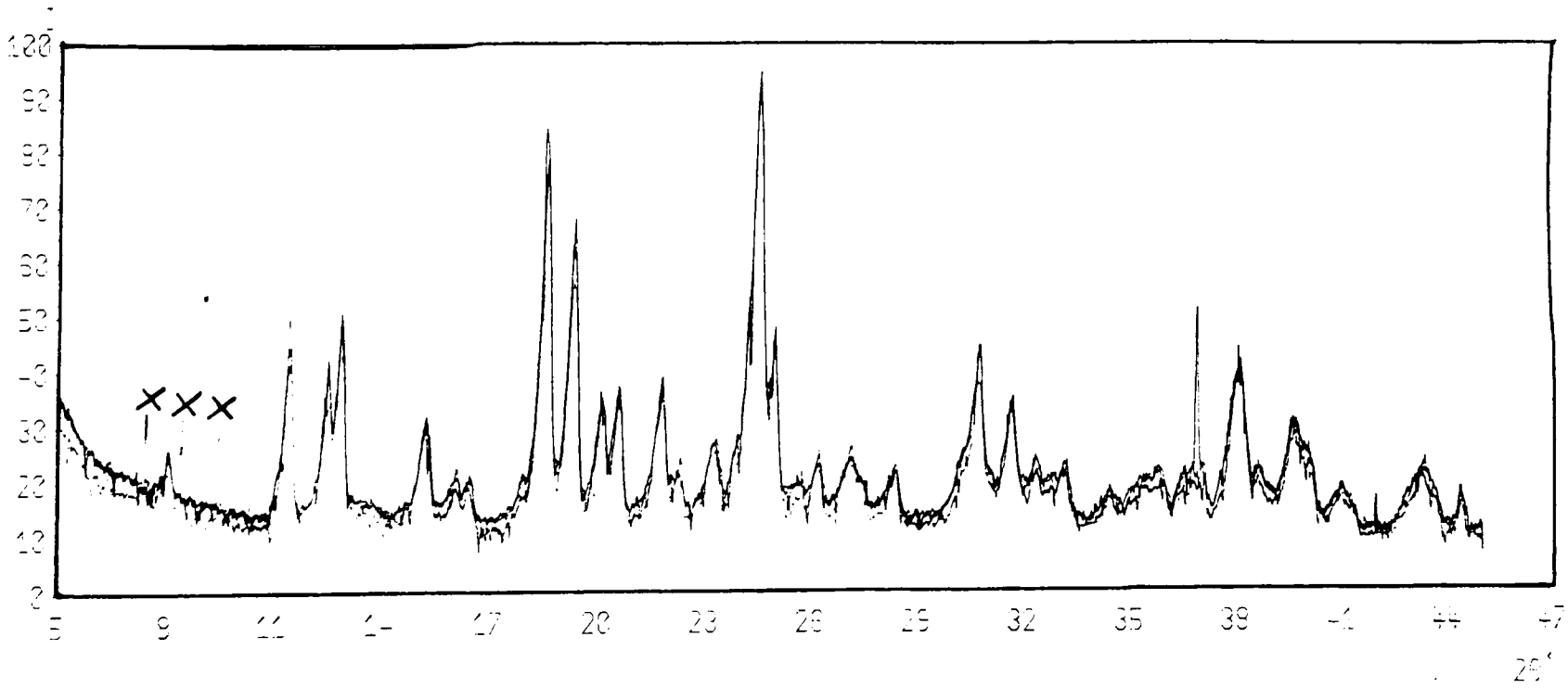

Figure 3.9(d) The ground sucrose was passed through a 45μm sieve. (The four "peaks" marked with crosses represent electrical surges encountered in the digital electronics)

significant even after grinding and sieving. The method used to load the sample holder can have the effect of ordering the random distribution of crystallites.

3.4.3 Sample loading

Excessive pressure when loading the sample holder can cause the crystallites to align in a common direction. To prevent this packing, it is essential that minimum force is applied when loading the sample. Several popular techniques were investigated, before a hybrid packing mechanism, based on the McCreery's was formulated which best suited the needs of the powder work involved[53,54]. This technique can be described with the aid of the sequence of diagrams in Figure 3.10.

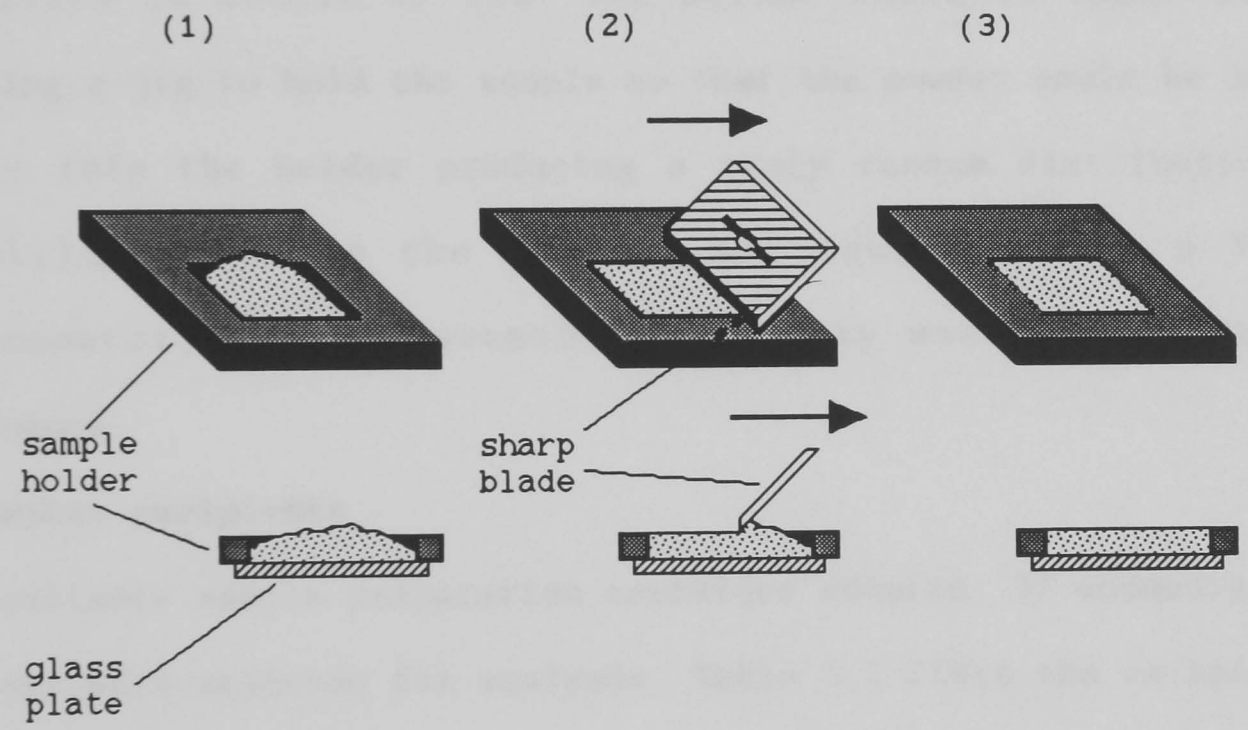

Figure 3.10 Sample preparation using a hybrid method.

(1) The sample is sieved directly into the sample holder. The glass plate used as a base is affixed by petroleum jelly.

(2) A fine edged blade is dragged across the surface of the powder, removing the excess.

(3) The processes described in (1) and (2) are repeated until the surface is even.

The thin rectangular aluminium sample holder is inverted and a thin

glass plate, smeared with a thin film of petroleum jelly, is fixed over the aperture. The jelly holds both the plate to the holder and the powder to the plate. The powder is loaded gently into the cavity of the holder, by spatula or direct sieving, until there is an excess. The surface of the powder is made planar by drawing a scalpel blade across the top of the sample holder, avoiding any unnecessary pressure. The result of the levelling will have produced a near perfect surface, however there can often be pits created by a "snowball" effect. These are removed by repeating the steps of loading and skimming until no further improvement can be made.

This method has proven to be capable of reproducing diffracted intensities to within +/-15%. The method could be improved, by fashioning a jig to hold the sample so that the powder could be sieved directly into the holder producing a truly random distribution of crystallites. Since the LRPD is not equipped with a X-ray monochromator, the improvement in quality would be of little significance.

3.2.4 Tablet excipients

With a reliable sample preparation technique adopted, 37 commonly used excipients were selected for analysis. Table 3.1 lists the excipients, using their common names.

The materials were all scanned over the 2Θ range of 5-45° with identical operating conditions. From experience, it has been observed that the majority of useful well defined peaks lie within this range, whilst using Cu Kα X-rays. The traces featured in Figure 3.11 represent typical diffractograms of the excipients analysed. All of the significant peaks were measured and then arranged in order of

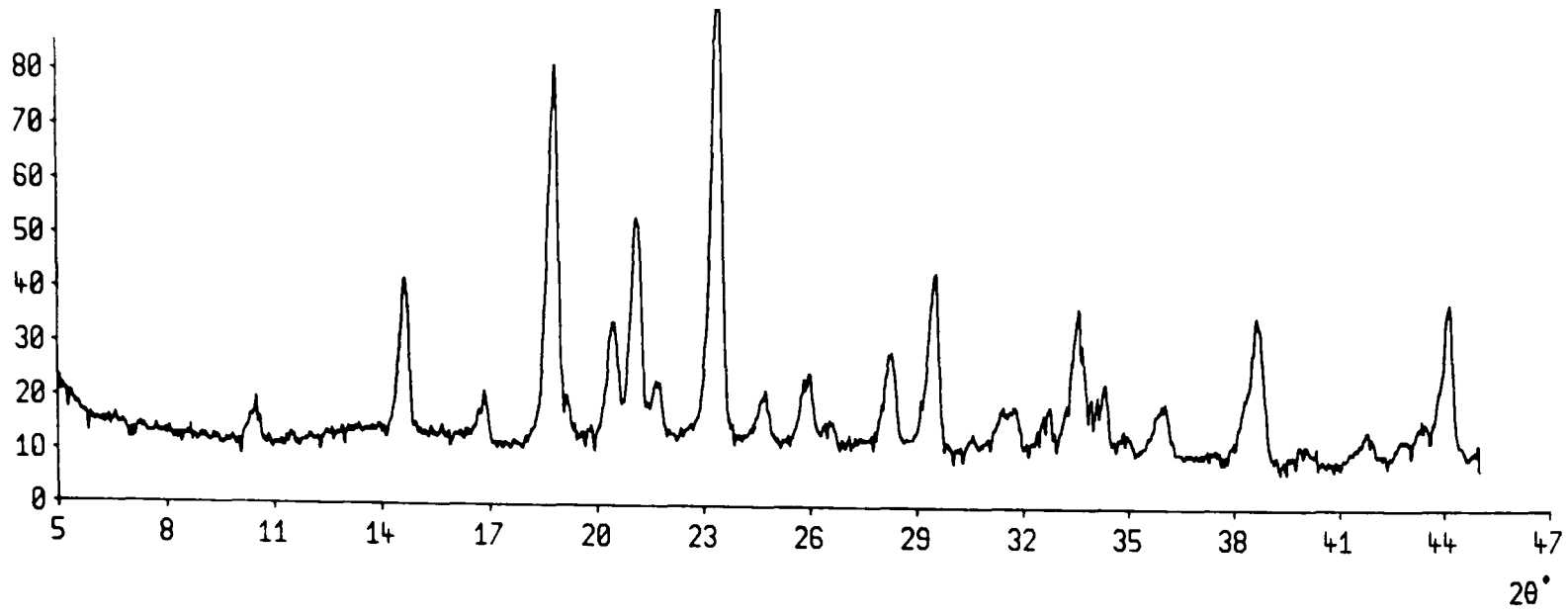

Figure 3.11(a) LRPD trace of mannitol over 2θ range 5-45°.

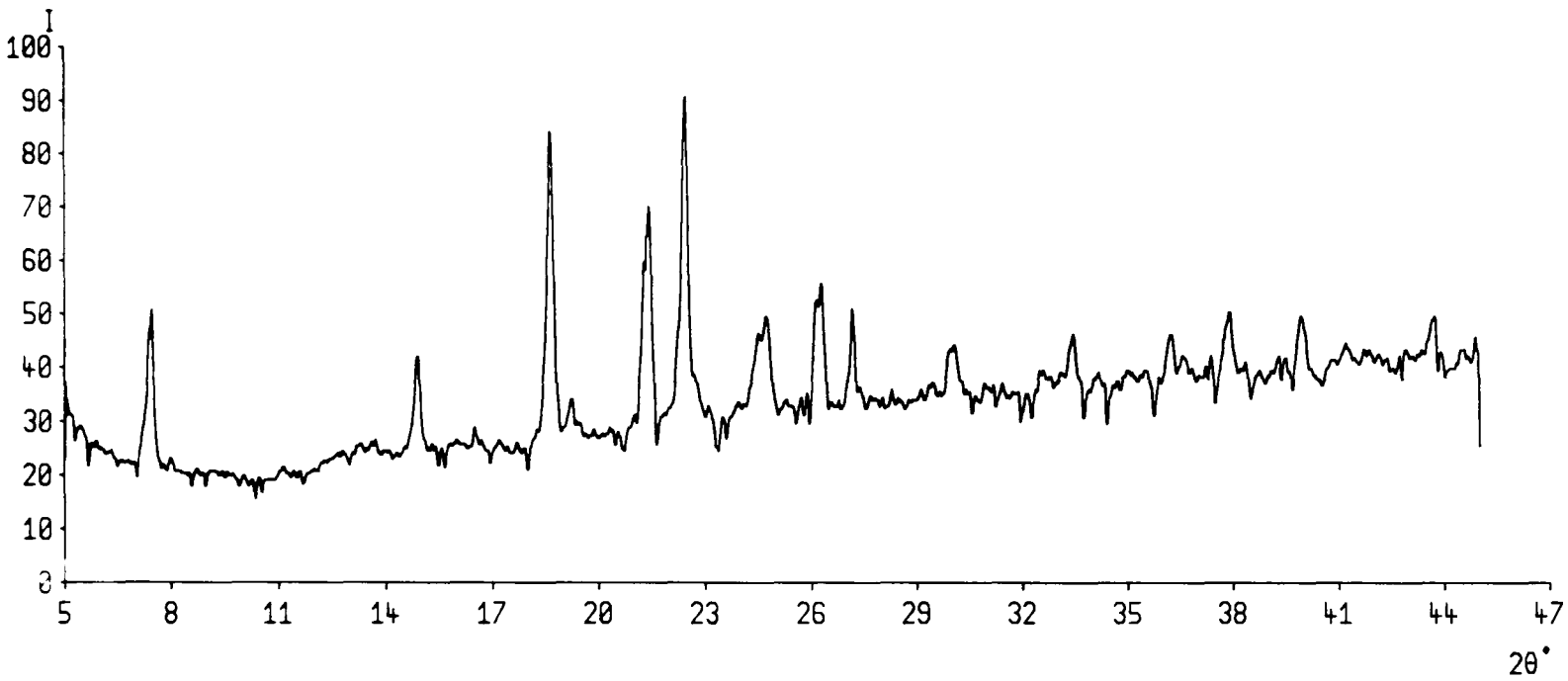

Figure 3.11(b) LRPD trace of cetrimide over 2θ range 5-45°.

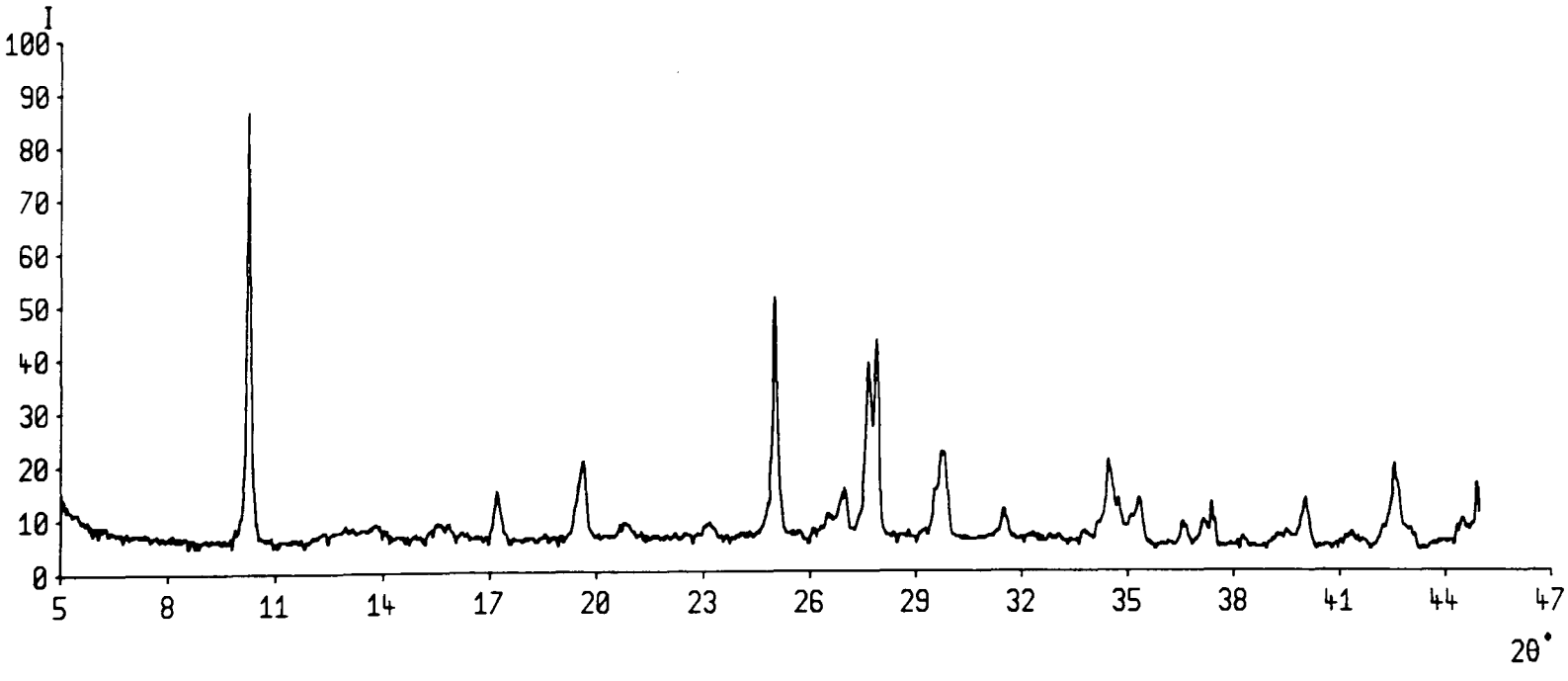

Figure 3.11(c) LRPD trace of L-ascorbic acid over 2θ range 5-45°.

decreasing intensity. Up to a maximum of 30 of the most intense peaks were selected for storage on the database. In most cases a sample can be identified with as few as 5 peaks. The JCPDS search manual displays only the 8 most intense peaks. The diffraction data was stored on disc with additional information regarding the scan conditions.

Table 3.1 Tablet excipients examined for the database.

L-ascorbic acid	magnesium stearate
benzoic acid	DL malic acid
butyl paraben	mannitol
calcium carbonate	methyl paraben
calcium phosphate	potassium chloride
calcium stearate	propyl paraben
cetrimide	saccharin sodium
cetyl alcohol	sodium benzoate
cholesterol	sodium chloride
citric acid	sodium hydrogen carbonate
dextrose anhydrous	sodium lauryl sulphate
dextrose monohydrate	sorbic acid
EDTA	sorbitol
ethyl paraben	stearic acid BP
lactose BP	sucrose
α-lactose monohydrate	tri potassium citrate
lactose monohydrate	tri sodium citrate
light kaolin	zinc stearate
magnesium carbonate	

The information stored on the disc is held in a random access file allowing rapid data retrieval making it ideal as a reference database. The information is presented in a way similar to the card system adopted by the powder index. A typical screen presentation is shown in Figure 3.12. To make reference quicker the diffraction data for the four most intense peaks is displayed in the top right hand corner.

The system can produce a hard copy of the diffraction data on request or even generate a synthetic diffraction trace based on the measured peaks. The other main purpose of the database was to develop an automated search and comparison routine for sample identification.

Such a system had to be able to pick out individual compounds from a mixed sample. The tablet excipients are used in varying quantities depending on their purpose. Many tablets have large quantities of sugar, which simply acts as a transport mechanism for the active drugs. The lesser used chemicals pose a problem for identification for the search routine, since their Bragg peaks may be masked by the scattering of other chemicals in the sample. To determine to what extent the system could identify powder mixtures, multi-phase compounds of known composition were examined.

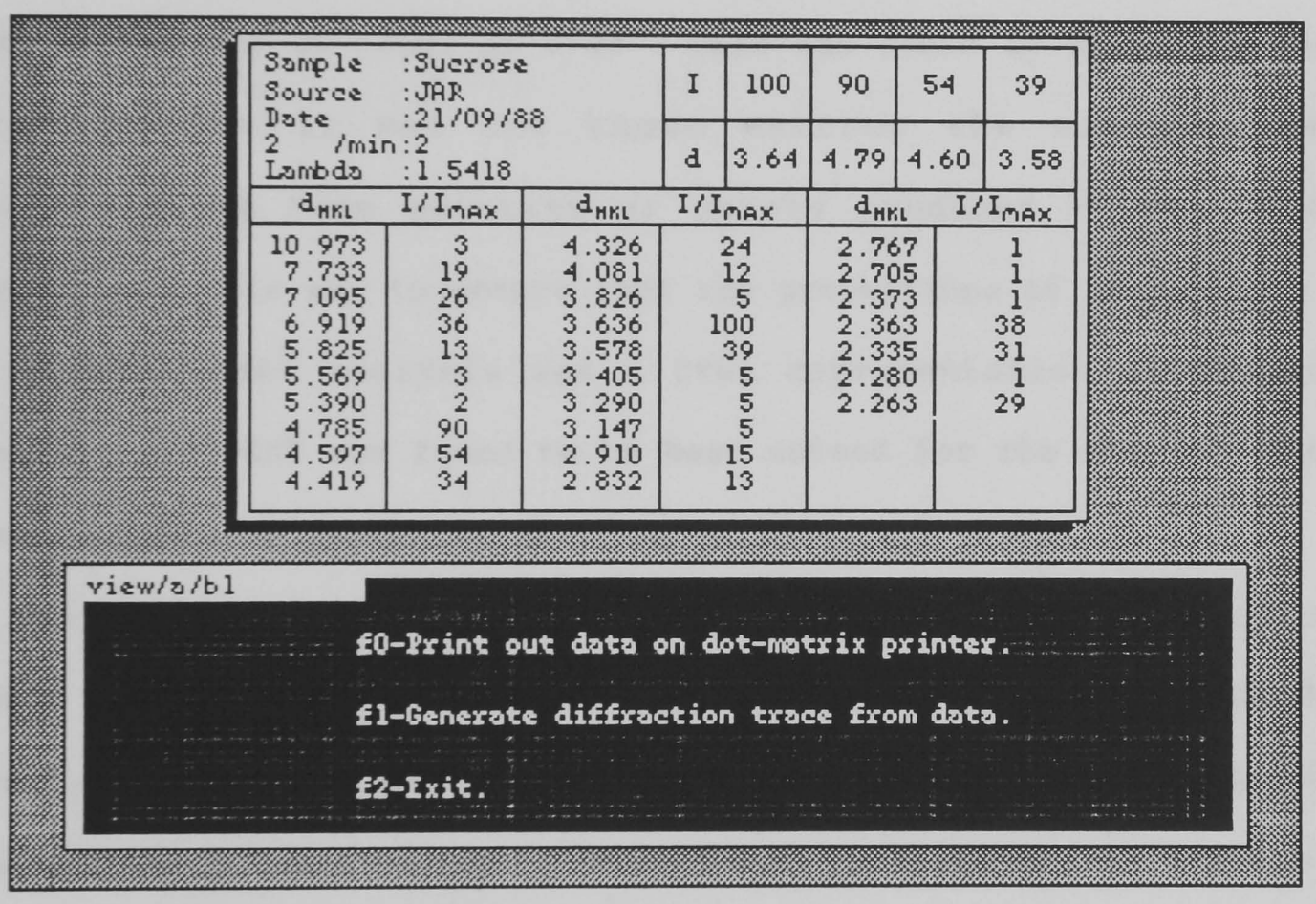

Figure 3.12 The presentation of diffraction data by CENPOD.

3.4.5 Qualitative multi-phase analysis

Two commercial pharmaceutical products REHIDRAT[55] and DIORALYTE[56] were selected for analysis. These are diuretic powders which contain simple sugars and salts, which exist in polycrystalline states. The

manufacturers stated dose of each of the chemical components for both products are listed in Table 3.2.

Table 3.2 Chemical compositions of Rehidrat and Dioralyte.

REHIDRAT		DIORALYTE	
compound	weight/g	compound	weight/g
sodium chloride	0.44	sodium chloride	0.2
potassium chloride	0.38	potassium chloride	0.3
sodium bicarbonate	0.42	sodium bicarbonate	0.3
citric acid	0.44	glucose	8.0
sugars	12.23		

Both samples were prepared in the manner previously discussed and scanned over the 2θ range of 5-45°. Care was taken to sieve the whole sample, since it was not known whether the mixtures were recrystallised from solution or merely produced by mixing dry ingredients. This was to ensure that the proportions of ingredients in the sample under analysis was a true representation of the bulk material. REHIDRAT was found to be best suited for the analysis since it was capable of producing numerous well defined peaks.

The auto-search routine revealed that the most probable match was either sucrose or dextrose anhydrous. It was noted that the matched peaks for both compounds related to independent peaks from the sample. On comparison of the original plots of sucrose and dextrose anhydrous, it was confirmed that both materials are present in the mixture. The other compounds in REHIDRAT were not detected by the first pass of the auto search routines, however by omitting the matched peaks from the sample file, the process was repeated and sodium chloride was eventually identified. The traces for REHIDRAT, sucrose, dextrose anhydrous and sodium chloride are plotted in Figure 3.13, with their

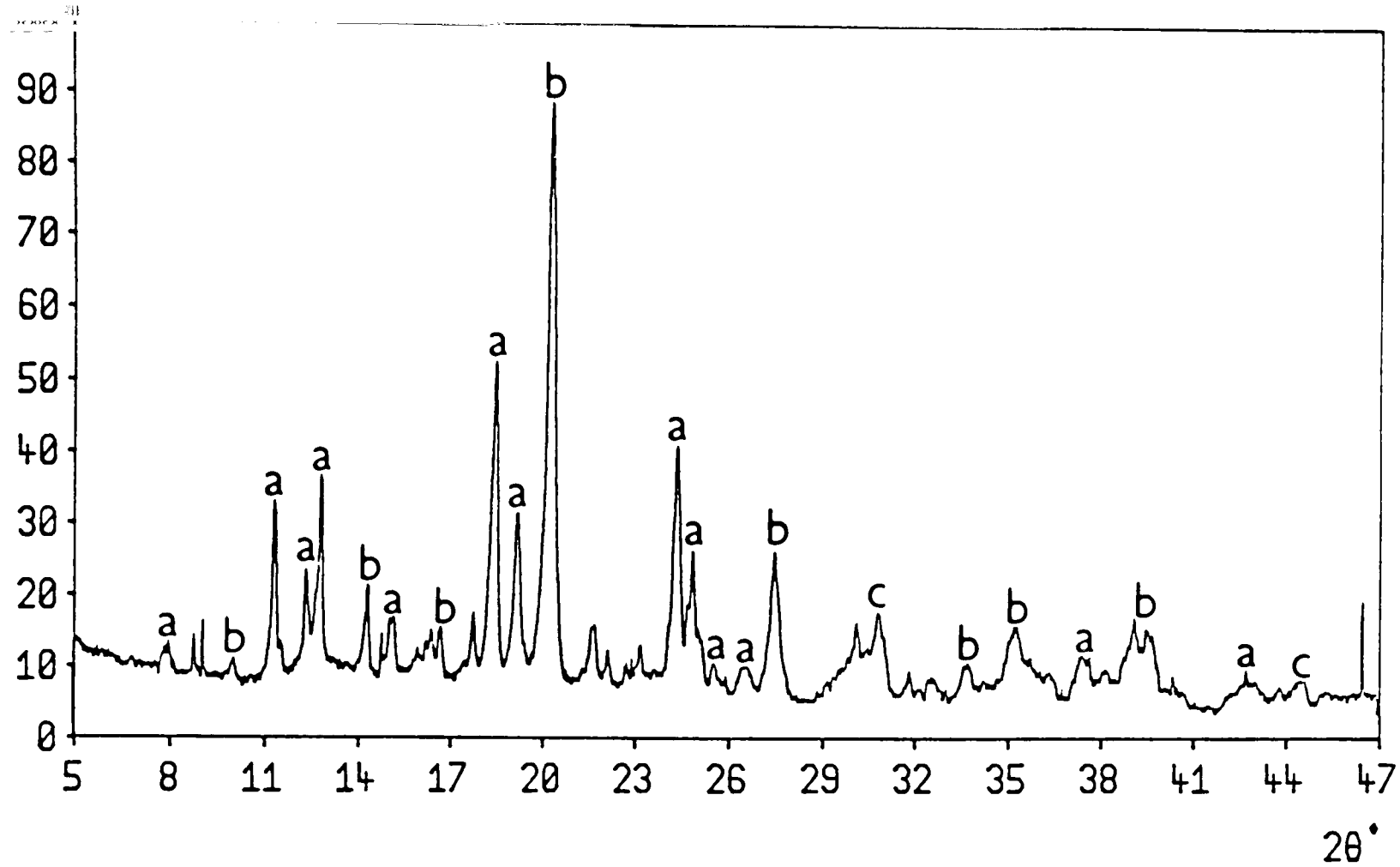

Figure 3.13(a) REHIDRAT. (**a**=sucrose, **b**=dextrose anhydrous & **c**=sodium chloride)

I

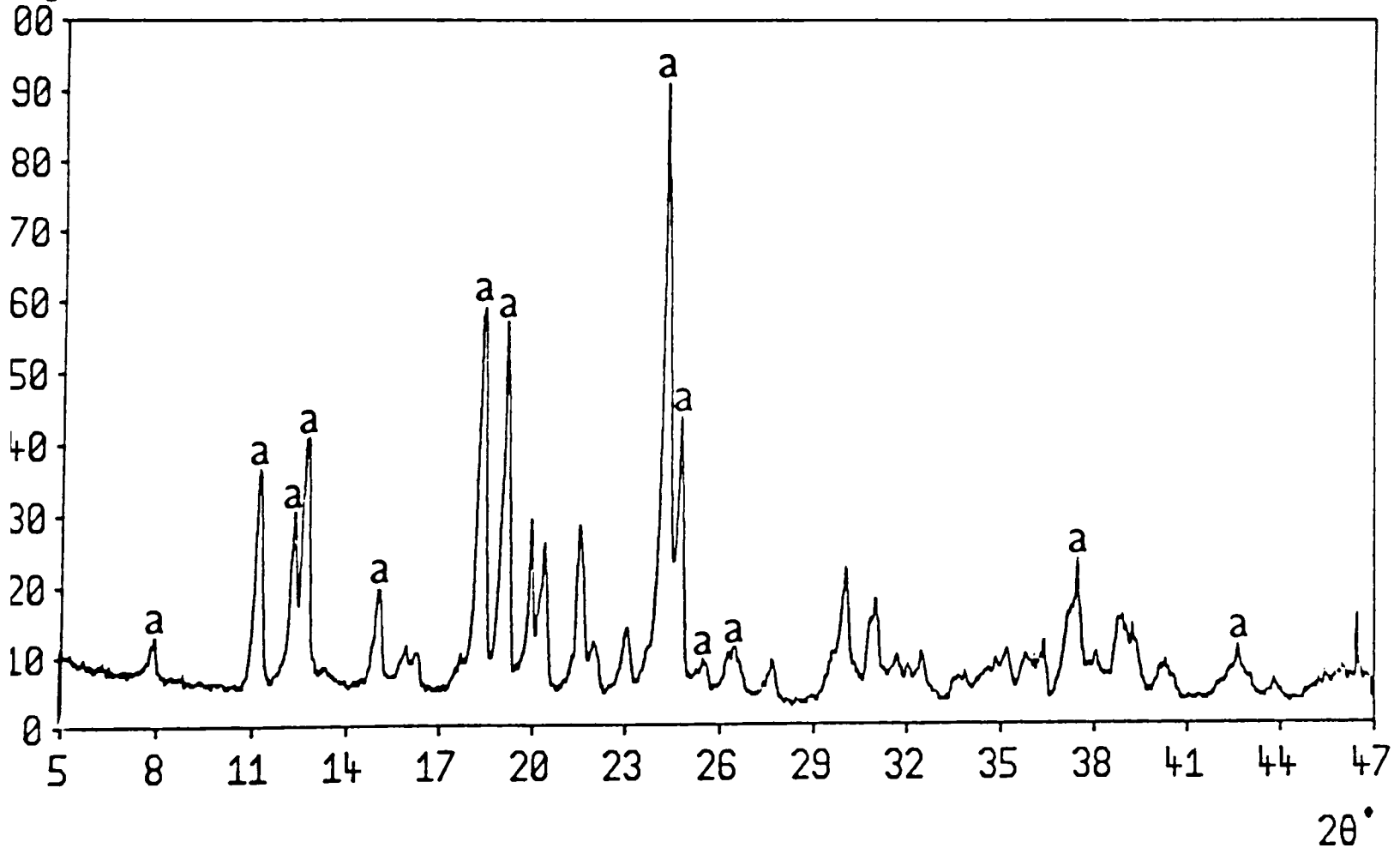

Figure 3.13(b) Sucrose.

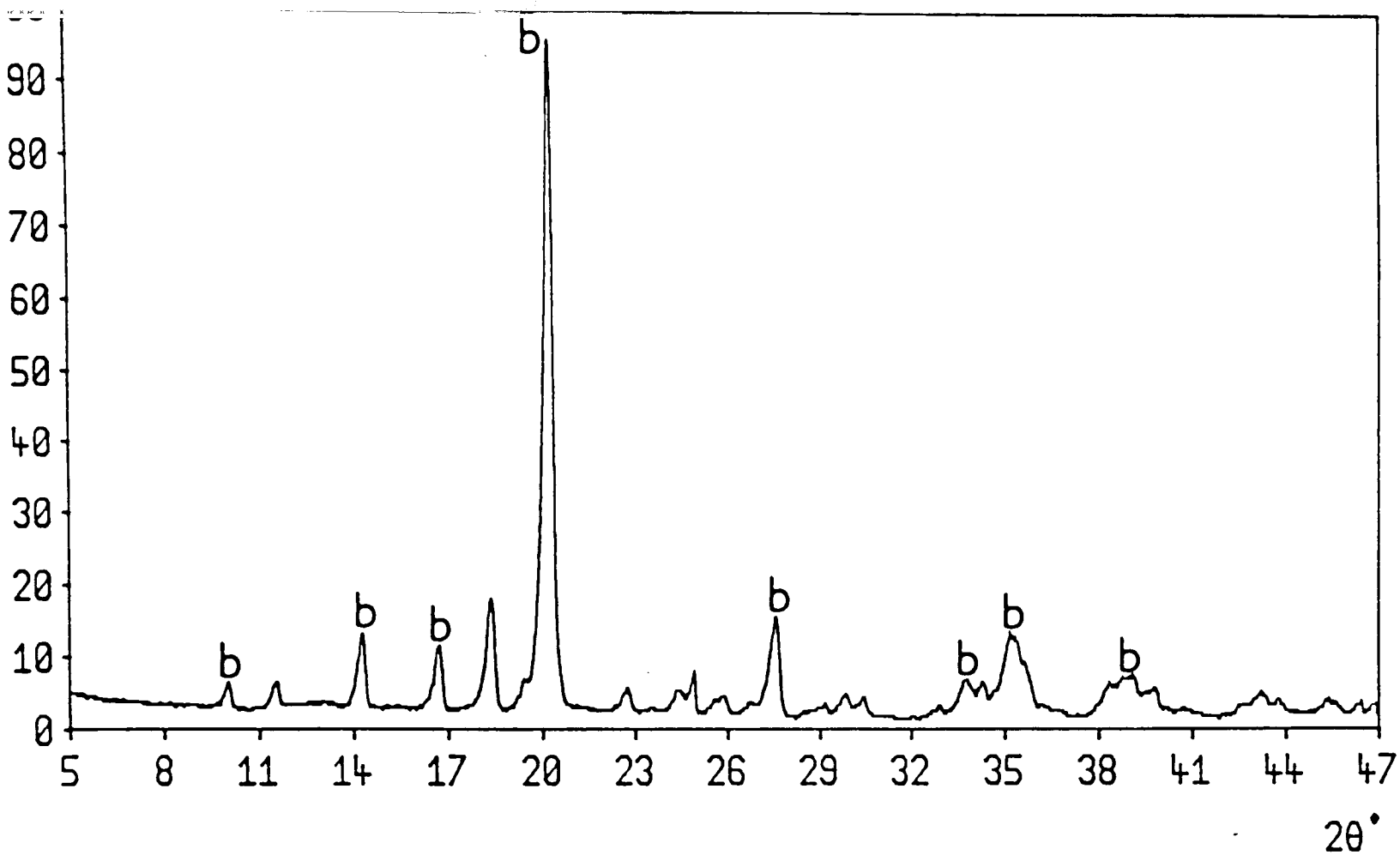

Figure 3.13(c) Dextrose anhydrous.

I

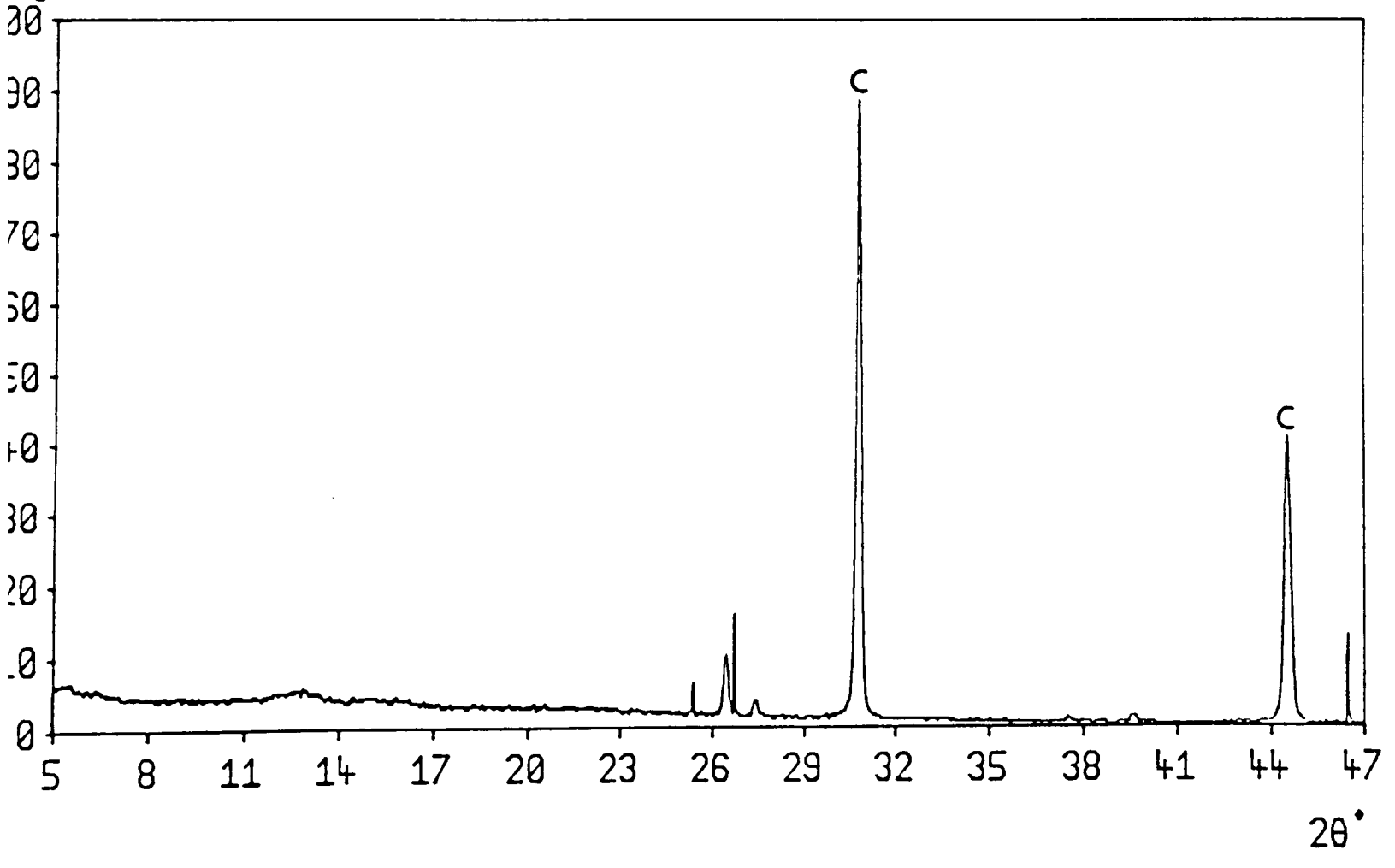

Figure 3.13(d) Sodium chloride.

contributing peaks marked for clarity.

This study has shown that the database package is capable of determining the components of a multi-phase sample. However it is not sensitive enough to detect the components in very small concentrations. Visual comparison of the traces for REHIDRAT and sucrose, indicate that the majority of the crystalline substance is indeed made up of sucrose. However it is not possible to say exactly what proportion of the mixture is sucrose using these methods.

3.4.6 Quantitative multi-phase analysis

The previous study was concerned only with identifying the components of a multiphase mixture. This prompted the question of whether quantitative analysis could be successfully achieved on simple two phase compounds.

The established method of producing a calibration graph from the relative intensities of two phase compounds with known concentrations was adopted[57-61]. Sodium chloride and potassium chloride were selected for the investigation. Both compounds readily crystallise in the same high symmetry cubic space group with high peak multiplicity, ensuring few significant overlapping peaks.

A selection of powders were produced from recrystallised infusion solutions with a constant %w/v of NaCl and varying %w/v of KCl. Samples of pure NaCl and KCl were scanned individually to determine the positions of suitable peaks for measurement. Fortunately, the most intense peaks for both compounds fell in the 2θ range of 26-33°. Each of the multiphase samples were scanned five times over this 2θ range. The superimposed traces are shown in Figure 3.14. The intensities of the KCl and NaCl peaks were measured and expressed as a ratio. The

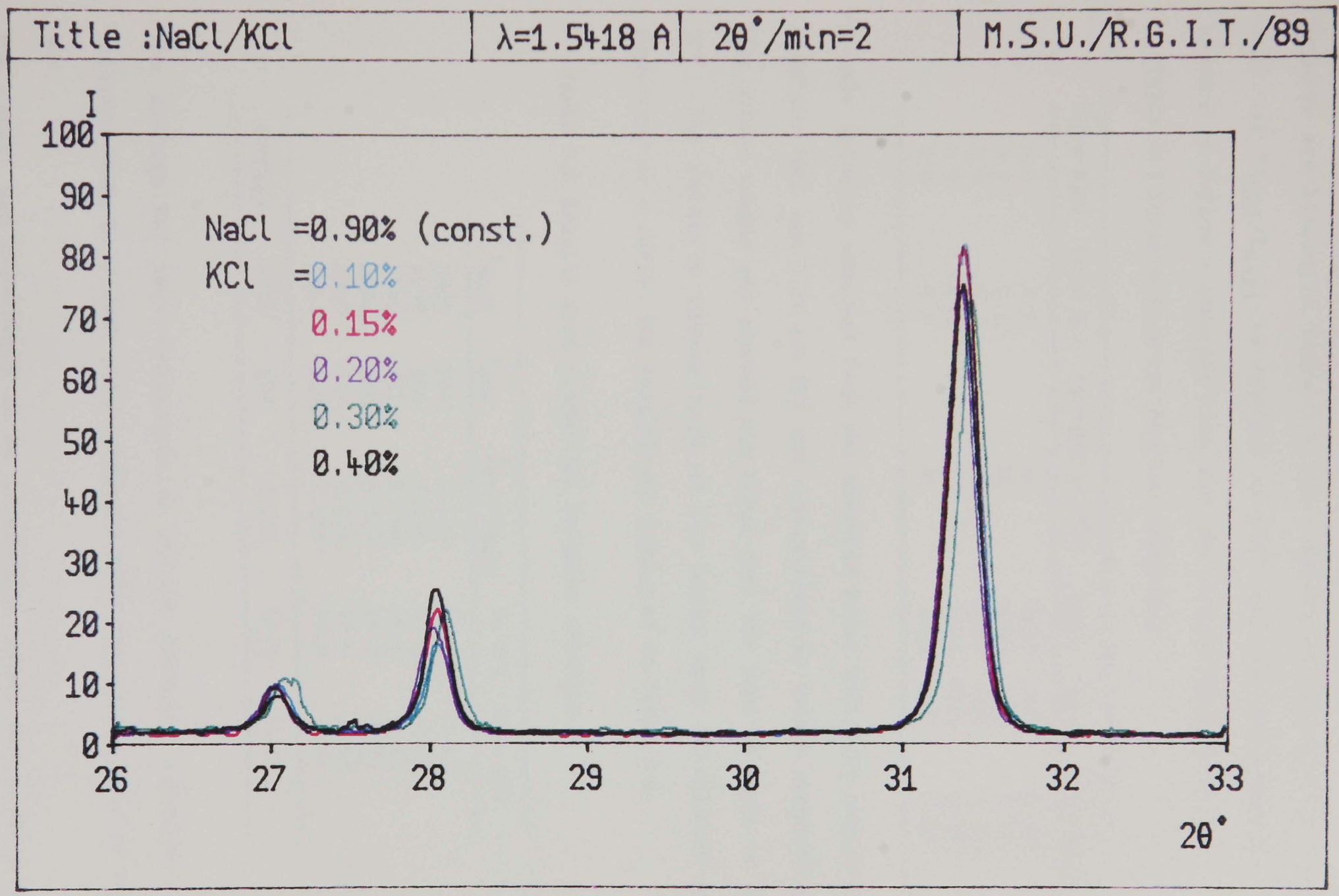

Figure 3.14 Superimposed plots of KCl/NaCl mixtures with constant NaCl.

results are listed in Table 3.3. The results are plotted in Figure 3.15. as "I_{KCl}/I_{NaCl} vs %weight of KCL" and the relationship was assumed to follow a straight line over the narrow range of values.

Table 3.3 Results from calibration experiment.

%w/v NaCl	%w/v KCl	%weight of KCl	I_{NaCl}	I_{KCl}	I_{KCl}/I_{NaCl}
0.9	0.1	10	4585	463	0.101
0.9	0.15	14	4087	513	0.126
0.9	0.2	18	3789	938	0.248
0.9	0.3	25	3673	1219	0.332
0.9	0.4	31	3312	1235	0.373

A salt infusion obtained from the Aberdeen Royal Infirmary containing 0.9% w/v NaCl and 0.2% w/v KCl was crystallised by rotary evaporation. The powder sample was scanned six times over the same 2θ range of 26-33°. The relative intensities of the peaks were calculated and expressed as a ratio. The results are tabulated in Table 3.4.

Table 3.4 Results from commercial infusion solution.

	I_{NaCl}	I_{KCl}	I_{KCl}/I_{NaCl}	%w KCl	%w/v KCl
	3889	594	0.153	19.3	0.22
	4249	666	0.156	19.6	0.22
	4194	621	0.148	18.8	0.21
	3494	536	0.153	19.3	0.22
	4040	621	0.154	19.4	0.22
	4242	635	0.150	19.0	0.21
Average	4018	612	0.152	19.2	0.216

The average KCl %w/v concentration of the infusion solution was calculated to be 0.216% which compares with the quoted dose of 0.2% w/v.

The result was considered to be favourable, since the problem was simplified by assuming a straight line relationship. The accuracy

could be further improved if a greater number of samples were prepared covering the entire range of possible concentrations and a establishing a polynomial relationship to describe the curve.

The quantitative and qualitative studies were performed in association with final year Pharmacy students. These projects were intended to test the software and to develop new facilities.

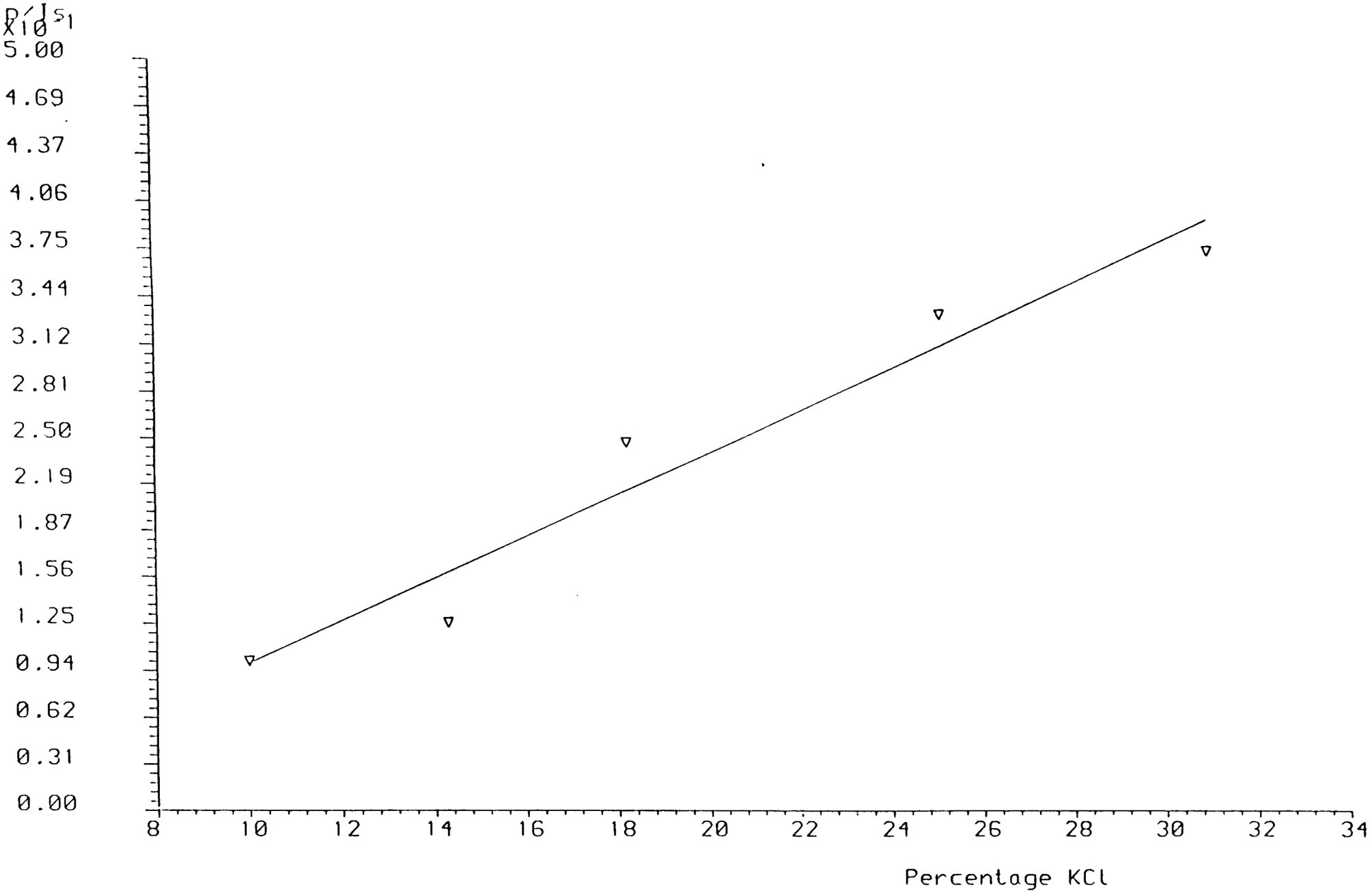

Figure 3.15 'I_{KCl}/I_{NaCl} vs %weight KCl' calibration plot. (y= 0.01x - 0.04)

Chapter 4. Enhanced single crystal diffractometer and applications.

4.1 Introduction

This instrument was previously enhanced by Dr I.T.Liddell incorporating the use of a microcomputer to store the diffraction data. It was proposed to develop the software further to deal with systematic absences therefore reducing the time for data collection. Furthermore a data set was to be collected on a crystal of 4,6,O-benzylidene-3-deoxy-3-triphenyl-tin-alpha-d-altropyranoside, $C_{32}H_{32}O_5Sn$, the structure of which had been previously solved[62]. The analysis of $C_{32}H_{32}O_5Sn$ was intended to develop practical experience with data collection techniques in association with the other diffractometers utilised in the research. A schematic diagram of the molecule (excluding H atoms) is shown in Figure 4.1.

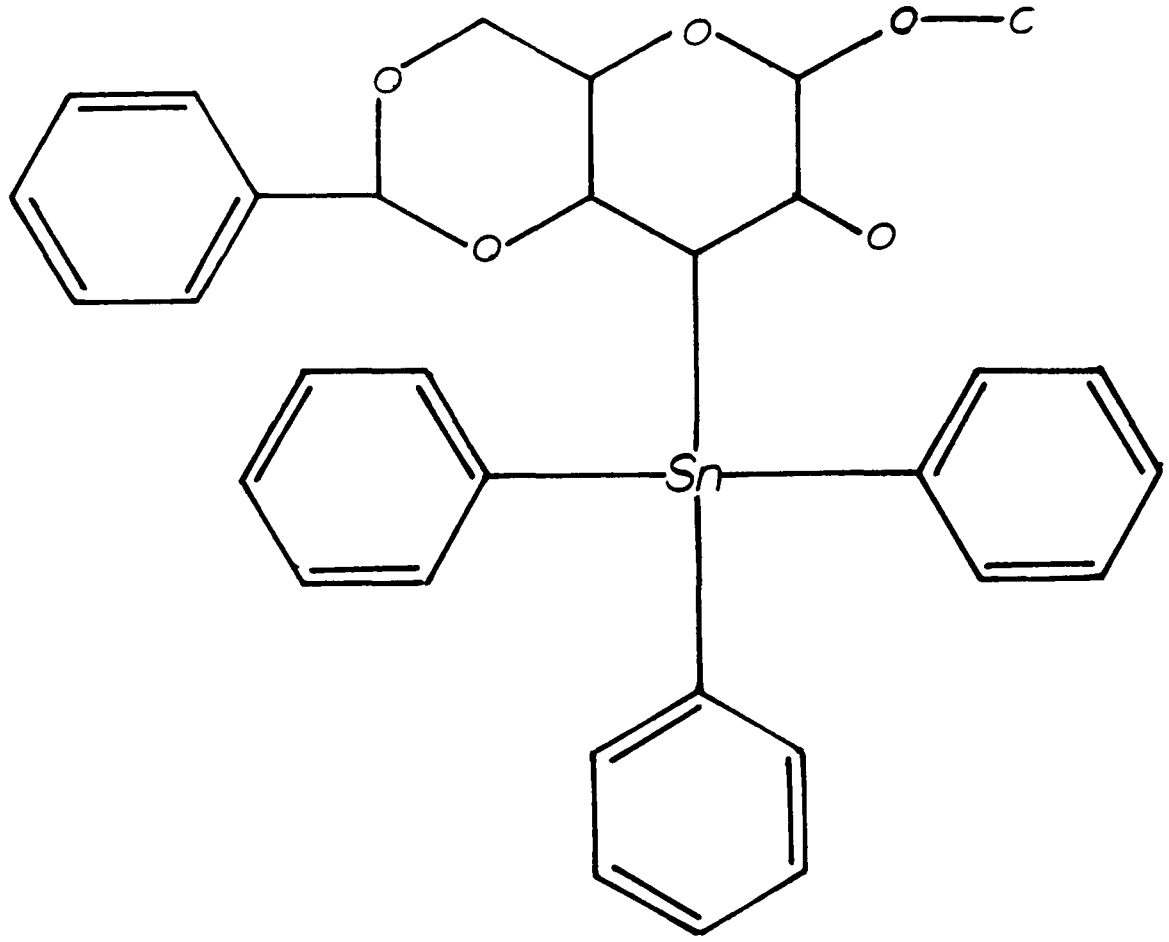

Figure 4.1 A schematic diagram of $C_{32}H_{32}O_5Sn$.

Unfortunately the quality of the Mo X-ray tube fitted to the instrument began to deteriorate to the extent that poor counting statistics were experienced. Therefore the quality of the data was subject to significant error. This event prompted a reappraisal of this particular aspect of the research and so no further instrument development was performed. What therefore follows is an account of the data collection process and a brief examination of the experimental data.

4.2 Instrument enhancement

The Stoe Stadi-2 two circle single crystal diffractometer, requires the external facilities of a DEC PDP8/II computer system to control the motor servos and to quantise the diffracted intensities. The computer was initially accessed through a simple terminal via a serial data line, which was used to issue simple commands. The dumb terminal was replaced by a BBC master microcomputer, which performed the same task. However, the additional processing power of the micro enabled more sophisticated procedures to be activated.

The original system utilised a paper tape streamer to read programs and to down load diffraction intensities. The BBC was used to transfer the control programs via the RS432 serial port and to relay any output to a magnetic disc storage device. This was far more reliable and convenient than the conventional paper tape.

The addition of the computer console permitted far more flexible operation of the instrument, and so greatly reducing the amount of labour expended in the process of mounting and aligning a crystal sample.

4.3 Data collection of $C_{32}H_{32}O_5Sn$

The selected crystal had dimensions of approximately 1.5 x 1 x 0.25 mm^3, which was initially recognised as being larger than is normally used for X-ray diffraction methods. This however was regarded as the best crystal from the comparatively restricted choice of crystals. The initial rotation photographs and zero order Weissenberg photographs indicated that the reflexions were well defined and relatively intense. In particular the (200), (204) and (104) were very strong. However the absolute centring of the crystal proved to be less convincing of crystal quality.

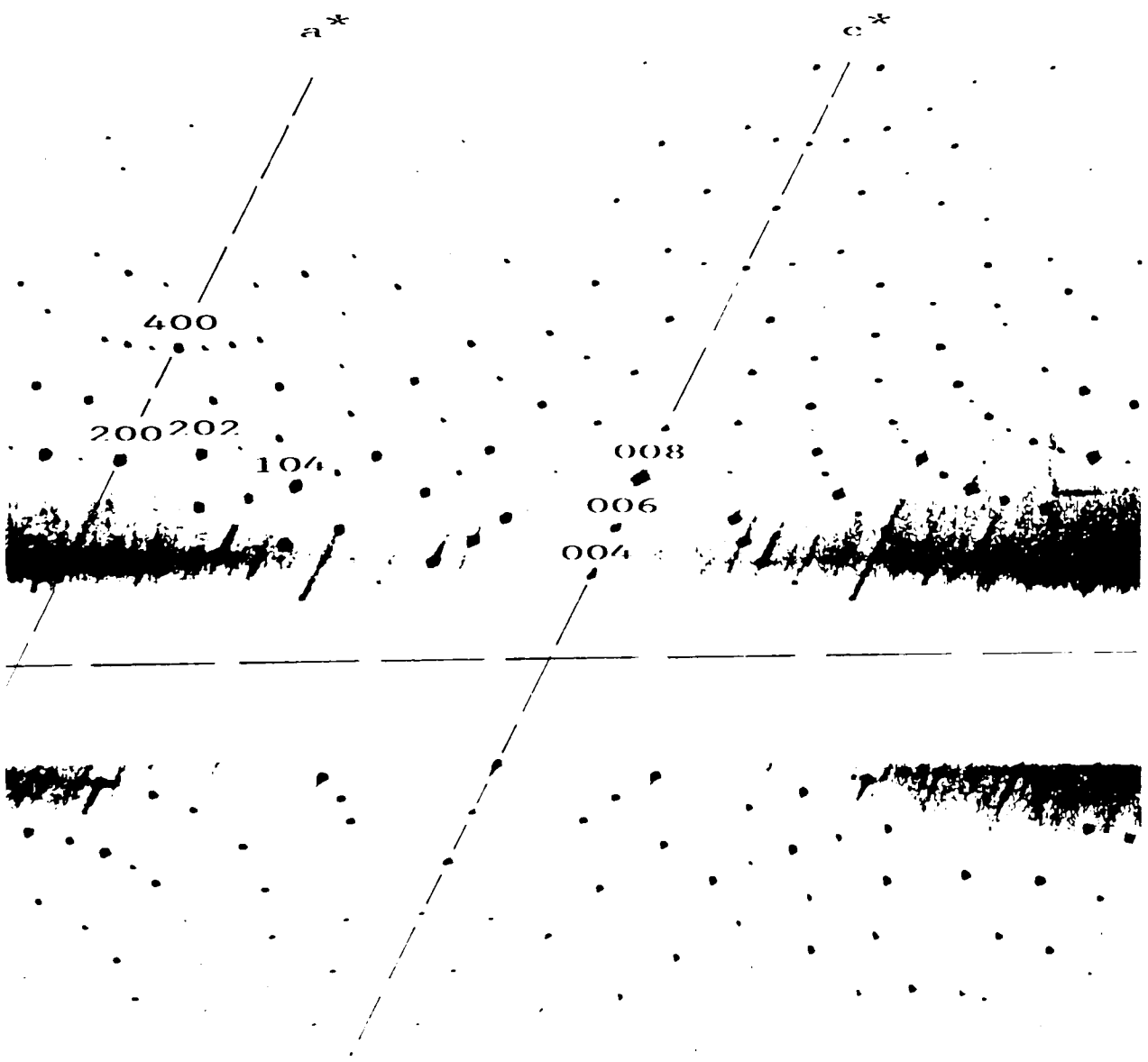

Figure 4.2 The zero order Weissenberg photograph.

The crystal was mounted about with the b-axis parallel to the ω axis of the diffractometer. The (0n0) reflexions were examined for suitability for crystal alignment; where n represents even integers. The (060) reflexion was selected as being the most suitable for the centring process since the (020) and (040) reflexions were virtually undetectable. The process of centring the crystal discussed in section 2.5.4 was performed. On a complete ω rotation there was a significant variation in diffracted intensity. This is shown in the plot in Figure 4.3 where the ω value relates to an arbitrary crystal orientation. The intensity characteristic appears to follow a sinusoidal function with the maximum peak intensities appearing 180° apart. This indicated that either the crystal was still incorrectly aligned or indeed that the X-rays were attenuated by the crystal. The very regular shape of the crystal suggested that the latter was more plausible. At this stage it was noted that the large degree of scatter was due to a degradation of tube quality.

Despite these setbacks, the computer was instructed to measure reflexions layer by layer, as $\omega/2\theta$ scans, over the range of **hkl** ; $0 \leq \mathbf{h} \leq 10$, $0 \leq \mathbf{k} \leq 13$, $0 \leq \mathbf{l} \leq 24$ with $2\theta_{max}=60^{\circ}$. A total of 2127 unique reflexions were measured. The individual layer data sets were combined into one overall file which was transferred to the Honeywell mainframe using the KERMIT file transfer protocol. The intensities were converted to structure factor amplitudes by DATRN[63], with corrections being applied for Lorentz/Polarisation effects. At this stage no absorption correction was performed.

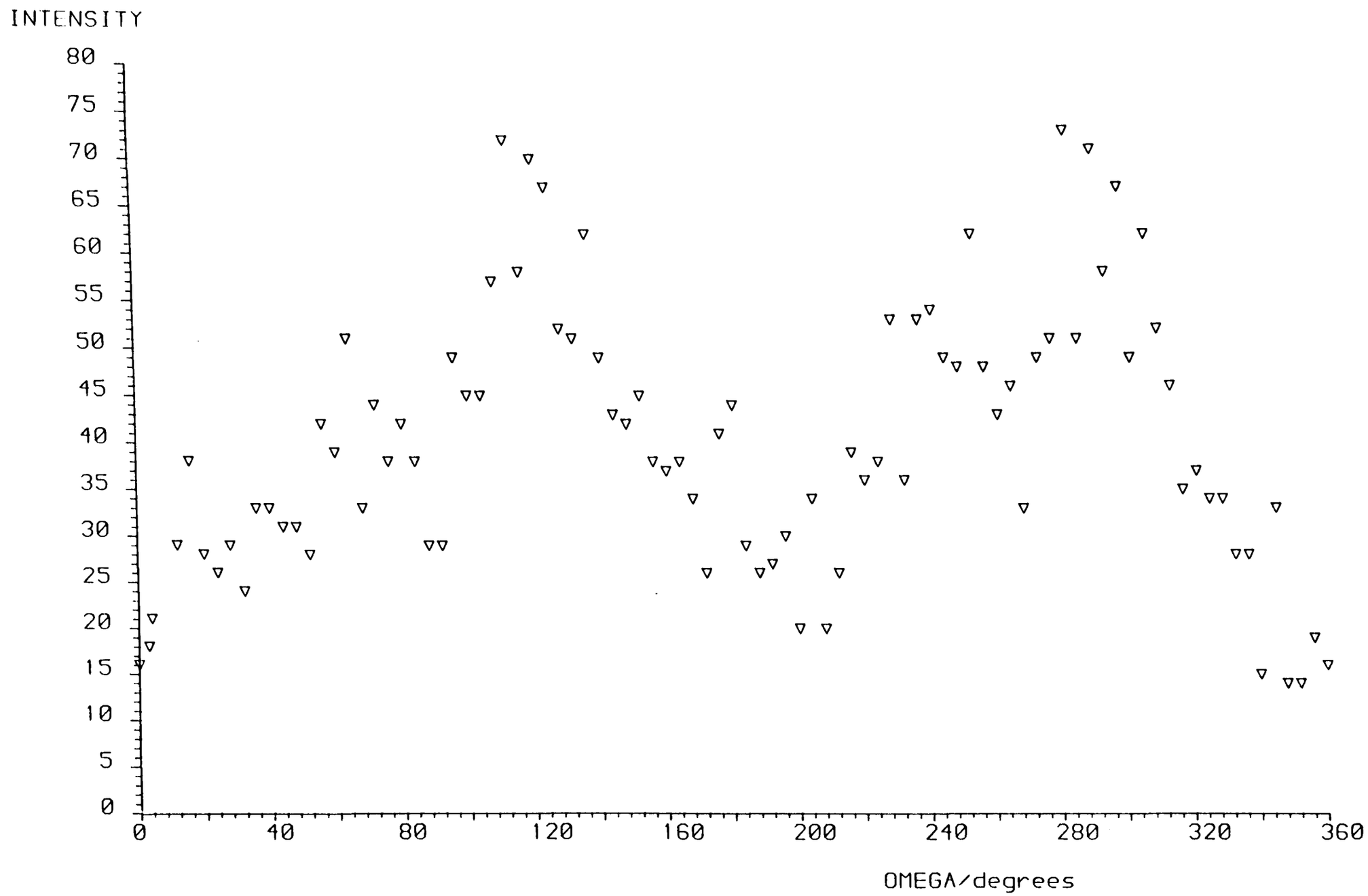

Figure 4.3 The intensity variation for the (060) reflexion through a complete ω-scan on the STADI-2 2C-SXD. The two maxima are separated by 180°.

4.4 Results

4.4.1 Crystal Data

$C_{32}H_{32}O_5Sn$, M_r=615.31, orthorhombic, $P2_12_12_1$, **a**=9.84(2), **b**=13.73(5), **c**=21.20(2) Å, **V**=2861(12) Å^3, **Z**=4, D_x=1.39 gcm^{-3}, Mo **Kα**, **λ**=0.71069 Å, **μ**=8.40 cm^{-1}, **F(000)**=1256, **T**=293 K, **R**=0.24 for 1707 unique reflexions.

4.4.2 Structure refinement

The atomic coordinates of the solved structure were used as an initial starting point for the refinement process, using SHELX-76[64]. The data used for the refinement was restricted to a limited set of 1707 reflexions with $F<\sigma(F)$. During the refinement the structure was unstable and atomic coordinates varied in the second decimal place. The best residual of 0.2762 was achieved. At this stage it was recognised that the quality of the data was unsuitable for further refinement.

A simple absorption correction was attempted to help produce a improved fit between observed and calculated structure factors. Using the basic sawtooth relationship of the ω scan, the reflexions were scaled based on the ω value at which the reflexions were measured. This had little overall effect on the final residual value of R=0.24. $\Delta\rho_{max}$=6.8 eÅ^{-1} and $\Delta\rho_{min}$=-6.1 eÅ^{-1}.

4.5 Discussion

Clearly the objectives of this study were not fully achieved. The combination of the oversized crystal and of the failing X-ray tube made it impossible to extract sufficient volumes of reliable data. There is still a little uncertainty over the absolute centring of the crystal, which was essential for successful data collection. Given the weak beam, it was not possible to conclusively say that the crystal

was perfectly aligned.

However, the process of solving the structure was purely academic. The process of selecting the crystal, orientating it by Weissenberg photographic methods and finally collecting a full data set, gave valuable 'hands on' experience with single crystal diffraction techniques. It also contrasted the levels of sophistication of the other single crystal instruments used in other areas of the research. That is not to say that excellent results will always be achieved on these instruments if in the first place the crystal quality is unsuitable.

The two circle diffractometer can still be regarded as a instrument capable of resolving structures with comparable accuracy of the present fully automated four circle diffractometers. The additional degrees of freedom gained with more modern instruments simply allow faster operation and places less emphasis on the initial crystal orientation.

The microcomputer enhancement has extended the lifetime of this instrument incorporating a magnetic data storage device. The data are now more transportable allowing a variety of software packages to be employed for structure solution. The software could be further improved by incorporating a least squares routine for cell parameter refinement and a data base of space group absences. This would bring the diffractometer closer to the integrated systems which are currently available.

CHAPTER 5. Qualitative analysis of thio-bis[triphenyltin(IV)], $C_{36}H_{30}SSn_2$, using high resolution powder diffraction.

5.1 Introduction

Thio-bis[triphenyltin(IV), $C_{36}H_{30}Sn_2S$ is an organometallic compound of known structure, solved by conventional single crystal X-ray methods[65]. A schematic diagram of the molecule is shown in Figure 5.1. The original structure solution was based on data collected from a Stoe Stadi-2 two circle diffractometer with Mo Kα X-rays in a $\omega/2\theta$ mode.

In this study the material was used to compare and contrast the levels of crystalline information available from a selection of powder diffractometers. The diffractometers ranged in sophistication from the basic LRPD , to the high resolution powder diffractometer instrument of station 9.1 at the SRS facility, both of which were discussed in Chapters 2 and 3. Emphasis was placed on the possibility of using powder data for structure solution and refinement.

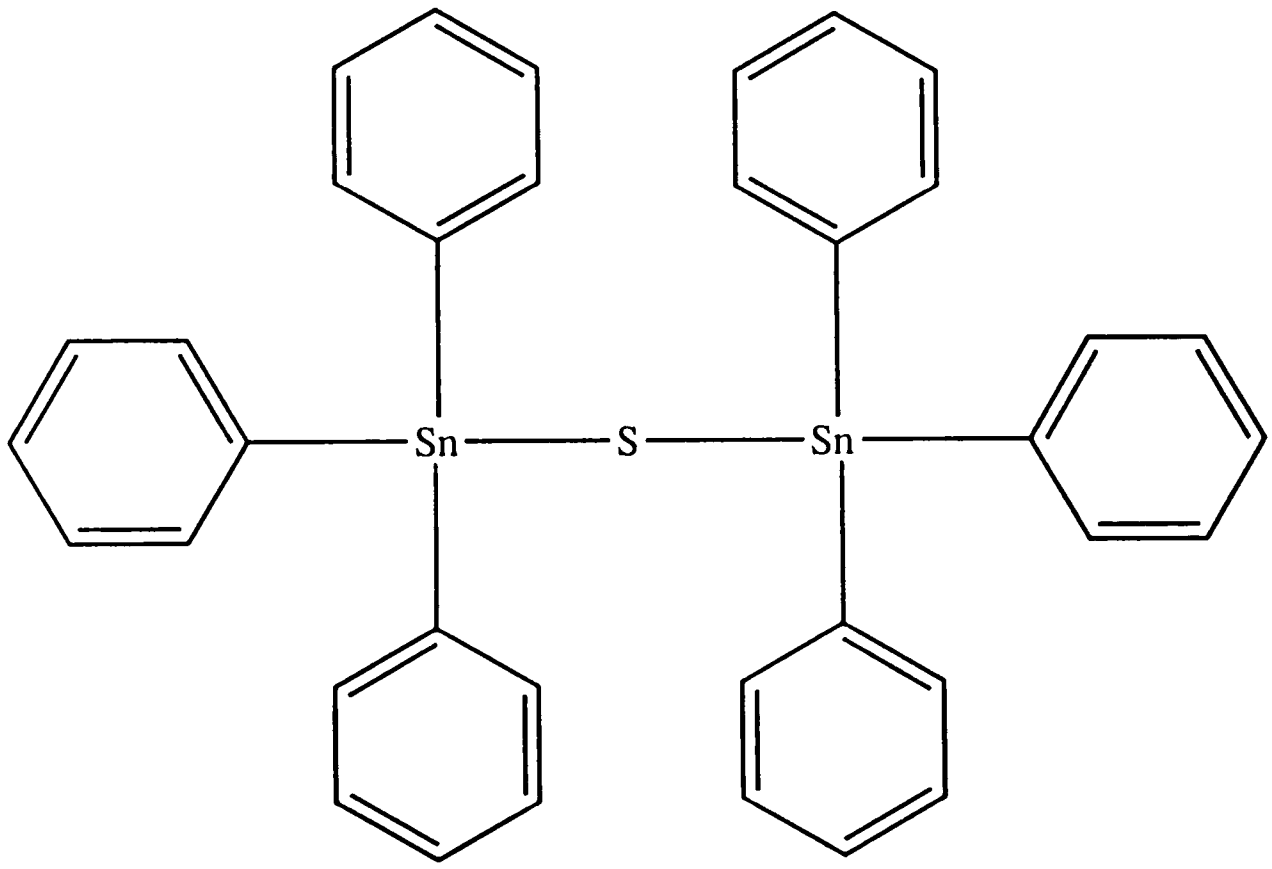

Figure 5.1 A schematic diagram of $C_{36}H_{30}Sn_2S$.

5.2 Data collection

A trace was collected on the LRPD at RGIT over the 2θ range 5-105°, with λ=1.5418 Å, to ascertain the 'useful' range of information. The trace indicated a high level of crystallinity with the majority of the scattering occurring in the low 2θ region. The same material was scanned over the 2θ range of 5-50° on the SRS high resolution powder diffractometer at the selected wavelength of λ=1.6008 Å.

To contrast the apparent high quality results from the SRS diffractometer, the sample was also run on POLARIS[66], a medium resolution high count neutron powder diffractometer also situated at RAL. It was anticipated that by using a neutron source more information relating to the lighter atoms' scattering contributions could be extracted from the sample. However, the level of information returned was poor both in the low angle and back scattering modes. The strong incoherent scattering of the H atoms prevented any useful structural information from being gathered.

5.3 Results

5.3.1 X-ray data

Thio-bis[triphenyltin(IV)], $C_{36}H_{30}Sn_2S$, M_r=732.08, orthorhombic, $P2_12_12_1$ (no.19), **a**=18.469(5), **b**=17.648(5), **c**=9.848(6) Å, **V**=3209.87 Å^3, **Z**=4, D_x=1.515 gcm^{-3}, **λ**=1.6008 Å.

5.3.2 Trace analysis

5.3.2.1 LRPD

The trace shown in Figure 5.2 represents a typical plot for a highly crystalline material on a low resolution instrument. The trace has been smoothed in an attempt to reduce the level of spurious scattering. The major peaks are well defined, but the less intense

peaks are still masked by the background noise. At the higher 2θ values, the peaks overlap, making the process of resolving them virtually impossible.

No further information could be extracted from the trace with the level of sophistication of the CENPOD software. However, the trace does manage to confirm the crystalline quality of the material, which was essential for the higher resolution analysis.

5.3.2.2 SRS, Daresbury.

The SRS trace shown in Figure 5.3 reveals a great deal of information, albeit in a one dimensional form. This represents a dramatic visible improvement on the LRPD trace. The trace has an excellent signal to noise ratio enabling all but the very weak peaks to identified.

The peaks have been described by a Voigt function which are essentially symmetric in form[67]. This is generally the case over the 2θ range of 30-130°. The plot in Figure 5.4 shows the observed and calculated line profiles over the 2θ range of 7-19°, which seem to be in good agreement. The high photon flux of the synchrotron ensures high count rates for crystalline materials, therefore ensuring reliable intensities, whilst retaining narrow peak widths.

Despite the high quality of the experimental data, there are too few peaks to gain further structural information with the reliability of a single crystal analysis performed with over 1000 unique reflexions. There were however, sufficient reflexions to index the trace and extract peak intensities. The significant structure factor amplitudes and standard deviations are listed in Table 5.1.

Table 5.1 Structure factors for significant reflexions.

h	k	l	$\|F_{hkl}\|$	$\sigma(F_{hkl})$	h	k	l	$\|F_{hkl}\|$	$\sigma(F_{hkl})$
1	1	0	2016.7	75.4	1	2	1	3779.8	139.1
2	0	0	47420.3	576.7	3	1	0	3772.7	229.1
0	2	0	12892.7	340.8	1	3	0	12649.3	386.9
1	0	1	1395.2	103.6	2	2	1	18759.7	325.9
0	1	1	7359.4	184.6	3	0	1	11395.8	413.9
1	1	1	53572.7	488.5	3	2	0	2959.3	732.9
2	0	1	7227.7	240.9	0	3	1	1020.9	714.0
0	2	1	14717.3	334.3	2	3	0	984.9	227.8
2	2	0	6796.7	271.0	0	0	2	6829.1	596.5
2	1	1	33204.6	348.4	1	3	1	9484.6	269.8

5.3.2.3 POLARIS

The powder traces from POLARIS operating in both forward and back scattering modes, shown in Figures 5.5 and 5.6 respectively, indicated the high level of incoherent scattering due to the hydrogen atom presence. The forward scattering trace features several significant peaks but with irregular line profiles. These differ considerably from traces produced by inorganic compounds or those with deuterated hydrogens. The level and quality of the data presented in these traces is so poor that very little could be ascertained regarding the structure other than the obvious presence of hydrogens. The incoherent scattering could be avoided if the sample could be deuterated, which is normally the case for organic samples. In this case it would almost certainly be possible to collect a high quality trace suitable for structure refinement.

5.4 Discussion

It is clear from these results that, while the data obtainable even from the highest resolution synchrotron data are more limited than a good single crystal data set, there is in principle much information available. Unfortunately, in terms of augmenting good single crystal

X-ray work on the type of materials here, the synchrotron remains limited. In order to add extra information from the powder data to that already gained from the single crystal study, it is really necessary to find out more about the hydrogen atoms. Recourse to neutron diffraction is the obvious way to do this, and given the difficulty in obtaining single crystals of sufficient size to allow single crystal neutron diffraction to be performed, neutron powder would appear to have a role to play. Unfortunately as the POLARIS results have shown, there are severe problems in studying hydrogenous materials in this way, and the information can still remain obscured under such circumstances. The solution to the problems outlined in this comparative study are to prepare larger single crystals in order to use single crystal neutron diffraction, to deuterate the material to allow the use of high resolution powder diffraction, to perform a single crystal X-ray study at low temperature, all of which may to some extent improve the precision of the structure, including the hydrogen atoms.

From this study it has been shown that the SRS facility represents a truly exceptional instrument capable of resolving a vast number of peaks in a narrow 2θ range. Given the cost to run such a facility, it is not advisable to carry out day-to-day structure solutions using data from this instrument. Generally the basic structures of novel compounds are solved by means of single crystal studies providing the atomic coordinates as a starting point for further refinement, however as recent experiments have shown, *ab initio* structure solutions of small structures are possible[68]. This is seen as a growth area in crystallography. Clearly with the revived interest in powder

techniques, there will be an accelerated rate of development in both instrumentation and data processing methods, which will be later incorporated into commercially available machines.

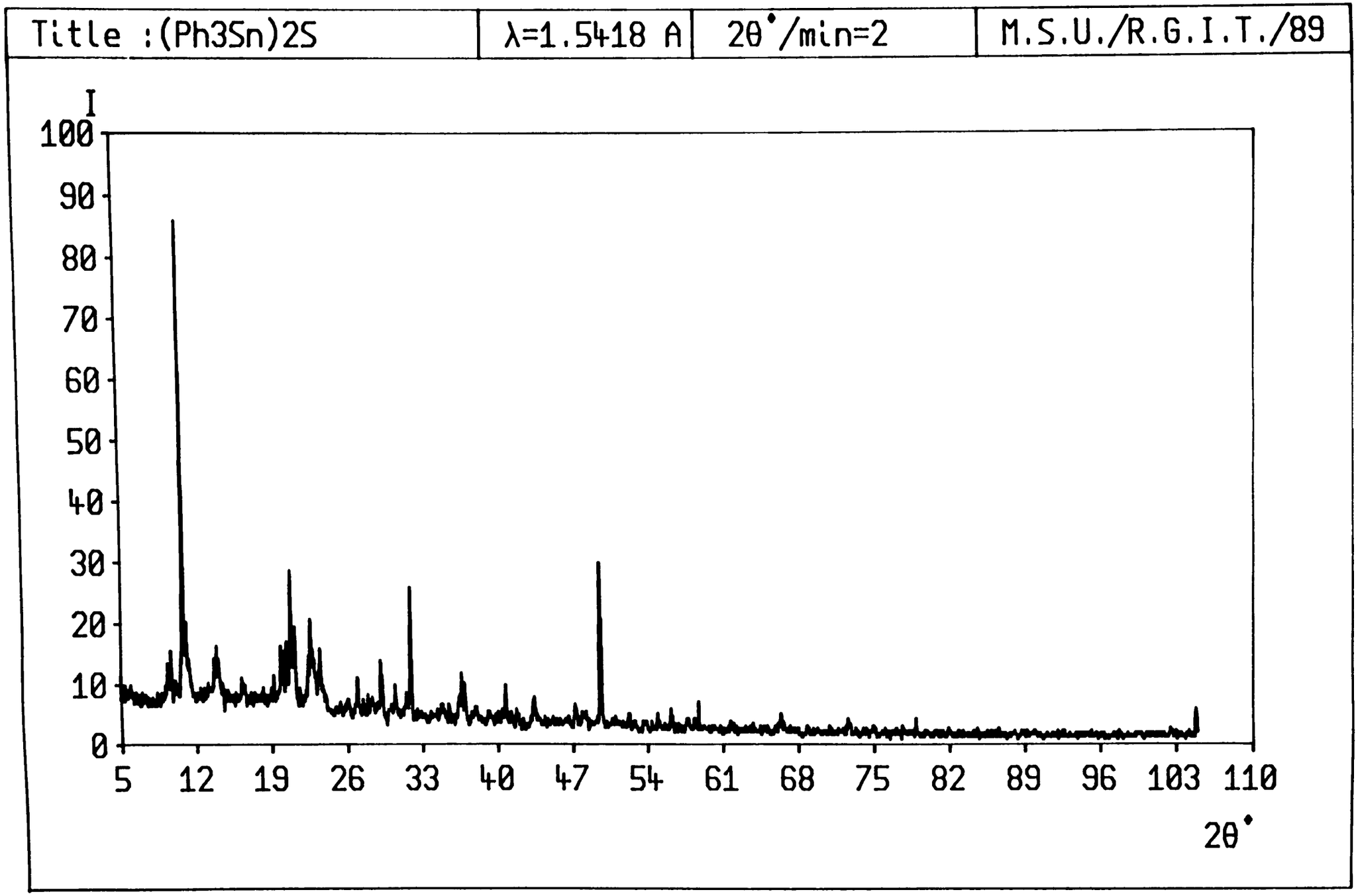

Figure 5.2 The powder trace of $C_{36}H_{30}Sn_2S$ over 2θ range 5-105°, produced by the LRPD.

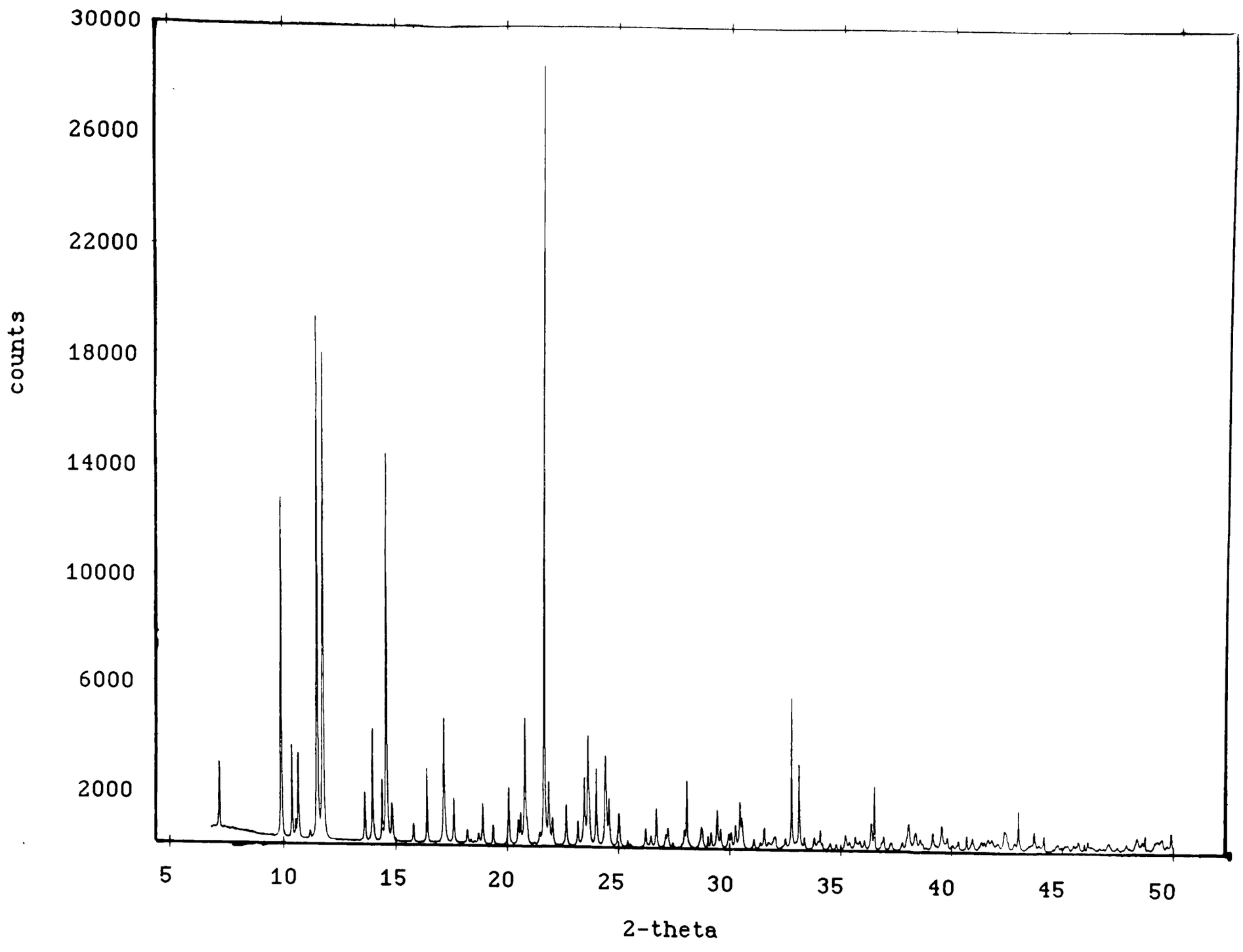

Figure 5.3 The high resolution trace of $C_{36}H_{30}Sn_2S$ over the 2θ range 5-50°, produced by station 9.1 at the SRS, Daresbury.

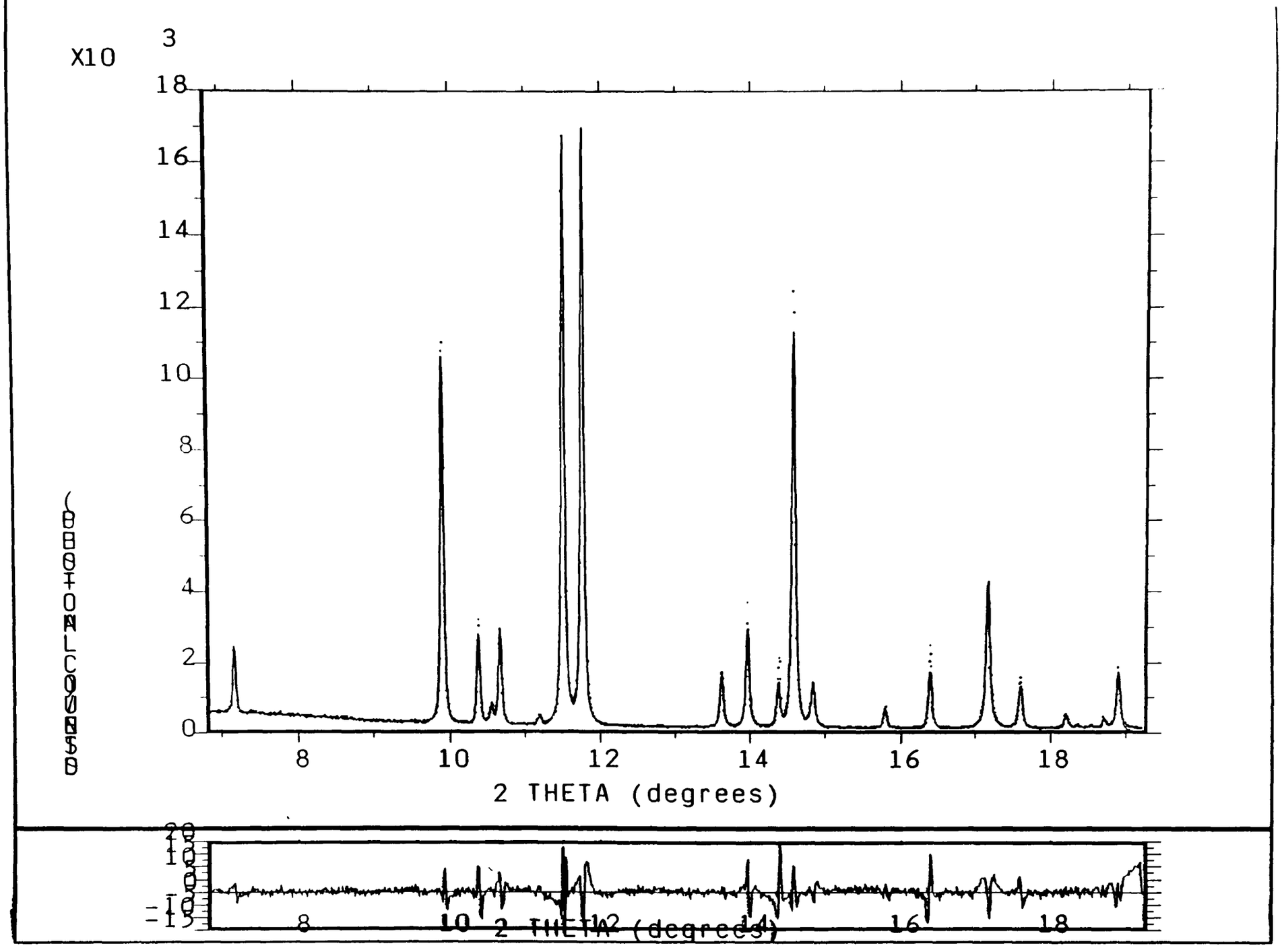

Figure 5.4 A condensed plot of the trace in Figure 5.3, with the profile fit included.

Figure 5.5 The medium resolution trace of $C_{36}H_{30}Sn_2S$ produced by POLARIS in the forward scattering mode.

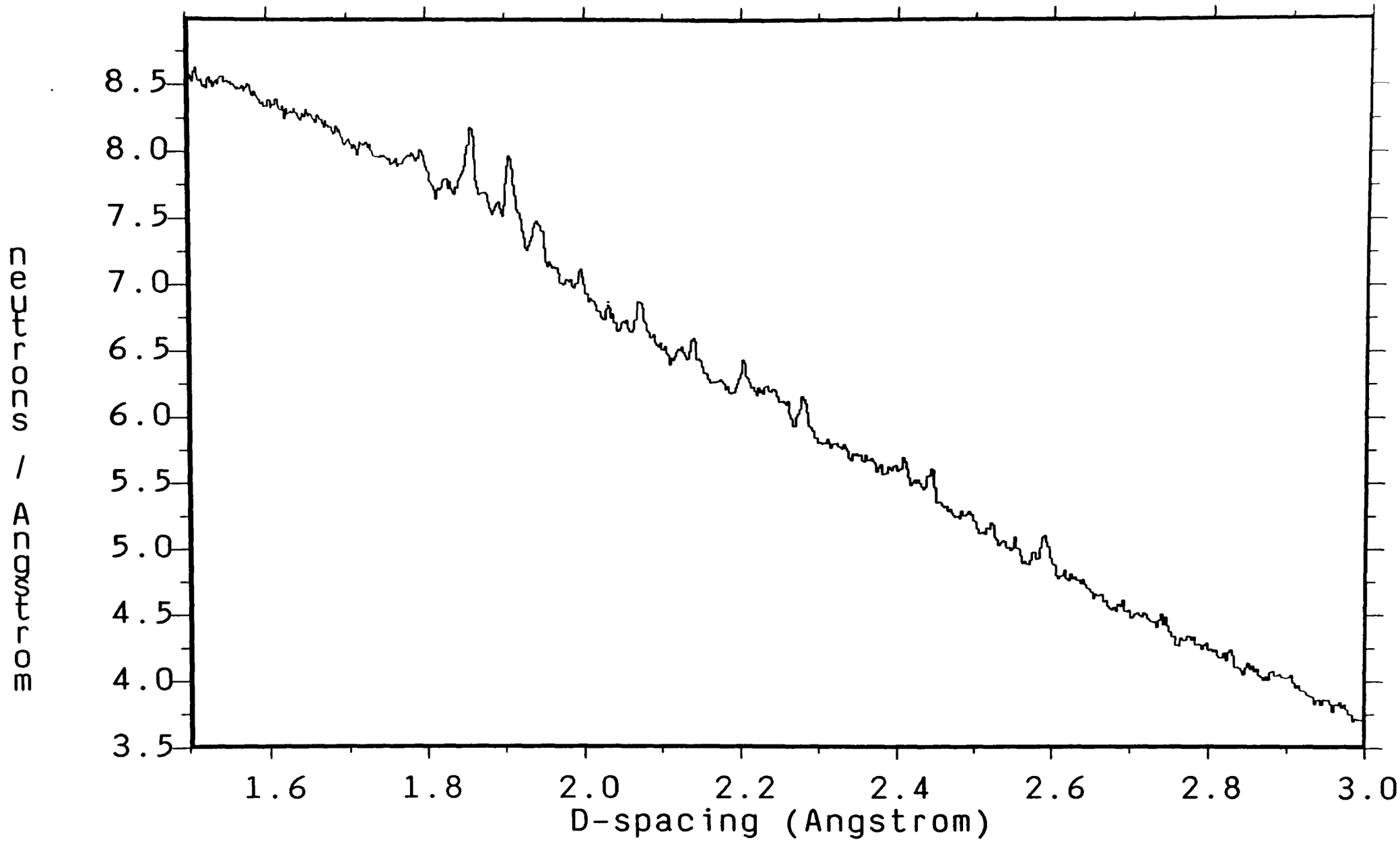

Figure 5.6 The medium resolution trace of $C_{36}H_{30}Sn_2S$ produced by POLARIS in the back scattering mode.

CHAPTER 6. X-ray crystal structure of 1a,2,3,7b-tetrahydro-1-phenyl-1H-cyclopropa[a]napthalene, $C_{17}H_{16}$.

6.1 Introduction

$C_{17}H_{16}$ is a steroid precursor currently being employed at Aberdeen University as a fundamental building block for steroid synthesis. To fully understand the synthetic processes involved in the development of steroids, using the precursor, the molecular arrangement of the compound was required. This compound has previously been the subject of a study using ultra-violet (UV) absorption techniques[69] and it was concluded that the molecule adopted the *trans* configuration. This was verified by comparisons with the UV spectrum belonging to that of *trans*-1,2-diphenylcyclopropane[70]. The UV study, however could not determine the atomic arrangement of the molecule. Thus a single crystal X-ray diffraction study was initiated to elaborate on the findings of the UV analysis.

The main feature of interest with the structure was the nature of the cyclopropyl ring (C(8)-C(9)-C(10)) and the relative position of the attached phenol ring.

6.2 Experimental

6.2.1 Data collection

The crystal used for the data collection was colourless with dimensions 0.5 x 0.4 x 0.2 mm^3. The approximate cell dimensions were determined with a Weissenberg camera using Cu Kα radiation. Diffraction data were collected on a Nicolet P3 automated 4C-SXD, using graphite monochromated Mo Kα radiation. The cell parameters were initially calculated from 12 independent reflexions with 2θ restricted to below 20°. More accurate measurements were performed at higher 2θ values. A total of 4183 unique reflexions were measured by $\theta/2\theta$ scans, with $2\theta_{max}<60^\circ$. The reflexions covered the **hkl** range; $-11 \leq \mathbf{h} \leq 11$,

$0 \leq \mathbf{k} \leq 11$, $0 \leq \mathbf{l} \leq 20$. During the data collection, two known strong reflexions were monitored periodically and no significant variation in intensity was detected. The data were corrected for Lorentz and polarisation effects. Absorption effects were considered to be negligible. After the data reduction process, 1710 reflexions were found to have $\mathbf{F}>5\sigma(\mathbf{F})$.

6.2.2 Structure solution and refinement

This compound represents a relatively simple organic compound with a commonly occurring space group. Given the light element composition of the precursor and the relatively small number of variables, Direct Methods was best suited for structure solution. With structures of this composition it is possible to fully establish correct phases for the experimental reflexions. The basic structure was solved using MITHRIL[71], giving an unambiguous projection of the molecule. The C atom positions were input to SHELX-76 for subsequent least squares refinement.

The basic structure was initially refined using full matrix least squares techniques with isotropic thermal parameters. Once the positional parameters had stabilised, the C atoms were permitted to refine with anisotropic parameters producing relatively spherical thermal ellipsoids.

A Fourier difference synthesis revealed all the H atom positions. All but three of the H atoms were however, placed in calculated positions and constrained to ride on their associated C atoms. This had the effect of reducing the number of variables involved in the least squares analysis. The cyclopropane H atoms were however permitted to refine freely as independent atoms, as their positions could not be

readily calculated. During the final cycles of refinement, the H atoms were assigned one overall isotropic thermal parameter, which proved satisfactory. The overall R factor for the stabilised model was 0.079. $\Delta/\sigma<0.01$, $\rho_{max}=0.3eÅ^{-3}$, $\rho_{min}=-0.3eÅ^{-3}$.

6.3 Results

6.3.1 Crystal and diffraction data

$C_{17}H_{16}$. $M_r=220.3$, monoclinic, $P2_1/c$ (no.14), $a=10.098(9)$, $b=11.315(10)$, $c=22.121(27)$ Å, $\beta=90.27(9)^\circ$, $V=2527.5Å^3$, $Z=8$, $D_x=1.16gcm^{-3}$, Mo $K\alpha$, $\lambda=0.71069$ Å, $\mu=0.32cm^{-1}$, $F(000)=944$, $T=293$ K, $R=0.079$ for 1710 observed reflexions.

6.3.2 Structure analysis

The basic asymmetric unit is composed of two whole molecules which have similar atomic arrangements in space. Figure 6.1 features a labelled ORTEP[72] plot showing the relative positioning of the two molecules. In both molecules the aromatic rings adopt the low energy *trans* configuration relative to the cyclopropane ring, with the torsion angles C(7)-C(8)-C(11)-C(12) equal to 146(1)°. The full list of C atom coordinates, thermal parameters, H atom coordinates, bond lengths, bond angles and torsion angles are listed in Tables 6.1, 6.2, 6.3, 6.4, 6.5 and 6.6 respectively.

The basic carbon-carbon bond lengths show an acceptable amount of deviation from the currently accepted values. The C(5)-C(10) bonds in molecules A and B have values 1.42(2) Å and 1.40(2) Å respectively. In the case of the bond in molecule A, the bond would appear to be a hybrid of a single bond and a double bond in terms of length. The two rings have undergone minor distortions to accommodate the intermediate bond. The bond angles around the two interconnecting rings are all

removed from the idealised angle of 120°. The largest deviations being C(6)-C(7)-C(8) at 112.9(7)° in molecule B and C(2)-C(1)-C(10) at 122.4(8)° in molecule A. Despite the geometrical distortions, the two rings remain fairly planar.

The cyclopropane ring was found to exist as an equilateral triangle, with an average bond length of 1.52 Å. The bond angles show only slight variation from the ideal value of 60°. These values are comparable to the bond geometries reported from the X-ray studies of dimethyl 1a,7b-*cis*-dihydro-1,1-demethyl-1H-cyclopropa[**a**]naphthalene-2,3- dicarboylate[73] and 1-carbomyl-1-carboxy-1a-methyl-1a,7a-dihydro-1H-cyclopropa[**b**]-naphthalene-2,7-dione[74]. Both of these structures have typical cyclopropane C-C bond lengths of 1.516(2) and 1.528(4) Å respectively. The three hydrogens of the cyclopropane ring were determined from the difference map and were therefore allowed to refine freely. The C-H bond lengths were found to be identical within experimental error, at 1.01 Å and each were inclined at approximately 135° to the ring plane.

6.4 Discussion

The final residual of 7.9% can be considered to be higher than ideal considering the simplicity of the structure itself. Examination of the atomic bond lengths and the list of angles indicates that these values are in reasonable agreement with the expected values given suitable error margins. The anisotropic temperature factors do not exhibit any unacceptable values and on the whole the electron distribution of the C atoms are approximate spheres. The high R value can only be accredited to poor crystal quality. However optical examination under a polarising microscope suggested that the crystal was of suitable

quality for single crystal X-ray analysis.

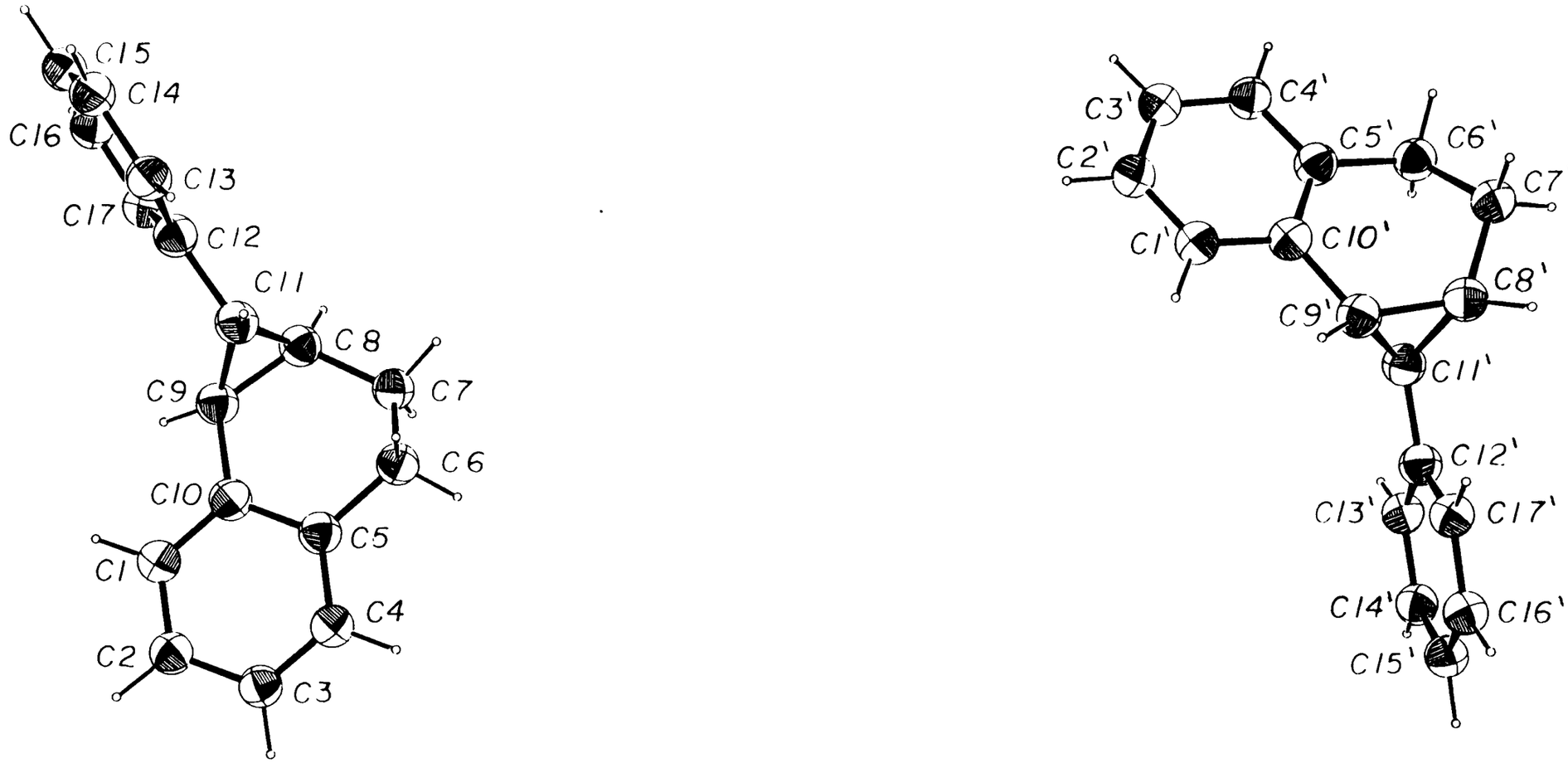

Figure 6.1 A labelled ORTEP plot of the basic asymmetric unit of $C_{17}H_{16}$, consisting of two molecules.

Table 6.1 Fractional atomic coordinates for the carbon atoms within the asymmetric unit. ($U_{eq}=1/3\sum_i\sum_j U_{ij}a_i^*a_j^*a_i\cdot a_j$)

MOLECULE A

	(X/A)	(Y/B)	(Z/C)	U_{eq}
C(1)	0.3547(9)	0.2171(8)	1.0277(4)	0.046
C(2)	0.3687(9)	0.3358(10)	1.0242(5)	0.062
C(3)	0.3689(9)	0.3915(9)	0.9679(6)	0.062
C(4)	0.3534(9)	0.3257(9)	0.9178(5)	0.057
C(5)	0.3379(8)	0.2056(8)	0.9206(4)	0.043
C(6)	0.3133(10)	0.1303(10)	0.8649(4)	0.069
C(7)	0.3725(9)	0.0097(10)	0.8670(4)	0.063
C(8)	0.3508(8)	-.0564(8)	0.9259(4)	0.050
C(9)	0.3359(8)	0.0169(8)	0.9821(4)	0.043
C(10)	0.3399(8)	0.1483(8)	0.9776(4)	0.040
C(11)	0.2176(8)	-.0527(8)	0.9569(4)	0.043
C(12)	0.1760(8)	-.1630(7)	0.9898(3)	0.039
C(13)	0.0398(8)	-.1913(8)	0.9923(4)	0.045
C(14)	0.0025(9)	-.2945(10)	1.0214(5)	0.067
C(15)	0.0923(11)	-.3700(10)	1.0478(4)	0.067
C(16)	0.2247(10)	-.3419(8)	1.0455(4)	0.056
C(17)	0.2651(9)	-.2400(8)	1.0172(4)	0.048

MOLECULE B

	(X/A)	(Y/B)	(Z/C)	U_{eq}
C(1)'	0.1322(8)	-.0012(8)	0.3328(4)	0.047
C(2)'	0.1418(9)	-.1033(9)	0.3658(4)	0.054
C(3)'	0.1701(9)	-.2074(10)	0.3388(5)	0.061
C(4)'	0.1874(8)	-.2106(9)	0.2772(5)	0.055
C(5)'	0.1792(8)	-.1075(8)	0.2423(4)	0.045
C(6)'	0.2048(10)	-.1084(10)	0.1743(5)	0.068
C(7)'	0.1296(10)	-.0150(10)	0.1395(4)	0.063
C(8)'	0.1401(8)	0.1074(9)	0.1679(4)	0.048
C(9)'	0.1450(8)	0.1128(8)	0.2361(4)	0.044
C(10)'	0.1512(7)	0.0002(8)	0.2705(4)	0.037
C(11)'	0.2667(8)	0.1484(8)	0.1984(4)	0.042
C(12)'	0.3047(9)	0.2753(8)	0.1951(4)	0.043
C(13)'	0.4393(9)	0.3071(9)	0.1960(4)	0.051
C(14)'	0.4772(9)	0.4240(9)	0.1928(4)	0.057
C(15)'	0.3863(11)	0.5128(9)	0.1909(5)	0.067
C(16)'	0.2517(10)	0.4843(9)	0.1904(5)	0.062
C(17)'	0.2137(9)	0.3670(9)	0.1926(4)	0.056

Table 6.2 Anisotropic thermal parameters.

MOLECULE A

	U11	U22	U33	U23	U13	U12
C(1)	0.049(6)	0.044(6)	0.046(6)	-.003(5)	-.003(4)	-.006(5)
C(2)	0.045(6)	0.070(8)	0.072(8)	-.009(6)	0.006(5)	-.022(6)
C(3)	0.040(6)	0.046(7)	0.101(9)	-.002(5)	0.010(6)	0.015(7)
C(4)	0.050(6)	0.058(8)	0.062(7)	-.006(5)	0.012(5)	0.018(6)
C(5)	0.038(5)	0.053(6)	0.037(6)	-.002(5)	0.006(4)	0.000(5)
C(6)	0.074(7)	0.084(8)	0.050(7)	-.012(7)	0.011(5)	0.015(6)
C(7)	0.064(7)	0.073(8)	0.053(6)	-.002(6)	0.025(5)	-.010(6)
C(8)	0.042(5)	0.058(6)	0.049(6)	0.012(5)	0.021(4)	-.006(5)
C(9)	0.034(5)	0.059(7)	0.035(5)	-.001(5)	-.003(4)	-.002(5)
C(10)	0.031(5)	0.042(6)	0.047(6)	-.004(4)	0.003(4)	0.007(5)
C(11)	0.038(5)	0.053(6)	0.037(5)	0.003(4)	0.005(4)	-.003(4)
C(12)	0.047(5)	0.041(6)	0.029(5)	0.005(4)	0.007(4)	-.008(4)
C(13)	0.034(5)	0.052(6)	0.049(6)	-.008(4)	0.010(4)	0.002(5)
C(14)	0.048(6)	0.076(8)	0.076(8)	-.016(6)	0.022(6)	-.003(7)
C(15)	0.076(8)	0.065(7)	0.062(7)	-.016(7)	0.029(6)	0.019(6)
C(16)	0.065(7)	0.041(6)	0.061(7)	0.011(5)	0.004(5)	0.005(5)
C(17)	0.045(5)	0.039(6)	0.059(6)	-.003(4)	-.001(5)	-.008(5)

MOLECULE B

	U11	U22	U33	U23	U13	U12
C(1)'	0.043(5)	0.050(6)	0.047(6)	0.000(5)	0.002(4)	-.003(5)
C(2)'	0.055(6)	0.059(7)	0.047(6)	0.006(5)	0.009(5)	0.010(6)
C(3)'	0.058(7)	0.063(7)	0.061(7)	0.001(6)	0.005(5)	0.017(6)
C(4)'	0.044(6)	0.049(6)	0.071(8)	-.002(5)	-.002(5)	-.004(6)
C(5)'	0.036(5)	0.058(7)	0.042(6)	-.004(5)	-.005(4)	-.006(5)
C(6)'	0.069(7)	0.072(8)	0.063(8)	-.014(6)	0.015(6)	-.021(6)
C(7)'	0.075(7)	0.077(8)	0.038(6)	-.003(6)	-.008(5)	-.012(6)
C(8)'	0.051(6)	0.069(7)	0.025(5)	-.002(4)	0.009(4)	0.011(5)
C(9)'	0.031(5)	0.056(6)	0.044(6)	-.002(4)	0.012(4)	0.010(5)
C(10)'	0.028(4)	0.045(6)	0.039(5)	0.000(4)	0.005(3)	-.004(5)
C(11)'	0.042(5)	0.051(6)	0.035(5)	0.006(5)	0.010(4)	0.001(4)
C(12)'	0.054(6)	0.042(6)	0.032(5)	-.002(5)	0.014(4)	0.001(4)
C(13)'	0.041(5)	0.054(6)	0.059(6)	-.001(5)	0.007(6)	0.002(5)
C(14)'	0.039(5)	0.061(7)	0.070(7)	-.015(5)	0.011(5)	0.000(6)
C(15)'	0.072(8)	0.053(7)	0.075(8)	-.023(6)	0.007(6)	0.006(6)
C(16)'	0.063(7)	0.049(7)	0.072(7)	0.002(6)	0.000(5)	0.006(6)
C(17)'	0.051(6)	0.059(7)	0.059(7)	-.003(5)	0.004(5)	-.004(5)

Table 6.3 Fractional atomic coordinates of hydrogen atoms with a common temperature factor. (* indicates atoms allowed to refine freely)

MOLECULE A

	(X/A)	(Y/B)	(Z/C)	Ueq
H(1)	0.35528	0.17861	1.06837	0.05
H(2)	0.37880	0.38367	1.06200	0.05
H(3)	0.38036	0.47911	0.96490	0.05
H(4)	0.35333	0.36542	0.87740	0.05
H(6a)	0.35092	0.17265	0.82922	0.05
H(6b)	0.21537	0.12151	0.85953	0.05
H(7a)	0.33294	-.03805	0.83348	0.05
H(7b)	0.47015	0.01742	0.86064	0.05
* H(8)	0.40927	-.12279	0.91250	0.05
* H(9)	0.38157	0.02119	1.02233	0.05
* H(11)	0.12475	-.03219	0.94479	0.05
H(13)	-.02804	-.13826	0.97352	0.05
H(14)	-.09380	-.31479	1.02330	0.05
H(15)	0.06198	-.44400	1.06822	0.05
H(16)	0.29163	-.39555	1.06457	0.05
H(17)	0.36169	-.22077	1.01623	0.05

MOLECULE B

	(X/A)	(Y/B)	(Z/C)	Ueq
H(1)'	0.11101	0.07444	0.35407	0.05
H(2)'	0.12753	-.10092	0.41050	0.05
H(3)'	0.17857	-.28127	0.36335	0.05
H(4)'	0.20600	-.28779	0.25698	0.05
H(6a)'	0.17863	-.18756	0.15806	0.05
H(6b)'	0.30157	-.09557	0.16762	0.05
H(7a)'	0.16575	-.01130	0.09755	0.05
H(7b)'	0.03409	-.03821	0.13787	0.05
* H(8)'	0.08388	0.14239	0.13503	0.05
* H(9)'	0.09015	0.15153	0.26811	0.05
* H(11)'	0.36187	0.12400	0.19685	0.05
H(13)'	0.50847	0.24407	0.19884	0.05
H(14)'	0.57360	0.44395	0.19194	0.05
H(15)'	0.41552	0.59718	0.18987	0.05
H(16)'	0.18338	0.54819	0.18842	0.05
H(17)'	0.11707	0.34753	0.19238	0.05

Table 6.4 Intramolecular bond lengths in angstroms.

MOLECULE A

C(1)	- C(2)	1.35(2)	C(1)	- C(10)	1.36(2)
C(2)	- C(3)	1.40(2)	C(3)	- C(4)	1.34(2)
C(4)	- C(5)	1.37(2)	C(5)	- C(6)	1.52(2)
C(5)	- C(10)	1.42(2)	C(6)	- C(7)	1.49(2)
C(7)	- C(8)	1.52(2)	C(8)	- C(9)	1.50(2)
C(8)	- C(11)	1.51(2)	C(9)	- C(10)	1.49(2)
C(9)	- C(11)	1.53(2)	C(11)	- C(12)	1.51(2)
C(12)	- C(13)	1.41(2)	C(12)	- C(17)	1.39(2)
C(13)	- C(14)	1.39(2)	C(14)	- C(15)	1.37(2)
C(15)	- C(16)	1.38(2)	C(16)	- C(17)	1.37(2)

MOLECULE B

C(1)'	- C(2)'	1.37(2)	C(1) '	- C(10)'	1.39(2)
C(2)'	- C(3)'	1.35(2)	C(3)'	- C(4)'	1.37(2)
C(4)'	- C(5)'	1.40(2)	C(5)'	- C(6)'	1.53(2)
C(5)'	- C(10)'	1.40(2)	C(6)'	- C(7)'	1.51(2)
C(7)'	- C(8)'	1.52(2)	C(8)'	- C(9)'	1.51(2)
C(8)'	- C(11)'	1.54(2)	C(9)'	- C(10)'	1.49(2)
C(9)'	- C(11)'	1.54(2)	C(11)'	- C(12)'	1.49(2)
C(12)'	- C(13)'	1.41(2)	C(12)'	- C(17)'	1.39(2)
C(13)'	- C(14)'	1.38(2)	C(14)'	- C(15)'	1.36(2)
C(15)'	- C(16)'	1.40(2)	C(16)'	- C(17)'	1.38(2)

Table 6.5 Intramolecular bond angles in degrees.

MOLECULE A

C(2)-C(1)-C(10)	122.2(9)	C(1)-C(2)-C(3)	119.9(10)
C(2)-C(3)-C(4)	119.0(10)	C(3)-C(4)-C(5)	121.7(10)
C(4)-C(5)-C(6)	122.6(9)	C(4)-C(5)-C(10)	119.6(9)
C(6)-C(5)-C(10)	117.8(9)	C(5)-C(6)-C(7)	116.1(9)
C(6)-C(7)-C(8)	114.7(8)	C(7)-C(8)-C(9)	116.9(8)
C(7)-C(8)-C(11)	120.5(8)	C(9)-C(8)-C(11)	61.1(6)
C(8)-C(9)-C(10)	119.5(8)	C(8)-C(9)-C(11)	59.7(6)
C(10)-C(9)-C(11)	120.6(7)	C(1)-C(10)-C(5)	117.6(9)
C(1)-C(10)-C(9)	121.3(8)	C(5)-C(10)-C(9)	121.0(8)
C(8)-C(11)-C(9)	59.1(6)	C(8)-C(11)-C(12)	116.5(8)
C(9)-C(11)-C(9)	117.9(7)	C(11)-C(12)-C(13)	118.7(8)
C(11)-C(12)-C(17)	123.3(8)	C(13)-C(12)-C(17)	118.0(8)
C(12)-C(13)-C(14)	118.4(8)	C(13)-C(14)-C(15)	122.7(10)
C(14)-C(15)-C(16)	118.7(10)	C(15)-C(16)-C(17)	120.1(9)
C(12)-C(17)-C(16)	122.1(9)		

MOLECULE B

C(2)'-C(1)'-C(10)'	121.8(9)	C(1)'-C(2)'-C(3)'	120.9(9)
C(2)'-C(3)'-C(4)'	119.3(10)	C(3)'-C(4)'-C(5)'	121.1(10)
C(4)'-C(5)'-C(6)'	121.8(9)	C(4)'-C(5)'-C(10)'	119.5(9)
C(6)'-C(5)'-C(10)'	118.7(9)	C(5)'-C(6)'-C(7)'	114.2(9)
C(6)'-C(7)'-C(8)'	113.1(8)	C(7)'-C(8)'-C(9)'	116.7(8)
C(7)'-C(8)'-C(11)'	121.2(8)	C(9)'-C(8)'-C(11)'	61.3(6)
C(8)'-C(9)'-C(10)'	118.5(8)	C(8)'-C(9)'-C(11)'	59.5(6)
C(10)'-C(9)'-C(11)'	118.0(7)	C(1)'-C(10)'-C(5)'	117.4(9)
C(1)'-C(10)'-C(9)'	120.7(8)	C(5)'-C(10)'-C(9)'	121.9(8)
C(8)'-C(11)'-C(9)'	59.3(6)	C(8)'-C(11)'-C(12)'	119.4(8)
C(9)'-C(11)'-C(9)'	119.0(8)	C(11)'-C(12)'-C(13)'	119.7(8)
C(11)'-C(12)'-C(17)'	123.6(8)	C(13)'-C(12)'-C(17)'	116.7(8)
C(12)'-C(13)'-C(14)'	120.9(9)	C(13)'-C(14)'-C(15)'	121.5(9)
C(14)'-C(15)'-C(16)'	119.0(10)	C(15)'-C(16)'-C(17)'	119.4(10)
C(12)'-C(17)'-C(16)'	122.4(9)		

Table 6.6 Intramolecular torsion angles in degrees.

MOLECULE A

C(1)-C(2)-C(3)-C(4)	0.8(10)	C(2)-C(3)-C(4)-C(5)	-.2(10)
C(3)-C(4)-C(5)-C(10)	-.9(10)	C(4)-C(5)-C(10)-C(1)	1.4(9)
C(2)-C(1)-C(10)-C(5)	-.8(9)	C(10)-C(1)-C(2)-C(3)	-.3(10)
C(6)-C(5)-C(10)-C(1)	-176.4(13)	C(4)-C(5)-C(10)-C(9)	-174.3(13)
C(5)-C(6)-C(7)-C(8)	45.8(9)	C(6)-C(7)-C(8)-C(9)	-28.7(9)
C(7)-C(8)-C(9)-C(10)	1.3(8)	C(8)-C(9)-C(10)-C(5)	9.4(8)
C(6)-C(5)-C(10)-C(9)	7.9(8)	C(10)-C(5)-C(6)-C(7)	-35.9(9)
C(7)-C(8)-C(9)-C(11)	111.7(9)	C(11)-C(8)-C(9)-C(10)	-110.3(9)
C(8)-C(11)-C(12)-C(13)	-147.8(11)	C(8)-C(11)-C(12)-C(17)	31.1(9)
C(9)-C(11)-C(12)-C(13)	144.8(11)	C(9)-C(11)-C(12)-C(17)	-36.3(9)
C(12)-C(13)-C(14)-C(15)	0.0(10)	C(13)-C(14)-C(15)-C(16)	0.3(10)
C(14)-C(15)-C(16)-C(17)	-.1(10)	C(15)-C(16)-C(17)-C(12)	-.4(9)
C(13)-C(12)-C(17)-C(16)	0.7(9)	C(17)-C(12)-C(13)-C(14)	-.5(9)

MOLECULE B

C(1)'-C(2)'-C(3)'-C(4)'	-1.0(10)	C(2)'-C(3)'-C(4)'-C(5)'	1.6(10)
C(3)'-C(4)'-C(5)'-C(10)'	-.9(9)	C(4)'-C(5)'-C(10)'-C(1)'	-.2(9)
C(2)'-C(1)'-C(10)'-C(5)'	0.7(9)	C(10)'-C(1)'-C(2)'-C(3)'	-.1(9)
C(6)'-C(5)'-C(10)'-C(1)'	-172.2(13)	C(4)'-C(5)'-C(10)'-C(9)'	178.3(13)
C(5)'-C(6)'-C(7)'-C(8)'	48.0(9)	C(6)'-C(7)'-C(8)'-C(9)'	-35.2(9)
C(7)'-C(8)'-C(9)'-C(10)'	5.3(8)	C(8)'-C(9)'-C(10)'-C(5)'	13.1(8)
C(6)'-C(5)'-C(10)'-C(9)'	0.3(8)	C(10)'-C(5)'-C(6)'-C(7)'	-31.4(9)
C(7)'-C(8)'-C(9)'-C(11)'	112.7(9)	C(11)'-C(8)'-C(9)'-C(10)'	-107.5(9)
C(8)'-C(11)'-C(12)'-C(13)'	-149.9(11)	C(8)'-C(11)'-C(12)'-C(17)'	31.8(9)
C(9)'-C(11)'-C(12)'-C(13)'	141.1(12)	C(9)'-C(11)'-C(12)'-C(17)'	-37.2(9)
C(12)'-C(13)'-C(14)'-C(15)'	2.4(10)	C(13)'-C(14)'-C(15)'-C(16)'	-1.9(10)
C(14)'-C(15)'-C(16)'-C(17)'	0.9(10)	C(15)'-C(16)'-C(17)'-C(12)'	-1.9(10)
C(13)'-C(12)'-C(17)'-C(16)'	0.7(10)	C(17)'-C(12)'-C(13)'-C(14)'	-1.7(9)

CHAPTER 7. X-ray crystal structure of 16-benzylidenyl-6-benzyloxy-3-dehydro-3,5-epiandrosterone, $C_{33}H_{38}O_2$.

7.1 Introduction

$C_{33}H_{38}O_2$ (16-benzylidenyl-6-benzyloxy-3-dehydro-3,5-epiandrosterone) belongs to the biochemical group of steroids formed by the solvolysis of dehydroepiandrosterone (DHEA). It was anticipated that the solvolysis process could follow two possible reaction paths and so the composition of the final product was uncertain. The crystalline material produced was later found to be a steroid byproduct of the main reaction. Initial spectroscopic analysis of this compound indicated the possible presence of a cyclopropane ring incorporated in the steroid.

The present X-ray diffraction analysis was therefore undertaken to resolve the crystal and molecular structure and to verify the existence of the three membered carbon ring. It is however beyond the scope of this report to explain the actual reaction mechanism leading to the final material.

7.2 Experimental

7.2.1 Data collection

Data were collected on a colourless crystal of dimensions 0.5 x 0.9 x 0.3 mm^3. The instrument used was the Nicolet P3 4C-SXD using graphite monochromated Mo Kα X-radiation. The initial cell parameters and crystal orientation were determined from 12 unique reflexions with $2\theta \approx 20^\circ$. A total of 3294 unique intensities were measured with $2\theta < 50^\circ$ as $\omega/2\theta$ scans over the **hkl** range; $-13 \leq \mathbf{h} \leq 13$, $0 \leq \mathbf{k} \leq 11$, $0 \leq \mathbf{l} \leq 18$. Of the 3294 measured, 1654 had $\mathbf{F} > 5\sigma(\mathbf{F})$. There was no significant variation in beam intensity throughout the data collection. The data were corrected for Lorentz and polarisation effects whilst diminished intensities due to absorption was considered

to be negligible.

7.2.2 Structure solution and refinement

Given the light element composition of the steroid molecule, Direct methods were initially employed. The information regarding the structure revealed by MITHRIL was limited. Only the positions of the C atoms from the steroid skeleton could be pinpointed. Fragments of the side chains were found on closer inspection of the two dimensional projections of the electron peaks, but the errors associated with these possible positions left a high degree of doubt about their authenticity. This method of approach was not pursued further.

Using the PC (personal computer) based SHELXS-86[75] software package a more automated direct methods routine was employed. This enabled the coordinates of the non-hydrogen atoms to be determined directly. The coordinates for the basic skeleton generated by MITHRIL agreed with those from SHELXS-86. The coordinates were then refined using the more familiar software of SHELX-76, performing full matrix least squares with anisotropic thermal parameters for C and O atoms and a common isotropic thermal parameter for the H atoms. All H atoms , excluding the cyclopropane H atom, H(3), were placed in calculated positions and constrained to ride on their attached C atoms. The position of the H(3) atom was however, located on a Fourier difference map and was allowed to refine freely. The refinement finally converged at R=0.071 using unit weights. $\Delta\rho_{max}$=0.13 eÅ^{-1}, $\Delta\rho_{min}$=-.09 eÅ^{-1}, Δ/σ<0.07.

7.3 Results

7.3.1 Crystal and diffraction data

$C_{33}H_{38}O_2$, M_r=466.6, monoclinic, $P2_1$ (no.4), **a**=10.509(6), **b**=9.100(9), **c**=14.056(16) Å, **ß**=93.56(7)°, **V**=1342(2)Å^3, **Z**=2, D_x=1.15(2) gcm^{-3}, Mo **Kα**,

λ=0.71069 Å, μ=0.37cm^{-1}, **F(000)**=504, **T**=293 K, **R**=0.071 for 1654 unique reflexions.

7.3.2 Structure analysis

The final structure is represented in the two ORTEP plots in Figures 7.1 and 7.2. For clarity Figure 7.1 features only labelled C atoms with ideal spherical electron density distributions. The molecule has been rotated to enable the cyclopropane ring to be viewed more clearly. Figure 7.2 represents the same molecular orientation as Figure 7.1, but with the inclusion of the H atoms and anisotropic thermal ellipsoids. The non-hydrogen atom fractional coordinates, non-hydrogen atom anisotropic thermal parameters and hydrogen atom fractional coordinates are listed in Table 7.1, 7.2 and 7.3 respectively. All bonds, angles and torsion angles are tabulated in Table 7.4, 7.5 and 7.6 respectively.

The most obvious and interesting feature of the solved structure is the position of the benzyloxy (-OCH_2Ph) group. The formation of the cyclopropane ring, C(3)-C(4)-C(5), has prevented the benzyloxy group from forming a bonded contact with C(3), as the initial synthesis work had predicted. As a result, the group is bonded at C(6) and is ß orientated with C(4)-C(5)-C(6)-O(1) equal to -84.7(10)°.

The cyclopropane ring has valence angles close to 60° of 60.3(8), 60.9(7) and 58.8(8)°. The well formed three membered ring has had the effect of distorting ring A, in which it is housed. Ring A has adopted a distorted boat conformation with C(1) and C(4) displaced from the mean plane, C(2)-C(3)-C(5)-C(10), by 0.48(1) and 1.21(1) Å respectively. The torsion angle C(4)-C(5)-C(10)-C(19) is 76.1(10)°. Similar studies of the cyclopropane steroids 3α,5-cycloandrostane-

6,17-dione[76] and 3,5-cycloandrostan-6ß-ol-17-one[77] have revealed virtually identical skeleton geometries. The angles of the cyclopropane ring in the former has angles of 58(2), 60(2) and 62(2)°. The bond lengths of the ring, at 1.61(4), 1.56(3) and 1.58(4) Å , show greater distortion than the title structure.

The bond lengths for the atoms composing the basic steroid framework, agree with the currently accepted values within experimental error. However the geometries of the phenyl groups of the side chains are in not such good agreement.

The basic steroid skeleton has proven to be rigid and so the atomic positions and thermal parameters are well defined. The two side chains, more notably the benzyloxy group, are long and flexible, thus permitting a high degree of movement. As a result the thermal ellipsoids for the side chain atoms are exaggerated rugby ball shaped. This feature is visibly noticeable from Figure 7.1. The thermal vibration has left some uncertainty about their atomic positions and this is reflected in the bond lengths for these atoms.

All the hydrogen atoms in the structure, except H(3), were placed in calculated positions with the C-H bond lengths constrained at 1.00 Å. However H(3) was refined freely relative to C(3) producing a bond length of 0.99(3)°. The bond angles C(4)-C(3)-H(3) and C(5)-C(3)-H(3) are 121.3(9) and 122.1(9)° which compares with the average value 135°, of the cyclopropane hydrogens of the steroid precursor discussed in Chapter 6.

The methyl groups at C(10) and C(13) adopt slightly distorted tetrahedral arrangements. The angles C(1)-C(10)-C(18), C(5)-C(10)-C(18) and C(9)-C(10)-C(19) are 111.0(8), 111.1(9) and 112.6(9)° (av.

111.2°). And C(12)-C(13)-C(18), C(14)-C(13)-C(18) and C(17)-C(13)-C(18) are 111.5(9), 112.7(8) and 105.6(8)° (av. 109.9°). These values compare favourably with the normal tetrahedral value of 109.5°.

Finally the 5 membered ring C(13)-C(14)-C(15)-C(16)-C(17) represents a moderately strained ring adopting a half-chair conformation. This is reflected by the atom bond angles which range from 101.2(7)° to 108.4(7)°.

7.3.3 Spectroscopic analysis

As part of the process of the synthesis, the novel compound was routinely analysed by various spectroscopic techniques, such as NMR, IR. Mass fragmentation and UV. Examination of the IR spectrum, shown in Figure 7.3. revealed the possibility of a cyclopropane ring at 1010 cm^{-1} which was not initially expected.

7.4 Discussion

The final structure and other related structures have provided valuable information regarding the reaction mechanism for cyclopropane steroids. Unfortunately, the high thermal vibration of the all important side chains cannot be accurately described. The packing diagram in Figure 7.4 indicates that despite the considerable size of the side chains, there is sufficient room for many degrees of freedom in movement. This has resulted in a high residual factor of R=0.071.

Despite the uncertainties, the X-ray analysis has shown that it is indeed the definitive structural tool for molecular and crystal structures. However, this is not to say that X-ray crystallography can be successful without other methods. They invariably help to initially restrict the number of feasible starting structures, hence reducing the overall computation time.

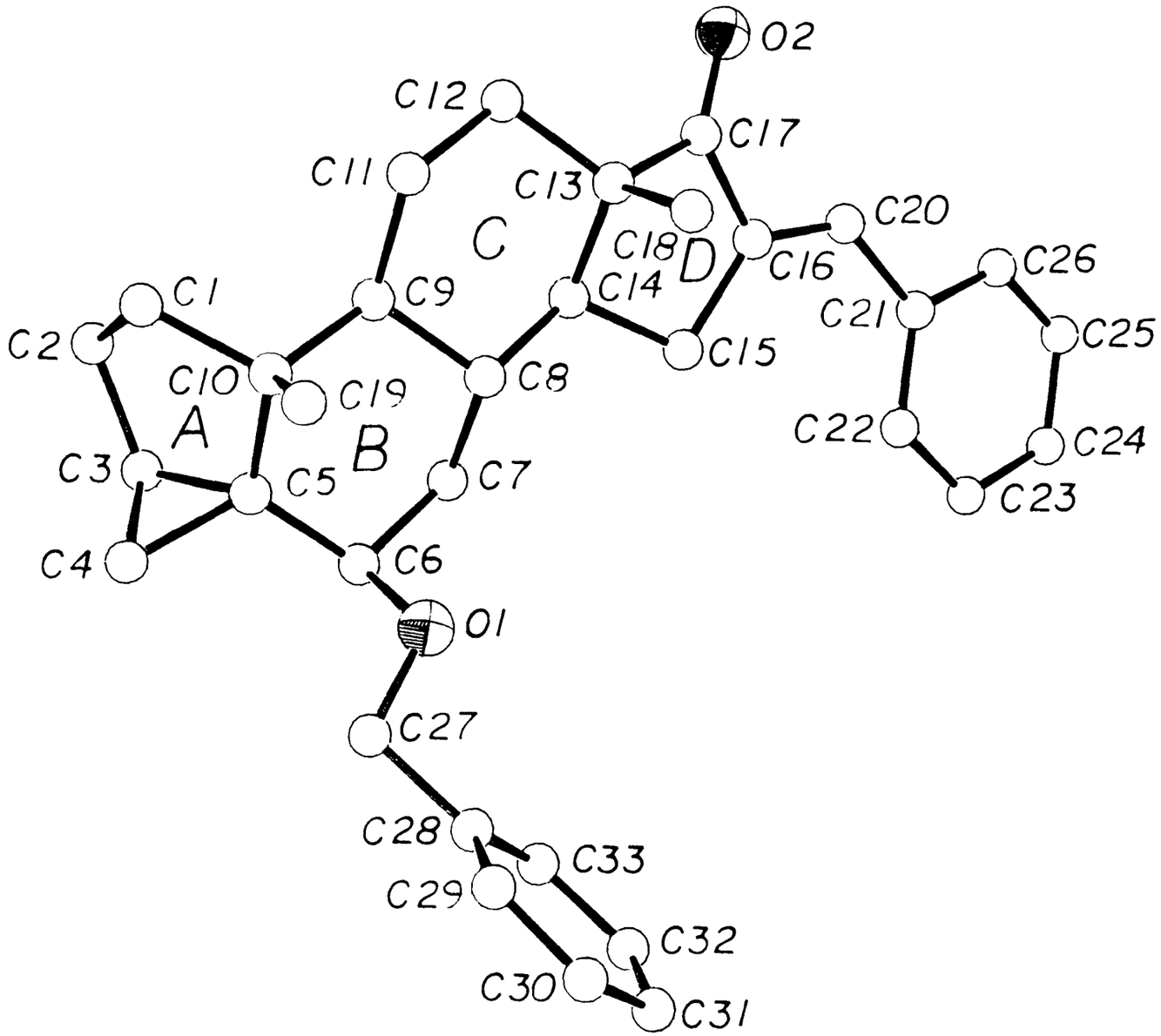

Figure 7.1 A labelled ORTEP plot of the steroid, $C_{33}H_{38}O_2$, minus the hydrogen atoms for improved clarity. All like atoms have been represented by fixed radii spheres.

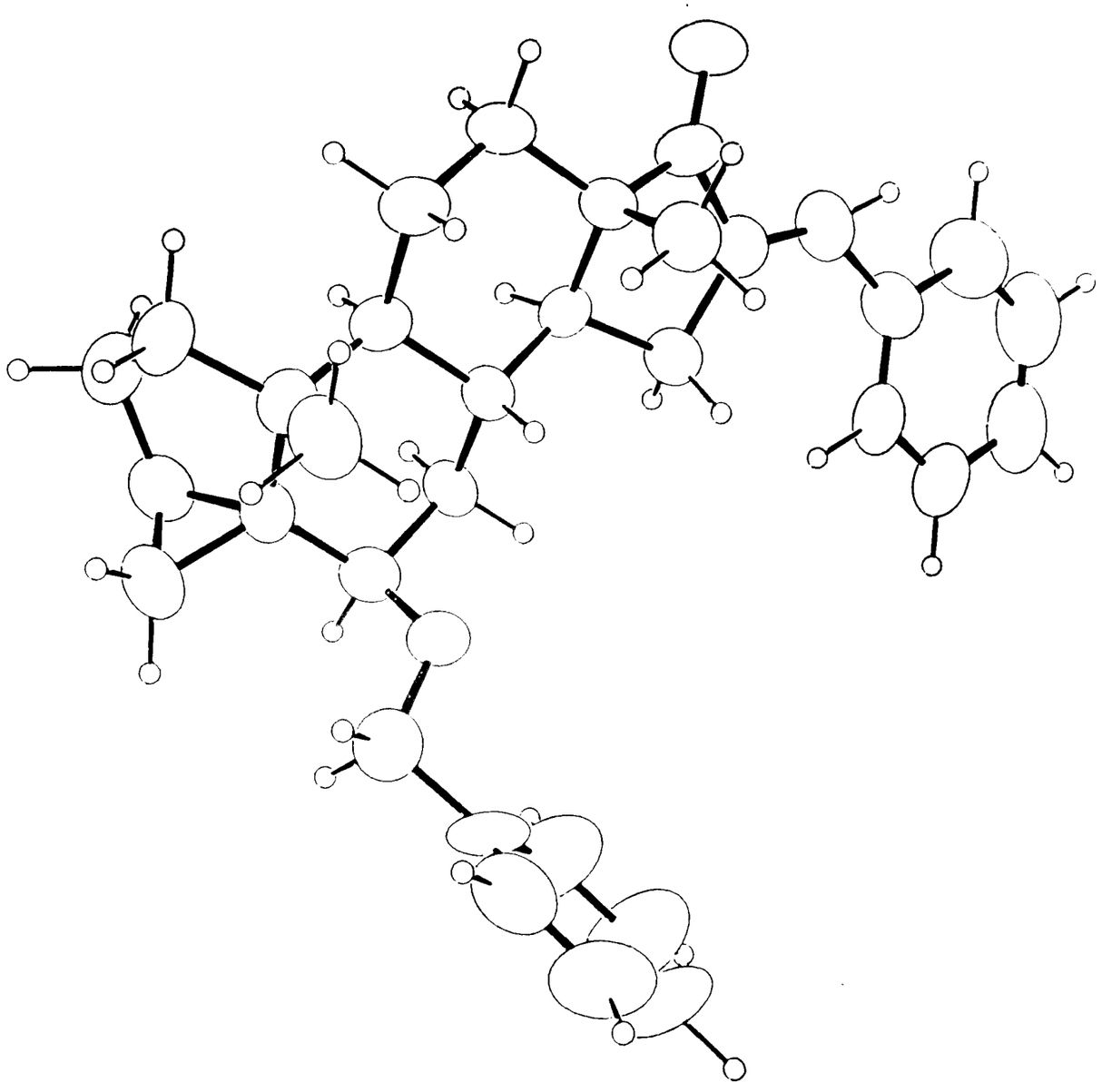

Figure 7.2 As Figure 7.1, including the H atoms. The atoms have been represented by thermal ellipsoids, contrasting the rigid steroid skeleton with the mobile side groups.

Table 7.1 Fractional atomic coordinates of non-hydrogen atoms. ($U_{eq}=1/3\sum_i\sum_j U_{ij}a_i^*a_j^*a_i\cdot a_j$)

	(X/A)	(Y/B)	(Z/C)	U_{eq}
C(1)	-.7724(9)	-.2833(15)	-1.0148(6)	0.067
C(2)	-.7030(10)	-.1434(15)	-.9832(8)	0.079
C(3)	-.6036(9)	-.1921(16)	-.9064(7)	0.068
C(4)	-.5263(8)	-.3250(15)	-.9310(7)	0.073
C(5)	-.6425(7)	-.3445(13)	-.8726(6)	0.050
C(6)	-.6204(7)	-.3843(13)	-.7684(6)	0.053
C(7)	-.7353(6)	-.3412(15)	-.7135(5)	0.049
C(8)	-.8583(7)	-.4042(13)	-.7599(5)	0.042
C(9)	-.8794(7)	-.3463(14)	-.8627(5)	0.044
C(10)	-.7690(8)	-.3851(14)	-.9269(5)	0.052
C(11)	-1.0121(7)	-.3875(14)	-.9082(5)	0.057
C(12)	-1.1220(7)	-.3458(14)	-.8480(5)	0.053
C(13)	-1.0991(7)	-.4120(12)	-.7476(6)	0.046
C(14)	-.9690(6)	-.3578(13)	-.7047(5)	0.040
C(15)	-.9731(7)	-.3963(14)	-.5974(5)	0.052
C(16)	-1.1133(8)	-.3728(13)	-.5791(6)	0.056
C(17)	-1.1869(8)	-.3615(14)	-.6727(6)	0.054
C(18)	-1.1094(9)	-.5806(13)	-.7497(7)	0.061
C(19)	-.7703(9)	-.5495(14)	-.9574(7)	0.068
C(20)	-1.1750(8)	-.3680(14)	-.5006(6)	0.063
C(21)	-1.1260(8)	-.3892(14)	-.3973(6)	0.058
C(22)	-1.0008(9)	-.4305(14)	-.3699(6)	0.063
C(23)	-.9650(10)	-.4482(15)	-.2749(7)	0.077
C(24)	-1.0567(13)	-.4245(15)	-.2074(7)	0.084
C(25)	-1.1783(13)	-.3848(17)	-.2358(8)	0.094
C(26)	-1.2123(10)	-.3657(18)	-.3272(7)	0.090
C(27)	-.4891(10)	-.6006(15)	-.7793(7)	0.079
C(28)	-.4544(9)	-.7226(15)	-.7090(9)	0.068
C(29)	-.4353(10)	-.8656(20)	-.7385(9)	0.090
C(30)	-.3987(14)	-.9707(22)	-.6760(14)	0.128
C(31)	-.3834(18)	-.9382(29)	-.5832(17)	0.156
C(32)	-.4050(18)	-.7999(29)	-.5556(11)	0.164
C(33)	-.4374(14)	-.6919(20)	-.6183(10)	0.119
O(1)	-.6050(5)	-.5408	-.7542(4)	0.067
O(2)	-1.2961(5)	-.3227(11)	-.6858(4)	0.073

Table 7.2 Anisotropic thermal parameters.

	U11	U22	U33	U23	U13	U12
C(1)	0.077(7)	0.086(9)	0.038(5)	0.008(6)	0.007(5)	0.011(6)
C(2)	0.074(7)	0.084(9)	0.079(7)	0.005(7)	0.012(6)	0.033(7)
C(3)	0.052(6)	0.079(9)	0.074(7)	-.004(6)	0.008(5)	0.008(7)
C(4)	0.057(6)	0.087(8)	0.077(7)	-.011(6)	0.017(5)	0.009(7)
C(5)	0.052(5)	0.043(5)	0.054(5)	0.006(5)	0.014(4)	0.008(5)
C(6)	0.039(4)	0.062(7)	0.056(5)	-.002(5)	-.002(4)	0.004(5)
C(7)	0.038(4)	0.077(7)	0.033(4)	-.003(5)	0.004(3)	-.001(5)
C(8)	0.037(4)	0.052(6)	0.037(4)	-.005(4)	0.000(3)	0.000(4)
C(9)	0.045(4)	0.046(5)	0.041(4)	-.001(4)	-.008(3)	-.004(4)
C(10)	0.057(5)	0.064(7)	0.035(4)	-.006(5)	-.003(4)	-.001(5)
C(11)	0.048(5)	0.071(7)	0.049(5)	0.006(5)	-.006(4)	-.003(5)
C(12)	0.038(4)	0.060(6)	0.060(5)	0.007(5)	-.007(4)	0.000(6)
C(13)	0.035(4)	0.054(6)	0.049(5)	0.002(4)	0.000(4)	0.003(5)
C(14)	0.043(4)	0.039(5)	0.039(4)	0.002(4)	-.002(3)	0.004(4)
C(15)	0.047(4)	0.065(7)	0.045(4)	0.001(5)	0.004(3)	0.000(5)
C(16)	0.055(5)	0.050(6)	0.062(5)	0.009(5)	0.012(4)	0.003(5)
C(17)	0.048(5)	0.048(6)	0.065(6)	0.008(5)	-.009(4)	0.005(6)
C(18)	0.058(6)	0.052(6)	0.074(7)	0.001(5)	0.009(5)	0.001(6)
C(19)	0.075(7)	0.068(7)	0.061(6)	-.002(6)	0.021(5)	-.019(6)
C(20)	0.066(5)	0.063(7)	0.060(6)	0.006(6)	0.027(4)	-.003(6)
C(21)	0.060(5)	0.057(7)	0.057(5)	-.001(5)	0.014(4)	-.014(5)
C(22)	0.082(7)	0.064(7)	0.044(5)	0.000(6)	0.020(5)	0.007(5)
C(23)	0.090(8)	0.064(8)	0.075(7)	-.013(6)	0.000(6)	0.020(6)
C(24)	0.13(1)	0.07(1)	0.05(1)	-.04(1)	0.01(1)	-.01(1)
C(25)	0.13(1)	0.10(1)	0.06(1)	-.02(1)	0.04(1)	-.02(1)
C(26)	0.093(8)	0.096(10)	0.081(7)	0.008(8)	0.027(6)	-.024(8)
C(27)	0.074(7)	0.086(9)	0.079(7)	0.007(7)	0.012(6)	0.015(7)
C(28)	0.039(5)	0.073(8)	0.090(8)	0.015(5)	-.021(5)	0.010(7)
C(29)	0.064(7)	0.097(11)	0.108(10)	-.009(8)	0.009(6)	-.005(10)
C(30)	0.10(1)	0.08(1)	0.20(2)	0.03(1)	0.02(1)	0.01(2)
C(31)	0.12(1)	0.15(2)	0.21(2)	0.05(1)	-.01(2)	0.10(2)
C(32)	0.19(2)	0.23(3)	0.06(1)	0.05(2)	-.03(1)	0.04(1)
C(33)	0.16(1)	0.10(1)	0.09(1)	0.04(1)	-.03(1)	-.01(1)
O(1)	0.050(4)	0.080(5)	0.072(4)	0.023(4)	0.014(3)	0.024(4)
O(2)	0.046(3)	0.087(6)	0.085(5)	0.025(4)	0.004(3)	0.006(4)

Table 7.3 Fractional atomic coordinates of hydrogen atoms, with a common temperature factor. (* denotes atom allowed to refine freely)

	(X/A)	(Y/B)	(Z/C)	Ueq
H(1a)	-.8626(9)	-.2609(15)	-1.0370(6)	0.075(5)
H(1b)	-.7280(9)	-.3309(15)	-1.0676(6)	0.075(5)
H(2a)	-.7637(10)	-.0721(15)	-.9563(8)	0.075(5)
H(2b)	-.6616(10)	-.0968(15)	-1.0378(8)	0.075(5)
* H(3)	-.569(8)	-.115(8)	-.862(5)	0.075(5)
H(4a)	-.5286(8)	-.3611(15)	-.9983(7)	0.075(5)
H(4b)	-.4388(8)	-.3391(15)	-.9003(7)	0.075(5)
H(6)	-.5413(7)	-.3306(13)	-.7455(6)	0.075(5)
H(7a)	-.7421(6)	-.2316(15)	-.7120(5)	0.075(5)
H(7b)	-.7232(6)	-.3795(15)	-.6469(5)	0.075(5)
H(8)	-.8514(7)	-.5138(13)	-.7606(5)	0.075(5)
H(9)	-.8778(7)	-.2367(14)	-.8576(5)	0.075(5)
H(11a)	-1.0143(7)	-.4962(14)	-.9185(5)	0.075(5)
H(11b)	-1.0242(7)	-.3361(14)	-.9710(5)	0.075(5)
H(12a)	-1.1275(7)	-.2363(14)	-.8433(5)	0.075(5)
H(12b)	-1.2035(7)	-.3851(14)	-.8785(5)	0.075(5)
H(14)	-.9537(6)	-.2498(13)	-.7101(5)	0.075(5)
H(15a)	-.9170(7)	-.3291(14)	-.5572(5)	0.075(5)
H(15b)	-.9467(7)	-.5004(14)	-.5849(5)	0.075(5)
H(18a)	-1.0531(9)	-.6206(13)	-.7982(7)	0.075(5)
H(18b)	-1.1998(9)	-.6096(13)	-.7667(7)	0.075(5)
H(18c)	-1.0822(9)	-.6211(13)	-.6855(7)	0.075(5)
H(19a)	-.8534(9)	-.5730(14)	-.9927(7)	0.075(5)
H(19b)	-.7592(9)	-.6132(14)	-.8995(7)	0.075(5)
H(19c)	-.6989(9)	-.5680(14)	-.9997(7)	0.075(5)
H(20)	-1.2359(8)	-.3555(14)	-.4493(6)	0.075(5)
H(22)	-.9378(9)	-.4474(14)	-.4192(6)	0.075(5)
H(23)	-.8758(10)	-.4773(15)	-.2542(7)	0.075(5)
H(24)	-1.0323(13)	-.4370(15)	-.1380(7)	0.075(5)
H(25)	-1.2423(13)	-.3695(17)	-.1869(8)	0.075(5)
H(26)	-1.3014(10)	-.3345(18)	-.3465(7)	0.075(5)
H(27a)	-.4988(10)	-.6413(15)	-.8484(7)	0.075(5)
H(27b)	-.4213(10)	-.5234(15)	-.7761(7)	0.075(5)
H(29)	-.4490(10)	-.8911(20)	-.8076(9)	0.075(5)
H(30)	-.3827(14)	-1.0703(22)	-.6984(14)	0.075(5)
H(31)	-.3568(18)	-1.0155(29)	-.5354(17)	0.075(5)
H(32)	-.3963(18)	-.7755(29)	-.4861(11)	0.075(5)
H(33)	-.4490(14)	-.5889(20)	-.5956(10)	0.075(5)

Table 7.4 Intramolecular bond lengths in angstroms.

C(1) - C(2)	1.52(2)	C(1) - C(10)	1.54(2)
C(2) - C(3)	1.52(2)	C(3) - C(4)	1.51(2)
C(3) - C(5)	1.53(2)	C(4) - C(5)	1.52(2)
C(5) - C(6)	1.51(2)	C(5) - C(10)	1.54(2)
C(6) - C(7)	1.52(2)	C(6) - O(1)	1.45(2)
C(7) - C(8)	1.52(2)	C(8) - C(9)	1.54(2)
C(8) - C(14)	1.50(2)	C(9) - C(10)	1.55(2)
C(9) - C(11)	1.54(2)	C(10) - C(19)	1.56(2)
C(11) - C(12)	1.52(2)	C(12) - C(13)	1.54(2)
C(13) - C(14)	1.54(2)	C(14) - C(15)	1.55(2)
C(13) - C(18)	1.54(2)	C(13) - C(17)	1.52(2)
C(15) - C(16)	1.53(2)	C(16) - C(17)	1.49(2)
C(16) - C(20)	1.32(2)	C(17) - O(2)	1.20(2)
C(20) - C(21)	1.52(2)	C(21) - C(22)	1.40(2)
C(21) - C(26)	1.40(2)	C(22) - C(23)	1.37(2)
C(23) - C(24)	1.41(2)	C(24) - C(25)	1.36(2)
C(25) - C(26)	1.32(2)	C(27) - C(28)	1.52(2)
C(27) - O(1)	1.40(2)	C(28) - C(29)	1.38(3)
C(28) - C(33)	1.31(2)	C(29) - C(30)	1.34(3)
C(30) - C(31)	1.34(4)	C(31) - C(32)	1.34(3)
C(32) - C(33)	1.35(3)	C(3) - H(3)	0.99(3)

Table 7.5 Intramolecular bond angles in degrees.

C(2)-C(1)-C(10)	106.4(8)	C(1)-C(2)-C(3)	105.0(11)
C(2)-C(3)-C(4)	115.2(10)	C(2)-C(3)-C(5)	107.4(9)
C(4)-C(3)-C(5)	60.2(8)	C(3)-C(4)-C(5)	60.6(8)
C(3)-C(5)-C(4)	59.2(8)	C(3)-C(5)-C(6)	119.3(9)
C(3)-C(5)-C(10)	107.6(9)	C(4)-C(5)-C(6)	118.0(7)
C(4)-C(5)-C(10)	117.2(7)	C(6)-C(5)-C(10)	120.0(8)
C(5)-C(6)-C(7)	110.5(7)	C(5)-C(6)-O(1)	112.2(9)
C(7)-C(6)-O(1)	105.6(8)	C(6)-C(7)-C(8)	111.3(8)
C(7)-C(8)-C(9)	110.0(8)	C(7)-C(8)-C(14)	109.7(8)
C(9)-C(8)-C(14)	108.6(7)	C(8)-C(9)-C(10)	113.5(8)
C(8)-C(9)-C(11)	112.2(8)	C(10)-C(9)-C(11)	113.1(7)
C(1)-C(10)-C(5)	103.3(9)	C(1)-C(10)-C(9)	110.4(9)
C(1)-C(10)-C(19)	111.0(8)	C(5)-C(10)-C(9)	108.1(7)
C(5)-C(10)-C(19)	111.1(9)	C(9)-C(10)-C(19)	112.6(9)
C(9)-C(11)-C(12)	114.0(8)	C(11)-C(12)-C(13)	109.3(8)
C(12)-C(13)-C(14)	108.6(8)	C(12)-C(13)-C(17)	116.9(8)
C(12)-C(13)-C(18)	111.5(9)	C(14)-C(13)-C(17)	101.2(7)
C(14)-C(13)-C(18)	112.7(8)	C(17)-C(13)-C(18)	105.6(8)
C(13)-C(14)-C(15)	103.4(7)	C(8)-C(14)-C(15)	120.6(8)
C(8)-C(14)-C(13)	113.9(8)	C(14)-C(15)-C(16)	102.5(7)
C(15)-C(16)-C(17)	108.4(7)	C(15)-C(16)-C(20)	132.6(8)
C(17)-C(16)-C(20)	118.9(8)	C(13)-C(17)-C(16)	106.7(7)
C(13)-C(17)-O(2)	126.7(8)	C(16)-C(17)-O(2)	126.5(8)
C(16)-C(20)-C(21)	129.9(8)	C(20)-C(21)-C(22)	123.6(8)
C(20)-C(21)-C(26)	117.2(9)	C(22)-C(21)-C(26)	119.1(9)
C(21)-C(26)-C(25)	121.1(11)	C(28)-C(27)-O(1)	107.4(9)
C(27)-C(28)-C(29)	121.8(12)	C(27)-C(28)-C(33)	119.5(14)
C(29)-C(30)-C(31)	119.6(20)	C(30)-C(31)-C(32)	118.5(22)
C(31)-C(32)-C(33)	122.3(18)	C(28)-C(33)-C(32)	119.7(18)
C(6)-O(1)-C(27)	116.1(8)	C(4)-C(3)-H(3)	121.3(5)
C(5)-C(3)-H(3)	122.1(5)		

Table 7.6 Intramolecular torsion angles in degrees.

C(10)-C(1)-C(2)-C(3)	30.6(9)	C(2)-C(2)-C(10)-C(5)	-31.5(9)
C(2)-C(1)-C(10)-C(9)	83.9(10)	C(2)-C(1)-C(10)-C(19)	-150.6(12)
C(1)-C(2)-C(3)-C(4)	47.2(10)	C(1)-C(2)-C(3)-C5)	-17.5(9)
C(2)-C(3)-C(4)-C(5)	-96.4(11)	C(2)-C(3)-C(5)-C(4)	109.6(11)
C(2)-C(3)-C(5)-C(4)	-143.4(13)	C(2)-C(3)-C(5)-C(10)	-2.1(9)
C(4)-C(3)-C(5)-C(6)	107.0(11)	C(4)-C(3)-C(5)-C(10)	-111.7(10)
C(3)-C(4)-C(5)-C(6)	-109.2(11)	C(3)-C(4)-C(5)-C(10)	95.2(10)
C(3)-C(5)-C(6)-C(7)	89.2(11)	C(3)-C(5)-C(6)-O(1)	-153.2(12)
C(3)-C(5)-C(10)-C(1)	20.4(9)	C(3)-C(5)-C(10)-C(9)	-96.6(10)
C(3)-C(5)-C(10)-C(19)	139.4(11)	C(4)-C(5)-C(6)-C(7)	157.7(12)
C(4)-C(5)-C(6)-O(1)	-84.7(10)	C(4)-C(5)-C(10)-C(1)	-43.5(9)
C(4)-C(5)-C(10)-C(9)	-160.5(12)	C(4)-C(5)-C(10)-C(19)	75.5(10)
C(6)-C(5)-C(10)-C(1)	161.3(12)	C(10)-C(5)-C(6)-C(7)	-47.4(9)
C(6)-C(5)-C(10)-C(9)	44.4(9)	C(6)-C(5)-C(10)-C(19)	-79.6(10)
C(10)-C(5)-C(6)-O(1)	70.2(10)	C(5)-C(6)-C(7)-C(8)	52.8(9)
C(5)-C(6)-O(1)-C(27)	73.7(9)	O(1)-C(6)-C(7)-C(8)	-68.8(8)
C(7)-C(6)-O(1)-C(27)	-165.9(10)	C(6)-C(7)-C(8)-C(9)	-59.9(9)
C(6)-C(7)-C(8)-C(14)	-179.3(11)	C(7)-C(8)-C(9)-C(10)	58.9(9)
C(7)-C(8)-C(9)-C(11)	-171.4(11)	C(7)-C(8)-C(14)-C(13)	178.2(11)
C(7)-C(8)-C(14)-C(15)	-58.0(9)	C(14)-C(8)-C(9)-C(10)	178.9(11)
C(14)-C(8)-C(9)-C(11)	-51.3(8)	C(9)-C(8)-C(14)-C(13)	58.0(8)
C(9)-C(8)-C(14)-C(15)	-178.2(12)	C(8)-C(9)-C(10)-C(1)	-160.8(11)
C(8)-C(9)-C(10)-C(5)	-48.5(9)	C(8)-C(9)-C(10)-C(19)	74.6(10)
C(8)-C(9)-C(11)-C(12)	52.0(9)	C(11)-C(9)-C(10)-C(1)	69.8(9)
C(11)-C(9)-C(10)-C(5)	-177.9(11)	C(10)-C(9)-C(11)-C(12)	-178.0(12)
C(11)-C(9)-C(10)-C(19)	-54.8(9)	C(9)-C(11)-C(12)-C(13)	-54.1(9)
C(11)-C(12)-C(13)-C(14)	56.5(9)	C(11)-C(12)-C(13)-C(17)	170.1(12)
C(11)-C(12)-C(13)-C(18)	-68.3(9)	C(12)-C(13)-C(14)-C(8)	-61.6(9)
C(12)-C(13)-C(14)-C(15)	165.7(10)	C(12)-C(13)-C(17)-C(16)	-151.4(11)
C(12)-C(13)-C(17)-O(2)	30.0(10)	C(17)-C(13)-C(14)-C(8)	174.8(10)
C(17)-C(13)-C(14)-C(15)	42.1(8)	C(14)-C(13)-C(17)-C(16)	-33.8(8)
C(14)-C(13)-C(17)-O(2)	147.7(13)	C(18)-C(13)-C(14)-C(8)	62.4(9)
C(18)-C(13)-C(14)-C(15)	-70.3(9)	C(18)-C(13)-C(17)-C(16)	83.9(9)
C(18)-C(13)-C(17)-O(2)	-94.7(12)	C(8)-C(14)-C(15)-C(16)	-163.3(11)
C(13)-C(14)-C(15)-C(16)	-34.6(8)	C(14)-C(15)-C(16)-C(17)	13.8(8)
C(14)-C(15)-C(16)-C(20)	-169.5(15)	C(15)-C(16)-C(17)-C(13)	12.6(8)
C(15)-C(16)-C(17)-O(2)	-168.8(14)	C(15)-C(16)-C(20)-C(21)	-1.9(10)
C(20)-C(16)-C(17)-C(13)	-164.6(13)	C(17)-C(16)-C(20)-C(21)	174.5(17)
C(20)-C(16)-C(17)-O(2)	14.0(11)	C(16)-C(20)-C(21)-C(22)	-5.3(11)
C(16)-C(20)-C(21)-C(26)	174.8(17)	C(20)-C(21)-C(22)-C(23)	-179.5(16)
C(20)-C(21)-C(26)-C(25)	178.6(18)	C(26)-C(21)-C(22)-C(23)	0.4(11)
C(22)-C(21)-C(26)-C(25)	-1.4(12)	C(21)-C(22)-C(23)-C(24)	0.3(11)
C(22)-C(23)-C(24)-C(25)	-.1(12)	C(23)-C(24)-C(25)-C(26)	-.8(13)
C(24)-C(25)-C(26)-C(21)	1.6(12)	C(28)-C(27)-O(1)-C(6)	144.8(11)
C(1)-C(27)-C(28)-C(29)	121.9(15)	O(1)-C(27)-C(28)-C(33)	-60.6(13)
C(27)-C(28)-C(29)-C(30)	176.8(21)	C(27)-C(28)-C(33)-C(32)	-1.7(16)
C(28)-C(29)-C(30)-C(31)	1.6(17)	C(29)-C(30)-C(31)-C(32)	-.2(19)
C(30)-C(31)-C(32)-C(33)	-2.3(20)	C(31)-C(32)-C(33)-C(28)	3.2(19)

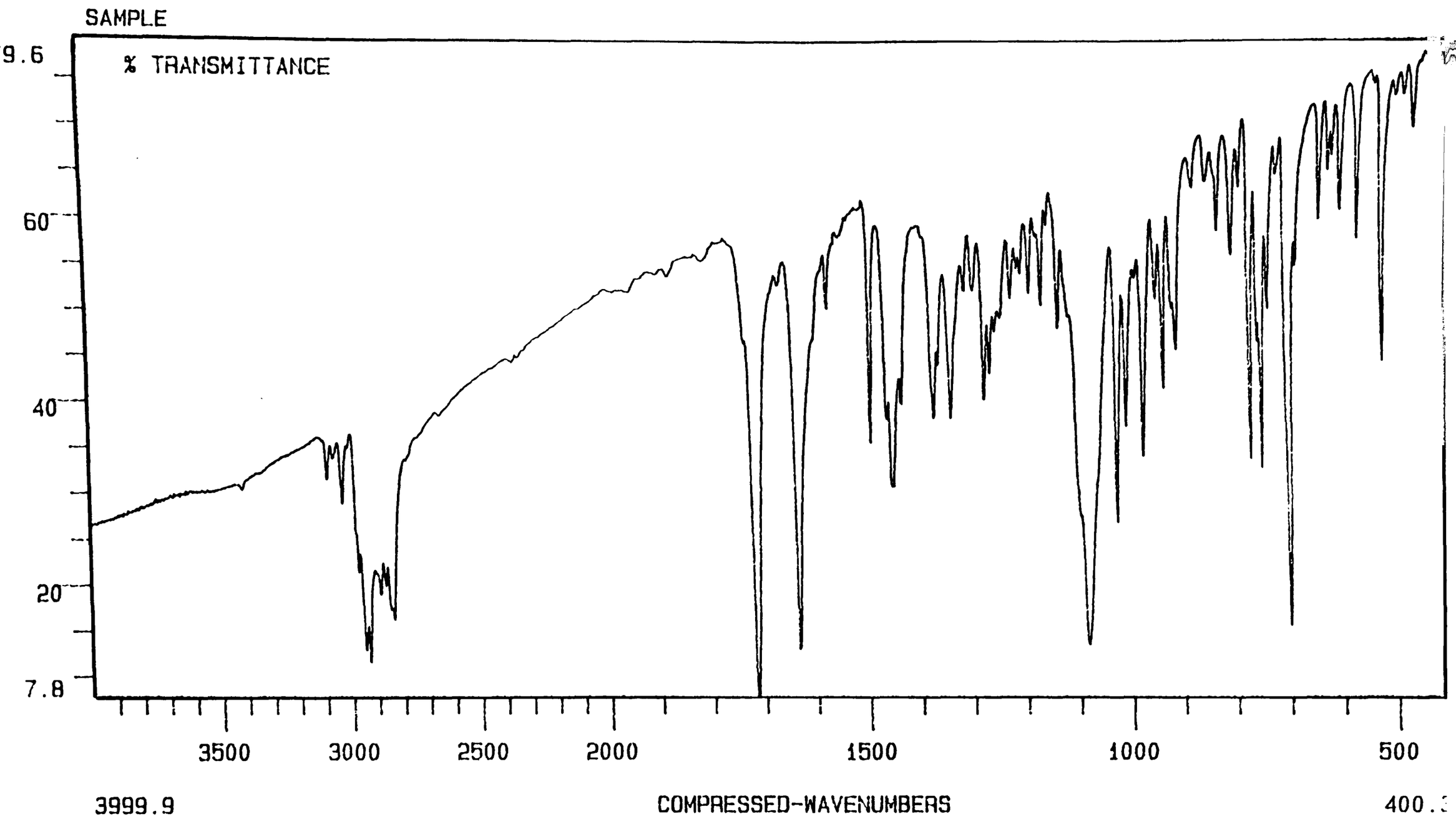

Figure 7.3 The steroid IR spectrum, identifying the presence of the isopropyl group.

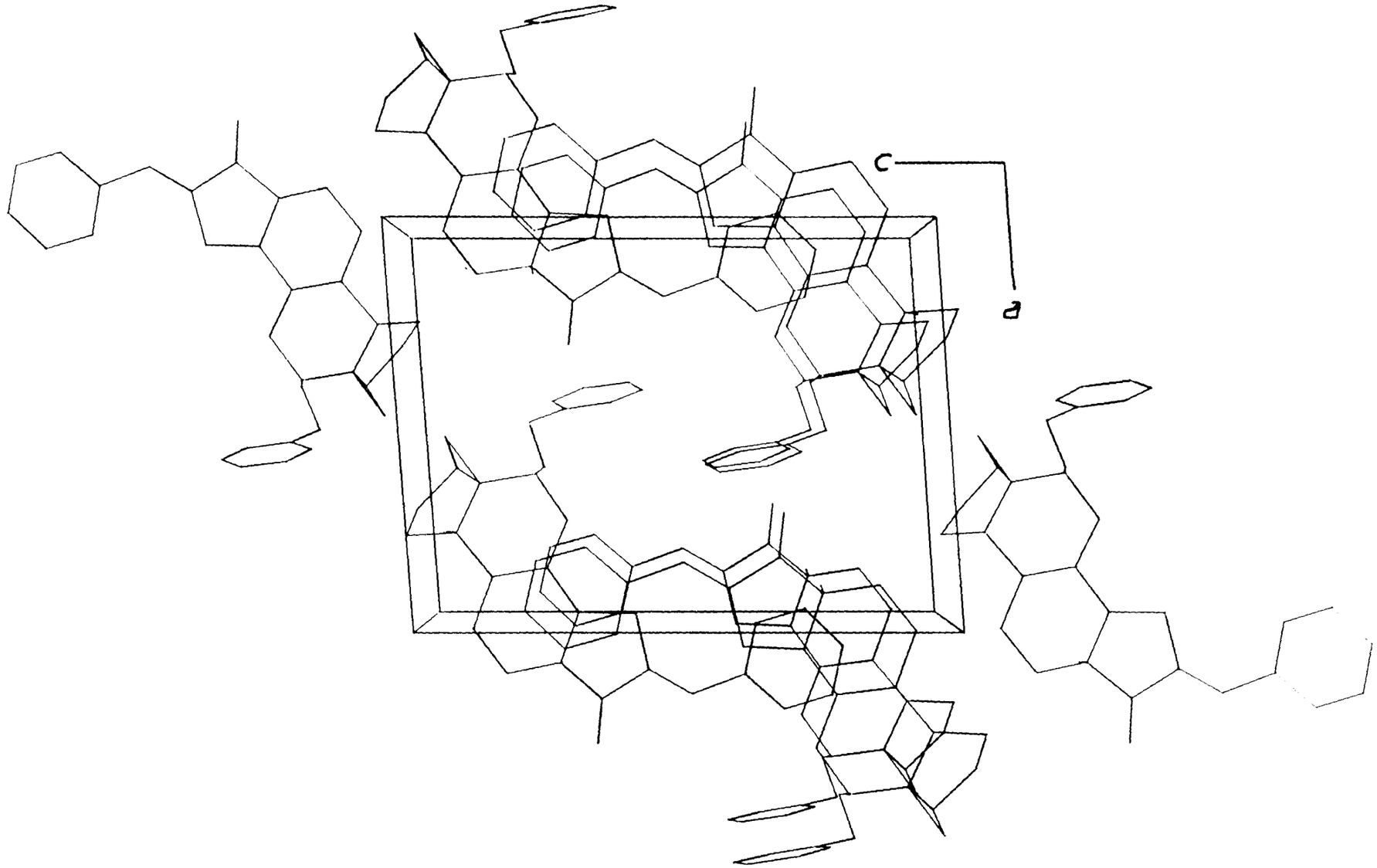

Figure 7.4 A packing diagram of the steroid viewed along the y-axis.

CHAPTER 8. X-ray crystal structure of Trineophyltin fluoride, $C_{30}H_{39}SnF$.

8.1 Introduction

$C_{30}H_{39}SnF$ is an organo-metallic compound, which is one of several multivalent tin atom structures synthesised in the Chemistry department of the University of Aberdeen. The main feature of interest of these compounds relates to the nature of the heavy atom bonding in the presence of various ligand groups.

The title material has been found to crystallise as a trigonal lattice system, but the absolute space group has yet to be determined unambiguously. The crystal system has exhibited signs of major disordering and so the final X-ray image produced by Fourier electron density maps is thought to represent a time averaged structure. The following analysis reviews several highly plausible scenarios, detailing the factors which led to their rejection and the final acceptance of the current structure. As will become clear, there are still possible alternative avenues of approach to the solution of this particular structure but given the obvious time restrictions of the research programme, not all have been pursued.

8.2 Experimental

8.2.1 Data collection

Data were collected on a colourless crystal of dimensions 0.24 x 0.18 x $0.8mm^3$, on a Nicolet P3 automated 4C-SXD using graphite monochromated Mo Kα X-radiation. The cell parameters and crystal orientation were determined from 14 independent reflexions with $2\theta<20^\circ$. A total of 2295 unique reflexions were measured over the hkl range ; $0 \leq \mathbf{h} \leq 22$, $0 \leq \mathbf{k} \leq 22$, $-15 \leq \mathbf{l} \leq 15$. The intensities were calculated from $\theta/2\theta$ scans, with $2\theta_{max}=60^\circ$. These data were corrected for Lorentz and polarisation effects. At the time of data

collection it was not thought that absorption effects were significant. Periodic monitoring of beam intensity during the data collection showed no signs of crystal decomposition. Data reduction techniques showed that 1069 reflexions had $\mathbf{F}>5\sigma(\mathbf{F})$. Examination of the final structure factor lists revealed that certain reflexions which are generally missing from trigonal crystal systems, due to systematic absences, had small non-zero values. To improve the quality of the data set all reflexions with $-h+k+l\neq 3n$ were removed.

8.2.2 Structure solution

The exact structure of this compound still remains uncertain, since there are several inconsistencies associated with the interpretation of the experimental data. All that can be ascertained is the best time averaged structure, which can describe the majority of the features discovered in the analysis. This is believed to have been largely due to a high level of disorder present in the crystal sample used for the data collection.

A systematic account of the steps involved in the determination of the most suitable space group is given below. In this case it is important to review all the trial structures used in the process of elimination which led to the currently preferred structure.

From the initial zero and first order Weissenberg photographs it was revealed that there were two possible sets of axes which could be assigned. These indicated that the crystal system could either be described by unique orthorhombic or trigonal cell parameters. The intensities and distribution of the spots along the festoons also suggested that the structure might have a centre of symmetry. The high symmetry trigonal lattice system was selected and data were collected

using indices based on the hexagonal axes.

It was assumed that the molecule would adopt a distorted bi-pyramidal arrangement with a 3-fold rotational symmetry. Similar arrangements were found in the related structures of chlorotrineophylstannane and chlorotris[(dimethylphenylsilyl)methyl]stannane[78]. Crystal density calculations based on the molecular formula found the number of molecules per unit cell to be equal to six. Given the high symmetry of the molecules and the number of molecules per unit cell, the number of suitable space groups was restricted to $R\bar{3}$ and R3.

Due to the presence of the Sn atoms in the structure and of the high symmetry space group, the most favourable analytical method for the elucidation of the structure was the Patterson vector map technique employing SHELX-76. The level of disordering present in the structure prevented Direct methods from producing consistent phases.

8.2.2.1 R3 (no.148)

Each of the ligands attached to the Sn atom were assumed to be identical, thus producing a 3-fold rotational symmetry axis about the Sn atom. All non-primitive trigonal lattice systems are characterised by the presence of the three fold symmetry axes, perpendicular to the z -axis, with the X and Y coordinates (0,0), (1/3,2/3) and (2/3,1/3). Therefore, it was concluded that pairs of molecules, positioned about a centre of symmetry, would occupy each of the special axes producing 18 asymmetric units per cell. A similar situation was found to exist for the related compound $[(CH_3)_3SiCH_2]_3SnF$ which lies on the (0,0) axis of a primitive trigonal lattice[79].

The solution of a strong Patterson vector revealed the coordinates of a large non-origin peak at (0,0,0.304). This was assumed to be a Sn

atom. Difference synthesis indicated that another sizable atom was located on the same symmetry axis at (0,0,0.1700). The separation of these two atom sites was 2.2 Å, which closely resembles the sum of covalent radii of Sn and F at 2.17 Å[79]. Both of these atoms were refined each with a site occupation factor (SOF) of 1/3. Repeated difference synthesis gradually revealed all of the C atoms of the ligand, which were given a SOF equal to unity. All atoms at this stage were refined with isotropic thermal parameters converging with R=0.12. At this point in the refinement there was still a great deal of unaccounted electron density around the Sn atom, despite having accounted for all 12 non-hydrogen atoms in the assumed asymmetric unit.

The most significant unaccounted peak was also positioned on the three fold axis at (0,0,0.473), with a separation from the Sn of approximately 2 Å. The weight of this peak indicated that it may be another F atom, F(2). The addition of F(2) to the asymmetric unit contradicted the molecular formula with the F site occupations held at 1/3. However, if the molecules formed polymeric chains extending along the z-axis, each F atom would be shared by adjoining molecules, giving SOF's of 1/6. In this arrangement the number of axial atoms per asymmetric unit satisfied the molecular formula.

The adapted model was refined, with F(1) and F(2) both assuming SOF's of 1/6, which resulted in improved temperature factors on account of effectively reducing the electron density by half. However, the bond lengths did not refine significantly and remained unequal, thus challenging the centre of symmetry.

The polymer chain model was therefore considered to be unsuitable.

This was verified by considering the repeat unit length extending along the z-axis. With a repeat unit every two molecules, the c-axis would measure approximately 8.7 Å. However, the c-axis was reliably determined, by a refinement process during the data collection on the 4C-SXD, to be 12.08 Å. This indicated that it was not possible to have a situation where both F atoms are shared by adjacent asymmetric units.

8.2.2.2 R3 (no.146)

From the evidence gathered from the $R\bar{3}$ model, it appeared that the asymmetric unit was greater than one ligand and possessed pseudo-symmetry. Assuming the space group R3, the asymmetric unit contained twice the number of atoms, incorporating two staggered ligands bonded to separate Sn atoms stacked one above the other on a symmetry axis. Solution of a few Patterson vectors revealed the presence of a strong peak at coordinates (2/3,1/3,1/3). Due to the peak height associated with these coordinates, it was assumed to be a Sn atom. The Sn atom, Sn(1), was positioned on the axis, with the X and Y coordinates fixed to prevent the atom from drifting away from the axis. Further difference synthesis revealed another Sn atom at coordinates (2/3,1/3,0.722) with a separation from Sn(1) of 4.7 Å. With the second Sn atom, Sn(2), introduced to the model, a difference synthesis revealed three other significant peaks with coordinates of (2/3,1/3,0.141), (2/3,1/3,0.526) and (2/3,1/3,0.913). The centre peak, positioned approximately midway between Sn(1) and Sn(2), was most intensely represented on the map being almost twice the amplitude of the other two. All three atoms were assumed to be F atoms.

The arrangement of the three F atoms, F(1), F(2) and F(3), per

asymmetric unit also contradicted the molecular formula. The fact that both $R\bar{3}$ and R3 produced models which disagreed with the molecular formula, was considered to be very significant. Both seemed to suggest that the X-ray structures were in fact time averaged images, produced by disordering. The centrally bonded three fluorine model is shown in Figure 8.1, with F(3) positioned in an ideal position.

Full matrix least squares calculations were performed on the five atoms, all with isotropic thermal parameters and the fine structure of the two ligands were successfully determined from repeated difference synthesis. The thermal parameters of the F atoms gave cause for concern due to their high values.

Satellite clusters of electron density were observed close to the Sn atoms along the 3-fold axis. By refining the structure with the Sn atoms described by anisotropic thermal parameters these pockets of surplus electron density were incorporated by the Sn atoms' thermal ellipsoids. However the temperature factors of the F atoms remained high and their positions along the 3-fold axis remained unstable. F(3) had virtually all its thermal motion in a plane perpendicular to the symmetry axis which contrasts with the anticipated spread of electron density along the axis between the Sn atoms. This fact further indicated that the model was incomplete. The thermal parameters of the C atoms were also found to be high and so it was concluded that disorder was indeed present in the crystal. It was expected that the flexible ligands would experience some freedom of movement, but this could not account for the imbalance of the F atoms.

Due to the greater density of electrons on the F(3) site, this indicated either the presence of another atom of twice the atomic mass

of F, or that the occupation of the site was twice that of the other F atoms.

By assuming as before, that F(3) had an occupancy of 1/3 and F(1) and F(2) had occupancies of 1/6, this agreed with the molecular formula and the symmetry conditions of R3. The physical interpretation of this can be explained by three possible scenarios.

(i) Discrete disordered molecules

This structure however does begin to make sense when it is considered to be a time averaged structure. It was proposed that two possible orientations of the molecules were possible, as shown in Figure 8.2. In the first case, orientation A, F(1) and F(2) are bonded to Sn(1) and Sn(2) respectively, with F(1) placed approximately midway between the two Sn atoms. The second model, B, has the same bonding as before, but features F(2) placed between the Sn atoms. In both orientations, there is always one F atom centrally placed between the Sn atoms. If both orientations were to be present in the crystal simultaneously, then both would contribute to the X-ray diffraction pattern. As a result four possible F positions would exist. The two positions in the centre would overlap, thus producing a large central region of electron density. If the occurrence of either conformation were equally likely, then the central peak would appear to be approximately twice the strength of the other two peaks.

(ii) The complex cation

One anomaly of the highly disordered discrete molecule model was the relatively well defined sites of the ligands. Comparison of the F(1)-Sn(1)-C(1) and F(2)-Sn(2)-C(1)' angles of 76.6 and 92.4° respectively, in orientation A gave a clue to a more plausible

explanation of the disorder mechanism. The two molecules were expected to adopt identical distorted bi-pyramidal arrangements. If the molecule were to be inverted, the positions of the ligand atoms would differ from those of the opposite orientation. However, no strong evidence of ligand disordering was detected.

An alternative disordered model was proposed, where the molecule was assumed to form the complex cation $[(C_{10}H_{13})_3\text{-Sn-F-Sn-}(C_{10}H_{13})_3]^+ F^-$ as shown in Figure 8.3. Previously, compounds of the form R_3SnF have shown mixed covalent/ionic bonding between adjacent Sn atoms with Sn-F bonds ranging from 2.15 to 2.565 Å[80-83]. In this case a F atom is bonded midway between the two Sn atoms with a typical Sn-F bond length of 2.38 Å. The cation is therefore electrostatically balanced by the F^- ion, which can occupy both peripheral sites with equal probabilities.

(iii) Trapped oxygen model

An IR analysis was performed (shown in Figure 8.4), revealing the possibility of a Sn-O bond at 491.91 cm^{-1}. It was proposed that the a H_2O molecule could have become trapped between the two Sn atoms restricting its movement to along the z-axis. In this configuration the two F atoms were assumed to occupy the positions of F(1) and F(2). A refinement of this model however, failed to produce any improvement over the centrally bonded model. Both F atom positions remained very unstable and the thermal parameters assumed unrealistically high values.

8.2.2.3 P3 (no.143)

To determine whether the disorder of the F atoms was a random long range effect throughout the crystal or if the two positions are

equally represented in all unit cells, the primitive cell P3 was selected. The primitive cell relaxes the symmetry operators and reduces the contents of the entire unit cell to one asymmetric unit. It was hoped that all six molecules could be identified and therefore establish the nature of the disorder.

Great difficulty was experienced in trying to reveal the entire unit cell contents. In total this amounted to 192 non-hydrogen atoms or approximately 770 variables when refined isotropically. The Sn atoms were found on the expected special positions, but the essential F and C positions could not be determined from the difference map. This refinement proved to be inconclusive.

8.2.3 Structure refinement

It was finally decided to refine the structure as the complex cation model with R3 space group (Figure 8.3). The central F atom, F(1) was constrained to occupy a position midway between the Sn atoms at (2/3,1/3,0.529) with a SOF of 1/3. The F ions, F(2) and F(2)', were fixed at (2/3,1/3,0.141) and (2/3,1/3,0.913) respectively, with SOF's of 1/6. Repeated Fourier difference synthesis maps revealed the positions of the remaining C atoms. The presence of the heavy atoms in the structure prevented the H atoms from being observed from the difference map and so were introduced to the model in calculated positions. The Sn atoms were refined with anisotropic thermal parameters, whilst the other remaining atoms were assigned isotropic parameters. The level of disorder in the crystal under analysis, prevented realistic anisotropic thermal parameters to be assigned to non-tin atoms.

The cyclic carbons in each ligand (C(6)-C(7)-C(8)-C(9)-C(10)) were

constrained to refine collectively as a regular hexagon, with bond lengths and angles of 1.395 Å and 120° respectively.

All H atoms were constrained to ride on their bonded C atoms and were refined with one common isotropic temperature factor. The final converged structure produced a residual of 0.08 for the reduced data set with unit weights. The value of Δ/σ=0.3 indicates that structure is unstable. This is to be expected, since the final model represents only one of the two structures described by the data set. Final $\Delta\rho_{max}$=0.1 eÅ^{-3} and $\Delta\rho_{min}$=-0.1 eÅ^{-3}.

8.3 Results

8.3.1 Crystal and diffraction data

$C_{30}H_{39}SnF$, **M**$_r$=537.33, trigonal, R3, **a**=19.837(14), **c**=12.088(7) Å, **γ**=120°. Mo **Kα**, **λ**=0.71069 Å, **V**=4119(5)Å^3, **Z**=6, **D**$_x$=1.30gcm^{-3}, **T**=293 K, **F(000)**=1668, **μ**=8.62 cm^{-1}, **R**=0.081 for 1069 unique reflexions.

8.3.2 Structure analysis

The final accepted structure of the asymmetric unit, shown in Figure 8.5, consists of two Sn atoms bridged by a F atom creating a complex cation. The F^- ion can assume the positions of either F(2) or F(2)'. The two hydrocarbon ligands (one bonded to either Sn) are staggered in a low energy conformation some 30° apart. Figure 8.6 presents the whole complex minus the hydrogen atoms, viewed along the z-axis, which exhibits the apparent pseudosymmetry reflected by the rotation photographs and the X-ray data set.

The fractional coordinates, anisotropic thermal parameters, relevant bond lengths, bond angles and torsion angles for the asymmetric unit are tabulated in Tables 8.1, 8.2, 8.3, 8.4 and 8.5 respectively.

The Sn-F(1) bond length was found to be 2.38(5) Å, which is

considerably longer than the sum of the covalent radii of 2.17 Å. The bridging F atom has a bond length more comparable with those of polymeric Sn..X..Sn..X chains where the bond is of a mixed covalent/ionic nature[79]. In these cases the Sn..Sn separation has been approximately 5 Å. and the strength of the Sn-F interaction has the effect of changing the coordination of the Sn to a trigonal bi-pyramidal. Where the Sn...Sn separation is longer, the central halide atom bonds covalently to one of the two Sn atoms in an off centre position[84]. In the title compound the Sn..Sn separation of only 4.74(5) Å suggests that the mixed covalent/ionic bonding is present inducing an overall positive charge. The two F-Sn-C(1) angles were found to be 87.6(9) and 76.6(1)° confirming the effect of Sn-F interaction. These values compare with other related halide-tin compounds, existing as discrete molecules, with C-Sn-Cl angles of 99.7(2) and 104.3(2)°[78] and C-Sn-F angles of 104.6(3), 98.9(4) and 99.5(4)°[85].

As previously mentioned, the anisotropic thermal ellipse of F(1) was found to be disc-like perpendicular to the z-axis. In the case of $[(CH_3)_3SiCH_2]_3SnF$[79], the electron distribution was found to be spread along the axis. No suitable explanation could be provided for this anomaly, but it is thought that the quality of the experimental data, which was not corrected for absorption effects, could be to blame.

The F ions, F(2) and F(2)', positioned at 2.32 and 2.27 Å from the Sn centres were closer than was expected, but given the poor thermal parameters and dramatic shifts along the z-axis during the refinement, these values are acceptable.

The bond lengths and bond angles in the cyclic rings were constrained

to assume perfect hexagons with C-C bond lengths of 1.395 Å. However the radii of the isotropic thermal spheres are noted to be abnormally large. This has been due to the highly flexible ligand permitting free movement, blurring the electron density. The other C bond lengths in the ligand groups correspond to accepted values within the normal error margins of three e.s.d's. Ligand B exhibits the majority of the questionable parameters. The H atom coordinates were not included in the tables, since their calculated positions relative to the constrained C atoms are purely theoretical.

8.4 Discussion

The relative merits of the structures were previously discussed in 8.2.2, describing the feasibility of each in terms of symmetry. Each of the structures can be simply compared by examining the final residuals listed in Table 8.6.

Although it is incorrect to simply judge the validity of a presumed crystal structure by the value of the residual factor, the values listed in Table 8.6 clearly indicate that the molecular symmetry is best described by the R3. However, the exact positioning of the F atoms and the disordering mechanism is less certain. Both of the possible mechanisms discussed could account for certain features of the calculated electron distribution, but neither model could be refined to give acceptable parameters without applying positional constraints.

With the level of information contained within the experimental structure factor amplitudes, the absolute molecular structure cannot be defined unambiguously. However from the final molecular geometries, it is thought that the molecule exists in the complex cation form.

The lack of systematic absences ($-h+k+l \neq 3n$) in the observed structure factor list seems to indicate that this was a direct effect of the disordering or that the crystal quality was poor. Clearly there is still sufficient scope for a future project to determine the absolute molecular configuration. It may be possible to re-examine this compound using a different sample and possibly a higher resolution diffractometer. The use of neutrons in a low temperature environment may provide the additional information regarding non-tin atom positions.

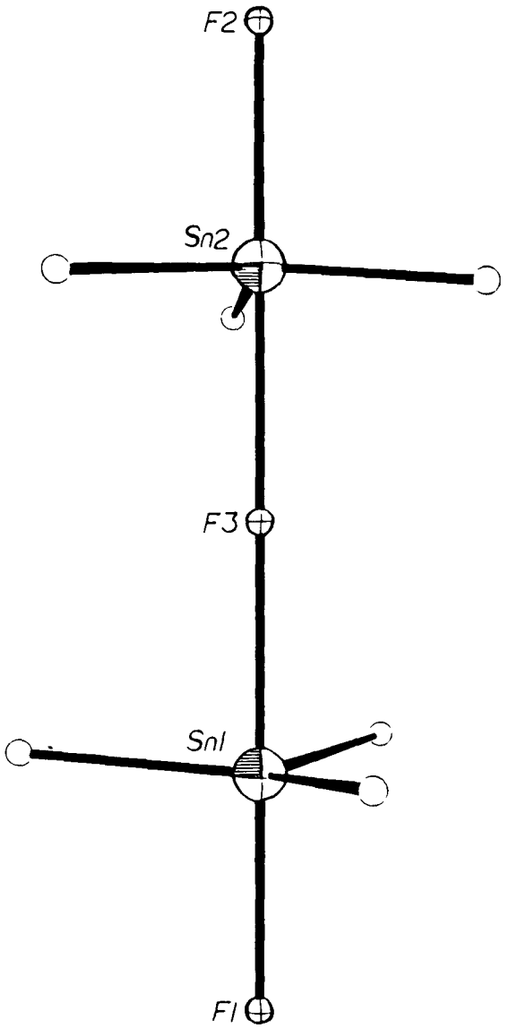

Figure 8.1 The three F model. The ligands are represented by single atoms.

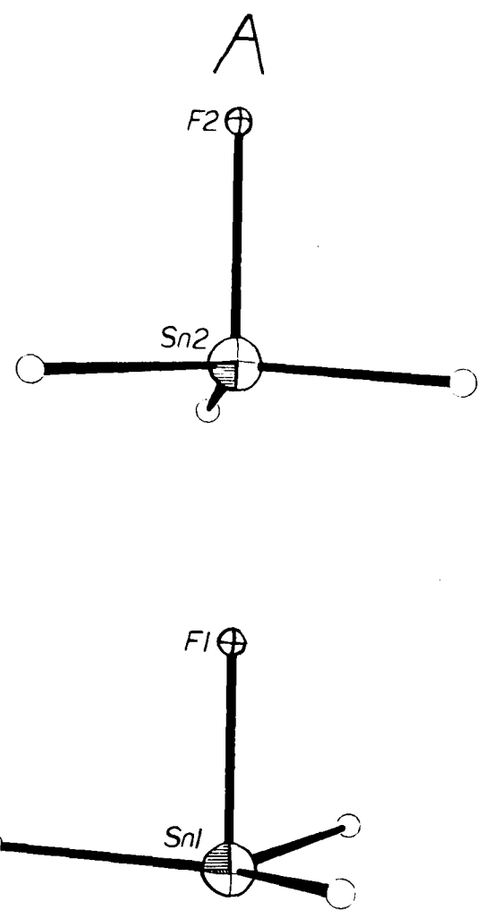

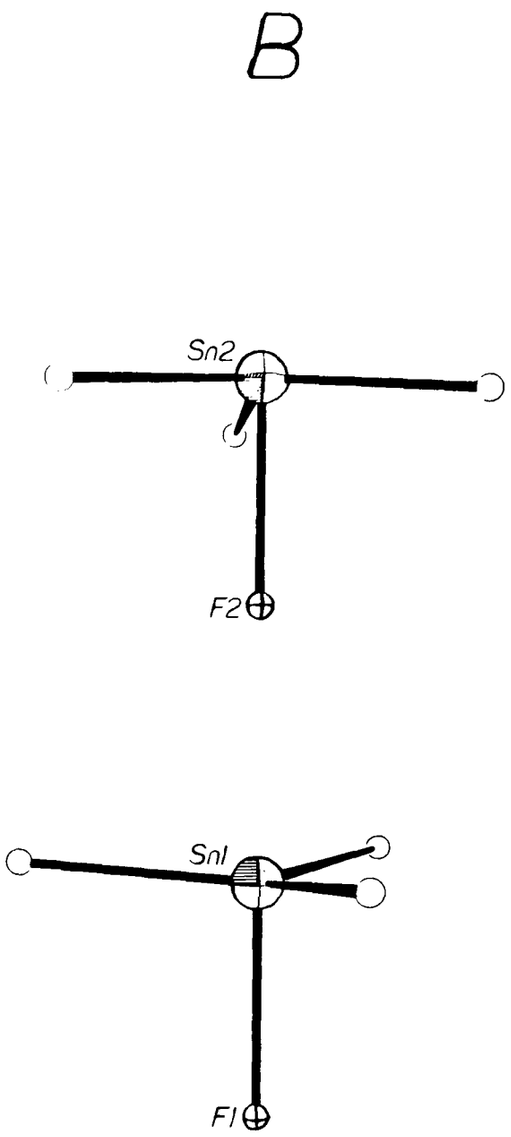

Figure 8.2 The two possible molecule orientations of the disordered discrete molecule model.

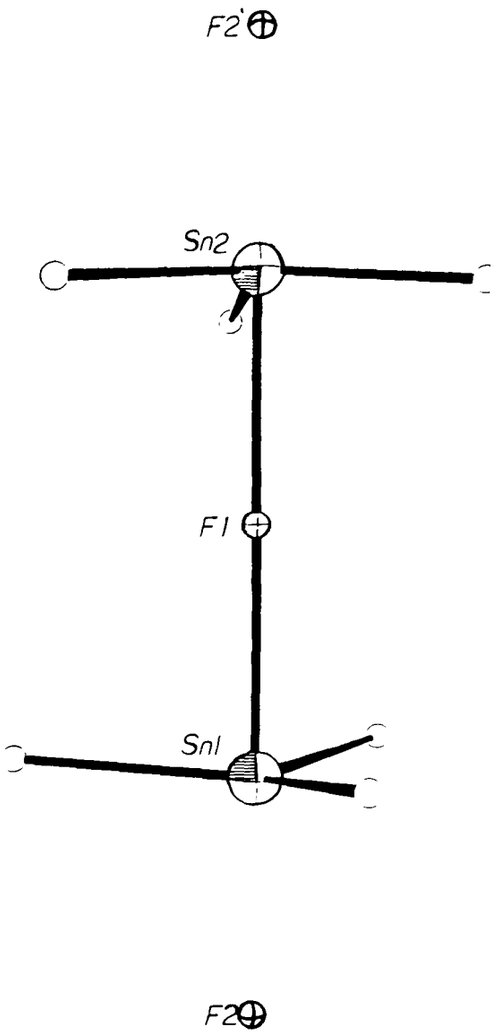

Figure 8.3 The complex cation model

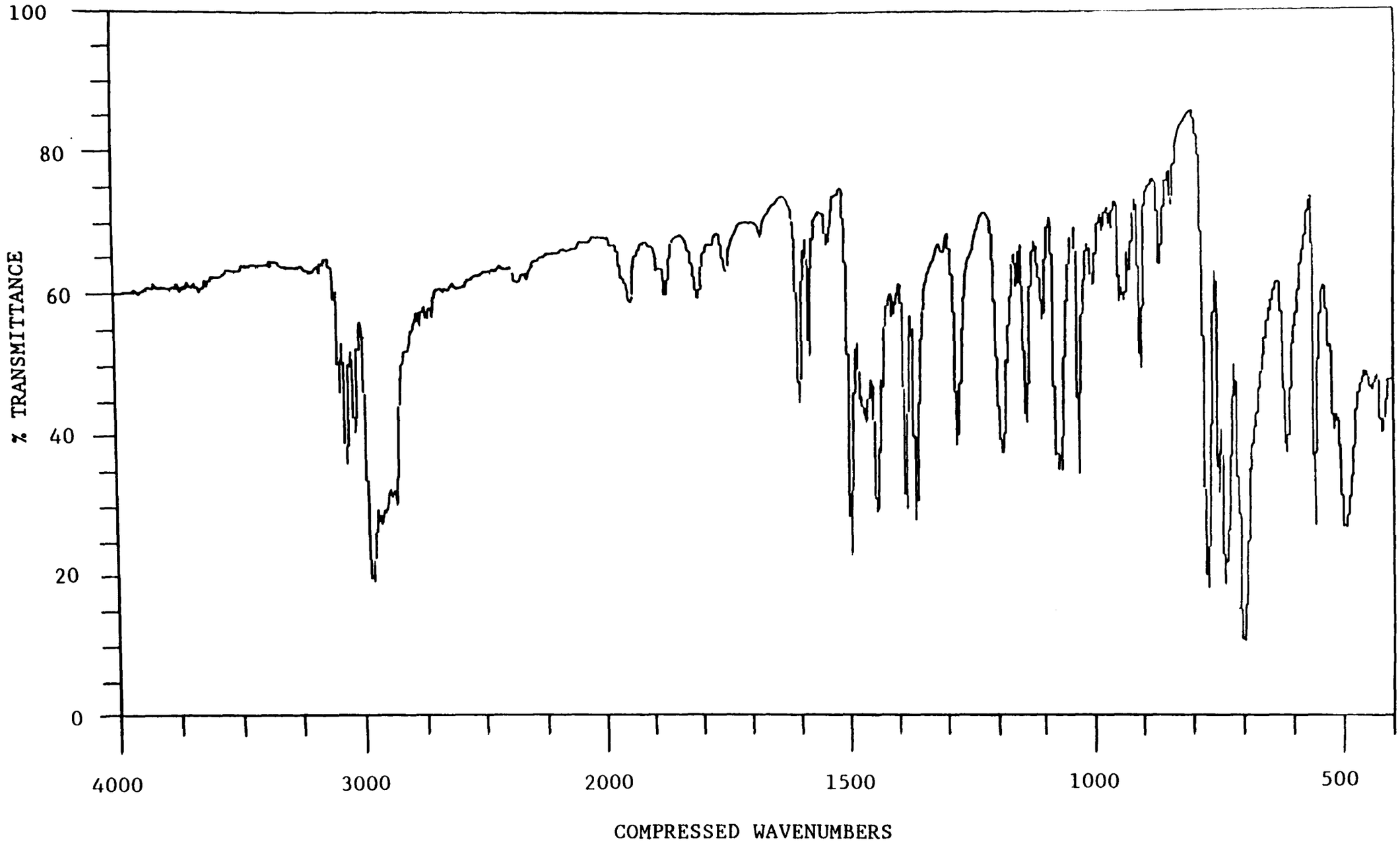

Figure 8.4 The IR spectrum which revealed the possibility of the Sn-O bond.

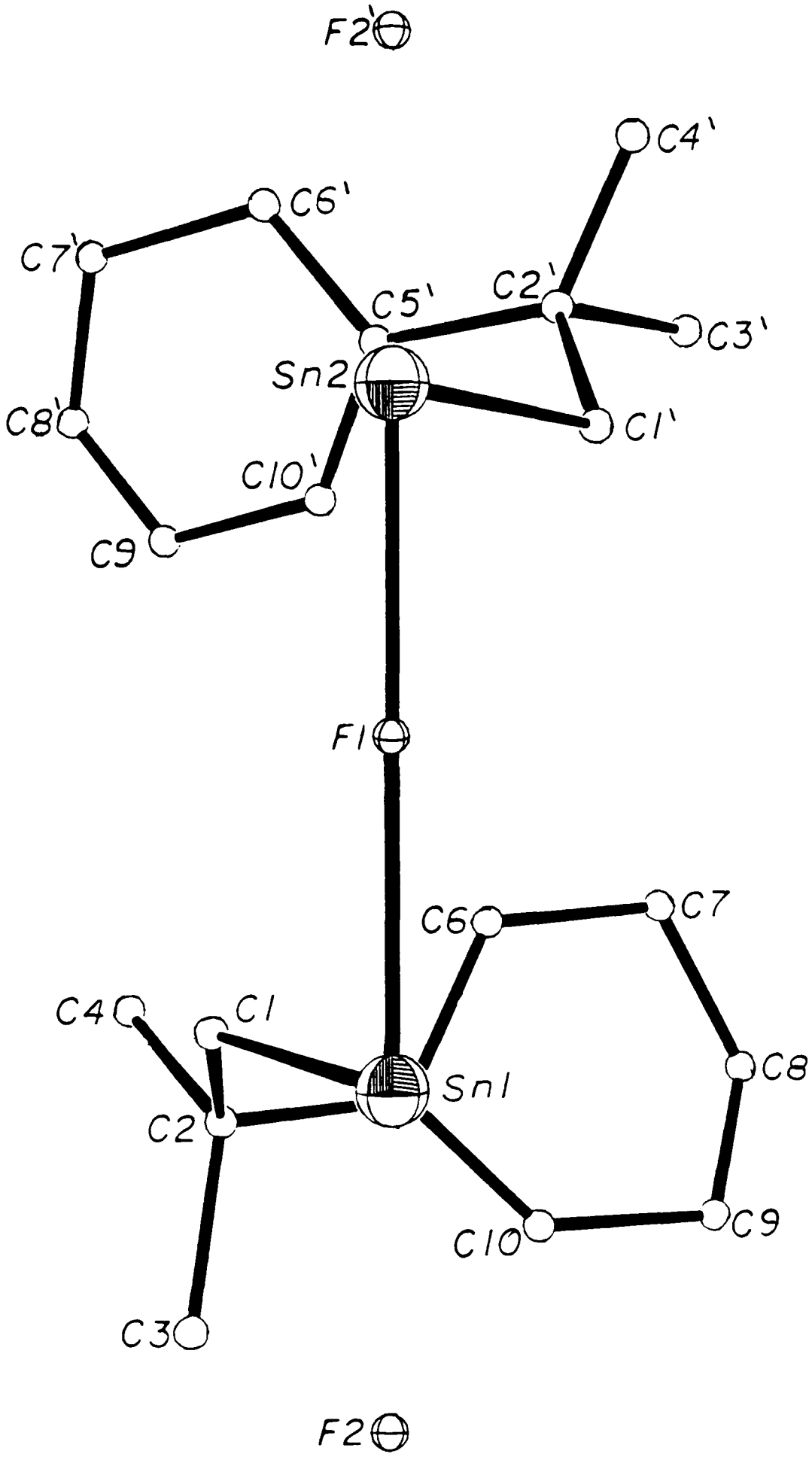

Figure 8.5 The complete asymmetric unit of the complex cation, minus the hydrogens.

Figure 8.6 The complex cation viewed along the z axis. A 3 fold rotation has been performed to generate the whole molecule.

Table 8.1 Fractional atomic coordinates and thermal parameters of the non-hydrogen atoms within the asymmetric unit, where * denotes one of two possible F locations. ($U_{eq}=1/3\sum_i\sum_j U_{ij}a_i{*}a_j{*}a_i{\bullet}a_j$)

	(X/A)	(Y/B)	(Z/C)	U_{eq}
Sn(1)	0.6666	0.3333	0.3333	0.092
Sn(2)	0.6667	0.3333	0.7254(5)	0.088
F(1)	0.667	0.333	0.529(4)	0.22(2)
F(2)*	0.667	0.333	0.141(2)	0.11(1)
C(1)	0.7502	0.4510	0.3742	0.17(2)
C(2)	0.810(2)	0.497(2)	0.276(3)	0.10(1)
C(3)	0.782(3)	0.493(3)	0.171(4)	0.13(2)
C(4)	0.856(4)	0.579(3)	0.294(5)	0.22(4)
C(5)	0.8683(16)	0.4261(15)	0.2856(20)	0.11(1)
C(6)	0.9024(16)	0.4623(15)	0.3866(20)	0.14(2)
C(7)	0.9452(16)	0.4243(15)	0.3967(20)	0.15(2)
C(8)	0.9538(16)	0.3860(15)	0.3058(20)	0.12(1)
C(9)	0.9197(16)	0.3857(15)	0.2047(20)	0.14(2)
C(10)	0.8789(16)	0.4238(15)	0.1946(20)	0.11(1)
C(1)'	0.6607(19)	0.4420(19)	0.7176(28)	0.082(9)
C(2)'	0.6050(16)	0.4506(15)	0.7807(24)	0.061(7)
C(3)'	0.6140(17)	0.5292(17)	0.7388(29)	0.071(9)
C(4)'	0.635(3)	0.476(3)	0.902(4)	0.12(2)
C(5)'	0.5236(9)	0.3842(9)	0.7672(11)	0.040(5)
C(6)'	0.4794(9)	0.3390(9)	0.8562(11)	0.060(7)
C(7)'	0.4037(9)	0.2780(9)	0.8389(11)	0.060(9)
C(8)'	0.3723(9)	0.2621(9)	0.7324(11)	0.07(1)
C(9)'	0.4165(9)	0.3073(9)	0.6434(11)	0.078(8)
C(10)'	0.4992(9)	0.3684(9)	0.6606(11)	0.063(7)

Table 8.2 Anisotropic thermal parameters of the Sn atoms within the asymmetric unit.

	U11	U22	U33	U23	U13	U12
Sn(1)	0.048(2)	0.048(2)	0.164(7)	0.024(1)	0.000	0.000
Sn(2)	0.047(2)	0.047(2)	0.155(6)	0.023(1)	0.000	0.000

Table 8.3 Intramolecular atom bond lengths in angstroms.

Sn(1)-F(1)	2.37	Sn(2)-F(1)	2.37
Sn(1)-F(2)	2.32	Sn(2)-F(2)'	2.27
Sn(1)-C(1)	2.13(8)	Sn(2)-C(1)'	2.22(4)
C(1)-C(2)	1.61(4)	C(1)'-C(2)'	1.42(5)
C(2)-C(3)	1.38(7)	C(2)'-C(3)'	1.56(5)
C(2)-C(4)	1.42(7)	C(2)'-C(4)'	1.57(6)
C(2)-C(5)	1.62(5)	C(2)'-C(5)'	1.50(4)
C(5)-C(6)	1.40(4)	C(5)'-C(6)'	1.39(3)
C(6)-C(7)	1.40(4)	C(6)'-C(7)'	1.39(3)
C(7)-C(8)	1.39(4)	C(7)'-C(8)'	1.39(3)
C(8)-C(9)	1.39(4)	C(8)'-C(9)'	1.40(3)
C(9)-C(10)	1.39(4)	C(9)'-C(10)'	1.49(3)
C(10)-C(5)	1.39(4)	C(10)'-C(5)'	1.36(3)

Table 8.4 Intramolecular bond angles in degrees.

F(1)-Sn(1)-C(1)	76.6(1)	F(1)-Sn(2)-C(1)'	87.6(9)
Sn(1)-C(1)-C(2)	113.7(14)	Sn(2)-C(1)'-C(2)'	121.0(22)
C(1)-C(2)-C(3)	118.7(32)	C(1)'-C(2)'-C(3)'	103.7(25)
C(1)-C(2)-C(4)	113.9(37)	C(1)'-C(2)'-C(4)'	110.8(28)
C(1)-C(2)-C(5)	100.6(23)	C(1)'-C(2)'-C(5)'	113.4(23)
C(3)-C(2)-C(4)	103.1(41)	C(3)'-C(2)'-C(4)'	98.1(26)
C(3)-C(2)-C(5)	113.3(33)	C(3)'-C(2)'-C(5)'	112.1(22)
C(4)-C(2)-C(5)	107.1(36)	C(4)'-C(2)'-C(5)'	116.9(26)
C(2)-C(5)-C(6)	120.6(25)	C(2)'-C(5)'-C(6)'	122.4(17)
C(2)-C(5)-C(10)	119.1(25)	C(2)'-C(5)'-C(10)'	114.2(17)
C(5)-C(6)-C(7)	120.0(24)	C(5)'-C(6)'-C(7)'	120.0(15)
C(6)-C(7)-C(8)	120.0(24)	C(6)'-C(7)'-C(8)'	120.0(14)
C(7)-C(8)-C(9)	120.0(26)	C(7)'-C(8)'-C(9)'	120.0(15)
C(8)-C(9)-C(10)	120.0(24)	C(8)'-C(9)'-C(10)'	119.9(13)
C(5)-C(10)-C(9)	120.0(24)	C(5)'-C(10)'-C(9)'	116.2(14)
C(6)-C(5)-C(10)	120.0(26)	C(6)'-C(5)'-C(10)'	123.2(15)

Table 8.5 Intramolecular torsion angles in degrees.

F(1)-Sn(1)-C(1)-C(2)	-20.9(16)	F(2)-Sn(2)-C(1)'-C(2)'	130.8(26)
Sn(1)-C(1)-C(2)-C(3)	46.8(31)	Sn(2)-C(1)'-C(2)'-C(3)'	-172.8(32)
Sn(1)-C(1)-C(2)-C(4)	168.5(40)	Sn(2)-C(1)'-C(2)'-C(4)'	82.9(30)
Sn(1)-C(1)-C(2)-C(5)	-77.3(19)	C(5)'-C(2)'-C(1)'-Sn(2)	-51.0(21)
C(1)-C(2)-C(5)-C(6)	-52.2(25)	C(1)'-C(2)'-C(5)'-C(6)'	121.2(30)
C(1)-C(2)-C(5)-C(10)	120.8(31)	C(1)'-C(2)'-C(5)'-C(10)'	-54.0(24)
C(2)-C(5)-C(6)-C(7)	173.0(40)	C(2)'-C(5)'-C(6)'-C(7)'	179.8(26)
C(2)-C(5)-C(10)-C(9)	-173.1(40)	C(2)'-C(5)'-C(10)'-C(9)'	-175.1(23)
C(3)-C(2)-C(5)-C(6)	-180.0(46)	C(3)'-C(2)'-C(5)'-C(6)'	-121.7(28)
C(3)-C(2)-C(5)-C(10)	-6.9(32)	C(3)'-C(2)'-C(5)'-C(10)'	63.1(22)
C(4)-C(2)-C(5)-C(6)	67.0(39)	C(4)'-C(2)'-C(5)'-C(6)'	-9.6(24)
C(4)-C(2)-C(5)-C(10)	-119.9(43)	C(4)'-C(2)'-C(5)'-C(10)'	175.2(32)
C(5)-C(6)-C(7)-C(8)	0.0(25)	C(5)'-C(6)'-C(7)'-C(8)'	0.2(15)
C(6)-C(7)-C(8)-C(9)	0.0(25)	C(6)'-C(7)'-C(8)'-C(9)'	-.2(15)
C(6)-C(5)-C(10)-C(9)	0.0(25)	C(6)'-C(5)'-C(10)'-C(9)'	9.8(15)
C(7)-C(8)-C(9)-C(10)	0.0(25)	C(7)'-C(8)'-C(9)'-C(10)'	4.8(15)
C(8)-C(9)-C(10)-C(5)	0.0(25)	C(8)'-C(9)'-C(10)'-C(5)'	-9.4(15)
C(10)-C(5)-C(6)-C(7)	0.0(25)	C(10)'-C(5)'-C(6)'-C(7)'	-5.5(16)

Table 8.6 Final residuals of the proposed models. (Note P3 model residual was calculated on Sn and selected F positions.)

SPACE GROUP	ASYMMETRIC UNIT	RESIDUAL
R3 (complex)	2 x Sn ; sof=1/3 1 x F ; sof=1/3 2 x F ; sof=1/6 20 x C ; sof=1 16 x H ; sof=1	8%
$R\bar{3}$	1 x Sn ; sof=1/3 2 x F ; sof=1/6 10 x C ; sof=1 13 x H ; sof=1	13%
P3	6 x Sn ; sof=1 6 x F ; sof=1 180 x C ; sof=1 234 x H ; sof=1	22%
R3 (trapped O)	2 x Sn ; sof=1/3 2 x F ; sof=1/3 1 x O ; sof=1/3 20 x C ; sof=1 16 x H ; sof=1	10%

CHAPTER 9. X-ray crystal structure of (2-carbomethyoxyethyl)-iododiphenylstannane, $C_{16}H_{17}O_2SnI$.

9.1 Introduction

In addition to the obvious covalent bonding in the molecular structure of a compound, there are other more subtle interactions between neighbouring atoms. Weak interactions arising from mild dipoles in molecules are obvious sites for attack in chemical reactions.

In $C_{16}H_{17}O_2SnI$ it is these fairly long range weak interactions which were of interest to both the chemists and the crystallographers involved. There exists an intramolecular complex, which is created by the mild dipole of the C(15)-O(1) double bond and the central Sn atom. The strongly electronegative oxygen atom creates a electron acceptor centre at the Sn atom. The strength and separation of this attraction was of prime interest, since this effects the molecules ability to behave as a reaction reagent.

This study discusses the crystal and molecular structure of $C_{16}H_{17}O_2SnI$, and how its coordination chemistry relates to its effectiveness as a reagent. It has been found that ester group ligands forming part of an organotin molecule were more likely to complex with the Sn nucleus of the molecule than the same ester group, forming a discrete molecule, would if the attraction were intermolecular[86-88]. The relative strengths of these chelated rings of similar compounds has been shown to be related to the size and composition of the side groups.

9.2 Experimental

9.2.1 Data collection

The X-ray analysis was performed on a colourless crystal of dimensions 0.31 x 0.14 x 0.25 mm^3. Data were collected using the Nicolet P3 4C-SXD using graphite monochromated Mo Kα radiation. The cell dimensions

and basic orientation of the crystal were determined as before using 14 low 2θ strong reflexions with a 2θ limit of 20°. A full data set of 3059 unique reflexions were measured, with θ limit of 25°, by θ/2θ scans over the **hkl** range; $0 \leq \mathbf{h} \leq 11$, $0 \leq \mathbf{k} \leq 21$, $-11 \leq \mathbf{l} \leq 11$. Of these 3059, 1958 reflexions had $\mathbf{F} > 5\sigma(\mathbf{F})$. The data were corrected for Lorentz and polarisation effects. Absorption was not considered to be significant. Periodic monitoring of the diffracted beam from reliable strong reflexions showed no signs of crystal deterioration.

9.2.2 Structure solution and refinement

Due to the presence of the Sn and I atoms, the Patterson method was adopted. From the Patterson vector peaks at (0.5,0.262,0.5) and (0.342,0.5,0.131), the atomic coordinates of the Sn atom were determined to be (-0.08,0.112,0.816). Successive difference synthesis Fourier maps revealed the I atom and the remaining lighter atoms. The H atoms were placed in calculated positions as they were unobserved from the difference map. The atomic coordinates and associated thermal parameters were refined to optimum values using the full matrix least squares technique. All non-hydrogen atoms were refined with anisotropic thermal parameters, with the H atoms initially refined with one common isotropic thermal parameter. Eventually the H atoms were assigned individual thermal parameters and were constrained to ride on their bonded C atoms. This resulted in a final residual of 5.2% with $\Delta\rho_{max}$=0.76 eÅ^{-3} and $\Delta\rho_{min}$=-0.66 eÅ^{-3}.

9.3 Results

9.3.1 Crystal and diffraction data

$C_{16}H_{17}O_2SnI$, $\mathbf{M_r}$=486.91, monoclinic, $P2_1/n$ (no.14), **a**=10.073(8), **b**=17.721(10), **c**=10.427(10) Å, **ß**=112.11(7)°, **V**=1725(2) Å^3, **Z**=4,

D_x=1.875 gcm^{-3}, **F(000)**=928, μ=3.26 mm^{-1}, Mo **K**α, λ=0.71069 Å, **T**=293 K, **R**=0.053 for 1958 reflexions.

9.3.2 Structure analysis

The atomic arrangement of the molecule is shown in a labelled ORTEP diagram in Figure 9.1, as a discrete molecule with a five membered chelated ring. All atoms have been represented as spheres with radii not necessarily to scale. The hydrogen atoms have been removed to help view the basic molecule structure. Figure 9.2 features the molecule with the hydrogens in calculated positions. Atomic coordinates are listed in Tables 9.1 and 9.3 and the anisotropic thermal parameters for the non-hydrogen atoms are listed in Table 9.2. The bond lengths, bond angles and torsion angles are listed in Tables 9.4, 9.5 and 9.6 respectively.

The molecule has been found to adopt a distorted bipyramidal geometry with the carbon atoms C(1), C(7) and C(13) lying in equatorial positions. The I-Sn-X angles (X representing C(1),C(7) & C(13)) have values of 96.9(5), 100.3(5) and 97.6(6)° respectively with an average of 98.3°. The Sn-O bond was of prime importance in trying to establish properties of the compound. The intramolecular Sn-O distances in other $RO_2(CH_2)_n$-Sn compounds, ranging in value from 2.347(5) Å to 2.847(4) Å, are given in Table 9.7[86, 89-93]. The Sn-O distance of 2.55(2) Å is comparable to those in $Cl_2Sn(CH_2CH_2CO_2Me)_2$[91], but is appreciably greater than $Cl_3SnCH_2CH_2CO_2CH_3$[86]. The sum of the covalent radii of Sn and O is 2.13 Å, while the sum of the Van der Waal's radii is 3.70 Å.

The Sn-I bond of 2.811(2) Å is relatively long when compared to other tetrahedral tin-iodine compounds. These have been found to range from 2.69(3) to 2.729(3) Å[94-97]. The O(1)-Sn-I angle of 170.5(3)° virtually

makes the three atoms co-linear thus effecting the positions of the ligand groups.

The formation of the Sn-O interaction places considerable stress on the $CH_2CH_2COOHCH_3$ ester ligand. The bond lengths are as expected but the angles exhibit significant distortions. The angles Sn-C(13)-C(14) and C(13)-C(14)-C(15) have values of 123.6(14) and 119.4(19)° respectively which differs considerably from the strain free angle of 109.5°

The six membered rings C(1)-C(2)-C(3)-C(4)-C(5)-C(6) and C(7)-C(8)-C(9)-C(10)-C(11)-C(12) are well formed with bond lengths ranging from 1.33(3) to 1.40(3) Å. The torsion angles also indicate that the rings are relatively planar with maximum values of 6.0(19)° and minimum values of -5.9(18)°.

9.4 Discussion

The Sn-O(1) bond of 2.55(2) Å has shown that the interaction between these two atoms is relatively strong, creating a rigid chelated ring. The presence of the I atom is thought to be the main reason for this effect. The structure solution has shown that the I-Sn-O(1) angle is approximately linear with a value of 170.5(3)°. This is reinforced by the Sn-O bond lengths of those compounds in Table 9.7, where the increasing presence of the halogen groups, about the Sn atom, has the effect of strengthening the interaction. The strongly electronegative halogen atoms have the effect of increasing the strength of the electrostatic interaction between the Sn and O atoms. It is thought that the Sn atom in $CH_3O_2CCH_2CH_2SnX_3$ (where X represents halides) would also be a greater acceptor centre for external esters.

This study has shown that accurate crystal structures can be

determined using heavy atom methods. In this case the ratio of light to heavy atoms allowed full anisotropic thermal parameters to be calculated for all non-hydrogen atoms. Clearly it was not possible to make further comment on the actual H atom positions.

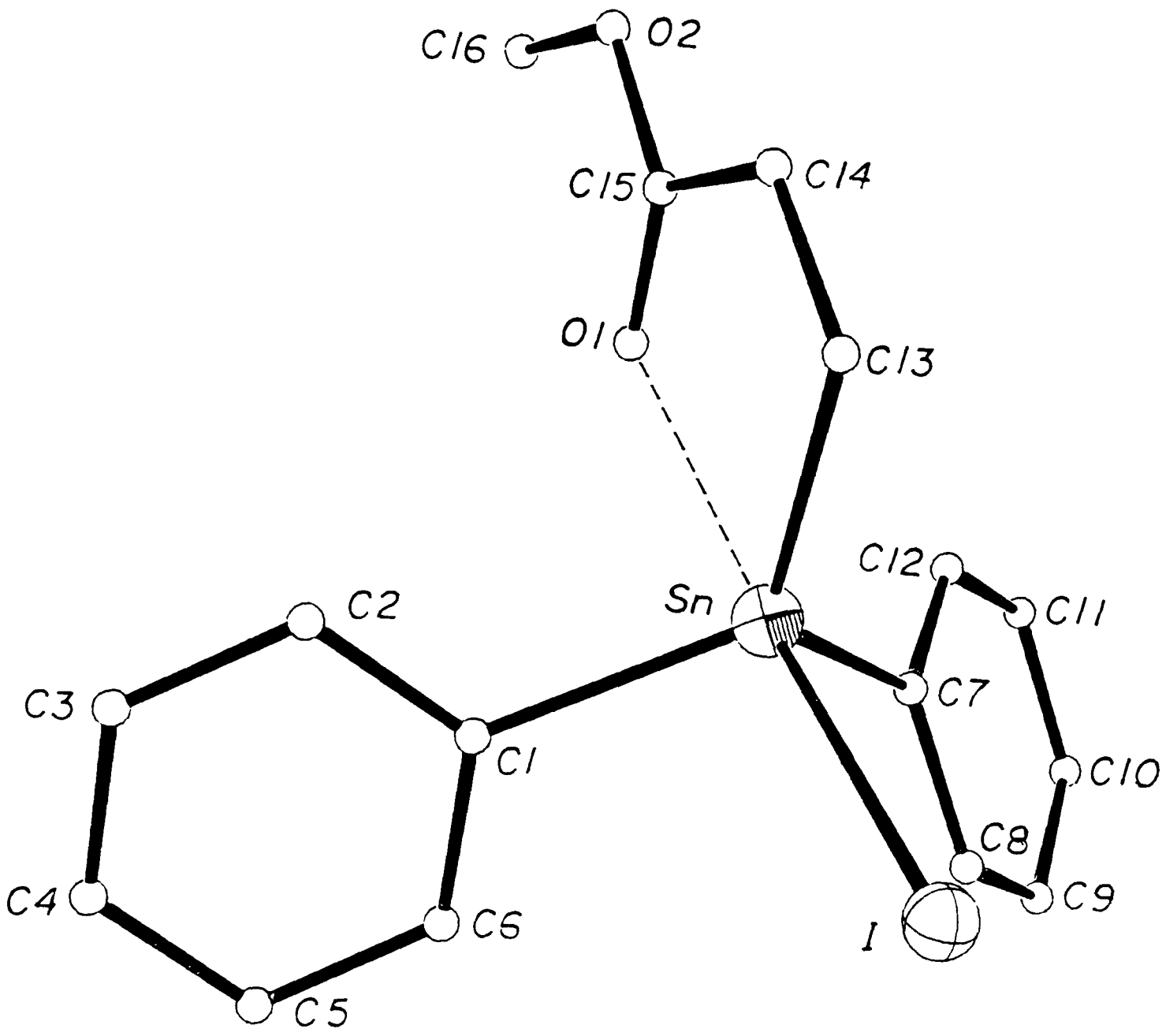

Figure 9.1 A labelled ORTEP plot of $C_{16}H_{17}O_2SnI$ minus the hydrogen atoms. All atoms have been represented by fixed radii spheres.

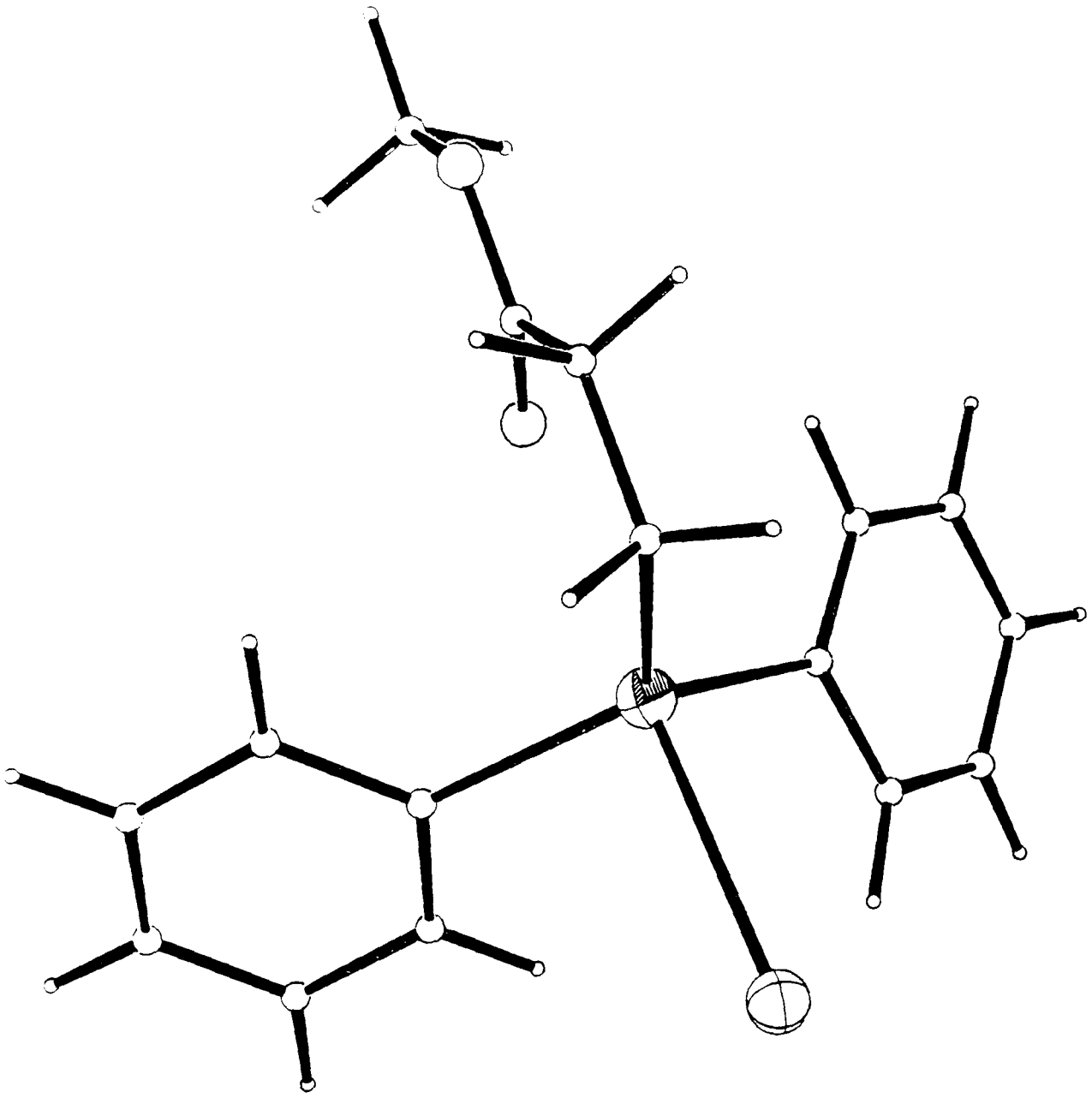

Figure 9.2 As Figure 9.1, but including the hydrogen atoms.

Table 9.1 Fractional atomic coordinates of non-hydrogen atoms. ($U_{eq}=1/3\sum_i\sum_j U_{ij}a_i^*a_j^*a_i \cdot a_j$)

	(X/A)	(Y/B)	(Z/C)	Ueq
Sn	-.08043(12)	-.11876(7)	0.81569(12)	0.047
I	0.08566(15)	-.00396(8)	0.76432(17)	0.090
O(1)	-.1925(11)	-.2298(7)	0.8938(11)	0.058
O(2)	-.1476(16)	-.3042(9)	1.0757(13)	0.090
C(1)	-.0970(17)	-.1884(9)	0.6426(17)	0.050
C(2)	-.0529(18)	-.2629(10)	0.6585(19)	0.063
C(3)	-.066(2)	-.305(1)	0.542(2)	0.077
C(4)	-.124(2)	-.276(1)	0.413(2)	0.078
C(5)	-.168(2)	-.203(1)	0.396(2)	0.067
C(6)	-.1556(18)	-.1603(10)	0.5110(16)	0.059
C(7)	-.1556(18)	-.1603(10)	0.7824(17)	0.050
C(8)	-.3112(19)	0.0030(10)	0.6909(19)	0.076
C(9)	-.442(2)	0.039(1)	0.665(2)	0.095
C(10)	-.528(2)	0.022(1)	0.733(2)	0.075
C(11)	-.488(2)	-.035(1)	0.824(2)	0.093
C(12)	-.3628(19)	-.0729(11)	0.8484(21)	0.076
C(13)	0.063(2)	-.148(1)	1.015(2)	0.070
C(14)	0.019(3)	-.210(2)	1.083(2)	0.124
C(15)	-.1170(15)	-.2498(11)	1.0077(16)	0.046
C(16)	-.286(2)	-.342(1)	1.005(2)	0.098

Table 9.2 Anisotropic thermal parameters.

	U11	U22	U33	U23	U13	U12
Sn	0.0379(5)	0.0498(7)	0.0467(6)	0.0005(6)	0.0145(4)	-.0058(7)
I	0.0720(9)	0.0655(9)	0.1265(13)	-.0217(7)	0.0598(9)	-.0178(9)
O(1)	0.044(6)	0.081(9)	0.036(7)	-.002(6)	0.001(6)	0.008(6)
O(2)	0.11(1)	0.10(1)	0.05(1)	0.00(1)	0.03(1)	0.04(1)
C(1)	0.044(9)	0.054(11)	0.048(11)	-.013(8)	0.023(8)	-.008(9)
C(2)	0.07(1)	0.06(1)	0.06(1)	0.02(1)	0.03(1)	0.00(1)
C(3)	0.09(1)	0.04(1)	0.09(2)	0.01(1)	0.04(1)	0.00(1)
C(4)	0.07(1)	0.09(2)	0.06(1)	0.00(1)	0.03(1)	0.00(1)
C(5)	0.08(1)	0.09(2)	0.02(1)	0.01(1)	0.01(1)	0.02(1)
C(6)	0.07(1)	0.06(1)	0.03(1)	0.02(1)	0.01(1)	0.00(1)
C(7)	0.040(9)	0.054(11)	0.049(10)	0.009(8)	0.015(8)	-.009(9)
C(8)	0.08(1)	0.07(1)	0.08(1)	0.05(1)	0.06(1)	0.04(1)
C(9)	0.08(2)	0.07(1)	0.12(2)	0.03(1)	0.03(1)	0.03(1)
C(10)	0.05(1)	0.07(1)	0.10(2)	0.01(1)	0.04(1)	0.00(1)
C(11)	0.06(1)	0.10(2)	0.11(2)	0.03(1)	0.05(1)	0.04(2)
C(12)	0.06(1)	0.08(1)	0.08(1)	0.04(1)	0.03(1)	0.02(1)
C(13)	0.07(1)	0.10(2)	0.03(1)	0.00(1)	0.01(1)	-.02(1)
C(14)	0.10(2)	0.16(3)	0.08(2)	-.02(2)	-.02(1)	0.06(2)
C(15)	0.022(7)	0.079(13)	0.028(9)	0.018(8)	-.004(7)	-.009(9)
C(16)	0.12(2)	0.08(2)	0.09(2)	-.01(1)	0.06(2)	0.00(1)

Table 9.3 Fractional atomic coordinates of hydrogen atoms.

	(X/A)	(Y/B)	(Z/C)	U_{eq}
H(2)	-.0123(18)	-.2863(10)	0.7526(19)	0.063
H(3)	-.031(2)	-.358(1)	0.554(2)	0.077
H(4)	-.135(2)	-.308(1)	0.331(2)	0.078
H(5)	-.209(2)	-.180(1)	0.302(2)	0.067
H(6)	-.1907(18)	-.1070(10)	0.4975(16)	0.059
H(8)	-.2452(19)	-.0202(10)	0.6453(19)	0.077
H(9)	-.474(2)	0.079(1)	0.592(2)	0.095
H(10)	-.618(2)	0.051(1)	0.717(2)	0.075
H(11)	-.551(2)	-.050(1)	0.875(2)	0.095
H(12)	-.3350(19)	-.1141(11)	0.9193(21)	0.076
H(13a)	0.078(2)	-.103(1)	1.075(2)	0.071
H(13b)	0.156(2)	-.163(1)	1.008(2)	0.071
H(14a)	0.097(3)	-.249(2)	1.108(2)	0.125
H(14b)	0.013(3)	-.189(2)	1.169(2)	0.125
H(16a)	-.298(2)	-.383(1)	1.066(2)	0.097
H(16b)	-.288(2)	-.365(1)	0.916(2)	0.097
H(16c)	-.365(2)	-.305(1)	0.984(2)	0.097

Table 9.4 Intramolecular bond lengths in angstroms.

Sn	- I	2.811(2)	Sn	- O(1)	2.55(2)
Sn	- C(1)	2.14(2)	Sn	- C(7)	2.16(2)
Sn	- C(13)	2.10(2)	O(1)	- C(15)	1.20(2)
O(2)	- C(15)	1.30(3)	O(2)	- C(16)	1.47(3)
C(1)	- C(2)	1.38(3)	C(1)	- C(6)	1.37(3)
C(2)	- C(3)	1.39(3)	C(3)	- C(4)	1.35(4)
C(4)	- C(5)	1.35(4)	C(5)	- C(6)	1.38(3)
C(7)	- C(8)	1.39(3)	C(7)	- C(12)	1.33(3)
C(8)	- C(9)	1.40(3)	C(9)	- C(10)	1.35(3)
C(10)	- C(11)	1.34(4)	C(11)	- C(12)	1.37(3)
C(13)	- C(14)	1.45(4)	C(14)	- C(15)	1.48(3)

Table 9.5 Intramolecular bond angles in degrees.

I-Sn-C(1)	96.9(5)	I-Sn-C(7)	100.3(5)
I-Sn-C(13)	97.6(6)	I-Sn-O(1)	170.5(3)
O(1)-Sn-C(1)	85.5(6)	O(1)-Sn-C(7)	87.2(5)
O(1)-Sn-C(13)	73.4(6)	C(1)-Sn-C(7)	112.1(7)
C(1)-Sn-C(13)	119.8(7)	C(7)-Sn-C(13)	121.9(7)
Sn-C(1)-C(2)	122.0(13)	Sn-C(1)-C(6)	120.2(13)
C(1)-C(2)-C(3)	118.9(17)	C(2)-C(3)-C(4)	122.1(19)
C(3)-C(4)-C(5)	119.6(20)	C(4)-C(5)-C(6)	119.2(17)
C(5)-C(6)-C(1)	122.4(18)	C(6)-C(2)-C(1)	117.8(16)
Sn-C(7)-C(8)	118.8(12)	Sn-C(7)-C(12)	123.6(14)
C(7)-C(8)-C(9)	117.9(17)	C(8)-C(9)-C(10)	122.6(20)
C(9)-C(10)-C(11)	117.7(17)	C(10)-C(11)-C(12)	120.7(19)
C(11)-C(12)-C(7)	123.3(19)	C(12)-C(7)-C(8)	117.5(16)
Sn-C(13)-C(14)	123.6(14)	Sn-O(1)-C(15)	110.7(11)
C(13)-C(14)-C(15)	119.4(19)	C(14)-C(15)-O(2)	115.4(16)
C(15)-O(2)-C(16)	116.0(15)	C(14)-C(15)-O(1)	120.0(18)

Table 9.6 Intramolecular torsion angles in degrees.

I-Sn-C(1)-C(2)	123.4(15)	I-Sn-C(1)-C(6)	-58.2(14)
I-Sn-C(7)-C(8)	28.5(13)	I-Sn-C(7)-C(12)	-149.1(16)
I-Sn-C(13)-C(14)	-178.5(16)	I-Sn-O(1)-C(15)	18.4(13)
Sn-O(1)-C(15)-O(2)	178.5(21)	Sn-O(1)-15-14	0.9(5)
Sn-C(1)-C(2)-C(3)	-179.6(24)	Sn-C(1)-C(6)-C(5)	179.7(24)
Sn-C(7)-C(8)-C(9)	176.4(23)	Sn-C(7)-C(12)-C(11)	-178.3(28)
Sn-C(13)-C(14)-C(15)	2.5(15)	C(1)-Sn-O(1)-C(15)	123.3(13)
C(7)-Sn-O(1)-C(15)	-124.5(7)	C(13)-Sn-O(1)-C(15)	0.3(12)
O(1)-Sn-C(7)-C(12)	25.1(6)	C(13)-Sn-C(1)-C(2)	20.5(14)
C(13)-Sn-C(1)-C(6)	-161.1(17)	C(13)-Sn-C(7)-C(8)	134.2(16)
C(13)-Sn-C(7)-C(12)	-43.3(15)	C(1)-Sn-C(7)-C(8)	-73.3(14)
C(1)-Sn-C(7)-C(12)	109.1(17)	C(1)-Sn-C(13)-C(14)	-76.0(17)
C(7)-Sn-C(13)-C(14)	74.4(7)	C(7)-Sn-C(1)-C(2)	-132.6(16)
C(7)-Sn-C(1)-C(6)	45.9(14)	C(1)-C(2)-C(3)-C(4)	-2.1(9)
C(2)-C(3)-C(4)-C(5)	2.0(20)	C(3)-C(4)-C(5)-C(6)	-1.8(19)
C(4)-C(5)-C(6)-C(1)	1.8(19)	C(2)-C(1)-C(6)-C(5)	-1.8(17)
C(6)-C(1)-C(2)-C(3)	1.9(17)	C(7)-C(8)-C(9)-C(10)	6.0(19)
C(8)-C(9)-C(10)-C(11)	-3.8(20)	C(9)-C(10)-C(11)-C(12)	1.7(21)
C(10)-C(11)-C(12)-C(7)	-2.1(20)	C(8)-C(7)-C(12)-C(11)	4.2(19)
C(12)-C(7)-C(8)-C(9)	-5.9(18)	C(13)-C(14)-C(15)-O(1)	-2.3(18)
C(13)-C(14)-C(15)-O(2)	179.9(29)	C(14)-C(15)-C(16)-O(2)	-4.7(26)
C(16)-O(2)-C(15)-O(1)	-.3(17)	C(16)-O(2)-C(15)-C(14)	177.4(24)

Table 9.7 Sn-O bond lengths for complexed compounds of the form $RO_2C(CH_2)_nSn$. (* represents this study)

Compound	Coordination No.	Sn-O bond (Å)	Ref.
$(CH_3O_2CCH_2CH_2)_2Sn(S_2CN(CH_3)_2)_2$	7	2.751(5)	90
$(CH_3O_2CCH_2CH_2)_2SnCl_2$	6	2.520(4) 2.524(4)	91
$(CH_3O_2CCH_2CH_2)_2SnCl$	6	2.847(4)	92
$CH_3O_2CCH_2CH_2SnCl_3$	5	2.347(5)	86
$CH_3O_2CCH_2CH_2SnCl_2(S_2CN(CH_3)_2)$	6	2.436(4)	93
$CH_3CH_2O_2CCH_2CH_2CH_2SnCl_3$	5	2.405(8)	89
$CH_3O_2CCH_2CH_2SnIPh_2$	5	2.55(2)	*

CHAPTER 10. Neutron refinement of 3-deazauracil, $C_5H_5O_2N$.

10.1 Introduction

3-deazauracil is a relatively simple organic structure with the orthorhombic space group, $P2_12_12_1$. The X-ray structure of 3-deazauracil is well established, but the H atom positions published are not known with any great deal of accuracy[98]. In many larger structures, the accurate positions of the H atoms is not usually of great importance and indeed the coordinates are often omitted from publications. However in the case of 3-deazauracil, the H atoms are believed to play an important role in the crystal structure and so accurate determination of their positions was desirable.

The modified nucleoside 3-deazauridine exhibits some biological activity, which is assumed to be associated with a very strong O-H...O hydrogen bond, observed in the X-ray structure[99]. Such a strong intermolecular hydrogen bond was also found in the related base, 3-deazauracil from the aforementioned X-ray study. However, X-ray studies for both compounds, failed to adequately determine the positions of the H atoms involved in the interaction. A previous high resolution neutron powder diffraction analysis managed to reveal the H atom positions but with limited accuracy[100]. Given the importance of the hydrogens in the structure, a neutron diffraction study using a limited data set, was performed in an attempt to produce a complete crystal and molecular model.

10.2 Experimental

10.2.1 Data collection

A large, pale brown single crystal of dimensions 3 x 3 x 2 mm^3 was selected for data collection. The cell dimensions and quality of the crystals, from the same recrystallisation batch, were verified by a

preliminary zero order Weissenberg photograph (Cu Kα X-ray), confirming that they were of the same polymorphic form as the crystal used in the previous X-ray study.

A restricted data set was collected on N-SXD, operated in a quasi-equatorial mode, with the crystal mounted on a set of conventional crystal arcs. The crystal was glued to an aluminium rod, clad in cadmium and fixed to the arcs with modelling clay. The crystal was orientated by eye, such that the b-axis was approximately parallel to the rotation axis of the arcs, ω.

The combination of the servo controlled ω rotation axis and the fixed arcs, to position the crystal for diffraction, prevented the full flexibility of the instrument to be utilised. However, an approximate quarter-sphere of reciprocal space was investigated, by successively rotating the crystal about the ω-axis, in 7° increments, collecting separate diffraction histograms for each ω setting. The small ZnS PSD used for data collection, measures 80 x 80 mm^2 and therefore restricts the area of any one histogram in the equatorial plane to a solid angle of approximately 20 x 20°. The collection of histograms effectively covered an arc of 105° about the ω axis.

The histograms were combined to form one overall data set of 124 reflexions with $(\sin\theta/\lambda)_{max}$ of 0.6 $Å^{-1}$ and a wavelength range of 0.96-4.8 Å. Of these 81 had $I>5\sigma(I)$. The measured peak intensities were extracted using the RAL crystallographic software, producing $|F_{hkl}|$ values.

10.2.2 Structure refinement

The non-hydrogen atoms were initially assigned the atomic coordinates previously determined in the X-ray study and were given arbitrary

isotropic thermal parameters. The atoms coordinates and thermal parameters were refined using the least squares refinement program SFLSQ[101], developed from the Cambridge Crystallographic Subroutine Library (CCSL). Given the poor ratio of observations to variables, the refinement was simplified by keeping all thermal parameters isotropic and using blocked matrix least squares techniques. All parameters were constrained to be constant and a difference map revealed the H atoms positions. These were assigned isotropic thermal parameters and the complete molecule was refined using unit weights. The refinement converged with a residual of 0.085.

10.3 Results

10.3.1 Crystal and diffraction data

3-Deazauracil, $C_5H_5NO_2$, M_r=111.1, orthorhombic , $P2_12_12_1$ (no.19), **a**=8.638(6), **b**=5.279(5), **c**=11.220(8) Å, **V**=511.61 Å^3, **Z**=4, D_x=1.44 gcm^{-3}, λ=0.48-4.8 Å, **T**=295 K, **R**=0.085 for 81 unique reflexions using unit weights.

10.3.2 Structure analysis

The molecular structure including the H atoms is shown in an ORTEP plot in Figure 10.1. Figure 10.2 features a SCHAKAL[102] plot showing a representation of the hydrogen bonding scheme involving the O(4)-H(4)...O(2) and N(1)-H(1)...O(2) interactions between adjacent molecules.

The final atomic parameters from this refinement are compared with those of the previous X-ray and neutron studies in Table 10.1. The H atom positions are remarkably close to those of the X-ray study, which were in calculated positions. These offer a significant improvement over the high resolution neutron powder analysis. The high estimated

errors provided in brackets reflect the limited nature of the data set. The intramolecular and intermolecular bond lengths are listed in Table 10.2. As expected the intramolecular bond lengths for non-hydrogen atom pairs are in good agreement with those of the X-ray structure. However, the H atom bonds have been found to vary significantly. The bonds for H(3), H(4), H(5) and H(6) range from 0.90(10) to 1.133(89) Å, which given the size of the errors are in agreement within the accepted neutron bond length of 1.08 Å. These are in general an improvement on the neutron powder values.

More significantly, the bond lengths of the H atoms involved in the intermolecular hydrogen bonding, have been found to yield consistent values. Previously the N(1)-H(1) separation of 0.81 Å was considered to be too short. A revised value of 0.922(65) Å seems to be more realistic and is comparable to the neutron powder result of 1.098(7) Å. The O(4)-H(4) bond length also coincides with the value from the neutron powder study of 1.10(13) Å, but the H(4)...O(2'') length of 1.42(8) Å has been found to be 0.18 Å shorter.

Selected intramolecular and intermolecular bond angles are tabulated in Table 10.3. In general there is very little difference between the values reported in this refinement and those of the X-ray structure analysis. The H(1)-N(1)-C(2) and N(1)-H(1)...O(2') angles measuring 113.6(60) and 157(8)° respectively, virtually duplicate the previous values of 113.7 and 156°. The angle of 171(9)° for O(4)-H(4)...O(2'') indicates a similar hydrogen bonding geometry.

10.4 Discussion

There is clearly good agreement between the atomic parameters found in the X-ray study and in the more limited neutron single crystal study

presented here. This refinement has additionally provided new accurate hydrogen atom parameter information which was unobtainable from the previous X-ray study. The refined hydrogen parameters clearly show H(4) to be bonded to O(4), with bond length of 1.10(13) Å. These results confirm the general conclusions obtained in the earlier neutron powder study, but give more accurate and reliable atomic parameters.

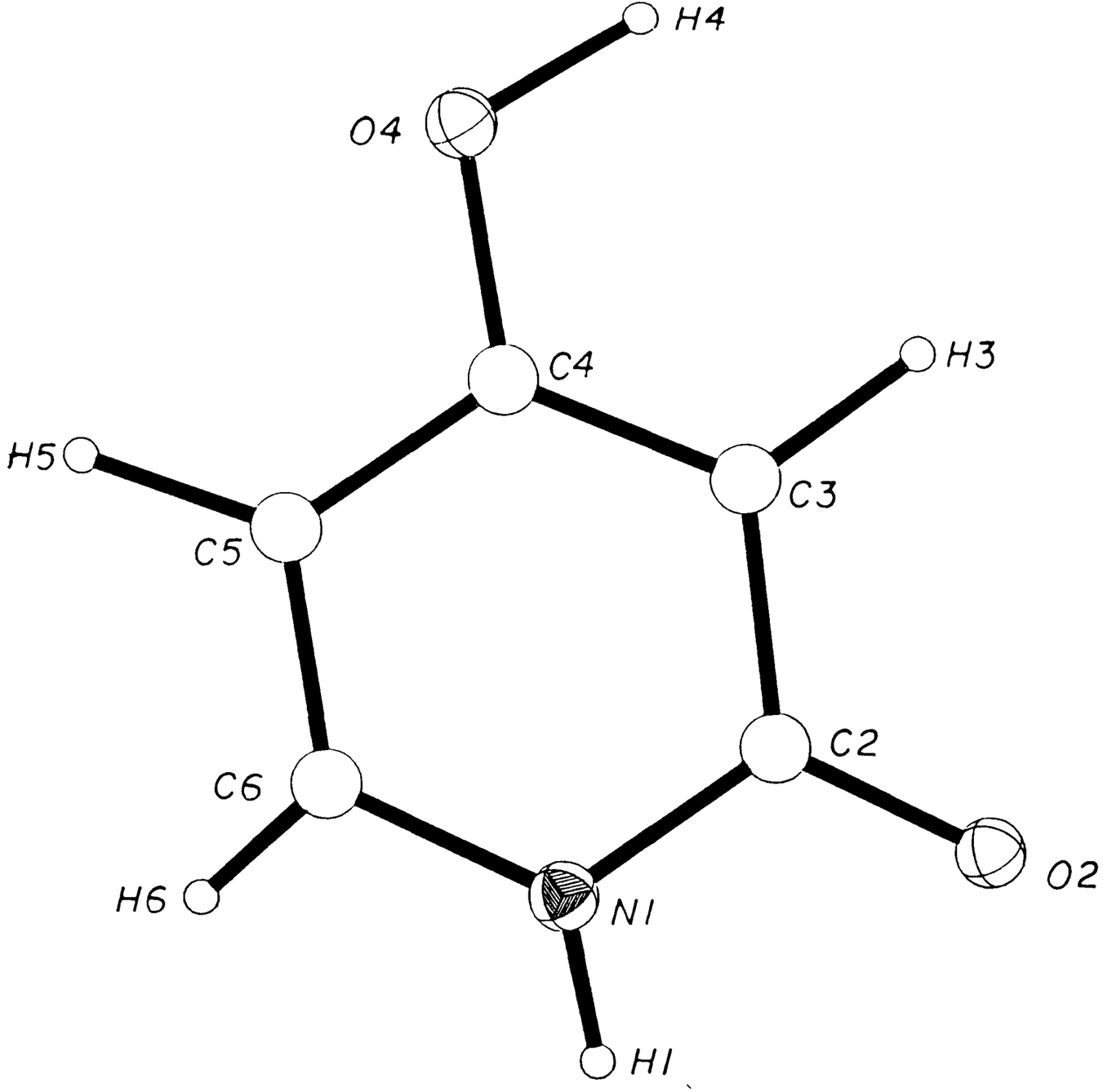

Figure 10.1 An ORTEP plot of the basic molecule of $C_5H_5O_2N$, viewed perpendicular to the plane of the six membered ring.

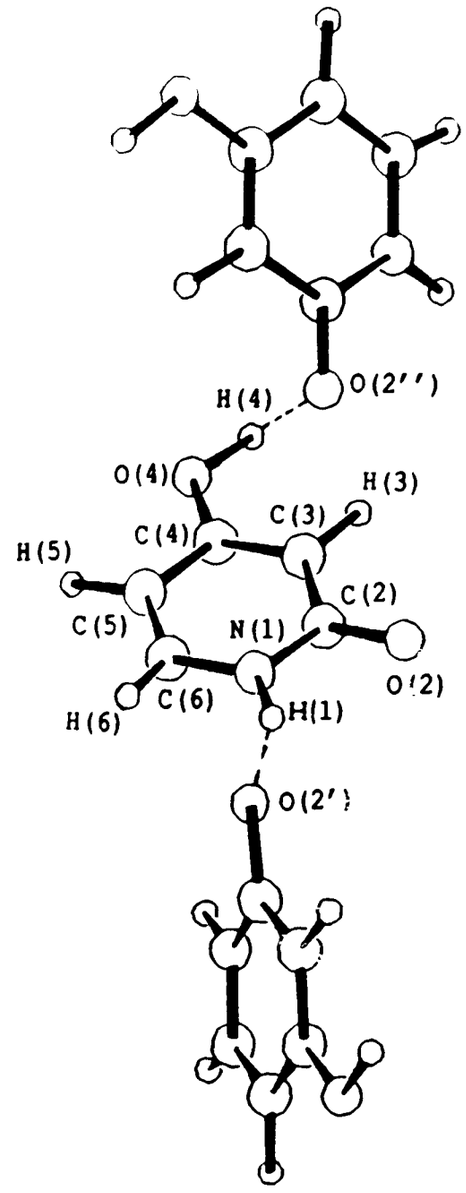

Figure 10.2 A SCHAKAL packing diagram revealing the hydrogen bonding creating chains of molecule extending along the z-axis.

Table 10.1(a) Refined fractional atomic coordinates from neutron study. ($U_{eq}=1/3\sum_i\sum_j U_{ij}a_i^*a_j^*a_i\cdot a_j$)

	(X/A)	(Y/B)	(Z/C)	U_{eq}
N(1)	0.3268(23)	0.3446(45)	0.7115(25)	0.010(5)
H(1)	0.4178(59)	0.329(18)	0.7538(73)	0.015(11)
C(2)	0.3279(38)	0.5392(60)	0.6334(42)	0.016(8)
O(2)	0.4417(29)	0.6901(86)	0.6303(42)	0.020(8)
C(3)	0.1921(26)	0.5798(53)	0.5644(29)	0.005(6)
H(3)	0.1847(67)	0.749(17)	0.5045(74)	0.024(15)
C(4)	0.0702(33)	0.4151(67)	0.5775(32)	0.012(8)
O(4)	-.0610(33)	0.4427(76)	0.5137(36)	0.014(8)
H(4)	-.0583(59)	0.611(24)	0.4565(75)	0.019(14)
C(5)	0.0735(34)	0.2074(75)	0.6524(36)	0.015(6)
H(5)	-.0231(60)	0.065(20)	0.665(10)	0.025(12)
C(6)	0.2043(27)	0.1781(73)	0.7175(42)	0.033(9)
H(6)	0.2192(63)	0.051(17)	0.7685(72)	0.048(18)

Table 10.1(b) Fractional atomic coordinates from X-ray study[98].

	(X/A)	(Y/B)	(Z/C)	U_{eq}
N(1)	0.3255(3)	0.3429(5)	0.7102(2)	0.027(1)
H(1)	0.4086	0.3167	0.403	-----
C(2)	0.3245(3)	0.5441(5)	0.6344(2)	0.026(1)
O(2)	0.4417(3)	0.6865(5)	0.6315(2)	0.036(1)
C(3)	0.1899(3)	0.5811(5)	0.5650(2)	0.024(1)
H(3)	0.1837	0.7406	0.5050	-----
C(4)	0.0671(3)	0.4147(5)	0.5735(2)	0.026(1)
O(4)	-.0671(3)	0.4432(5)	0.5143(2)	0.037(1)
C(5)	0.0761(4)	0.2074(6)	0.6526(3)	0.032(1)
H(5)	-.0188	0.0752	0.6602	-----
C(6)	0.2055(4)	0.1774(6)	0.7184(2)	0.032(1)
H(6)	0.2138	0.0187	0.7789	-----

Table 10.1(c) Refined fractional coordinates from high resolution neutron powder study[100].

	(X/A)	(Y/B)	(Z/C)
N(1)	0.3339(4)	0.3265(6)	0.7037(3)
H(1)	0.4082(8)	0.3413(13)	0.7642(6)
C(2)	0.3236(5)	0.5394(6)	0.6370(3)
O(2)	0.4406(6)	0.6868(8)	0.6317(4)
C(3)	0.1956(4)	0.5927(7)	0.5631(4)
H(3)	0.2094(9)	0.7256(14)	0.4985(6)
C(4)	0.0821(5)	0.4206(7)	0.5822(3)
O(4)	-.0504(5)	0.4192(8)	0.5235(4)
H(4)	-.0651(9)	0.5909(12)	0.4359(75)
C(5)	0.0639(5)	0.2068(8)	0.6558(3)
H(5)	-.0121(8)	0.0712(13)	0.6446(6)
C(6)	0.2019(4)	0.1836(7)	0.7105(3)
H(6)	0.2227(8)	0.0572(12)	0.7743(5)

Table 10.2 Refined intermolecular bond lengths (Å) with values from previous studies for comparison.

	SXD	X-RAY	NEUTRON POWDER
N(1)-C(2)	1.354(47)	1.360	1.382(4)
N(1)-C(6)	1.376(38)	1.359	1.362(4)
C(2)-O(2)	1.267(48)	1.262	1.313(4)
C(2)-C(3)	1.422(46)	1.412	1.404(4)
C(3)-C(4)	1.374(41)	1.381	1.413(5)
C(4)-O(4)	1.361(60)	1.319	1.366(5)
C(4)-C(5)	1.376(54)	1.411	1.456(5)
C(5)-C(6)	1.356(47)	1.348	1.382(5)
C(3)-H(3)	1.109(93)	-----	1.023(7)
O(4)-H(4)	1.10(13)	-----	1.025(7)
C(5)-H(5)	1.133(89)	-----	1.001(7)
C(6)-H(6)	0.90(10)	-----	1.100(8)
N(1)-H(1)	0.922(65)	0.81	1.098(7)
H(1)...O(2')	1.92(8)	2.05	--------
N(1)-H(1)...O(2')	2.789(44)	2.807	--------
O(4)-H(4)	1.10(13)	-----	1.100(8)
H(4)...O(2'')	1.42(11)	-----	1.603(8)
O(4)-H(4)...O(2'')	2.52(8)	-----	2.703(6)

Table 10.3 Refined intramolecular bond angles (degrees) with X-ray values for comparison.

	NEUTRON	X-RAY
H(1)-N(1)-C(2)	113.6(60)	113.7
C(2)-N(1)-C(6)	120.9(29)	122.7(2)
N(1)-C(2)-C(3)	118.0(28)	117.2(2)
C(2)-C(3)-H(3)	119.8(41)	-----
H(3)-C(3)-C(4)	122.2(41)	-----
C(3)-C(4)-C(5)	124.4(29)	119.6(3)
C(4)-O(4)-H(4)	112.1(42)	-----
C(4)-C(5)-C(6)	115.1(32)	118.8(3)
N(1)-C(6)-C(5)	123.5(37)	121.3(2)
C(5)-C(6)-H(6)	123.2(52)	-----
H(1)-N(1)-C(6)	125.3(63)	122.7(2)
N(1)-C(2)-O(2)	119.8(37)	-----
O(2)-C(2)-C(3)	122.0(37)	124.3(2)
C(2)-C(3)-C(4)	117.9(30)	120.4(2)
C(3)-C(4)-O(4)	120.6(36)	123.4(2)
O(4)-C(4)-C(5)	114.9(34)	116.9(3)
C(4)-C(5)-H(5)	126.1(58)	-----
H(5)-C(5)-C(6)	118.8(61)	-----
N(1)-C(6)-H(6)	113.3(50)	-----
N(1)-H(1)...O(2')	157(8)	156
O(4)-H(4)...O(2'')	171(9)	-----

CHAPTER 11. Neutron refinement of Schultenite, $PbHAsO_4$

11.1 Introduction

Lead Hydrogen Arsenate (LHA, $PbHAsO_4$) is a naturally occurring mineral, known more commonly as Schultenite. The general molecular structure for LHA and other related compounds (Lead Hydrogen Phosphate, LHP, and a deuterated potassium derivative $KH(D)_2PO_4$) have been previously established by X-ray and Raman studies[103-106]. However, the presence of the heavy atoms in these structures has left a degree of uncertainty about the H positions, due to their dominant scattering.

The Raman studies of both LHA and LHP have detected paraelectric phase transitions at ambient temperatures[106]. The phase transition in LHP involves a change of symmetry from P2/c in the high temperature paraelectric phase to Pc in the ferroelectric phase[107]. In P2/c the strongly hydrogen bonded H atom is positioned on a centre of symmetry and the heavy atoms reside on a two fold axis. As the temperature is reduced through the critical temperature, T_c, the heavy atoms move away from the two fold axes and the H orders onto one of the two symmetry related sites. The change from one state to the other is a gradual one and it has been discovered that on cooling LHP the ordering becomes complete at around 110° below T_c. It has been found that this loss of symmetry can be evident even at temperatures in excess of T_c. Clearly the transition is not dramatic and the mechanism is not well understood.

The critical temperature of the paraelectric-ferroelectric phase transition occurring in LHA was determined to be T_c=312 K , which compares with T_c=310 K for LHP. These physical similarities would seem to indicate that the phase transition mechanism for both materials

would likewise be similar. The principal interest in these materials lies with the nature of the hydrogen ordering at the phase transition and hence of the precise potentials in which these hydrogen-bonded H atoms sit. These potentials are believed to be strongly coupled to the separation of the two O atoms in the O-H...O bond[108]. The phase transition temperature is also thought to be dependent on O atom separation and of the level of disordering of the H atoms from the centre of symmetry. High pressure studies have allowed the separations to be varied hence changing T_c[108,109]. In this study, a comparison between the atom separations of LHA and LHP may allow the mechanisms to be understood more fully.

The nature of this study was two fold. Initially, the process of data collection and structure refinement was intended as a commissioning experiment for the neutron SXD at RAL. Secondly it was used to demonstrate the advantages of using neutrons for fine detail structural refinements.

11.2 Experimental

11.2.1 Data collection

The crystal used for the data collection was colourless with dimensions 4 x 3 x 1 mm^3. The plate-like crystal had a small green inclusion, thought to be the mineral Mimetite, measuring approximately 0.75 x 0.75 x 0.25 mm^3. Removal of the inclusion was considered to be futile given the tendency of LHA crystals to cleave along the (010) plane. The volume of the inclusion was approximately 1% of the total sample volume and so its presence was not considered to be significantly detrimental to diffraction intensities.

The crystal was mounted on a set of arcs fixed to a shaft, which was

capable of rotation through 360°. A total of 20 histograms were collected for three arbitrary arc settings. Figure 11.1 shows the TOF profile for the (hhh) principal row. The unit cell was determined from 64 strong reflexions taken from six of the histograms. The cell parameters were already known, but they were redetermined as part of the instrument commissioning. A total of 541 independent reflexions were measured over the **hkl** range : $0 \leq \mathbf{h} \leq 8$, $0 \leq \mathbf{k} \leq 12$, $0 \leq \mathbf{l} \leq 7$. Figure 11.2 presents the TOF profiles for adjacent pixels on the PSD, grouped together displaying the three dimensional nature of the diffraction data produced by SXD. The time of flight limits restricted the wavelength range to 0.48 - 4.8 Å. Due to the PSD overlap, reflexions for certain **hkl** were measured twice which were treated as independent reflexions. Of the 541 reflexions, 467 had $I>3\sigma(I)$.

11.2.2 Structure refinement

Initially the higher symmetry space group P2/c was assumed and the atomic coordinates of the non-hydrogen atoms were assigned the values determined from the previous X-ray work. A Fourier map revealed a region of strong negative scattering density located close to the centre of symmetry between the two O atoms. Initial refinements were carried out by SFLSQ.

The structure was initially refined without the H atom, so as to refine the atomic coordinates of the non-hydrogen atoms thus producing a stable structure. This produced a residual factor R=11.2%. The H atom was introduced to the model and placed on the centre of symmetry with coordinates (0.5,0.5,0.5). The H coordinates were constrained to comply with the symmetry operators during the refinement. An improved

residual of 7.3% resulted. All non-hydrogen atoms were refined with anisotropic thermal parameters whilst the H atom was kept isotropic. The exaggerated thermal motion of the H atom indicated that its position might be represented better than being fixed at a centre of symmetry. By removing the centre of symmetry constraint, the H atom disordered onto two sites equidistant from the centre. The new H positions were assumed to have equal site occupation factors. This resulted in an improved thermal parameter and R was further reduced to 7.1%. An improved model was sought by refining the H atom with anisotropic thermal parameters. This had the effect of producing a marginally improved R factor, but it also had the result of producing a very exaggerated disc-like thermal ellipsoid. An acceptable explanation for such behaviour could not be readily obtained and so the final structure was refined with H isotropic. Final R=7.13%.

The experimental data were collected on SXD at room temperature, just below the published transition temperature for LHA. Therefore it would not be unreasonable to expect the lower symmetry phase to be present in the test sample. To determine what extent the low temperature phase was present, the refinement was repeated using the symmetry operators of Pc (no.7). The atomic coordinates from the P2/c refinement were used as the initial starting values. Subsequent cycles of least squares refinement resulted in a minor deviation in the positions of the heavy atoms from the two fold axis. The shifts were however small and so cannot be taken as conclusive evidence. The H atoms eventually stabilised on two positions equidistant from the symmetry centre with equal occupancies. This model produced an improved R value of 6.9%, which initially seemed to indicate that the lower symmetry model was

indeed the correct structure. However the errors associated with the atomic and thermal parameters still leave an element of uncertainty to their reliability.

11.3 Results

11.3.1 Crystal and diffraction data (Combined X-ray and neutron Data)

$PbHAsO_4$, Schultenite, M_r=347.2, monoclinic, P2/c (no.13), **a**=4.930(10), **b**=6.772(16), **c**=5.859(17) Å, **ß**=96.07(19)°, **V**=194.51(84)Å^3, **Z**=2, D_x=5.97 gcm^{-3}, **λ**=0.48 - 4.8 Å, 467 unique reflexions with **I**>3**σ**(I), **R**=7.13%, **T**=300-305 K.

11.3.2 Structure analysis

The atomic arrangement of the unit cell contents of $PbHAsO_4$ adopting the P2/c space group is featured in an ORTEP plot in Figure 11.3. The two possible disordered sites for the H atom (H and H′) are shown together. The refined non-hydrogen atom positions of both molecular states do not differ significantly from previously published figures. Table 11.1 compares the atomic coordinates with the most recent X-ray study. Table 11.2 lists the anisotropic thermal parameters for the atoms of the P2/c refinement, with those of the H atom omitted.

The intermolecular and intramolecular bond lengths and angles are given in Tables 11.3 and 11.4 respectively.

The As-O lengths of 1.711(5) Å are equal, within experimental error, to those of LHP at 1.714(7) Å. The molecular geometries of both compounds are further related by the O(1)-As-O(1)′ angle of 108.7(3)° which compares with the equivalent LHP angle of 107.9(3)°

Comparison of the main bonding parameters for LHA and LHP show that they are in good agreement but the O...O separations differ significantly. The greater separation may account for a less rapid

ordering during the transition. The O(1)-H...O(1)' angle of 176.9(19)° and the H atom shift of 0.166(19) Å indicates that the H disordering from the centre of symmetry is fairly subtle. It is expected that like LHP, the H atom of LHA will undergo complete ordering onto one of the two sites, as the crystal temperature is lowered below T_c.

11.4 Discussion

The use of the SXD has permitted the extraction of new structural data regarding the H atom position, which previous to this was unknown. Considering the close proximity to the transition temperature, the absolute H position is still in some doubt. The absolute space group at room temperature has been shown to be a hybrid of the low and high symmetry phases, although the statistics relating to the validity of the molecular parameters would tend to favour P2/c. At this temperature there appears to be very little lattice distortion, despite the expected movement of the heavy atoms from their special positions on the 2-fold axis. The final residual value of 7.1%, is encouraging considering the poor crystal quality and the relatively small data set collected.

This may be verified using SXD, since it has the capabilities for data collection under non-ambient conditions. The crystal goniometer can be immersed in a custom made cryostat and the temperature accurately monitored. The deep penetrating power of the neutrons will permit their passage through the body of the cryostat without significant effect. With the rapid data collection and processing of the SXD software, it would be possible to collect numerous data sets as the crystal environment temperature is dropped well below T_c. This would permit the H atom positions to be refined at various stages throughout

the phase change, forming a detailed account of the disordering.

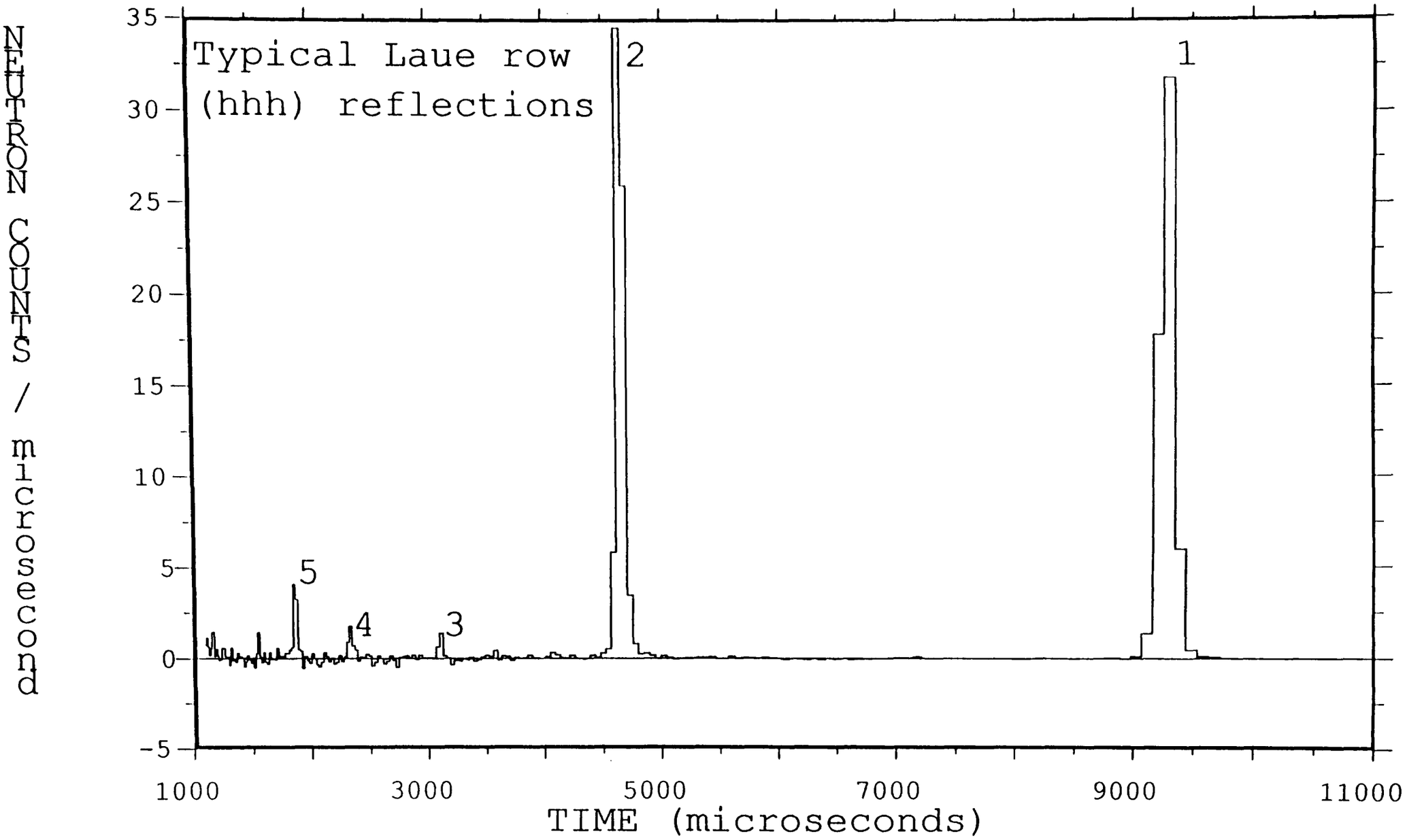

Figure 11.1 A time of flight profile showing the principal row reflexions (hhh) for schultenite.

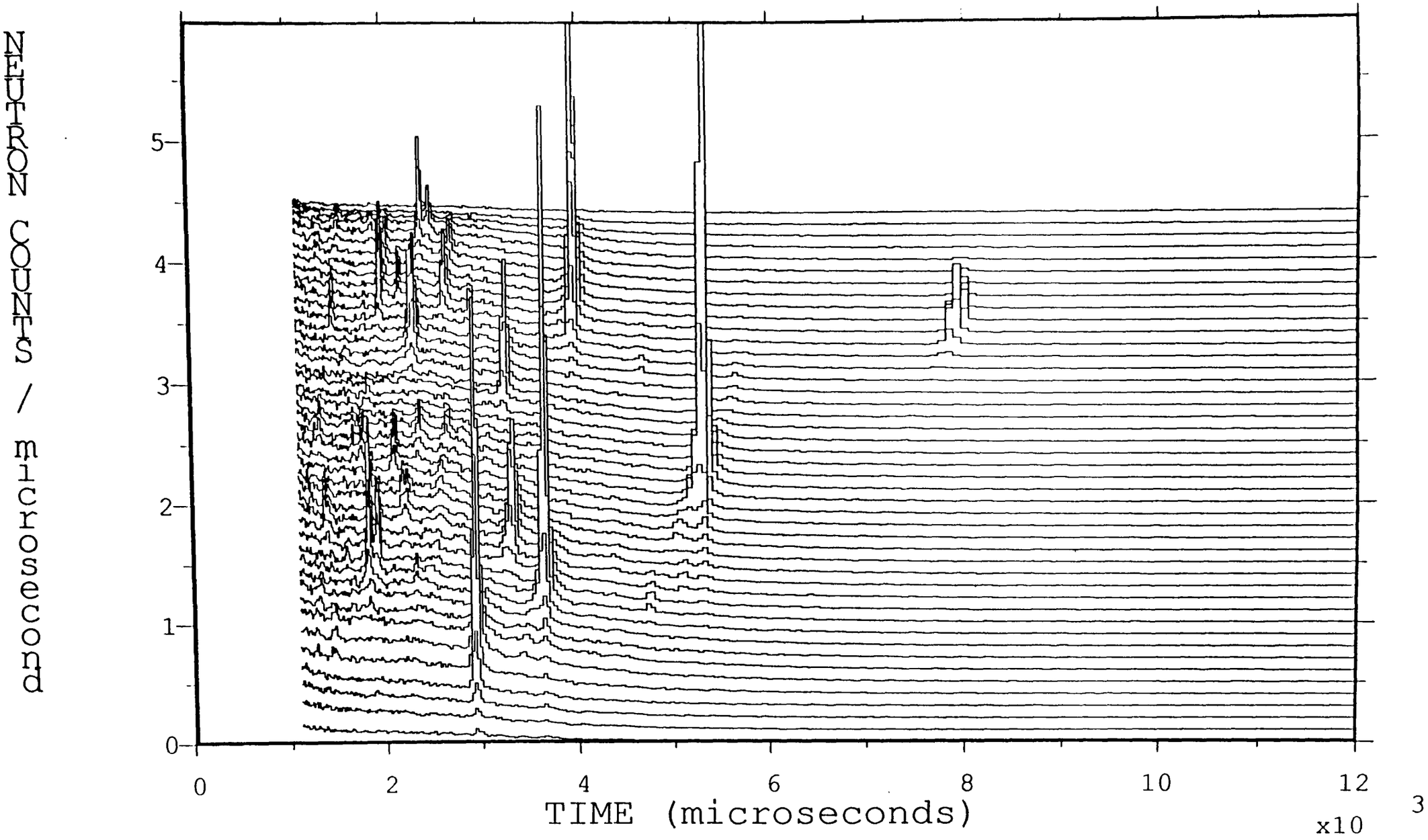

Figure 11.2 The grouped time of flight profiles for adjacent pixels reveals the area of reciprocal space close to the (hh0) direction for schultenite.

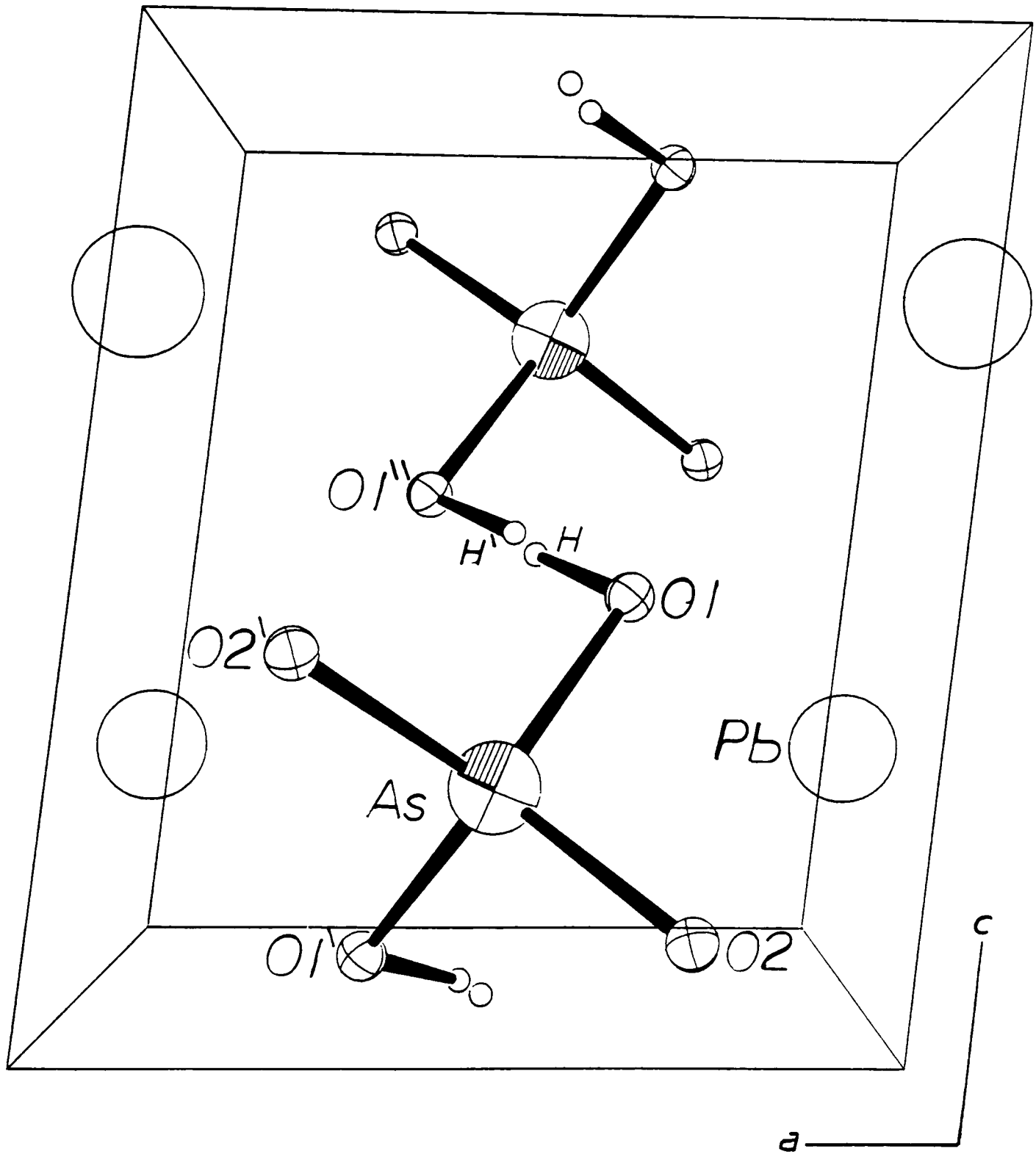

Figure 11.3 The basic cell contents of $PbHAsO_4$ in a disordered state, viewed along the y axis. H and H′ represent the two stable disordered positions for hydrogen in P2/c.

Table 11.1(a) Fractional atomic coordinates from neutron study, refined as P2/c. ($U_{eq}=1/3\sum_i\sum_j U_{ij}a_i^*a_j^*a_i\cdot a_j$)

NEUTRON (P2/c)

	(X/A)	(Y/B)	(Z/C)	U_{eq}
Pb	0.0000	0.2027(3)	0.2500	0.013
As	0.5000	0.7966(4)	0.2500	0.009
O(1)	0.3591(8)	0.6494(4)	0.4433(10)	0.016
O(2)	0.2492(7)	0.9318(4)	0.1089(9)	0.012
H	0.484(4)	0.5245(23)	0.488(5)	0.030(3)

Table 11.1(b) Fractional atomic coordinates from neutron study, refined as Pc.

NEUTRON (Pc)

	(X/A)	(Y/B)	(Z/C)	U_{eq}
Pb	-.0003(3)	0.2028(3)	0.2496(44)	0.011(5)
As	0.5019(35)	0.7965(4)	0.2422(51)	0.008(6)
O(1)	0.3625(34)	0.6489(13)	0.4309(48)	0.015(2)
O(2)	0.2429(30)	0.9264(10)	0.1093(45)	0.01(2)
O(3)	0.6437(33)	0.6494(16)	0.0449(51)	0.017(2)
O(4)	0.7436(33)	0.9373(11)	0.3919(49)	0.01(2)
H(1)	0.458(8)	0.514(6)	0.478(8)	0.022(6)
H(2)	0.497(6)	0.472(5)	0.508(7)	0.017(6)

Table 11.1(c) Fractional atomic coordinates from X-ray study of Effenberger and Pertlik.

X-RAY (P2/C)

	(X/A)	(Y/B)	(Z/C)
Pb	0.0000	0.2032(1)	0.2500
As	0.5000	0.7963(1)	0.2500
O(1)	0.3609(13)	0.6473(9)	0.4435(11)
O(2)	0.2479(11)	0.9322(8)	0.1098(8)

Table 11.2 Anisotropic thermal parameters from P2/c refinement.

	U11	U22	U33	U23	U13	U12
Pb	0.012(1)	0.012(1)	0.014(3)	0.000	0.001(19)	0.000
As	0.008(2)	0.008(1)	0.011(4)	0.000	0.0001(24)	0.000
O(1)	0.017(2)	0.015(10)	0.015(5)	0.007(1)	0.014(3)	0.0035(10)
O(2)	0.01(1)	0.017(10)	0.008(4)	0.001(1)	0.0015(21)	0.004(8)

Table 11.3 Selected intramolecular and intermolecular bond lengths. Values in angstroms.

	LHA		
	NEUTRON	X-RAY	LHP
Pb-O(1)	2.836(5)	2.860	2.845(7)
Pb-O(2)	2.402(4)	2.454	2.398(6)
As-O(1)	1.711(5)	-----	1.714(7)
As-O(2)	1.683(4)	-----	1.688(6)
O(1)-H	1.061(15)	1.048	--------
O(1)...O(1)''	2.503(5)	2.70	2.471(9)
H...O(1)''	1.443(15)	1.424	--------
H...H''	0.388(19)	0.392	--------

Table 11.4 Selected intramolecular and intermolecular bond angles. Values in degrees.

	NEUTRON	X-RAY
O(1)-As-O(1)'	108.7(3)	107.9(3)
O(1)-As-O(2)	108.3(2)	108.5(3)
O(1)-As-O(2)'	108.7(3)	108.9(3)
O(2)-As-O(2)'	114.1(3)	113.9(3)
O(1)-H-O(1)''	176.9(19)	--------

Chapter 12. A critical evaluation of some current computerised diffractometers

12.1 Introduction

Over the course of the research programme several diffractometers were employed to analyse crystal compounds. These have represented a wide range of operational geometries and advancements in instrument design. In addition to these systems there are a multitude of other instruments currently being used by the crystallographic community. This chapter endeavours to review and compare a selection of the most prevalent instruments highlighting the uses and benefits of each.

12.2 Powder diffractometers

In recent years the method of powder diffraction has been re-established for fine structure analysis of crystalline samples. Many scientific institutions are now in the dilemma of whether to upgrade their existing systems or to invest in modern technology.

12.2.1 Enhanced systems

There are several commercial packages specifically designed for diffractometer upgrading, however they all tend to simply perform the operation of goniometer control and data logging. The Hiltonbrooks[110] and Sietronics Sieray 112[111] systems both incorporate stepper motor controllers and data interfaces which are programmed by a remote IBM PC clone computer. The Hiltonbrooks system offers a collection of pulleys, belts and mounting plates to allow almost all diffractometers to be upgraded. The final step size and the absolute resolution of the goniometer arm is dictated by the choice of pulley mechanisms.

The SieRay 112 system can be used as a basic mechanical upgrade, but additional software and hardware including a detector amplifier/analyser can be added to create an completely integrated package. The bundled software performs the same tasks as the CENPOD

system with access to a database for automatic comparison.

The cost of these upgrades range to about £7000, which in comparison with new instruments is small, but it still represents a considerable outlay for smaller institutions.

Several other systems have been developed by individuals for a fraction of the cost of the commercial systems[112-114]. Again these systems ultimately perform the basic task of controlling the data logging process. However, they can offer step sizes of 0.001° 2Θ which represents a very significant improvement in resolution, comparable with other modern instruments. These systems have been reported to have been successful in their operation allowing fairly sophisticated data analysis to be carried out, such as Reitveld profile fitting. The cost of implementing the upgrades was however, far cheaper than the commercially available ones.

12.2.2 Current commercial systems

The range of commercial powder systems in quite extensive, but there are a few instruments which deserve recognition.

12.2.2.1 Siemens D5000 X-ray diffractometer[115]

The D5000 is a very versatile instrument which seems to have inherited many of the features incorporated in the custom built instruments such as those at SRS.

It is based on a simple 2-circle goniometer design with independent computer control over the sample, detector and X-ray tube positions. This permits operation in Θ/2Θ, Θ, 2Θ and Θ/Θ modes. The Θ/Θ mode moves the detector and tube whilst maintaining the sample position. This is important when liquid samples are being used for amorphous scattering experiments.

The instrument is heavily automated allowing control over the sample turntable, sample loading and adjusting the slit width. The slit width can be programmed to vary as a function of θ, thereby maintaining beam focus. The monochromator can be installed in either a incident or receiving mode, depending on the particular application.

The variable geometry of the instrument allows the incorporation of non-ambient sample apparatus. Clearly this is a highly desirable facility to have at ones disposal. In addition the goniometer table is designed to allow the addition of other devices such as Eulerian cradles and position sensitive detectors.

The instrument can be controlled via a dedicated microcomputer, allowing the diffraction data to be processed. There is provision for direct access to the JCPDS file on floppy disc or CD-ROM.

The exact price for the dedicated generator and instrument is unknown, but due to it shear flexibility, it represents a valuable piece of apparatus for any institutions involved in X-ray diffraction studies.

The D5000 boasts a step size in theta of 0.001°, a reproducibility of theta of ±0.0005° and an accuracy of ±0.005°. A maximum scanning speed of 1000°/min allows fast initial scans and in the step mode more accurate data can be collected.

12.2.2.2 Enraf-Nonius PDS120[116]

This represents a basic powder diffractometer with a fixed tube position arrangement. The main feature of note is the Inel CPS120 PSD which is used to collect the experimental data[117]. (The operational principles of the PSD will be dealt with in 12.4.1.)

The CPS120 allows traces of up to 120° of 2θ to be collected simultaneously in a very short time scale. The sample is generally

mounted in a capillary tube allowing X-rays to be emitted radially in plane perpendicular to the capillary. The manufacturer quotes a minimum data collection period of 1 minute, however longer periods are required to achieve reliable counting statistics. This does however, permit the sample to be viewed quickly to ascertain the regions of most intense diffraction.In normal operation only the sample holder is rotated (to help reduce the effects of preferred orientation) and so this allows non-ambient temperature and pressure vessels to be attached. The present temperature range is quoted as 4 to 1700K.

As with the D5000 a sample cartridge holding 30 plus samples can be fitted, allowing jobs to be queued. This obviously makes sound economical sense, permitting the instrument to be used 24 hours per day.

Control is achieved by a microcomputer providing a link with other computer systems and databases. Although no numerical information regarding accuracy was available, the instrument cannot be realistically compared with the D5000. The PDS120 is more suited to phase analysis.

12.2.2.3 Philips PW1840 compact diffractometer[118]

This represents the successor to the PW1050 powder diffractometer. The operational geometry has changed little. The paper scroll plotter is still incorporated, but there is provision for a VDU.

Philips have placed a lot of emphasis on safety and ease of operation. The entire goniometer is now enclosed and sample loading is automatic. It still operates in a $\theta/2\theta$ mode using a stepper motor rather than the continuous drive system of the PW1050.

The slits can now be computer controlled allowing synchronisation to

the movement of the goniometer. This allows very low angles approaching 1° of 2θ to be measured whilst retaining a relatively good signal to noise ratio.

The 2θ range is limited to 0-120° with an incremental step size of 0.01°, giving an accuracy of 0.02°. This is comparable to the enhanced system described in 2.2. With this level of resolution, the instrument is intended for qualitative and semi-quantative work.

For institutions, such as RGIT, who are already in possession of a PW1050 or equivalent, which is employed mainly for quantitative and semi-qualitative analysis, there would be little sense in purchasing such an instrument, since for a fraction of the cost the existing system could be upgraded.

12.2.2.4 Philips PW1800[118]

The PW1800 can best be described as an upgraded PW1840 with full software support. The system is supplied with APD 1700, a software package to run via the current edition of MS-DOS on an IBM PC. The software allows automatic peak identification and profile fitting to asymmetric, broadened, single or overlapping peaks. This is essentially a vastly improved version of the CENPOD system, giving greater effectivity in all aspects of operation.

The goniometer and the X-ray generator can be programmed giving even greater flexibility. The θ and 2θ circles are computer controlled and are independent of one another. A minimum step size of 0.005° provides greater 2θ resolution than the PW1840.

The instrument can be supplied with the JCPDS powder index on magnetic disc or CD-ROM, making the instrument ideal for educational purposes. Again the resolution cannot compare with the D5000, but it is a

considerable improvement over the PW1840.

12.2.2.5 Philips MPD1880/HR[118]

This instrument is primarily intended to be used for wafer surface examination, but it also has the capability to be converted into a high resolution powder diffractometer.

Its main difference from the PW1800 is the use of the unique four crystal monochromator. The monochromator uses a series of four crystals of germanium to remove undesirable X-ray components giving a highly monochromated beam with $\Delta\lambda/\lambda=2 \times 10^{-5}$. This is comparable with the narrow range of wavelengths produced by the synchrotron at SRS. The performance of such an instrument obviously makes it a good choice for profile fitting, stress measurements and other high resolution work, but it still lacks the overall flexibility of the D5000.

12.3 Single crystal diffractometers

Single crystal diffractometers have seen vast improvements since the days of manually operated goniometers. The Nicolet P3 instrument used as a standard in this current research programme has proved its abilities in the collection of quality data, but perhaps more modern instruments are beginning to set the standard for single crystal diffraction for the 1990's and beyond.

12.3.1 Enraf-Nonius CAD4[116]

This instrument is currently regarded as the crystallographic community standard and has become the best selling single crystal diffractometer to date.

Its success can be attributed to the introduction of the Kappa (κ) axis developed by Enraf-Nonius. This arrangement dispenses with the bulky Eulerian cradle which is common on most diffractometers. The X-

ray source and detector positions are still located in the same plane, but the crystal is mounted on the κ axis, inclined at 45° to the detector/tube plane. The κ axis geometry has the advantage of producing a completely open instrument, allowing full rotational freedom of the crystal and detector. Conventional 4-circle diffractometers equipped with Eulerian cradles can often experience blind spots, where the orientation of the χ circle can obscure the path of the incident/diffracted beam. The spacious environment of the CAD4 enables crystal conditioning apparatus, such as low temperature probes, to be positioned with ease. The system has been designed to be modular so that it may be tailored to suit the individual needs of the operators.

The system is linked to a dedicated MicroVax computer, which attends to the crystal orientation and the operation of the X-ray generator. The MoIEN crystallographic program library comes supplied which has full capabilities for data processing and analysis. This includes direct methods, Patterson vector and least squares routines as well as graphics packages to produce molecular plots. The problem of applying absorption corrections can be dealt with by collecting absorption profiles relative to rotations of the crystal.

The κ axis has a rotational range of -180° to +180° with step size of 0.01°. The ω axis has an accuracy of 0.005° and the 2θ and ϕ axes have accuracies of 0.01°. This results in a combined reproducibility of 0.002° for any given reflexion.

12.3.2 Siemens R3 Series II[115]

This represents one of the latest Eulerian cradle based 4-circle diffractometers with dedicated computer control. The basic operational

geometry does not differ from the Nicolet P3 system at Aberdeen University, but it has more sophisticated computer routines for structure elucidation, such as SHELXTL PLUS. The package also allows complete automated control over the diffractometer and generator. Although no data was available regarding the accuracy and reproducibility of the rotation axes, the instrument is likely to have similar capabilities as the CAD4. What is clear though, is that the R3 cannot offer the same level of flexibility as the CAD4. The Eulerian cradle despite its effectivity, can be now regarded as obsolete especially in systems which are used for non-ambient studies.

12.4 Additional hardware

The emergence of κ axis diffractometers represents the latest advancement in instrument geometries, but as the neutron SXD at RAL and the SRS, Daresbury has demonstrated, the most significant area of development has been with detector instrumentation and beam source.

12.4.1 Position sensitive detectors

PSD's are becoming increasingly more widespread in both powder and single crystal diffractometry. They offer numerous advantages over conventional rotating detectors, but it is arguable whether they are more accurate.

12.4.1.1 STOE PSD[119]

STOE manufacture several one dimensional PSD's which range in 2Θ angle from 4° to 45°. They use a curved wire anode sealed in an chamber with a gas mixture of 90% argon and 10% methane. On the event of a photon entering the chamber, the resulting gas ionisation causes a surge of electrons on the anode. The charge is dissipated along the anode in both directions and the times of flight for the surges indicates

the position of the photon event.

This style of curved PSD has the advantage of being able to collect a range of 2θ simultaneously, making analysis very rapid. This allows samples which undergo deterioration in the presence of a X-ray beam to be analysed rapidly. More importantly, real time spectra can be collected for samples being exposed to varying conditions, such as pressure and temperature. In addition the focusing geometry of the detector, ensures symmetric peaks throughout the 2θ range, making peak fitting simple.

However, this convenience is balanced by a loss of accuracy compared to the conventional rotating detector diffractometers.

12.4.1.2 Spectrolab Series 3000X PSD[120]

This PSD operates in a similar fashion to the STOE instruments, but has the extended 2θ range of 120°. A 2θ resolution of better than 0.02° is quoted, which is only suited to qualitative and quantitative work. In this particular aspect the PSD excels since it is capable of scanning the entire 2θ range at great speed.

12.4.1.3 Enraf-Nonius FAST PSD[116]

Both of the PSDs mentioned above are one dimensional and are ideally suited for powder analysis, although they can be used for single crystal work also. The Enraf-Nonius represents the very latest development in two dimensional X-ray PSDs.

The detector records the diffraction intensities on an Eu^{2+} doped barium halide imaging plate, producing an image analogous to a Laue photograph. The plate is divided into an array of pixels which are connected to fibre optic cables. The event of a photon striking the plate causes the molecules in the plate to absorb the quantum of

energy. By scanning the plate with a laser, the energy is released as a photon of light, which is transmitted down the fibre optic cable to a photomultiplier tube. The mode of operation is similar to the neutron ZnS detector discussed in chapter 2, but only stores the information in two dimensions.

The main advantage of the FAST system is that plates may be removed from the diffractometer and put to one side to be examined later, thus accelerating the rate of data collection. Clearly this type of detector represents the future for rapid data collection. The combination of speed and flexibility offered surpasses all other previous commercial detectors.

11.4.2 X-ray sources

The main advantage of synchrotron radiation for X-ray analysis, lies in the enormous flux and highly monochromatic beams, but the basic economics of operating a synchrotron prevents small institutions from gaining access to these facilities on a daily basis.

The Siroflux Primary Beam X-ray Optical System can offer an alternative to the synchrotron for high resolution diffractometry[121]. Using a high power rated X-ray tube and unique optical X-ray focussing components, a highly monochromatic beam can be produced. The manufacturers quote a wavelength spread of $\Delta\lambda/\lambda=2 \times 10^{-4}$ with a typical flux of 3×10^{6} cps.

11.5 Conclusions

All of the diffractometers and peripheral devices described have benefited in some way by the incorporation of microprocessor devices. They have added increased accuracy, but with improved operational efficiency and in some cases have become more "user friendly". With

the increased level of sophistication, new more exciting projects have been made possible. However with most technological advances, there reaches a point of diminishing return where vast sums of money have to be spent to produce significant progress. It is hard to estimate when this stage of development will occur in the field of crystallography, since there has been a wide diversification of techniques in the past decade. What is certain is that the next generation of ever increasingly powerful computers will be involved in all aspects.

REFERENCES

1. H.A.Klug and L.E.Alexander, "X-ray diffraction procedures for polycrystalline and amorphous materials", pp138, Wiley, USA (1974).

2. B.T.M.Willis and A.W.Pryor, "Thermal vibrations in Crystallography", Chpt.4, Cambridge University Press, England (1975).

3. G.E.Bacon (1972) *Acta Cryst.*, **A28**, 357.

4. M.J.Buerger, "Crystal-structure analysis", pp152-192, 2nd Edition, Wiley, USA (1967).

5. S.C.Abrahams (1973) *Acta Cryst.*, **A29**, 111.

6. M.J.Beurger, "Crystal-structure analysis", pp370-404, 2nd Edition, Wiley, USA (1967).

7. C.E.Nordman and K.Nakatsu (1963) *J.Am.Chem.Soc.*, **85**, 353.

8. C.E.Nordman (1965) *J.Am.Chem.Soc.*, **87**, 2059.

9. C.Bokhoven, J.C.Schoone and J.M.Bijvoet (1951) *Acta Cryst.*, **4**, 275.

10. D.W.Green, V.M.Ingram and M.F.Perutz (1954) *Proc.Roy.Soc.A*, **225**, 287.

11. D.Harker and J.S.Kasper (1948) *Acta Cryst.*, **1**, 70.

12. J.Karle and H.Hauptman (1950) *Acta Cryst.*, **3**, 181.

13. J.P.Glusker and K.N.Trueblood, "Crystal structure analysis", pp104, 2nd Edition, Oxford University Press, England (1985).

14. D.Sayre (1952) *Acta Cryst.*, **5**, 60.

15. W.Cochran (1955) *Acta Cryst.*, **8**, 473.

16. J.Karle and H.Hauptman (1956) *Acta Cryst.*, **9**, 635.

17. W.Cochran and M.M.Woolfson (1955) *Acta Cryst.*, **8**, 1.

18. I.L.Karle and J.Karle (1964) *Acta Cryst.*, **17**, 835.

19. A.L.Patterson (1935) *Z.Krist.*, **A90**, 517.

20. G.H.Stout and L.H.Jensen, "X-ray structure determination", 2nd Edition, pp349, Wiley, USA (1989).

21. G.H.Stout and L.H.Jensen, "X-ray structure determination", 2nd Edition, pp358-368, Wiley, USA (1989).

22. L.H.Hodgsen and J.S.Rollet (1963) *Acta Cryst.*, **16**, 329.

23. W.C.Hamilton (1965) *Acta Cryst.*, **18**, 502.

24. A.J.C.Wilson (1950) *Acta Cryst.*, **3**, 397.

25. J.Donohue and K.N.Trueblood (1956) *Acta Cryst.*, **9**, 615.

26. B.D.Cullity, "Elements of X-ray diffraction", Chapt.9, Addison-Wesley, USA (1977).

27. B.D.Cullity, "Elements of X-ray diffraction", Chapt.7, Addison-Wesley, USA (1977).

28. G.J.Stanisz, J.M.Holender and J.Soltys (1989) *Powder Diffraction*, **Vol.4**, **No.2**, 70.

29. G.Will, M.Bellotto, W.Parrish and M.Hart (1988) *J.Appl.Cryst.*, **21**, 182.

30. N.P.Pyrros and C.R.Hubbard (1983) *J.Appl.Cryst.*, **16**, 289.

31. H.M.Rietveld (1969) *J.Appl.Cryst.*, **2**, 65.

32. "Reference guide to Philips PW1025/25 goniometer", Philips, Eindhoven, Netherlands, 1969.

33. SERC Bulletin (1988) **Vol.3**, **No.12**, 14.

34. "The Stoe on-line Automatic 2-Circle X-ray Diffractometer STADI 2", Stoe, Darmstadt, Germany.

35. Nicolet P3 data collection tutorial, Department of Chemistry, Aberdeen University.

36. C.C.Wilson (1990) *Neutron News*, **Vol.1**, **No.1**, 14.

37. H.D.Anger (1958) *Rev.Sci.Instr.*, **29**, 27.

38. J.B.Forsyth, R.T.Lawrence and C.C.Wilson (1988) *Nuclear Instrum.Meth.*, **A273**, 741.

39. J.B.Forsyth, C.C.Wilson, A.M.Stringer, J.A.K.Howard and O.Johnson (1986) *Journal de Physique* **C5**, 143.

40. B.Buras and L.Gerward (1975) *Acta Cryst.*, **A31**, 372.

41. M.L.DeJong, "Programming and interfacing the 6502, with experiments", H.W.Sams and Co., Indianapolis, USA (1980).

42. A.C.Bray, A.C.Dickens and M.A.Holmes, "The advanced user guide for the BBC micro", Chapt.28, Cambridge Computer Centre, England (1983).

43. "BBC Master user guide", Volume 2, Acorn Computers, Cambridge, England (1985).

44. D.M.A.Guerin, R.D.Bonetto and A.G.Alvarez (1988) *Powder Diffraction*, **Vol.3**, **No.2**, 84.

45. J.M.Stewart and Y.Zhang (1989) *J.Appl.Cryst.*, **22**, 640.

46. K.E.Wiedemann, J.Unnam and R.K.Clark (1987) *Powder Diffraction*, **Vol.2**, **No.3**, 137.

47. E.A.Armstrong and D.G.Cameron (1989) *Powder Diffraction*, **Vol.4**, **No.3**, 144.

48. H.Toraya (1988) *J.Appl.Cryst.*, **21**, 192.

49. **JCPDS**, International Centre for Diffraction Data, National Bureau of Standards, Washington, DC 20234.

50. E.Hadicke, F.Frickel and A.Franke (1978) *Chem.Ber.*, **111**, 3222.

51. L.Parkanyi, A.Kalman, B.Hegedus, K.Harsanyi and J.Kreidl (1984) *Acta Cryst. C*, **40**, 676.

52. L.E.Alexander, H.P.Klug and E.Kummer (1948) *J.Appl.Phys.* **19**, 742.

53. L.S.Dent Glasser, "Crystallography and its applications", Chapt.6, Van Nostrand Reinhold, USA (1977).

54. G.L.McCreery (1949) *J.Am.Ceram.Soc.*, **32**, 141.

55. **REHIDRAT**, Searle Pharmaceutics, Searle and Co., England.

56. **DIORALYTE**, Rorer Pharmaceutics, England.

57. J.W.Shell (1963) *J.Pharm.Sci.*, **Vol.52**, **No.1**, 24.

58. G.J.Papariello, H.Letterman and R.E.Huettermann (1964) *J.Pharm.Sci.*, **Vol.53**, **No.6**, 663.

59. L.S.Zevin and S.L.Zevin (1989) *Powder Diffraction*, **Vol.4**, **No.4**, 196.

60. L.E.Alexander and H.P.Klug (1989) *Powder Diffraction*, **Vol.4**, **No.2**, 66.

61. P.M.de Woolf and J.W.Visser (1988) *Powder Diffraction*, **Vol.3**, **No.4**, 202.

62. S.M.S.V.Doidge-Harrison, I.W.Nowell, P.J.Cox, R.A.Howie, O.J.Taylor and J.L.Wardell (1991) *J.Organomet.Chem.* **401**, 273.

63. **DATRN**, Program for calculating structure factor amplitudes from single crystal X-ray diffraction data, University of Leicester, England.

64. G.M.Sheldrick (1976) **SHELX-76**, Program for Crystal Structure Determinations, University of Cambridge, England.

65. C.Glidewell and D.C.Liles (1982) *J.Organomet.Chem.*, **224**, 237.

66. ISIS Annual Report 1990, *RAL-90-050*, Didcot, Oxon, England.

67. J.I.Langford and P.D.Hatton (1986) *High Resolution Powder Diffraction. Materials Science Forum*, **9**, 31-38.

68. J.Plevert, M.Louer and D.Louer (1989) *J.Appl.Cryst.*, **22**, 470.

69. H.G.Heller and R.A.N.Morris (1966) *J.Chem.Soc.*, 1004.

70. D.Y.Curtin, H.Gruen, Y.G.Hendrickson and H.E.Knipmeyer (1961) *J.Am.Chem.Soc.* **83**, 4838.

71. C.J.Gilmore (1984) **MITHRIL** - an integrated direct-methods program, *J.Appl.Cryst.*, **17**, 42.

72. C.K.Johnson (1965) **ORTEP**. *Oak Ridge National Laboratory Report ORNL-3794*, Oak Ridge, Tennessee, USA.

73. W.E.Noland and V.Kameswaran (1981) *J.Org.Chem.*, **46**, 1318.

74. P.H.Boyle, M.J.O'Mahoney and C.J.Cardin (1984) *J.Chem.Soc., Perkin Trans.*, 593.

75. G.M.Sheldrick (1986) **SHELXS-86**, Program for the solution of crystal structures from diffraction data. (PC Version)

76. P.J.Cox, S.M.McManus, B.C.Gibb, I.W.Nowell, A.B.Turner and R.A.Howie (1990) *J.Cryst.Spect.Res.*, (in press)

77. S.B.Hanson, P.B.Hitchcock, P.B.Reese and A.Trunneh (1988) *J.Chem.Soc.Perkin Trans.*, **1**, 1465.

78. D.Schomberg, M.Link, H.Linoh and R.Tacke (1988) *J.Organomet.Chem.*, **339**, 71.

79. L.N.Zakarov, Yu.T.Struchov, E.A.Kuz'min and B.I.Petrov (1983) *Sov.Phys.Crystallogr.*, **28**, 158.

80. S.Vilminot, W.Grainer, Z.Al'Orabi and L.Cot (1978) *Acta Cryst.*, **B34**, 3308.

81. H.C.Clark, R.J.O'Brien and J.Trotter (1963) *Proc.Chem.Soc.*, 85.

82. H.C.Clark, R.J.O'Brien and J.Trotter (1964) *J.Chem.Soc.*, 2332.

83. S.Calogero, P.Ganis, V.Peruzzo, G.Tagliavini and G.Vale (1981) *J.Organomet.Chem.*, **220**, 11.

84. L.N.Zakarov, V.A.Lebedev, E.A.Kuz'min and N.V.Belov (1978) *Kristallografia*, **23**, 1049.

85. S.S.Al-Juaid, S.M.Dhaher, C.Eaborn and P.B.Hithcock (1989) *J.Organomet.Chem.*, **366**, 39.

86. P.G.Harrison, T.J.King and M.A.Healy (1979) *J.Organomet.Chem.*, **182**, 17.

87. R.A.Howie, E.S.Paterson, J.L.Wardell and J.W.Burley (1983) *Organomet.Chem.*, **259**, 71.

88. R.A.Howie, E.S.Paterson, J.L.Wardell and J.W.Burley (1986) *Organomet.Chem.*, **304**, 301.

89. R.E.Hutton, J.W.Burley and V.Oakes (1978) *J.Organomet.Chem.*, **156**, 369.

90. R.M.Haigh, A.G.Davies and M.-W.Tse (1979) *J.Organomet.Chem.*, **174**, 163.

91. O.-S.Jung, J.H.Jeong and Y.S.Sohn (1989) *Polyhedron*, **8**, 1413.

92. O.-S.Jung, J.H.Jeong and Y.S.Sohn (1989) *Acta Cryst.*, **C46**, 31.

93. P.J.Cox, S.M.S.V.Doidge-Harrison, R.A.Howie, I.W.Nowell, O.J.Taylor and J.W.Wardell (1989) *J.Chem.Soc., Perkin Trans. I*, 2017.

94. F.Meller and I.Fankucken (1955) *Acta Cryst.*, **8**, 343.

95. N.W.Alcock and J.F.Sawyer (1977) *J.Chem.Soc., Dalton Trans.*, 1090.

96. V.Cody and E.R.Corey (1969) *J.Organomet.Chem.*, **19**, 359.

97. H.A.Skinner and L.E.Sutton (1944) *Trans.Faraday Soc.*, **90**, 164.

98. J.N.Low and C.C.Wilson (1983) *Acta Cryst.*, **C39**, 1688.

99. C.H.Schwalbe and W.Saenger (1973) *Acta Cryst.*, **B29**, 61.

100. J.W.Wadsworth, C.C.Wilson and W.I.F.David (1989) *Nucleosides & Nucleotides*, **8**, 537.

101. P.J.Brown and J.C.Matthewman (1987) *Rutherford Appleton Laboratory Report RAL-87-010*, Didcot, Oxon, England.

102. E.Keller (1988) **SCHAKAL88**. A FORTRAN program for the graphical representation of molecular and crystallographic models. Albert-Ludwigs University, Freiburg, Germany.

103. G.F.Claringbull (1950) *Min.Mag.*, **29**, 157.

104. H.Effenberger and F.Pertlik (1986) *Tschermarks Min.Petr.Mitt.*, **35**, 157.

105. B.B.Lavrencic and J.Petzelt (1977) *J.Chem.Phys.*, **67**, 3890.

106. D.J.Lockwood, D.Ohno, R.J.Nelmes and H.Arend (1985) *J.Phys.C.*, **18**, 559.

107. T.J.Negran, A.M.Glass, C.S.Brickenkamp, R.D.Rosenstein, R.K.Osterheld and R.Susott (1974) *Ferroelectrics*, **6**, 179.

108. R.Restori, Z.Tun, R.J.Nelmes and C.J.McIntyre (1987) *J.Phys.C.*, **20**, 591.

109. R.J.Nelmes (1988) *J.Phys.C.*, **21**, 881

110. Hiltonbrooks Ltd, Yew Tree Cottage, Knutsford Road, Cranage, Holmes Chapel, Cheshire, England.

111. SieRay Ltd, Hawker A.C.T., 2614 Australia.

112. J.C.Madsen, H.J.Skov and S.E.Rasmussen (1988) *Powder Diffraction*, **Vol.3**, **No.2**, 91.

113. K.D.Rogers and D.W.Lane (1987) *Powder Diffraction*, **Vol.2**, **No.4**, 227.

114. G.J.Van Hummel and H.Graafsma (1989) *J.Appl.Cryst.*, **22**, 75.

115. Siemens AG, Analytical Systems, E689, Postfach 21 1262, D7500 Karlsruhe 21, Germany.

116. B.V.Enraf-Nonius Delft, PO Box 483, 2600 AL Delft, Netherlands.

117. INEL Ltd, France. (Distributed through Spectrolab Ltd - see ref.120)

118. Philips Nederland B.V., Afd. Analysetechnieken, VB3 Postbus 90050, 5600 PB, Eindhoven, Netherlands.

119. STOE & CIE Gmbh, Hilperstraße 10, PO Box 4110, D-6100 Darmstadt, Germany.

120. Spectrolab Ltd, PO Box 25, Newbury, Berkshire, England.

121. C.S.I.R.O., Division of Materials Science & Technology, Melbourne, Austrailia. (Distributed through Spectrolab Ltd.)

APPENDIX A

CENPOD manual with program listings.

CENPOD

SOFTWARE ROUTINES FOR POWDER DIFFRACTION ANALYSIS

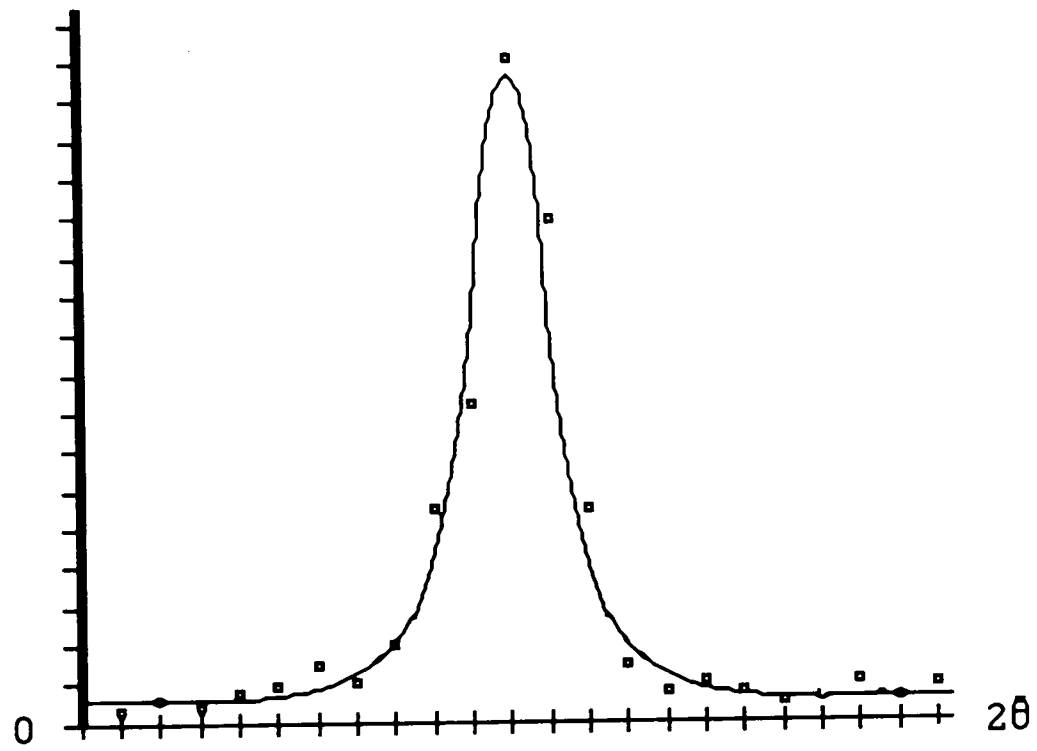

BY

NEIL S STEWART

ROBERT GORDON'S INSTITUTE OF TECHNOLOGY

CONTENTS

1. INTRODUCTION

CENPOD (Computer **EN**hanced **PO**wder **D**iffractometer) is a software package written to be used for the enhanced operation of the Phillips PW1050 powder diffractometer (PD). The software is written to be as straight-forward as possible and only requires a basic knowledge of powder diffraction techniques to operate it. However, to carry out more elaborate studies, the user will require a greater knowledge of both powder diffraction and **CENPOD**.

For users who are unfamiliar with the instrument, Figure 1 presents a labelled schematic diagram of the diffractometer. The instrument and processing electronics look fairly complicated, but there are only a few basic features that you need to be familiar with.

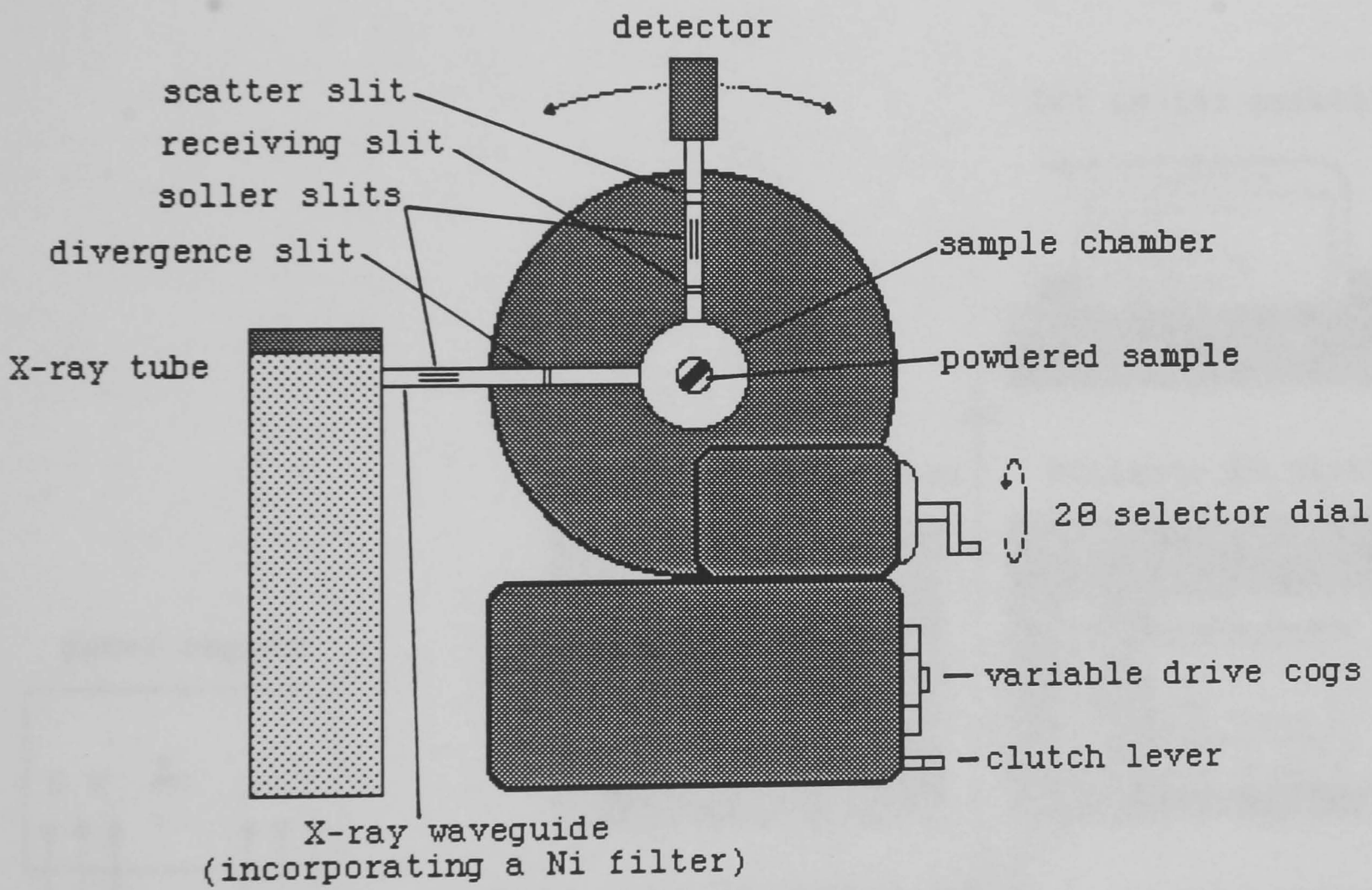

Figure 1 Philips PW1050 powder diffractometer.

The significance of each of the features and the basic operation of the PD will be discussed in the following chapters of the manual. If further information is required you can consult the user manuals stored in the X-ray lab or one of many books under the Crystallography heading in the St.Andrews St. library.

2.HARDWARE REQUIREMENTS AND CONNECTIONS

The software is a fairly specific package and will only run successfully with the correct hardware. Everything which the user is likely to need is tabulated below:-

12V/5V power supply.
BBC Master 128K microcomputer.
Diffractometer data-logger interface.
80 track double-sided disc drive.
Med/High resolution monitor.
Epson compatible dot-matrix printer.
Plotmate A3 XY plotter.

Figure 2 shows a schematic diagram of the connections for the apparatus.

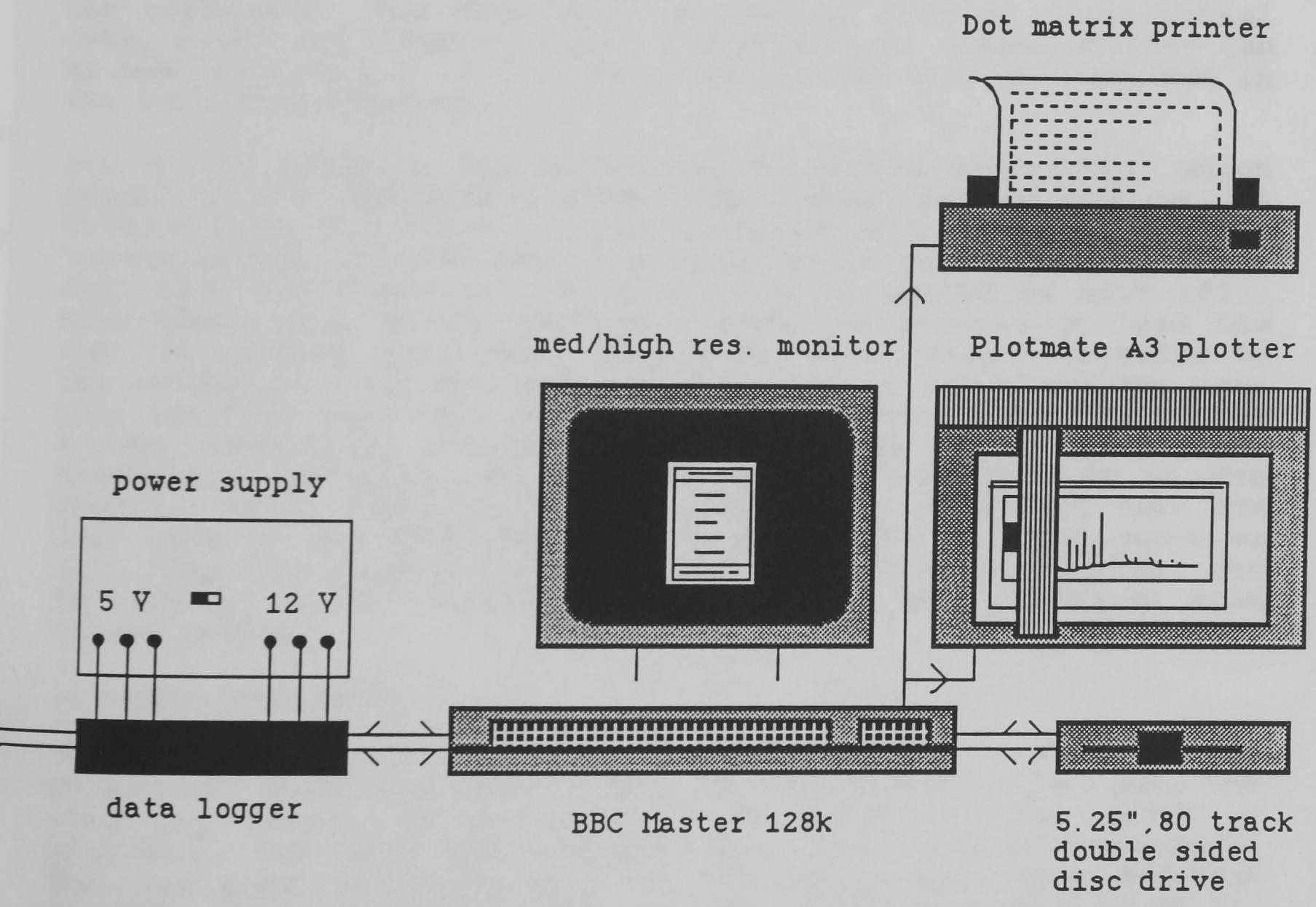

Figure 2 Hardware connections for the enhanced system.

3 OPERATING PRINCIPLES OF SOFTWARE

3.1 The black box approach

In this manual each of the programs will be explained giving tips on how to use them most effectively and how to avoid making simple mistakes. It will explain what each function will do, but it will not go into unnecessary detail of what is actually happening in the program. Therefore the package can be treated as a 'black box'. However should the user wish to involve themselves in the code and perhaps update the routines, there are complete listings of all the programs in Appendix B. Further details on the theory behind the code and also full technical explanations concerning the interface are discussed in my thesis.

3.2 The working environment

A feature which is common to all program units in **CENPOD**, is the **instruction window**. This is a text window positioned at the bottom of the screen and it is from here that instructions are issued. The area directly above the instruction window is called the **workspace**. The workspace is used to display experimental data, plots and command files. A hypothetical screen display can be seen in Figure 3. All of these facilities will be discussed in the following chapters.

All of the programs are controlled by nested mini-menus, which appear in the instruction window. The menus list several options controlling the flow of the program and by pressing the corresponding function key, the function is activated. All menus will have two functions (f0 & f1) and an option to exit (f2). Mini-menus will either perform a specific process or lead the user to another mini-menu, displaying more options relating to the selection from the previous menu. If at any stage the user realises that they have selected the wrong menu or that they have accomplished their desired task and now wish to utilise another facility, the **Exit** option will return program flow to the previous menu. Repeating this procedure will eventually take the user back to the first menu, where the option to start again or exit from the program is permitted. The mini-menu structure can be likened to the sub-directory hierarchy of a computer disc filing system.

3.3 Menu path route

To remind the user of their current position in the menu structure, each menu has a label which describes the route the user has taken. In the example in Figure 3, the label is **prog/a/b1**. The label can be broken down into separate components. The name **prog**, indicates that the current program being executed is **PROG**. The root menu of any program is always indicated by **/a**, where the letter **a** relates to the first menu level. The extension **/b1** indicates the current menu is in the second (**b**) level and the number **1** states that this menu was selected from the previous

menu by pressing f(1). Therefore, should the user select f(0) from the menu, in Figure 3, the resulting menu would be **prog/a/b1/c0**.

3.4 Menu descriptions

There are numerous different routes through the program and to cover every one would be laborious and confusing. Instead each of the menus will be examined in order of possible selection. This will however cause a certain amount of confusion in itself. Each menu option will be discussed under a separate sub-heading, which will quote the menu label and the function description. The following text will describe the function and give instructions on how to reply to any prompts issued. Where the selection of one option simply produces another menu, a short description will be given of the new options presented by the new menu.

The brief description given here may have seem a little vague, but it is strongly advised to run the software and try pressing a few buttons!. All being well there should be a diffraction trace stored in memory, which you can experiment with.

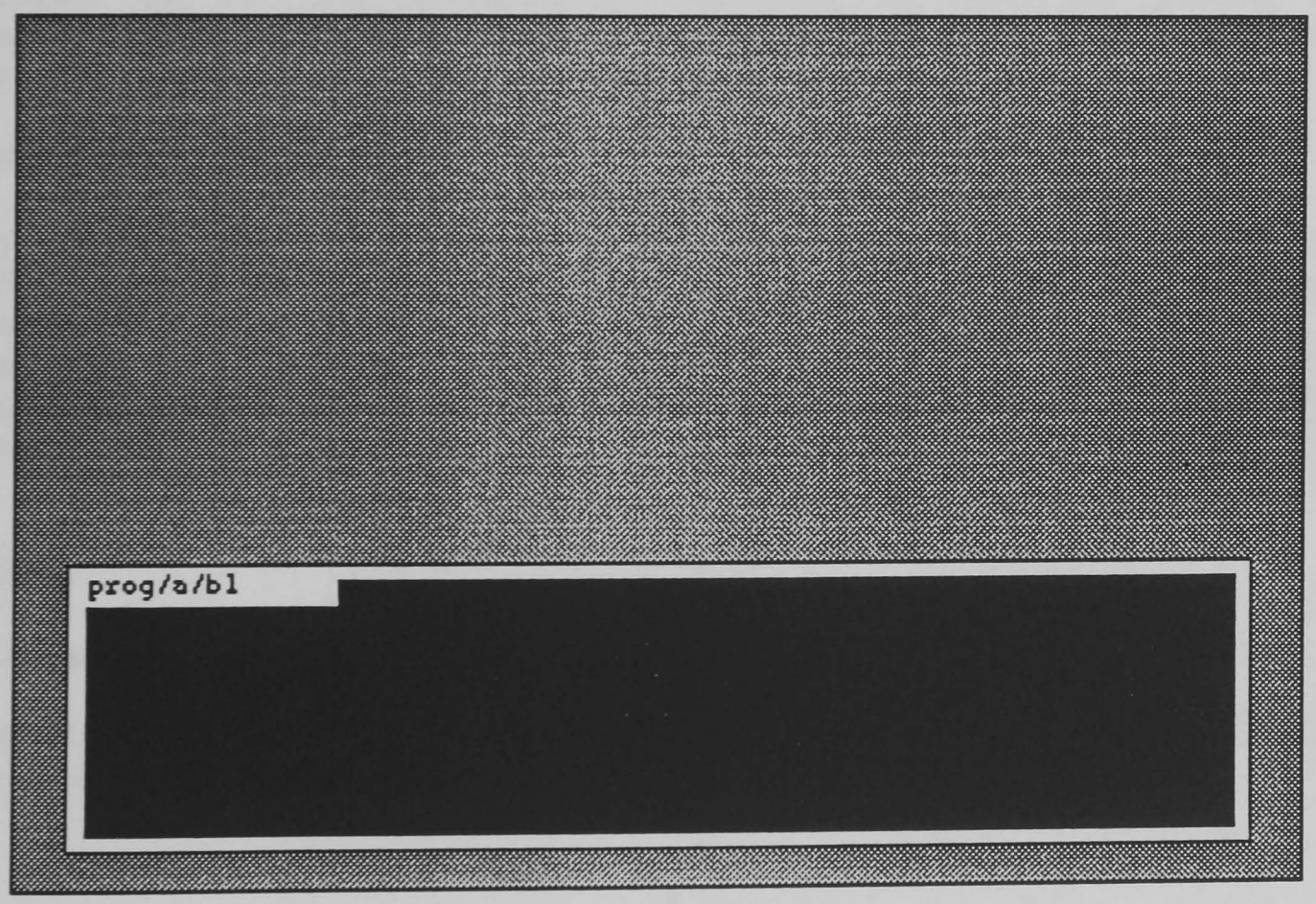

Figure 3 The working enviroment of **CENPOD**.

4.RUNNING THE SOFTWARE

The program is "booted" from the magnetic disc, by holding **SHIFT** and pressing **BREAK**. Assuming the disc drive is switched on and the correct disc inserted, the main menu will appear on the screen as shown in Figure 4. To select any one of the options the user need only press the key which corresponds to the program required. A carriage return is not necessary in this case. A brief description of each of the routines is given below:-

<1> SCAN.

This program performs the task of monitoring the movement of the goniometer and storing the diffraction trace on disc.

<2> PROFILE.

This is the largest and most complex of the routines. It has numerous functions regarding the data processing of the data. The data-file produced by **SCAN** can be examined and the relevant data extracted.

The diffraction data can be compared with one of several powder databases or if the sample is novel, it may be added to the database. Hard copies of the comparison routines, diffraction traces and reflexion intensities are fully supported.

<3> DATABASE.

As the name suggests this is the database for the PD and can be compared to a small computer version of the JCPDS file. It allows the user to input diffraction data, edit existing records, examine records and produce hard copies of the information. To assist with identification or with teaching methods, the information from any record may be used to generate a theoretical powder trace.

<4> EXIT.

This leaves CENPOD and takes user back to the BASIC editor.

Each of the programs listed above are explained in greater detail on the following pages.

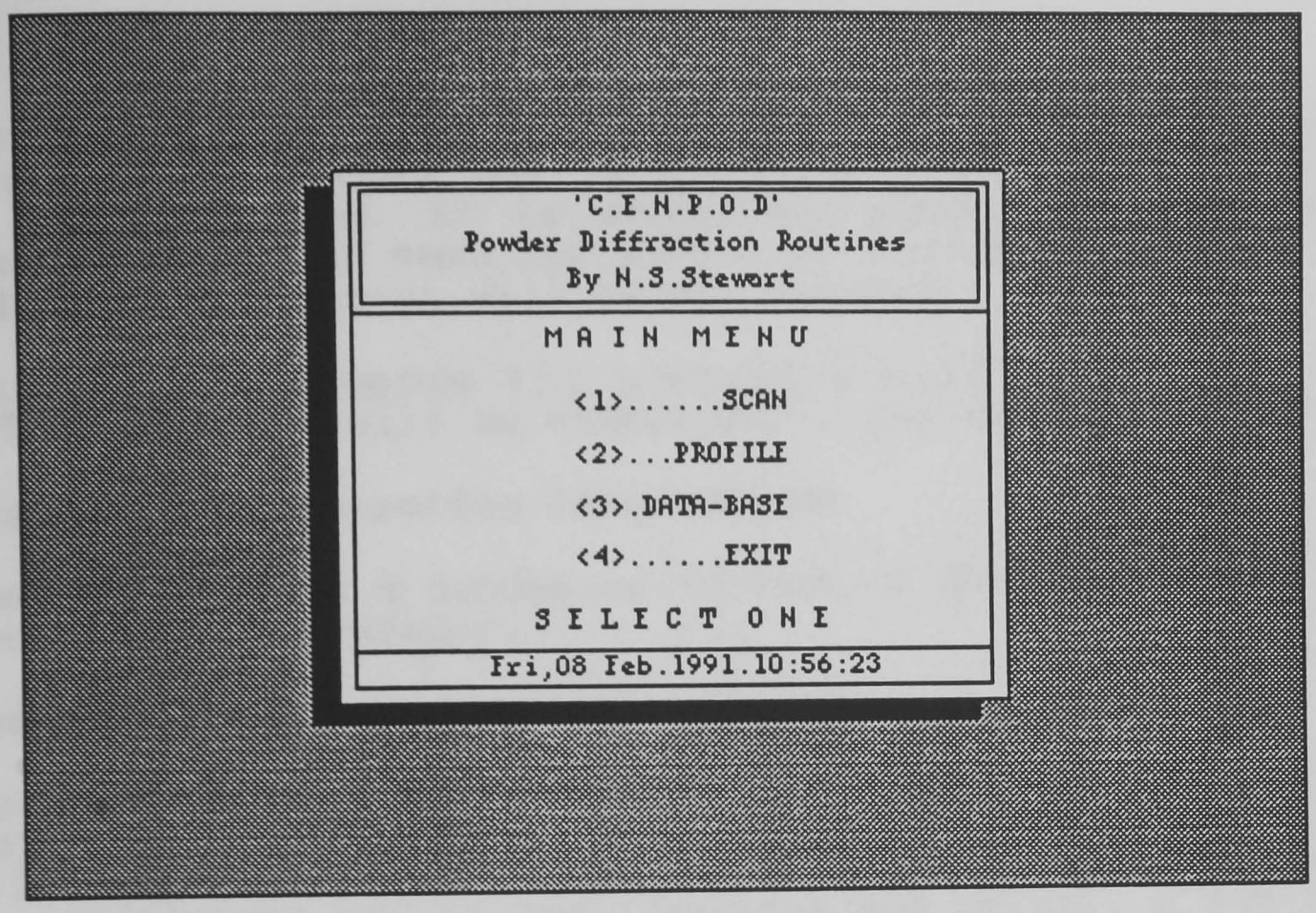

Figure 4 The main menu of **CENPOD.**

5.SCAN

To ensure that the system will perform to its full abilities it is necessary to follow the correct power-up sequence for the micro and interface. **It is essential that the interface is switched on first and then the micro.** If the sequence is reversed then the data collection will be unsuccessful.

On entry to the program the workspace will be clear and the following mini-menu will be displayed in the instruction window.

5.1 scan/a : (f0) Operating instructions

The instructions are a condensed version of what is written below and included as a reminder.

5.2 scan/a : (f1) Commence scan

The scan parameters are stored in the scan file which will be displayed in the workspace on selection of f(1). The user is asked if they wish to edit the file. In general cases, the start, finish, wavelength may be kept constant and so only a few of the parameters will need to be changed.

To edit the scan file, the instructions will be prompted in the instruction window at the foot of the screen. Figure 5 shows an example of the scan card being edited. Initially, the title displayed on the scan file card will be printed in reverse video, indicating that this parameter is currently selected. To select other parameters, the highlighted bar is moved by pressing the ↑ and ↓ keys. These keys are programed to move only one space per key press and so holding your finger on the key to move several spaces will result in the advancement of only one space. To change the parameter press the **RETURN** key and the user will be prompted in the instruction window to input the new value.

The scan parameters are discussed below:-

Title : the response to this prompt will be a string of alphanumeric characters which somehow indicate unambiguously what is being scanned. Inputs such as "FRED1" are acceptable, but they do not say much about the sample. The title will be truncated or padded to 16 characters.

Start : this represents the proposed starting position of the goniometer arm, which must be a positive integer greater than 5°. If an unsuitable value is input, the user will be prompted to try again.

Finish : this is the 2θ value at which the data collection is to terminate. Again, the value must be a positive integer. The software is set up to accept only those values which satisfy (**Start**+5) < **Finish** < 180°. Failure to meet these requirements will result in the question being

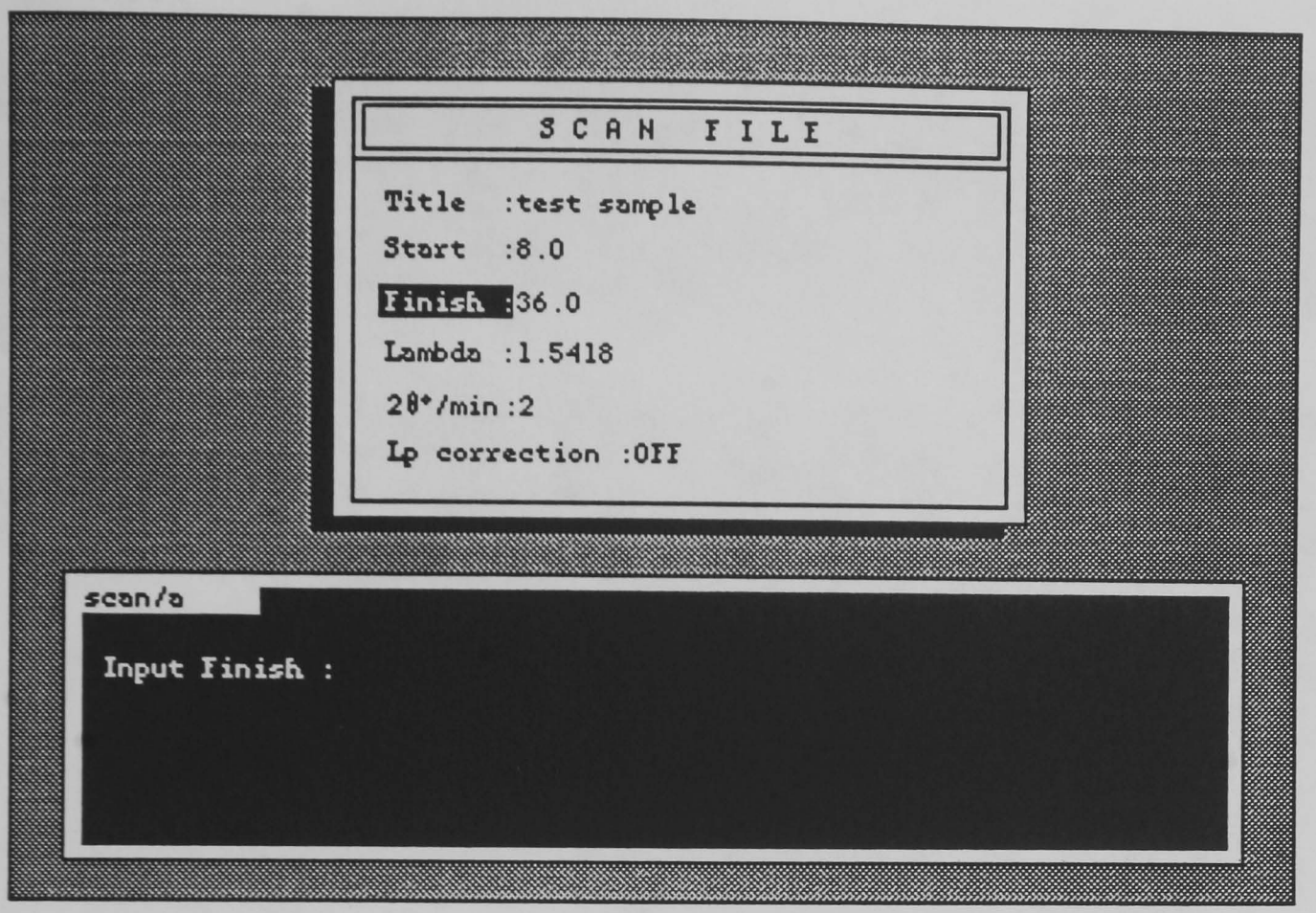

Figure 5 Editing a scan card.

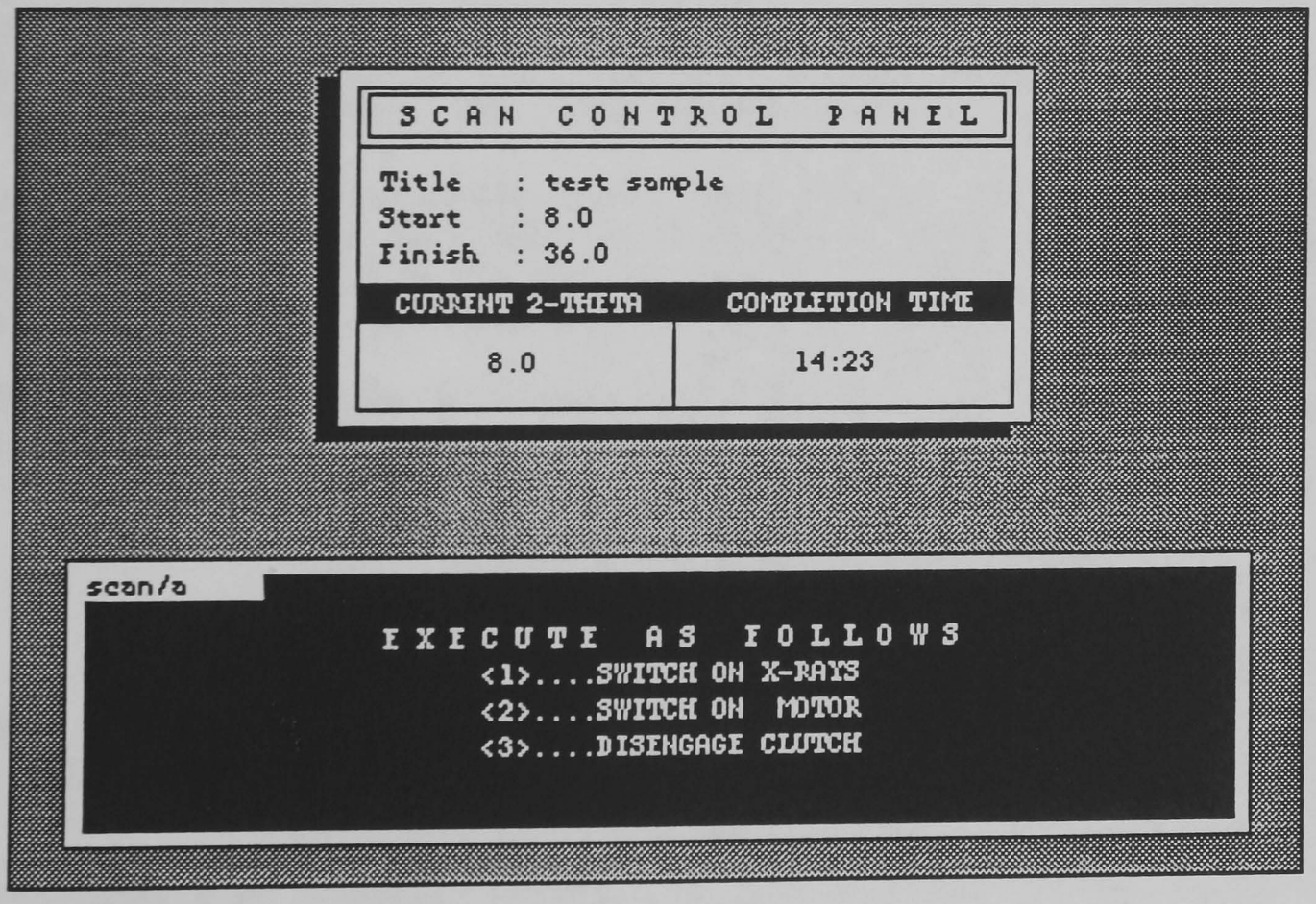

Figure 6 The control card displaying the current 2θ position.

repeated.

Lambda : the user is requested to input the wavelength, in angströms, of the X-radiation being used for the scan. In general this will be **1.5418 Å**, corresponding to a copper tube. The response is expected to be a positive number and so it is up to the user to ensure that a suitable value is input. If unsure, check the top of the tube or ask a technician.

Scanning rate : this input must comply to certain fixed values. These are governed by the ratio of the drive cogs. All the possible scanning rates are tabulated in Table 1. An incorrect input will result in the user being asked again.

motor shaft	driven shaft	scanning rate, 2θ°/min
24	96	0.125
40	80	0.250
60	60	0.500
80	40	1.000
96	24	2.000

Table 1 Cog ratios for scanning rates.

Lp correction : this allows a Lorentz/polarisation correction to be applied to the data. There is no input necessary to change this option. Pressing **RETURN** will simply toggle between the two possible states.

Once all the scan information has been input, pressing **SPACE** will exit from the editor and the information will be redisplayed on the control card. The control card, as shown in Figure 6, displays the current operational state of the diffractometer.

With the scan parameters accepted, the PD is ready to be used. The instruction window will clear and more instructions will appear.

<1> SWITCH ON X-RAYS.
<2> OPEN SHUTTER.
<3> DISENGAGE CLUTCH.

The order in which these requests are carried out is important. Firstly rotate the 2θ shaft around to the **Start** position and then rotate anti-clockwise until an audible click is heard. Clear the scaler counter on the PD instrumentation panel. Open the shutter and disengage the clutch. When the shaft passes the zero point the data collection is initiated.

The expected completion time is indicated on the control card. When the scan is completed the micro will stop logging data, but

the goniometer will continue to rotate. It is up to the user to return in time, before the scan is complete. However there are safety shut-off micro switches which will stop the goniometer from going too far, thus preventing any damage. **DO NOT RELY ON THESE.**

Should the user decide that they wish to discontinue the data logging, but retain the data collected so far, pressing **ESCAPE** will cause the program to halt at the next whole degree.

At the end of the data collection the maximum number of counts per data point is displayed. This value is the reference to which all other data values are scaled. The user is prompted to accept this value or select another value of their own choosing. In general the true experimental value will be required, and so the user replies "Y" to the question. If however the nature of the work requires that the trace be scaled to some other value, the facilities are there to do so. Answer "N" to the prompt and then input your new value. The new value must be equal to or greater than the experimental value, otherwise some strange effects will be produced!. Regardless of your answer the data is then stored on the disc. The data is stored on up to two files "RAWDAT1" and "RAWDAT2". Program flow now returns to the main menu.

6.PROFILE

PROFILE represents the most powerful of all the routines available in **CENPOD**. It also has the greatest number of nested mini-menus and so this chapter is liable to cause some confusion.

6.1 profile/a : (f0) Examine trace

On execution, the program reads in the data files and sets up the parameter lists. This process takes some time to complete, so please be patient. An example of the screen presentation is shown in Figure 7. The entire trace is plotted in a graphics window at the top and in a lower but larger screen the first 5° section is plotted. In a typical trace of 45° degrees there is too much information to be displayed on screen at once, therefore the trace can be broken down and viewed section by section. The condensed plot is there to assist in the location of the diffraction peaks.

Along the right-hand-side of the screen there is a **status** window, a **result** window and a list of **function** key definitions. On depression of any of the programmed function keys, the "button" will illuminate. If there is no change or it flashes and releases a sound then that key is presently disabled.

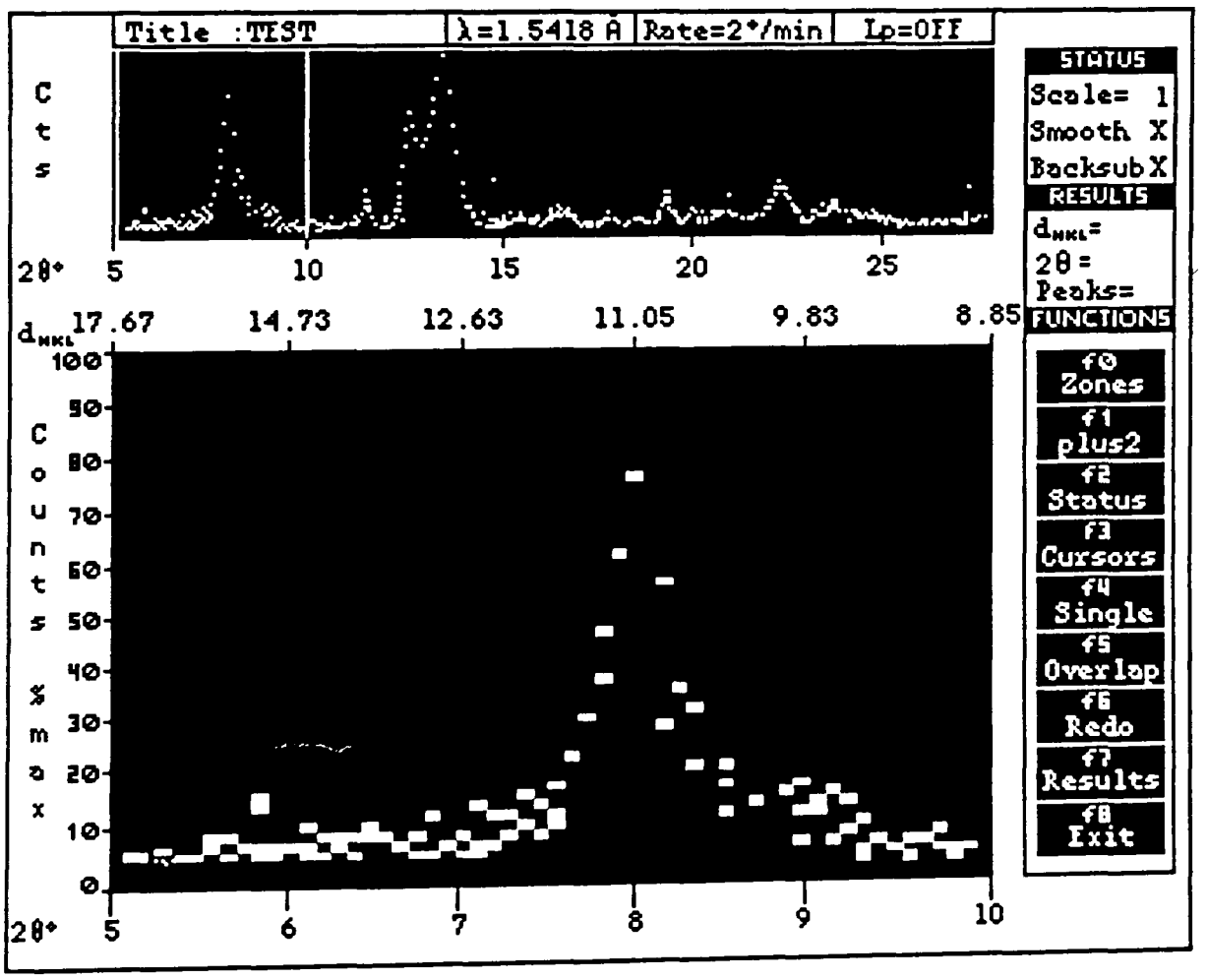

Figure 7 A typical screen representation of a trace by **PROFILE**.

Function Key Definitions.

(f0) Zone : this key allows the user to select any 5 degree section for fine detail examination. Using the ← and → cursor keys, the indicator lines in the upper graphics window will move either left or right. Once the particular section of interest has been identified, pressing **RETURN** will instruct the computer to plot the corresponding trace in the lower graphics window.

f(1) plus2 : it is possible that a peak may be positioned such that it straddles two adjacent five degree zones. This makes it impossible to measure the whole peak. However, the trace can be moved two degrees to the left with this function which will generally be sufficient to reveal the whole of the peak. This function can be used repeatedly, each time moving the trace by successive 2° intervals.

f(2) Status : at the top left hand side of the screen there is the status window. This reflects the way in which the experimental data is to be displayed in the five degree window. Each of the options may be altered by selecting f(2). As with the scan editor, the currently selected parameter is highlighted in a reverse video format and the individual effect is selected by the ↑ and the ↓ keys. To change the parameter, the ← and → keys will change the value. When all the changes have been made, pressing **RETURN** will exit from the status editor and redisplay the five degree plot as requested.

The status window has three plotting functions, which are discussed below:-

(a) Smooth : the experimental data usually has a high level of noise associated with it which can often mask some fine detail and so is undesirable. The random fluctuation can be suppressed to a certain extent by carrying out the smoothing routine. Pressing either the ← or → will switch on/off the smoothing function. In Figure 8 the effect of smoothing the trace is clearly visible.

The smoothing function has the additional effect of slightly diminishing the absolute intensities of the peaks. Therefore once one or more peaks have been measured, the smoothing function cannot be altered. However, it is possible to overcome this problem with the **redo** key. (see later)

(b) Scale : on entry to the routine the scaling factor for the data is set to the maximum peak height. This was set when the diffraction data was being saved to disc in SCAN. Scaling the data ensures that the maximum peak always fills the screen vertically. However, the scaling can often prevent small peaks from being distinguished from the

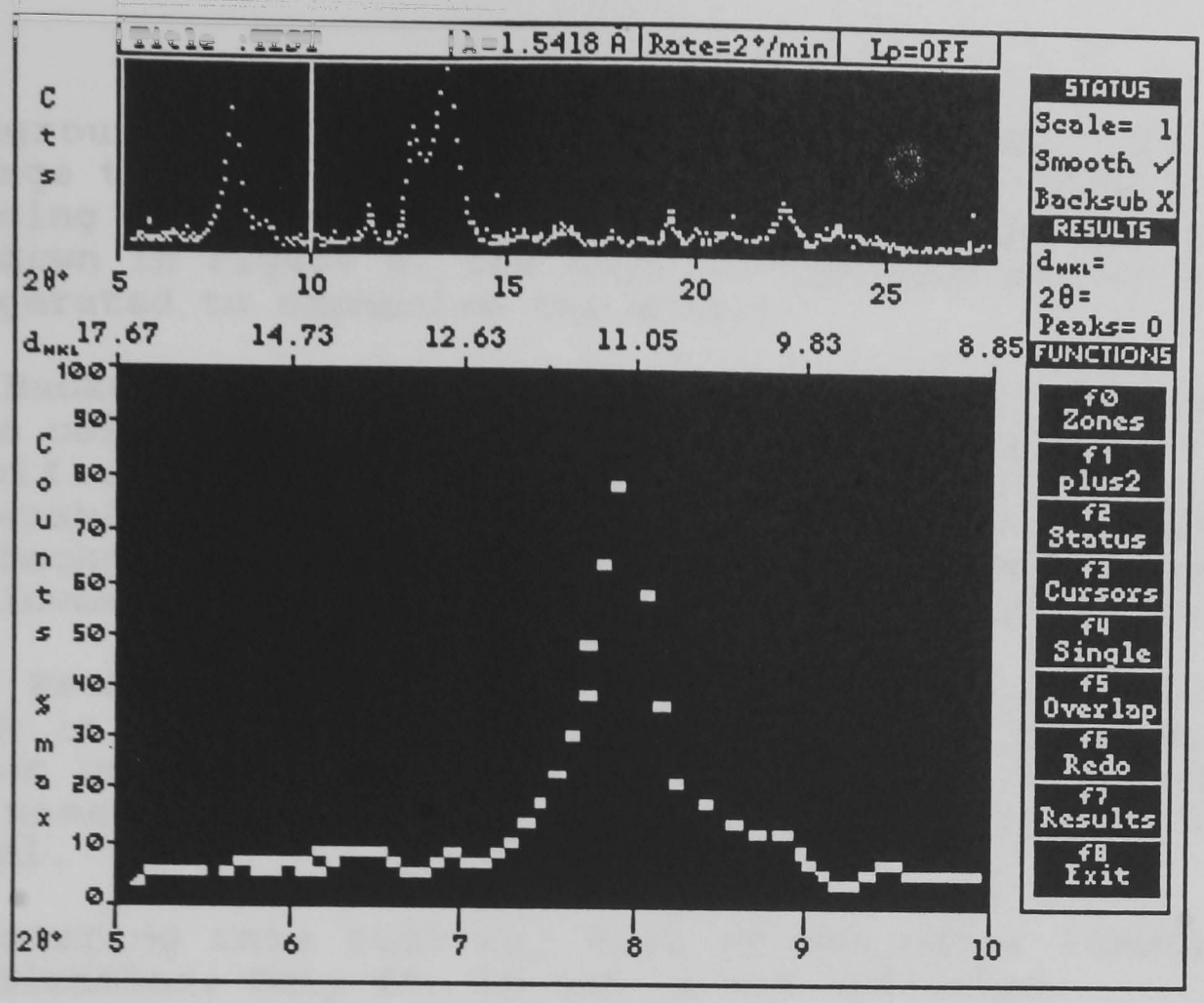

Figure 8 Activating the smooth function can reveal more information, than is distinguishable from the raw data. (Compare with Figure 7.)

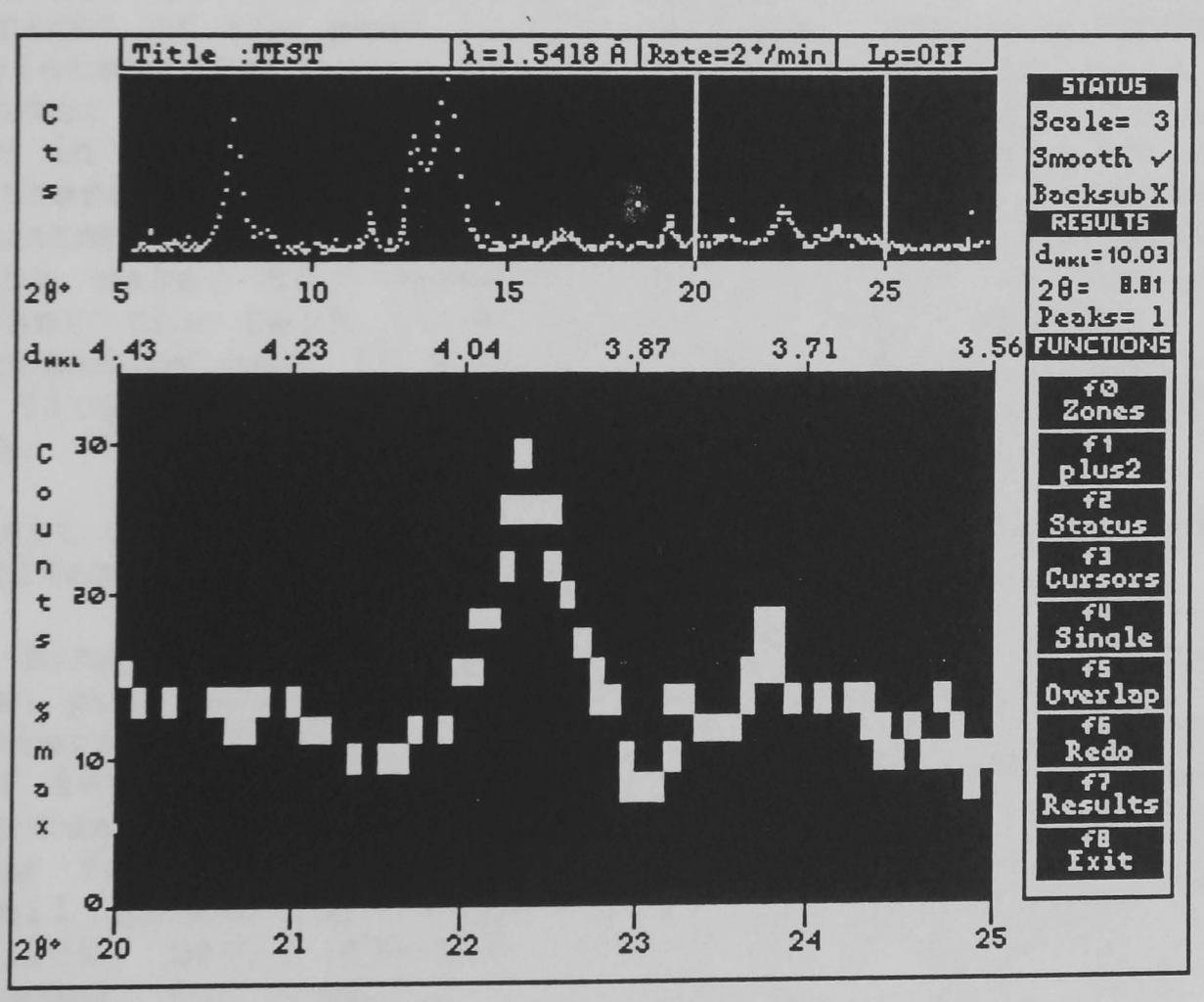

Figure 9 Low level information can be viewed under magnification. In the figure the trace has been increased by 200%.

background scatter. The scale feature allows the user to enlarge the trace by up to 5x magnification. This is done by pressing either ← or → keys. The effect of x3 magnification is shown in Figure 9. The size of the data points have been exaggerated to emphasise the effect.

(c) Background Subtraction : as a result of enlarging the trace using the scale facility, the background level is also magnified. To fully utilise the scale function it is preferable to "pull down" the background level. Activating the background subtraction has this effect and ensures that the lowest value in the five degree window is set to zero.

(f3) Peaks : this initiates an vertical on-screen cursor which is used to locate the proximity of a Bragg peak. The cursor is manipulated by the ← and → keys. Pressing **SHIFT** at the same time has the effect of increasing the speed of travel.

On entering this routine, most of the other function keys are disabled. Only f4, f5 and f6 are activated.

The cursor is first positioned to the left hand side of the peak, close to the base. Pressing **RETURN** "freezes" the cursor in that position and displays a second cursor to the right of the first one. The second cursor is positioned to the right of the peak in the same way. Pressing **RETURN** again completes the process and identifies the peak to the computer. The final result should be similar to the case shown in Figure 10. In most cases the peak will be singular, but there are cases when two or more peaks overlap and so the unambiguous identification is less straight forward. In either case, the user has to identify to the computer whether the peak is **singular** or **overlapping**. This is performed by keys f5 and f6. Note any peaks to be measured, must first be identified to the computer **before** pressing f5 or f6.

To exit from this routine press the **SPACE** bar. This will reactivate the other function keys.

(f4) Single : a horizontal cursor appears midway on the screen positioned between the two vertical cursors. This is to determine the background level of the peak. Using the ↑ and ↓ keys the cursor can be positioned at the estimated background level. See Figure 11. It is important that this cursor is carefully positioned since it will effect the overall intensity calculation. Once satisfied with the position, press **RETURN**. When the calculation has been completed, the computer will generate a short tone and the 2θ and dhkl values will be displayed in the result window. The intensity value is stored in memory which will be saved to a file when the analysis is complete.

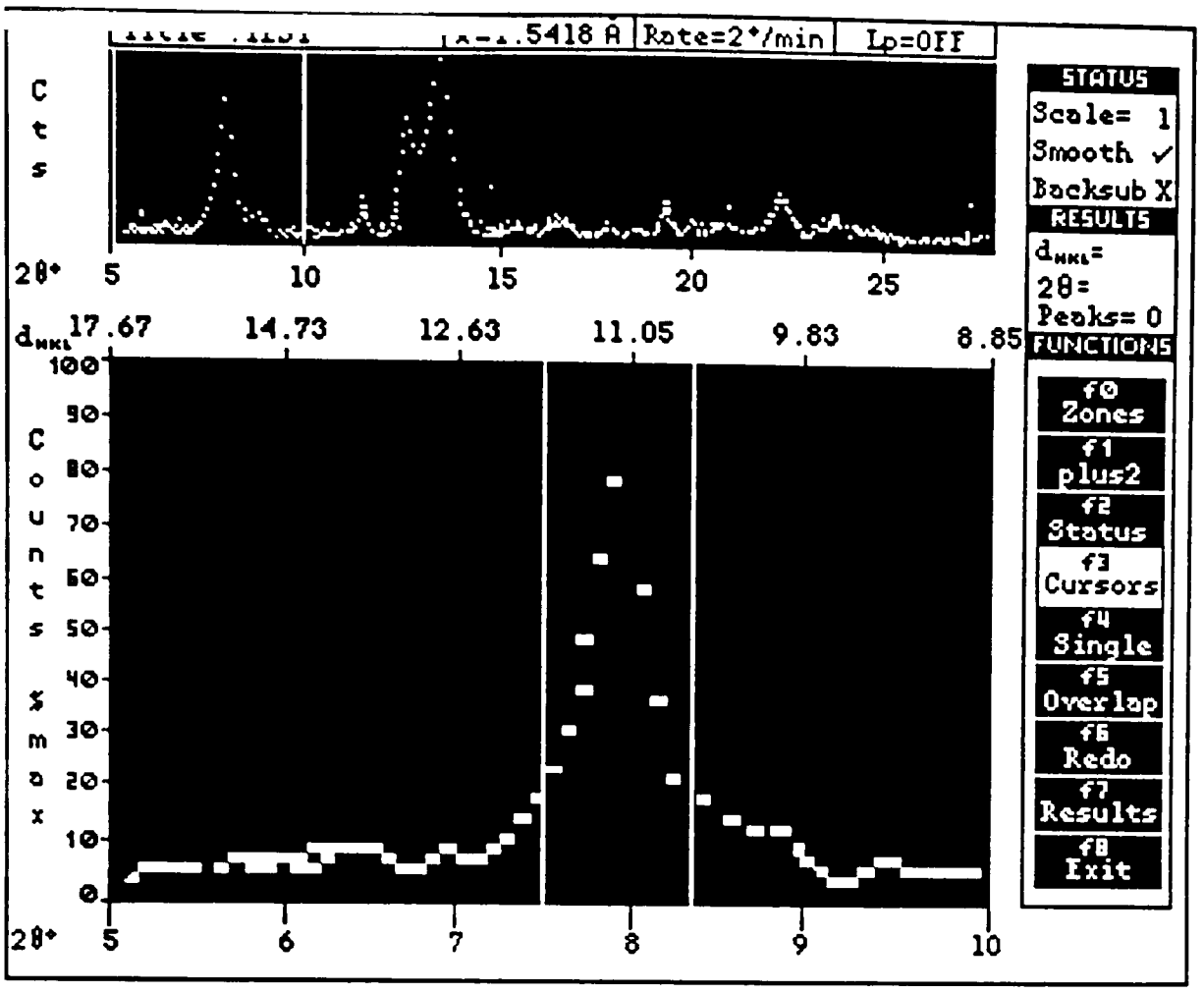

Figure 10 A single peak is identified by the two vertical cursors.

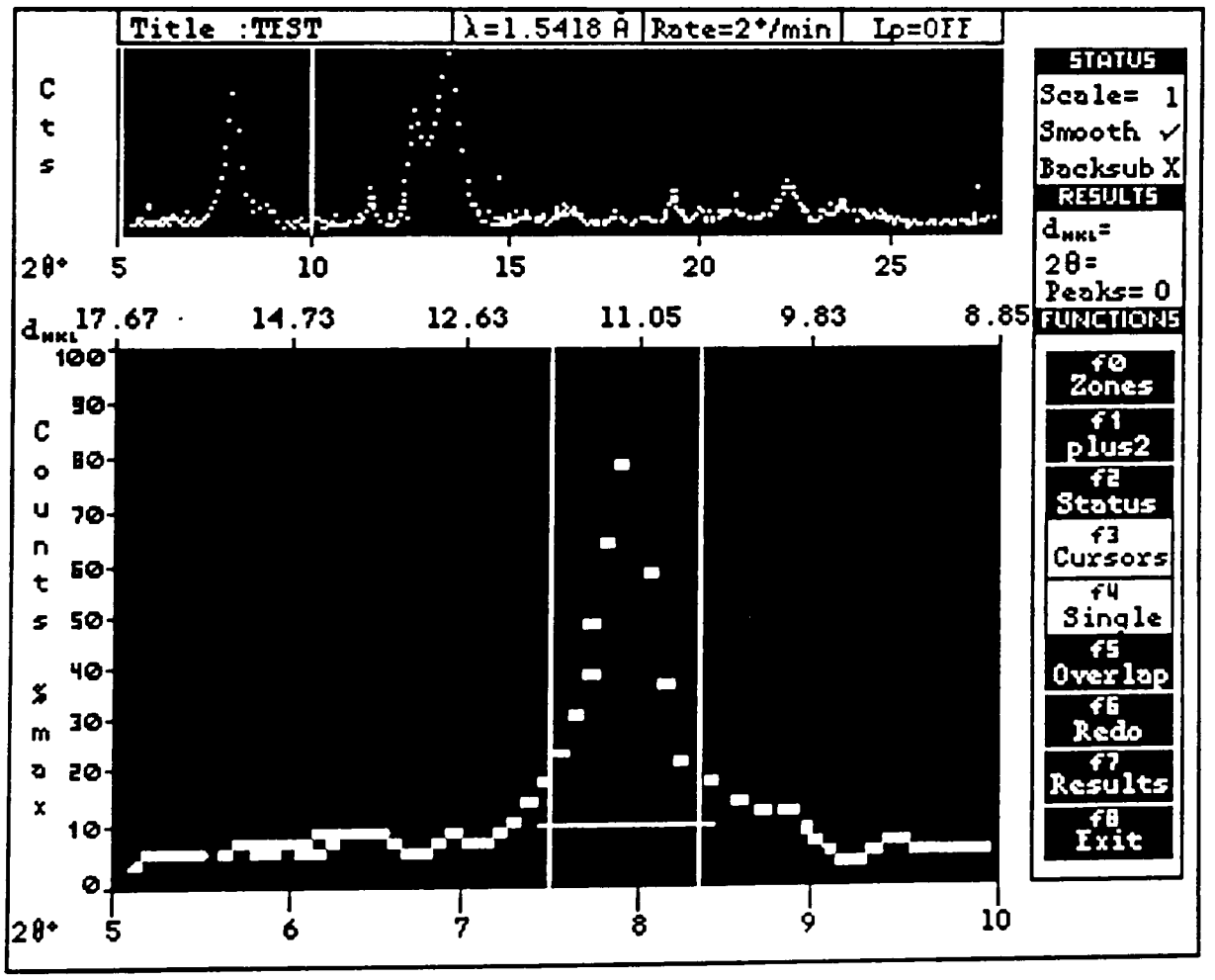

Figure 11 Positioning of the background level cursor.

(f5) Overlap : once the peak of interest has been identified by the first two cursors, a third vertical cursor will appear. This cursor is to be positioned beyond the apex of the second peak. This is shown in Figure 12, where the right hand peak is being measured. If this procedure has been carried out correctly there should be a cursor between the overlapping peaks, and one on either side of the pair of peaks. When satisfied with the positioning, pressing **RETURN** will reveal the horizontal background cursor. It does not matter whether the peak to be measured is on the left or the right of the pair, since the positioning of the first two cursors identifies the peak to be measured. This routine can be applied to adjacent pairs in a group of overlapping peaks.

N.B. The overlapping routine at this stage is still a little simplistic and so errors can be introduced. The resulting intensities should not be considered to be as accurate as singular peaks.

f(6) Redo : this key simply erases the intensity and interplanar spacing of the last peak to be measured. Notice that on each depression of this key, the number of measured peaks in the result window, decrements by one. When this value is reset to zero, the user can change the smooth rate, as described above.

f(7) Results : prints out the intensities and interplanar spacings of the 16 most intense peaks. A hard copy of all the peak values can be obtained using **PROFILE**.

f(8) Exit : leave this routine to the first mini-menu. If any peaks have been measured, the interplanar data is stored in the present sample file, which can be later extracted.

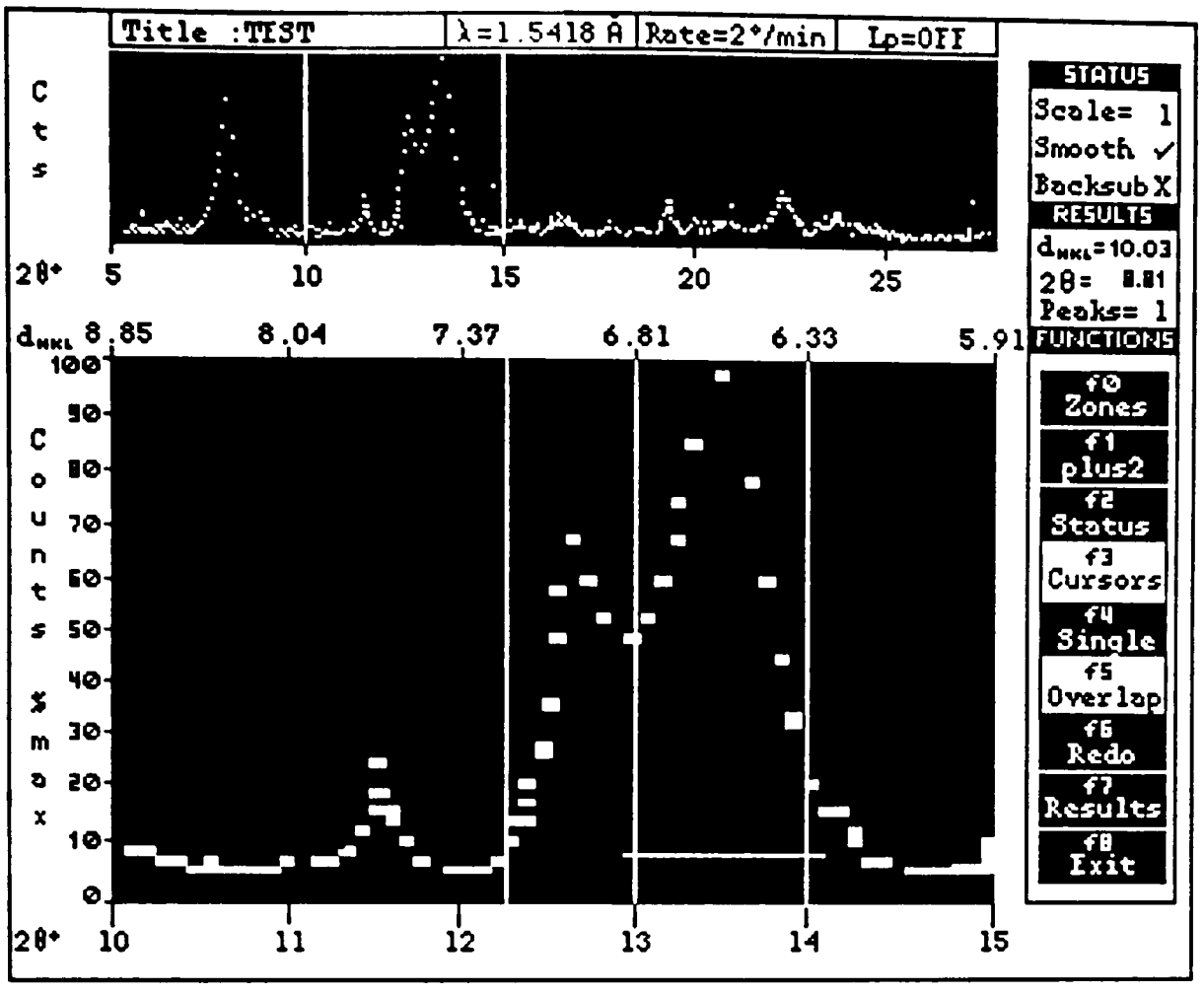

Figure 12 Multiple cursor positioning for overlapping peaks.

6.2 profile/a : f(1) View results

This part of the program uses the information obtained by the trace analysis. There are several processes which can be called upon to analyse the experimental data.

6.2.1 profile/a/b1 : f(0) Identify sample

The sample can be identified by either comparing the data with the limited database, with the purpose of finding a matching pattern or to identify it to the data base by inputting the data to the database, thus increasing the number of records.

6.2.1.1 profile/a/b1/c0 : (f0) Compare data with database

This feature allows the user to compare the experimental data with the **CENPOD** crystallographic database. The program searches through the records comparing the interplanar spacings and the intensities. In the majority of cases the d_{hkl} values are of the greatest interest. During the data collection of the powder trace, the measured 2θ values will have a positional error either created by the instrument or by the user. The magnitude of the error when translated into d_{hkl} terms will vary depending on the 2θ position of the peak. Since the relationship between d_{hkl} and 2θ is not linear a standard error of delta-d_{hkl} can not be used. Therefore, given a rather pessimistic maximum error in 2θ of 0.1°, the permissible error for each d_{hkl} value is calculated. If the two values being compared agree to within the error margin then the value is accepted. The reliability of the match is indicated by the closeness of the two intensity values. If the intensities are in good agreement then the match is considered to be good.

Once all the records have been checked they are placed in a list in order of merit. The top three results (or less) are displayed to the user in the workspace. Figure 13 shows a typical screen output presenting three possible matches. The data values highlighted in reverse video indicate a successful match. The user is required to decide which one of the displayed samples has the best match. A hard copy of this result table can be produced on the dot-matrix printer.

On some occasions the sample being identified will not be a pure single phase powder. In this case it may be possible to identify the different phases depending upon the relative concentrations of the phases. In the result table, there may be two or more samples with significant and unique matches with the test data, therefore indicating that there is indeed several different species in the sample.

When there is one predominant phase in the sample, the other phase will not appear in the printout due to a low figure of merit. To identify both phases, the peaks from the prominent phase are noted from the result table and the trace remeasured

avoiding the already matched reflexions. The new data set should then only represent the other unidentified phases and the comparison routine is repeated. All being well these compounds will be selected as suitable matches.

Users should note that the database only holds a small number of specific records and so it will probably fail to identify most samples. What use then is this facility?. The database is intended for routine samples which will be encountered regularly.

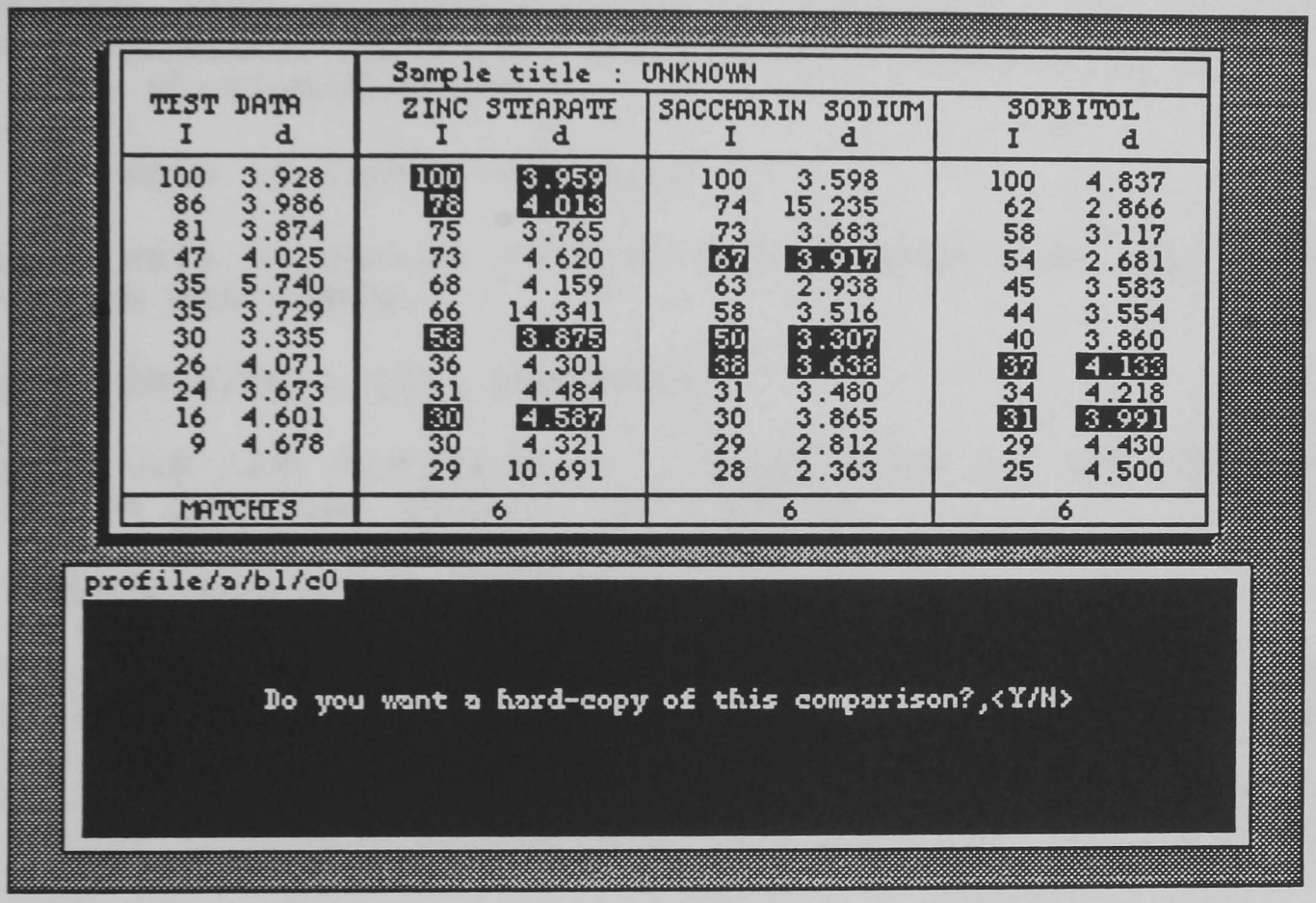

Figure 13 The output of a comparison, with three possible matches.

6.2.1.2 profile/a/b1/c0 : (f1) Input data to database

Alternatively, the experimental data can be stored on the crystallographic database, thus expanding the number of records.

The experimental data is displayed in the workspace on a record card, which resembles the type used for the Powder Index. The user is prompted to input additional data relating the conditions of data collection.

Source : this is a 3 letter acronym for the source of the sample. The letters used is entirely up to the user, but they should adopt a consistent approach, making any future reference of the record more straightforward.

Date : the date in format dd/mm/yy

The record will be stored to disc and program flow will return to the previous mini-menu.

6.2.2 profile/a/b1 : (f1) Hardcopy

Hardcopies of the diffraction intensities or the diffraction trace can be produced through this option.

6.2.2.1 profile/a/b1/c1 : f(0) Dot-matrix

This function outputs the 2θ, d_{hkl}, I_{hkl} and the absolute intensities of all the measured peaks. The user is prompted to place the printer on-line and press **RETURN** when ready. The user may also wish to ensure the printer is indeed connected to the micro, since it shares the same output line as the XY plotter.

6.2.2.2 profile/a/b1/c1 : f(1) Plotmate

Plotmate is an XY plotter which has been incorporated to produce diffraction traces of superior quality to that of the scroll plotter originally installed with the PD. There are several options which determine the overall presentation of the final trace. These are selected by editing the plotfile, in the same fashion as the scan file in **SCAN**. The default parameters are obtained from the scan file and are displayed as shown in Figure 14. The parameters are listed and explained below:-

(a) Title : generally the user will retain the title carried through from **SCAN** but the option to change it, for whatever reasons, is facilitated.

(b) Start : the user may which to plot only a portion of the original trace and so the new limits are required. The value input must be a positive integer, less than the current finish value.

(c) Finish :as above. The limiting value must be greater than

Start and less than 180°.

(d) **Smoothing** : generally the trace is visibly less complicated if it is smoothed and so this option is recommended.

(e) **Background Subtraction** : as previously described, more useful information can be presented on the plot if the background level is diminished. This is most useful when a trace exhibits a low crystalline state and therefore has a high level of amorphous scattering.

(f) **Scale** : this will allow sections to be enlarged revealing fine detail. The upper limit is set at x5.

(g) **Superimpose** : this allows a trace to be plotted on top of an existing trace for comparative purposes. The Start and Finish limits must therefore be the same as the previous plot.

(h) **Paper** : both A3 and A4 leaves are supported by the software.

Once satisfied with the plot parameters, the edit is recorded by pressing **SPACE**. As the program runs, it will issue commands to change pens when needed and so your presence will be required!. Given practice, the system can be used to produce high quality plots. One example is featured in Figure 15.

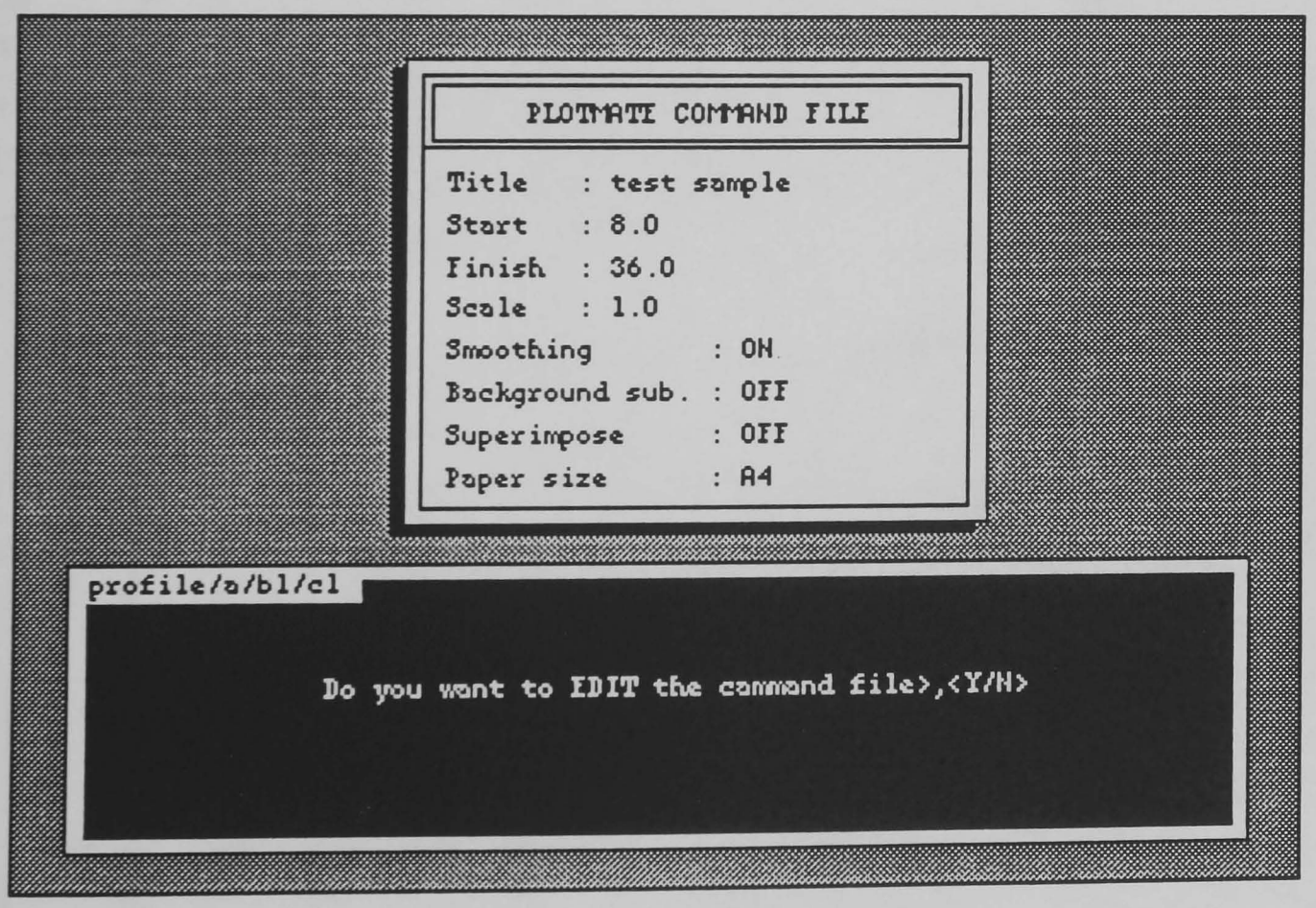

Figure 14 A typical plotfile

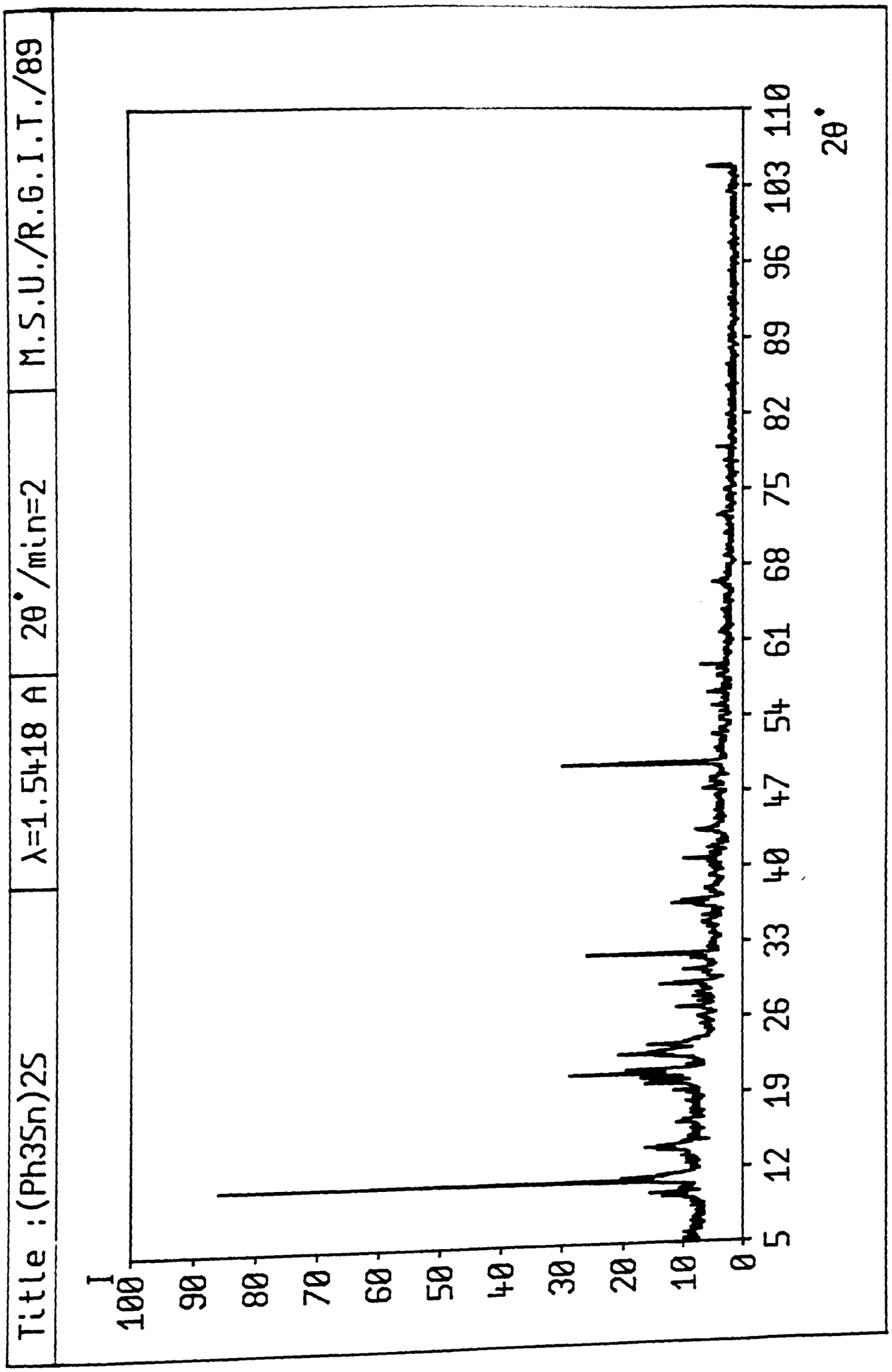

Figure 15 A trace of $(Ph_3Sn)_2S$ over the 2θ range of 5-105°.

7.DATABASE

On selection of this option a second menu will appear on the screen displaying three database programs. All three programs have been written so that the presentation and operational principles are virtually the same. Therefore one chapter covering all three will be sufficient to cover all of the facilities.

7.1 VIEW

VIEW is a search and retrieval program which allows the user to examine the contents of the crystallographic database. Essentially the routine will be used to retrieve the interplanar spacings to be compared with experimental data. The information can be output to the printer in a numerical format and also graphically as a simulated diffraction trace.

7.1.1 view/a : (f0) View entire database

This routine will display a list of the current contents on the disc. The information is restricted to the record title, source, date of input, scanning rate and the number of Bragg peaks.

7.1.1.1 view/a/b0 : f(0) Scroll data on screen

The stream of information regarding the database records is printed on the screen. This is done in a page mode fashion with the operator controlling the rate of scrolling.

7.1.1.2 view/a/b1 : f(1) Scroll data on dot-matrix

This produces an identical function as f(0), but in this case the output is directed to the dot-matrix printer. This process is continuous. The user must ensure that the printer is connected and placed "on-line".

7.1.2 view/a : (f1) View one specific record

This prompts the user to input the name of the record to be displayed. The user must be careful to input the name exactly, as any slight mistake will result in a failure to locate the record. If it is successful in finding the record, the information will be displayed in a pull-down window, in a style similar to the Powder Diffraction Index. In the top left hand corner the name and scan details appear. To the right of this, the four most intense reflexions are displayed. In the lower half the other reflexions are tabulated in order of decreasing d_{hkl} values. The powder data for sucrose is displayed in Figure 16.

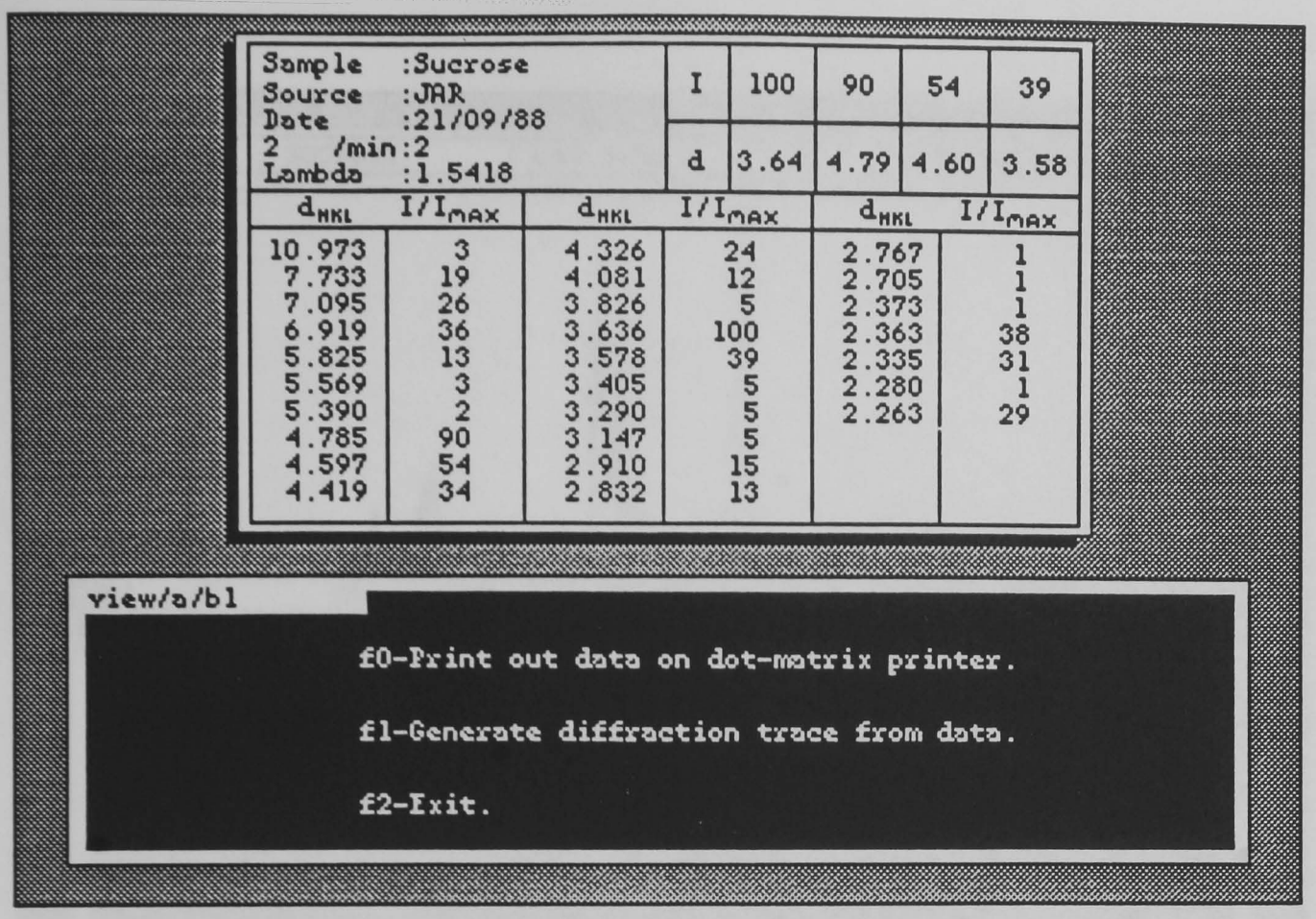

Figure 16 Graphical presentation of records stored on the database.

The diffraction data can be output in two ways, as indicated by the following mini-menu.

7.1.2.1 view/a/b1 : f(0) Hardcopy of data

This produces an approximate copy of the card on the dot-matrix printer.

7.1.2.2 view/a/b1 : f(1) Generate trace

This option allows a artificial trace to be generated based on the d_{hkl} values stored in the data base. The experimental data for a scan is held in two files occupying 14Kbytes, and so it was impossible to store all the traces on the present disc drive. By regenerating the trace from the information stored on the database, a temporary file can be set up. The trace is plotted on the screen, as shown in Figure 17. If the user is satisfied with the plot, it can be submitted to the plotter. The plotfile can be edited in the same fashion as the plotfile for the experimental data. (Refer to editing plotfile in section 5)

Please note that the plot produced will not be identical to the original trace. This is because certain simplifications and assumptions have been made in the mathematical model. The purpose of the facility is to produce a plot which represents the trace so that users can visually interpret the data.

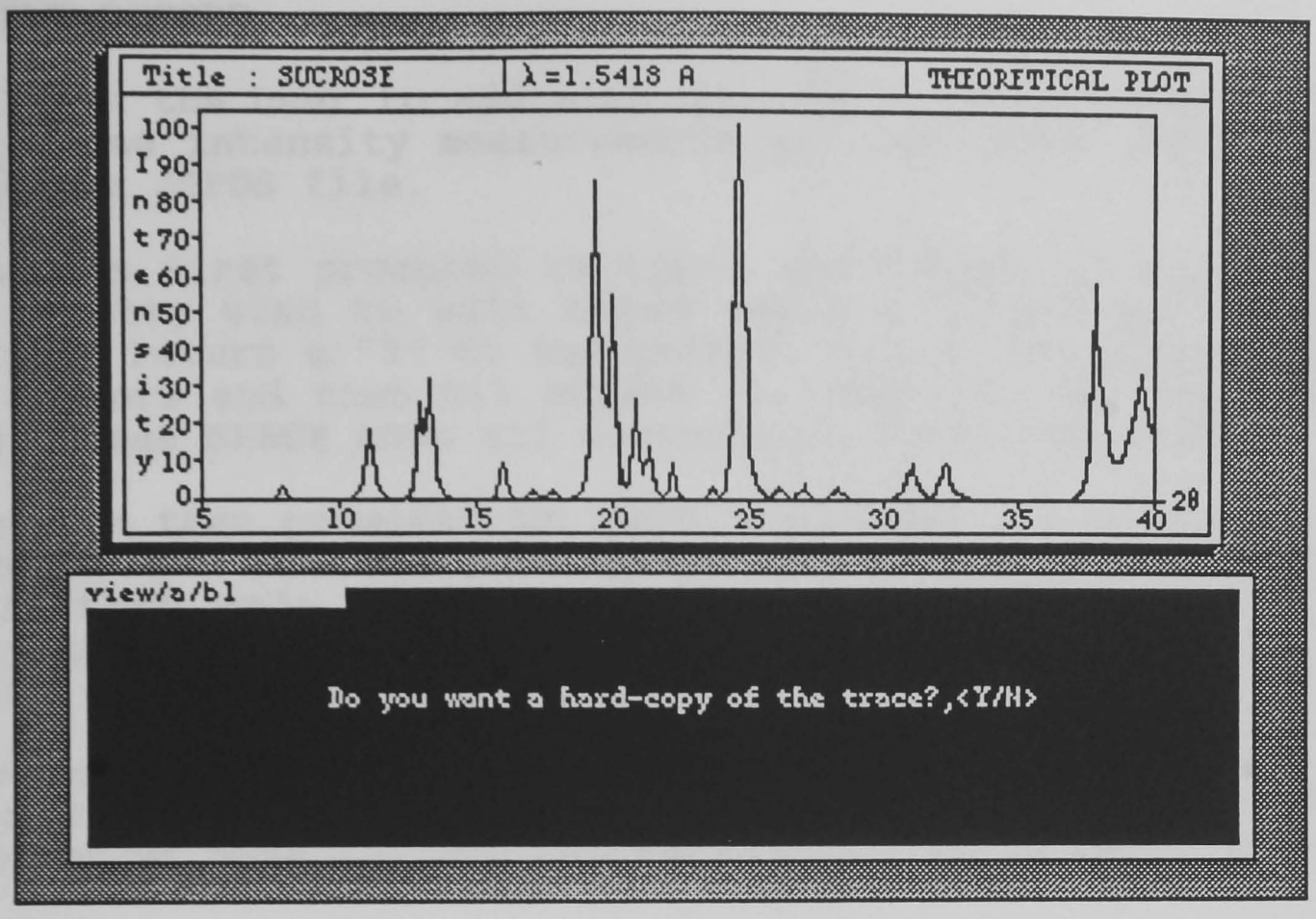

Figure 17 A theoretical plot using the diffraction data from the database.

7.2 INPUT RECORD

This allows the user to add more records to the database by hand. The d_{hkl} and intensity measurements may come from other sources, such as the JCPDS file.

The user is first prompted to input identifying details and then asked if they wish to edit these values. If mistakes have been made, then return a "Y" to the prompt. Select the item with the ↑ and ↓ cursors and then hit **RETURN** to input the revised character string. Press **SPACE** when all corrections have been made.

The user is then prompted to input the number of reflexions which are to be entered. The maximum number is 30. If you have more than 30 then only input the 30 most significant reflexions. Usually the lower 2θ reflexions will be most important, since the majority of scans on organic samples will be carried out over the range of 5-45°. Once all the reflexions have been input in the manner indicated, the user will again be prompted if there are any corrections to be made. The method of selection and correction of data follows the same procedure as mentioned above.

7.3 UPDATE RECORD

This facility allows the user to change the contents of a record stored on the database. Should values be found to be erroneous, new values published or for any reason why the file should be updated, the relevant changes can be made here. The editing functions are identical to those described in 7.2. The scan details and the diffraction data are edited separately by selecting the appropriate function key.

7.3.1 update record/a : f(0) Update details

The functions used for selecting and editing are the same as the other file editors discussed in 7.2.

7.3.2 update record/a : f(1) Update data

As above.

Once the necessary amendments have been made, pressing f(2) will save the new values to disc and return the user to the database main menu.

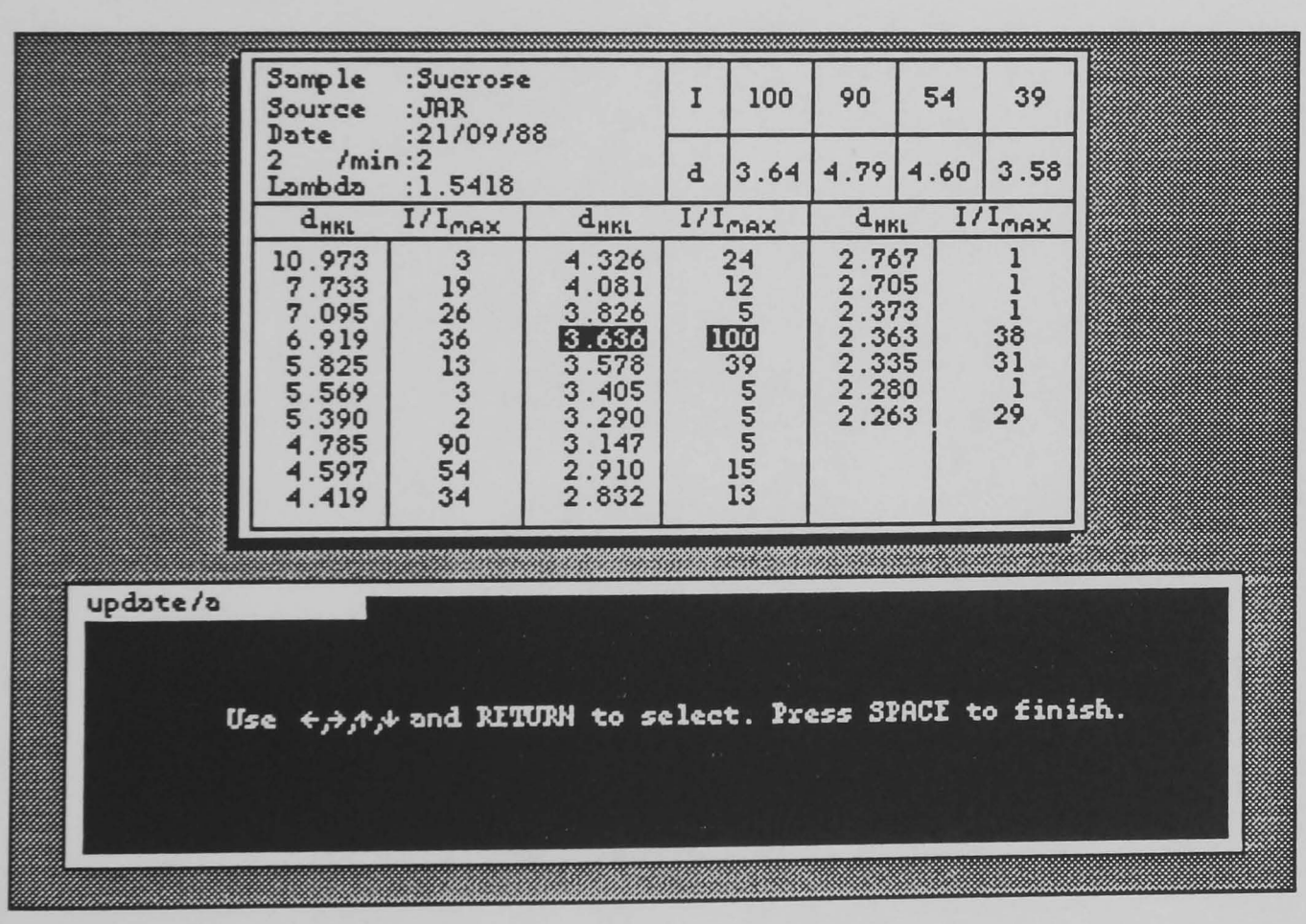

Figure 18 Editing an existing record on the database.

A P P E N D I X A

Digital Interface

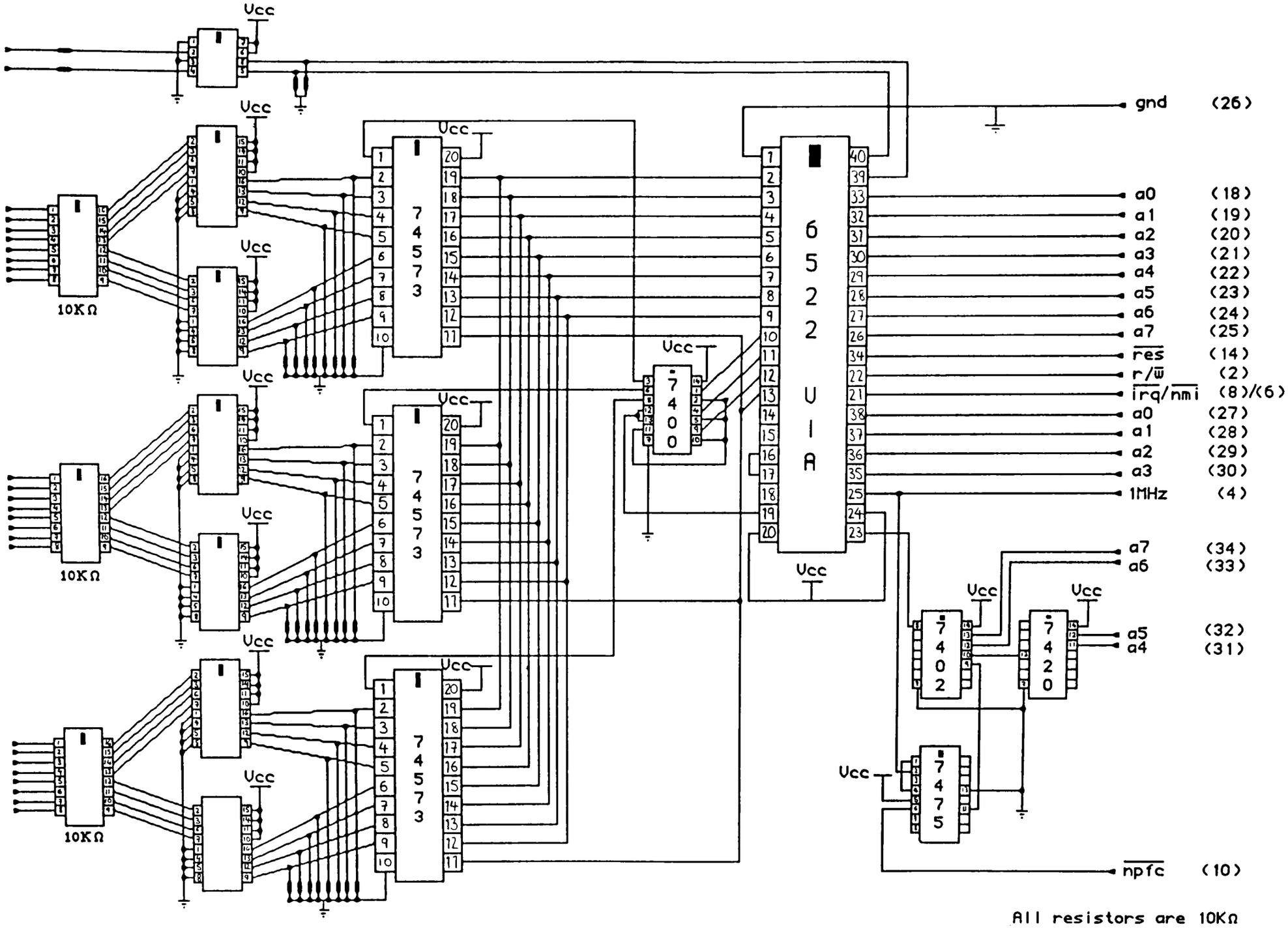
Vcc
10KΩ
7 4 5 7 3
7 4 0 0
6 5 2 2 U I A
gnd (26)
a0 (18)
a1 (19)
a2 (20)
a3 (21)
a4 (22)
a5 (23)
a6 (24)
a7 (25)
res (14)
r/w (2)
irq/nmi (8)/(6)
a0 (27)
a1 (28)
a2 (29)
a3 (30)
1MHz (4)
a7 (34)
a6 (33)
7 4 0 2
7 4 2 0
a5 (32)
a4 (31)
7 4 7 5
npfc (10)
All resistors are 10KΩ

A P P E N D I X B

Program listings for CENPOD

```
   10 REM ************************************************************************
   20 REM * CENPOD is the main menu program from where all other programs        *
   30 REM * are loaded and executed. All the programs have been written in       *
   40 REM * a similar style and even use the same routines. The database         *
   50 REM * programs all use the same routines, but in different ways. The       *
   60 REM * programs have been commented, describing their basic function.       *
   70 REM * However these do not go into detail about individual variables.      *
   80 REM *                                                                      *
   90 REM * SEE THE CENPOD MANUAL FOR FURTHER DETAILS ON SOFTWARE OPERATION     *
  100 REM *                                                Neil S Stewart, RGIT *
  110 REM ************************************************************************
  120 REM
  130PROCwindow
  140DIM A$(4):A$(1)="<1>.....SCAN":A$(2)="<2>...PROFILE":A$(3)="<3>.DATA-BASE"
:A$(4)="<4>.....EXIT":VDU23,1,0;0;0;0;
  150PROCmenu:OSCLI("FX4,0")
  160END
  170DEFPROCmenu
  180 REM MENU LOADS AND EXECUTES INDIVIDUAL PROGRAMS
  190VDU5:GCOL0,0:MOVE512,650:PRINT"M A I N  M E N U":FORT%=1TO4:MOVE536,590-(T%
-1)*64:PRINTA$(T%):NEXT:MOVE488,326:PRINT"S E L E C T  O N E":VDU4:COLOUR0:COLO
UR129:TIME=100
  200 IFTIME>=100 THEN PRINTTAB(28,24)TIME$:TIME=0
  210 IFINKEY(-49)PROChigh_light(1):CHAIN"SCAN"
  220 IFINKEY(-50)PROChigh_light(2):K%=0:CHAIN"PROFILE"
  230 IFINKEY(-18)PROChigh_light(3):A%=1:CHAIN"DBASE"
  240 IFINKEY(-19)PROChigh_light(4) ELSE 200
  250 OSCLI"FX15,0":A%=0:COLOUR1:COLOUR128:CLS
  260 ENDPROC
  270DEFPROChigh_light(T%)
  280VDU5:GCOL0,0:MOVE520,590-(T%-1)*64:PRINTSTRING$(15,CHR$255):GCOL0,1:MOVE536
,590-(T%-1)*64:PRINTA$(T%):VDU4
  290ENDPROC
  300 DEFPROCwindow
  310 IF A%=1 THEN GCOL0,1:VDU26:MOVE370,670:VDU25,101,920;360;:ENDPROC ELSE VDU
22,128
  320OSCLI("FX14,6"):OSCLI("FX21,0"):*KEY10 CH."CENPOD"|M
  330VDU23,2,85,85,85,85,85,85,85,85:VDU19,1,6;0;
  340VDU18,16,128:CLG:GCOL0,0:MOVE325,185:VDU25,101,925;830;:GCOL0,1:MOVE340,200
:VDU25,101,940;846;:MOVE0,0:DRAW0,1023:DRAW1279,1023:DRAW1279,0:DRAW0,0
  350 GCOL0,0:MOVE 356,216:DRAW 356,830:DRAW 924,830:DRAW924,216:DRAW356,216
  360 MOVE340,200:DRAW340,846:DRAW940,846:DRAW940,200:DRAW340,200
  370 MOVE 356,680:DRAW924,680:MOVE356,265:DRAW924,265
  380 MOVE362,688:DRAW362,822:DRAW918,822:DRAW918,688:DRAW362,688
  390 VDU5:MOVE536,810:PRINT"'C.E.N.P.O.D'"
  400 MOVE400,770:PRINT"Powder Diffractometer Routines"
  410 MOVE528,730:PRINT"by N.S.Stewart"
  420 VDU4:VDU24,5;5;1274;1018;
  430 ENDPROC
```

```
   10 REM ***********************************************************
   20 REM * SCAN controls the flow of data from the powder           *
   30 REM * diffractometer via the interface board. The data         *
   40 REM * can be scaled, corrected for Lp and stored in two        *
   50 REM * datafiles; RAWDAT1 and RAWDAT2. S-INFO stores the       *
   60 REM * scan parameters.                                         *
   70 REM *                                  Neil S Stewart, RGIT    *
   80 REM ***********************************************************
   90 REM
  100 MODE128:CLEAR:HIMEM=&3FFF:OSCLI("CLOSE")
  110 OSCLI("LOAD LOGGER DEA0")
  120 PROCsetup:PROCdisplay:PROCmenu
  130 A%=0:CHAIN"CENFOD"
  140 END
  150 DEFPROCsetup
  160 REM SET UP VARIABLES AND PARAMETERS FOR 6522
  170 FORT%=4TO7:OSCLI("SRROM "+STR$T%):NEXT
  180 Peak%=0:Ram%=4:Smooth%=0:S%=&3FFF:Max%=0:N%=0:Old_max%=0:I%=0:DIM Hdeg%(2)
,A$(5)
  190 orb=&FCC0:ira=&FCC1:ddrb=&FCC2:ddra=&FCC3:acr=&FCCB:pcr=&FCCC:ifr=&FCCD:ie
r=&FCCE
  200 ?ier=&7F:?pcr=&E2:?acr=&FC:?ddra=&00:?ddrb=&FF:?ifr=&7F
  210 decode_process=&DD00:ux=406:uy=866:lx=906:ly=492
  220 A$(0)="Title  :":A$(1)="Start  :":A$(2)="Finish :":A$(3)="Lambda :":A$(4)=
"2"+CHR$232+CHR$160+"/min:":A$(5)="Lp correction :"
  230 ENDPROC
  240 DEFPROCdisplay
  250 REM SCREEN DISPLAY
  260 VDU19,1,6;0;:VDU23,2,85,85,85,85,85,85,85,85:VDU18,16,129:@%=&02008:CLG
  270 GCOL0,1:MOVE0,0:DRAW0,1023:DRAW1279,1023:DRAW1279,0:DRAW0,0
  280 MOVE50,35:VDU25,101,1230;423;:GCOL0,0:MOVE66,51:VDU25,101,1214;407;
  290 MOVE50,35:DRAW50,423:DRAW1230,423:DRAW1230,35:DRAW50,35
  300 COLOUR0:COLOUR129:VDU28,0,31,79,0:PRINTTAB(4,19)"scan/a "
  310 ENDPROC
  320 DEFPROCmenu
  330 COLOUR1:COLOUR128:VDU28,5,29,75,20:CLS
  340 PRINTTAB(22,2)"f0-Operating Instructions."
  350 PRINTTAB(22,4)"f1-Commence Scan."
  360 PRINTTAB(22,6)"f2-Exit."
  370 IFINKEY-33 PROCselect(22,2,"f0-Operating Instructions.",33):PROCinstructio
ns:PROCscan:ENDPROC
  380 IFINKEY-114 PROCselect(22,4,"f1-Commence Scan.",114):PROCscan:ENDPROC
  390 IFINKEY-115 PROCselect(22,6,"f2-Exit.",115):ENDPROC ELSE370
  400 ENDPROC
  410 DEFPROCinstructions
  420 CLS:PRINTTAB(0,1);:PRINT"  Using this program ,the POWDER DIFFRACTOMETER c
an download it's data"
  430 PRINT"into a BBC MASTER 128K micro via  a  6522 interface.By instructing t
he"
  440 PRINT"micro of the START and FINISH positions  of  the  goniometer arm,for
 a"
  450 PRINT"particular scan width,the diffracted intensities of the beam , betwe
en"
  460 PRINT"these points , can be stored on disc. Once on disc the information m
ay"
  470 PRINT"be further manipulated  by  other  software to retrieve  the  data
of"
  480 PRINT"interest."
  490 PRINTTAB(21,8);"<Press  ";:COLOUR0:COLOUR129:PRINT"RETURN";:COLOUR1:COLOUR
```

```
128:PRINT"    to continue>"
  500 REPEAT:G=GET:UNTILG=13:CLS
  510 PRINTTAB(0,1);:PRINT" Having placed the sample in the holder and put the X
-ray generator on"
  520 PRINT"stand-by,set the GONIOMETER arm to the desired START position,ensuri
ng"
  530 PRINT"that the 2-THETA value is an integer. Then manually rotate  the  sca
le"
  540 PRINT"anti-clockwise until there is an audible click."
  550 PRINTTAB(21,8);"<Press  ";:COLOUR0:COLOUR129:PRINT"RETURN";:COLOUR1:COLOUR
128:PRINT"    to continue>"
  560 REPEAT:G=GET:UNTILG=13:CLS
  570 ENDPROC
  580 DEFPROCscan_card
  590 REM CONTROL PANEL, DISPLAYING START,FINISH, CURRENT 2-THETA AND TIME
  600 GCOL16,1:MOVE200,900:VDU25,101,1000;450;:GCOL0,0:MOVE304,848:VDU25,101,975
;500;:GCOL0,1:MOVE320,864:VDU25,101,991;512;
  610 GCOL0,0:MOVE336,848:DRAW975,848:DRAW975,528:DRAW336,528:DRAW336,848:MOVE31
9,864:DRAW991,864:DRAW991,512:DRAW319,512:DRAW319,864:MOVE336,641:DRAW975,641:MO
VE344,840:DRAW967,840:DRAW967,792:DRAW344,792:DRAW344,840
  620 VDU28,0,31,79,0:COLOUR1:COLOUR128:PRINTTAB(21,12)"  CURRENT 2-THETA      C
OMPLETION TIME  ":VDU28,5,29,75,20
  630 MOVE336,784:DRAW975,784:MOVE655,607:DRAW655,528:VDU5:MOVE376,830:PRINT"S C
 A N   C O N T R O L   P A N E L":FORT%=0TO2:MOVE350,764-T%*40:PRINTA$(T%):NEXT
  640@%=&020105:MOVE494,764:PRINT;Title$:MOVE494,724:PRINT;Start%:MOVE494,684:PR
INT;Finish%:VDU4
  650 ENDPROC
  660 DEFPROClimits
  670 REM ROUTINE ALLOWS EDITING OF THE SCAN PARAMETERS
  680 CLS:PROCcommand_window:PROCedit:PROCscan_card
  690 T%=40/Rate
  700 CLS:PRINTTAB(15,1);"  E X E C U T E   A S   F O L L O W S"
  710 PRINTTAB(23,3);"<1>....SWITCH ON X-RAYS"
  720 PRINTTAB(23,5);"<2>....SWITCH ON  MOTOR"
  730 PRINTTAB(23,7);"<3>....DISENGAGE CLUTCH"
  740 ENDPROC
  750 DEFPROCtime
  760 REM CALCULATION OF ESTIMATED COMPLETION TIME
  770 Hour=VAL(MID$(TIME$,17,2)):Min=VAL(MID$(TIME$,20,2)):Minutes=(Finish%-Star
t%)/Rate
  780 Hr=(Minutes DIV 60):Hour=Hour+Hr:Mn=(Minutes MOD 60):Min=Min+Mn
  790 IF Min>59 THEN Hour=Hour+1:Min=Min-60
  800 IF Min<10 THEN  Z$="0" ELSE Z$=""
  810 ENDPROC
  820 DEFPROCscan
  830 REM MAIN CONTROL ROUTINE. PROG. MICRO LOGS DATA FROM INTERFACE WAITING FOR
  840 REM INITIAL ca2 INTERRUPT.
  850 PROClimits:PROCtime:REPEAT:CALL &DEA0:UNTIL ?ifr AND &01:PROCstart
  860 OSCLI("FX229,1"):VDU5:PROCcontrol:VDU4:PROCreport_end:PROCsave:*FX229,0
  870 ENDPROC
  880 DEFPROCstart
  890 REM CALCULATES INITIAL READING FROM SCALAR.
  900 A%=?&70:B%=?&71:C%=?&72:Zero=(A%DIV16)*10+(A%MOD16)+(B%DIV16)*1000+(B%MOD1
6)*100+(C%DIV16)*100000+(C%MOD16)*10000:?ifr=&01:Theta=Start%:@%=&902:VDU5:GCOL0
,0:MOVE767,582:PRINTHour;":";Z$;Min:@%=&020105:MOVE440,582:PRINTTheta:VDU4
  910 VDU28,5,28,75,20:COLOUR1:COLOUR128:CLS:PRINTTAB(18,3)"<<<  PROGRAM RUNNING
:X-RAYS ON  >>>":TIME=1000
  920 ENDPROC
  930 DEFPROCcontrol
  940 REM POLLS INTERRUPT REGISTER AND ACTS ON SET FLAGS.
```

```
  950 REPEAT
  960 IFINKEY-113 SOUND1,-15,80,1:Finish%=Theta+1
  970 IF ?ifr AND &02 THEN PROCca1
  980 IF ?ifr AND &01 THEN PROCca2
  990 UNTIL Theta=Finish%
 1000 ENDPROC
 1010 DEFPROCca1
 1020 REM 1/96 DEG. INTERRUPT SERVICE ROUTINE.
 1030 IF TIME<T% THEN 1120
 1040 TIME=0:CALL &DEA0:A%=?&70:B%=?&71:C%=?&72
 1050 Int=(A%DIV16)*10+(A%MOD16)+(B%DIV16)*1000+(B%MOD16)*100+(C%DIV16)*100000+(
C%MOD16)*10000
 1060 IF (Int-Zero)<0 THEN SOUND1,-15,120,1:PROCneg_data:GOTO1110
 1070 I%=(Int-Zero)
 1080 IF Lp%=1 THEN I%=I%*FNlorentz(Theta+N%*0.01041666)
 1090 IF I%>65535 THEN I%=65535
 1100 S%=S%+1:?S%=I% DIV256:S%=S%+1:?S%=I% MOD256:IF I%>Max% THEN Old_max%=Max%:
Max%=I%
 1110 N%=N%+1
 1120 Zero=Int:?ifr=&02
 1130 ENDPROC
 1140 DEFPROCca2
 1150 REM HALF DEGREE MARKER INTERRUPT. SELECTS FIRST 48 INTENSITY READINGS
 1160IF N%<48 THEN FORN%=N%+1 TO 48:S%=S%+1:?S%=I% DIV256:S%=S%+1:?S%=I% MOD256:
NEXT
 1170MOVE440,582:GCOL0,1:PRINTTheta:Theta=Theta+0.5:GCOL0,0:MOVE440,582:PRINTThe
ta
 1180 IF Hdeg%(Ram%-3)=160 THEN Ram%=Ram%+1:Hdeg%(Ram%-3)=0
 1190 OSCLI("SRWRITE 4000 4060 "+STR$~(&8000+96*Hdeg%(Ram%-3))+" "+STR$~Ram%)
 1200 Hdeg%(Ram%-3)=Hdeg%(Ram%-3)+1:?ifr=&01:N%=0:S%=&3FFF
 1210 ENDPROC
 1220 DEFPROCreport_end
 1230SOUND1,-15,87,2:SOUND1,-15,40,2:CLS:PRINTTAB(22,1)"S C A N   C O M P L E T
E"TAB(18,3)"Turn off X-rays and engage clutch"TAB(23,6)"Press ";:COLOUR0:COLOUR1
29:PRINT"RETURN";:COLOUR1:COLOUR128:PRINT" when ready":REPEAT:G=GET:UNTIL G=13
 1240 ENDPROC
 1250 DEFPROCsave
 1260 REM ALLOWS DATA TO BE SCALED TO A PREFERRED MAXIMUM.
 1270@%=&90A:CLS:PRINTTAB(2,1)"Maximum value of trace=";Max%
 1280PRINTTAB(2,3)"Do you wish to scale the data relative to this maxima?,<Y/N>"
 1290REPEAT:G=GET:UNTIL G=89 OR G=78:IF G=89 THEN 1320
 1300PRINTTAB(2,5)"Input the reference value for scaling :";:INPUT""New_max%
 1310IF New_max%<Max% THEN PRINTTAB(41,5)STRING$(5," "):PROCincorrect_response:G
OTO1300 ELSE Max%=New_max%
 1320 CLS:PRINTTAB(17,3)"DATA BEING SAVED TO DISC"
 1330 REM SAVES DIFFRCTION DATA IN TWO FILES; RAWDAT1 AND RAWDAT2
 1340 OSCLI("SRREAD 4000 8000 8000 4"):OSCLI("SAVE RAWDAT1 4000 8000")
 1350 OSCLI("SRREAD 4000 8000 8000 5"):OSCLI("SAVE RAWDAT2 4000 8000")
 1360 REM S-INFO HOLDS SCAN DETAILS. THIS IS USED THROUGHOUT SOFTWARE TO
 1370 REM TRANSFER PARAMETERS.
 1380 Int%=-2:Dhkl=0:X=OPENUP"S-INFO":PRINT#X,Title$,Start%,Finish%,Lambda,Rate,
Lp%,Smooth%,Max%,Ram%,Peak%:FORT%=1TO30:PRINT#X,Int%,Dhkl:NEXT:CLOSE#X
 1390 VDU4:@%=&02008
 1400 ENDPROC
 1410 DEFPROCneg_data
 1420 REM CORRECTS FOR NEGATIVE VALUES CAUSED BY INTERFACE GLITCH.
 1430 IF ?S%=&FF AND ?(S%-1)=&FF THEN 1460
 1440 Pointer=S%-3:IF ?Pointer=&FF AND ?(Pointer+1)=&FF THEN Pointer=Pointer-2
 1450 ?(S%+1)=?Pointer:?(S%+2)=?(Pointer+1):?(S%-1)=?Pointer:?S%=?(Pointer+1):GO
TO1470
```

```
 1460 Pointer=S%-5:?(S%+1)=?Pointer:?(S%+2)=?(Pointer+1):?(S%-3)=?Pointer:?(S%-2
)=?(Pointer+1)
 1470 I%=?(S%+1)*256+?(S%+2):Max%=Old_max%:S%=S%+2
 1480 ENDPROC
 1490 DEFPROCincorrect_response
 1500 SOUND1,-12,40,2:SOUND2,-12,47,2:TIME=0:REPEATUNTILTIME>25
 1510 ENDPROC
 1520 DEFPROCselect(Xcoord%,Ycoord%,Phrase$,Key%)
 1530 COLOUR0:COLOUR129:PRINTTAB(Xcoord%,Ycoord%)Phrase$
 1540 Now%=TIME:REPEAT:REPEATUNTILNOTINKEY(-Key%):UNTIL(TIME-Now%)>50:COLOUR1:CO
LOUR128
 1550 ENDPROC
 1560DEFPROCcommand_window
 1570X=OPENUP"S-INFO":INPUT#X,Title$,Start%,Finish%,Lambda,Rate,Lp%:CLOSE#X
 1580PROCwindow("S C A N   F I L E")
 1590ENDPROC
 1600DEFPROCedit
 1610 REM ALLOWS COMMAND FILE TO BE ALTERED.
 1620CLS:PRINTTAB(13,1)"Do you want to EDIT the command file?,<Y/N>";:REPEAT:G=G
ET:UNTILG=89 OR G=78:IF G=78 THEN ENDPROC
 1630 T%=0:PROCupdown
 1640 ENDPROC
 1650 DEFPROCupdown
 1660 REM CURSOR CONTROL FOR EDITING.
 1670 PROCon
 1680 CLS:PRINTTAB(11,1)"Use ";:COLOUR0:COLOUR129:PRINTCHR$139;:COLOUR1:COLOUR12
8:PRINT",";:COLOUR0:COLOUR129:PRINTCHR$138;:COLOUR1:COLOUR128:PRINT" & ";:COLOUR
0:COLOUR129:PRINT"RETURN";
 1690 COLOUR1:COLOUR128:PRINT" to select.Press ";:COLOUR0:COLOUR129:PRINT"SPACE"
;:COLOUR1:COLOUR128:PRINT" to finish."
 1700 IFINKEY-58 AND T%>0:PROCoff:T%=T%-1:PROCon:PROCfinger_off(58)
 1710 IFINKEY-42 AND T%<5:PROCoff:T%=T%+1:PROCon:PROCfinger_off(42)
 1720 IFINKEY-74:PROCfinger_off(74):PROCchange:GOTO1680
 1730 IFINKEY-99 THEN PROCoff ELSE 1700
 1740 ENDPROC
 1750 DEFPROCon
 1760 REM HIGHLIGHTS A STRING PARAMETER ON SCREEN. USED FOR EDITOR SELECTION.
 1770 VDU5:GCOL0,0:MOVEux+34,uy-108-T%*40:PRINTSTRING$(LEN(A$(T%)),CHR$255)
 1780 GCOL0,1:MOVEux+34,uy-108-T%*40:PRINTA$(T%):VDU4
 1790 ENDPROC
 1800 DEFPROCoff
 1810 REM REMOVES HIGHLIGHT ON STRING.
 1820 VDU5:GCOL0,1:MOVEux+34,uy-108-T%*40:PRINTSTRING$(LEN(A$(T%)),CHR$255)
 1830 GCOL0,0:MOVEux+34,uy-108-T%*40:PRINTA$(T%):VDU4
 1840 ENDPROC
 1850 DEFPROCchange
 1860 REM PARAMETER ALTERATIONS ARE PERFORMED.
 1870 CLS:ON T%+1 GOTO 1880,1920,1940,1960,1980,2000
 1880 PRINTTAB(0,2)"Input Title :";:INPUT""Title$
 1890 IF Title$="" THEN 1870
 1900 IF LEN(Title$)>16 THEN Title$=LEFT$(Title$,16) ELSE Title$=Title$+STRING$(
16-LEN(Title$)," ")
 1910 PROCnewdat(Title$,178,0,0,16):GOTO2010
 1920 PRINTTAB(0,2)"Input Start :";:INPUT""Start%
 1930 IF Start%<160 AND Start%>0 THEN PROCnewdat("",178,Start%,&020105,5):GOTO20
10 ELSE 1870
 1940 PRINTTAB(0,2)"Input Finish :";:INPUT""Finish%
 1950 IF Finish%>=(Start%+5) AND Finish%<160 THEN PROCnewdat("",178,Finish%,&020
105,5):GOTO2010 ELSE 1870
 1960 PRINTTAB(0,2)"Input Lambda :";:INPUT""Lambda
```

```
 1970 IF Lambda>0.7 AND Lambda<3.0 THEN PROCnewdat("",178,Lambda,&020406,6):GOTO
2010 ELSE 1870
 1980 PRINTTAB(0,2)"Input Rate    :";:INPUT""Rate
 1990 IF Rate>0 AND Rate<3 THEN PROCnewdat("",178,Rate,&020305,5):GOTO2010 ELSE
1870
 2000 IF Lp%=1 THEN Lp%=0:PROCnewdat("OFF",290,0,0,3) ELSE Lp%=1:PROCnewdat("ON"
,290,0,0,3)
 2010 PROCfinger_off(74)
 2020 ENDPROC
 2030 DEFPROCnewdat(A$,A,B,C,L)
 2040 REM USED FOR PRINTING NEW VALUE IN THE SCAN CARD.
 2050 VDU5:GCOL0,1:MOVEux+A,uy-108-T%*40:PRINTSTRING$(L,CHR$255)
 2060 GCOL0,0:MOVEux+A,uy-108-T%*40:IF C=0 PRINT;A$ ELSE @%=C:PRINT;B
 2070 VDU4
 2080 ENDPROC
 2090DEFPROCwindow(Banner$)
 2100 REM FULL DOWN WINDOW.
 2110VDU5:GCOL0,0:MOVEux-16,uy-16:VDU25,101,lx-16;ly-16;
 2120GCOL0,1:MOVEux,uy:VDU25,101,lx;ly;
 2130GCOL0,0:MOVEux,uy:DRAWlx,uy:DRAWlx,ly:DRAWux,ly:DRAWux,uy
 2140MOVEux+16,uy-16:DRAWlx-16,uy-16:DRAWlx-16,ly+16:DRAWux+16,ly+16:DRAWux+16,u
y-16
 2150MOVEux+16,uy-80:DRAWlx-16,uy-80:MOVEux+24,uy-72:DRAWux+24,uy-24:DRAWlx-24,u
y-24:DRAWlx-24,uy-72:DRAWux+24,uy-72:MOVE ux+((lx-ux)/2)-8*LEN(Banner$),uy-36:PR
INT;Banner$
 2160FORT%=0TO5:MOVEux+34,uy-108-T%*40:PRINTA$(T%):NEXT
 2170@%=&020105
 2180MOVEux+178,uy-108:PRINT;Title$
 2190MOVEux+178,uy-148:PRINT;Start%
 2200MOVEux+178,uy-188:PRINT;Finish%
 2210@%=&020406
 2220MOVEux+178,uy-228:PRINT;Lambda
 2230@%=&020305
 2240MOVEux+178,uy-268:PRINT;Rate
 2250MOVEux+290,uy-308:IF Lp%=1 PRINT;"ON" ELSE PRINT;"OFF"
 2260VDU4
 2270ENDPROC
 2280DEFPROCfinger_off(A)
 2290 REM ENSURES OPERATOR'S FINGER HAS BEEN RELEASED FROM KEY AND FLUSHES
 2300 REM THE KEYBORD BUFFER.
 2310REPEATUNTILNOTINKEY(-A):OSCLI"FX15,0"
 2320ENDPROC
 2330DEFFNlorentz(0)
 2340 REM LORENTZ/POLARISATION FUNCTION.
 2350=(1+COS(RAD(0))^2)/SIN(RAD(0))
```

```
  10 REM ***************************************************************
  20 REM * PROFILE is a driver program for two subroutine libraries;     *
  30 REM * P-LIB1 and P-LIB2. It controls the loading and locating of    *
  40 REM * the various files required for the subroutines. From here     *
  50 REM * the user can examine the trace, compare the experimental data *
  60 REM * with the database, input the data to the database and also    *
  70 REM * produce hard copies of the trace.                            *
  80 REM *                                          Neil S Stewart/RGIT *
  90 REM ***************************************************************
 100 REM
 110FORT%=4TO7:OSCLI("SRROM "+STR$T%):NEXT
 120X=OPENUP"S-INFO":PTR#X=55:INPUT#X,Ram%:CLOSE#X:FORT%=1TO(Ram%-3):OSCLI("LOA
D RAWDAT"+STR$(T%)+" 4000"):OSCLI("SRWRITE 4000 7FFF 8000 "+STR$~(T%+3)):NEXT
 130OSCLI("LOAD P-LIB1 4000"):OSCLI("SRWRITE 4000 7400 8000 6")
 140OSCLI("LOAD P-LIB2 4000"):OSCLI("SRWRITE 4000 7800 8000 7")
 150 REM SMCODE IS THE DATA SMOOTHING ROUTINE
 160 REM MICODE IS A MINIMUM TURNING POINT ROUTINE
 170OSCLI("LOAD SMCODE DD00"):OSCLI("LOAD MICODE DD70")
 180PROCbox(0)
 190PROCmenu_pos("profile/a ",0):CLS:PRINTTAB(25,0)"f0-Examine trace."
 200PRINTTAB(25,2)"f1-View results."
 210PRINTTAB(25,4)"f2-Exit."
 220 REM ON SELECTING ANY OF THESE OPTIONS, ALL ARRAYS/VARIABLES ARE RESET
 230IFINKEY-33 PROCselect(25,0,"f0-Examine trace.",33):CLEAR:HIMEM=&7000:PROCtr
ace:GOTO180
 240IFINKEY-114 PROCselect(25,2,"f1-View results.",114):CLEAR:HIMEM=&8000:PROCr
esults:GOTO190
 250IFINKEY-115 PROCselect(25,4,"f2-Exit.",115) ELSE 230
 260CHAIN"CENPOD"
 270END
 280DEFPROCbox(T%)
 290VDU18,16,128:VDU23,2,85,85,85,85,85,85,85,85:VDU19,1,6;0;:GCOL16,1:CLG:MOVE
50,34:GCOL0,1:VDU25,101,1230;327+T%*192;:GCOL0,0:MOVE66,50:VDU25,101,1214;311+T%
*192;:MOVE50,34:DRAW50,327+T%*192:DRAW1230,327+T%*192:DRAW1230,34:DRAW50,34
 300ENDPROC
 310DEFPROCmenu_pos(A$,T%)
 320VDU28,0,31,79,0:COLOUR0:COLOUR129:PRINTTAB(4,22-T%*6)STRING$(16," ");TAB(4,
22-T%*6)A$:COLOUR1:COLOUR128:VDU28,5,29,75,24-T%*6
 330ENDPROC
 340DEFPROCtrace
 350 REM MAIN ROUTINE FOR TRACE EXAMINATION
 360LOMEM=TOP-2+&3400:OSCLI("SRREAD "+STR$~(TOP-2)+" "+STR$~(TOP-2+&3400)+" 800
0 6"):PROCpeak_id
 370ENDPROC
 380DEFPROCresults
 390 REM USED FOR TREATING THE RESULTS FROM peak_id
 400LOMEM=TOP-2+&3800:OSCLI("SRREAD "+STR$~(TOP-2)+" "+STR$~(TOP-2+&3800)+" 800
0 7")
 410DIM Int%(30),Dhkl(30),Itest%(30),Dtest(30),Match_stat%(50,2),ResultI%(4,30)
,Resultd(4,30),Name$(4),IlibI%(30),IlibII%(30),Dlib(30),Lib_match%(4,30),Xinc%(5
),A$(15)
 420X=OPENIN"S-INFO":INPUT#X,Title$,Start%,Finish%,Lambda,Rate,Lp%,Son%,Max%,Ra
m%,Peak%:FORT%=1TO30:INPUT#X,Int%(T%),Dhkl(T%):NEXT:CLOSE#X:LoS%=Start%:HiS%=Fin
ish%:zoom=1:Sheet%=4:Super$="OFF":Backsub$="OFF"
 430CLS:PROCmenu_pos("profile/a/b1 ",0):PRINTTAB(25,0)"f0-Identify sample."
 440PRINTTAB(25,2)"f1-Hardcopy/plot."
 450PRINTTAB(25,4)"f2-Exit."
 460IFINKEY-33 PROCselect(25,0,"f0-Identify sample.",33):PROCidentify:GOTO400
 470IFINKEY-114 PROCselect(25,2,"f1-Hardcopy/plot.",114):PROCcopy:GOTO400
```

```
480IFINKEY-115 PROCselect(25,4,"f2-Exit.",115):ENDPROC ELSE 460
490ENDPROC
500DEFPROCselect(Xcoord%,Ycoord%,Phrase$,Key%)
510COLOUR0:COLOUR129:PRINTTAB(Xcoord%,Ycoord%)Phrase$
520Now%=TIME:REPEAT:REPEATUNTILNOTINKEY(-Key%):UNTIL(TIME-Now%)>50:COLOUR1:COL
OUR128:*FX15,0
530ENDPROC
```

```
 1000 REM ************************************************************
 1010 REM * F-LIB1 contains all the trace manipulation routines *
 1020 REM ************************************************************
 1030DEFPROCpeak_id
 1040PROCsetup:PROCscreen:PROCdefault_plot:PROCmenu
 1050ENDPROC
 1060DEFPROCsetup
 1070 REM SETS UP ALL VARIABLES REQUIRED INITIALLY
 1080OSCLI"FX14,6":DIM A$(15),B%(3),Dhkl(50),Int%(50)
 1090VDU23,240,0,0,0,132,133,230,165,164:VDU23,241,0,0,0,16,16,16,16,152
 1100A$(1)="Zones":A$(2)="plus2":A$(3)="Status":A$(4)="Cursors":A$(5)="Single":A
$(6)="Overlap":A$(7)="Re-Do":A$(8)="Results":A$(9)="Exit":A$(10)="Scale":A$(11)=
"Smooth":A$(12)="Backsub"
 1110X=OPENIN"S-INFO":INPUT#X,Title$,Start%,Finish%,Lambda,Rate,Lp%,Son%,Max%,Ra
m%:CLOSE#X:Z%=1:O%=0:P%=0:Q%=0:disp%=0:zoom%=1
 1120 IF ((Finish%-Start%)DIV 5)>16 THEN Sinc%=10 ELSE Sinc%=5
 1130Begin%=(Start% DIV5)*5:origin%=Begin%:End%=Begin%+((Finish%-Begin%+Sinc%-1)
DIV Sinc%)*Sinc%
 1140 Xoff_set%=(Start%-Begin%)*192:Zones%=(End%-Begin%)/5:Low%=0:Min%=0:Son%=0:
Bon%=0:lower%=&8000:upper%=lower%+1+(5+Begin%-Start%)*192
 1150ENDPROC
 1160DEFPROCscreen
 1170 REM PRINTS THE WORKING ENVIROMENT FOR TRACE ANALYSIS
 1180VDU26:VDU18,1,129:CLG:GCOL0,0:MOVE100,775:VDU25,101,1076;975;:MOVE100,52:VD
U25,101,1076;680;
 1190MOVE1106,998:DRAW1268,998:DRAW1268,26:DRAW1106,26:DRAW1106,998:MOVE1108,994
:DRAW1266,994:DRAW1266,26:MOVE1108,26:DRAW1108,994
 1200VDU5:GCOL0,0:MOVE1108,994:PRINTSTRING$(10,CHR$255):GCOL0,1:MOVE1139,994:PRI
NT"STATUS":GCOL0,0:MOVE1116,958:PRINT"Scale  x1":MOVE1116,926:PRINT"Smooth  X":M
OVE1116,894:PRINT"Backsub X"
 1210GCOL0,0:MOVE1108,862:DRAW1266,862:MOVE1108,858:PRINTSTRING$(10,CHR$255):GCO
L0,1:MOVE1116,858:PRINT"PEAK DATA":GCOL0,0:MOVE1116,822:PRINT"2"CHR$200"=":MOVE1
116,790:PRINT"d"CHR$240CHR$241"=":MOVE1116,758:PRINT"Peaks="
 1220MOVE1108,722:PRINTSTRING$(10,CHR$255):MOVE1108,726:DRAW1266,726:GCOL0,1:MOV
E1116,722:PRINT"FUNCTIONS":VDU4
 1230GCOL0,0:MOVE1116,682:VDU25,101,1258;38;:GCOL0,1:FORT%=1TO8:MOVE1116,682-T%*
72:DRAW1258,682-T%*72:NEXT
 1240VDU5:GCOL0,1:FORT%=1TO9:MOVE1171,674-(T%-1)*72:PRINT"f";T%-1:MOVE1187-8*LEN
(A$(T%)),642-(T%-1)*72:PRINTA$(T%):NEXT:VDU4
 1250GCOL0,0:MOVE100,1019:VDU25,101,1076;987;:GCOL0,1:MOVE516,1019:DRAW516,987:M
OVE708,1019:DRAW708,987:MOVE932,1019:DRAW932,987
 1260@%=&020406:VDU5:MOVE108,1014:PRINT"Title: ";Title$:MOVE532,1014:PRINTCHR$23
5"=";Lambda;" "CHR$129:MOVE724,1014:@%=&020204:PRINT"2"CHR$200"/min=";Rate;CHR$1
60:MOVE956,1014:PRINT"Lp ";:IF Lp%=1 THEN PRINT" ON" ELSE PRINT"OFF"
 1270GCOL0,0:PROCvert_banner("Cts",940):PROCvert_banner("Counts %Max",632)
 1280@%=&90A:Step=960/(End%-Begin%):FORT%=Begin% TO End% STEP Sinc%:D%=8*(LEN(ST
R$(T%)))
 1290MOVE108+(T%-Begin%)*Step,775:DRAW108+(T%-Begin%)*Step,767:MOVE(108-D%)+(T%-
Begin%)*Step,763:PRINT;T%:NEXT
 1300FORT%=0TO50:IF(T% MOD10)=0 THEN PROCfrac(52,-8):PROCfrac(680,8):PROCaxis_nu
mber ELSE PROCfrac(52,-4)
 1310NEXT
 1320PROCvert_scale:VDU5
 1330 A$=STRING$(3,CHR$255):GCOL0,0:MOVE4,36:PRINTA$:MOVE4,723:PRINTA$:MOVE4,763
:PRINTA$:GCOL0,1:MOVE4,36:PRINT"2"CHR$200CHR$160:MOVE4,723:PRINT"d"CHR$240CHR$24
1:MOVE4,763:PRINT"2"CHR$200CHR$160:VDU4
 1340ENDPROC
 1350DEFPROCdefault_plot
 1360 REM PLOT THE ENTIRE TRACE IN THE TOP GRAPHICS WINDOW
```

```
1370GCOL0,1:Xinc=960/((End%-Begin%)*96):Xpos=108+(Start%-Begin%)*96*Xinc
1380FORT%=1TO(Finish%-Start%)
1390IF T%>80 THEN OSCLI"SRREAD 7A00 7AC0 "+STR$~(&8000+(T%-81)*192)+" 5" ELSE O
SCLI"SRREAD 7A00 7AC0 "+STR$~(&8000+(T%-1)*192)+" 4"
1400Scale=192/Max%:FORV%=&7A00 TO &7ABF STEP2:DD=Scale*(256*?V%+?(V%+1))
1410IF DD>192 THEN DD=192
1420PLOT69,Xpos,783+DD:Xpos=Xpos+Xinc:NEXT:NEXT
1430PROCwindow_limits:PROCload_window:PROCplotII
1440ENDPROC
1450DEFPROCmenu
1460 REM BASIC MENU FOR FUNCTION KEYS
1470IFINKEY-33 PROCzone
1480IFINKEY-114 PROCplus2
1490IFINKEY-115 PROCstatus
1500IFINKEY-116 PROCpeaks
1510IFINKEY-23 PROCresultsI
1520IFINKEY-119 THEN PROChighlight(8):GOTO1550:ELSEGOTO1470
1530 REM ON EXIT EXPERIMENTAL DATA IS STORED IN S-INFO
1540 REM IF NO PEAKS HAVE BEEN MEASURED THEN S-INFO IS NOT UPDATED
1550X=OPENUP"S-INFO":IFP%=0 THEN1630 ELSE IF P%=1 THEN Int%(1)=100:GOTO1610
1560M%=0:REPEAT:swap=0:FORT%=1TOP%-1:IF Int%(T%)<Int%(T%+1) THEN PROCswapI
1570NEXT:UNTILswap=0
1580FORT%=1TOP%:IF Int%(T%)>M% THEN M%=Int%(T%)
1590NEXT
1600FORT%=1TOP%:Int%(T%)=Int%(T%)*100/M%:NEXT
1610IF P%>30 THEN P%=30 ELSE FORT%=(P%+1)TO30:Int%(T%)=-2:NEXT
1620 PTR#X=60:PRINT#X,P%:FORT%=1TO30:PRINT#X,Int%(T%),Dhkl(T%):NEXT
1630 PTR#X=45:PRINT#X,Son%:CLOSE#X
1640ENDPROC
1650DEFPROCerror
1660 REM INDICATES THAT A FUNCTION HAS BEEN CALLED WHILST IT IS UNAVAILABLE
1670SOUND1,-12,47,2:SOUND2,-12,40,2:PROCtime_fill
1680ENDPROC
1690DEFPROChighlight(M%)
1700VDU24,1120;42+72*(8-M%);1254;98+72*(8-M%);:GCOL4,128:CLG:VDU24,0;0;1279;102
3;
1710ENDPROC
1720DEFPROCtime_fill
1730TIME=0:REPEATUNTILTIME>25
1740ENDPROC
1750DEFPROCzone
1760 REM SELECTS THE 5 DEGREE ZONE
1770Step=4800/(End%-Begin%):disp%=0:PROChighlight(0):VDU24,0;0;1279;1023;:GCOL0
,1:PROCparallel(0,-1):GCOL4,1
1780IFINKEY-26 AND Z%>1 THEN Z%=Z%-1:PROCparallel(1,-1)
1790IFINKEY-122 AND Z%<Zones% THEN Z%=Z%+1:PROCparallel(-2,0)
1800IFINKEY-74 THEN 1810 ELSE GOTO1780
1810origin%=Begin%+(Z%-1)*5:PROCwindow_limits:IF (origin%-Start%)<=0 THEN lower
%=&8000 ELSE lower%=&8000+(origin%-Start%)*192
1820upper%=lower%+1+192*chunk%:PROCload_window:PROCsmooth:PROCbacksub:PROChor_s
cale:PROCvert_scale:PROCplotII:PROChighlight(0):VDU24,0;0;1279;1023;
1830ENDPROC
1840DEFPROCparallel(M%,N%)
1850 REM PRODUCES THE PARALLEL LINES BORDERING THE CURRENTLY SELECTED ZONE
1860MOVE108+(Z%+M%)*Step,775:DRAW108+(Z%+M%)*Step,975:MOVE108+(Z%+N%)*Step,775:
DRAW108+(Z%+N%)*Step,975:PROCtime_fill
1870ENDPROC
1880DEFPROCsmooth
1890 REM SMOOTHS DATA HELD IN TRACE WORKSPACE,.i.e., &7A00 TO &7DC0
1900 REM CALLS SMCODE
```

```
 1910IF Son%=0 THEN 1950
 1920IF lower%=&8000 THEN ?&73=0:?&74=&7A ELSE ?&73=&FA:?&74=&79
 1930IF upper%=(&8000+(Finish%-Start%)*192) THEN ?&75=(&7A00+chunk%*192)MOD256:?
&76=(&7A00+chunk%*192)DIV256 ELSE ?&75=(&7A08+chunk%*192)MOD256:?&76=(&7A08+chun
k%*192)DIV256
 1940CALL &DD00
 1950ENDPROC
 1960DEFPROCplotII
 1970 REM PLOTS DATA IN LOWER GRAPHICS WINDOW
 1980Scale=zoom%*612/Max%:GCOL0,1:VDU24,108;52;1068;680;:VDU18,0,128:CLG:GCOL0,1
:FORT%=&7A00TO(&7A00+chunk%*192) STEP2:PLOT69,108+Xoff_set%+(T%-&7A00),60+Scale*
((256*?T%+?(T%+1))-Min%):NEXT
 1990ENDPROC
 2000DEFPROCplus2
 2010 REM SHIFTS THE TRACE BY 2 DEG. TO THE RIGHT
 2020PROChighlight(1):IF(Finish%-origin%)<5 THEN PROCerror:GOTO2060
 2030 origin%=origin%+2:IF Xoff_set%<=192 THEN lower%=lower%+(384-Xoff_set%)
 2040 PROCwindow_limits:upper%=lower%-1+chunk%*192
 2050 PROCload_window:PROCsmooth:PROCbacksub:PROChor_scale:PROCvert_scale:PROCpl
otII
 2060PROChighlight(1)
 2070ENDPROC
 2080DEFPROChor_scale
 2090 REM PRINTS HORIZONTAL SCALE ALONG GRAPHICS WINDOW
 2100VDU24,0;0;1279;1023;:VDU5:GCOL0,1:MOVE54,36:VDU25,101,1100;0;:MOVE54,723:VD
U25,101,1100;691;:GCOL0,0:FORT%=0TO50STEP10:PROCaxis_number:NEXT:VDU4:VDU23,1,0;
0;0;0;
 2110ENDPROC
 2120DEFPROCresultsI
 2130PROChighlight(7):IF P%=0 THEN PROCerror:PROChighlight(7):ENDPROC ELSE IF P%
=1 THEN N%=1:M%=Int%(1):GOTO2180
 2140REPEAT:swap=0:FORT%=1TOP%-1:IF Int%(T%)<Int%(T%+1) THEN PROCswapI
 2150NEXT:UNTILswap=0
 2160M%=0:FORT%=1TOP%:IF Int%(T%)>M% THEN M%=Int%(T%)
 2170NEXT:IF P%>15 THEN N%=15 ELSE N%=P%
 2180PROCtable:FORT%=1TON%:@%=&905:PRINTTAB(49,T%+13),Int%(T%):@%=&903:PRINTTAB(
55,T%+13),INT(Int%(T%)*100/M%):@%=&020205:PRINTTAB(59,T%+13),2*DEG(ASN(Lambda/(2
*Dhkl(T%)))):NEXT:@%=&90A:PROChighlight(7)
 2190ENDPROC
 2200DEFPROCswapI
 2210 REM BUBBLE SORT
 2220Q=Int%(T%):Int%(T%)=Int%(T%+1):Int%(T%+1)=Q:Q=Dhkl(T%):Dhkl(T%)=Dhkl(T%+1):
Dhkl(T%+1)=Q:swap=swap+1
 2230ENDPROC
 2240DEFPROCtable
 2250 REM TABLE FOR INTENSITY OUTPUT ON SCREEN
 2260GCOL0,0:MOVE768,611:VDU25,101,1038;575-32*N%;:COLOUR129:COLOUR0:PRINTTAB(48
,13)"   Ia   In  2"CHR$232CHR$160"  ":GCOL0,1:MOVE768,611:DRAW768,575-32*N%:DRAW
1038,575-32*N%:DRAW1038,611:DRAW768,611:COLOUR128:COLOUR1
 2270ENDPROC
 2280DEFPROCwindow_limits
 2290 REM CALCULATES SIZE OF TRACE WORKSPACE
 2300 IF (origin%-Start%)>=0 THEN Xoff_set%=0 ELSE Xoff_set%=(Start%-origin%)*19
2
 2310 IF (origin%+5-Finish%)<=0 THEN chunk%=5 ELSE chunk%=Finish%-origin%
 2320 IF Xoff_set%>0 THEN chunk%=chunk%-(Xoff_set%/192)
 2330ENDPROC
 2340DEFPROCload_window
 2350 REM TRANSFERS DATA FROM SIDEWAYS RAM TO TRACE WORKSPACE
 2360IF lower%=&8000 THEN OSCLI"SRREAD 7A00 7DC8 8000 4":GOTO2420
```

```
 2370IF upper%<&BC00 THEN OSCLI"SRREAD 79FA 7DC8 "+STR$~(lower%-6)+" 4":GOTO2420
 2380IF upper%=&BC00 THEN OSCLI"SRREAD 79FA 7DC0 "+STR$~(lower%-6)+" 4":OSCLI"SR
READ "+STR$~(&7A00+chunk%*192)+" "+STR$~(&7A00+chunk%*192+8)+" 8000 5":GOTO2420
 2390IF lower%=&BC00 THEN OSCLI"SRREAD 79FA 7A00 BBFA 4":OSCLI"SRREAD 7A00 "+STR
$~(&7A08+chunk%*192)+" 8000 5":GOTO2420
 2400IF lower%>&BC00 THEN OSCLI"SRREAD 79FA 7DC8 "+STR$~(lower%-&3C06)+" 5":GOTO
2420
 2410OSCLI"SRREAD 79FA "+STR$~(&7A00+&BC00-lower%)+" "+STR$~(lower%-6)+" 4":OSCL
I"SRREAD "+STR$~(&7A00+&BC00-lower%)+" 7DC8 8000 5"
 2420ENDPROC
 2430DEFPROCpeaks
 2440 REM DISABLES PREVIOUS MENU AND PASSES CONTROL TO CURSOR MOVEMENT
 2450PROChighlight(3):IF P%>49 THEN PROCerror:GOTO2520
 2460Xpos=480:GCOL4,1:PROCvert_line
 2470PROCboundaries
 2480IFV%=1 THEN 2520
 2490IFINKEY-21 PROChighlight(4):PROCsingle:PROCline_clear:PROChighlight(4):PROC
display:GOTO2470
 2500IFINKEY-117 PROChighlight(5):PROCmultiple:PROChighlight(5):PROCdisplay:GOTO
2470
 2510GOTO2490
 2520PROChighlight(3)
 2530ENDPROC
 2540DEFPROCboundaries
 2550 REM ESTABLISHES THE BOUDARIES OF THE SELECTED PEAK
 2560V%=0:T%=0
 2570PROCcursors:IF V%=1 THEN ENDPROC
 2580ZZ%=1:IFT%=1 THEN Xpos=Xpos+8:PROCvert_line:PROCcursors
 2590IFB%(1)>B%(2) THEN PROCerror:Xpos=B%(1):PROCvert_line:Xpos=B%(2):T%=0:GOTO2
570
 2600P%=P%+1:Q%=1:SOUND1,-12,40,2
 2610ENDPROC
 2620DEFPROCcursors
 2630 REM CURSOR CONTROL
 2640IFINKEY-1 I%=16 ELSE I%=2
 2650IFINKEY-26 AND (Xpos-I%)>=0 THEN PROCvert_line:Xpos=Xpos-I%:PROCvert_line
 2660IFINKEY-122 AND (Xpos+I%)<=960 THEN PROCvert_line:Xpos=Xpos+I%:PROCvert_lin
e
 2670IFINKEY-118 PROCredo
 2680IFINKEY-99 PROCvert_line:V%=1:@%=&90A:VDU24,94;68;1054;616;:ENDPROC
 2690IFINKEY-74 THEN T%=T%+1:B%(T%)=Xpos:PROCtime_fill:ENDPROC:ELSEGOTO2640
 2700ENDPROC
 2710DEFPROCline_clear
 2720Xpos=B%(1):PROCvert_line:Xpos=B%(2):SOUND1,-12,40,2
 2730ENDPROC
 2740DEFPROCvert_line
 2750MOVE108+Xpos,52:DRAW108+Xpos,680
 2760ENDPROC
 2770DEFPROCbackground
 2780 REM CONTROLS A VERTICAL CURSOR TO ESTABLISH A SUITABLE BACKGROUND LEVEL
 2790VDU24,108;52;1068;680;:GCOL4,1:Ypos%=304:PROChoriz_line
 2800IFINKEY-1 I%=16 ELSE I%=4
 2810IFINKEY-58 AND (Ypos%+I%)<=612:PROChoriz_line:Ypos%=Ypos%+I%:PROChoriz_line
 2820IFINKEY-42 AND (Ypos%-I%)>=0:PROChoriz_line:Ypos%=Ypos%-I%:PROChoriz_line
 2830IFINKEY-74 THEN B%=Ypos%*Max%/(612*zoom%)+Min%:GOTO2840 ELSE2800
 2840ENDPROC
 2850DEFPROChoriz_line
 2860MOVE108+B%(1)-10,60+Ypos%:DRAW108+B%(2)+10,60+Ypos%
 2870ENDPROC
 2880DEFPROCsingle
```

```
 2890 REM SINGLE PEAK MEASUREMENT
 2900PROCbackground:PROCmaxima(B%(1),B%(2)):PROChalf_power:var=(L%-Mu%)^2/LN(2):
PROCintegrate:PROChoriz_line
 2910ENDPROC
 2920DEFPROCintegrate
 2930 REM CALCULATES THE PEAK AREA BETWEEN TWO CALCULATED LIMITS
 2940sum=0:FORT%=Mu%-SQR(var/LN(50)) TO Mu%:sum=sum+(M%-B%)*EXP(-(T%-Mu%)^2/var)
:NEXT:Int%(P%)=(2*sum)+0.5
 2950ENDPROC
 2960DEFPROCmultiple
 2970 REM OVERLAPPING PEAKS
 2980Xpos=Xpos+8:PROCvert_line:REPEAT:T%=2:PROCcursors:UNTIL B%(3)<B%(1) OR B%(3
)>B%(1)
 2990PROCbackground:PROCmaxima(B%(1),B%(2)):M1=M%:Mi1=Mi:IF B%(3)>B%(1) THEN PRO
Cmaxima(B%(2),B%(3)):M2=M%:Mi2=Mi:Trough%=B%(2) ELSE PROCmaxima(B%(3),B%(1)):M2=
M%:Mi2=Mi:Trough=B%(1)
 3000 IF Mi1<Mi2 THEN Xa=Mi1+(((Mi2-Mi1)/3)DIV2)*2:Xb=Mi1+((2*(Mi2-Mi1)/3)DIV2)*
2 ELSE Xa=Mi2+(((Mi1-Mi2)/3)DIV2)*2:Xb=Mi2+((2*(Mi1-Mi2)/3)DIV2)*2
 3010Ia=256*?(&7A00+Xa-Xoff_set%)+?(&7A01+Xa-Xoff_set%)-B%:Ib=256*?(&7A00+Xb-Xof
f_set%)+?(&7A01+Xb-Xoff_set%)-B%
 3020Z1=LN(Ia)-LN(M1)-LN(M2):Z2=LN(Ib)-LN(M1)-LN(M2):Z3=(Xa-Mi2)^2:Z4=(Xb-Mi2)^2
:Y1=(Xb-Mi1)^2:Y2=(Xa-Mi1)^2:var=(Z3*Y1-Z4*Y2)/(Z1*Z4-Z2*Z3)
 3030Mu%=Mi1:M%=M1:PROCintegrate
 3040FORT%=1TO2:Xpos=B%(T%):PROCvert_line:NEXT:PROChoriz_line:Xpos=B%(3):GCOL4,1
 3050Dhkl(P%)=0.5*Lambda/SIN(RAD((origin%+Mi1/192)/2)):Last_peak=2:SOUND1,-12,40
,2
 3060ENDPROC
 3070DEFPROCmaxima(A,B)
 3080 REM SEARCHES BETWEEN TWO CURSOR POSITIONS FOR MAXIMUM TURNING POINT
 3090M%=0:FORT%=A TO B STEP2:Mem%=&7A00+T%-Xoff_set%
 3100V%=256*?Mem%+?(Mem%+1):IF V%>M% THEN M%=V%:Mamp=Mem%:Mi=T%
 3110NEXT
 3120ENDPROC
 3130DEFPROCredo
 3140 REM SCRATCHES LAST DATA PAIR AND DECREMENTS PEAK COUNTER BY 1
 3150PROChighlight(6):IF P%=0 OR ZZ%=0 THEN PROCerror:GOTO3180
 3160Int%(P%)=0:P%=P%-1:T%=0:PROCupdate(1212,758,0,P%,3,3):GCOL4,1:SOUND1,-12,40
,2
 3170T%=0:PROCupdate(1212,758,0,P%,3,3):GCOL4,1:SOUND1,-12,40,2
 3180PROChighlight(6)
 3190ENDPROC
 3200DEFPROCdisplay
 3210 REM PRINTS OUT Dhkl AND 2-THETA RESULTS WINDOW
 3220twothet=2*DEG(ASN(0.5*Lambda/Dhkl(P%))):PROCupdate(1164,822,0,twothet,&0202
06,6):PROCupdate(1180,790,0,Dhkl(P%),&020205,5):PROCupdate(1212,758,0,P%,3,3):GC
OL4,1
 3230ENDPROC
 3240DEFPROCfrac(A,B)
 3250 REM AXIS DIVISION MARKER
 3260MOVE108+T%*19.2,A:DRAW108+T%*19.2,A+B
 3270ENDPROC
 3280DEFPROCaxis_number
 3290 REM NUMBER AXIS
 3300@%=&90A:theta=T%/10+origin%:D%=LEN(STR$(theta))*8:MOVE(108-D%)+T%*19.2,36:P
RINT;theta
 3310dhkl=Lambda/(2*SIN(RAD((origin%+(T%/10))/2))):@%=&020205:IF dhkl>10 THEN D%
=40 ELSE D%=32
 3320MOVE(108-D%)+T%*19.2,723:PRINT;dhkl
 3330ENDPROC
 3340DEFPROCdigoff(A)
```

```
 3350 REM PAUSES UNTIL KEY IS RELEASED
 3360REPEATUNTILNOTINKEY(-A)
 3370ENDPROC
 3380DEFPROCvert_banner(V$,N%)
 3390 REM PRINTS VERTICAL BANNERS, LABELLING THE Y AXES OF WINDOWS
 3400V1$="Counts %Max":V2$="Counts"
 3410FORT%=1 TO LEN(V$):MOVE20,N%-T%*32:PRINT;MID$(V$,T%,1):NEXT
 3420ENDPROC
 3430DEFPROCbacksub
 3440 REM IF REQUESTED THE TRACE WORK SPACE IS SEARCHED FOR MINIMUM.
 3450 CALLS MICODE
 3460IF Bon%=0 THEN Min%=0:ENDPROC
 3470?&70=0:?&71=&7A:?&72=255:?&73=255:?&76=&C0:?&77=&7D:CALL &DD70:Min%=?&72+25
6*?&73
 3480ENDPROC
 3490DEFPROCvert_scale
 3500 REM CALCULATES VERT SCALE FOR LOWER G WINDOW.
 3510low%=100*Min%/Max%:high%=low%+100/zoom%:diff%=high%-low%
 3520 A$="20100504030201"
 3530 T%=-1:REPEAT
 3540 T%=T%+2:step%=VAL(MID$(A$,T%,2))
 3550 UNTIL (diff%/step%)>=5 OR T%=13
 3560 VDU5:GCOL0,1:MOVE44,691:VDU25,101,98;48;:GCOL0,0
 3570 @%=&903:FORT%=0TO(INT(diff%/step%)):Step=T%*615*step%/diff%:IF Step>615 OR
(low%+T%*step%)>100 THEN 3590
 3580 MOVE100,60+Step:DRAW94,60+Step:MOVE44,72+Step:PRINT,low%+T%*step%
 3590 NEXT:VDU4
 3600 ENDPROC
 3610DEFPROCstatus
 3620 REM ALLOWS EDITING OF STATUS WINDOW
 3630PROChighlight(2):minus%=0:plus%=0:up%=1:PROCillum(0)
 3640REPEAT
 3650IFINKEY-58 AND up%<>1:PROCdigoff(58):PROCillum(1):up%=up%-1:PROCillum(0)
 3660IFINKEY-42 AND up%<>3:PROCdigoff(42):PROCillum(1):up%=up%+1:PROCillum(0)
 3670IFINKEY-26:PROCdigoff(26):minus%=1:PROCstatus_edit
 3680IFINKEY-122:PROCdigoff(122):plus%=1:PROCstatus_edit
 3690UNTILINKEY-74:PROCillum(1)
 3700PROCload_window:PROCsmooth:PROCbacksub:PROCvert_scale:PROCplotII
 3710PROChighlight(2)
 3720ENDPROC
 3730DEFPROCstatus_edit
 3740ONup% GOTO3750,3780,3800
 3750IF minus% AND zoom%<>1 THEN zoom%=zoom%-1:minus%=0:PROCupdate(1244,958,zoom
%+48,0,0,0)
 3760IF plus% AND zoom%<>5 THEN zoom%=zoom%+1:plus%=0:PROCupdate(1244,958,zoom%+
48,0,0,0)
 3770GOTO3810
 3780minus%=0:plus%=0:IF P%<>0 THEN PROCerror:GOTO3810 ELSE:IF Son% THEN Son%=0:
PROCupdate(1244,926,88,0,0,0) ELSE Son%=1:PROCupdate(1244,926,190,0,0,0)
 3790GOTO3810
 3800minus%=0:plus%=0:IF Bon% THEN Bon%=0:PROCupdate(1244,894,88,0,0,0) ELSE Bon
%=1:PROCupdate(1244,894,190,0,0,0)
 3810ENDPROC
 3820DEFPROCupdate(X,Y,Ch,Dat,Fd,Tp)
 3830 REM TEXT/NUMBER RE-WRITE
 3840VDU5:IF Ch=0 THEN @%=Fd:GCOL0,1:MOVEX,Y:PRINTSTRING$(Tp,CHR$255):GCOL0,0:MO
VEX,Y:PRINT;Dat:GOTO3860
 3850GCOL0,1:MOVEX,Y:PRINTSTRING$(1,CHR$255):GCOL0,0:MOVEX,Y:PRINTCHR$(Ch)
 3860VDU4
 3870ENDPROC
```

```
3880DEFPROCillum(A%)
3890 REM PRINTS STRING IN INVERSE VIDEO
3900VDU5:GCOL0,A%:MOVE1116,958-(up%-1)*32:PRINTSTRING$(7,CHR$255)
3910GCOL0,A%+1:MOVE1116,958-(up%-1)*32:PRINTA$(9+up%):VDU4
3920ENDPROC
3930DEFPROChalf_power
3940 REM CALCULATES THE HALF POWER POINTS FOR SINGLE PEAKS
3950T%=Mi:REPEAT:Mem%=&7A00+T%-Xoff_set%
3960V%=256*?Mem%+?(Mem%+1):T%=T%-2
3970UNTIL (V%-B%)<=(M%-B%)/2 OR T%=0
3980L%=T%+2
3990T%=Mi:REPEAT:Mem%=&7A00+T%-Xoff_set%
4000V%=256*?Mem%+?(Mem%+1):T%=T%+2
4010UNTIL (V%-B%)<=(M%-B%)/2 OR T%=960
4020R%=T%-2
4030Mu%=(R%+L%)/2:Dhkl(P%)=0.5*Lambda/SIN(RAD((origin%+Mu%/192)/2)):GOTO2950
4040ENDPROC
```

```
 1000 REM ************************************************
 1010 REM * P-LIB2 contains all the result processing routines *
 1020 REM ************************************************
 1030 DEFPROCidentify
 1040 REM EITHER COMPARE DATA WITH DATABASE OR INPUT DATA AS NEW RECORD
 1050 IF Peak%=0 THEN PROCdeny:ENDPROC
 1060 CLS:PROCmenu_pos("profile/a/b1/c0 ",0):PRINTTAB(20,0)"f0-Compare test data
 with DATA-BASE."
 1070 PRINTTAB(20,2)"f1-Input test data to DATA-BASE."
 1080 PRINTTAB(20,4)"f2-Exit."
 1090 IFINKEY-33 PROCselect(20,0,"f0-Compare test data with DATA-BASE.",33):PROC
dbase_match:GOTO1060
 1100 IFINKEY-114 PROCselect(20,2,"f1-Input test data to DATA-BASE.",114):PROCte
st_input:GOTO1060
 1110 IFINKEY-115 PROCselect(20,4,"f2-Exit.",115):ENDPROC ELSE 1090
 1120 ENDPROC
 1130 DEFPROCcopy
 1140 REM PRODUCES HARD COPIES OF THE RESULTS
 1150 CLS:PROCmenu_pos("profile/a/b1/c1 ",0):PRINTTAB(24,0)"f0-Plot trace on PLO
TMATE."
 1160 PRINTTAB(24,2)"f1-Printout experimental data."
 1170 PRINTTAB(24,4)"f2-Exit."
 1180 IFINKEY-33 PROCselect(24,0,"f0-Plot trace on PLOTMATE.",33):PROCplotmate:G
OTO1150
 1190 IFINKEY-114 PROCselect(24,2,"f1-Printout experimental data.",114):PROChard
_copyII:GOTO1150
 1200 IFINKEY-115 PROCselect(24,4,"f2-Exit.",115):ENDPROC ELSE 1180
 1210 ENDPROC
 1220DEFPROCtest_input
 1230 REM ADD TO DATABASE
 1240PROCcard:PROCdisplay_data:VDU28,5,29,75,24:COLOUR1:COLOUR128:PROCinput_deta
 ils:X=OPENUP":2.PDFILE":INPUT#X,Disc$,Entries%:PTR#X=PTR#X+Entries%*380:Entries%
 =Entries%+1:PROCdisc_poker
 1250ENDPROC
 1260DEFPROCdbase_match
 1270 REM COMPARISON WITH DATABASE
 1280PROCcompare:IF Top3%=0 THEN VDU28,5,29,75,24:COLOUR1:COLOUR128:CLS:PRINTTAB
(20,1)"CANNOT FIND A SIGNIFICANT MATCH!":TIME=0:REPEATUNTILTIME>300:ENDPROC ELSE
 PROCresult_table:VDU28,0,31,79,0:PROCresultsII:VDU28,5,29,75,24
 1290CLS:PRINTTAB(10,2)"Do you want a hard-copy of this comparison?,<Y/N>";:REPE
AT:G=GET:UNTIL(G=89 OR G=78):IF G=89 THEN PROCcompare_print
 1300ENDPROC
 1310DEFPROCcompare
 1320X=OPENUP":2.PDFILE":INPUT#X,Disc$,Entries%:Record%=0
 1330@%=&90003:CLS:PRINTTAB(3,0)"Comparing Test-Data with contents of data-file "
:Disc$;TAB(3,1)"There are ";Entries%;" records on this disc."
 1340FORT%=1TOEntries%:PRINTTAB(30,3)"Record #";T%:PTR#X=22+(T%-1)*380:Pointer%=
PTR#X:PTR#X=PTR#X+45:INPUT#X,Pair%
 1350FORV%=1TOPair%:INPUT#X,IlibI%(V%),Dlib(V%):IlibII%(V%)=IlibI%(V%):NEXT
 1360IF Pair%<8 THEN Lib%=Pair% ELSE Lib%=8
 1370IF Peak%<8 THEN Test%=Peak% ELSE Test%=8
 1380PROCcheck(Lib%,Test%):IF Match%=0 THEN 1410
 1390FORV%=1TOLib%:IlibII%(V%)=IlibI%(V%):NEXT
 1400Record%=Record%+1:PROCcheck(Pair%,Peak%):Match_stat%(Record%,0)=Pointer%:Ma
tch_stat%(Record%,1)=Match%
 1410NEXT
 1420IF Record%=0 THEN Top3%=0:GOTO1550
 1430IF Record%=1 THEN 1470
 1440Bubble%=1:REPEAT:swap%=0:FORT%=1TO(Record%-Bubble%)
```

```
 1450IF Match_stat%(T%,1)<Match_stat%(T%+1,1) THEN swap%=swap%+1:Q%=Match_stat%(
T%,1):Match_stat%(T%,1)=Match_stat%(T%+1,1):Match_stat%(T%+1,1)=Q%:Q%=Match_stat
%(T%,0):Match_stat%(T%,0)=Match_stat%(T%+1,0):Match_stat%(T%+1,0)=Q%
 1460NEXT:Bubble%=Bubble%+1:UNTIL swap%=0
 1470IF Record%>3 THEN Top3%=3 ELSE Top3%=Record%
 1480PRINTTAB(16,4)"Selecting the top 3 possible matches."
 1490FORT%=1TOTop3%:PTR#X=Match_stat%(T%,0):INPUT#X,Name$(T%):PTR#X=PTR#X+27:INP
UT#X,Pair%:Match_stat%(T%,2)=Pair%
 1500FORV%=1TOPair%:INPUT#X,ResultI%(T%,V%),Resultd(T%,V%):IlibII%(V%)=ResultI%(
T%,V%):Dlib(V%)=Resultd(T%,V%):NEXT
 1510FORA%=1TOPeak%:Dtol=RAD(0.2)*Lambda/(2*SIN(ASN(Lambda/(2*Dhkl(A%))))*TAN(AS
N(Lambda/(2*Dhkl(A%))))):FORB%=1TOPair%:IF IlibII%(B%)=-999 THEN 1530
 1520IF (ABS(Int%(A%)-IlibII%(B%))<25) AND (ABS(Dhkl(A%)-Dlib(B%))<Dtol) THEN Li
b_match%(T%,B%)=Lib_match%(T%,B%)+1:IlibII%(B%)=-999:B%=Pair%
 1530NEXT:NEXT
 1540NEXT:CLOSE#X
 1550ENDPROC
 1560DEFPROCresultsII
 1570 REM OUTPUT OF COMPARISON RESULTS
 1580IF Peak%>12 THEN Test12%=12 ELSE Test12%=Peak%
 1590COLOUR0:COLOUR129:FORT%=1TOTest12%:@%=&9003:PRINTTAB(10,T%+5)Int%(T%):@%=&0
20306:PRINTTAB(14,T%+5)Dhkl(T%):NEXT
 1600FORT%=1TOTop3%:IF Match_stat%(T%,2)>12 THEN Top12%=12 ELSE Top12%=Match_sta
t%(T%,2)
 1610FORV%=1TOTop12%:IF Lib_match%(T%,V%)=1 THEN COLOUR1:COLOUR128:ELSE COLOUR0:
COLOUR129
 1620@%=&9003:PRINTTAB(25+17*(T%-1),V%+5)ResultI%(T%,V%):@%=&020306:PRINTTAB(30+
17*(T%-1),V%+5)Resultd(T%,V%):NEXT
 1630@%=&9002:VDU5:Y%=17:REPEAT:Y%=Y%-1:UNTIL MID$(Name$(T%),Y%,1)<>" ":Length=Y
%
 1640MOVE490+(T%-1)*272-8*Length,921:PRINTName$(T%):MOVE470+(T%-1)*272,431:PRINT
;Match_stat%(T%,1):VDU4:NEXT:COLOUR1:COLOUR128
 1650ENDPROC
 1660DEFPROCcheck(Lib%,Test%)
 1670 REM COMPARES Dhkl VALUES
 1680Match%=0:FORA%=1TOTest%:Dtol=RAD(0.2)*Lambda/(2*SIN(ASN(Lambda/(2*Dhkl(A%))
))*TAN(ASN(Lambda/(2*Dhkl(A%))))):FORB%=1TOLib%:IF IlibII%(B%)=-999 THEN 1700
 1690IF (ABS(Dhkl(A%)-Dlib(B%))<Dtol) THEN IlibII%(B%)=-999:Match%=Match%+1:B%=L
ib%
 1700NEXT:NEXT
 1710ENDPROC
 1720DEFPROCbox(A$)
 1730GCOL0,0:MOVE15,15:DRAW15,1008:DRAW1266,1008:DRAW1266,15:DRAW15,15:GCOL0,1:M
OVE50,34:VDU25,101,1230;327;:GCOL0,0:MOVE66,51:VDU25,101,1214;311;:MOVE50,34:DRA
W50,327:DRAW1230,327:DRAW1230,34:DRAW50,34
 1740COLOUR0:COLOUR129:PRINTTAB(4,22)A$;"INSTRUCTIONS:";VDU28,5,29,75,24:COLOUR1
:COLOUR128
 1750ENDPROC
 1760DEFPROCswapII
 1770 REM BUBBLE SORT
 17800=Int%(T%):Int%(T%)=Int%(T%+1):Int%(T%+1)=0:0=Dhkl(T%):Dhkl(T%)=Dhkl(T%+1):
Dhkl(T%+1)=0
 1790ENDPROC
 1800DEFPROCresult_table
 1810 REM COMPARISON OUTPUT WINDOW
 1820GCOL16,1:MOVE50,1000:VDU25,101,1260;330;:GCOL0,0:MOVE100,368:VDU25,101,1176
;981;:GCOL0,1:MOVE110,378:VDU25,101,1186;995;:GCOL0,0:MOVE110,378:DRAW110,995:DR
AW1186,995:DRAW1186,378:DRAW110,378
 1830MOVE128,398:DRAW128,975:DRAW1168,975:DRAW1168,398:DRAW128,398:MOVE352,975:D
RAW352,398:MOVE348,975:DRAW348,398:MOVE352,935:DRAW1168,935:MOVE128,851:DRAW1168
```

```
,851:MOVE128,439:DRAW1168,439
 1840FORT=1TO3:MOVE352+T*272,935:DRAW352+T*272,398:NEXT:@%=&90A:VDU5:MOVE184,431
:PRINT"MATCHES":MOVE160,921:PRINT"TEST DATA":MOVE176,881:PRINT"I      d":FORT=0TO
2:MOVE431+T*272,881:PRINT"I      d":NEXT
 1850MOVE370,965:PRINT"Sample title: ";Title$:VDU4
 1860ENDPROC
 1870DEFPROCcard
 1880 REM POWDER INDEX CARD
 1890VDU23,240,0,0,0,132,133,230,165,164:VDU23,241,0,0,0,16,16,16,16,152
 1900VDU23,242,0,0,0,251,168,171,138,139:VDU23,243,0,0,0,162,148,136,148,162
 1910GCOL16,1:MOVE50,1000:VDU25,101,1260;330;
 1920VDU28,0,31,79,0:GCOL0,0:MOVE190,348:VDU25,101,1090;967;:GCOL0,1:MOVE198,356
:VDU25,101,1098;975;:GCOL0,0:MOVE198,356:DRAW198,975:DRAW1098,975:DRAW1098,356:D
RAW198,356:MOVE216,373:DRAW216,959:DRAW1082,959:DRAW1082,372:DRAW216,372
 1930MOVE216,767:DRAW1082,767:MOVE216,719:DRAW1082,719:MOVE648,959:DRAW648,767:M
OVE648,863:DRAW1082,863:FORT=1TO2:MOVE216+T*288,767:DRAW216+T*288,372:NEXT:FORT=
0TO3:MOVE700+T*96,959:DRAW700+T*96,767:NEXT
 1940A$(0)="Sample :":A$(1)="Source :":A$(2)="Date    :":A$(3)="2"+CHR$232+CHR$16
0+"/min:":A$(4)="Lambda :":GCOL0,0:VDU5:FORT%=0TO4:MOVE224,939-T%*32:PRINT;A$(T%
):NEXT:MOVE666,927:PRINT"I":MOVE666,831:PRINT"d"
 1950FORT%=0TO2:MOVE248+T%*288,752:PRINT" d"CHR$240CHR$241:MOVE398+T%*288,752:PR
INT"I/I"CHR$242CHR$243:NEXT:VDU4:FORT%=0TO2:MOVE360+T%*288,719:DRAW360+T%*288,37
2:NEXT
 1960 FORT=0TO2:MOVE360+T*288,719:DRAW360+T*288,372:NEXT
 1970ENDPROC
 1980DEFPROCdisplay_data
 1990 REM DISPLAYS EXPERIMENTAL RESULTS ON INDEX CARD
 2000VDU23,1;0;0;0;0;:COLOUR0:COLOUR129:IF Peak%<4 THEN Top4=Peak% ELSE Top4=4
 2010FORT=1TOTop4:VDU5:@%=&9A03:MOVE644-INT(LOG(Int%(T)))*8+T*96,927:PRINT;Int%(
T):@%=&020204:MOVE620-INT(LOG(Dhkl(T)))*8+T*96,831:PRINT;Dhkl(T):NEXT:VDU4
 2020Bubble%=1:REPEAT:swap%=0:FORT%=1TO(30-Bubble%):IF Dhkl(T%)<Dhkl(T%+1) THEN
PROCswapII:swap%=swap%+1
 2030NEXT:Bubble%=Bubble%+1:UNTIL swap%=0
 2040Y=0:Z=0:FORT%=1TOPeak%:Z=Z+1:IF T%=11 THEN Y=1:Z=1
 2050IF T%=21 THEN Y=2:Z=1
 2060@%=&020306:PRINTTAB(15+Y*18,9+Z),Dhkl(T%):@%=&9A03:PRINTTAB(25+Y*18,9+Z),In
t%(T%):NEXT
 2070ENDPROC
 2080DEFPROCdisc_poker
 2090 REM WRITES DATA TO DISC
 2100VDU28,5,29,75,24:COLOUR1:COLOUR128:CLS:PRINTTAB(29,2)"SAVING RECORD!":REPEA
T:swap%=0:FORT%=1TO29:IF Int%(T%)<Int%(T%+1) THEN PROCswapII:swap%=swap%+1
 2110NEXT:UNTIL swap%=0
 2120PRINT#X,Title$,Source$,Date$,Rate,Lambda,Peak%:FORT%=1TO30:PRINT#X,Int%(T%)
,Dhkl(T%):NEXT:PTR#X=17:PRINT#X,Entries%:CLOSE#X
 2130ENDPROC
 2140DEFPROCinput_details
 2150PROCnewdat2(Title$,0,0,0,16):PROCnewdat2("",3,Rate,&020204,4):PROCnewdat2("
",4,Lambda,&020406,6)
 2160VDU23,1,1;0;0;0;:COLOUR1:COLOUR128:VDU28,5,29,75,24:*FX21,0
 2170CLS:PRINTTAB(0,2)"Sample source :";:INPUT""Source$
 2180IF Source$="" THEN2170
 2190IF LEN(Source$)>3 THEN Source$=LEFT$(Source$,3) ELSE Source$=Source$+STRING
$(3-LEN(Source$)," ")
 2200PROCnewdat2(Source$,1,0,0,3)
 2210CLS:PRINTTAB(0,2)"Date           :";:INPUT""Date$
 2220IFDate$="" THEN2210
 2230PROCnewdat2(Date$,2,0,0,8)
 2240ENDPROC
 2250DEFPROChard_copyII
```

```
 2260 REM HARD COPY OF EXPERIMENTAL DATA
 2270*FX21,0
 2280IFPeak%=0 THEN PROCdeny:ENDPROC
 2290PROCon_line("printer")
 2300VDU2:VDU21:PRINTSTRING$(51,"="):PRINT"¦ POWDER DIFFRACTOMETER DATA       MSU
/RGIT/NSS/88 ¦":PRINTSTRING$(51,"="):PRINT"¦ Sample name:";Title$;SPC(36-LEN(Tit
le$));"¦":PRINT"¦ Date        :";MID$(TIME$,5,11);SPC(25);"¦"
 2310@%=&020204:PRINT"¦ deg/min    :";Rate;SPC(32);"¦":@%=&020406:PRINT"¦ Lambda
    :";Lambda;SPC(30);"¦":PRINTSTRING$(51,"="):PRINT"¦ Intensity              D
hkl              2-Theta ¦":PRINTSTRING$(51,"=")
 2320FORT%=1TOPeak%:PRINT"¦     ";:@%=&903:PRINTInt%(T%);:@%=&020306:PRINTSPC(15)
Dhkl(T%);:@%=&020205:PRINTSPC(14)2*DEG(ASN(Lambda/(2*Dhkl(T%))));"  ¦":NEXT:PRIN
TSTRING$(51,"="):VDU6:VDU3
 2330ENDPROC
 2340DEFPROCdeny
 2350SOUND1,-12,40,2:SOUND2,-12,47,2:TIME=0:REPEATUNTILTIME>25
 2360ENDPROC
 2370DEFPROCcompare_print
 2380 REM HARD COPY OF COMPARISON
 2390PROCon_line("printer")
 2400 Rows%=Peak%:FORT%=1TOTop3%:IF Match_stat%(T%,2)>Rows% THEN Rows%=Match_sta
t%(T%,2)
 2410 NEXT
 2420VDU2:VDU21
 2430PRINTSTRING$(20+Top3%*19,"=")
 2440PRINT"¦ COMPARISON WITH "Disc$;SPC((20+Top3%*19)-33);"¦":PRINTSTRING$(20+To
p3%*19,"-")
 2450PRINT"¦     TEST DATA      ¦";
 2460FORT%=1TOTop3%:Y%=17:REPEAT:Y%=Y%-1:UNTIL MID$(Name$(T%),Y%,1)<>" ":PRINTSP
C((18-Y%)/2):LEFT$(Name$(T%),Y%);SPC(INT(((18-Y%)/2)+0.5));"¦";:NEXT:PRINT""
 2470PRINTSTRING$(20+Top3%*19,"-")
 2480FORT%=1TORows%:@%=&9003:PRINT"¦   ";:IF Int%(T%)=-2 THEN PRINTSPC(14);"  ¦
"; ELSE PRINTInt%(T%);SPC(5);:@%=&020306:PRINTDhkl(T%);"  ¦  ";
 2490FORV%=1TOTop3%:@%=&9003:IF Resultd(V%,T%)=0 THEN PRINTSPC(14);"  ¦  "; ELSE
 PRINTResultI%(V%,T%);SPC(5);:@%=&020306:PRINTResultd(V%,T%);:IF Lib_match%(V%,T
%)=1 THEN PRINT"* ¦  "; ELSE PRINT"  ¦  ";
 2500NEXT:PRINT"":NEXT:PRINTSTRING$(20+Top3%*19,"-")
 2510PRINT"¦ MATCHED PEAKS (*) ¦";:@%=&9002:FORT%=1TOTop3%:PRINTSPC(9)Match_stat%
(T%,1);SPC(8);"¦";:NEXT:PRINT"":PRINTSTRING$(20+Top3%*19,"=")
 2520VDU6:VDU3
 2530ENDPROC
 2540DEFPROCon_line(A$)
 2550OSCLI"FX21,0":CLS:PRINTTAB(16,0)"Place the ";A$;" ON LINE & hit RETURN":REP
EAT:G=GET:UNTILG=13
 2560ENDPROC
 2570DEFPROCplotmate
 2580 REM PLOTMATE DRIVER
 2590OSCLI"FX21.0"
 2600PROCcommand_window:PROCedit:VDU28,0,31,79,0:GCOL0,1:CLS
 2610PROCon_line("plotter")
 2620Xinc%(1)=1:Xinc%(2)=5:Xinc%(3)=10:Xinc%(4)=20
 2630IF Sheet%=3 Xdim%=3400:Ydim%=2400 ELSE Xdim%=2300:Ydim%=1550
 2640T%=0:REPEAT:T%=T%+1:Xdiv=((HiS%-LoS%)/Xinc%(T%)):UNTIL Xdiv<16
 2650IF INT(Xdiv)<Xdiv THEN Xdiv=INT(Xdiv+1)
 2660step_size%=Xinc%(T%)
 2670Xdeg=Xdim%/(HiS%-LoS%):Inc=Xdeg/96:@%=&903
 2680IF Super$="ON" THEN 2720
 2690OSCLI"FX21,0":CLS:PRINTTAB(10,1)"Select the desired pen for the AXIS & hit
RETURN":REPEAT:G=GET:UNTILG=13
 2700VDU21:OSCLI("PLOT")
```

```
 2710MOVE0,Ydim%+150:DRAW0,Ydim%+250:DRAW Xdim%+400,Ydim%+250:DRAW Xdim%+400,Ydi
m%+150:DRAW0,Ydim%+150:DRAW0,0:DRAW Xdim%+400,0:DRAW Xdim%+400,Ydim%+150
 2720IF LoS%>=Start% THEN LT%=LoS%:Xpos=200
 2730IF LoS%<Start% THEN LT%=Start%:Xpos=200+(Start%-LoS%)*Xdeg
 2740IF HiS%>=Finish% THEN HT%=Finish%
 2750IF HiS%<Finish% THEN HT%=HiS%
 2760IF LoS%>=Start% THEN Xpos=200 ELSE Xpos=200+(Start%-LoS%)*96*Inc
 2770Scale=zoom*(Ydim%-200)/Max%
 2780IF Backsub$="OFF" THEN Min%=0:GOTO2840 ELSE Min%=65535
 2790FORT%=LT% TO HT%-1:mem=&8000+(T%-Start%)*192
 2800PROCdata_load
 2810?&70=0:?&71=&7A:?&72=Min% MOD 256:?&73=Min% DIV 256:?&76=&C0:?&77=&7A:CALL
&DD70:Min%=?&72+256*?&73
 2820NEXT
 2830IF Super$="ON" THEN 2920
 2840MOVE Xdim%+200,Ydim%:DRAW Xdim%+200,200:DRAW200,200:DRAW200,Ydim%:DRAW Xdim
%+200,Ydim%
 2850VDU5:@%=&90A:FORX%=0TO Xdiv*step_size%:Xval=LoS%+X%:IF Xval>HiS% THEN 2870
 2860 IF ((Xval-LoS%) MOD step_size%)=0 THEN PROClabel(200,20,30,200,16) ELSE PR
OCmark(200,11,200)
 2870 NEXT:MOVE Xdim%+220,240:PRINT"2"CHR$157CHR$211
 2880PROCvert_scale
 2890MOVE50,Ydim%+240:PRINT"Title :";Title$:MOVE950,Ydim%+250:DRAW950,Ydim%+150:
MOVE1000,Ydim%+240:@%=&020406:PRINT"L=";Lambda:MOVE1375,Ydim%+250:DRAW1375,Ydim%
+150:MOVE1425,Ydim%+240:@%=&020204:PRINT"Rate=";Rate;" deg/min"
 2900MOVE2065,Ydim%+250:DRAW2065,Ydim%+150:MOVE2115,Ydim%+240:PRINTMID$(TIME$,5,
11):MOVE Xdim%+200,Ydim%+250:DRAWXdim%+200,Ydim%+150
 2910VDU4:VDU1,16:OSCLI("PLOTOFF"):OSCLI("FX21,0")
 2920VDU6:CLS:PRINTTAB(10,1)"Select the desired pen for the TRACE & hit RETURN":
REPEAT:G=GET:UNTILG=13
 2930VDU21:OSCLI("PLOT")
 2940FORT%=LT% TO HT%-1:mem=&8000+(T%-Start%)*192
 2950PROCdata_load
 2960IF T%<>LT% THEN 2990
 2970DD=200+Scale*(?&7A00*256+?&7A01-Min%):IF DD>Ydim% THEN DD=Ydim%
 2980MOVE Xpos,DD
 2990FORV%=1TO192 STEP2:DD=200+Scale*(?(&79FF+V%)*256+?(&7A00+V%)-Min%):IF DD>Yd
im% THEN DD=Ydim%
 3000DRAW Xpos,DD:Xpos=Xpos+Inc:NEXT
 3010NEXT
 3020VDU1,6:VDU1,16:OSCLI("PLOTOFF")
 3030VDU6
 3040ENDPROC
 3050DEFPROClabel(A,B,C,D,E)
 3060 REM AXIS LABELLING FOR TRACE PLOTS
 3070 IF Xval<10 THEN Xp=D-E ELSE Xp=D-(INT(LOG(Xval)+1))*E
 3080 MOVE D+Xdeg*X%,A:DRAW D+Xdeg*X%,A-B:MOVEXp+Xdeg*X%,A-C:PRINT;Xval;
 3090 ENDPROC
 3100 DEFPROCmark(A,B,C)
 3110 REM DIVISON MARKERS
 3120 MOVE C+Xdeg*X%,A:DRAW C+Xdeg*X%,A-B
 3130 ENDPROC
 3140DEFPROCerror(A,B)
 3150SOUND1,-12,40,2:SOUND2,-12,47,2:PRINTTAB(13,A)SPC(LEN(STR$(B)))
 3160ENDPROC
 3170DEFPROCcommand_window
 3180 REM PLOTMATE PLOT FILE
 3190PROCwindow(406,866,906,432)
 3200MOVE424,786:DRAW890,786:MOVE430,794:DRAW430,842:DRAW884,842:DRAW884,794:DRA
W430,794:VDU5:MOVE489,830:PRINT"PLOTMATE COMMAND FILE"
```

```
 3210A$(0)="Title  :":A$(1)="Start  :":A$(2)="Finish :":A$(3)="Scale  :":A$(4)="
Smoothing       :":A$(5)="Background sub. :":A$(6)="Superimpose     :":A$(7)="Pa
per size      : A"
 3220FORT%=0TO7:MOVE440,770-T%*40:PRINTA$(T%):NEXT
 3230@%=&020105
 3240MOVE584,770:PRINT;Title$
 3250MOVE584,730:PRINT;LoS%
 3260MOVE584,690:PRINT;HiS%
 3270@%=&020204
 3280MOVE584,650:PRINT;zoom
 3290MOVE728,610:IF Son%=1 THEN PRINT;"ON" ELSE PRINT;"OFF"
 3300MOVE728,570:PRINT;Backsub$
 3310MOVE728,530:PRINT;Super$
 3320@%=&90A
 3330MOVE744,490:PRINT;Sheet%
 3340VDU4
 3350ENDPROC
 3360DEFPROCedit
 3370 REM PLOTMATE PLOT FILE EDITOR
 3380CLS:PRINTTAB(13,1)"Do you want to EDIT the command file?,<Y/N>";:REPEAT:G=G
ET:UNTILG=89 OR G=78:IF G=78 THEN ENDPROC
 3390 T%=0:PROCupdown
 3400 ENDPROC
 3410 DEFPROCupdown
 3420 PROCon
 3430 CLS:PRINTTAB(11,1)"Use ";:COLOUR0:COLOUR129:PRINTCHR$139;:COLOUR1:COLOUR12
8:PRINT",";:COLOUR0:COLOUR129:PRINTCHR$138;:COLOUR1:COLOUR128:PRINT" & ";:COLOUR
0:COLOUR129:PRINT"RETURN";
 3440 COLOUR1:COLOUR128:PRINT" to select.Press ";:COLOUR0:COLOUR129:PRINT"SPACE"
;:COLOUR1:COLOUR128:PRINT" to finish."
 3450 IFINKEY-58 AND T%>0:PROCoff:T%=T%-1:PROCon:PROCfinger_off(58)
 3460 IFINKEY-42 AND T%<7:PROCoff:T%=T%+1:PROCon:PROCfinger_off(42)
 3470 IFINKEY-74:PROCfinger_off(74):PROCchange:GOTO3430
 3480 IFINKEY-99:PROCfinger_off(99):PROCoff:ENDPROC ELSE 3450
 3490 ENDPROC
 3500 DEFPROCon
 3510 REM HIGHLIGHTS A STRING
 3520 VDU5:GCOL0,0:MOVE440,770-T%*40:PRINTSTRING$(LEN(A$(T%)),CHR$255)
 3530 GCOL0,1:MOVE440,770-T%*40:PRINTA$(T%):VDU4
 3540 ENDPROC
 3550 DEFPROCoff
 3560 REM REMOVES HIGHLIGHT
 3570 VDU5:GCOL0,1:MOVE440,770-T%*40:PRINTSTRING$(LEN(A$(T%)),CHR$255)
 3580 GCOL0,0:MOVE440,770-T%*40:PRINTA$(T%):VDU4
 3590 ENDPROC
 3600 DEFPROCchange
 3610 REM INPUT NEW PARAMETER VALUE
 3620 CLS:ON T%+1 GOTO 3630,3670,3690,3710,3730,3740,3760,3780
 3630PRINTTAB(0,2)"Input Title :";:INPUT""Title$
 3640IF Title$=""THEN 3620
 3650IF LEN(Title$)>16 THEN Title$=LEFT$(Title$,16) ELSE Title$=Title$+STRING$(1
6-LEN(Title$)," ")
 3660PROCnewdat(Title$,584,0,0,16):GOTO3800
 3670PRINTTAB(0,2)"Input Start :";:INPUT""LoS%
 3680IFLoS%<0 OR LoS%>Finish% OR LoS%>HiS% THEN 3620 ELSE PROCnewdat("",584,LoS%
,&020105,5):GOTO3800
 3690PRINTTAB(0,2)"Input Finish :";:INPUT""HiS%
 3700IF HiS%>180 OR HiS%<=LoS% THEN 3620 ELSE PROCnewdat("",584,HiS%,&020105,5):
GOTO3800
```

```
 3710PRINTTAB(0,2)"Input Scaling Factor :";:INPUT""zoom
 3720IF zoom<=0 OR zoom>5 THEN 3620 ELSE PROCnewdat("",584,zoom,&020205,5):GOTO3
800
 3730IF Son%=1 THEN PROCnewdat("OFF",728,0,0,3):Son%=0:GOTO3800 ELSE PROCnewdat(
"ON",728,0,0,3):Son%=1:GOTO3800
 3740 IF Backsub$="OFF" THEN Backsub$="ON" ELSE Backsub$="OFF"
 3750 PROCnewdat(Backsub$,728,0,0,3):GOTO3800
 3760 IF Super$="OFF" THEN Super$="ON" ELSE Super$="OFF"
 3770 PROCnewdat(Super$,728,0,0,3):GOTO3800
 3780 IF Sheet%=4 THEN Sheet%=3 ELSE Sheet%=4
 3790 PROCnewdat("",744,Sheet%,&901,1)
 3800PROCfinger_off(74)
 3810ENDPROC
 3820 DEFPROCnewdat(A$,A,B,C,L)
 3830 REM PRINT NEW VALUE
 3840 VDU5:GCOL0,1:MOVEA,770-T%*40:PRINT;STRING$(L,CHR$255)
 3850 GCOL0,0:MOVEA,770-T%*40: IF A$="" THEN @%=C:PRINT;B ELSE PRINT;A$
 3860 VDU4
 3870 ENDPROC
 3880DEFPROCwindow(ux,uy,lx,ly)
 3890 REM PULL DOWN WINDOW
 3900GCOL0,0:MOVEux-16,uy-16:VDU25,101,lx-16;ly-16;
 3910GCOL0,1:MOVEux,uy:VDU25,101,lx;ly;
 3920GCOL0,0:MOVEux,uy:DRAWlx,uy:DRAWlx,ly:DRAWux,ly:DRAWux,uy
 3930MOVEux+16,uy-16:DRAWlx-16,uy-16:DRAWlx-16,ly+16:DRAWux+16,ly+16:DRAWux+16,u
y-16
 3940ENDPROC
 3950DEFPROCfinger_off(A)
 3960REPEATUNTILNOTINKEY(-A):OSCLI"FX21,0"
 3970ENDPROC
 3980 DEFPROCnewdat2(A$,A,B,C,L)
 3990VDU5:GCOL0,1:MOVE352,939-A*32:PRINT;STRING$(L,CHR$255)
 4000GCOL0,0:MOVE352,939-A*32: IF A$="" THEN @%=C:PRINT;B ELSE PRINT;A$
 4010VDU4
 4020ENDPROC
 4030DEFPROCdata_load
 4040 REM TRANSFERS DATA TO &7A00 DEGREE BY DEGREE
 4050IF mem=&8000 THEN OSCLI"SRREAD 7A00 7AC8 8000 4":LO=&7A00:HI=&7ABA
 4060IF mem>&8000 AND mem<&BB40 THEN OSCLI"SRREAD 79FA 7AC8 "+STR$~(mem-6)+" 4":
LO=&79FA:HI=&7ABA
 4070IF mem=&BB40 THEN OSCLI"SRREAD 79FA 7AC0 BB3A 4":OSCLI"SRREAD 7AC0 7AC8 800
0 5":LO=&79FA:HI=&7ABA
 4080IF mem=&BC00 THEN OSCLI"SRREAD 79FA 7A00 BBFA 4":OSCLI"SRREAD 7A00 7AC8 800
0 5":LO=&79FA:HI=&7ABA
 4090IF mem>&BC00 AND mem<(&8000+(Finish%-Start%)*192) THEN OSCLI"SRREAD 79FA 7A
C8 "+STR$~(mem-&3C06)+" 5":LO=&79FA:HI=&7ABA
 4100IF mem=(&8000-(Finish%-Start%)*192) THEN OSCLI"SRREAD 79FA 7AC0 "+STR$~(mem
-&3C06)+" 5":LO=&79FA:HI=&7AB2
 4110IF Son% THEN ?&73=LO MOD 256:?&74=LO DIV 256:?&75=HI MOD 256:?&76=HI DIV 25
6:CALL &DD00
 4120ENDPROC
 4130DEFPROCvert_scale
 4140 REM VERTICAL SCALE USED FOR PLOTMATE
 4150low%=100*Min%/Max%:high%=low%+100/zoom:diff%=high%-low%
 4160 A$="20100504030201"
 4170 T%=-1:REPEAT
 4180 T%=T%+2:step%=VAL(MID$(A$,T%,2))
 4190 UNTIL (diff%/step%)>=5 OR T%=13
 4200 @%=&903:FORT%=0TO(INT(diff%/step%)):Step=T%*(Ydim%-200)*step%/diff%:IF Ste
p>(Ydim%-200) OR (low%+T%*step%)>100 THEN 4220
```

```
4210 MOVE200,200+Step:DRAW190,200+Step:MOVE65,240+Step:PRINT,low%+T%*step%
4220 NEXT
4230 ENDPROC
```

```
   10 REM ************************************************************
   20 REM * DBASE is a simple menu driver to load and execute VIEW, INPUT *
   30 REM * and UPDATE. Program flow returns to DBASE after exiting from  *
   40 REM * either program.                                              *
   50 REM *                                                 Neil S Stewart,RGIT *
   60 REM ************************************************************
   70 REM
   80 VDU26
   90DIM A$(5):A$(1)="<1>...VIEW RECORD":A$(2)="<2>..INPUT RECORD":A$(3)="<3>.UP
DATE RECORD":A$(4)="<4>.....EXIT":VDU23,1,0;0;0;0;
  100OSCLI("FX14,6"):OSCLI("FX21,0"):*KEY10 CH."CENPOD"|M
  110 VDU23,2,85,85,85,85,85,85,85,85:VDU19,1,6;0;
  120PROCwindow
  130PROCmenu:OSCLI("FX4,0")
  140END
  150DEFPROCmenu
  160VDU5:GCOL0,0:MOVE512,650:PRINT"D A T A  B A S E":FORT%=1TO5:MOVE504,590-(T%
-1)*64:PRINTA$(T%):NEXT:MOVE488,326:PRINT"S E L E C T  O N E":VDU4:COLOUR0:COLO
UR129:TIME=100
  170 IFTIME>=100 THEN PRINTTAB(28,24)TIME$:TIME=0
  180 IFINKEY(-49)PROChigh_light(1):CHAIN"VIEW"
  190 IFINKEY(-50)PROChigh_light(2):CHAIN"INPUT"
  200 IFINKEY(-18)PROChigh_light(3):CHAIN"UPDATE"
  210 IFINKEY(-19)PROChigh_light(4):CHAIN"CENPOD" ELSE 170
  220 OSCLI"FX15,0":COLOUR1:COLOUR128:CLS
  230DEFPROChigh_light(T%)
  240VDU5:GCOL0,0:MOVE488,590-(T%-1)*64:PRINTSTRING$(19,CHR$255):GCOL0,1:MOVE504
,590-(T%-1)*64:PRINTA$(T%):VDU4
  250ENDPROC
  260 DEFPROCwindow
  270 IF A%=1 THEN GCOL0,1:MOVE370,670:VDU25,101,920;360;:ENDPROC ELSE A%=1
  280VDU18,16,128:CLG:GCOL0,0:MOVE325,185:VDU25,101,925;830;:GCOL0,1:MOVE340,200
:VDU25,101,940;846;
  290 GCOL0,0:MOVE 356,216:DRAW 356,830:DRAW 924,830:DRAW924,216:DRAW356,216
  300 MOVE340,200:DRAW340,846:DRAW940,846:DRAW940,200:DRAW340,200
  310 MOVE 356,680:DRAW924,680:MOVE356,265:DRAW924,265
  320 MOVE362,688:DRAW362,822:DRAW916,822:DRAW916,688:DRAW362,688
  330 VDU5:MOVE536,810:PRINT"'C.E.N.P.O.D'"
  340 MOVE400,770:PRINT"Powder Diffractometer Routines"
  350 MOVE528,730:PRINT"by N.S.Stewart"
  360 VDU4
  370 ENDPROC
```

```
  10 REM ************************************************************
  20 REM * VIEW is the main database program. Its prime use is to let    *
  30 REM * users extract the diffraction parameters for a given material.*
  40 REM * The data can be presented in two ways. Initially the data is  *
  50 REM * printed in a format similar to the Powder index. In addition  *
  60 REM * the data can be used to re-generate a theoretical trace. Both *
  70 REM * formats can be printed out on a dot-matrix printer and the    *
  80 REM * Plotmate plotter.                                             *
  90 REM *                                              Neil S Stewart, RGIT *
 100 REM ************************************************************
 110 REM
 120 MODE128:DIM Int%(30),Dhkl(30),A$(7),Xaxis(2410),TT(50),sigma(50),deltaT(50
),Xinc%(4)
 130 Xinc%(1)=1:Xinc%(2)=5:Xinc%(3)=10
 140 REM BINARY PATTERNS FOR SPECIAL TEXT CHARACTERS.
 150 VDU23,240,0,0,0,132,133,230,165,164:VDU23,241,0,0,0,16,16,16,16,152
 160 VDU23,242,0,0,0,251,168,171,138,139:VDU23,243,0,0,0,162,148,136,148,162
 170 PROCview
 180 A%=0:CHAIN"DBASE"
 190 END
 200 :
 210 DEFPROCview
 220 PROCbox
 230 PROCroots("view/a"):CLS:PRINTTAB(23,0)"f0-View entire disc contents."
 240 PRINTTAB(23,2)"f1-View one specific record."
 250 PRINTTAB(23,4)"f2-Exit."
 260 IFINKEY-33 PROCselect(23,0,"f0-View entire disc contents."):PROCscroll:GOT
0230
 270 IFINKEY-114 PROCselect(23,2,"f1-View one specific record."):PROCspecific:G
OTO230
 280 IFINKEY-115 PROCselect(23,4,"f2-Exit.") ELSE 260
 290 ENDPROC
 300 DEFPROCspecific
 310 REM PROMPTS MICRO TO SEARCH DATABASE FOR ONE RECORD. CARE MUST BE TAKEN
 320 REM TO SPELL THE COMPOUND NAME AS IS STORED ON THE FILE.
 330*FX15,0
 340CLS:PRINTTAB(1,0)"Name of the sample to be viewed :";:INPUT""Name$
 350 IFName$=""THEN330
 360IF LEN(Name$)>16 THEN Name$=LEFT$(Name$,16) ELSE Name$=Name$+STRING$(16-LEN
(Name$)," ")
 370X=OPENUP":2.PDFILE":INPUT#X,Disc$,Entries%
 380PROCsearch:CLOSE#X:IF Success=0 THEN 460 ELSE GCOL16,1:MOVE20,1000:VDU25,10
1,1250;330;:PROCcard:PROCdisplay_details:PROCdisplay_data
 390PROCroots("view/a/b1"):CLS
 400 PRINTTAB(15,0)"f0-Print out data on dot-matrix printer."
 410 PRINTTAB(15,2)"f1-Generate diffraction trace from data."
 420 PRINTTAB(15,4)"f2-Exit."
 430 IFINKEY-33 PROCselect(15,0,"f0-Print out data on dot-matrix printer."):PRO
Chard_copy:GOTO390
 440 IFINKEY-114 PROCselect(15,2,"f1-Generate diffraction trace from data."):PR
OCcreate_trace:GOTO390
 450 IFINKEY-115 PROCselect(15,4,"f2-Exit."):GOTO470 ELSE 430
 460COLOUR1:COLOUR128:PRINTTAB(15,1)"NO SUCH COMPOUND IS STORED ON THIS DISC";T
AB(19,3)"Do you wish to try again?,<Y/N>":REPEAT:G=GET:UNTILG=89 OR G=78:IF G=89
 THEN 340
 470ENDPROC
 480DEFPROCcard
 490 REM POWDER INDEX STYLE CARD FOR DATA DISPLAY
 500VDU28,0,31,79,0:GCOL0,0:MOVE190,348:VDU25,101,1090;967;:GCOL0,1:MOVE198,356
```

```
:VDU25,101,1098;975;:GCOL0,0:MOVE198,356:DRAW198,975:DRAW1098,975:DRAW1098,356:D
RAW198,356:MOVE216,372:DRAW216,959:DRAW1082,959:DRAW1082,372:DRAW216,372
  510MOVE216,767:DRAW1082,767:MOVE216,719:DRAW1082,719:MOVE648,959:DRAW648,767:M
OVE648,863:DRAW1082,863:FORT%=1TO2:MOVE216+T%*288,767:DRAW216+T%*288,372:NEXT:FO
RT%=0TO3:MOVE700+T%*96,959:DRAW700+T%*96,767:NEXT
  520A$(0)="Sample :":A$(1)="Source :":A$(2)="Date    :":A$(3)="2"+CHR$232+CHR$16
0+"/min:":A$(4)="Lambda :":GCOL0,0:VDU5:FORT%=0TO4:MOVE224,939-T%*32:PRINT;A$(T%
):NEXT:MOVE666,927:PRINT"I":MOVE666,831:PRINT"d"
  530FORT%=0TO2:MOVE248+T%*288,752:PRINT" d"CHR$240CHR$241:MOVE398+T%*288,752:PR
INT"I/I"CHR$242CHR$243:NEXT:VDU4:FORT%=0TO2:MOVE360+T%*288,719:DRAW360+T%*288,37
2:NEXT
  540ENDPROC
  550DEFPROCdisplay_data
  560 REM PRINTS DATA ON THE CARD.
  570VDU23,1;0;0;0;0;:COLOUR0:COLOUR129:IF Pair%<4 THEN Top4=Pair% ELSE Top4=4
  580VDU5:FORT%=1TOTop4:@%=&9A03:MOVE644-INT(LOG(Int%(T%)))*8+T%*96,927:PRINT;In
t%(T%):@%=&020204:MOVE620-INT(LOG(Dhkl(T%)))*8+T%*96,831:PRINT;Dhkl(T%):NEXT:VDU
4
  590REPEAT:swap=0:FORT%=1TO29:IF Dhkl(T%)<Dhkl(T%+1) THEN PROCswapII:swap=swap+
1
  600NEXT:UNTILswap=0
  610FORP%=1TOPair%:PROCprint_data:NEXT
  620ENDPROC
  630DEFPROCdisplay_details
  640 REM SAMPLE PARAMETERS
  650VDU23,1;0;0;0;0;:VDU5:GCOL0,0:MOVE352,939:PRINT;Title$:MOVE352,907:PRINT;So
urce$:MOVE352,875:PRINT;Date$
  660MOVE352,843:IF Rate=0 THEN PRINT;"N/A":ELSE @%=&020204:PRINT,Rate
  670@%=&020406:MOVE352,811:PRINT,Lambda;" "CHR$129
  680ENDPROC
  690DEFPROCscroll
  700 REM PRINTS OUT ENTIRE DATABASE RECORDS TO EITHER SCREEN OR PRINTER
  710 GCOL16,1:MOVE20,980:VDU25,101,1250;330;
  720PROCroots("view/a/b0"):CLS:PRINTTAB(10,0)"f0-Scrolls the contents of the DA
TA-BASE on screen."
  730 PRINTTAB(10,2)"f1-Prints the contents of the DATA-BASE on printer."
  740 PRINTTAB(10,4)"f2-Exit."
  750IFINKEY-33 PROCselect(10,0,"f0-Scrolls the contents of the DATA-BASE on scr
een."):PROCscreen_display:GOTO720
  760IFINKEY-114 PROCselect(10,2,"f1-Prints the contents of the DATA-BASE on pri
nter."):PROCprinter_display:GOTO720
  770IFINKEY-115 REPEATUNTILNOTINKEY-115:PROCselect(10,4,"f2-Exit."):ENDPROC ELS
E 750
  780 ENDPROC
  790 DEFPROCscreen_display
  800 REM OUTPUT DETAILS TO SCREEN
  810CLS:PRINTTAB(15,1)"Press SHIFT to scroll or SPACE to finish."
  820VDU28,0,31,79,0:GCOL0,0:MOVE52,945:VDU25,101,1214;976;:GCOL0,1:MOVE66,359:V
DU25,101,1230;990;:@%=&90A:GCOL0,0:MOVE66,359:DRAW66,990:DRAW1230,990:DRAW1230,3
59:DRAW66,359
  830 MOVE82,372:DRAW82,974:DRAW1214,974:DRAW1214,372:DRAW82,372:MOVE82,916:DRAW
1214,916
  840COLOUR0:COLOUR129:PRINTTAB(7,2)"  COMPOUND NAME";SPC(8)"SOURCE";SPC(7)"deg/
min";SPC(9)"DATE";SPC(5)"PEAKS  ":VDU28,6,19,74,4
  850X=OPENUP":2.PDFILE":INPUT#X,Disc$,Entries%
  860V=0
  870T%=0:REPEAT:T%=T%+1
  880INPUT#X,Title$,Source$,Date$,Rate,Lambda,Pair%
  890PRINT"  ";Title$;SPC(6+(17-LEN(Title$)));Source$;SPC(10+(3-LEN(Source$)));
  900IF Rate=0 THEN PRINT" N/A";SPC(9);:ELSE @%=&020305:PRINT;Rate;SPC(8);
```

```
  910PRINTDate$;SPC(5+(8-LEN(Date$)));:@%=&902:PRINT,Pair%
  920PTR#X=PTR#X+330:UNTIL T%=15 OR (T%+V*15)=Entries%
  930IF (T%+V*15)=Entries% THEN CLOSE#X:VDU28,5,29,75,24:ENDPROC
  940V=V+1
  950 IFINKEY-1 THEN870
  960 IFINKEY-99 THEN CLOSE#X:VDU28,5,29,75,24:ENDPROC ELSE 950
  970 ENDPROC
  980 DEFPROCprinter_display
  990 REM PRINTS OUTPUT TO THE PRINTER.
 1000PROCon_line("printer"):X=OPENUP":2.PDFILE":INPUT#X,Disc$,Entries%:VDU2:VDU2
1:PRINT:PRINT" DISC TITLE :";Disc$
 1010PRINT" COMPOUND NAME";SPC(8)"SOURCE";SPC(7)"deg/min";SPC(9)"DATE";SPC(6)"PE
AKS":PRINTSTRING$(66,"-")
 1020FORT%=1TOEntries%:INPUT#X,Title$,Source$,Date$,Rate,Lambda,Pair%:PRINTTitle
$;SPC(6+(17-LEN(Title$)));Source$;SPC(10+(3-LEN(Source$)));
 1030IF Rate=0 THEN PRINT" N/A";SPC(9);:ELSE @%=&020305:PRINT;Rate;SPC(8);
 1040PRINTDate$;SPC(5+(8-LEN(Date$)));:@%=&902:PRINT,Pair%
 1050PTR#X=PTR#X+330:NEXT:PRINTSTRING$(66,"-")
 1060CLOSE#X:VDU6:VDU3
 1070ENDPROC
 1080DEFPROCbox
 1090 REM TEXT WINDOW
 1100VDU23,2,85,85,85,85,85,85,85,85:VDU18,16,129:VDU19,1,6;0;:VDU28,0,31,79,0:C
LG
 1110GCOL0,1:MOVE0,0:DRAW0,1023:DRAW1279,1023:DRAW1279,0:DRAW0,0:MOVE50,34:VDU25
,101,1230;327;:GCOL0,0:MOVE66,51:VDU25,101,1214;311;:MOVE50,34:DRAW50,327:DRAW12
30,327:DRAW1230,34:DRAW50,34
 1120ENDPROC
 1130DEFPROCroots(A$)
 1140 REM PRINTSINSTRUCTION WINDOW LABEL. INDICATES POSITION IN MENU SYSTEM.
 1150VDU28,0,31,79,0:COLOUR0:COLOUR129:PRINTTAB(4,22)STRING$(10," ");TAB(4,22)A$
:VDU28,5,29,75,24:COLOUR1:COLOUR128
 1160ENDPROC
 1170DEFPROCsearch
 1180 REM COMPARES REQUESTED SAMPLE NAME WITH DATA BASE. IF SUCCESSFUL, THE
 1190 REM REMAINDER OF THE DATA IS TAKEN FROM THE DISC.
 1200Success=0:CLS:PRINTTAB(30,1)"SEARCHING!"
 1210T%=0:REPEAT:T%=T%+1
 1220INPUT#X,Title$
 1230IF Title$=Name$ THEN Success=1:Pointer%=PTR#X-18:GOTO1260
 1240PTR#X=PTR#X+362:UNTIL T%=Entries%
 1250GOTO1280
 1260INPUT#X,Source$,Date$,Rate,Lambda,Pair%
 1270FOR T%=1TO30:INPUT#X,Int%(T%),Dhkl(T%):NEXT
 1280ENDPROC
 1290DEFPROCswapII
 1300 REM BUBBLE SORT ROUTINE FOR ORDERING DIFFRACTION DATA.
 1310Q=Int%(T%):Int%(T%)=Int%(T%+1):Int%(T%+1)=Q:Q=Dhkl(T%):Dhkl(T%)=Dhkl(T%+1):
Dhkl(T%+1)=Q
 1320ENDPROC
 1330DEFPROChard_copy
 1340 REM DOT-MATRIX DRIVER FOR INDIVIDUAL RECORD HARDCOPY.
 1350PROCon_line("printer"):VDU2:VDU21:PRINTSTRING$(41,"=")
 1360REPEAT:swap=0:FORT%=1TO29:IF Int%(T%)<Int%(T%+1) THEN PROCswapII:swap=swap+
1
 1370NEXT:UNTILswap=0
 1380PRINT"¦ ";A$(0);Title$;SPC(14);"¦":PRINT"¦ ";A$(1);Source$;SPC(27);"¦":PRIN
T"¦ ";A$(2);Date$;SPC(22);"¦":PRINT;"¦ deg/min:";
 1390IF Rate=0 THEN PRINT"N/A";SPC(27);"¦":ELSE @%=&020204:PRINTRate;SPC(26);"¦"
 1400@%=&020406:PRINT"¦ ";A$(4);Lambda;SPC(24);"¦":PRINTSTRING$(41,"=")
```

```
 1410@%=&90006:PRINT"¦  I  ¦ ";:FORT%=1TO4:IFInt%(T%)=-2 THEN PRINTSPC(7);"¦";:ELS
E PRINTInt%(T%);" ¦ ";
 1420NEXT:PRINT"":PRINTSTRING$(41,"-")
 1430@%=&020306:PRINT"¦ d  ¦ ";:FORT%=1TO4:IFDhkl(T%)=0 THEN PRINTSPC(7);"¦";:ELS
E PRINTDhkl(T%);" ¦ ";
 1440NEXT:PRINT"":PRINTSTRING$(41,"="):PRINTSTRING$(2,"¦   dhkl     I/Imax  ");"¦
":PRINTSTRING$(41,"-")
 1450REPEAT:swap=0:FORT%=1TO29:IF Dhkl(T%)<Dhkl(T%+1) THEN PROCswapII:swap=swap+
1
 1460NEXT:UNTILswap=0
 1470FORT%=1TO15:IF Int%(T%)=-2 THEN 1510
 1480PRINT"¦   ";:@%=&020306:PRINTDhkl(T%);:@%=&90007:PRINTInt%(T%);SPC(4);
 1490IF Int%(T%+15)=-2 THEN PRINT"¦";SPC(19);"¦" ELSE PRINT"¦   ";:@%=&020306:PRI
NTDhkl(T%+15);:@%=&90007:PRINTInt%(T%+15);SPC(4);"¦"
 1500NEXT
 1510PRINTSTRING$(41,"="):VDU6:VDU3
 1520ENDPROC
 1530DEFPROCselect(Xcoord%,Ycoord%,Phrase$)
 1540COLOUR0:COLOUR129:PRINTTAB(Xcoord%,Ycoord%)Phrase$
 1550Now%=TIME:REPEATUNTIL(TIME-Now%)>25:COLOUR1:COLOUR128
 1560ENDPROC
 1570DEFPROCon_line(A$)
 1580CLS:PRINTTAB(16,0)"Place the ";A$;" ON LINE & hit RETURN":REPEAT:G=GET:UNTI
LG=13
 1590ENDPROC
 1600 DEFPROCcreate_trace
 1610 REM GENERATES A ROUGH DIFFRACTION TRACE FROM THE DATA STORED ON DISC.
 1620 CLS:PRINTTAB(20,2)"PLEASE WAIT : GENERATING TRACE":PROCinput:PROCcalculate
:PROCplot
 1630 CLS:PRINTTAB(13,2)"Do you want a hard copy of the trace?,<Y/N>";:REPEAT:G=
GET:UNTILG=89 OR G=78:IF G=89 THEN PROCplotmate
 1640 ENDPROC
 1650 DEFPROCinput
 1660 LoT%=180:HiT%=0
 1670 FOR T%=1TO Pair%
 1680 TT(T%)=2*DEG(ASN(1.5418/(2*Dhkl(T%))))
 1690 IF TT(T%)>HiT% THEN HiT%=TT(T%)
 1700 IF TT(T%)<LoT% THEN LoT%=TT(T%)
 1710 NEXT
 1720 LoT%=(LoT% DIV 5)*5
 1730 HiT%=(HiT% DIV 5)*5+5
 1740 LoS%=LoT%:HiS%=HiT%
 1750 step=(HiT%-LoT%)/2400
 1760 ENDPROC
 1770 DEFPROCcalculate
 1780 FOR T%=1TO Pair%
 1790 deltaD=Dhkl(T%)/100
 1800 sigma(T%)=TT(T%)/100
 1810 deltaT(T%)=ABS(LN(0.05)*sigma(T%))
 1820 NEXT
 1830 FOR T%=1TO Pair%
 1840 M%=(TT(T%)-LoT%)/step
 1850 A%=M%-deltaT(T%)/step:B%=M%+deltaT(T%)/step
 1860 IF B%<1 OR A%>2400 THEN 1920
 1870 IF A%<1 THEN A%=1
 1880 IF B%>2400 THEN B%=2400
 1890 FOR V%=A% TO B%
 1900 Xaxis(V%)=Xaxis(V%)+Int%(T%)*EXP(-((((V%-M%)*step)/sigma(T%))^2))
 1910 NEXT
 1920 NEXT
```

```
 1930 Max%=0:FORT%=1TO (HiT%-LoT%)/step:IF Xaxis(T%)>Max% THEN Max%=Xaxis(T%)
 1940 NEXT
 1950 ENDPROC
 1960 DEFPROCplot
 1970 REM PLOTS THE THEORETICAL TRACE ON THE SCREEN.
 1980 GCOL0,0:MOVE50,350:VDU25,101,1214;964;:GCOL0,1:MOVE66,356:VDU25,101,1230;9
80;
 1990 GCOL0,0:MOVE66,356:DRAW66,980:DRAW1230,980:DRAW1230,356:DRAW66,356:MOVE82,
372:DRAW82,964:DRAW1214,964:DRAW1214,372:DRAW82,372:MOVE180,420:DRAW180,900:DRAW
1165,900:DRAW1165,420:DRAW180,420:MOVE82,920:DRAW1214,920
 2000 VDU5:MOVE100,958:PRINT"Title : ";Title$:MOVE484,964:DRAW484,920:MOVE500,95
8:PRINTCHR$235" = ";Lambda;" "CHR$129:MOVE926,964:DRAW926,920:MOVE942,958:PRINT"
THEORETICAL PLOT":MOVE1168,436:PRINT"2"CHR$232CHR$160
 2010 A$="Intensity":FORT%=1TOLEN(A$):MOVE98,890-T%*44:PRINT;MID$(A$,T%,1):NEXT:
VDU4
 2020 PROCstep_calc(HiT%,LoT%)
 2030Xdeg=985/(Xdiv*step_size%):Inc=Xdeg*step
 2040 @%=&90A:VDU5:FORX%=0 TO Xdiv*step_size%:Xval=LoT%+X%
 2050 IF ((Xval-LoT%) MOD step_size%)=0 THEN PROClabel(420,12,16,180,8) ELSE PRO
Cmark(420,4,180)
 2060 NEXT
 2070 Ystep=4.65:FORY%=0TO100 STEP10:Ypos=430+Y%*Ystep:Xpos=172-(INT(LOG(Y%+1))+
1)*16:MOVE180,Ypos:DRAW176,Ypos:MOVEXpos,Ypos+16:PRINT;Y%;:NEXT:VDU4
 2080 GCOL0,0:MOVE165,430+465*Xaxis.(1)/Max%:FOR T%=1TO (HiT%-LoT%)/step
 2090 DRAW180+(T%-1)*985/((Xdiv*step_size%)/step),430+465*Xaxis(T%)/Max%
 2100 NEXT
 2110 ENDPROC
 2120 DEFPROCinput_ansa
 2130 A$=""
 2140 G=GET:IF G=13 THEN ENDPROC
 2150 IF G<>127 THEN A$=A$+CHR$G:PRINTCHR$G; ELSE IF LEN(A$)<>0 THEN PRINTCHR$G;
:A$=LEFT$(A$,LEN(A$)-1)
 2160 GOTO2140
 2170 ENDPROC
 2180DEFPROCplotmate
 2190 REM DIRECTS THEORETICAL PLOT TO THE PLOTMATE. USER CAN SELECT RANGE OF
 2200 REM TRACE AND HOW IT IS PLOTTED.i.e. SUPERIMPOSED.
 2210*FX21,0
 2220PROCcommand_window:PROCedit:PROCstep_calc(HiS%,LoS%):VDU28,0,31,79,0:CLS:GC
OL0,1
 2230IF Sheet%=3 Xdim%=1000:Ydim%=800 ELSE Xdim%=800:Ydim%=600
 2240REM IF Sheet%=3 Xdim%=3400:Ydim%=2400 ELSE Xdim%=2300:Ydim%=1550
 2250Xdeg=Xdim%/(HiS%-LoS%):Inc=Xdeg*step:@%=&903
 2260IF Super$="ON" THEN2270
 2270REM CLS:PRINTTAB(10,1)"Select the desired pen for the AXIS & hit RETURN":RE
PEAT:G=GET:UNTILG=13
 2280REM VDU21:OSCLI("PLOT")
 2290MOVE0,Ydim%+150:DRAW0,Ydim%+250:DRAW Xdim%+400,Ydim%+250:DRAW Xdim%+400,Ydi
m%+150:DRAW0,Ydim%+150:DRAW0,0:DRAW Xdim%+400,0:DRAW Xdim%+400,Ydim%+150
 2300MOVE Xdim%+200,Ydim%:DRAW Xdim%+200,200:DRAW200,200:DRAW200,Ydim%:DRAW Xdim
%+200,Ydim%
 2310VDU5:FORX%=0TO Xdiv*step_size%:Xval=LoS%+X%
 2320 IF ((Xval-LoS%) MOD step_size%)=0 THEN PROClabel(200,20,30,200,16) ELSE PR
OCmark(200,11,200)
 2330 NEXT:MOVE Xdim%+220,240:PRINT"2"CHR$157CHR$211
 2340Ystep=(Ydim%-200)/100:FORY=0TO100 STEP 10:Ypos=200+Y*Ystep:Xpos=170-(INT(LO
G(Y+1))+1)*35:MOVE200,Ypos:DRAW190,Ypos:MOVEXpos,Ypos+40:PRINT;Y;:NEXT:MOVE175,Y
dim%+100:PRINT"I"
 2350MOVE50,Ydim%+240:PRINT"Title :":MOVE950,Ydim%+250:DRAW950,Ydim%+150:MOVE100
0,Ydim%+240:@%=&020406:PRINTCHR$140"=";" A";:MOVE1410,Ydim%+250:DRAW1410,Ydim%+1
```

```
50:MOVE1480,Ydim%+240:@%=&020204:PRINT"2"CHR$157"-Rate="
 2360PRINTCHR$211"/min";:MOVE2230,Ydim%+250:DRAW2230,Ydim%+150:MOVE2280,Ydim%+24
0:PRINTMID$(TIME$,5,11);:MOVE2700,Ydim%+250:DRAW2700,Ydim%+150:VDU4:VDU1,16:OSCL
I("PLOTOFF"):OSCLI("FX21,0")
 2370REM VDU6:CLS:PRINTTAB(10,1)"Select the desired pen for the TRACE & hit RETU
RN":REPEAT:G=GET:UNTILG=13
 2380REM VDU21:OSCLI("PLOT")
 2390IF LoS%<=LoT% THEN LT%=0:Xpos=200+(LoT%-LoS%)*Xdeg
 2400IF LoS%>LoT% THEN LT%=(LoS%-LoT%)/step:Xpos=200
 2410IF HiS%>=HiT% THEN HT%=2400
 2420IF HiS%<HiT% THEN HT%=2400-(HiT%-HiS%)/step
 2430Scale=(Ydim%-200)/Max%:MOVE Xpos,200+Scale*Xaxis(LT%):FORT%=LT% TO HT%:DRAW
Xpos,200+Scale*Xaxis(T%):Xpos=Xpos+Inc:NEXT
 2440VDU1,6:VDU1,16:OSCLI("PLOTOFF")
 2450VDU6
 2460ENDPROC
 2470 DEFPROClabel(A,B,C,D,E)
 2480 REM AXIS LABELLING ROUTINE.
 2490 IF Xval<10 THEN Xpos=D-E ELSE Xpos=D-(INT(LOG(Xval)+1))*E
 2500 MOVE D+Xdeg*X%,A:DRAW D+Xdeg*X%,A-B:MOVE Xpos+Xdeg*X%,A-C:PRINT;Xval;
 2510 ENDPROC
 2520 DEFPROCmark(A,B,C)
 2530 REM CREATES DIVISION MARKERS ON AXIS
 2540 MOVE C+Xdeg*X%,A:DRAW C+Xdeg*X%,A-B
 2550 ENDPROC
 2560DEFPROCerror(A,B)
 2570 REM MAKES NOISE WHEN USER ABUSES PROGRAM!?.
 2580SOUND1,-12,40,2:SOUND2,-12,47,2
 2590PROCwob:PRINTTAB(12,A)SPC(LEN(STR$(B))):PROCbow
 2600ENDPROC
 2610DEFPROCwob
 2620 REM CHANGES TEXT TO White On Black.
 2630COLOUR1:COLOUR128
 2640ENDPROC
 2650DEFPROCbow
 2660 REM CHANGES TEXT TO Black on White.
 2670COLOUR0:COLOUR129
 2680ENDPROC
 2690DEFPROCcommand_window
 2700 REM DISPLAYS PLOTTER PARAMETERS FOR EDITING.
 2710PROCwindow(406,866,906,548)
 2720MOVE424,786:DRAW890,786:MOVE430,794:DRAW430,842:DRAW884,842:DRAW884,794:DRA
W430,794:VDU5:MOVE489,830:PRINT"PLOTMATE COMMAND FILE"
 2730A$(0)="Title  :":A$(1)="Start  :":A$(2)="Finish :":A$(3)="Superimpose   :":
A$(4)="Paper size    : A":Sheet%=4:Super$="OFF"
 2740FORT%=0TO4:MOVE440,770-T%*40:PRINTA$(T%):NEXT
 2750@%=&020105
 2760MOVE584,770:PRINT;Name$
 2770MOVE584,730:PRINT,LoT%
 2780MOVE584,690:PRINT,HiT%
 2790MOVE696,650:PRINT;Super$
 2800@%=&90A
 2810MOVE712,610:PRINT;Sheet%
 2820VDU4
 2830ENDPROC
 2840DEFPROCedit
 2850CLS:PRINTTAB(13,1)"Do you want to EDIT the command file?,<Y/N>";:REPEAT:G=G
ET:UNTILG=89 OR G=78:IF G=78 THEN ENDPROC
 2860 T%=0:PROCupdown
 2870 ENDPROC
```

```
 2880 DEFPROCupdown
 2890 REM CURSOR CONTROL FOR SELECTING PARAMETER.
 2900 PROCon
 2910 CLS:PRINTTAB(11,1)"Use ";:COLOUR0:COLOUR129:PRINTCHR$139;:COLOUR1:COLOUR12
8:PRINT",";:COLOUR0:COLOUR129:PRINTCHR$138;:COLOUR1:COLOUR128:PRINT" & ";:COLOUR
0:COLOUR129:PRINT"RETURN";
 2920 COLOUR1:COLOUR128:PRINT" to select.Press ";:COLOUR0:COLOUR129:PRINT"SPACE"
;:COLOUR1:COLOUR128:PRINT" to finish."
 2930 IFINKEY-58 AND T%>0:PROCoff:T%=T%-1:PROCon:PROCfinger(58)
 2940 IFINKEY-42 AND T%<4:PROCoff:T%=T%+1:PROCon:PROCfinger(42)
 2950 IFINKEY-74:PROCfinger(74):PROCchange:GOTO2910
 2960 IFINKEY-99:PROCfinger(99):PROCoff:ENDPROC ELSE 2930
 2970 ENDPROC
 2980 DEFPROCon
 2990 REM HIGHLIGHTS TEXT.
 3000 VDU5:GCOL0,0:MOVE440,770-T%*40:PRINTSTRING$(LEN(A$(T%)),CHR$255)
 3010 GCOL0,1:MOVE440,770-T%*40:PRINTA$(T%):VDU4
 3020 ENDPROC
 3030 DEFPROCoff
 3040 REM REMOVES HIGHLIGHT FROM TEXT.
 3050 VDU5:GCOL0,1:MOVE440,770-T%*40:PRINTSTRING$(LEN(A$(T%)),CHR$255)
 3060 GCOL0,0:MOVE440,770-T%*40:PRINTA$(T%):VDU4
 3070 ENDPROC
 3080 DEFPROCchange
 3090 REM PARAMETERS UPDATED.
 3100 ON T%+1 GOTO 3110,3150,3170,3190,3210
 3110CLS:PRINTTAB(0,2)"Input Title :";:INPUT""Name$
 3120IF Name$=""THEN 3110
 3130IF LEN(Name$)>16 THEN Name$=LEFT$(Name$,16) ELSE Name$=Name$+STRING$(16-LEN
(Name$)," ")
 3140PROCnewdat(Name$,584,0,0,16):GOTO3230
 3150CLS:PRINTTAB(0,2)"Input Start :";:INPUT""LoS%
 3160IF LoS%<0 OR LoS%>=HiT% THEN 3150 ELSE PROCnewdat("",584,LoS%,&020105,5):GO
TO3230
 3170CLS:PRINTTAB(0,2)"Input Finish :";:INPUT""HiS%
 3180IF HiS%<=LoS% OR HiS%<=LoT% OR HiS%>180 THEN 3170 ELSE PROCnewdat("",584,Hi
S%,&020105,5):GOTO3230
 3190 IF Super$="OFF" THEN Super$="ON" ELSE Super$="OFF"
 3200 PROCnewdat(Super$,696,0,0,3):GOTO3230
 3210 IF Sheet%=4 THEN Sheet%=3 ELSE Sheet%=4
 3220 PROCnewdat("",712,Sheet%,&901,1)
 3230PROCfinger(74)
 3240ENDPROC
 3250 DEFPROCnewdat(A$,A,B,C,L)
 3260 REM PRINTS NEW PARAMETER.
 3270 VDU5:GCOL0,1:MOVEA,770-T%*40:PRINT;STRING$(L,CHR$255)
 3280 GCOL0,0:MOVEA,770-T%*40:IF A$="" THEN @%=C:PRINT,B ELSE PRINT;A$
 3290 VDU4
 3300 ENDPROC
 3310DEFPROCwindow(ux,uy,lx,ly)
 3320 REM PULL DOWN WINDOW
 3330GCOL0,0:MOVEux-16,uy-16:VDU25,101,lx-16;ly-16;
 3340GCOL0,1:MOVEux,uy:VDU25,101,lx;ly;
 3350GCOL0,0:MOVEux,uy:DRAWlx,uy:DRAWlx,ly:DRAWux,ly:DRAWux,uy
 3360MOVEux+16,uy-16:DRAWlx-16,uy-16:DRAWlx-16,ly+16:DRAWux+16,ly+16:DRAWux+16,u
y-16
 3370ENDPROC
 3380DEFPROCfinger(A)
 3390REPEATUNTILNOTINKEY(-A):OSCLI"FX15,0"
 3400ENDPROC
```

```
3410DEFPROCprint_data
3420 REM PRINTS OUT DATA ONTO CARD, OVERWRITING PREVIOUS OUTPUT.
3430X%=((P%-1)DIV10)+1:Y%=((P%-1)MOD10)+1
3440VDU5:GCOL0,1:MOVE240+(X%-1)*288,700-(Y%-1)*32:PRINTSTRING$(6,CHR$255):MOVE4
00+(X%-1)*288,700-(Y%-1)*32:PRINTSTRING$(3,CHR$255)
3450GCOL0,0:@%=&020306:MOVE240+(X%-1)*288,700-(Y%-1)*32:PRINT,Dhkl(P%):@%=&903:
MOVE400+(X%-1)*288,700-(Y%-1)*32:PRINT,Int%(P%):VDU4
3460ENDPROC
3470DEFPROCstep_calc(A,B)
3480 REM CALCULATES SUITABLE AXIS INCREMENT FOR PLOTS.
3490T%=0:REPEAT:T%=T%+1:Xdiv=((A-B)/Xinc%(T%)):UNTIL Xdiv<16
3500IF INT(Xdiv)<Xdiv THEN Xdiv=INT(Xdiv+1)
3510step_size%=Xinc%(T%)
3520ENDPROC
```

```
  10 REM ************************************************************************
  20 REM * INPUT allows the user to input new records to the database.          *
  30 REM * The data is input by hand, following the micros prompts. Editing     *
  40 REM * facilities allow mistakes to be corrected.                           *
  50 REM *                                                  Neil S Stewart/RGIT *
  60 REM ************************************************************************
  70 REM
  80 REM THE ROUTINES ARE ALMOST IDENTICAL TO THOSE IN VIEW AND UPDATE
  90 REM
 100 MODE128:DIM Int%(30),Dhkl(30),A$(5)
 110 REM BINARY PATTERNS FOR USER DEFINED CHARACTERS/
 120VDU23,240,0,0,0,132,133,230,165,164:VDU23,241,0,0,0,16,16,16,16,152
 130VDU23,242,0,0,0,251,168,171,138,139:VDU23,243,0,0,0,162,148,136,148,162
 140 PROCinput
 150 A%=0:CHAIN"DBASE"
 160 END
 170 :
 180DEFPROCinput
 190PROCbox("input/a "):PROCcard
 200PROCinput_details
 210 REM USER IS PROMPTED TO INPUT THE NAME,SOURCE etc.
 220VDU28,5,29,75,24:COLOUR1:COLOUR128:CLS:PRINTTAB(16,1)"Do you wish to change
 anything?,<Y/N>";:REPEAT:G=GET:UNTIL G=89 OR G=78:IF G=89 THEN PROCupdate_detai
ls
 230 REM USER IS PROMPTED TO INPUT THE DATA
 240PROCinput_data
 250VDU28,5,29,75,24:COLOUR1:COLOUR128:CLS:PRINTTAB(16,1)"Do you wish to change
 anything?,<Y/N>";:REPEAT:G=GET:UNTIL G=89 OR G=78:IF G=89 THEN PROCupdate_data
 260CLS:PRINTTAB(25,2)"SAVING DATA TO DISC"
 270X=OPENUP":2.PDFILE":INPUT#X,Disc$,Entries%:PTR#X=PTR#X+Entries%*380:Entries
%=Entries%+1:PROCdisc_poker:CLS
 280ENDPROC
 290DEFPROCcard
 310VDU28,0,31,79,0:GCOL0,0:MOVE190,348:VDU25,101,1090;967;:GCOL0,1:MOVE198,356
:VDU25,101,1098;975;:GCOL0,0:MOVE198,356:DRAW198,975:DRAW1098,975:DRAW1098,356:D
RAW198,356:MOVE216,372:DRAW216,959:DRAW1082,959:DRAW1082,372:DRAW216,372
 320MOVE216,767:DRAW1082,767:MOVE216,719:DRAW1082,719:MOVE648,959:DRAW648,767:M
OVE648,863:DRAW1082,863:FORT%=1TO2:MOVE216+T%*288,767:DRAW216+T%*288,372:NEXT:FO
RT%=0TO3:MOVE700+T%*96,959:DRAW700+T%*96,767:NEXT
 330COLOUR0:COLOUR129:A$(0)="Sample :":A$(1)="Source :":A$(2)="Date    :":A$(3)=
"2"+CHR$232+CHR$160+"/min:":A$(4)="Lambda :":GCOL0,0:VDU5:FORT%=0TO4:MOVE224,939
-T%*32:PRINT;A$(T%):NEXT:MOVE666,927:PRINT"I":MOVE666,831:PRINT"d"
 340FORT%=0TO2:MOVE248+T%*288,752:PRINT" d"CHR$240CHR$241:MOVE398+T%*288,752:PR
INT"I/I"CHR$242CHR$243:NEXT:VDU4:FORT%=0TO2:MOVE360+T%*288,719:DRAW360+T%*288,37
2:NEXT
 350ENDPROC
 360DEFPROCdisc_poker
 370 REM POKES DATA TO DISC AT NEXT RECORD ON DISC.
 380REPEAT:swap=0:FORT%=1TO29:IF Int%(T%)<Int%(T%+1) THEN PROCswapII:swap=swap+
1
 390NEXT:UNTILswap=0
 400PRINT#X,Title$,Source$,Date$,Rate,Lambda,Pair%
 410FORT%=1TO30:PRINT#X,Int%(T%),Dhkl(T%):NEXT:PTR#X=17:PRINT#X,Entries%:CLOSE#
X
 420ENDPROC
 430DEFPROCinput_details
 440FORT%=0TO4:PROCon2:PROCedit_details:PROCoff2:NEXT:T%=0
 450ENDPROC
 460DEFPROCinput_data
```

```
 470VDU23,1,1;0;0;0;:VDU28,5,29,75,24:COLOUR1:COLOUR128:CLS:PRINT"How many data
 pairs?,<MAX=30>:";:INPUT""Number
 480IF Number<=0 OR Number>30 THEN PROCerror:GOTO470
 490@%=&902:FORP%=1TONumber
 500CLS:PRINTTAB(0,1)"Peak #";P%;";";TAB(11,1);"d"CHR$240CHR$241;"=";TAB(11,2);
"Int=";
 510PRINTTAB(15,1)STRING$(LEN(STR$(Dhkl(P%)))," ");TAB(15,1);
 520INPUT""Dhkl(P%)
 530IFDhkl(P%)<=0 THEN510
 540PRINTTAB(15,2)STRING$(LEN(STR$(Int%(P%)))," ");TAB(15,2);
 550INPUT""Int%(P%)
 560IF Int%(P%)<0 OR Int%(P%)>100 THEN 540
 570PROCoff1
 580NEXT:IF Number<30 THEN FORT%=(Number+1)TO30:Int%(T%)=-2:NEXT
 590Pair%=Number
 600ENDPROC
 610DEFPROCedit_details
 620 REM USER CAN EDIT INPUT VALUES IF MISTAKES HAVE BEEN MADE.
 630*FX15,0
 640VDU28,5,29,75,24:COLOUR1:COLOUR128:CLS:VDU23,1,0;0;0;0;
 650ON T%+1 GOTO 660,700,740,780,810
 660CLS:PRINTTAB(0,2)"Sample name  :";:INPUT""Title$
 670IF Title$=""THEN660
 680IF LEN(Title$)>16 THEN Title$=LEFT$(Title$,16) ELSE Title$=Title$+STRING$(1
6-LEN(Title$)," ")
 690PROCnewdat(Title$,0,0,0,16):GOTO840
 700CLS:PRINTTAB(0,2)"Sample source:";:INPUT""Source$
 710IF Source$=""THEN700
 720IF LEN(Source$)>3 THEN Source$=LEFT$(Source$,3) ELSE Source$=Source$+STRING
$(3-LEN(Source$)," ")
 730PROCnewdat(Source$,1,0,0,3):GOTO840
 740CLS:PRINTTAB(0,2)"Date         :";:INPUT""Date$
 750IF Date$=""THEN740
 760IF LEN(Date$)>8 THEN Date$=LEFT$(Date$,8) ELSE Date$=Date$+STRING$(8-LEN(Da
te$)," ")
 770PROCnewdat(Date$,2,0,0,8):GOTO840
 780CLS:PRINTTAB(0,2)"Scanning rate:";:INPUT""Rate
 790IF Rate<=0 THEN Rate=0:PROCnewdat("N/A",3,0,0,4):GOTO840
 800PROCnewdat("",3,Rate,&020204,4):GOTO840
 810CLS:PRINTTAB(0,2)"Lambda          :";:INPUT""Lambda
 820IF Lambda<=0 THEN810
 830PROCnewdat("",4,Lambda,&020406,6)
 840PROCfinger(74)
 850ENDPROC
 860DEFPROCbox(A$)
 880VDU23,2,85,85,85,85,85,85,85,85:VDU18,16,129:VDU19,1,6;0;:VDU28,0,31,79,0:C
LG
 890GCOL0,0:MOVE15,15:DRAW15,1008:DRAW1266,1008:DRAW1266,15:DRAW15,15:GCOL0,1:M
OVE50,34:VDU25,101,1230;327;:GCOL0,0:MOVE66,51:VDU25,101,1214;311;:MOVE50,34:DRA
W50,327:DRAW1230,327:DRAW1230,34:DRAW50,34
 900COLOUR0:COLOUR129:PRINTTAB(4,22)A$:VDU28,5,29,75,24:COLOUR1:COLOUR128
 910ENDPROC
 920DEFPROCswapII
 930 REM BUBBLE SORT
 9400=Int%(T%):Int%(T%)=Int%(T%+1):Int%(T%+1)=0:0=Dhkl(T%):Dhkl(T%)=Dhkl(T%+1):
Dhkl(T%+1)=0
 950ENDPROC
 960DEFPROCerror
 980SOUND1,-12,40,2:SOUND2,-12,47,2:TIME=0:REPEATUNTILTIME>25
 990ENDPROC
```

```
 1000DEFPROCupdate_data
 1010 REM SELECTION OF DATA PAIR FOR EDITING
 1020P%=1:PROCon1
 1030VDU28,5,29,75,24:COLOUR1:COLOUR128:CLS:PRINTTAB(8,1)" Use ";:COLOUR0:COLOUR
129:PRINTCHR$136;:COLOUR1:COLOUR128:PRINT",";:COLOUR0:COLOUR129:PRINTCHR$137;
 1040COLOUR1:COLOUR128:PRINT",";:COLOUR0:COLOUR129:PRINTCHR$138;:COLOUR1:COLOUR1
28:PRINT",";:COLOUR0:COLOUR129:PRINTCHR$139;
 1050COLOUR1:COLOUR128:PRINT" & ";:COLOUR0:COLOUR129:PRINT"RETURN";:COLOUR1:COLO
UR128:PRINT" to select.Press ";:COLOUR0:COLOUR129:PRINT"SPACE";:COLOUR1:COLOUR12
8:PRINT" to finish."
 1060IFINKEY-122 AND (P%+10)<=Pair% PROCoff1:P%=P%+10:PROCon1:PROCfinger(122)
 1070IFINKEY-26 AND (P%-10)>0 PROCoff1:P%=P%-10:PROCon1:PROCfinger(26)
 1080IFINKEY-42  AND (P%+1)<=Pair% PROCoff1:P%=P%+1:PROCon1:PROCfinger(42)
 1090IFINKEY-58 AND P%>1 PROCoff1:P%=P%-1:PROCon1:PROCfinger(58)
 1100IFINKEY-74 PROCfinger(74):GOTO1130
 1110IFINKEY-99 PROCoff1:GOTO1200
 1120GOTO1060
 1130*FX15,0
 1140CLS:PRINTTAB(0,1)"New data-pair ; d"CHR$240CHR$241;"=";:INPUT""Dhkl(P%)
 1150IF Dhkl(P%)<=0 THEN 1140
 1160PRINTTAB(20,2)STRING$(LEN(STR$(Int%(P%)))," ");TAB(16,2)"Int=";:INPUT""Int%
(P%)
 1170IF Int%(P%)>100 OR Int%(P%)<0 THEN 1160
 1180PROCfinger(74)
 1190PROCon1:GOTO1030
 1200ENDPROC
 1210DEFPROCon1
 1220 REM HIGHLIGHTS DATA PAIR
 1230X%=((P%-1)DIV10)+1:Y%=((P%-1)MOD10)+1
 1240VDU5:GCOL0,0:MOVE240+(X%-1)*288,700-(Y%-1)*32:PRINTSTRING$(6,CHR$255):MOVE4
00+(X%-1)*288,700-(Y%-1)*32:PRINTSTRING$(3,CHR$255)
 1250GCOL0,1:@%=&020306:MOVE240+(X%-1)*288,700-(Y%-1)*32:PRINT,Dhkl(P%):@%=&903:
MOVE400+(X%-1)*288,700-(Y%-1)*32:PRINT,Int%(P%):VDU4
 1260ENDPROC
 1270DEFPROCoff1
 1280 REM REMOVES HIGHLIGHT SET BY on1
 1290X%=((P%-1)DIV10)+1:Y%=((P%-1)MOD10)+1
 1300VDU5:GCOL0,1:MOVE240+(X%-1)*288,700-(Y%-1)*32:PRINTSTRING$(6,CHR$255):MOVE4
00+(X%-1)*288,700-(Y%-1)*32:PRINTSTRING$(3,CHR$255)
 1310GCOL0,0:@%=&020306:MOVE240+(X%-1)*288,700-(Y%-1)*32:PRINT,Dhkl(P%):@%=&903:
MOVE400+(X%-1)*288,700-(Y%-1)*32:PRINT,Int%(P%):VDU4
 1320ENDPROC
 1330 DEFPROCupdate_details
 1340 REM SELECTS STRING FOR EDITING
 1350 T%=0:PROCon2
 1360 CLS:PRINTTAB(11,1)"Use ";:COLOUR0:COLOUR129:PRINTCHR$139;:COLOUR1:COLOUR12
8:PRINT",";:COLOUR0:COLOUR129:PRINTCHR$138;:COLOUR1:COLOUR128:PRINT" & ";:COLOUR
0:COLOUR129:PRINT"RETURN";
 1370 COLOUR1:COLOUR128:PRINT" to select.Press ";:COLOUR0:COLOUR129:PRINT"SPACE"
;:COLOUR1:COLOUR128:PRINT" to finish."
 1380 IFINKEY-58 AND T%>0:PROCoff2:T%=T%-1:PROCon2:PROCfinger(58)
 1390 IFINKEY-42 AND T%<4:PROCoff2:T%=T%+1:PROCon2:PROCfinger(42)
 1400 IFINKEY-74:PROCfinger(74):PROCedit_details:GOTO1360
 1410 IFINKEY-99 THEN PROCoff2 ELSE 1380
 1420 ENDPROC
 1430 DEFPROCon2
 1440 REM HIGHLIGHTS STRING FOR EDITING
 1450 VDU5:GCOL0,0:MOVE224,939-T%*32:PRINTSTRING$(LEN(A$(T%)),CHR$255)
 1460 GCOL0,1:MOVE224,939-T%*32:PRINTA$(T%):VDU4
 1470 ENDPROC
```

```
 1480 DEFPROCoff2
 1490 REM REMOVES HIGHLIGHT
 1500 VDU5:GCOL0,1:MOVE224,939-T%*32:PRINTSTRING$(LEN(A$(T%)),CHR$255)
 1510 GCOL0,0:MOVE224,939-T%*32:PRINTA$(T%):VDU4
 1520 ENDPROC
 1530DEFPROCfinger(A)
 1540 REM CLEARS BUFFER AFTER KEY IS RELEASED
 1550REPEATUNTILNOTINKEY(-A):*FX15,0
 1560ENDPROC
 1570DEFPROCedit_details
 1580*FX15,0
 1590VDU28,5,29,75,24:COLOUR1:COLOUR128:CLS:VDU23,1,0;0;0;0;
 1600ON T%+1 GOTO 1610,1650,1690,1730,1760
 1610CLS:PRINTTAB(0,2)"Sample name  :";:INPUT""Title$
 1620IF Title$=""THEN1610
 1630IF LEN(Title$)>16 THEN Title$=LEFT$(Title$,16) ELSE Title$=Title$+STRING$(1
6-LEN(Title$)," ")
 1640PROCnewdat(Title$,0,0,0,16):GOTO1790
 1650CLS:PRINTTAB(0,2)"Sample source:";:INPUT""Source$
 1660IF Source$=""THEN1650
 1670IF LEN(Source$)>3 THEN Source$=LEFT$(Source$,3) ELSE Source$=Source$+STRING
$(3-LEN(Source$)," ")
 1680PROCnewdat(Source$,1,0,0,3):GOTO1790
 1690CLS:PRINTTAB(0,2)"Date         .:";:INPUT""Date$
 1700IF Date$=""THEN1690
 1710IF LEN(Date$)>8 THEN Date$=LEFT$(Date$,8) ELSE Date$=Date$+STRING$(8-LEN(Da
te$)," ")
 1720PROCnewdat(Date$,2,0,0,8):GOTO1790
 1730CLS:PRINTTAB(0,2)"Scanning rate:";:INPUT""Rate
 1740IF Rate<=0 THEN Rate=0:PROCnewdat("N/A",3,0,0,4):GOTO1790
 1750PROCnewdat("",3,Rate,&020204,4):GOTO1790
 1760CLS:PRINTTAB(0,2)"Lambda          :";:INPUT""Lambda
 1770IF Lambda<=0 THEN1760
 1780PROCnewdat("",4,Lambda,&020406,6)
 1790PROCfinger(74)
 1800ENDPROC
 1810 DEFPROCnewdat(A$,A,B,C,L)
 1820 REM REPLACES OLD TEXT WITH NEW
 1830 VDU5:GCOL0,1:MOVE352,939-A*32:PRINT;STRING$(L,CHR$255)
 1840 GCOL0,0:MOVE352,939-A*32:IF A$="" THEN @%=C:PRINT;B ELSE PRINT;A$
 1850 VDU4
 1860 ENDPROC
```

```
  10 REM ************************************************************
  20 REM * UPDATE allows the user to edit an existing record on the   *
  30 REM * database.                                                  *
  40 REM *                                                           *
  50 REM *                                        Neil S Stewart/RGIT *
  60 REM ************************************************************
  70 REM
  80 REM THE ROUTINES ARE ALMOST IDENTICAL WITH VIEW AND INPUT
  90 REM
  90 DIM Int%(30),Dhkl(30),A$(5):OSCLI"FX15,0"
 100VDU23,240,0,0,0,132,133,230,165,164:VDU23,241,0,0,0,16,16,16,16,152
 110VDU23,242,0,0,0,251,168,171,138,139:VDU23,243,0,0,0,162,148,136,148,162
 120 PROCupdate
 130 A%=0:CHAIN"DBASE"
 140 END
 150 :
 160DEFPROCupdate
 170 REM INPUT NAME OF RECORD TO BE UPDATED
 180PROCbox("update/a "):*FX15,0
 190CLS:PRINTTAB(1,0)"Name of the sample to be updated :";:INPUT""Name$
 200IFName$=""THEN 190
 210IF LEN(Name$)>16 THEN Name$=LEFT$(Name$,16) ELSE Name$=Name$+STRING$(16-LEN
(Name$)," ")
 220 X=OPENUP":2.PDFILE":INPUT#X,Disc$,Entries%
 230PROCsearch:IF Success=0 THEN 290 ELSE PROCcard:PROCdisplay_details:PROCdisp
lay_data
 240VDU28,5,29,75,24:COLOUR1:COLOUR128:CLS:PRINTTAB(23,0)"f0-Update compound de
tails.";TAB(23,2)"f1-Update compound data.";TAB(23,4)"f2-Save and Exit.":PTR#X=P
ointer
 250IFINKEY-33 PROCselect(23,0,"f0-Update compound details."):PROCupdate_detail
s:GOTO240
 260IFINKEY-114 PROCselect(23,2,"f1-Update compound data."):PROCupdate_data:GOT
0240
 270IFINKEY-115 PROCselect(23,4,"f2-Save and Exit."):PROCdisc_poker:GOTO300
 280GOTO250
 290CLOSE#X:COLOUR1:COLOUR128:PRINTTAB(15,1)"NO SUCH COMPOUND IS STORED ON THIS
 DISC";TAB(19,3)"Do you wish to try again?,<Y/N>":REPEAT:G=GET:UNTILG=89 OR G=78
:IF G=89 THEN 190
 300ENDPROC
 310DEFPROCcard
 320VDU28,0,31,79,0:GCOL0,0:MOVE190,348:VDU25,101,1090;967;:GCOL0,1:MOVE198,356
:VDU25,101,1098;975;:GCOL0,0:MOVE198,356:DRAW198,975:DRAW1098,975:DRAW1098,356:D
RAW198,356:MOVE216,372:DRAW216,959:DRAW1082,959:DRAW1082,372:DRAW216,372
 330MOVE216,767:DRAW1082,767:MOVE216,719:DRAW1082,719:MOVE648,959:DRAW648,767:M
OVE648,863:DRAW1082,863:FORT%=1TO2:MOVE216+T%*288,767:DRAW216+T%*288,372:NEXT:FO
RT%=0TO3:MOVE700+T%*96,959:DRAW700+T%*96,767:NEXT
 340COLOUR0:COLOUR129:A$(0)="Sample :":A$(1)="Source :":A$(2)="Date   :":A$(3)=
"2"+CHR$232+CHR$160+"/min:":A$(4)="Lambda :":GCOL0,0:VDU5:FORT%=0TO4:MOVE224,939
-T%*32:PRINT;A$(T%):NEXT:MOVE666,927:PRINT"I":MOVE666,831:PRINT"d"
 350FORT%=0TO2:MOVE248+T%*288,752:PRINT" d"CHR$240CHR$241:MOVE398+T%*288,752:PR
INT"I/I"CHR$242CHR$243:NEXT:VDU4:FORT%=0TO2:MOVE360+T%*288,719:DRAW360+T%*288,37
2:NEXT
 360ENDPROC
 370DEFPROCdisplay_data
 380VDU23,1;0;0;0;0;:COLOUR0:COLOUR129:IF Pair%<4 THEN Top4=Pair% ELSE Top4=4
 390VDU5:FORT%=1TOTop4:@%=&9A03:MOVE644-INT(LOG(Int%(T%)))*8+T%*96,927:PRINT;In
t%(T%):@%=&020204:MOVE620-INT(LOG(Dhkl(T%)))*8+T%*96,831:PRINT;Dhkl(T%):NEXT:VDU
4
 400REPEAT:swap=0:FORT%=1TO29:IF Dhkl(T%)<Dhkl(T%+1) THEN PROCswapII:swap=swap+
1
```

```
  410NEXT:UNTILswap=0
  420FORP%=1TOPair%:PROCoff1:NEXT
  430ENDPROC
  440DEFPROCdisplay_details
  450VDU23,1;0;0;0;0;:GCOL0,0:VDU5
  460MOVE352,939:PRINT;Title$
  470MOVE352,907:PRINT;Source$
  480MOVE352,875:PRINT;Date$
  490MOVE352,843:IF Rate=0 THEN PRINT;"N/A" ELSE @%=020305:PRINT;Rate
  500MOVE352,811:@%=&020406:PRINT,Lambda
  510ENDPROC
  520DEFPROCdisc_poker
  530REPEAT:swap=0:FORT%=1TO29:IF Int%(T%)<Int%(T%+1) THEN PROCswapII:swap=swap+
1
  540NEXT:UNTILswap=0
  550PRINT#X,Title$,Source$,Date$,Rate,Lambda,Pair%
  560FORT%=1TO30:PRINT#X,Int%(T%),Dhkl(T%):NEXT:PTR#X=17:PRINT#X,Entries%:CLOSE#
X
  570ENDPROC
  580DEFPROCupdate_data
  590P%=1:PROCon1
  600VDU28,5,29,75,24:COLOUR1:COLOUR128:CLS:PRINTTAB(8,1)" Use ";:COLOUR0:COLOUR
129:PRINTCHR$136;:COLOUR1:COLOUR128:PRINT",";:COLOUR0:COLOUR129:PRINTCHR$137;
  610COLOUR1:COLOUR128:PRINT",";:COLOUR0:COLOUR129:PRINTCHR$138;:COLOUR1:COLOUR1
28:PRINT",";:COLOUR0:COLOUR129:PRINTCHR$139;
  620COLOUR1:COLOUR128:PRINT" & ";:COLOUR0:COLOUR129:PRINT"RETURN";:COLOUR1:COLO
UR128:PRINT" to select.Press ";:COLOUR0:COLOUR129:PRINT"SPACE";:COLOUR1:COLOUR12
8:PRINT" to finish."
  630IFINKEY-122 AND (P%+10)<=Pair% PROCoff1:P%=P%+10:PROCon1:PROCfinger(122)
  640IFINKEY-26 AND (P%-10)>0 PROCoff1:P%=P%-10:PROCon1:PROCfinger(26)
  650IFINKEY-42  AND (P%+1)<=Pair% PROCoff1:P%=P%+1:PROCon1:PROCfinger(42)
  660IFINKEY-58 AND P%>1 PROCoff1:P%=P%-1:PROCon1:PROCfinger(58)
  670IFINKEY-74 PROCfinger(74):GOTO700
  680IFINKEY-99 PROCoff1:GOTO770
  690GOTO630
  700*FX15,0
  710CLS:PRINTTAB(0,1)"New data-pair ; d"CHR$240CHR$241;"=";:INPUT""Dhkl(P%)
  720IF Dhkl(P%)<=0 THEN 710
  730PRINTTAB(20,2)STRING$(LEN(STR$(Int%(P%)))," ");TAB(16,2)"Int=";:INPUT""Int%
(P%)
  740IF Int%(P%)>100 OR Int%(P%)<0 THEN 730
  750PROCfinger(74)
  760PROCon1:GOTO600
  770ENDPROC
  780DEFPROCon1
  790X%=((P%-1)DIV10)+1:Y%=((P%-1)MOD10)+1
  800VDU5:GCOL0,0:MOVE240+(X%-1)*288,700-(Y%-1)*32:PRINTSTRING$(6,CHR$255):MOVE4
00+(X%-1)*288,700-(Y%-1)*32:PRINTSTRING$(3,CHR$255)
  810GCOL0,1:@%=&020306:MOVE240+(X%-1)*288,700-(Y%-1)*32:PRINT,Dhkl(P%):@%=&903:
MOVE400+(X%-1)*288,700-(Y%-1)*32:PRINT,Int%(P%):VDU4
  820ENDPROC
  830DEFPROCoff1
  840X%=((P%-1)DIV10)+1:Y%=((P%-1)MOD10)+1
  850VDU5:GCOL0,1:MOVE240+(X%-1)*288,700-(Y%-1)*32:PRINTSTRING$(6,CHR$255):MOVE4
00+(X%-1)*288,700-(Y%-1)*32:PRINTSTRING$(3,CHR$255)
  860GCOL0,0:@%=&020306:MOVE240+(X%-1)*288,700-(Y%-1)*32:PRINT,Dhkl(P%):@%=&903:
MOVE400+(X%-1)*288,700-(Y%-1)*32:PRINT,Int%(P%):VDU4
  870ENDPROC
  880DEFPROCbox(A$)
  890VDU23,2,85,85,85,85,85,85,85,85:VDU18,16,129:VDU19,1,6;0;:VDU28,0,31,79,0:C
```

```
LG
  900GCOL0,0:MOVE15,15:DRAW15,1008:DRAW1266,1008:DRAW1266,15:DRAW15,15:GCOL0,1:M
OVE50,34:VDU25,101,1230;327;:GCOL0,0:MOVE66,51:VDU25,101,1214;311;:MOVE50,34:DRA
W50,327:DRAW1230,327:DRAW1230,34:DRAW50,34
  910COLOUR0:COLOUR129:PRINTTAB(4,22)A$:VDU28,5,29,75,24:COLOUR1:COLOUR128
  920ENDPROC
  930DEFPROCsearch
  940Success=0:CLS:PRINTTAB(30,1)"SEARCHING!"
  950T%=0:REPEAT:T%=T%+1
  960INPUT#X,Title$
  970IF Title$=Name$ THEN Success=1:Pointer=PTR#X-18:GOTO1000
  980PTR#X=PTR#X+362:UNTIL T%=Entries%
  990GOTO1020
 1000INPUT#X,Source$,Date$,Rate,Lambda,Fair%
 1010FOR T%=1TO30:INPUT#X,Int%(T%),Dhkl(T%):NEXT
 1020ENDPROC
 1030DEFPROCswapII
 1040Q=Int%(T%):Int%(T%)=Int%(T%+1):Int%(T%+1)=Q:Q=Dhkl(T%):Dhkl(T%)=Dhkl(T%+1):
Dhkl(T%+1)=Q
 1050ENDPROC
 1060DEFPROCselect(Xcoord%,Ycoord%,Phrase$)
 1070COLOUR0:COLOUR129:PRINTTAB(Xcoord%,Ycoord%)Phrase$
 1080Now%=TIME:REPEATUNTIL(TIME-Now%)>25:COLOUR1:COLOUR128
 1090ENDPROC
 1100 DEFPROCupdate_details
 1110 T%=0:PROCon2
 1120 CLS:PRINTTAB(11,1)"Use ";:COLOUR0:COLOUR129:PRINTCHR$139;:COLOUR1:COLOUR12
8:PRINT",";:COLOUR0:COLOUR129:PRINTCHR$138;:COLOUR1:COLOUR128:PRINT" & ";:COLOUR
0:COLOUR129:PRINT"RETURN";
 1130 COLOUR1:COLOUR128:PRINT" to select.Press ";:COLOUR0:COLOUR129:PRINT"SPACE"
;:COLOUR1:COLOUR128:PRINT" to finish."
 1140 IFINKEY-58 AND T%>0:PROCoff2:T%=T%-1:PROCon2:PROCfinger(58)
 1150 IFINKEY-42 AND T%<4:PROCoff2:T%=T%+1:PROCon2:PROCfinger(42)
 1160 IFINKEY-74:PROCfinger(74):PROCedit_details:GOTO1120
 1170 IFINKEY-99 THEN PROCoff2 ELSE 1140
 1180 ENDPROC
 1190 DEFPROCon2
 1200 VDU5:GCOL0,0:MOVE224,939-T%*32:PRINTSTRING$(LEN(A$(T%)),CHR$255)
 1210 GCOL0,1:MOVE224,939-T%*32:PRINTA$(T%):VDU4
 1220 ENDPROC
 1230 DEFPROCoff2
 1240 VDU5:GCOL0,1:MOVE224,939-T%*32:PRINTSTRING$(LEN(A$(T%)),CHR$255)
 1250 GCOL0,0:MOVE224,939-T%*32:PRINTA$(T%):VDU4
 1260 ENDPROC
 1270DEFPROCfinger(A)
 1280REPEATUNTILNOTINKEY(-A):*FX15,0
 1290ENDPROC
 1300DEFPROCedit_details
 1310*FX15,0
 1320VDU28,5,29,75,24:COLOUR1:COLOUR128:CLS:VDU23,1,0;0;0;0;
 1330ON T%+1 GOTO 1340,1380,1420,1460,1490
 1340CLS:PRINTTAB(0,2)"Sample name  :";:INPUT""Title$
 1350IF Title$=""THEN1340
 1360IF LEN(Title$)>16 THEN Title$=LEFT$(Title$,16) ELSE Title$=Title$+STRING$(1
6-LEN(Title$)," ")
 1370PROCnewdat(Title$,0,0,0,16):GOTO1520
 1380CLS:PRINTTAB(0,2)"Sample source:";:INPUT""Source$
 1390IF Source$=""THEN1380
 1400IF LEN(Source$)>3 THEN Source$=LEFT$(Source$,3) ELSE Source$=Source$+STRING
$(3-LEN(Source$)," ")
```

```
1410PROCnewdat(Source$,1,0,0,3):GOTO1520
1420CLS:PRINTTAB(0,2)"Date          :";:INPUT""Date$
1430IF Date$=""THEN1420
1440IF LEN(Date$)>8 THEN Date$=LEFT$(Date$,8) ELSE Date$=Date$+STRING$(8-LEN(Da
te$)," ")
1450PROCnewdat(Date$,2,0,0,8):GOTO1520
1460CLS:PRINTTAB(0,2)"Scanning rate:";:INPUT""Rate
1470IF Rate<=0 THEN Rate=0:PROCnewdat("N/A",3,0,0,4):GOTO1520
1480PROCnewdat("",3,Rate,&020204,4):GOTO1520
1490CLS:PRINTTAB(0,2)"Lambda          :";:INPUT""Lambda
1500IF Lambda<=0 THEN1490
1510PROCnewdat("",4,Lambda,&020406,6)
1520PROCfinger(74)
1530ENDPROC
1540 DEFPROCnewdat(A$,A,B,C,L)
1550 VDU5:GCOL0,1:MOVE352,939-A*32:PRINT;STRING$(L,CHR$255)
1560 GCOL0,0:MOVE352,939-A*32:IF A$="" THEN @%=C:PRINT;B ELSE PRINT;A$
1570 VDU4
1580 ENDPROC
```

```
 10 MODE128
 20 REM lo, mid AND hi ARE TEMPORARY REGISTERS USED TO HOLD THE SUM OF 8
 30 REM 16 BIT NUMBERS.
 40 lo=&70
 50 mid=&71
 60 hi=&72
 70 REM mem_lo AND mem_hi HOLD THE INITIAL START POSITION IN MEMORY
 80 mem_lo=&73
 90 mem_hi=&74
100 REM limit_lo AND limit_hi HOLD THE FINAL POSITIONS IN MEMORY
110 limit_lo=&75
120 limit_hi=&76
130 REM THIS ROUTINE MAKES USE OF THE LSR COMMAND (LOGICAL SHIFT RIGHT).
140 REM IT SHIFTS THE BINARY PATTERN OF AN 8 BIT LOCATION TO THE RIGHT.
150 REM IN BINARY, THIS IS EQUIVALENT BY A DIVISION BY 2. REPEATING THIS
160 REM PROCESS 3 TIMES WILL DIVIDE BY 8. THE CONTENTS OF 256*mem_lo+mem_hi
170 REM THROUGH TO 256*(mem_hi)+mem_lo+15 ARE SUMMED AND STORED IN lo, mid AND
180 REM hi. THIS IS LSR'ED 3 TIMES AND THE RESULTING VALUE IS STORED IN
190 REM 256*mem_hi+mem_lo+6 AND 256*mem_hi+mem_lo+7.
200 REM AND mem_hi
210 START%=&DD00
220 FOR T%=0TO3 STEP3
230 P%=START%
240 [
250 OPT T%
260 .skip
270 LDA #0
280 STA lo
290 STA mid
300 STA hi
310 LDY #0
320 .skip1
330 CLC
340 INY
350 LDA (mem_lo),Y
360 ADC lo
370 STA lo
380 DEY
390 LDA (mem_lo),Y
400 ADC mid
410 STA mid
420 LDA #0
430 ADC hi
440 STA hi
450 INY
460 INY
470 CPY #16
480 BNE skip1
490 LDY #0
500 .skip2
510 LSR lo
520 CLC
530 LSR mid
540 BCC skip3
550 CLC
560 LDA #128
570 ADC lo
580 STA lo
590 .skip3
600 LSR hi
610 BCC skip4
620 CLC
630 LDA #128
640 ADC mid
650 STA mid
660 .skip4
670 INY
680 CPY #3
690 BNE skip2
700 LDY #6
710 LDA mid
720 STA (mem_lo),Y
730 INY
740 LDA lo
750 STA (mem_lo),Y
760 CLC
770 LDA mem_lo
780 ADC #2
790 STA mem_lo
800 BCC skip5
810 CLC
820 INC mem_hi
830 .skip5
840 LDA limit_hi
850 CMP mem_hi
860 BNE skip
870 LDA limit_lo
880 CMP mem_lo
890 BNE skip
900 RTS
910 ]
920 NEXT
```

```
 10 MODE128
 20 REM lo_mem AND hi_mem HOLD MEMORY LOCATION OF START OF DATA
 30 lo_mem=&70
 40 hi_mem=&71
 50 REM lo_min AND hi_min HOLD THE MINIMUM VALUE
 60 lo_min=&72
 70 hi_min=&73
 80 REM lo_dat AND hi_dat ARE TEMPORARY REGISTERS HOLDING PRESENT 16 BIT WORD
 90 lo_dat=&74
100 hi_dat=&75
110 REM lo_limit AND hi_limit HOLD THE LOCATION OF FINAL DATA PAIR
120 lo_limit=&76
130 hi_limit=&77
140 REM THE ROUTINE WORKS BY INITIALLY COMPARING THE HI-BYTES OF THE 16 BIT
150 REM WORD. IF THIS VALUE IS GREATER THAN MIN HI-BYTE THEN THE ROUTINE
160 REM INCREMENTS THE MEMORY POINTER AND CONTINUES. IF THE VALUE IS SMALLER
170 REM THEN, THERE IS NO NEED TO CHECK FURTHER. THE NEW VALUE OF MIN IS STORE
D.
180 REM ONLY WHEN THE HI-BYTES ARE THE SAME DOES THE LO-BYTES NEED TO BE
190 REM COMPARED. THE PROCESS IS CONTINUED UNTIL THE LIMITS ARE MET.
200 START%=&DD70
210 FORT%=0TO3STEP3
220 P%=START%
230 [
240 OPT T%
250 .begin
260 LDY #0
270 LDA (lo_mem),Y
280 STA hi_dat
290 INY
300 LDA (lo_mem),Y
310 STA lo_dat
320 :
330 LDA hi_min
340 CMP hi_dat
350 BCC next
360 BEQ lo_check
370 LDA hi_dat
380 STA hi_min
390 LDA lo_dat
400 STA lo_min
410 BRA next
420 .lo_check
430 LDA lo_dat
440 CMP lo_min
450 BCS next
460 LDA lo_dat
470 STA lo_min
480 .next
490 :
500 CLC
510 LDA lo_mem
520 ADC #2
530 STA lo_mem
540 BCC skip
550 CLC
560 INC hi_mem
570 .skip
580 LDA hi_mem
590 CMP hi_limit
600 BNE begin
610 LDA lo_mem
620 CMP lo_limit
630 BNE begin
640 RTS
650 ]
660 NEXT
```

APPENDIX B

Observed and calculated structure factor lists.

1a,2,3,7b-Tetrahydro-1-phenyl-1H-cyclopropa[a]napthalene, $C_{17}H_{16}$

h	k	l	10Fo	10Fc	h	k	l	10Fo	10Fc	h	k	l	10Fo	10Fc	h	k	l	10Fo	10Fc	h	k	l	10Fo	10Fc
2	0	0	2050	-1928	2	5	0	276	-259	2	1	1	1880	-1969	4	3	1	201	-192	-4	6	1	137	-127
4	0	0	1225	-1138	5	5	0	130	-161	3	1	1	180	120	5	3	1	130	107	-2	6	1	191	-229
5	0	0	379	364	6	5	0	94	78	4	1	1	246	243	6	3	1	182	172	-1	6	1	156	-159
6	0	0	761	761	7	5	0	111	-92	5	1	1	496	494	7	3	1	177	-205	0	6	1	217	255
7	0	0	183	-192	0	6	0	576	558	6	1	1	510	514	8	3	1	135	149	1	6	1	122	130
8	0	0	188	187	2	6	0	99	-92	7	1	1	146	-143	9	3	1	145	146	2	6	1	238	299
10	0	0	217	-246	3	6	0	179	188	8	1	1	348	-385	10	3	1	119	-92	3	6	1	99	-91
1	1	0	278	-310	4	6	0	231	-232	-10	2	1	175	188	-8	4	1	287	307	5	6	1	96	67
2	1	0	1901	1934	5	6	0	92	116	-8	2	1	233	-218	-6	4	1	143	-122	6	6	1	92	-120
3	1	0	504	-489	10	6	0	93	-85	-7	2	1	85	-98	-4	4	1	217	197	7	6	1	133	137
4	1	0	751	-745	2	7	0	212	211	-6	2	1	176	-129	-3	4	1	208	216	-7	7	1	148	174
5	1	0	388	393	6	7	0	95	91	-5	2	1	129	133	-2	4	1	270	287	-6	7	1	121	-111
6	1	0	233	190	0	8	0	297	307	-4	2	1	554	518	-1	4	1	187	-190	-2	7	1	134	133
7	1	0	81	71	2	8	0	242	-258	-3	2	1	470	-463	0	4	1	172	-158	0	7	1	83	-76
8	1	0	227	229	3	8	0	121	-113	-2	2	1	177	95	1	4	1	277	262	3	7	1	84	-116
9	1	0	116	-163	4	8	0	175	-181	-1	2	1	188	-189	3	4	1	255	-270	6	7	1	320	341
0	2	0	58	72	5	8	0	98	-104	0	2	1	534	518	4	4	1	209	215	7	7	1	113	108
3	2	0	538	-552	7	8	0	105	106	1	2	1	187	-223	5	4	1	123	-130	8	7	1	101	-80
4	2	0	558	-545	1	9	0	98	-100	2	2	1	461	-513	8	4	1	104	-80	-5	8	1	116	120
5	2	0	93	-92	3	9	0	129	118	3	2	1	303	-314	-7	5	1	122	-98	0	8	1	192	-217
6	2	0	90	-65	0	10	0	237	223	5	2	1	226	212	-5	5	1	133	-146	1	8	1	89	64
8	2	0	209	231	1	10	0	106	81	6	2	1	443	458	-4	5	1	226	-235	2	8	1	193	221
11	2	0	145	-127	3	10	0	108	-124	8	2	1	206	-205	-3	5	1	173	146	3	8	1	115	102
2	3	0	103	-118	4	10	0	204	-208	-10	3	1	192	206	-2	5	1	268	285	4	8	1	146	-137
3	3	0	122	91	6	10	0	142	135	-8	3	1	97	100	-1	5	1	352	-374	5	8	1	162	-168
5	3	0	77	-117	1	11	0	93	-73	-7	3	1	95	-64	0	5	1	285	276	9	8	1	101	67
6	3	0	104	68	-11	1	1	101	-103	-6	3	1	277	-272	1	5	1	170	124	-6	9	1	95	-65
8	3	0	119	-119	-9	1	1	135	162	-5	3	1	163	152	2	5	1	244	-251	-5	9	1	181	-202
9	3	0	140	-144	-8	1	1	132	137	-4	3	1	85	-109	3	5	1	204	214	-4	9	1	201	-202
0	4	0	157	-181	-5	1	1	499	-500	-3	3	1	211	203	4	5	1	202	-218	-3	9	1	116	146
1	4	0	211	-231	-4	1	1	320	-311	-2	3	1	227	243	5	5	1	99	-70	-2	9	1	290	303
2	4	0	146	144	-3	1	1	472	465	-1	3	1	354	-389	7	5	1	197	-206	1	9	1	258	-256
3	4	0	288	295	-2	1	1	1197	1118	0	3	1	376	385	-10	6	1	113	-112	2	9	1	316	-328
5	4	0	89	-41	-1	1	1	208	189	1	3	1	188	184	-7	6	1	182	196	4	9	1	186	202
7	4	0	135	143	0	1	1	408	434	2	3	1	137	-161	-6	6	1	95	92	5	9	1	104	127
1	5	0	525	533	1	1	1	419	-460	3	3	1	145	-125	-5	6	1	263	-281	-5	10	1	107	-106

h	k	l	10Fo	10Fc	h	k	l	10Fo	10Fc	h	k	l	10Fo	10Fc	h	k	l	10Fo	10Fc	h	k	l	10Fo	10Fc
-4	10	1	93	87	-5	1	2	727	-719	4	3	2	171	-169	8	6	2	113	-122	-7	1	3	144	-118
-3	10	1	124	137	-3	1	2	906	863	5	3	2	72	-38	-5	7	2	187	-214	-5	1	3	285	254
-2	10	1	211	-217	-2	1	2	759	-741	8	3	2	256	-266	2	7	2	136	150	-3	1	3	181	-180
-1	10	1	96	131	-1	1	2	338	-323	10	3	2	98	105	3	7	2	82	-72	-2	1	3	258	-241
0	10	1	111	101	0	1	2	301	-306	-6	4	2	99	-84	4	7	2	267	-289	-1	1	3	920	-919
2	10	1	128	-104	1	1	2	123	80	-4	4	2	492	477	6	7	2	229	238	0	1	3	520	504
3	10	1	88	-90	2	1	2	621	645	-2	4	2	433	-431	-5	8	2	120	-116	1	1	3	554	566
5	10	1	123	140	3	1	2	424	381	-1	4	2	111	-90	-2	8	2	175	161	2	1	3	127	115
7	10	1	100	-90	5	1	2	628	612	0	4	2	79	-63	-1	8	2	99	-52	3	1	3	325	-344
-5	11	1	99	-104	6	1	2	344	-318	1	4	2	264	251	0	8	2	252	-253	5	1	3	200	-191
-2	11	1	161	160	7	1	2	259	-252	2	4	2	207	200	1	8	2	326	-328	6	1	3	172	153
-1	11	1	179	179	8	1	2	174	190	6	4	2	109	100	3	8	2	155	167	7	1	3	97	99
0	11	1	93	-101	-9	2	2	97	72	8	4	2	85	-51	5	8	2	98	-106	11	1	3	100	-128
8	11	1	103	-58	-8	2	2	223	-219	-9	5	2	117	-125	6	8	2	155	-165	-11	2	3	99	-75
-11	0	2	117	155	-4	2	2	66	-32	-8	5	2	124	132	11	8	2	101	76	-9	2	3	120	-165
-10	0	2	101	-102	-3	2	2	224	-222	-7	5	2	134	139	-7	9	2	101	107	-8	2	3	224	-198
-9	0	2	122	134	-2	2	2	171	154	-6	5	2	107	-91	-3	9	2	132	112	-7	2	3	311	313
-8	0	2	159	203	-1	2	2	320	-350	-4	5	2	154	-160	-1	9	2	139	-159	-5	2	3	153	52
-7	0	2	679	-688	0	2	2	825	-875	-3	5	2	83	-64	0	9	2	134	100	-4	2	3	146	-125
-5	0	2	891	827	1	2	2	240	-246	-2	5	2	501	522	1	9	2	130	123	-3	2	3	109	-77
-4	0	2	474	-445	2	2	2	390	-437	-1	5	2	190	208	2	9	2	172	175	-2	2	3	103	-115
-3	0	2	1770	1630	3	2	2	72	-76	0	5	2	243	-223	3	9	2	197	-226	-1	2	3	305	-301
-2	0	2	860	807	4	2	2	163	186	1	5	2	152	129	4	9	2	107	-132	0	2	3	646	-660
-1	0	2	404	-396	6	2	2	89	-90	2	5	2	295	-236	7	9	2	113	-68	1	2	3	339	337
0	0	2	233	245	7	2	2	155	-168	3	5	2	151	-152	-3	10	2	184	216	2	2	3	149	170
1	0	2	203	-179	8	2	2	236	-257	4	5	2	133	136	-2	10	2	121	97	3	2	3	297	284
2	0	2	258	-172	9	2	2	106	117	6	5	2	87	-85	-1	10	2	86	-80	4	2	3	132	-141
3	0	2	2147	2148	10	2	2	150	146	-7	6	2	238	-237	0	10	2	253	-234	5	2	3	564	-565
5	0	2	611	-595	-5	3	2	159	151	-6	6	2	262	278	2	10	2	198	221	7	2	3	200	177
6	0	2	225	215	-4	3	2	175	179	-5	6	2	186	186	3	10	2	210	211	8	2	3	317	340
7	0	2	367	-325	-3	3	2	98	96	-4	6	2	127	-109	-4	11	2	100	-84	10	2	3	136	-152
9	0	2	213	238	-2	3	2	460	-506	-2	6	2	160	161	-1	11	2	118	85	-8	3	3	248	262
-9	1	2	101	84	-1	3	2	186	-197	0	6	2	202	170	1	11	2	193	-203	-6	3	3	175	-169
-8	1	2	159	-168	1	3	2	149	140	3	6	2	71	63	3	11	2	148	152	-5	3	3	75	54
-7	1	2	116	-88	2	3	2	338	340	5	6	2	113	-89	6	11	2	102	-46	-3	3	3	81	-30
-6	1	2	335	341	3	3	2	131	155	6	6	2	213	201	7	11	2	96	-72	-1	3	3	203	182

h	k	l	10Fo	10Fc	h	k	l	10Fo	10Fc	h	k	l	10Fo	10Fc	h	k	l	10Fo	10Fc	h	k	l	10Fo	10Fc
0	3	3	315	311	2	6	3	288	301	-1	0	4	1081	-1066	7	2	4	126	-117	0	5	4	311	-325
1	3	3	237	-262	3	6	3	123	-115	0	0	4	1244	1220	8	2	4	185	-194	1	5	4	122	-106
2	3	3	495	-542	4	6	3	152	-144	1	0	4	1312	1375	9	2	4	88	78	2	5	4	116	96
3	3	3	312	333	5	6	3	114	114	2	0	4	1035	-1065	-9	3	4	91	77	3	5	4	74	-69
5	3	3	187	-171	6	6	3	198	206	3	0	4	104	66	-8	3	4	177	201	6	5	4	96	53
6	3	3	117	-114	9	6	3	102	-87	4	0	4	253	226	-6	3	4	115	-112	-5	6	4	82	-54
8	3	3	203	175	-10	7	3	97	40	5	0	4	418	403	-5	3	4	228	-209	-4	6	4	119	-116
-10	4	3	98	-100	-6	7	3	175	175	6	0	4	201	178	-3	3	4	117	-83	-2	6	4	212	215
-7	4	3	193	205	0	7	3	245	-238	8	0	4	207	-213	-2	3	4	309	288	-1	6	4	123	135
-5	4	3	179	161	1	7	3	206	214	-9	1	4	143	159	-1	3	4	248	263	0	6	4	95	107
-3	4	3	166	-171	8	7	3	109	71	-8	1	4	83	-69	0	3	4	270	-276	1	6	4	88	87
-2	4	3	404	381	9	7	3	130	96	-5	1	4	449	-447	1	3	4	192	-190	2	6	4	196	-214
-1	4	3	187	214	-2	8	3	178	170	-4	1	4	134	116	2	3	4	321	330	5	6	4	120	147
0	4	3	75	60	1	8	3	113	-100	-3	1	4	257	244	3	3	4	193	-186	6	6	4	109	106
1	4	3	151	148	2	8	3	132	-127	-2	1	4	644	-651	4	3	4	179	-164	-6	7	4	102	-126
2	4	3	224	-182	9	8	3	102	-84	-1	1	4	217	-230	5	3	4	146	-143	-4	7	4	175	192
4	4	3	100	-70	11	8	3	108	100	0	1	4	1587	1516	8	3	4	121	102	-2	7	4	90	-93
8	4	3	111	-117	-2	9	3	186	-208	1	1	4	161	140	9	3	4	134	-164	-1	7	4	76	-51
10	4	3	110	115	3	9	3	133	118	3	1	4	392	-409	-9	4	4	130	137	3	7	4	92	83
-8	5	3	91	-81	4	9	3	97	-67	4	1	4	97	108	-7	4	4	140	158	4	7	4	107	83
-5	5	3	85	68	5	9	3	143	-149	5	1	4	149	126	-5	4	4	308	-299	9	7	4	102	111
-4	5	3	209	-223	7	9	3	109	115	6	1	4	125	148	-3	4	4	158	140	-3	8	4	111	118
-2	5	3	406	-408	1	10	3	107	-115	7	1	4	197	195	-2	4	4	239	205	-2	8	4	129	-101
-1	5	3	105	97	-1	11	3	102	86	-7	2	4	94	65	-1	4	4	232	231	-1	8	4	102	-87
0	5	3	819	796	2	11	3	97	122	-6	2	4	242	-250	0	4	4	84	-60	2	8	4	101	-137
1	5	3	122	-99	7	11	3	121	81	-5	2	4	78	-109	1	4	4	312	-342	3	8	4	96	-102
2	5	3	336	-338	-11	0	4	108	102	-4	2	4	196	190	2	4	4	404	-412	6	8	4	130	131
4	5	3	239	-215	-10	0	4	113	-127	-2	2	4	99	-100	3	4	4	238	227	-4	9	4	132	137
6	5	3	97	118	-9	0	4	107	-143	-1	2	4	697	-693	4	4	4	485	499	-2	9	4	155	-152
8	5	3	96	-107	-8	0	4	132	149	0	2	4	906	-861	5	4	4	90	65	-1	9	4	94	88
10	5	3	110	-99	-7	0	4	211	-207	1	2	4	255	193	-9	5	4	102	-142	2	9	4	133	-144
-6	6	3	283	-296	-6	0	4	78	77	2	2	4	162	-150	-7	5	4	276	290	6	9	4	146	-120
-5	6	3	87	-108	-5	0	4	387	342	3	2	4	315	-328	-5	5	4	163	-156	-2	10	4	145	166
-4	6	3	113	117	-4	0	4	340	303	4	2	4	255	-263	-4	5	4	103	145	-1	11	4	95	94
-2	6	3	212	-217	-3	0	4	370	349	5	2	4	72	-23	-2	5	4	306	315	2	11	4	87	-57
0	6	3	184	-193	-2	0	4	736	681	6	2	4	307	313	-1	5	4	76	-57	6	11	4	97	84

h	k	l	10Fo	10Fc	h	k	l	10Fo	10Fc	h	k	l	10Fo	10Fc	h	k	l	10Fo	10Fc	h	k	l	10Fo	10Fc
-10	1	5	179	-179	1	3	5	251	-239	5	6	5	123	109	-5	0	6	336	340	-8	3	6	116	-142
-6	1	5	164	150	2	3	5	224	240	6	6	5	223	-223	-4	0	6	233	175	-6	3	6	97	96
-5	1	5	94	-91	3	3	5	79	85	11	6	5	102	-61	-2	0	6	570	-578	-5	3	6	81	-81
-3	1	5	80	60	4	3	5	231	244	-6	7	5	190	207	-1	0	6	1098	1083	-4	3	6	263	-220
-2	1	5	817	-792	6	3	5	98	-121	-4	7	5	89	46	0	0	6	1610	1631	-3	3	6	103	116
0	1	5	577	-585	8	3	5	178	-195	-1	7	5	122	-111	1	0	6	853	-866	-1	3	6	353	356
1	1	5	733	782	9	3	5	142	130	0	7	5	73	82	2	0	6	295	303	1	3	6	432	-442
2	1	5	405	375	10	3	5	170	159	1	7	5	101	-118	3	0	6	115	103	2	3	6	110	120
3	1	5	146	157	-10	4	5	93	94	3	7	5	122	112	4	0	6	121	119	3	3	6	95	60
4	1	5	134	146	-7	4	5	163	154	4	7	5	100	121	5	0	6	244	-243	4	3	6	458	-438
5	1	5	122	-118	-4	4	5	162	177	6	7	5	132	126	6	0	6	118	121	-4	4	6	121	105
8	1	5	224	-240	-3	4	5	186	201	8	7	5	160	-166	7	0	6	232	236	-3	4	6	167	145
10	1	5	113	122	-1	4	5	261	283	-4	8	5	97	93	10	0	6	94	58	-2	4	6	677	-621
-7	2	5	94	-62	1	4	5	111	87	-3	8	5	119	121	-6	1	6	107	-137	-1	4	6	347	-344
-5	2	5	233	-233	2	4	5	171	154	-2	8	5	136	-136	-3	1	6	64	44	0	4	6	192	189
-4	2	5	260	227	3	4	5	237	-249	-1	8	5	83	27	-2	1	6	111	-70	1	4	6	333	331
-3	2	5	73	86	-7	5	5	317	-322	1	8	5	176	-178	-1	1	6	446	447	2	4	6	698	683
-1	2	5	463	-474	-5	5	5	82	-50	2	8	5	254	273	0	1	6	528	-485	3	4	6	95	61
0	2	5	1166	-1108	-4	5	5	151	149	3	8	5	125	126	1	1	6	471	484	4	4	6	189	-217
2	2	5	385	440	-3	5	5	281	287	4	8	5	248	-234	2	1	6	425	427	5	4	6	109	-111
3	2	5	75	64	-2	5	5	104	76	6	8	5	107	131	8	1	6	173	195	6	4	6	126	-154
4	2	5	278	-231	-1	5	5	173	-155	-9	9	5	107	53	9	1	6	97	76	7	4	6	153	156
5	2	5	148	143	0	5	5	494	-474	-6	9	5	116	109	-9	2	6	101	97	-9	5	6	95	-66
6	2	5	111	84	1	5	5	181	-178	-5	9	5	84	-58	-8	2	6	109	92	-7	5	6	268	259
7	2	5	147	162	2	5	5	242	279	-1	9	5	147	145	-7	2	6	167	-132	-3	5	6	162	162
9	2	5	90	-110	3	5	5	212	219	0	9	5	144	-159	-4	2	6	347	-328	0	5	6	162	-197
11	2	5	117	118	4	5	5	134	145	1	9	5	202	-199	-3	2	6	124	109	5	5	6	90	78
-9	3	5	176	185	5	5	5	108	-115	2	9	5	154	183	-1	2	6	720	-721	6	5	6	79	-64
-8	3	5	140	-135	7	5	5	145	-141	6	9	5	165	-184	1	2	6	181	138	7	5	6	92	43
-7	3	5	98	-66	-8	6	5	120	-109	3	10	5	117	-128	2	2	6	71	-95	9	5	6	110	-106
-6	3	5	108	94	-6	6	5	122	137	4	10	5	113	136	3	2	6	69	-84	-7	6	6	156	-156
-4	3	5	117	97	-5	6	5	303	-335	5	10	5	97	75	4	2	6	121	-85	-6	6	6	222	247
-3	3	5	143	112	-4	6	5	182	-171	-8	11	5	124	-98	5	2	6	171	-186	-5	6	6	254	248
-2	3	5	170	175	1	6	5	70	-45	-8	0	6	112	129	6	2	6	144	-129	-4	6	6	154	-141
-1	3	5	113	-66	2	6	5	105	-138	-7	0	6	84	-62	9	2	6	133	142	-2	6	6	257	-259
0	3	5	599	-558	4	6	5	127	121	-6	0	6	165	-148	-9	3	6	85	68	-1	6	6	101	86

h	k	l	10Fo	10Fc	h	k	l	10Fo	10Fc	h	k	l	10Fo	10Fc	h	k	l	10Fo	10Fc	h	k	l	10Fo	10Fc
0	6	6	199	184	1	1	7	467	473	3	4	7	144	135	2	8	7	170	170	-1	1	8	336	-362
1	6	6	74	37	2	1	7	79	111	4	4	7	219	245	3	8	7	181	159	0	1	8	193	302
2	6	6	227	228	3	1	7	66	-54	-10	5	7	109	-133	4	8	7	241	-236	1	1	8	393	415
3	6	6	83	103	4	1	7	198	-198	-9	5	7	100	-80	-3	9	7	100	96	2	1	8	98	-102
5	6	6	104	-111	6	1	7	118	128	-4	5	7	242	-243	-2	9	7	127	-159	4	1	8	269	238
6	6	6	153	-147	8	1	7	118	-126	-2	5	7	171	158	1	9	7	189	-178	6	1	8	175	-176
7	6	6	146	142	-8	2	7	128	-168	-1	5	7	86	-91	6	9	7	150	-141	7	1	8	178	184
-7	7	6	102	-113	-5	2	7	219	-194	0	5	7	512	473	-4	10	7	96	117	-8	2	8	96	83
0	7	6	208	-208	-3	2	7	91	65	1	5	7	110	111	-2	10	7	125	-120	-7	2	8	128	133
2	7	6	112	114	-2	2	7	269	-223	2	5	7	319	-337	-1	10	7	111	107	-6	2	8	77	-72
3	7	6	151	155	-1	2	7	354	-329	4	5	7	140	-109	2	10	7	103	-113	-5	2	8	91	-76
5	7	6	154	-155	0	2	7	221	-206	5	5	7	146	164	4	10	7	98	81	-4	2	8	325	-323
6	7	6	115	125	1	2	7	506	-521	-8	6	7	90	-76	-2	11	7	117	88	-3	2	8	68	82
-7	8	6	131	-163	2	2	7	324	322	-6	6	7	125	-116	-10	0	8	115	-98	-2	2	8	341	333
-2	8	6	140	-137	5	2	7	76	64	-5	6	7	148	-130	-9	0	8	119	-135	-1	2	8	548	-541
0	8	6	151	154	6	2	7	93	100	-3	6	7	82	-61	-8	0	8	95	-95	0	2	8	104	-99
1	8	6	305	-311	7	2	7	96	-115	-2	6	7	163	-173	-7	0	8	91	87	1	2	8	232	239
2	8	6	230	-237	10	2	7	112	-75	-1	6	7	85	-72	-6	0	8	402	435	2	2	8	389	-392
3	8	6	259	279	-8	3	7	135	138	0	6	7	80	69	-4	0	8	259	-215	4	2	8	136	-124
4	8	6	106	-90	-7	3	7	158	171	2	6	7	128	133	-2	0	8	250	231	5	2	8	175	-206
5	8	6	96	-116	-4	3	7	175	-154	5	6	7	149	-138	-1	0	8	618	602	6	2	8	252	279
9	8	6	106	113	-3	3	7	310	289	7	6	7	153	170	0	0	8	390	-394	8	2	8	224	-230
-6	9	6	93	79	-2	3	7	158	141	-8	7	7	95	75	1	0	8	667	672	-7	3	8	135	-144
1	9	6	170	-167	-1	3	7	69	-86	-7	7	7	90	-71	2	0	8	179	183	-6	3	8	146	164
2	9	6	131	125	1	3	7	113	-132	-5	7	7	183	192	4	0	8	381	-335	-3	3	8	227	240
4	9	6	137	-125	3	3	7	202	-172	-4	7	7	192	-195	5	0	8	114	87	-2	3	8	379	-327
7	9	6	115	-104	4	3	7	87	-92	-2	7	7	91	-75	6	0	8	211	233	0	3	8	292	238
-4	10	6	91	-71	8	3	7	195	203	-1	7	7	179	-164	7	0	8	232	246	1	3	8	525	-575
-3	10	6	100	90	-6	4	7	146	152	0	7	7	236	224	9	0	8	182	-177	2	3	8	322	305
2	10	6	111	135	-5	4	7	79	-87	1	7	7	209	219	-10	1	8	111	111	3	3	8	245	237
-7	1	7	127	-167	-4	4	7	270	251	2	7	7	122	-106	-8	1	8	104	-107	4	3	8	498	-514
-4	1	7	166	116	-2	4	7	216	210	4	7	7	140	-140	-6	1	8	88	-76	5	3	8	76	-48
-3	1	7	73	88	-1	4	7	364	378	5	7	7	124	-114	-5	1	8	148	-151	7	3	8	159	-170
-2	1	7	164	-180	0	4	7	141	-120	6	7	7	228	232	-4	1	8	439	413	10	3	8	108	-122
-1	1	7	716	-693	1	4	7	156	-149	-6	8	7	172	171	-3	1	8	102	84	-8	4	8	152	147
0	1	7	818	819	2	4	7	82	48	-3	8	7	129	141	-2	1	8	133	-98	-7	4	8	86	-72

h	k	l	10Fo	10Fc	h	k	l	10Fo	10Fc	h	k	l	10Fo	10Fc	h	k	l	10Fo	10Fc	h	k	l	10Fo	10Fc
-6	4	8	146	-148	1	8	8	114	-77	-4	3	9	80	59	-8	7	9	114	119	-3	0	10	578	570
-4	4	8	114	110	2	8	8	205	-203	-2	3	9	102	97	-7	7	9	182	-207	-2	0	10	70	-30
-3	4	8	90	-94	5	8	8	177	-187	0	3	9	201	-228	-5	7	9	140	152	-1	0	10	939	-935
-1	4	8	212	189	6	8	8	136	149	1	3	9	379	-375	-4	7	9	229	-237	1	0	10	242	-209
1	4	8	123	-126	-3	9	8	215	253	2	3	9	69	86	-2	7	9	242	225	2	0	10	264	297
2	4	8	86	115	-2	9	8	179	-163	3	3	9	170	174	-1	7	9	255	-271	3	0	10	323	326
4	4	8	146	130	0	9	8	173	157	4	3	9	168	-193	0	7	9	245	224	4	0	10	253	196
5	4	8	138	126	3	9	8	99	-77	7	3	9	117	105	1	7	9	235	255	7	0	10	105	119
6	4	8	125	-95	7	9	8	96	-111	-9	4	9	103	126	2	7	9	395	-416	9	0	10	107	-93
7	4	8	126	-123	-1	10	8	106	109	-7	4	9	120	125	4	7	9	158	136	-10	1	10	94	60
-6	5	8	230	252	1	10	8	97	74	-6	4	9	224	234	5	7	9	106	-95	-7	1	10	133	144
-5	5	8	96	-113	-6	1	9	135	-167	-4	4	9	108	-94	-8	8	9	98	69	-6	1	10	129	-152
-4	5	8	196	-185	-5	1	9	177	-141	-3	4	9	133	125	-6	8	9	110	90	-4	1	10	120	124
-3	5	8	79	70	-4	1	9	342	-320	-2	4	9	122	123	-5	8	9	99	-94	-3	1	10	84	-58
-2	5	8	100	94	-3	1	9	344	350	-1	4	9	414	445	-3	8	9	305	323	-1	1	10	383	398
1	5	8	96	-84	-2	1	9	382	354	0	4	9	271	241	-1	8	9	212	-202	1	1	10	361	-367
2	5	8	108	116	-1	1	9	203	207	1	4	9	159	-149	0	8	9	279	263	2	1	10	93	58
4	5	8	80	61	1	1	9	187	-213	3	4	9	100	105	1	8	9	214	-191	3	1	10	213	202
6	5	8	92	-84	2	1	9	224	-226	4	4	9	103	-76	2	8	9	92	94	4	1	10	292	283
-9	6	8	91	26	3	1	9	136	-147	-6	5	9	149	-144	3	8	9	282	285	5	1	10	171	-177
-7	6	8	96	-84	4	1	9	192	199	-5	5	9	123	124	4	8	9	221	-226	7	1	10	102	118
-6	6	8	247	273	8	1	9	88	-92	-4	5	9	93	84	5	8	9	102	-71	-9	2	10	111	-133
-4	6	8	134	-125	9	1	9	92	-88	-2	5	9	134	-145	6	8	9	168	168	-6	2	10	158	-171
-3	6	8	92	91	-6	2	9	92	118	-1	5	9	92	102	-9	9	9	104	58	-5	2	10	161	177
-2	6	8	170	160	-5	2	9	181	-175	0	5	9	140	163	-5	9	9	125	-137	-2	2	10	450	433
6	6	8	117	122	-4	2	9	277	-259	4	5	9	99	-88	-1	9	9	223	228	-1	2	10	504	-499
-5	7	8	93	-111	-3	2	9	203	153	6	5	9	80	98	1	9	9	302	-326	0	2	10	414	-431
-3	7	8	115	-111	-2	2	9	505	-485	9	5	9	101	51	3	9	9	96	83	1	2	10	217	203
-1	7	8	93	94	-1	2	9	215	-223	-7	6	9	118	-151	-3	10	9	111	-103	2	2	10	350	-364
0	7	8	131	-139	1	2	9	148	-152	-4	6	9	165	-175	-5	11	9	93	60	4	2	10	97	127
-6	8	8	99	47	3	2	9	423	416	-3	6	9	158	-143	-2	11	9	102	73	7	2	10	129	-119
-5	8	8	115	107	4	2	9	213	-219	-2	6	9	88	86	-8	0	10	100	-110	-8	3	10	95	-94
-4	8	8	152	-190	5	2	9	125	-85	-1	6	9	108	124	-7	0	10	86	-110	-7	3	10	224	-247
-2	8	8	187	171	6	2	9	92	100	0	6	9	173	-180	-6	0	10	91	-125	-6	3	10	223	217
-1	8	8	212	-221	-9	3	9	164	158	3	6	9	122	-115	-5	0	10	116	-94	-5	3	10	140	128
0	8	8	89	92	-8	3	9	97	109	8	6	9	103	122	-4	0	10	675	660	-4	3	10	307	-315

h	k	l	10Fo	10Fc	h	k	l	10Fo	10Fc	h	k	l	10Fo	10Fc	h	k	l	10Fo	10Fc	h	k	l	10Fo	10Fc
-3	3	10	136	125	7	7	10	99	102	-2	2	11	134	-128	4	5	11	195	199	1	0	12	257	-263
-2	3	10	160	182	-6	8	10	148	-177	-1	2	11	599	-585	6	5	11	120	110	2	0	12	285	238
-1	3	10	192	-179	-5	8	10	201	232	0	2	11	106	73	-8	6	11	115	-128	4	0	12	124	-90
0	3	10	240	236	-4	8	10	91	69	1	2	11	199	173	-6	6	11	118	-119	5	0	12	92	-92
1	3	10	362	-348	-1	8	10	192	-202	2	2	11	212	200	-5	6	11	102	-86	6	0	12	247	260
2	3	10	194	-195	0	8	10	97	-103	4	2	11	205	-192	-1	6	11	78	-39	7	0	12	123	151
3	3	10	313	306	1	8	10	111	84	5	2	11	123	-117	1	6	11	223	-231	9	0	12	92	-92
4	3	10	182	-177	2	8	10	331	-347	9	2	11	93	90	2	6	11	173	-203	-2	1	12	128	98
5	3	10	167	-160	4	8	10	188	180	-7	3	11	259	270	4	6	11	118	115	1	1	12	286	314
6	3	10	83	61	5	8	10	97	-97	-6	3	11	215	228	-5	7	11	203	218	2	1	12	89	-80
7	3	10	159	-159	-2	9	10	92	-37	-5	3	11	180	-180	-3	7	11	166	-159	3	1	12	104	-96
-6	4	10	99	-62	0	9	10	181	167	-4	3	11	145	-134	-2	7	11	116	126	5	1	12	137	140
-5	4	10	138	-138	1	9	10	106	-72	-3	3	11	192	168	-1	7	11	188	-174	7	1	12	121	133
-3	4	10	81	70	2	9	10	200	-203	-2	3	11	144	120	1	7	11	196	196	8	1	12	120	128
-1	4	10	176	215	3	9	10	133	126	-1	3	11	109	-97	2	7	11	120	-114	-9	2	12	119	112
0	4	10	253	227	4	9	10	90	-92	0	3	11	442	-444	4	7	11	119	120	-6	2	12	97	64
1	4	10	232	-211	10	9	10	107	-64	1	3	11	200	-207	5	7	11	189	-197	-5	2	12	83	-90
2	4	10	119	-122	3	10	10	92	78	4	3	11	98	127	8	7	11	117	-105	-4	2	12	114	-108
3	4	10	157	135	5	10	10	85	38	7	3	11	93	-73	-7	8	11	141	-130	-3	2	12	76	50
4	4	10	101	-89	-10	1	11	106	-93	-7	4	11	100	75	-4	8	11	130	-108	-2	2	12	92	90
-11	5	10	111	82	-6	1	11	114	103	-6	4	11	269	283	-3	8	11	184	176	-1	2	12	120	-142
-8	5	10	92	90	-5	1	11	110	108	-2	4	11	154	165	0	8	11	116	113	0	2	12	101	-97
-7	5	10	175	156	-4	1	11	129	126	-1	4	11	361	370	3	8	11	150	130	1	2	12	123	143
-5	5	10	97	-74	-3	1	11	81	-64	0	4	11	141	144	4	8	11	109	-113	2	2	12	118	-114
0	5	10	145	122	-2	1	11	256	-233	1	4	11	98	-70	6	8	11	118	146	3	2	12	96	-94
-11	6	10	108	112	-1	1	11	217	-204	2	4	11	99	-65	7	8	11	137	-130	4	2	12	105	96
-5	6	10	124	132	0	1	11	168	-188	4	4	11	115	107	-2	9	11	113	-104	5	2	12	122	-140
-3	6	10	104	89	1	1	11	596	582	5	4	11	102	-85	2	9	11	106	143	-4	3	12	307	-310
0	6	10	121	129	2	1	11	229	214	-8	5	11	156	-173	3	9	11	104	-57	-3	3	12	245	221
1	6	10	84	119	4	1	11	201	-234	-6	5	11	164	141	1	11	11	95	103	-2	3	12	278	265
2	6	10	171	-166	5	1	11	150	-175	-4	5	11	112	87	-10	0	12	173	-204	-1	3	12	134	-99
5	6	10	112	107	7	1	11	100	124	-3	5	11	192	-167	-5	0	12	134	138	1	3	12	163	-135
-9	7	10	131	97	-9	2	11	91	107	-2	5	11	104	103	-4	0	12	377	-347	2	3	12	231	-231
-3	7	10	100	-103	-7	2	11	115	-150	0	5	11	71	-81	-3	0	12	290	-267	3	3	12	120	93
-1	7	10	133	128	-5	2	11	174	-178	1	5	11	142	138	-2	0	12	297	-293	4	3	12	222	-197
2	7	10	107	83	-4	2	11	145	-126	2	5	11	166	-156	-1	0	12	828	775	6	3	12	156	160

h	k	l	10Fo	10Fc	h	k	l	10Fo	10Fc	h	k	l	10Fo	10Fc	h	k	l	10Fo	10Fc	h	k	l	10Fo	10Fc
10	3	12	123	-113	-1	10	12	108	104	-6	5	13	170	-184	-2	0	14	171	149	-5	4	14	275	304
-10	4	12	105	-90	0	10	12	102	101	-4	5	13	157	159	-1	0	14	424	-403	-3	4	14	179	-186
-8	4	12	112	117	2	10	12	111	-97	-3	5	13	298	298	1	0	14	424	426	-2	4	14	166	-153
-5	4	12	266	-261	3	10	12	95	-87	-1	5	13	206	-220	3	0	14	154	152	-1	4	14	91	-60
-3	4	12	129	134	4	10	12	123	97	2	5	13	125	132	5	0	14	116	-109	0	4	14	136	140
-1	4	12	247	242	-7	1	13	118	-122	3	5	13	220	218	7	0	14	202	180	1	4	14	192	187
1	4	12	200	-187	-4	1	13	182	-174	4	5	13	117	136	8	0	14	129	-127	2	4	14	119	127
-5	5	12	136	157	-2	1	13	109	110	6	5	13	128	-99	-4	1	14	201	219	5	4	14	157	-174
-3	5	12	104	-95	0	1	13	354	374	-9	6	13	123	-121	-3	1	14	113	84	6	4	14	88	-76
-2	5	12	92	-82	1	1	13	240	-252	-7	6	13	97	111	-1	1	14	253	-251	-3	5	14	89	-56
0	5	12	160	157	2	1	13	74	-65	-3	6	13	148	-166	1	1	14	146	-160	0	5	14	132	140
2	5	12	172	-180	-7	2	13	157	-156	1	6	13	117	-106	3	1	14	341	313	1	5	14	80	74
3	5	12	108	81	-6	2	13	155	-183	5	6	13	153	-143	4	1	14	158	159	2	5	14	87	-89
4	5	12	117	113	-4	2	13	111	-95	-7	7	13	137	-122	5	1	14	162	-171	4	5	14	121	112
5	5	12	83	30	-2	2	13	133	-110	-5	7	13	191	214	9	1	14	122	130	-9	6	14	121	-99
-7	6	12	105	-102	-1	2	13	89	-95	0	7	13	78	-59	-9	2	14	114	-98	-6	6	14	95	88
-6	6	12	130	146	1	2	13	132	-116	1	7	13	166	154	-7	2	14	134	115	-5	6	14	117	108
-4	6	12	190	-167	2	2	13	164	-164	2	7	13	176	-176	-6	2	14	125	101	-2	6	14	155	-177
7	6	12	94	65	4	2	13	227	222	3	7	13	105	-110	-4	2	14	188	-154	-1	6	14	300	-312
-8	7	12	151	-150	7	2	13	147	-165	5	7	13	122	73	-3	2	14	81	60	0	6	14	95	95
-6	7	12	182	178	-11	3	13	124	105	-7	8	13	112	-86	-2	2	14	92	105	1	6	14	351	383
-2	7	12	105	-120	-8	3	13	132	122	-3	8	13	120	107	1	2	14	80	-74	2	6	14	135	151
2	7	12	131	118	-3	3	13	248	240	-1	8	13	172	-178	3	2	14	94	101	3	6	14	90	-85
3	7	12	179	189	-1	3	13	235	-223	0	8	13	105	115	7	2	14	99	-81	4	6	14	98	-82
-8	8	12	122	76	0	3	13	222	-197	1	8	13	124	113	9	2	14	100	116	-9	7	14	137	130
-5	8	12	94	90	1	3	13	114	-123	3	8	13	126	117	-9	3	14	123	-139	-5	7	14	90	-88
-4	8	12	97	73	3	3	13	127	117	5	8	13	97	-87	-7	3	14	113	-122	2	7	14	110	95
-3	8	12	271	-288	6	3	13	107	-122	-5	9	13	107	-128	-6	3	14	119	105	-7	8	14	123	103
-1	8	12	102	103	-6	4	13	117	113	-1	9	13	123	100	-5	3	14	245	237	0	8	14	119	-113
0	8	12	95	-78	-5	4	13	219	231	1	9	13	156	-148	-3	3	14	272	-261	2	9	14	92	-92
1	8	12	79	-30	-4	4	13	126	106	-1	10	13	110	102	2	3	14	88	-69	7	11	14	105	-48
8	8	12	97	-60	-2	4	13	149	146	1	10	13	93	-72	4	3	14	107	108	-7	1	15	107	-134
-2	9	12	134	127	0	4	13	73	53	-7	0	14	103	-92	7	3	14	163	-169	-4	1	15	242	-233
-1	9	12	139	-119	1	4	13	79	47	-5	0	14	133	-167	-8	4	14	119	-124	-3	1	15	173	174
1	9	12	88	-68	3	4	13	113	97	-4	0	14	160	-173	-7	4	14	194	-199	-2	1	15	157	168
5	9	12	93	-68	-7	5	13	97	-99	-3	0	14	110	117	-6	4	14	161	170	3	1	15	122	133

h	k	l	10Fo	10Fc	h	k	l	10Fo	10Fc	h	k	l	10Fo	10Fc	h	k	l	10Fo	10Fc	h	k	l	10Fo	10Fc
5	1	15	192	-178	-2	6	15	112	-75	-1	2	16	110	-102	-7	7	16	128	-104	-2	5	17	108	71
7	1	15	159	139	-1	6	15	112	-112	2	2	16	232	-235	-4	7	16	106	-111	-1	5	17	246	-252
-7	2	15	111	-109	1	6	15	114	120	5	2	16	101	98	-2	8	16	95	-113	0	5	17	169	-151
-5	2	15	92	-70	2	6	15	202	-190	-7	3	16	89	29	4	8	16	96	-45	1	5	17	135	133
-2	2	15	199	-195	3	6	15	135	-126	-1	3	16	105	-89	0	11	16	103	67	2	5	17	135	113
3	2	15	175	159	5	6	15	101	81	5	3	16	124	-137	-5	1	17	257	258	3	5	17	186	185
4	2	15	133	-132	-1	7	15	84	-88	-8	4	16	107	107	-3	1	17	175	-153	4	5	17	89	105
5	2	15	119	-114	0	7	15	156	150	-6	4	16	186	-217	-2	1	17	234	222	-4	6	17	87	59
-9	3	15	119	101	2	7	15	96	-79	-5	4	16	150	-172	-1	1	17	150	-194	1	6	17	146	-129
-8	3	15	134	145	3	7	15	81	-78	-4	4	16	132	-140	1	1	17	197	218	3	6	17	131	129
-6	3	15	103	109	7	7	15	136	110	-3	4	16	193	204	2	1	17	126	-151	5	6	17	120	-110
-4	3	15	284	-309	0	8	15	93	82	-2	4	16	387	405	-9	2	17	135	135	-5	7	17	97	106
-3	3	15	132	-142	1	8	15	82	-56	-1	4	16	218	231	-7	2	17	114	-119	-7	8	17	104	-70
-1	3	15	91	67	2	8	15	94	56	0	4	16	86	-97	-5	2	17	119	-133	4	8	17	74	34
0	3	15	108	79	-6	10	15	105	63	1	4	16	438	-433	-1	2	17	89	-86	1	9	17	144	117
3	3	15	169	-162	-7	0	16	105	-118	2	4	16	232	-239	0	2	17	221	228	2	10	17	143	-134
4	3	15	173	-187	-6	0	16	222	-236	3	4	16	137	114	3	2	17	147	-170	0	11	17	87	57
-8	4	15	89	32	-5	0	16	232	249	4	4	16	85	110	-7	3	17	134	103	-6	0	18	103	-91
-7	4	15	131	147	-3	0	16	181	-176	5	4	16	118	112	-3	3	17	103	90	-5	0	18	171	159
-2	4	15	104	122	-1	0	16	210	-200	-5	5	16	100	89	-1	3	17	114	-126	-4	0	18	112	-116
-1	4	15	212	212	0	0	16	129	135	-4	5	16	93	78	0	3	17	203	-207	-3	0	18	489	-487
3	4	15	81	50	1	0	16	108	85	-3	5	16	99	-123	3	3	17	147	143	-2	0	18	196	193
-10	5	15	110	-94	4	0	16	280	245	-2	5	16	101	-76	4	3	17	143	155	-1	0	18	264	282
-8	5	15	137	125	5	0	16	261	-258	-1	5	16	139	146	6	3	17	90	-88	0	0	18	440	-447
-6	5	15	174	178	7	0	16	204	201	0	5	16	198	190	7	3	17	166	-169	1	0	18	415	404
-4	5	15	273	-273	8	0	16	105	-123	2	5	16	134	-135	-8	4	17	94	56	3	0	18	241	-246
-3	5	15	371	-365	-8	1	16	92	95	3	5	16	111	-89	-4	4	17	95	88	4	0	18	201	179
-1	5	15	410	401	-5	1	16	97	100	4	5	16	102	104	-3	4	17	134	-175	7	0	18	153	164
0	5	15	315	324	-4	1	16	155	-148	7	5	16	97	-47	-1	4	17	177	178	-2	1	18	108	125
1	5	15	151	132	3	1	16	225	222	-6	6	16	188	-200	0	4	17	142	123	-1	1	18	388	-404
2	5	15	99	-96	5	1	16	168	-174	-3	6	16	115	100	3	4	17	167	-172	1	1	18	166	227
3	5	15	274	-252	6	1	16	161	169	-2	6	16	128	146	5	4	17	88	81	2	1	18	222	-247
6	5	15	129	149	9	1	16	122	103	2	6	16	187	-188	-8	5	17	98	-100	3	1	18	105	65
-7	6	15	147	-116	-4	2	16	115	-126	3	6	16	86	-65	-5	5	17	93	100	4	1	18	111	135
-5	6	15	107	65	-3	2	16	128	114	4	6	16	112	121	-4	5	17	162	167	-7	2	18	97	104
-3	6	15	90	-123	-2	2	16	204	214	5	6	16	113	100	-3	5	17	90	74	2	2	18	90	-89

h	k	l	10Fo	10Fc	h	k	l	10Fo	10Fc	h	k	l	10Fo	10Fc	h	k	l	10Fo	10Fc	h	k	l	10Fo	10Fc
3	2	18	104	127	-10	1	19	101	50	-2	10	19	128	105	7	2	20	108	-106	3	3	21	116	-97
5	2	18	125	-146	-2	1	19	117	148	-6	0	20	188	-216	-4	4	20	91	-88	6	3	21	96	-84
3	3	18	86	-89	4	1	19	169	190	-4	0	20	311	339	3	4	20	88	93	-3	4	21	87	53
5	3	18	185	189	-7	2	19	110	-138	-3	0	20	194	-187	-4	5	20	115	122	-2	4	21	106	-101
7	3	18	114	-101	1	2	19	80	-65	0	0	20	134	-132	-3	5	20	94	69	1	5	21	147	153
8	3	18	116	-104	4	2	19	101	126	1	0	20	158	159	-2	5	20	100	-97	5	7	21	105	-113
-5	4	18	103	138	6	2	19	141	-114	2	0	20	104	135	0	5	20	92	92	-6	0	22	115	-116
-3	4	18	128	-170	-9	3	19	117	98	4	0	20	167	173	-4	6	20	106	101	-3	0	22	168	-182
5	4	18	98	-76	2	3	19	135	-119	6	0	20	154	-157	1	6	20	140	144	-2	0	22	106	-113
6	4	18	101	42	9	3	19	101	-37	7	0	20	103	104	-1	7	20	95	-97	-1	0	22	277	305
-3	5	18	96	-93	-8	4	19	106	-95	9	0	20	97	-46	-2	8	20	88	-28	3	0	22	129	-120
-2	5	18	91	-64	-4	4	19	118	112	-8	1	20	116	120	0	10	20	95	-57	0	1	22	115	-115
-1	5	18	148	169	2	4	19	85	77	-6	1	20	146	-164	-5	1	21	92	102	-4	2	22	87	-72
-1	6	18	93	-96	-1	5	19	90	89	-3	1	20	90	-105	-3	1	21	99	-129	0	2	22	114	126
1	6	18	216	228	4	5	19	129	123	3	1	20	110	118	-2	1	21	99	-95	3	2	22	93	-87
2	6	18	99	63	6	6	19	99	121	4	1	20	102	116	1	1	21	100	140	0	5	22	108	117
3	6	18	109	-117	-3	8	19	102	97	5	1	20	152	-174	-7	2	21	137	-139	7	6	22	102	79
-3	9	18	105	98	-1	9	19	109	109	6	2	20	96	-60	-4	3	21	91	-75	-4	10	22	118	-81

16-benzylidenyl-6-benzyloxy-3-dehydro-3,5-epiandrosterone, $C_{33}H_{38}O_2$

h	k	l	10Fo	10Fc	h	k	l	10Fo	10Fc	h	k	l	10Fo	10Fc	h	k	l	10Fo	10Fc	h	k	l	10Fo	10Fc
1	0	0	224	240	3	3	0	57	54	8	6	0	60	50	7	0	1	27	7	3	2	1	80	72
2	0	0	300	301	4	3	0	185	175	9	6	0	45	44	9	0	1	68	69	4	2	1	186	180
3	0	0	125	119	5	3	0	91	79	1	7	0	28	34	12	0	1	41	43	5	2	1	61	53
4	0	0	97	113	6	3	0	64	34	2	7	0	63	69	13	0	1	39	22	6	2	1	91	70
5	0	0	181	183	8	3	0	82	89	3	7	0	105	110	-10	1	1	51	57	7	2	1	79	74
6	0	0	106	89	9	3	0	126	131	4	7	0	35	40	-8	1	1	229	238	8	2	1	77	81
7	0	0	142	128	11	3	0	40	34	5	7	0	62	67	-7	1	1	95	92	9	2	1	68	74
8	0	0	176	176	0	4	0	856	825	6	7	0	29	26	-6	1	1	133	103	10	2	1	34	38
9	0	0	42	40	1	4	0	369	355	9	7	0	34	21	-5	1	1	91	95	-13	3	1	40	21
10	0	0	73	68	2	4	0	283	281	0	8	0	68	66	-4	1	1	61	71	-11	3	1	37	32
12	0	0	66	68	3	4	0	170	163	1	8	0	47	48	-3	1	1	423	417	-9	3	1	43	59
1	1	0	271	272	4	4	0	48	40	2	8	0	34	36	-2	1	1	486	504	-8	3	1	101	116
2	1	0	950	957	5	4	0	130	129	3	8	0	62	59	-1	1	1	251	266	-7	3	1	37	36
3	1	0	390	411	6	4	0	118	104	5	8	0	39	33	0	1	1	635	605	-6	3	1	139	150
4	1	0	147	144	7	4	0	50	43	6	8	0	30	31	1	1	1	778	782	-5	3	1	89	93
5	1	0	274	271	8	4	0	63	76	4	9	0	59	63	2	1	1	271	280	-4	3	1	155	158
6	1	0	225	222	9	4	0	34	37	1	11	0	35	8	3	1	1	336	339	-3	3	1	78	74
7	1	0	79	76	10	4	0	30	28	5	11	0	37	17	4	1	1	342	345	-2	3	1	121	137
8	1	0	78	88	12	4	0	36	30	-12	0	1	48	44	5	1	1	288	273	-1	3	1	62	71
9	1	0	165	161	1	5	0	82	80	-11	0	1	43	43	6	1	1	89	86	0	3	1	596	562
12	1	0	41	38	2	5	0	272	279	-9	0	1	155	156	7	1	1	41	36	1	3	1	336	340
1	2	0	840	857	3	5	0	65	62	-8	0	1	177	180	8	1	1	39	38	2	3	1	168	178
2	2	0	201	201	4	5	0	65	68	-7	0	1	150	159	9	1	1	46	55	3	3	1	139	124
3	2	0	166	168	5	5	0	77	74	-6	0	1	224	231	12	1	1	60	48	4	3	1	108	102
4	2	0	119	118	6	5	0	38	48	-5	0	1	132	151	-10	2	1	40	39	5	3	1	192	184
5	2	0	199	194	7	5	0	53	52	-4	0	1	202	215	-9	2	1	166	175	6	3	1	86	68
6	2	0	100	91	8	5	0	57	66	-3	0	1	292	306	-8	2	1	46	34	7	3	1	53	55
7	2	0	96	89	9	5	0	52	51	-2	0	1	222	204	-7	2	1	53	55	8	3	1	38	40
8	2	0	98	102	0	6	0	327	311	-1	0	1	103	100	-6	2	1	67	60	10	3	1	51	43
9	2	0	55	59	1	6	0	150	151	0	0	1	43	69	-4	2	1	57	60	-9	4	1	104	114
10	2	0	34	29	2	6	0	92	92	1	0	1	307	329	-3	2	1	86	93	-8	4	1	54	59
11	2	0	44	35	3	6	0	108	106	2	0	1	303	320	-2	2	1	431	424	-7	4	1	45	52
12	2	0	40	45	4	6	0	101	94	3	0	1	179	197	-1	2	1	97	95	-6	4	1	97	101
13	2	0	41	28	5	6	0	86	81	4	0	1	174	165	0	2	1	415	400	-5	4	1	83	77
1	3	0	367	384	6	6	0	27	13	5	0	1	37	21	1	2	1	339	350	-3	4	1	76	69
2	3	0	190	206	7	6	0	32	34	6	0	1	285	283	2	2	1	60	52	-2	4	1	80	89

h	k	l	10Fo	10Fo	h	k	l	10Fo	10Fc	h	k	l	10Fo	10Fc	h	k	l	10Fo	10Fc	h	k	l	10Fo	10Fc
-1	4	1	37	39	1	6	1	158	153	-4	9	1	35	39	1	1	2	79	77	-5	3	2	76	83
0	4	1	187	179	2	6	1	72	74	-2	9	1	32	21	2	1	2	358	368	-4	3	2	48	57
1	4	1	301	307	3	6	1	45	45	0	9	1	33	28	3	1	2	351	348	-3	3	2	175	181
2	4	1	201	209	4	6	1	61	69	1	9	1	70	70	4	1	2	189	178	-2	3	2	34	35
3	4	1	172	168	5	6	1	79	80	2	9	1	63	71	5	1	2	189	177	-1	3	2	201	205
4	4	1	73	65	6	6	1	116	112	-4	10	1	35	30	6	1	2	39	30	0	3	2	111	93
5	4	1	67	65	7	6	1	52	53	-1	11	1	37	18	8	1	2	67	71	1	3	2	97	100
6	4	1	89	86	8	6	1	85	81	-10	0	2	75	71	12	1	2	57	41	2	3	2	151	151
8	4	1	67	68	9	6	1	33	31	-8	0	2	66	63	-12	2	2	39	18	3	3	2	134	130
9	4	1	82	82	11	6	1	47	34	-7	0	2	129	128	-10	2	2	46	47	4	3	2	155	143
12	4	1	44	29	-8	7	1	34	38	-6	0	2	117	60	-8	2	2	43	46	5	3	2	102	91
-10	5	1	38	33	-7	7	1	39	38	-4	0	2	38	36	-7	2	2	81	80	6	3	2	84	73
-8	5	1	101	105	-6	7	1	34	19	-3	0	2	330	328	-6	2	2	122	121	7	3	2	66	59
-7	5	1	40	32	-5	7	1	109	121	-2	0	2	884	900	-5	2	2	137	141	8	3	2	48	47
-5	5	1	91	87	-4	7	1	33	26	-1	0	2	414	427	-4	2	2	213	222	9	3	2	36	35
-4	5	1	34	27	-3	7	1	74	75	0	0	2	807	787	-3	2	2	165	171	-10	4	2	46	44
-3	5	1	119	122	-1	7	1	56	56	1	0	2	597	590	-2	2	2	154	173	-9	4	2	46	58
-2	5	1	94	92	0	7	1	75	74	2	0	2	109	107	-1	2	2	68	83	-8	4	2	74	89
-1	5	1	148	141	1	7	1	130	128	3	0	2	202	206	0	2	2	481	466	-6	4	2	48	32
0	5	1	433	406	2	7	1	86	91	4	0	2	387	385	1	2	2	194	201	-5	4	2	79	76
1	5	1	278	286	3	7	1	114	120	5	0	2	115	97	2	2	2	395	388	-4	4	2	90	77
2	5	1	97	108	4	7	1	55	64	6	0	2	85	68	3	2	2	192	182	-3	4	2	175	175
3	5	1	131	131	5	7	1	84	82	8	0	2	36	41	4	2	2	159	153	-2	4	2	95	90
4	5	1	128	130	6	7	1	71	62	9	0	2	95	94	5	2	2	153	167	-1	4	2	129	126
5	5	1	55	56	7	7	1	40	33	12	0	2	59	55	6	2	2	52	48	0	4	2	165	169
6	5	1	30	17	-4	8	1	51	58	13	0	2	41	25	7	2	2	87	94	1	4	2	162	161
7	5	1	107	103	-3	8	1	53	63	-9	1	2	159	166	8	2	2	118	117	2	4	2	29	34
8	5	1	76	73	-2	8	1	34	34	-8	1	2	285	299	9	2	2	56	66	3	4	2	122	98
-9	6	1	42	43	-1	8	1	38	37	-7	1	2	57	51	10	2	2	71	74	4	4	2	27	33
-8	6	1	90	86	1	8	1	48	59	-6	1	2	98	90	11	2	2	49	42	5	4	2	104	105
-7	6	1	59	61	2	8	1	44	45	-5	1	2	97	114	12	2	2	40	31	6	4	2	57	47
-6	6	1	52	61	3	8	1	69	69	-4	1	2	272	288	-10	3	2	43	42	7	4	2	98	94
-3	6	1	105	103	4	8	1	81	85	-3	1	2	194	202	-9	3	2	111	122	8	4	2	35	32
-2	6	1	63	64	5	8	1	38	32	-2	1	2	426	435	-8	3	2	133	143	9	4	2	42	49
-1	6	1	91	89	6	8	1	32	6	-1	1	2	439	440	-7	3	2	72	74	10	4	2	35	42
0	6	1	48	45	-5	9	1	36	26	0	1	2	683	679	-6	3	2	53	44	-9	5	2	59	63

h	k	l	10Fo	10Fo	h	k	l	10Fo	10Fc	h	k	l	10Fo	10Fc	h	k	l	10Fo	10Fc	h	k	l	10Fo	10Fc
-8	5	2	97	104	-1	7	2	66	55	8	0	3	41	42	5	2	3	38	22	6	4	3	59	56
-7	5	2	93	98	0	7	2	48	52	10	0	3	34	18	6	2	3	72	52	7	4	3	75	64
-6	5	2	52	46	1	7	2	104	108	-13	1	3	40	30	7	2	3	49	47	9	4	3	44	54
-4	5	2	66	80	2	7	2	42	30	-10	1	3	49	62	8	2	3	86	85	-9	5	3	35	41
-3	5	2	53	51	3	7	2	92	97	-8	1	3	98	100	-13	3	3	44	34	-8	5	3	47	58
-2	5	2	136	135	4	7	2	86	94	-7	1	3	68	63	-8	3	3	69	83	-6	5	3	61	63
-1	5	2	32	37	5	7	2	70	82	-6	1	3	56	48	-6	3	3	37	21	-5	5	3	104	106
0	5	2	115	108	6	7	2	38	42	-5	1	3	149	136	-5	3	3	43	32	-4	5	3	70	68
1	5	2	44	49	-5	8	2	50	54	-4	1	3	345	345	-4	3	3	41	35	-3	5	3	68	71
2	5	2	31	38	-4	8	2	67	66	-3	1	3	135	139	-3	3	3	86	82	-2	5	3	64	66
3	5	2	156	154	-1	8	2	37	45	-2	1	3	169	172	-2	3	3	91	100	-1	5	3	36	53
4	5	2	82	85	0	8	2	41	55	-1	1	3	217	236	-1	3	3	190	183	0	5	3	46	47
5	5	2	43	50	1	8	2	58	65	0	1	3	312	296	0	3	3	228	220	2	5	3	44	48
6	5	2	79	73	3	8	2	71	71	1	1	3	254	266	1	3	3	230	239	3	5	3	135	139
7	5	2	39	37	4	8	2	61	57	2	1	3	362	370	2	3	3	263	277	4	5	3	124	135
-8	6	2	52	45	4	9	2	44	40	3	1	3	117	119	3	3	3	147	141	5	5	3	144	145
-7	6	2	43	38	5	9	2	55	54	4	1	3	278	273	4	3	3	266	258	6	5	3	68	69
-6	6	2	49	20	-5	10	2	45	42	5	1	3	252	255	5	3	3	83	77	7	5	3	78	74
-5	6	2	109	103	4	10	2	34	31	6	1	3	118	116	6	3	3	61	39	8	5	3	56	51
-4	6	2	60	61	4	11	2	39	31	8	1	3	41	29	7	3	3	29	26	9	5	3	65	63
-2	6	2	37	38	-10	0	3	47	55	9	1	3	133	137	8	3	3	62	64	-11	6	3	38	28
-1	6	2	127	125	-8	0	3	214	208	10	1	3	41	37	9	3	3	95	97	-9	6	3	37	33
0	6	2	99	91	-7	0	3	94	101	-10	2	3	68	61	-10	4	3	44	40	-8	6	3	60	67
1	6	2	58	55	-6	0	3	165	178	-9	2	3	38	45	-8	4	3	107	118	-7	6	3	41	44
2	6	2	126	119	-5	0	3	244	227	-8	2	3	70	72	-6	4	3	82	82	-5	6	3	84	79
3	6	2	100	101	-4	0	3	530	516	-7	2	3	33	32	-5	4	3	64	61	-4	6	3	41	53
4	6	2	130	128	-3	0	3	197	191	-5	2	3	193	189	-4	4	3	125	131	-3	6	3	72	82
5	6	2	41	30	-2	0	3	118	125	-4	2	3	308	314	-3	4	3	112	116	-2	6	3	87	90
6	6	2	38	40	-1	0	3	30	12	-3	2	3	130	122	-2	4	3	135	145	-1	6	3	53	50
7	6	2	37	40	0	0	3	526	495	-2	2	3	317	325	-1	4	3	93	95	0	6	3	37	34
8	6	2	58	61	1	0	3	84	75	-1	2	3	185	186	0	4	3	83	64	1	6	3	39	45
-6	7	2	65	60	2	0	3	386	405	0	2	3	28	51	1	4	3	24	13	2	6	3	52	58
-5	7	2	60	60	3	0	3	214	219	1	2	3	178	173	2	4	3	206	209	4	6	3	110	119
-4	7	2	32	29	4	0	3	387	377	2	2	3	177	192	3	4	3	92	102	5	6	3	62	72
-3	7	2	62	65	5	0	3	73	86	3	2	3	154	163	4	4	3	160	158	8	6	3	60	63
-2	7	2	104	107	6	0	3	88	93	4	2	3	358	355	5	4	3	38	36	9	6	3	64	56

h	k	l	10Fo	10Fc	h	k	l	10Fo	10Fc	h	k	l	10Fo	10Fc	h	k	l	10Fo	10Fc	h	k	l	10Fo	10Fc
10	6	3	46	38	-2	0	4	255	248	-8	2	4	155	161	6	3	4	37	48	-4	6	4	133	139
11	6	3	38	25	-1	0	4	62	48	-7	2	4	61	60	8	3	4	40	37	-3	6	4	130	141
-6	7	3	33	22	0	0	4	378	374	-6	2	4	131	130	9	3	4	44	44	-2	6	4	31	38
-4	7	3	113	111	1	0	4	211	207	-5	2	4	147	139	-10	4	4	34	37	0	6	4	114	123
-3	7	3	90	91	2	0	4	91	95	-4	2	4	259	255	-9	4	4	58	54	1	6	4	110	113
-2	7	3	39	34	3	0	4	56	58	-3	2	4	284	288	-8	4	4	69	75	2	6	4	37	41
0	7	3	90	84	4	0	4	94	89	-2	2	4	46	47	-7	4	4	51	47	3	6	4	38	37
1	7	3	62	59	5	0	4	110	87	-1	2	4	223	216	-5	4	4	203	205	4	6	4	129	132
3	7	3	40	35	6	0	4	92	99	0	2	4	241	248	-4	4	4	57	54	6	6	4	51	46
4	7	3	150	157	7	0	4	91	80	1	2	4	82	74	-3	4	4	132	136	7	6	4	43	42
6	7	3	54	39	9	0	4	109	102	2	2	4	27	34	-2	4	4	118	132	8	6	4	53	44
8	7	3	57	56	-12	1	4	55	44	3	2	4	143	153	-1	4	4	81	84	9	6	4	66	66
9	7	3	48	52	-10	1	4	40	44	4	2	4	190	174	0	4	4	126	132	-6	7	4	61	59
-8	8	3	34	32	-9	1	4	100	105	5	2	4	38	55	1	4	4	141	135	-5	7	4	55	59
-3	8	3	70	65	-8	1	4	97	105	6	2	4	71	54	2	4	4	44	36	-4	7	4	56	50
1	8	3	57	50	-7	1	4	46	58	7	2	4	66	52	4	4	4	88	86	-3	7	4	78	82
2	8	3	60	56	-6	1	4	144	130	8	2	4	79	73	5	4	4	127	119	-2	7	4	42	51
3	8	3	46	35	-5	1	4	88	96	9	2	4	97	105	6	4	4	61	50	-1	7	4	43	41
4	8	3	52	52	-4	1	4	341	329	10	2	4	59	56	7	4	4	44	32	1	7	4	85	86
5	8	3	65	57	-3	1	4	218	214	11	2	4	35	28	9	4	4	104	109	2	7	4	63	66
8	8	3	37	34	-2	1	4	73	80	-10	3	4	44	41	-8	5	4	46	44	3	7	4	66	81
-5	9	3	43	39	-1	1	4	279	280	-9	3	4	47	50	-7	5	4	48	60	4	7	4	55	59
-4	9	3	50	49	0	1	4	373	368	-8	3	4	60	64	-6	5	4	43	40	5	7	4	64	72
-3	9	3	44	39	1	1	4	128	149	-7	3	4	79	89	-5	5	4	121	122	7	7	4	54	60
0	9	3	36	26	2	1	4	225	258	-6	3	4	129	136	-4	5	4	116	123	-5	8	4	39	41
-4	10	3	41	24	3	1	4	132	136	-5	3	4	76	74	-2	5	4	28	35	-4	8	4	98	102
-4	11	3	41	41	4	1	4	158	156	-4	3	4	187	198	-1	5	4	151	148	-2	8	4	72	75
-3	11	3	37	18	5	1	4	122	106	-3	3	4	113	116	0	5	4	122	130	-1	8	4	41	40
-13	0	4	40	37	6	1	4	84	64	-2	3	4	52	41	2	5	4	103	111	0	8	4	51	56
-9	0	4	36	36	7	1	4	48	46	-1	3	4	60	60	4	5	4	123	128	1	8	4	53	56
-8	0	4	141	142	8	1	4	43	51	0	3	4	178	187	5	5	4	47	51	4	8	4	63	64
-7	0	4	117	129	9	1	4	63	56	1	3	4	70	80	6	5	4	56	51	8	8	4	40	35
-6	0	4	81	85	10	1	4	45	50	2	3	4	72	92	7	5	4	47	33	-5	9	4	38	41
-5	0	4	72	73	-13	2	4	36	27	3	3	4	112	109	9	5	4	65	54	-4	9	4	33	21
-4	0	4	113	129	-10	2	4	33	40	4	3	4	103	110	-7	6	4	46	56	3	9	4	44	14
-3	0	4	323	321	-9	2	4	53	51	5	3	4	89	80	-5	6	4	127	127	4	9	4	41	43

h	k	l	10Fo	10Fc	h	k	l	10Fo	10Fc	h	k	l	10Fo	10Fc	h	k	l	10Fo	10Fc	h	k	l	10Fo	10Fc
5	9	4	54	53	4	1	5	125	132	2	3	5	120	134	4	5	5	56	62	-5	9	5	40	36
-4	10	4	51	50	5	1	5	36	39	3	3	5	58	71	5	5	5	63	65	-4	9	5	42	58
-12	0	5	64	69	6	1	5	45	31	4	3	5	84	79	6	5	5	63	52	0	9	5	42	41
-11	0	5	48	30	7	1	5	47	44	5	3	5	67	61	7	5	5	43	41	7	9	5	36	27
-10	0	5	46	33	8	1	5	111	112	6	3	5	69	73	8	5	5	82	79	-12	0	6	36	27
-8	0	5	151	158	9	1	5	72	76	7	3	5	79	84	9	5	5	70	73	-9	0	6	43	39
-6	0	5	62	59	-12	2	5	51	48	8	3	5	48	46	-8	6	5	48	50	-8	0	6	113	120
-5	0	5	125	116	-10	2	5	56	38	9	3	5	70	63	-6	6	5	75	75	-6	0	6	63	58
-4	0	5	290	264	-9	2	5	60	63	10	3	5	40	45	-5	6	5	68	72	-4	0	6	142	132
-3	0	5	251	253	-8	2	5	77	77	-9	4	5	33	17	-4	6	5	122	120	-3	0	6	32	56
-2	0	5	23	31	-7	2	5	56	51	-8	4	5	57	52	-1	6	5	77	69	-2	0	6	352	338
-1	0	5	261	273	-6	2	5	142	144	-7	4	5	85	91	0	6	5	170	172	-1	0	6	158	153
0	0	5	140	117	-5	2	5	64	64	-6	4	5	40	35	1	6	5	71	70	0	0	6	441	420
1	0	5	72	79	-4	2	5	307	299	-5	4	5	165	172	3	6	5	61	58	1	0	6	154	133
2	0	5	201	196	-3	2	5	94	95	-4	4	5	110	109	5	6	5	53	71	2	0	6	396	388
3	0	5	105	97	-2	2	5	278	276	-3	4	5	126	135	6	6	5	92	87	3	0	6	86	81
5	0	5	55	72	-1	2	5	115	124	-2	4	5	170	172	9	6	5	45	47	4	0	6	151	148
6	0	5	63	65	0	2	5	359	337	-1	4	5	46	48	-7	7	5	36	45	5	0	6	95	83
7	0	5	45	38	1	2	5	168	155	0	4	5	142	138	-6	7	5	75	84	6	0	6	102	105
8	0	5	32	39	2	2	5	148	161	1	4	5	110	106	-5	7	5	50	52	7	0	6	39	50
10	0	5	39	37	3	2	5	67	70	2	4	5	77	74	-4	7	5	71	87	8	0	6	113	111
11	0	5	45	47	4	2	5	161	167	3	4	5	88	83	-3	7	5	43	47	-13	1	6	39	24
12	0	5	52	49	5	2	5	48	41	4	4	5	77	77	-1	7	5	34	31	-10	1	6	40	39
-10	1	5	46	51	6	2	5	74	71	5	4	5	65	78	0	7	5	100	108	-8	1	6	64	72
-9	1	5	72	65	7	2	5	90	83	6	4	5	50	56	1	7	5	98	91	-7	1	6	32	38
-8	1	5	82	80	9	2	5	33	29	7	4	5	50	41	2	7	5	45	47	-6	1	6	59	58
-7	1	5	98	106	-9	3	5	59	54	9	4	5	41	46	3	7	5	43	35	-5	1	6	124	119
-6	1	5	144	143	-7	3	5	96	97	-10	5	5	39	32	4	7	5	52	54	-4	1	6	113	104
-5	1	5	107	109	-6	3	5	49	44	-8	5	5	34	48	6	7	5	33	31	-3	1	6	137	130
-4	1	5	175	161	-5	3	5	31	28	-7	5	5	98	104	8	7	5	56	50	-2	1	6	104	109
-3	1	5	270	269	-4	3	5	216	215	-6	5	5	86	87	9	7	5	59	57	-1	1	6	50	45
-2	1	5	150	165	-3	3	5	28	25	-4	5	5	78	89	-5	8	5	75	61	0	1	6	359	323
-1	1	5	67	51	-2	3	5	133	129	-3	5	5	45	44	-1	8	5	49	55	1	1	6	486	482
0	1	5	325	318	-1	3	5	144	150	-1	5	5	142	139	0	8	5	109	108	2	1	6	192	199
1	1	5	65	61	0	3	5	229	219	0	5	5	146	136	1	8	5	42	32	3	1	6	59	58
3	1	5	141	137	1	3	5	76	86	2	5	5	32	24	2	8	5	34	25	4	1	6	119	125

h	k	l	10Fo	10Fc	h	k	l	10Fo	10Fc	h	k	l	10Fo	10Fc	h	k	l	10Fo	10Fc	h	k	l	10Fo	10Fc
5	1	6	51	58	2	3	6	183	193	7	5	6	39	30	3	9	6	41	38	1	1	7	124	120
6	1	6	110	107	3	3	6	110	110	9	5	6	35	27	0	10	6	57	50	2	1	7	49	53
7	1	6	99	103	4	3	6	35	38	-8	6	6	73	77	1	10	6	43	43	3	1	7	44	48
8	1	6	91	102	5	3	6	47	53	-7	6	6	59	66	5	10	6	44	29	4	1	7	126	126
9	1	6	36	33	6	3	6	93	85	-6	6	6	58	48	-9	0	7	42	26	5	1	7	41	47
12	1	6	36	33	7	3	6	88	94	-5	6	6	52	47	-8	0	7	91	84	6	1	7	115	117
-10	2	6	32	30	9	3	6	55	55	-4	6	6	65	71	-7	0	7	84	77	7	1	7	110	112
-9	2	6	54	59	-9	4	6	73	75	-3	6	6	91	91	-6	0	7	128	134	-8	2	7	74	84
-7	2	6	51	58	-8	4	6	72	71	-2	6	6	35	33	-5	0	7	39	8	-7	2	7	36	29
-6	2	6	101	104	-4	4	6	77	84	-1	6	6	47	50	-4	0	7	39	25	-6	2	7	36	12
-5	2	6	65	55	-3	4	6	44	45	0	6	6	177	187	-3	0	7	32	20	-4	2	7	90	68
-4	2	6	97	101	-2	4	6	130	137	1	6	6	151	157	-2	0	7	98	90	-3	2	7	87	101
-3	2	6	76	76	-1	4	6	95	101	2	6	6	39	35	-1	0	7	121	92	-2	2	7	101	104
-2	2	6	201	182	0	4	6	169	162	3	6	6	50	52	0	0	7	98	105	-1	2	7	163	173
-1	2	6	50	47	1	4	6	169	178	4	6	6	90	86	1	0	7	245	234	0	2	7	192	188
0	2	6	301	286	2	4	6	97	96	5	6	6	37	26	2	0	7	94	117	1	2	7	207	199
1	2	6	270	275	3	4	6	47	53	6	6	6	62	62	3	0	7	126	132	2	2	7	107	125
2	2	6	162	167	4	4	6	31	27	8	6	6	57	39	4	0	7	145	138	3	2	7	39	49
3	2	6	172	188	5	4	6	49	55	9	6	6	57	50	5	0	7	266	269	4	2	7	99	111
4	2	6	44	33	6	4	6	52	44	-9	7	6	40	22	6	0	7	42	35	5	2	7	153	158
5	2	6	32	28	7	4	6	42	43	-8	7	6	38	42	7	0	7	37	56	6	2	7	98	97
6	2	6	57	67	8	4	6	66	76	-4	7	6	41	34	8	0	7	81	79	8	2	7	67	67
-	2	6	36	50	9	4	6	58	51	-2	7	6	79	83	9	0	7	63	62	-12	3	7	43	33
8	2	6	75	75	-8	5	6	45	42	-1	7	6	48	52	10	0	7	41	46	-10	3	7	36	38
9	2	6	40	26	-6	5	6	106	102	0	7	6	77	77	12	0	7	65	65	-9	3	7	47	48
10	2	6	49	44	-4	5	6	53	59	1	7	6	72	72	-12	1	7	51	51	-8	3	7	88	95
-9	3	6	37	21	-3	5	6	69	68	3	7	6	35	34	-9	1	7	34	27	-7	3	7	70	59
-7	3	6	65	72	-2	5	6	108	117	4	7	6	58	56	-8	1	7	126	131	-6	3	7	100	102
-6	3	6	48	38	-1	5	6	78	69	6	7	6	59	51	-7	1	7	74	68	-4	3	7	79	78
-5	3	6	97	92	0	5	6	77	74	-7	8	6	37	40	-6	1	7	69	51	-3	3	7	68	79
-4	3	6	77	74	1	5	6	132	133	-5	8	6	35	27	-5	1	7	146	144	-2	3	7	40	29
-3	3	6	170	167	2	5	6	39	37	-4	8	6	69	70	-4	1	7	64	74	-1	3	7	96	91
-2	3	6	108	116	3	5	6	51	43	0	8	6	67	61	-3	1	7	96	110	1	3	7	76	82
-1	3	6	44	44	4	5	6	139	138	1	8	6	80	86	-2	1	7	110	114	4	3	7	61	69
0	3	6	253	242	5	5	6	37	37	6	8	6	40	29	-1	1	7	137	125	5	3	7	39	33
1	3	6	267	259	6	5	6	91	105	-3	9	6	38	28	0	1	7	167	169	6	3	7	67	73

h	k	l	10Fo	10Fo	h	k	l	10Fo	10Fc	h	k	l	10Fo	10Fc	h	k	l	10Fo	10Fc	h	k	l	10Fo	10Fc
7	3	7	56	52	-1	6	7	31	23	4	0	8	275	278	10	2	8	35	26	-2	5	8	57	58
8	3	7	46	35	0	6	7	102	106	5	0	8	38	36	-9	3	8	40	34	-1	5	8	107	117
9	3	7	38	26	1	6	7	87	96	-8	1	8	44	42	-8	3	8	57	54	0	5	8	105	104
-9	4	7	39	38	2	6	7	51	57	-7	1	8	34	39	-7	3	8	48	53	1	5	8	89	93
-7	4	7	36	35	3	6	7	60	62	-6	1	8	81	71	-6	3	8	40	32	2	5	8	92	93
-6	4	7	38	48	5	6	7	112	117	-5	1	8	69	69	-5	3	8	34	30	3	5	8	51	56
-4	4	7	107	108	8	6	7	44	25	-3	1	8	52	65	-4	3	8	76	78	5	5	8	83	94
-3	4	7	86	88	9	6	7	40	32	-2	1	8	48	62	-3	3	8	72	61	-7	6	8	46	54
-2	4	7	31	39	-7	7	7	50	52	-1	1	8	116	76	-2	3	8	48	53	-6	6	8	49	41
-1	4	7	39	49	-3	7	7	56	61	0	1	8	39	29	-1	3	8	34	24	-5	6	8	36	40
0	4	7	99	98	0	7	7	62	49	1	1	8	225	221	0	3	8	89	84	-4	6	8	36	49
1	4	7	119	127	1	7	7	56	59	2	1	8	80	79	1	3	8	80	78	-3	6	8	36	28
2	4	7	104	102	2	7	7	37	34	3	1	8	35	39	2	3	8	88	87	-2	6	8	72	77
3	4	7	70	71	3	7	7	52	56	5	1	8	131	142	4	3	8	40	38	-1	6	8	62	57
4	4	7	75	80	-8	8	7	43	42	6	1	8	40	39	5	3	8	89	91	0	6	8	41	54
5	4	7	130	143	0	8	7	51	61	10	1	8	34	20	6	3	8	55	63	1	6	8	92	99
7	4	7	67	70	1	8	7	37	43	-12	2	8	48	43	7	3	8	43	33	4	6	8	100	101
8	4	7	43	46	2	8	7	63	64	-10	2	8	45	49	-11	4	8	43	38	5	6	8	39	36
9	4	7	36	38	3	8	7	34	22	-9	2	8	37	40	-10	4	8	38	23	9	6	8	40	36
-8	5	7	73	79	0	9	7	41	34	-8	2	8	77	91	-9	4	8	35	20	-8	7	8	69	66
-7	5	7	79	85	1	9	7	41	41	-7	2	8	41	49	-8	4	8	45	52	-4	7	8	47	45
-6	5	7	36	18	0	10	7	49	42	-6	2	8	76	77	-7	4	8	93	97	-3	7	8	41	48
-4	5	7	31	37	-12	0	8	50	40	-5	2	8	51	61	-5	4	8	56	60	1	7	8	44	47
-3	5	7	46	56	-9	0	8	37	37	-4	2	8	118	116	-4	4	8	92	101	3	7	8	34	44
-2	5	7	52	56	-8	0	8	92	100	-3	2	8	30	27	0	4	8	64	68	5	7	8	40	46
0	5	7	85	80	-7	0	8	99	101	-2	2	8	40	44	1	4	8	85	93	-3	8	8	32	18
1	5	7	103	97	-6	0	8	32	22	-1	2	8	44	35	3	4	8	40	42	0	8	8	37	35
2	5	7	40	60	-5	0	8	122	87	0	2	8	87	95	4	4	8	118	129	6	9	8	36	9
3	5	7	79	84	-4	0	8	120	125	1	2	8	134	150	5	4	8	83	88	3	10	8	37	22
4	5	7	52	54	-3	0	8	159	166	2	2	8	96	99	6	4	8	36	36	-12	0	9	37	22
5	5	7	77	75	-2	0	8	72	79	3	2	8	64	59	7	4	8	49	47	-9	0	9	57	46
7	5	7	63	63	-1	0	8	52	17	4	2	8	98	119	-9	5	8	49	38	-7	0	9	54	56
-8	6	7	54	58	0	0	8	182	168	5	2	8	47	45	-8	5	8	46	47	-5	0	9	96	97
-7	6	7	34	43	1	0	8	108	112	6	2	8	42	26	-7	5	8	45	55	-4	0	9	103	118
-3	6	7	52	57	2	0	8	33	36	7	2	8	35	37	-4	5	8	44	37	-2	0	9	175	187
-2	6	7	79	83	3	0	8	80	62	8	2	8	40	39	-3	5	8	58	55	-1	0	9	70	43

h	k	l	10Fo	10Fo	h	k	l	10Fo	10Fc	h	k	l	10Fo	10Fc	h	k	l	10Fo	10Fc	h	k	l	10Fo	10Fc
1	0	9	140	141	-8	3	9	42	49	-4	6	9	65	68	2	1	10	85	90	5	4	10	75	74
4	0	9	65	68	-6	3	9	42	41	-3	6	9	64	57	4	1	10	74	76	7	4	10	36	41
5	0	9	139	144	-5	3	9	40	45	-1	6	9	53	44	5	1	10	40	39	9	4	10	38	28
6	0	9	72	62	-4	3	9	112	117	2	6	9	34	33	6	1	10	59	64	-8	5	10	49	31
7	0	9	58	55	-3	3	9	103	106	5	6	9	41	41	-6	2	10	79	80	-5	5	10	48	41
9	0	9	39	34	-1	3	9	51	50	-5	7	9	34	36	-5	2	10	53	28	-4	5	10	118	121
10	0	9	64	60	0	3	9	100	101	-4	7	9	33	13	-4	2	10	72	71	-3	5	10	46	53
-7	1	9	42	40	1	3	9	53	57	-1	7	9	48	43	-3	2	10	151	153	-2	5	10	92	100
-6	1	9	36	33	2	3	9	72	71	1	7	9	44	47	-2	2	10	58	65	0	5	10	48	38
-5	1	9	91	103	3	3	9	51	47	-7	8	9	36	20	-1	2	10	105	92	1	5	10	45	56
-4	1	9	214	218	4	3	9	150	170	0	9	9	39	29	0	2	10	77	75	-1	6	10	41	42
-3	1	9	157	164	5	3	9	116	130	-8	0	10	32	22	1	2	10	120	124	2	6	10	63	65
-1	1	9	35	16	6	3	9	76	92	-7	0	10	42	47	2	2	10	36	16	4	6	10	40	42
0	1	9	95	101	7	3	9	43	42	-6	0	10	87	87	4	2	10	42	85	6	6	10	37	24
1	1	9	75	84	10	3	9	36	20	-5	0	10	59	39	5	2	10	103	96	7	6	10	36	34
2	1	9	63	53	-7	4	9	45	41	-4	0	10	156	155	9	2	10	47	40	-8	7	10	40	29
4	1	9	232	250	-6	4	9	55	57	-3	0	10	211	199	-6	3	10	46	38	-7	7	10	38	36
5	1	9	215	227	-5	4	9	62	70	-2	0	10	40	35	-5	3	10	66	71	-5	7	10	47	41
6	1	9	92	96	-4	4	9	44	32	-1	0	10	50	41	-4	3	10	132	139	-4	7	10	54	55
7	1	9	96	96	-3	4	9	40	40	1	0	10	47	45	-3	3	10	71	78	-1	7	10	35	23
-8	2	9	37	28	-1	4	9	39	40	2	0	10	58	48	-2	3	10	58	62	1	7	10	56	55
-7	2	9	62	66	0	4	9	48	40	4	0	10	154	145	-1	3	10	76	76	-1	8	10	41	34
-6	2	9	56	66	1	4	9	67	71	5	0	10	92	83	0	3	10	36	31	-4	9	10	40	31
-5	2	9	80	88	2	4	9	70	70	6	0	10	39	41	2	3	10	46	51	-6	0	11	73	80
-4	2	9	126	122	5	4	9	74	82	8	0	10	56	49	4	3	10	73	72	-4	0	11	236	244
-3	2	9	52	58	6	4	9	53	46	9	0	10	54	44	6	3	10	72	81	-3	0	11	171	184
-2	2	9	78	80	-5	5	9	48	58	-8	1	10	46	54	-6	4	10	64	63	-2	0	11	152	154
-1	2	9	39	32	-4	5	9	93	93	-7	1	10	54	54	-5	4	10	63	70	0	0	11	126	114
1	2	9	84	85	-3	5	9	85	91	-6	1	10	51	40	-4	4	10	39	47	1	0	11	50	49
2	2	9	104	101	1	5	9	37	29	-5	1	10	127	107	-3	4	10	72	83	3	0	11	37	28
4	2	9	69	73	2	5	9	50	59	-4	1	10	146	154	-2	4	10	53	44	5	0	11	54	54
5	2	9	168	175	3	5	9	64	67	-3	1	10	83	98	-1	4	10	47	49	6	0	11	32	23
6	2	9	54	52	4	5	9	38	42	-2	1	10	56	54	0	4	10	80	80	7	0	11	44	31
7	2	9	47	38	5	5	9	116	127	-1	1	10	82	77	1	4	10	40	50	-7	1	11	42	45
8	2	9	42	47	7	5	9	42	36	0	1	10	66	58	2	4	10	48	56	-6	1	11	74	61
-9	3	9	40	32	-8	6	9	40	37	1	1	10	52	36	4	4	10	46	49	-5	1	11	32	29

h	k	l	10Fo	10Fo	h	k	l	10Fo	10Fc	h	k	l	10Fo	10Fc	h	k	l	10Fo	10Fc	h	k	l	10Fo	10Fc
-4	1	11	117	122	-6	4	11	57	58	-1	1	12	75	72	-1	8	12	38	20	2	3	13	52	57
-3	1	11	166	163	-4	4	11	99	108	0	1	12	111	119	0	8	12	50	42	4	3	13	40	35
-2	1	11	64	68	-3	4	11	124	125	1	1	12	62	72	1	8	12	41	36	5	3	13	38	22
-1	1	11	130	131	0	4	11	141	129	2	1	12	74	76	-8	0	13	60	66	6	3	13	59	48
0	1	11	109	100	1	4	11	53	60	8	1	12	42	16	-4	0	13	51	40	-3	4	13	36	41
1	1	11	94	79	4	4	11	34	35	-8	2	12	37	27	-2	0	13	49	38	-2	4	13	35	24
2	1	11	57	45	-5	5	11	53	57	-4	2	12	73	72	-1	0	13	44	53	-1	4	13	43	42
3	1	11	57	63	-4	5	11	93	101	-3	2	12	152	166	0	0	13	74	84	1	4	13	62	54
4	1	11	44	52	-3	5	11	70	68	-2	2	12	60	68	2	0	13	54	64	2	4	13	40	34
5	1	11	74	73	-1	5	11	60	47	-1	2	12	74	73	3	0	13	38	43	4	4	13	35	11
8	1	11	39	37	0	5	11	61	63	0	2	12	63	59	5	0	13	43	32	-1	5	13	35	35
9	1	11	78	72	-3	6	11	46	60	1	2	12	86	84	-10	1	13	39	34	0	5	13	56	64
-8	2	11	47	52	-2	6	11	55	55	6	2	12	40	37	-7	1	13	46	36	1	5	13	73	74
-5	2	11	36	22	-1	6	11	39	45	9	2	12	65	51	-5	1	13	40	38	-1	7	13	43	34
-4	2	11	166	188	0	6	11	75	67	-5	3	12	59	50	-4	1	13	38	26	0	7	13	61	54
-3	2	11	156	158	1	6	11	56	53	-2	3	12	43	42	-3	1	13	34	34	-8	0	14	53	41
-2	2	11	96	94	-5	7	11	36	31	-1	3	12	94	103	-2	1	13	71	72	-5	0	14	41	41
-1	2	11	68	68	-4	7	11	57	56	0	3	12	82	87	-1	1	13	65	61	-4	0	14	50	41
0	2	11	105	96	0	7	11	47	43	1	3	12	40	43	0	1	13	37	27	4	0	14	42	44
1	2	11	72	67	1	7	11	50	47	-4	4	12	37	27	1	1	13	69	69	-7	1	14	35	37
2	2	11	48	46	0	8	11	42	32	-3	4	12	88	104	2	1	13	80	89	-5	1	14	48	48
4	2	11	79	87	-9	0	12	41	42	-2	4	12	86	86	3	1	13	37	43	-3	1	14	51	54
5	2	11	53	57	-6	0	12	64	50	0	4	12	48	53	4	1	13	33	32	-1	1	14	41	43
6	2	11	44	49	-5	0	12	38	13	1	4	12	62	67	5	1	13	39	38	1	1	14	67	68
-5	3	11	49	49	-3	0	12	154	157	8	4	12	41	33	-9	2	13	36	15	2	1	14	36	35
-4	3	11	74	83	-2	0	12	111	109	-1	5	12	69	79	-4	2	13	37	27	7	1	14	37	12
-3	3	11	133	140	-1	0	12	39	35	1	5	12	52	45	-3	2	13	37	28	-8	2	14	43	35
-2	3	11	52	54	0	0	12	70	57	2	5	12	48	56	-1	2	13	41	30	0	2	14	62	62
-1	3	11	103	102	1	0	12	91	94	3	5	12	36	33	0	2	13	55	49	1	2	14	36	29
0	3	11	35	34	4	0	12	84	90	-5	6	12	35	33	1	2	13	77	85	6	2	14	38	37
1	3	11	63	53	6	0	12	38	42	-3	6	12	42	32	5	2	13	40	35	-1	3	14	35	37
2	3	11	83	92	9	0	12	54	46	-1	6	12	37	22	-5	3	13	33	18	0	3	14	35	28
5	3	11	60	58	-8	1	12	50	38	0	6	12	48	50	-4	3	13	51	48	1	3	14	55	63
6	3	11	34	19	-5	1	12	50	35	1	6	12	72	74	-1	3	13	50	45	6	3	14	40	18
8	3	11	37	36	-3	1	12	44	47	-1	7	12	46	36	0	3	13	103	93	-1	4	14	41	37
9	3	11	57	43	-2	1	12	50	41	1	7	12	51	44	1	3	13	79	76	1	4	14	49	52

h	k	l	10Fo	10Fo	h	k	l	10Fo	10Fc	h	k	l	10Fo	10Fc	h	k	l	10Fo	10Fc	h	k	l	10Fo	10Fc
5	4	14	44	33	0	1	15	40	32	1	3	15	39	30	4	0	16	51	44	-4	1	17	54	60
-3	5	14	36	28	-8	2	15	45	31	-7	4	15	41	24	-2	1	16	34	16	-3	1	17	44	35
-6	0	15	42	42	-7	2	15	36	30	-3	4	15	40	24	5	1	16	41	26	1	1	17	39	31
-4	0	15	48	34	-5	2	15	38	20	-1	4	15	35	21	-4	3	16	40	33	-3	3	17	45	42
5	0	15	46	44	-2	2	15	37	36	1	4	15	37	20	-3	3	16	37	36	1	3	17	39	30
-8	1	15	43	28	-6	3	15	38	33	-3	5	15	45	35	-3	4	16	38	38	1	0	18	63	61
-6	1	15	35	16	-4	3	15	38	39	-3	6	15	38	30	-5	1	17	53	40					

Trineophyltin Fluoride, $C_{30}H_{39}SnF$

h	k	l	10Fo	10Fc	h	k	l	10Fo	10Fc	h	k	l	10Fo	10Fc	h	k	l	10Fo	10Fc	h	k	l	10Fo	10Fc
3	8	-14	237	17	-11	9	-8	253	262	2	9	-7	269	372	0	9	-6	380	356	-9	8	-5	1095	1009
1	5	-13	236	14	1	9	-8	456	419	5	9	-7	232	247	6	9	-6	402	293	0	8	-5	942	934
2	7	-11	232	156	-10	10	-8	372	359	-12	10	-7	260	292	1	10	-6	558	503	3	8	-5	982	937
-17	9	-11	226	24	5	10	-8	251	302	0	10	-7	386	405	7	10	-6	288	241	6	8	-5	723	694
-2	2	-10	297	346	-12	11	-8	266	200	3	10	-7	288	306	10	10	-6	229	171	-17	9	-5	520	501
-4	3	-10	226	356	0	11	-8	350	335	-11	11	-7	241	277	-13	11	-6	303	266	-14	9	-5	501	569
0	4	-10	214	375	-13	13	-8	309	254	1	11	-7	218	285	2	11	-6	233	97	-11	9	-5	904	921
-8	5	-10	209	164	2	13	-8	232	201	-16	12	-7	218	207	5	11	-6	335	319	1	9	-5	978	929
3	13	-10	241	111	-18	14	-8	252	228	-13	12	-7	305	374	-15	12	-6	243	275	4	9	-5	694	699
-3	3	-9	286	221	1	15	-8	237	171	-18	13	-7	232	187	0	12	-6	268	275	7	9	-5	503	519
3	6	-9	216	176	0	1	-7	584	608	-14	14	-7	278	307	3	12	-6	456	350	-19	10	-5	448	436
-8	7	-9	209	38	-2	2	-7	330	232	1	1	-6	759	672	-14	13	-6	272	251	-16	10	-5	367	440
-3	2	-8	496	454	1	2	-7	705	677	2	2	-6	1050	1003	-18	18	-6	227	127	-13	10	-5	670	710
0	2	-8	383	364	-4	3	-7	374	375	-3	3	-6	328	471	-1	1	-5	1754	1693	-10	10	-5	648	724
-5	3	-8	343	461	2	3	-7	434	322	0	3	-6	879	763	-3	2	-5	1974	1961	2	10	-5	709	655
1	3	-8	426	396	-6	4	-7	405	463	-5	4	-6	713	799	0	2	-5	2126	2052	5	10	-5	545	579
-4	4	-8	514	497	0	4	-7	585	594	1	4	-6	443	457	-5	3	-5	1025	1177	8	10	-5	462	471
-9	5	-8	319	319	3	4	-7	282	368	4	4	-6	340	342	1	3	-5	1591	1579	-21	11	-5	316	260
-6	5	-8	248	317	-8	5	-7	421	470	-7	5	-6	328	430	-7	4	-5	1134	1206	-18	11	-5	377	427
0	5	-8	267	205	-5	5	-7	346	336	2	5	-6	266	173	-4	4	-5	1052	1172	-15	11	-5	303	397
3	5	-8	356	369	1	5	-7	352	346	5	5	-6	424	436	2	4	-5	928	856	-12	11	-5	690	728
-11	6	-8	340	318	-10	6	-7	280	324	-9	6	-6	357	382	-9	5	-5	912	918	0	11	-5	853	774
-8	6	-8	248	302	-7	6	-7	496	522	-6	6	-6	262	379	-6	5	-5	1218	1262	3	11	-5	763	743
1	6	-8	221	262	2	6	-7	306	259	0	6	-6	411	331	0	5	-5	907	942	6	11	-5	260	305
4	6	-8	352	279	5	6	-7	349	376	3	6	-6	401	303	3	5	-5	1183	1124	9	11	-5	344	391
-13	7	-8	313	294	-12	7	-7	365	377	6	6	-6	418	353	-11	6	-5	877	805	-20	12	-5	364	335
-10	7	-8	279	239	-9	7	-7	378	381	-11	7	-6	374	281	-8	6	-5	1490	1440	-17	12	-5	474	479
-7	7	-8	260	277	0	7	-7	360	404	-8	7	-6	412	358	1	6	-5	1343	1243	-14	12	-5	667	663
2	7	-8	400	384	3	7	-7	338	385	1	7	-6	519	511	4	6	-5	1064	969	1	12	-5	653	678
5	7	-8	234	262	6	7	-7	364	405	4	7	-6	239	270	-13	7	-5	731	678	4	12	-5	396	449
-15	8	-8	233	180	-14	8	-7	233	220	-13	8	-6	376	345	-10	7	-5	880	896	7	12	-5	499	459
-12	8	-8	288	226	-11	8	-7	376	370	-10	8	-6	361	318	-7	7	-5	1335	1257	-19	13	-5	345	403
-9	8	-8	329	324	-8	8	-7	303	303	2	8	-6	313	224	2	7	-5	1167	1110	-16	13	-5	447	509
0	8	-8	355	386	1	8	-7	329	314	8	8	-6	340	217	5	7	-5	931	843	-13	13	-5	828	853
3	8	-8	273	158	4	8	-7	301	294	-12	9	-6	236	192	-15	8	-5	701	727	2	13	-5	618	624
6	8	-8	244	192	7	8	-7	291	286	-9	9	-6	607	543	-12	8	-5	979	918	5	13	-5	404	427

h	k	l	10Fo	10Fc	h	k	l	10Fo	10Fc	h	k	l	10Fo	10Fc	h	k	l	10Fo	10Fc	h	k	l	10Fo	10Fc
8	13	-5	259	258	6	7	-4	302	305	4	7	-3	1117	982	12	12	-3	261	227	0	2	-2	1376	1416
-18	14	-5	328	374	-11	8	-4	372	404	7	7	-3	601	699	-20	13	-3	432	410	-5	3	-2	2003	2094
-15	14	-5	486	535	1	8	-4	187	168	-13	8	-3	882	932	-17	13	-3	484	527	1	3	-2	435	557
0	14	-5	455	496	4	8	-4	305	206	-10	8	-3	1200	1215	-14	13	-3	855	884	-7	4	-2	930	1141
3	14	-5	475	431	7	8	-4	224	97	2	8	-3	1041	1000	1	13	-3	684	700	-4	4	-2	2058	1978
6	14	-5	327	324	2	9	-4	270	273	5	8	-3	771	802	4	13	-3	625	595	2	4	-2	1666	1486
9	14	-5	250	213	5	9	-4	518	485	8	8	-3	880	830	7	13	-3	467	416	-9	5	-2	663	624
-20	15	-5	359	345	-18	10	-4	244	254	-15	9	-3	565	638	10	13	-3	274	273	-6	5	-2	1466	1601
-17	15	-5	253	354	-15	10	-4	337	301	-12	9	-3	1034	1089	-19	14	-3	359	384	0	5	-2	1893	1733
1	15	-5	444	395	-12	10	-4	340	380	-9	9	-3	1249	1229	-16	14	-3	412	498	3	5	-2	1859	1709
4	15	-5	338	344	0	10	-4	215	89	0	9	-3	1167	1157	2	14	-3	684	659	-11	6	-2	1421	1387
-19	16	-5	269	302	3	10	-4	405	331	3	9	-3	1034	965	5	14	-3	416	417	-8	6	-2	1506	1497
-16	16	-5	402	400	-11	11	-4	209	217	6	9	-3	524	648	8	14	-3	282	265	1	6	-2	1295	1181
2	16	-5	368	333	0	13	-4	267	265	9	9	-3	578	529	-21	15	-3	376	319	4	6	-2	857	944
5	16	-5	271	259	4	14	-4	258	197	-17	10	-3	590	474	-18	15	-3	405	393	-13	7	-2	938	888
-18	17	-5	321	368	2	15	-4	227	110	-14	10	-3	464	523	-15	15	-3	345	366	-10	7	-2	1553	1607
0	17	-5	404	367	0	16	-4	238	231	-11	10	-3	820	799	0	15	-3	542	493	-7	7	-2	1382	1432
3	17	-5	251	269	1	1	-3	1645	1748	1	10	-3	1029	922	3	15	-3	468	450	2	7	-2	879	887
6	17	-5	252	215	2	2	-3	1939	2136	4	10	-3	628	700	6	15	-3	269	281	5	7	-2	1204	1193
-20	18	-5	282	236	-3	3	-3	1374	1456	7	10	-3	660	601	-23	16	-3	244	247	-15	8	-2	544	593
4	18	-5	249	242	0	3	-3	2007	1998	10	10	-3	334	386	-20	16	-3	280	322	-12	8	-2	1040	942
-22	19	-5	242	225	3	3	-3	849	923	-19	11	-3	497	425	-17	16	-3	489	444	-9	8	-2	1334	1372
-19	19	-5	249	244	-5	4	-3	1042	1152	-16	11	-3	372	458	1	16	-3	422	344	0	8	-2	763	733
2	19	-5	293	242	1	4	-3	1343	1297	-13	11	-3	830	870	4	16	-3	318	256	3	8	-2	908	888
-2	2	-4	623	586	4	4	-3	1305	1226	2	11	-3	589	637	-19	17	-3	401	376	6	8	-2	801	798
1	2	-4	208	528	-7	5	-3	912	827	5	11	-3	367	349	2	17	-3	312	311	-17	9	-2	600	680
2	3	-4	321	275	2	5	-3	1640	1432	8	11	-3	476	521	5	17	-3	268	286	-14	9	-2	785	732
-6	4	-4	185	295	5	5	-3	1074	1059	11	11	-3	353	289	-18	18	-3	385	374	-11	9	-2	1074	1057
3	4	-4	770	689	-9	6	-3	1269	1318	-21	12	-3	314	258	0	18	-3	328	307	1	9	-2	1472	1350
1	5	-4	445	576	-6	6	-3	1052	1149	-18	12	-3	568	567	3	18	-3	338	332	4	9	-2	1190	1142
-10	6	-4	245	461	0	6	-3	836	870	-15	12	-3	611	662	6	18	-3	271	219	7	9	-2	299	367
-7	6	-4	379	519	3	6	-3	963	928	-12	12	-3	781	759	-20	19	-3	280	242	-19	10	-2	493	521
2	6	-4	288	332	6	6	-3	975	874	0	12	-3	723	705	1	19	-3	262	246	-16	10	-2	693	719
5	6	-4	284	276	-11	7	-3	935	996	3	12	-3	824	792	0	21	-3	319	225	-13	10	-2	1057	974
0	7	-4	234	280	-8	7	-3	1371	1360	6	12	-3	398	389	-1	1	-2	4573	4369	-10	10	-2	805	734
3	7	-4	245	253	1	7	-3	1439	1383	9	12	-3	358	318	-3	2	-2	1033	1024	2	10	-2	1367	1271

h	k	l	10Fo	10Fc	h	k	l	10Fo	10Fc	h	k	l	10Fo	10Fc	h	k	l	10Fo	10Fc	h	k	l	10Fo	10Fc
5	10	-2	924	950	1	15	-2	666	697	-9	7	-1	742	743	1	14	-1	354	255	0	9	0	1796	1787
8	10	-2	552	550	4	15	-2	410	542	0	7	-1	1134	905	4	14	-1	242	255	3	9	0	1899	1859
-21	11	-2	307	282	7	15	-2	300	290	3	7	-1	485	428	-19	15	-1	215	132	6	9	0	980	1020
-18	11	-2	584	566	-22	16	-2	285	289	6	7	-1	306	463	2	15	-1	236	209	9	9	0	779	824
-15	11	-2	747	768	-19	16	-2	392	411	-14	8	-1	271	333	-18	16	-1	226	172	-17	10	0	940	1039
-12	11	-2	650	636	-16	16	-2	607	569	-11	8	-1	353	407	-17	17	-1	255	180	-14	10	0	1291	1317
0	11	-2	1016	987	2	16	-2	367	336	-8	8	-1	229	287	-19	18	-1	242	135	-11	10	0	1304	1345
3	11	-2	658	636	5	16	-2	400	365	1	8	-1	989	895	1	1	0	3701	3456	1	10	0	2144	2017
6	11	-2	559	621	-21	17	-2	331	349	4	8	-1	865	717	2	2	0	1445	1707	4	10	0	1145	1205
9	11	-2	436	410	-18	17	-2	322	340	7	8	-1	192	213	-3	3	0	1619	2191	7	10	0	870	880
-23	12	-2	256	272	0	17	-2	573	508	-16	9	-1	262	247	0	3	0	1701	2321	10	10	0	529	594
-20	12	-2	435	433	3	17	-2	312	278	-13	9	-1	496	452	3	3	0	2230	2442	-19	11	0	751	778
-17	12	-2	375	385	-23	18	-2	234	228	-10	9	-1	657	596	-5	4	0	5303	4928	-16	11	0	884	964
-14	12	-2	568	627	-20	18	-2	313	296	2	9	-1	587	675	1	4	0	2235	1974	-13	11	0	1360	1395
1	12	-2	561	542	1	18	-2	246	260	8	9	-1	494	439	4	4	0	2042	2084	2	11	0	1273	1330
4	12	-2	475	533	4	18	-2	271	235	-18	10	-1	286	212	-7	5	0	2087	2240	5	11	0	975	1018
7	12	-2	527	432	-19	19	-2	259	306	-12	10	-1	358	341	2	5	0	3588	3329	8	11	0	695	667
10	12	-2	294	314	2	19	-2	332	280	0	10	-1	439	441	5	5	0	1364	1398	11	11	0	448	467
-22	13	-2	311	345	-21	20	-2	268	262	3	10	-1	217	331	-9	6	0	2584	2529	-21	12	0	492	534
-19	13	-2	420	363	0	20	-2	367	339	6	10	-1	224	185	-6	6	0	2177	2298	-18	12	0	686	681
-16	13	-2	631	668	3	20	-2	288	235	-17	11	-1	324	310	0	6	0	2216	2235	-15	12	0	1142	1188
-13	13	-2	578	616	0	1	-1	1076	1006	-14	11	-1	254	306	3	6	0	1902	1931	-12	12	0	914	1026
2	13	-2	221	329	-2	2	-1	1108	1291	-11	11	-1	288	222	6	6	0	2011	1875	0	12	0	971	1026
5	13	-2	575	556	1	2	-1	188	394	1	11	-1	279	295	-11	7	0	1745	1594	3	12	0	750	810
8	13	-2	433	340	-4	3	-1	1105	1389	7	11	-1	266	237	-8	7	0	2839	2815	6	12	0	760	795
11	13	-2	264	269	2	3	-1	3160	2982	-19	12	-1	241	236	1	7	0	1522	1523	9	12	0	533	569
-24	14	-2	276	209	-6	4	-1	441	752	-13	12	-1	403	422	4	7	0	1363	1383	12	12	0	296	358
-21	14	-2	293	335	0	4	-1	2402	2110	2	12	-1	218	433	7	7	0	1093	1191	-23	13	0	367	388
-18	14	-2	341	445	3	4	-1	1094	1025	11	12	-1	222	118	-13	8	0	1171	1201	-20	13	0	529	551
-15	14	-2	667	641	-8	5	-1	1165	938	-18	13	-1	263	260	-10	8	0	2391	2371	-17	13	0	678	728
0	14	-2	716	671	-5	5	-1	403	605	-15	13	-1	369	364	2	8	0	1525	1493	-14	13	0	874	964
3	14	-2	568	576	1	5	-1	1157	1396	0	13	-1	304	283	5	8	0	1425	1442	1	13	0	844	896
6	14	-2	347	388	4	5	-1	378	438	3	13	-1	589	537	8	8	0	887	979	4	13	0	761	833
-23	15	-2	298	314	-10	6	-1	996	926	9	13	-1	223	137	-15	9	0	878	990	7	13	0	619	611
-20	15	-2	393	377	5	6	-1	301	276	-23	14	-1	221	100	-12	9	0	1442	1441	10	13	0	336	414
-17	15	-2	365	504	-12	7	-1	454	487	-14	14	-1	241	283	-9	9	0	1793	1770	-25	14	0	270	303

h	k	l	10Fo	10Fc	h	k	l	10Fo	10Fc	h	k	l	10Fo	10Fc	h	k	l	10Fo	10Fc	h	k	l	10Fo	10Fc
-22	14	0	395	479	-21	21	0	340	379	5	10	1	417	393	3	7	2	878	897	11	12	2	238	284
-19	14	0	514	561	0	21	0	354	379	-15	11	1	351	290	6	7	2	1111	1159	-24	13	2	290	247
-16	14	0	741	801	-1	1	1	1036	1007	-12	11	1	433	402	-14	8	2	726	779	-21	13	2	230	310
2	14	0	861	887	-3	2	1	1526	1408	0	11	1	218	226	-11	8	2	1000	1004	-18	13	2	379	405
5	14	0	665	702	0	2	1	1092	1297	3	11	1	541	487	-8	8	2	744	710	-15	13	2	585	571
8	14	0	409	439	-5	3	1	149	445	6	11	1	214	206	1	8	2	843	809	0	13	2	626	612
11	14	0	244	327	1	3	1	605	399	1	12	1	337	355	4	8	2	1020	959	3	13	2	543	516
-24	15	0	327	357	-4	4	1	2356	2125	7	12	1	250	239	7	8	2	773	787	6	13	2	597	559
-21	15	0	502	541	2	4	1	270	314	-19	13	1	219	236	-16	9	2	728	738	9	13	2	333	309
-18	15	0	554	653	-9	5	1	266	152	-13	13	1	241	275	-13	9	2	820	840	-23	14	2	326	289
-15	15	0	913	976	-6	5	1	165	306	-15	14	1	203	213	-10	9	2	1308	1321	-20	14	2	272	336
0	15	0	999	966	0	5	1	378	653	0	14	1	297	283	2	9	2	1374	1253	-17	14	2	360	416
3	15	0	668	679	3	5	1	1411	1322	-17	15	1	239	287	5	9	2	609	598	-14	14	2	654	676
6	15	0	499	537	-11	6	1	383	403	4	15	1	234	212	8	9	2	543	542	1	14	2	772	712
9	15	0	365	320	-8	6	1	278	326	2	16	1	226	217	-18	10	2	685	673	4	14	2	428	416
-23	16	0	379	380	1	6	1	756	898	0	17	1	276	188	-15	10	2	581	633	7	14	2	365	320
-20	16	0	544	595	4	6	1	1245	1193	0	20	1	233	96	-12	10	2	1054	1039	10	14	2	299	220
-17	16	0	696	767	-13	7	1	236	245	0	1	2	4499	4374	0	10	2	830	745	-22	15	2	287	307
1	16	0	742	747	-10	7	1	610	670	-2	2	2	1360	1366	3	10	2	922	930	-19	15	2	359	450
4	16	0	512	555	-7	7	1	1059	909	1	2	2	167	225	6	10	2	602	604	-16	15	2	585	616
-22	17	0	380	463	2	7	1	1134	1148	-4	3	2	2352	2296	9	10	2	411	415	2	15	2	483	457
-19	17	0	477	539	5	7	1	193	286	2	3	2	885	899	-20	11	2	402	429	5	15	2	397	411
2	17	0	452	458	-15	8	1	449	484	-6	4	2	1683	1888	-17	11	2	685	645	-21	16	2	309	412
5	17	0	296	379	-12	8	1	431	439	0	4	2	2011	2007	-14	11	2	917	979	-18	16	2	418	422
8	17	0	312	316	-9	8	1	1176	1122	3	4	2	1800	1841	-11	11	2	1012	1008	0	16	2	606	572
-21	18	0	388	406	0	8	1	260	244	-8	5	2	1547	1577	1	11	2	1067	1058	3	16	2	410	363
-18	18	0	501	549	3	8	1	478	462	-5	5	2	1837	1736	4	11	2	610	594	9	16	2	255	221
0	18	0	595	552	6	8	1	451	383	1	5	2	1559	1428	7	11	2	535	539	-23	17	2	254	270
3	18	0	436	428	-14	9	1	288	289	4	5	2	1126	1203	10	11	2	299	383	-20	17	2	314	269
6	18	0	292	314	-11	9	1	414	545	-10	6	2	773	688	-22	12	2	296	285	-17	17	2	514	510
-23	19	0	255	319	1	9	1	319	430	-7	6	2	1271	1371	-19	12	2	452	410	1	17	2	437	436
-20	19	0	461	464	7	9	1	304	334	2	6	2	1963	1897	-16	12	2	678	653	4	17	2	270	297
1	19	0	435	461	-16	10	1	221	277	5	6	2	897	875	-13	12	2	765	683	7	17	2	235	223
4	19	0	252	331	-13	10	1	326	292	-12	7	2	817	720	2	12	2	850	892	-22	18	2	262	285
-22	20	0	381	330	-10	10	1	376	455	-9	7	2	1925	1841	5	12	2	637	615	-19	18	2	343	366
2	20	0	285	358	2	10	1	389	459	0	7	2	1423	1433	8	12	2	398	407	2	18	2	313	297

h	k	l	10Fo	10Fc	h	k	l	10Fo	10Fc	h	k	l	10Fo	10Fc	h	k	l	10Fo	10Fc	h	k	l	10Fo	10Fc
5	18	2	242	222	-9	9	3	1106	1151	-22	14	3	324	286	3	5	4	683	807	-9	7	5	1101	1137
-21	19	2	234	251	0	9	3	1262	1229	-19	14	3	347	359	-11	6	4	227	301	0	7	5	1350	1245
0	19	2	345	313	3	9	3	791	751	-16	14	3	529	574	-8	6	4	558	625	3	7	5	851	880
3	19	2	261	220	6	9	3	707	723	2	14	3	435	427	1	6	4	800	746	6	7	5	659	650
-20	20	2	327	342	9	9	3	466	490	5	14	3	311	386	-7	7	4	247	287	-14	8	5	555	653
1	20	2	328	299	-17	10	3	482	480	8	14	3	268	320	5	7	4	209	220	-11	8	5	1018	1058
0	22	2	253	212	-14	10	3	766	740	-21	15	3	228	325	-15	8	4	230	271	-8	8	5	892	930
0	0	3	2069	2309	-11	10	3	1004	1051	-18	15	3	385	389	-12	8	4	196	250	1	8	5	1073	1062
1	1	3	1296	1293	1	10	3	762	712	-15	15	3	501	509	3	8	4	225	270	4	8	5	796	783
2	2	3	1273	1334	4	10	3	760	735	0	15	3	375	365	-11	9	4	357	402	7	8	5	563	540
-3	3	3	1940	1986	7	10	3	577	583	3	15	3	480	472	-13	10	4	246	235	-16	9	5	578	621
0	3	3	1324	1436	10	10	3	253	296	6	15	3	363	289	-10	10	4	185	78	-13	9	5	712	736
3	3	3	1432	1451	-19	11	3	488	464	-23	16	3	270	244	2	10	4	201	246	-10	9	5	1000	991
-5	4	3	1082	1100	-16	11	3	596	606	-20	16	3	313	316	0	11	4	217	217	2	9	5	708	777
1	4	3	1451	1525	-13	11	3	619	637	-17	16	3	567	550	3	11	4	231	277	5	9	5	807	804
4	4	3	954	893	2	11	3	905	869	1	16	3	473	461	1	12	4	287	237	8	9	5	411	445
-7	5	3	695	687	5	11	3	566	507	4	16	3	343	288	-13	13	4	291	268	-18	10	5	392	472
2	5	3	1618	1638	8	11	3	437	431	-22	17	3	252	212	-17	15	4	242	60	-15	10	5	681	684
5	5	3	1071	1070	11	11	3	374	289	-19	17	3	383	412	-16	16	4	290	232	-12	10	5	954	958
-9	6	3	1258	1251	-21	12	3	334	357	2	17	3	375	383	0	1	5	1760	1706	0	10	5	694	731
-6	6	3	828	852	-18	12	3	454	431	-18	18	3	331	308	-2	2	5	2072	2063	3	10	5	729	762
0	6	3	1046	1105	-15	12	3	527	570	0	18	3	450	374	1	2	5	1069	1018	6	10	5	495	467
3	6	3	1332	1353	-12	12	3	664	701	3	18	3	312	287	-4	3	5	1401	1504	9	10	5	382	388
6	6	3	770	752	0	12	3	793	749	-23	19	3	254	150	2	3	5	1333	1400	-20	11	5	299	339
-11	7	3	1147	1159	3	12	3	488	518	-20	19	3	309	294	-6	4	5	1349	1409	-17	11	5	451	430
-8	7	3	1282	1374	6	12	3	656	595	1	19	3	234	258	0	4	5	1056	1149	-14	11	5	484	505
1	7	3	1103	1222	9	12	3	367	281	-21	21	3	261	225	3	4	5	1448	1519	-11	11	5	782	766
4	7	3	923	956	-23	13	3	241	261	0	21	3	259	185	-8	5	5	1231	1144	1	11	5	595	619
7	7	3	816	816	-20	13	3	455	420	-1	1	4	460	220	-5	5	5	882	896	4	11	5	521	585
-13	8	3	613	634	-17	13	3	435	487	-3	2	4	941	855	1	5	5	1499	1578	7	11	5	552	517
-10	8	3	1240	1368	-14	13	3	389	484	0	2	4	635	577	4	5	5	883	833	10	11	5	300	229
2	8	3	1122	1167	1	13	3	749	699	-5	3	4	286	390	-10	6	5	968	934	-22	12	5	263	278
5	8	3	738	733	4	13	3	519	528	1	3	4	861	914	-7	6	5	1337	1345	-19	12	5	345	385
8	8	3	655	702	7	13	3	345	368	-7	4	4	674	657	2	6	5	1101	1133	-16	12	5	517	562
-15	9	3	767	735	10	13	3	274	293	2	4	4	381	270	5	6	5	844	909	-13	12	5	325	358
-12	9	3	1001	1019	-25	14	3	239	168	-6	5	4	230	439	-12	7	5	482	565	2	12	5	455	558

h	k	l	10Fo	10Fc	h	k	l	10Fo	10Fc	h	k	l	10Fo	10Fc	h	k	l	10Fo	10Fc	h	k	l	10Fo	10Fc
5	12	5	525	507	1	1	6	182	294	2	14	6	223	245	6	11	7	245	173	-15	10	8	224	201
8	12	5	247	272	-3	3	6	850	773	-15	15	6	223	179	-17	12	7	250	146	-12	10	8	276	277
11	12	5	279	289	0	3	6	362	449	7	16	6	244	116	4	12	7	241	168	0	10	8	391	362
-21	13	5	248	288	3	3	6	385	430	-1	1	7	550	612	-16	13	7	243	291	6	10	8	270	289
-18	13	5	333	330	-5	4	6	633	541	-3	2	7	432	393	-15	14	7	253	182	9	10	8	237	113
-15	13	5	410	471	1	4	6	403	376	0	2	7	286	218	0	14	7	270	304	-11	11	8	350	331
0	13	5	830	843	-7	5	6	185	253	-5	3	7	339	378	-17	15	7	260	220	1	11	8	295	280
3	13	5	344	330	2	5	6	171	201	-7	4	7	459	441	0	1	8	244	125	4	11	8	264	261
6	13	5	261	394	5	5	6	625	608	-4	4	7	573	591	-2	2	8	402	390	-19	12	8	218	127
-20	14	5	230	276	-9	6	6	386	393	2	4	7	548	579	1	2	8	588	669	5	12	8	283	210
-17	14	5	476	478	-6	6	6	400	347	-9	5	7	265	265	-4	3	8	591	667	0	13	8	264	263
-14	14	5	427	488	0	6	6	282	369	-6	5	7	501	537	2	3	8	360	263	-17	14	8	239	143
1	14	5	376	384	3	6	6	505	450	0	5	7	326	352	-6	4	8	304	343	1	14	8	243	222
4	14	5	462	455	6	6	6	407	406	3	5	7	619	676	0	4	8	504	491	0	16	8	269	150
-19	15	5	268	307	-11	7	6	342	347	-8	6	7	430	425	3	4	8	267	175	1	1	9	231	136
-16	15	5	452	494	-8	7	6	361	328	1	6	7	572	562	-8	5	8	298	272	0	3	9	201	227
2	15	5	450	402	1	7	6	337	284	4	6	7	334	325	1	5	8	254	325	-5	4	9	188	250
-21	16	5	242	276	4	7	6	328	201	-10	7	7	203	237	4	5	8	444	417	-7	5	9	241	237
-18	16	5	341	366	7	7	6	297	374	-7	7	7	322	389	-10	6	8	344	255	2	5	9	262	306
0	16	5	433	404	-10	8	6	224	225	2	7	7	369	343	-7	6	8	239	241	-9	6	9	218	90
3	16	5	317	328	2	8	6	509	405	5	7	7	260	313	2	6	8	420	460	-3	2	10	413	508
6	16	5	290	256	-9	9	6	410	359	-9	8	7	399	387	5	6	8	446	449	0	2	10	273	334
-23	17	5	237	209	0	9	6	602	551	0	8	7	317	305	-12	7	8	279	246	1	3	10	405	388
-20	17	5	296	310	9	9	6	227	143	3	8	7	231	287	-9	7	8	292	311	3	5	10	299	307
-17	17	5	338	372	-14	10	6	341	277	-14	9	7	253	334	0	7	8	272	271	-8	6	10	217	225
1	17	5	345	393	-11	10	6	512	504	-11	9	7	465	511	3	7	8	368	435	1	6	10	274	194
4	17	5	319	225	1	10	6	326	315	1	9	7	250	302	6	7	8	227	331	4	6	10	207	267
-22	18	5	234	187	7	10	6	239	217	4	9	7	416	460	-14	8	8	321	230	2	7	10	213	219
-19	18	5	240	268	-13	11	6	287	195	-16	10	7	278	294	-11	8	8	196	189	-12	8	10	224	129
2	18	5	296	279	5	11	6	342	303	-10	10	7	341	391	-8	8	8	352	388	-9	8	10	223	271
0	19	5	258	243	-15	12	6	260	176	5	10	7	384	388	1	8	8	412	335	-16	15	11	218	63
-20	20	5	275	253	-12	12	6	259	264	8	10	7	246	211	-16	9	8	237	200	-12	11	13	216	42
1	20	5	233	208	0	12	6	222	270	-15	11	7	262	207	-13	9	8	213	153	-10	9	14	224	24
0	0	6	570	560	-14	13	6	193	112	3	11	7	213	277	-10	9	8	345	314					

(2-carbomethyoxyethyl)-iododiphenylstannane, $C_{16}H_{17}O_2SnI$

h	k	l	10Fo	10Fc	h	k	l	10Fo	10Fc	h	k	l	10Fo	10Fc	h	k	l	10Fo	10Fc	h	k	l	10Fo	10Fc
2	0	0	1981	2007	4	5	0	539	527	6	10	0	636	-641	-6	1	1	331	-336	-4	3	1	1723	-1733
4	0	0	1469	-1454	6	5	0	206	-148	8	10	0	246	-268	-5	1	1	650	654	-3	3	1	564	522
6	0	0	1575	-1589	8	5	0	228	-267	9	10	0	272	301	-4	1	1	336	-323	-2	3	1	3350	-3357
8	0	0	585	-585	0	6	0	1414	1366	1	11	0	481	500	-3	1	1	422	-368	-1	3	1	813	-805
1	1	0	2167	2206	1	6	0	700	679	2	11	0	553	-557	-2	1	1	153	-134	0	3	1	217	-177
2	1	0	2049	-2068	2	6	0	505	492	4	11	0	472	-471	-1	1	1	743	-732	1	3	1	1297	-1306
3	1	0	199	-163	3	6	0	1704	1665	5	11	0	323	-311	0	1	1	671	639	2	3	1	1741	1732
4	1	0	695	-692	4	6	0	332	-329	6	11	0	220	-229	1	1	1	1331	-1334	3	3	1	582	-579
5	1	0	1697	-1717	5	6	0	423	461	3	12	0	324	-291	2	1	1	1295	1303	4	3	1	1288	1286
7	1	0	1014	-1050	6	6	0	409	-399	2	13	0	340	341	5	1	1	552	569	5	3	1	442	470
8	1	0	367	329	7	6	0	417	-412	1	14	0	388	401	6	1	1	376	-400	6	3	1	290	269
10	1	0	258	279	9	6	0	457	-426	3	14	0	552	566	7	1	1	631	648	7	3	1	444	464
11	1	0	434	339	1	7	0	1987	1925	5	14	0	240	205	-10	2	1	343	-341	8	3	1	443	-439
0	2	0	1150	1090	2	7	0	1110	1071	7	14	0	238	-282	-9	2	1	344	292	10	3	1	296	-328
1	2	0	911	-866	4	7	0	816	815	1	15	0	483	487	-6	2	1	1082	1072	-9	4	1	834	844
2	2	0	974	957	5	7	0	1192	-1201	2	15	0	636	702	-5	2	1	855	-847	-7	4	1	986	993
3	2	0	1205	-1203	7	7	0	645	-644	4	15	0	535	567	-4	2	1	1217	1241	-5	4	1	508	-510
4	2	0	238	-210	8	7	0	443	-427	5	15	0	319	-359	-3	2	1	1738	-1632	-3	4	1	3246	-3241
5	2	0	433	-447	0	8	0	2134	2140	0	16	0	757	800	-2	2	1	511	-482	-1	4	1	1704	-1711
6	2	0	835	-825	1	8	0	479	455	1	16	0	275	269	-1	2	1	290	-301	0	4	1	559	-507
7	2	0	300	278	2	8	0	1176	1128	2	16	0	326	353	0	2	1	2015	-1975	1	4	1	982	970
9	2	0	488	474	3	8	0	320	338	3	16	0	329	315	1	2	1	662	666	2	4	1	199	-208
1	3	0	318	-296	4	8	0	712	-751	4	16	0	295	-320	2	2	1	616	-656	3	4	1	2065	2083
4	3	0	1077	-1064	6	8	0	1161	-1197	6	16	0	388	-483	3	2	1	1422	1404	5	4	1	1103	1125
5	3	0	635	-608	7	8	0	246	-217	1	17	0	619	634	4	2	1	210	244	7	4	1	327	-308
8	3	0	262	307	8	8	0	476	-463	5	17	0	465	-436	5	2	1	275	257	9	4	1	500	-479
10	3	0	307	357	9	8	0	290	-249	0	18	0	412	463	6	2	1	667	714	-10	5	1	530	502
0	4	0	1180	1107	1	9	0	1783	1717	-7	0	1	247	-236	7	2	1	315	-308	-8	5	1	843	844
1	4	0	374	-361	4	9	0	231	-214	-3	0	1	154	136	8	2	1	523	489	-7	5	1	215	-184
2	4	0	183	186	5	9	0	985	-1026	-1	0	1	1247	1214	9	2	1	318	-277	-5	5	1	512	-513
3	4	0	234	-216	7	9	0	785	-824	1	0	1	251	272	-11	3	1	268	-317	-4	5	1	1441	-1434
5	4	0	229	-197	0	10	0	1254	1280	5	0	1	742	-774	-10	3	1	416	406	-3	5	1	179	-124
6	4	0	303	262	2	10	0	633	648	7	0	1	355	-359	-8	3	1	983	959	-2	5	1	1951	-1986
8	4	0	253	197	3	10	0	516	-522	9	0	1	235	239	-7	3	1	449	399	-1	5	1	535	513
2	5	0	656	641	4	10	0	516	-553	-11	1	1	275	-200	-6	3	1	276	300	0	5	1	500	-500
3	5	0	269	-257	5	10	0	407	-455	-7	1	1	539	486	-5	3	1	1271	1222	1	5	1	368	370

h	k	l	10Fo	10Fc	h	k	l	10Fo	10Fc	h	k	l	10Fo	10Fc	h	k	l	10Fo	10Fc	h	k	l	10Fo	10Fc
2	5	1	1920	1904	7	7	1	567	-542	-5	11	1	770	794	-1	14	1	421	-447	-5	1	2	2013	2017
3	5	1	247	161	-5	8	1	406	-375	-4	11	1	605	-592	0	14	1	366	372	-4	1	2	412	-384
4	5	1	1758	1792	-4	8	1	199	-166	-3	11	1	377	317	1	14	1	294	281	-3	1	2	470	488
6	5	1	230	264	-3	8	1	282	-269	-2	11	1	890	-903	2	14	1	416	399	-1	1	2	1249	-1227
7	5	1	308	-308	-2	8	1	195	-240	-1	11	1	879	-816	3	14	1	795	753	0	1	2	809	-816
8	5	1	514	-478	-1	8	1	668	627	0	11	1	297	-306	5	14	1	411	402	1	1	2	1834	-1877
10	5	1	359	-394	0	8	1	258	271	1	11	1	911	-913	-5	15	1	372	-289	2	1	2	343	310
-9	6	1	333	350	1	8	1	685	678	2	11	1	801	825	1	15	1	476	464	3	1	2	496	-541
-8	6	1	335	-287	2	8	1	366	402	4	11	1	579	580	2	15	1	354	342	4	1	2	833	870
-7	6	1	379	374	5	8	1	361	-386	5	11	1	376	432	3	15	1	338	339	5	1	2	913	904
-6	6	1	660	-673	7	8	1	248	-318	7	11	1	348	374	7	15	1	322	-274	6	1	2	461	477
-5	6	1	596	-594	8	8	1	222	-199	-9	12	1	470	477	2	16	1	251	226	7	1	2	707	621
-4	6	1	517	-475	-6	9	1	227	-200	-7	12	1	427	441	3	17	1	248	37	10	1	2	344	-251
-3	6	1	1350	-1366	-5	9	1	508	515	-6	12	1	392	386	-6	18	1	279	262	-10	2	2	245	-241
-2	6	1	386	390	-4	9	1	320	-278	-5	12	1	426	-496	-4	18	1	359	338	-9	2	2	433	475
-1	6	1	1179	-1082	-3	9	1	335	296	-4	12	1	521	547	0	18	1	359	-382	-8	2	2	284	250
0	6	1	1028	995	-1	9	1	579	-548	-3	12	1	1246	-1221	-5	19	1	335	339	-7	2	2	763	782
1	6	1	905	862	0	9	1	772	711	-2	12	1	309	-298	-2	19	1	258	-175	-6	2	2	917	932
2	6	1	1323	1294	1	9	1	818	-824	-1	12	1	782	-789	-1	19	1	290	-259	-4	2	2	1049	1063
3	6	1	1412	1415	4	9	1	238	-210	0	12	1	430	-436	1	19	1	401	-357	-3	2	2	959	-958
5	6	1	431	448	5	9	1	232	193	1	12	1	388	384	-3	20	1	262	-327	-2	2	2	1092	-1062
6	6	1	619	-603	6	9	1	291	-348	2	12	1	281	-275	0	20	1	259	-266	-1	2	2	1714	-1687
7	6	1	234	-208	-10	10	1	318	-293	3	12	1	1111	1075	3	20	1	320	272	0	2	2	3091	-3117
8	6	1	513	-501	-6	10	1	619	598	4	12	1	254	232	-10	0	2	622	-641	2	2	2	468	-457
9	6	1	283	-286	-4	10	1	720	714	5	12	1	585	640	-8	0	2	233	209	3	2	2	962	966
-7	7	1	275	-323	-3	10	1	544	-496	6	12	1	283	308	-6	0	2	1904	1912	4	2	2	257	319
-6	7	1	258	-164	-1	10	1	277	-277	-8	13	1	507	496	-4	0	2	1082	1094	5	2	2	1014	1026
-5	7	1	381	-356	0	10	1	922	-911	-4	13	1	877	-890	-2	0	2	879	-874	6	2	2	464	469
-4	7	1	555	-520	1	10	1	461	469	-2	13	1	1155	-1169	0	0	2	2268	-2300	7	2	2	344	293
-3	7	1	443	-443	2	10	1	760	-777	2	13	1	876	886	2	0	2	1882	-1977	-9	3	2	279	301
-2	7	1	302	-337	3	10	1	328	354	3	13	1	267	194	6	0	2	789	823	-8	3	2	465	440
-1	7	1	369	362	4	10	1	305	322	4	13	1	736	807	8	0	2	550	565	-7	3	2	390	375
1	7	1	1120	1090	6	10	1	511	525	8	13	1	314	-287	-11	1	2	513	-474	-6	3	2	655	643
2	7	1	820	812	8	10	1	260	265	-6	14	1	263	-237	-9	1	2	208	-150	-5	3	2	258	249
3	7	1	572	610	-8	11	1	354	385	-5	14	1	291	-292	-8	1	2	449	486	-4	3	2	335	-319
6	7	1	268	-280	-7	11	1	386	428	-3	14	1	772	-765	-7	1	2	907	905	-3	3	2	676	-636

h	k	l	10Fo	10Fc	h	k	l	10Fo	10Fc	h	k	l	10Fo	10Fc	h	k	l	10Fo	10Fc	h	k	l	10Fo	10Fc
-2	3	2	1841	-1831	6	5	2	292	-285	-9	8	2	240	-225	4	10	2	361	390	5	14	2	274	-272
-1	3	2	1512	-1489	7	5	2	325	-325	-7	8	2	487	-444	5	10	2	606	623	-8	15	2	373	-349
0	3	2	1499	-1457	9	5	2	315	-314	-6	8	2	1081	1074	6	10	2	363	376	-6	15	2	272	-323
1	3	2	269	273	-9	6	2	443	-438	-4	8	2	1059	1088	7	10	2	299	312	-5	15	2	314	295
2	3	2	175	-110	-8	6	2	237	292	-3	8	2	468	511	-8	11	2	274	317	-2	15	2	610	598
3	3	2	891	907	-7	6	2	746	-776	-2	8	2	205	-204	-7	11	2	323	346	-1	15	2	425	-451
4	3	2	730	764	-6	6	2	622	615	-1	8	2	542	531	-6	11	2	325	322	0	15	2	231	233
5	3	2	504	531	-5	6	2	234	-226	0	8	2	1770	-1742	-5	11	2	248	227	1	15	2	472	-471
6	3	2	535	513	-3	6	2	1360	1304	2	8	2	1471	-1488	-3	11	2	367	-328	2	15	2	289	-239
9	3	2	263	-241	-2	6	2	1078	-1065	3	8	2	378	-393	-2	11	2	665	-638	4	15	2	360	-352
-10	4	2	291	278	-1	6	2	1388	1367	6	8	2	685	642	-1	11	2	874	-868	5	15	2	282	217
-8	4	2	497	482	0	6	2	859	-862	8	8	2	523	528	0	11	2	653	-659	-7	16	2	339	-313
-5	4	2	303	256	1	6	2	482	493	-9	9	2	321	-245	1	11	2	316	-301	-6	16	2	356	420
-4	4	2	1278	-1282	3	6	2	461	-456	-7	9	2	719	698	4	11	2	340	417	-4	16	2	349	376
-2	4	2	1135	-1139	4	6	2	523	518	-5	9	2	1353	1357	5	11	2	326	316	-1	16	2	279	282
-1	4	2	208	219	5	6	2	766	-762	-3	9	2	618	639	6	11	2	382	395	0	16	2	586	-617
0	4	2	941	-903	6	6	2	289	279	-2	9	2	382	-382	-8	12	2	291	280	2	16	2	342	-324
2	4	2	656	669	9	6	2	331	288	-1	9	2	1201	-1158	-4	12	2	383	-409	-5	17	2	564	528
3	4	2	328	-320	-11	7	2	364	-294	0	9	2	614	-643	-2	12	2	658	-649	-1	17	2	362	-375
4	4	2	918	932	-8	7	2	562	-524	1	9	2	1682	-1644	1	12	2	252	-265	1	17	2	580	-584
5	4	2	265	269	-7	7	2	569	546	3	9	2	472	-461	2	12	2	403	436	-6	18	2	354	322
8	4	2	363	-346	-6	7	2	567	-492	4	9	2	262	248	3	12	2	282	244	-4	18	2	259	275
-9	5	2	303	282	-5	7	2	1267	1231	5	9	2	388	434	4	12	2	451	457	-1	18	2	237	-245
-8	5	2	559	-533	-4	7	2	225	244	6	9	2	389	397	5	12	2	286	325	0	18	2	441	-420
-7	5	2	583	566	-3	7	2	246	250	7	9	2	534	509	-3	13	2	544	-556	2	18	2	337	-329
-6	5	2	420	-451	-2	7	2	1096	1086	-10	10	2	272	-195	-2	13	2	346	313	0	19	2	307	-301
-5	5	2	202	193	-1	7	2	1492	-1461	-7	10	2	367	304	1	13	2	276	265	-11	0	3	340	-351
-4	5	2	303	260	0	7	2	750	715	-6	10	2	768	773	2	13	2	251	-270	-7	0	3	782	796
-3	5	2	922	-899	1	7	2	862	-860	-4	10	2	513	529	3	13	2	339	341	-5	0	3	1473	1487
-2	5	2	1250	1222	2	7	2	494	-521	-3	10	2	349	-277	6	13	2	242	70	-3	0	3	1309	1275
-1	5	2	955	-916	3	7	2	406	-364	-2	10	2	482	-469	-7	14	2	351	-408	-1	0	3	1013	-971
1	5	2	179	123	4	7	2	753	-847	-1	10	2	770	-757	-3	14	2	460	501	1	0	3	1380	-1460
2	5	2	381	-398	5	7	2	413	407	0	10	2	1124	-1115	-1	14	2	603	608	3	0	3	524	-502
3	5	2	1013	1037	6	7	2	436	-399	1	10	2	554	-593	0	14	2	203	-232	5	0	3	392	391
4	5	2	465	-469	7	7	2	528	516	2	10	2	450	-478	3	14	2	264	-348	7	0	3	500	552
5	5	2	576	562	-10	8	2	338	-386	3	10	2	462	524	4	14	2	280	306	-11	1	3	292	249

h	k	l	10Fo	10Fc	h	k	l	10Fo	10Fc	h	k	l	10Fo	10Fc	h	k	l	10Fo	10Fc	h	k	l	10Fo	10Fc
-10	1	3	348	-342	-8	3	3	951	-941	1	5	3	256	-297	6	7	3	414	398	2	10	3	691	725
-9	1	3	368	370	-6	3	3	190	-187	2	5	3	814	-831	7	7	3	346	324	3	10	3	368	-411
-8	1	3	302	-285	-5	3	3	783	-806	3	5	3	802	-813	9	7	3	328	294	4	10	3	310	237
-6	1	3	751	742	-4	3	3	1081	1056	4	5	3	931	-851	-11	8	3	285	-291	-9	11	3	422	394
-5	1	3	747	-789	-3	3	3	1310	-1291	5	5	3	214	-251	-7	8	3	442	451	-8	11	3	332	-367
-4	1	3	1163	1188	-2	3	3	1123	1112	6	5	3	399	-410	-5	8	3	870	886	-5	11	3	669	-679
-3	1	3	976	-927	-1	3	3	567	-559	7	5	3	250	288	-3	8	3	676	673	-4	11	3	653	597
-2	1	3	510	492	0	3	3	625	638	-10	6	3	372	-336	-1	8	3	525	-557	-3	11	3	692	-709
-1	1	3	242	233	1	3	3	1004	1021	-9	6	3	440	-458	1	8	3	1263	-1295	-2	11	3	573	597
0	1	3	1464	-1467	2	3	3	759	-803	-8	6	3	290	-341	2	8	3	416	-423	-1	11	3	230	201
1	1	3	900	928	3	3	3	953	985	-7	6	3	483	-484	3	8	3	194	-117	0	11	3	277	224
2	1	3	1091	-1134	4	3	3	828	-772	-5	6	3	591	578	4	8	3	325	-345	1	11	3	594	605
3	1	3	589	599	7	3	3	384	-388	-4	6	3	1319	1239	5	8	3	465	415	2	11	3	346	-387
6	1	3	574	527	-9	4	3	659	-677	-3	6	3	1564	1516	7	8	3	432	395	3	11	3	389	373
8	1	3	324	252	-8	4	3	226	188	-2	6	3	1175	1148	-10	9	3	248	-249	4	11	3	371	-363
9	1	3	253	-246	-7	4	3	900	-881	-1	6	3	336	318	-9	9	3	300	312	5	11	3	242	177
-10	2	3	504	527	-6	4	3	209	-180	0	6	3	460	-410	-6	9	3	788	777	-9	12	3	267	-336
-9	2	3	338	-311	-5	4	3	271	183	1	6	3	662	-654	-5	9	3	465	-501	-7	12	3	464	-517
-8	2	3	262	275	-4	4	3	438	-436	2	6	3	1173	-1223	-4	9	3	793	813	-6	12	3	261	-221
-7	2	3	270	-177	-3	4	3	1785	1735	3	6	3	719	-679	-3	9	3	202	-205	-4	12	3	345	-339
-6	2	3	551	-527	-2	4	3	233	-187	4	6	3	714	-674	-2	9	3	197	-162	-3	12	3	837	855
-5	2	3	830	801	-1	4	3	1752	1749	5	6	3	304	-322	0	9	3	907	-885	-1	12	3	931	915
-4	2	3	1113	-1108	0	4	3	332	332	8	6	3	405	416	1	9	3	293	309	0	12	3	258	264
-3	2	3	1651	1600	1	4	3	190	200	-10	7	3	358	-356	2	9	3	927	-939	3	12	3	454	-432
-2	2	3	652	-689	2	4	3	237	-234	-9	7	3	367	-366	6	9	3	568	576	5	12	3	539	-511
0	2	3	525	494	3	4	3	893	-938	-8	7	3	237	-151	-10	10	3	365	367	-8	13	3	446	-464
1	2	3	1121	-1100	5	4	3	1001	-938	-6	7	3	568	540	-9	10	3	281	-209	-4	13	3	436	437
2	2	3	1184	1278	-10	5	3	260	-281	-5	7	3	555	517	-8	10	3	328	305	-3	13	3	370	280
3	2	3	834	-872	-9	5	3	239	-175	-4	7	3	1085	1083	-6	10	3	459	-410	-2	13	3	892	910
4	2	3	724	754	-8	5	3	930	-935	-3	7	3	693	699	-5	10	3	661	681	-1	13	3	273	285
5	2	3	235	257	-6	5	3	646	-660	-2	7	3	186	212	-4	10	3	876	-883	0	13	3	339	329
7	2	3	315	261	-4	5	3	701	715	-1	7	3	374	381	-3	10	3	497	525	2	13	3	240	-297
8	2	3	428	-369	-3	5	3	1112	1067	0	7	3	642	-626	-2	10	3	440	-435	3	13	3	315	-295
-11	3	3	255	294	-2	5	3	2017	2011	1	7	3	603	-584	-1	10	3	269	-306	4	13	3	395	-422
-10	3	3	373	-378	-1	5	3	346	339	2	7	3	728	-753	0	10	3	297	270	6	13	3	335	-288
-9	3	3	356	331	0	5	3	966	957	3	7	3	751	-833	1	10	3	608	-651	-7	14	3	306	-280

h	k	l	10Fo	10Fc	h	k	l	10Fo	10Fc	h	k	l	10Fo	10Fc	h	k	l	10Fo	10Fc	h	k	l	10Fo	10Fc
-5	14	3	278	148	-3	1	4	602	-612	3	3	4	686	-665	-4	6	4	182	183	1	9	4	502	528
-3	14	3	571	562	-2	1	4	172	212	5	3	4	573	-574	-2	6	4	649	634	2	9	4	345	325
-2	14	3	322	356	-1	1	4	761	809	6	3	4	502	-508	-1	6	4	1172	-1178	3	9	4	637	662
-1	14	3	385	374	0	1	4	1140	1128	8	3	4	277	-251	0	6	4	1002	1050	-8	10	4	274	-231
2	14	3	369	-349	1	1	4	902	939	-10	4	4	257	-237	1	6	4	906	-916	-7	10	4	355	-337
3	14	3	293	-335	2	1	4	723	764	-8	4	4	813	-798	4	6	4	529	-497	-6	10	4	603	-600
4	14	3	366	-397	3	1	4	360	378	-6	4	4	811	-832	5	6	4	256	243	-5	10	4	676	-678
-5	15	3	269	228	4	1	4	274	-249	-4	4	4	774	776	7	6	4	424	387	-4	10	4	250	-262
-4	15	3	396	377	6	1	4	325	-275	-3	4	4	320	-290	-8	7	4	458	441	-1	10	4	684	690
-3	15	3	366	390	-11	2	4	331	294	-2	4	4	2082	2119	-7	7	4	551	-561	0	10	4	327	339
-1	15	3	252	249	-10	2	4	274	244	-1	4	4	342	370	-6	7	4	781	799	1	10	4	786	851
1	15	3	265	-238	-8	2	4	434	-453	0	4	4	615	633	-5	7	4	586	-620	2	10	4	435	405
2	15	3	278	-280	-7	2	4	667	-681	2	4	4	679	-665	-4	7	4	245	261	5	10	4	497	-477
3	15	3	366	-422	-6	2	4	947	-945	4	4	4	1077	-1086	-3	7	4	379	-374	7	10	4	306	-278
-5	16	3	380	363	-5	2	4	990	-1000	5	4	4	315	-271	-2	7	4	546	-554	-10	11	4	249	120
1	16	3	321	-343	-4	2	4	268	-249	6	4	4	343	-377	-1	7	4	643	665	-7	11	4	507	-495
2	16	3	269	-323	-3	2	4	176	-66	8	4	4	323	323	0	7	4	372	-405	-6	11	4	342	-344
-6	17	3	356	356	-2	2	4	642	645	-9	5	4	639	-600	1	7	4	694	683	-5	11	4	246	-187
-4	17	3	260	234	-1	2	4	801	828	-8	5	4	326	299	4	7	4	296	315	-4	11	4	351	-378
0	17	3	399	-431	0	2	4	1274	1243	-7	5	4	899	-895	6	7	4	305	301	-3	11	4	388	384
-4	18	3	295	-301	1	2	4	1101	1102	-6	5	4	346	373	-10	8	4	421	388	-2	11	4	228	252
-5	19	3	339	-266	3	2	4	311	295	-5	5	4	360	-348	-8	8	4	242	199	-1	11	4	673	712
1	19	3	306	252	4	2	4	210	-207	-4	5	4	430	411	-7	8	4	356	352	0	11	4	818	830
-10	0	4	596	617	5	2	4	572	-552	-3	5	4	1344	1334	-6	8	4	649	-630	2	11	4	639	637
-6	0	4	988	-976	7	2	4	450	-462	-2	5	4	351	-329	-4	8	4	921	-900	6	11	4	467	-475
-4	0	4	1085	-1039	-9	3	4	534	-507	-1	5	4	1598	1668	-3	8	4	406	-396	-9	12	4	258	103
-2	0	4	239	-241	-7	3	4	962	-995	0	5	4	484	-490	-1	8	4	277	-268	-8	12	4	495	-523
0	0	4	789	790	-6	3	4	772	-743	1	5	4	303	-293	0	8	4	698	669	-6	12	4	381	-367
2	0	4	832	943	-5	3	4	499	-500	2	5	4	250	-195	2	8	4	713	756	-4	12	4	365	389
4	0	4	426	442	-4	3	4	705	-720	3	5	4	922	-919	-9	9	4	302	310	-3	12	4	263	-207
-11	1	4	337	357	-3	3	4	1082	1084	5	5	4	617	-611	-6	9	4	401	-390	-2	12	4	874	873
-8	1	4	230	-160	-2	3	4	652	627	6	5	4	304	321	-5	9	4	919	-985	-1	12	4	232	176
-7	1	4	415	-404	-1	3	4	1344	1358	-8	6	4	558	-589	-4	9	4	325	-365	0	12	4	565	604
-6	1	4	817	-817	0	3	4	1411	1404	-7	6	4	668	715	-3	9	4	616	-611	1	12	4	240	289
-5	1	4	1286	-1269	1	3	4	431	368	-6	6	4	630	-673	-1	9	4	345	315	2	12	4	311	-351
-4	1	4	357	-334	2	3	4	336	370	-5	6	4	795	788	0	9	4	442	447	4	12	4	575	-642

h	k	l	10Fo	10Fc	h	k	l	10Fo	10Fc	h	k	l	10Fo	10Fc	h	k	l	10Fo	10Fc	h	k	l	10Fo	10Fc
-9	13	4	359	-363	1	0	5	1755	1768	-9	3	5	443	-492	-6	6	5	327	367	3	8	5	512	523
-7	13	4	452	-460	3	0	5	962	944	-8	3	5	564	539	-5	6	5	297	-279	4	8	5	254	286
-3	13	4	561	545	5	0	5	438	-490	-7	3	5	478	-418	-4	6	5	386	-396	7	8	5	312	-323
-1	13	4	749	766	7	0	5	476	-476	-6	3	5	305	293	-3	6	5	527	-543	-10	9	5	462	476
3	13	4	426	-421	-10	1	5	602	666	-5	3	5	329	293	-2	6	5	886	-879	-7	9	5	248	-217
5	13	4	331	-402	-9	1	5	327	-311	-3	3	5	581	594	-1	6	5	235	-200	-6	9	5	706	-714
-8	14	4	303	-346	-8	1	5	485	523	-2	3	5	622	-639	0	6	5	425	-445	-4	9	5	1139	-1159
-7	14	4	373	358	-7	1	5	603	-600	-1	3	5	538	508	1	6	5	229	224	-2	9	5	223	-245
-6	14	4	358	-328	-6	1	5	949	-968	0	3	5	211	-299	2	6	5	469	448	0	9	5	705	701
-5	14	4	243	237	-4	1	5	1542	-1538	1	3	5	280	-240	3	6	5	231	215	2	9	5	819	844
-4	14	4	242	212	-3	1	5	656	661	3	3	5	294	-302	4	6	5	619	606	6	9	5	305	-327
-2	14	4	529	569	-2	1	5	274	-268	5	3	5	385	-420	6	6	5	248	282	-10	10	5	250	-263
-1	14	4	271	-250	-1	1	5	772	798	8	3	5	237	153	-10	7	5	410	451	-9	10	5	357	318
0	14	4	275	294	0	1	5	1037	1028	-11	4	5	212	-151	-9	7	5	270	318	-8	10	5	321	-343
4	14	4	269	-256	1	1	5	235	218	-9	4	5	337	299	-8	7	5	263	269	-5	10	5	442	-439
-8	15	4	274	245	2	1	5	954	1030	-7	4	5	554	523	-7	7	5	523	536	-4	10	5	533	511
-6	15	4	392	362	3	1	5	506	-536	-6	4	5	243	211	-6	7	5	507	-507	-3	10	5	611	-630
-2	15	4	264	-259	5	1	5	428	-376	-3	4	5	716	-703	-4	7	5	1029	-1053	-2	10	5	396	460
0	15	4	353	-347	6	1	5	387	-407	-1	4	5	731	-741	-3	7	5	1087	-1062	0	10	5	261	228
-7	16	4	314	262	8	1	5	283	-312	1	4	5	343	-339	-2	7	5	293	-307	1	10	5	526	538
-6	16	4	300	-228	-11	2	5	244	275	4	4	5	233	-113	-1	7	5	807	-810	3	10	5	238	214
-4	16	4	319	-294	-10	2	5	268	-318	7	4	5	419	370	0	7	5	480	502	4	10	5	299	-301
2	16	4	305	297	-9	2	5	343	331	-9	5	5	299	251	2	7	5	807	848	-9	11	5	309	-357
-5	17	4	388	-327	-8	2	5	565	-612	-8	5	5	567	594	3	7	5	576	642	-4	11	5	497	-484
0	17	4	200	137	-6	2	5	342	-376	-7	5	5	211	202	5	7	5	295	295	-3	11	5	404	405
3	17	4	277	270	-5	2	5	647	-655	-6	5	5	387	397	6	7	5	267	-270	-2	11	5	274	-320
-1	18	4	268	188	-4	2	5	583	600	-4	5	5	402	-407	-11	8	5	456	419	-1	11	5	303	300
-4	19	4	288	-185	-3	2	5	1051	-1059	-3	5	5	389	-370	-9	8	5	539	536	3	11	5	325	-340
-1	19	4	226	185	-2	2	5	1241	1253	-2	5	5	535	-488	-7	8	5	333	-328	5	11	5	284	-274
0	19	4	282	296	-1	2	5	179	118	-1	5	5	451	-468	-6	8	5	243	216	-2	12	5	351	312
-11	0	5	537	547	0	2	5	592	591	0	5	5	552	-545	-5	8	5	1294	-1316	-1	12	5	341	-334
-9	0	5	607	591	1	2	5	581	602	3	5	5	303	299	-3	8	5	977	-1003	-7	13	5	243	168
-7	0	5	313	-349	2	2	5	274	-255	5	5	5	285	310	-2	8	5	370	-414	-5	13	5	222	70
-5	0	5	1939	-1962	3	2	5	397	362	8	5	5	284	131	-1	8	5	450	471	-1	13	5	292	-263
-3	0	5	1610	-1597	4	2	5	670	-679	-9	6	5	359	356	1	8	5	1230	1179	0	13	5	422	-458
-1	0	5	336	344	6	2	5	304	-268	-8	6	5	688	658	2	8	5	296	306	-8	14	5	266	269

h	k	l	10Fo	10Fc	h	k	l	10Fo	10Fc	h	k	l	10Fo	10Fc	h	k	l	10Fo	10Fc	h	k	l	10Fo	10Fc
-6	14	5	352	322	-9	2	6	333	-328	-4	5	6	290	-279	-5	10	6	596	575	-9	0	7	687	-708
-2	14	5	631	-636	-8	2	6	451	428	-3	5	6	740	-723	-3	10	6	368	427	-5	0	7	1075	1083
4	14	5	291	301	-6	2	6	730	780	-1	5	6	1325	-1283	0	10	6	320	-320	-3	0	7	1613	1564
-7	15	5	303	302	-5	2	6	808	825	1	5	6	388	-359	1	10	6	444	-433	-1	0	7	205	134
-6	15	5	255	-184	-3	2	6	772	814	2	5	6	273	307	3	10	6	334	-350	1	0	7	883	-887
-4	15	5	437	-469	-2	2	6	429	-480	3	5	6	247	282	-10	11	6	341	-300	3	0	7	741	-745
-3	15	5	443	-428	0	2	6	252	-270	5	5	6	365	367	-7	11	6	402	470	5	0	7	243	-169
-2	15	5	269	-296	1	2	6	851	-824	-11	6	6	260	285	-6	11	6	386	376	-10	1	7	639	-674
-1	15	5	477	-505	3	2	6	552	-606	-9	6	6	291	274	-5	11	6	336	318	-8	1	7	480	-531
0	15	5	208	206	4	2	6	249	253	-8	6	6	346	357	-4	11	6	696	675	-7	1	7	346	342
3	15	5	337	406	7	2	6	277	283	-7	6	6	248	-263	-1	11	6	460	-455	-6	1	7	435	484
-5	16	5	387	-381	-11	3	6	243	-237	-6	6	6	681	697	0	11	6	429	-444	-5	1	7	380	383
-3	16	5	447	-418	-10	3	6	362	-382	-5	6	6	505	-535	1	11	6	288	-232	-4	1	7	1071	1097
1	16	5	433	437	-9	3	6	458	467	-3	6	6	525	-504	2	11	6	366	-412	-3	1	7	257	-204
-6	17	5	334	-346	-7	3	6	1039	1051	-2	6	6	788	-761	-8	12	6	502	529	-2	1	7	690	652
-4	17	5	445	-391	-6	3	6	457	433	0	6	6	427	-422	-6	12	6	573	657	-1	1	7	632	-648
0	17	5	289	280	-5	3	6	611	586	1	6	6	539	561	-5	12	6	301	359	0	1	7	374	-360
2	17	5	422	354	-4	3	6	498	488	3	6	6	392	355	-2	12	6	697	-709	1	1	7	326	-341
-5	18	5	297	-289	-3	3	6	683	-669	4	6	6	305	322	0	12	6	411	-414	2	1	7	575	-577
-8	0	6	249	-201	-2	3	6	382	396	-7	7	6	314	234	1	12	6	411	-407	4	1	7	328	-307
-4	0	6	325	319	-1	3	6	1437	-1398	-6	7	6	375	-364	4	12	6	337	284	5	1	7	240	275
-2	0	6	331	339	0	3	6	693	-667	-5	7	6	218	214	-9	13	6	295	321	-9	2	7	385	-434
0	0	6	329	367	1	3	6	474	-544	-4	7	6	581	-562	-7	13	6	532	572	-8	2	7	322	334
4	0	6	444	-541	2	3	6	565	-517	0	7	6	312	264	-5	13	6	274	272	-6	2	7	600	601
6	0	6	271	-310	3	3	6	530	505	2	7	6	553	542	-3	13	6	434	-427	-5	2	7	598	613
-10	1	6	234	-305	5	3	6	496	486	6	7	6	245	-149	-1	13	6	702	-739	-3	2	7	451	424
-6	1	6	476	471	-8	4	6	931	968	-6	8	6	214	129	3	13	6	340	273	-2	2	7	649	-599
-5	1	6	396	372	-6	4	6	1040	1062	-2	8	6	269	262	-8	14	6	351	326	0	2	7	728	-723
-4	1	6	801	823	-5	4	6	199	177	0	8	6	322	296	-6	14	6	369	317	1	2	7	335	-301
-3	1	6	185	130	-2	4	6	1354	-1398	-4	9	6	383	362	-5	14	6	247	-269	4	2	7	323	335
0	1	6	213	-190	0	4	6	1254	-1219	-3	9	6	318	327	-2	14	6	359	-424	-7	3	7	525	558
2	1	6	521	-537	4	4	6	649	606	-2	9	6	211	244	0	14	6	361	-345	-5	3	7	318	307
4	1	6	273	-318	6	4	6	404	361	0	9	6	214	-240	-4	15	6	284	-251	-1	3	7	463	-531
5	1	6	261	-302	-9	5	6	553	559	2	9	6	335	-359	0	15	6	215	163	4	3	7	224	155
6	1	6	259	234	-7	5	6	1071	1068	5	9	6	293	-259	1	15	6	253	-20	-3	4	7	378	-391
-11	2	6	303	-350	-5	5	6	463	463	-9	10	6	336	-316	-11	0	7	502	-556	-1	4	7	237	-259

h	k	l	10Fo	10Fc	h	k	l	10Fo	10Fc	h	k	l	10Fo	10Fc	h	k	l	10Fo	10Fc	h	k	l	10Fo	10Fc
3	4	7	283	262	1	8	7	486	-400	2	0	8	252	-255	-7	5	8	758	-745	-7	13	8	362	-438
-11	5	7	250	194	3	8	7	513	-531	4	0	8	275	-63	-5	5	8	517	-472	-5	13	8	301	-288
-7	5	7	348	-339	5	8	7	286	-198	-10	1	8	250	230	-4	5	8	233	250	-1	13	8	490	393
-5	5	7	342	-320	-10	9	7	490	-463	-8	1	8	226	212	-2	5	8	346	340	1	13	8	281	253
-3	5	7	298	312	-8	9	7	385	-394	-5	1	8	333	284	-1	5	8	633	609	-3	14	8	293	237
-2	5	7	386	-327	-6	9	7	326	292	-4	1	8	477	-471	1	5	8	592	568	-9	0	9	617	569
-1	5	7	485	481	-4	9	7	954	972	-3	1	8	279	227	2	5	8	269	-259	-7	0	9	291	262
2	5	7	223	240	-2	9	7	389	339	-2	1	8	399	-391	-9	6	8	362	-347	-5	0	9	447	-419
4	5	7	297	251	0	9	7	227	-204	0	1	8	278	180	-8	6	8	244	-307	-3	0	9	435	-392
-9	6	7	283	-341	2	9	7	483	-499	1	1	8	228	-207	-6	6	8	408	-433	-1	0	9	269	-247
-8	6	7	460	-453	-9	10	7	379	-388	4	1	8	254	235	-3	6	8	486	517	-10	1	9	392	371
-6	6	7	633	-652	-6	10	7	272	294	-11	2	8	226	179	-2	6	8	455	437	-8	1	9	377	367
-5	6	7	272	255	-5	10	7	393	447	-9	2	8	377	422	-1	6	8	419	473	-5	1	9	239	-241
-3	6	7	387	382	-3	10	7	423	441	-8	2	8	282	-306	0	6	8	234	264	-4	1	9	483	-476
-2	6	7	551	552	-2	10	7	297	-295	-7	2	8	288	324	3	6	8	357	-454	-2	1	9	471	-439
0	6	7	604	643	0	10	7	344	-369	-5	2	8	380	-414	-10	7	8	259	-194	-9	2	9	230	246
1	6	7	261	-224	1	10	7	432	-427	-3	2	8	677	-711	-9	7	8	305	-239	-6	2	9	462	-455
3	6	7	218	93	-7	11	7	353	343	-2	2	8	522	504	-4	7	8	333	376	-5	2	9	278	-246
4	6	7	270	-273	-6	11	7	225	200	3	2	8	278	337	-2	7	8	340	346	-4	2	9	472	-452
6	6	7	308	-314	-5	11	7	293	333	-11	3	8	315	294	1	7	8	303	-224	-3	2	9	264	-280
-10	7	7	406	-399	-1	11	7	484	-440	-8	3	8	365	386	-4	8	8	339	329	0	2	9	353	396
-8	7	7	317	-373	1	11	7	393	-319	-7	3	8	648	-657	0	8	8	220	-250	2	2	9	426	399
-7	7	7	366	-359	0	12	7	280	-239	-5	3	8	655	-614	-8	9	8	236	232	-8	3	9	231	-158
-4	7	7	845	875	-8	14	7	257	-248	-4	3	8	379	-356	-5	9	8	324	297	-6	3	9	329	-299
-3	7	7	342	316	-6	14	7	286	-277	-3	3	8	265	241	-2	9	8	221	-139	-5	3	9	504	-472
-2	7	7	518	543	-2	14	7	264	240	-2	3	8	566	-553	-9	10	8	268	308	-3	3	9	345	-352
-1	7	7	498	487	0	14	7	388	293	-1	3	8	490	488	-3	10	8	452	-453	0	3	9	249	283
0	7	7	197	-158	-7	15	7	311	-342	2	3	8	366	359	0	10	8	206	-147	1	3	9	393	428
1	7	7	443	390	-1	15	7	349	357	4	3	8	333	309	3	10	8	305	275	-7	4	9	425	-442
2	7	7	369	-411	-5	16	7	304	307	-8	4	8	481	-474	-8	11	8	296	260	-1	4	9	452	486
5	7	7	350	-331	-3	16	7	320	304	-6	4	8	931	-936	-7	11	8	295	-273	-7	5	9	226	164
-9	8	7	501	-548	-2	16	7	261	207	-4	4	8	390	-345	-4	11	8	376	-386	-6	5	9	296	-316
-8	8	7	236	-240	-4	17	7	410	367	-2	4	8	456	418	-2	11	8	322	-365	-5	5	9	233	241
-5	8	7	616	669	-6	0	8	216	254	0	4	8	676	688	-8	12	8	302	-240	0	5	9	300	238
-3	8	7	782	767	-4	0	8	429	410	2	4	8	296	312	-6	12	8	421	-435	1	5	9	272	-318
-1	8	7	244	179	0	0	8	256	-302	-8	5	8	261	-228	0	12	8	407	412	-6	6	9	424	405

h	k	l	10Fo	10Fc	h	k	l	10Fo	10Fc	h	k	l	10Fo	10Fc	h	k	l	10Fo	10Fc	h	k	l	10Fo	10Fc
-4	6	9	421	394	-5	9	9	256	-255	-3	1	10	403	-385	-7	6	10	379	358	-4	2	11	306	285
0	6	9	318	-305	-4	9	9	388	-424	-2	1	10	341	360	-3	6	10	243	-259	-6	3	11	270	288
2	6	9	297	-308	-2	9	9	537	-476	0	1	10	201	216	-1	6	10	312	-333	-5	3	11	296	228
-8	7	9	239	264	-4	10	9	323	-374	-7	2	10	328	-334	-9	7	10	237	239	0	3	11	264	-197
-5	7	9	423	415	0	10	9	294	294	-1	2	10	478	453	-6	7	10	305	268	-7	4	11	301	309
-4	7	9	374	-344	-7	12	9	266	-223	-2	3	10	251	245	0	7	10	233	-220	-5	4	11	317	325
-1	7	9	263	-314	-10	0	10	330	313	0	3	10	252	237	-8	8	10	283	200	-1	4	11	361	-285
1	7	9	295	-275	-8	0	10	362	330	1	3	10	257	-259	-4	8	10	356	-392	-6	5	11	291	313
-9	8	9	383	420	-4	0	10	491	-512	-6	4	10	439	414	-5	9	10	269	-298	-4	6	11	312	-297
-7	8	9	238	221	-2	0	10	386	-420	-4	4	10	284	262	-3	9	10	292	-243	-2	0	12	288	371
-3	8	9	596	-566	0	0	10	324	303	2	4	10	306	-293	-7	0	11	258	-285	-7	1	12	257	-224
-1	8	9	294	-315	-7	1	10	265	185	-5	5	10	403	415	-1	0	11	338	344	-7	2	12	260	206
-8	9	9	313	331	-6	1	10	320	-323	0	5	10	269	-260	-3	1	11	316	296					

3-deazauracil, $C_5H_5O_2N$

h	k	l	10Fo	10Fc	h	k	l	10Fo	10Fc
0	3	7	36.1	36.9	4	1	3	37.0	35.6
0	1	3	11.2	8.0	3	1	2	24.6	23.8
0	3	8	41.1	37.1	6	2	4	54.8	51.2
0	2	6	18.7	15.8	6	2	3	55.3	56.0
0	2	5	16.0	13.2	7	2	5	31.6	28.8
1	2	6	23.5	21.2	4	1	2	44.9	49.2
1	3	8	38.1	34.6	5	1	3	41.9	39.7
1	5	13	55.6	56.0	5	1	2	39.8	39.0
1	2	5	43.4	40.9	7	2	3	50.5	53.8
1	2	6	22.7	21.2	6	1	3	16.6	15.0
3	4	9	35.4	35.9	9	2	4	35.4	39.0
1	1	3	45.8	47.8	11	3	5	37.8	38.5
2	2	6	67.4	65.6	7	1	3	54.8	53.7
3	3	7	78.2	76.3	5	1	2	37.6	39.0
1	1	3	45.8	47.8	6	1	2	39.3	38.1
3	3	9	35.7	40.1	7	1	2	43.8	48.2
4	4	10	72.5	71.1	9	1	3	40.5	43.2
3	3	8	27.6	28.6	5	1	1	15.6	16.3
2	2	5	11.3	7.2	8	1	2	56.4	62.5
4	3	6	69.3	71.3	7	1	1	37.6	44.4
4	3	8	62.9	60.7	9	1	3	49.7	43.2
3	2	5	28.4	26.4	6	1	1	28.1	28.6
3	2	6	33.6	29.7	8	1	1	35.7	50.9
4	3	9	43.5	41.7	8	1	0	42.0	37.8
5	3	9	26.7	32.2	9	1	0	46.2	41.1
2	1	3	35.6	33.6	8	0	0	123.5	133.2
4	2	6	67.5	71.2	4	0	0	36.3	35.9
4	2	5	55.1	52.7	7	0	-1	67.1	67.6
3	2	4	37.8	38.0	9	0	-1	34.6	34.2
4	3	6	72.5	71.3	3	0	-1	32.4	32.1
5	3	7	56.8	55.1	5	0	-1	55.1	51.4
5	3	6	46.4	48.9	6	0	-2	62.5	59.3
2	1	2	16.3	7.8	7	0	-2	73.0	65.9
4	2	5	53.8	52.7	7	0	-1	62.1	67.6
5	2	6	62.8	61.0	4	0	-1	21.4	27.2
5	2	5	57.6	58.7	9	0	-2	62.7	58.4
4	2	4	26.9	27.7	9	0	-3	38.3	30.7
6	3	6	38.3	40.8	9	0	-1	34.4	34.2
3	1	3	64.0	64.4	6	0	-1	18.0	15.0
5	2	4	48.9	42.7	8	0	-1	34.3	33.3
5	2	5	57.3	58.7	8	-1	-1	77.5	50.9
6	2	6	54.0	49.8	7	-1	-1	55.0	44.4
6	2	5	24.6	26.5	9	-1	-2	26.5	27.1

Schultenite, $PbHAsO_4$

h	k	l	10Fo	10Fc	h	k	l	10Fo	10Fc	h	k	l	10Fo	10Fc	h	k	l	10Fo	10Fc	h	k	l	10Fo	10Fc
-1	10	-6	274	226	-1	7	-2	265	262	-1	5	-1	529	519	2	2	0	843	827	1	10	0	199	195
-1	8	-5	451	415	0	7	-2	189	186	0	5	-1	116	56	3	2	0	89	67	2	10	0	473	470
0	8	-5	182	172	0	7	-2	214	186	0	5	-1	71	56	6	2	0	616	632	3	-6	1	659	580
1	8	-5	349	361	2	7	-2	358	341	1	5	-1	502	467	0	3	0	212	175	2	-5	1	478	483
-1	9	-5	456	415	4	7	-2	678	610	2	5	-1	167	177	1	3	0	454	434	4	-4	1	227	191
0	9	-5	196	206	6	7	-2	326	371	2	5	-1	158	177	1	3	0	431	434	5	-4	1	901	770
-1	7	-4	134	134	-1	8	-2	341	357	4	5	-1	156	160	1	3	0	405	434	1	-3	1	513	540
0	7	-4	106	101	-1	8	-2	370	357	6	5	-1	301	366	2	3	0	479	504	1	-3	1	567	540
-1	8	-4	172	174	0	8	-2	245	268	-1	6	-1	536	555	3	3	0	188	159	2	-3	1	127	100
0	9	-4	390	413	0	8	-2	232	268	0	6	-1	132	133	3	3	0	148	159	4	-3	1	149	152
0	10	-4	385	367	1	8	-2	299	265	0	6	-1	119	133	4	3	0	464	497	6	-3	1	181	172
0	6	-3	384	406	1	8	-2	267	265	1	6	-1	585	529	0	4	0	303	261	1	-2	1	311	280
1	6	-3	451	464	3	8	-2	318	327	2	6	-1	354	369	1	4	0	367	314	1	-2	1	280	280
2	6	-3	240	204	3	8	-2	319	327	2	6	-1	347	369	1	4	0	326	314	2	-2	1	628	529
3	6	-3	554	575	1	9	-2	349	347	-1	7	-1	249	261	2	4	0	196	231	2	-2	1	573	529
-1	7	-3	117	102	-2	10	-2	191	215	1	7	-1	267	210	2	4	0	261	231	3	-2	1	495	503
1	7	-3	235	254	-2	10	-2	219	215	1	7	-1	230	210	3	4	0	137	127	4	-2	1	355	328
0	8	-3	291	292	0	10	-2	563	556	2	7	-1	136	128	4	4	0	345	301	5	-2	1	320	301
1	8	-3	286	300	0	10	-2	555	556	-1	8	-1	475	473	4	4	0	262	301	1	-1	1	671	725
3	8	-3	455	486	2	10	-2	448	446	1	8	-1	244	224	0	5	0	437	424	2	-1	1	89	64
-1	9	-3	399	421	1	2	-1	824	758	2	8	-1	323	341	2	5	0	657	756	3	-1	1	666	682
-1	9	-3	382	421	3	2	-1	394	348	2	8	-1	373	341	2	5	0	759	756	2	1	1	64	64
0	10	-3	152	178	4	2	-1	176	117	2	8	-1	346	341	2	5	0	732	756	2	1	1	66	64
-1	11	-3	562	542	0	3	-1	310	349	-2	9	-1	236	249	4	5	0	303	346	3	1	1	622	682
-1	11	-3	615	542	1	3	-1	140	121	3	9	-1	341	370	-1	6	0	102	94	4	1	1	126	156
0	4	-2	513	530	2	3	-1	353	306	3	9	-1	391	370	2	6	0	289	263	6	1	1	218	233
2	4	-2	511	447	3	3	-1	734	681	-1	10	-1	198	211	2	6	0	251	263	7	1	1	498	495
6	4	-2	183	190	4	3	-1	293	298	-1	11	-1	347	331	3	6	0	243	293	1	2	1	293	280
0	5	-2	426	489	0	4	-1	391	395	3	0	0	573	521	3	6	0	326	293	2	2	1	489	529
2	5	-2	364	387	0	4	-1	389	395	4	0	0	541	500	4	6	0	335	405	2	2	1	520	529
5	5	-2	288	261	1	4	-1	321	332	6	0	0	229	212	0	7	0	995	959	3	2	1	508	503
6	5	-2	340	342	2	4	-1	354	380	3	1	0	299	274	3	7	0	406	309	4	2	1	399	328
-1	6	-2	270	287	2	4	-1	347	380	6	1	0	197	218	0	8	0	549	521	4	2	1	280	328
1	6	-2	499	487	3	4	-1	931	914	0	2	0	508	466	2	9	0	368	372	7	2	1	341	343
3	6	-2	339	390	3	4	-1	862	914	1	2	0	139	124	6	9	0	331	316	1	3	1	488	540
-1	7	-2	279	262	4	4	-1	271	267	1	2	0	174	124	-2	10	0	527	470	2	3	1	125	100

h	k	l	10Fo	10Fc	h	k	l	10Fo	10Fc	h	k	l	10Fo	10Fc	h	k	l	10Fo	10Fc	h	k	l	10Fo	10Fc
2	3	1	96	100	2	-6	2	208	244	4	0	2	658	597	1	6	2	243	287	1	-3	3	625	576
4	3	1	138	152	4	-6	2	312	286	4	0	2	605	597	4	6	2	262	286	2	-3	3	417	378
4	3	1	221	152	4	-6	2	298	286	5	0	2	483	444	5	6	2	164	180	4	-3	3	144	165
1	4	1	564	582	2	-5	2	382	399	5	0	2	467	444	1	7	2	242	262	5	-3	3	402	354
4	4	1	169	191	2	-5	2	366	399	6	0	2	293	337	2	7	2	657	698	5	-3	3	378	354
4	4	1	158	191	3	-5	2	286	286	3	1	2	85	59	3	7	2	473	468	6	-3	3	205	255
5	4	1	710	770	3	-5	2	298	286	3	1	2	78	59	4	7	2	365	386	2	-2	3	294	284
1	5	1	494	519	3	-4	2	253	225	5	1	2	355	300	4	7	2	334	386	2	-2	3	288	284
2	5	1	482	483	3	-4	2	231	225	5	1	2	276	300	5	7	2	309	318	3	-2	3	229	235
3	5	1	212	199	4	-4	2	177	188	6	1	2	276	260	6	7	2	304	231	3	-2	3	254	235
3	5	1	199	199	6	-4	2	273	261	2	2	2	399	383	1	8	2	329	357	3	-2	3	253	235
4	5	1	301	336	1	-3	2	145	135	3	2	2	289	291	6	8	2	347	295	4	-2	3	487	502
4	5	1	333	336	1	-3	2	145	135	4	2	2	436	437	4	9	2	244	235	4	-2	3	538	502
4	5	1	337	336	1	-3	2	157	135	4	2	2	462	437	0	12	2	361	343	6	-2	3	182	190
0	6	1	157	133	2	-3	2	280	240	4	2	2	490	437	3	-8	3	334	375	7	-2	3	346	355
1	6	1	553	555	2	-3	2	236	240	6	2	2	242	232	3	-8	3	384	375	3	-1	3	667	674
3	6	1	612	580	2	-3	2	252	240	6	2	2	192	232	5	-8	3	363	361	3	-1	3	592	674
5	6	1	165	192	3	-3	2	353	370	7	2	2	257	263	5	-8	3	365	361	5	-1	3	506	482
5	6	1	256	192	3	-3	2	389	370	2	3	2	236	240	5	-7	3	175	191	5	-1	3	456	482
1	7	1	253	261	4	-3	2	362	309	3	3	2	350	370	3	-6	3	579	603	3	1	3	673	674
3	7	1	226	246	4	-3	2	281	309	3	3	2	397	370	3	-6	3	541	603	3	1	3	641	674
-1	8	1	225	224	5	-3	2	155	164	4	3	2	287	309	1	-5	3	215	212	5	1	3	458	482
1	8	1	442	473	6	-3	2	497	497	4	3	2	294	309	1	-5	3	227	212	5	1	3	524	482
3	8	1	362	382	2	-2	2	420	383	5	3	2	207	164	2	-5	3	325	341	5	1	3	519	482
-1	9	1	574	572	2	-2	2	364	383	5	3	2	165	164	2	-5	3	308	341	7	1	3	294	304
2	9	1	243	249	3	-2	2	317	291	6	3	2	469	497	2	-5	3	305	341	2	2	3	307	284
1	10	1	223	211	3	-2	2	275	291	3	4	2	209	225	1	-4	3	734	842	3	2	3	289	235
1	11	1	322	331	4	-2	2	372	437	3	4	2	195	225	1	-4	3	911	842	3	2	3	234	235
1	12	1	390	372	6	-2	2	211	232	4	4	2	138	188	2	-4	3	268	279	4	2	3	518	502
4	-8	2	223	223	7	-2	2	250	263	4	4	2	183	188	2	-4	3	269	279	4	2	3	497	502
2	-7	2	703	698	1	-1	2	470	527	4	4	2	243	188	2	-4	3	261	279	6	2	3	197	190
3	-7	2	432	468	3	-1	2	77	59	2	5	2	325	399	3	-4	3	238	246	7	2	3	433	355
3	-7	2	459	468	2	0	2	1117	1023	3	5	2	289	286	3	-4	3	238	246	7	2	3	385	355
4	-7	2	376	386	3	0	2	684	685	3	5	2	228	286	5	-4	3	467	438	2	3	3	439	378
4	-7	2	379	386	3	0	2	634	685	4	5	2	390	433	5	-4	3	393	438	4	3	3	151	165
5	-7	2	347	318	4	0	2	614	597	6	5	2	232	278	6	-4	3	307	271	5	3	3	334	354

h	k	l	10Fo	10Fc	h	k	l	10Fo	10Fc	h	k	l	10Fo	10Fc	h	k	l	10Fo	10Fc	h	k	l	10Fo	10Fc
6	3	3	242	255	1	-6	4	383	287	3	0	4	382	412	3	-4	5	826	762	4	-7	6	318	319
6	3	3	275	255	2	-6	4	340	358	4	0	4	177	151	3	-4	5	728	762	4	-7	6	335	319
3	4	3	252	246	2	-6	4	345	358	4	0	4	160	151	3	-3	5	636	657	2	-6	6	328	358
3	4	3	190	246	2	-6	4	378	358	5	0	4	214	200	3	-3	5	705	657	3	-6	6	184	187
5	4	3	392	438	4	-6	4	234	258	6	0	4	709	731	7	-3	5	414	391	2	-5	6	448	432
6	4	3	249	271	4	-6	4	252	258	4	1	4	136	151	3	-2	5	222	194	4	-3	6	330	369
2	5	3	299	341	1	-5	4	147	129	4	1	4	156	151	5	-2	5	430	438	4	-3	6	428	369
4	5	3	346	397	2	-5	4	321	344	6	1	4	307	298	4	-1	5	189	191	4	-1	6	342	321
4	5	3	355	397	2	-5	4	342	344	6	1	4	337	298	4	-1	5	174	191	4	-1	6	287	321
6	5	3	231	210	2	-5	4	321	344	4	2	4	568	606	4	1	5	213	191	4	0	6	512	474
3	6	3	557	603	4	-5	4	675	595	4	2	4	620	606	4	1	5	197	191	4	1	6	334	321
5	6	3	316	299	2	-4	4	303	299	6	2	4	192	187	5	1	5	437	475	5	1	6	252	244
5	6	3	283	299	2	-3	4	469	474	4	3	4	356	356	5	1	5	524	475	6	2	6	321	326
3	8	3	360	375	4	-3	4	358	356	4	3	4	361	356	5	2	5	500	438	4	4	6	204	200
5	8	3	346	361	4	-3	4	344	356	5	3	4	178	196	5	2	5	466	438	4	5	6	201	208
2	-8	4	562	563	4	-3	4	363	356	5	4	4	194	190	3	3	5	643	657	4	7	6	334	319
6	-8	4	335	362	4	-2	4	685	606	4	5	4	599	595	7	3	5	349	391	5	-4	7	241	280
2	-7	4	360	366	4	-2	4	520	606	4	5	4	560	595	5	5	5	220	226	5	2	7	213	219
2	-7	4	329	366	8	-2	4	317	372	3	7	4	216	246	5	6	5	467	478	5	1	7	313	272
2	-7	4	338	366	4	-1	4	128	151	6	7	4	541	519	4	-8	6	351	353					
3	-7	4	252	246	6	-1	4	291	298	2	10	4	462	389	4	-8	6	310	353					
3	-7	4	242	246	6	-1	4	300	298	1	-6	5	541	594	2	-7	6	270	282					

APPENDIX C

Postgraduate Courses attended
&
Publications and Communications.

Postgraduate Courses Attended

1. Radiation hazards course at the University of Aberdeen.

2. A 3rd year undergraduate course of nine X-ray analysis lectures at the University of Aberdeen.

3. 10 data acquisition lectures forming part of a postgraduate diploma course from the School of Electrical and Electronic Engineering at the Robert Gordon Institute of Technology, Aberdeen.

4. The 1990 British Crystallographic Association spring conference at Exeter University, England.

Publications and Communications

1. **Structure of 1a,2,3,7b-Tetrahydro-1-phenyl-1H-cyclopropa[a]naphthalene.**
   P.J.Cox, S.M.S.V.Doidge-Harrison, I.W.Nowell, N.S.Stewart, R.A.Howie and A.B.Turner (1989) *Acta Cryst.*, **C45**, 1452.

2. **Crystal and molecular structure of the product from solvolysis of DHEA tosylate in benzyl alcohol.**
   P.J.Cox, N.S.Stewart, A.B.Turner and R.A.Howie (1990) *J.Cryst.Spect.Res.*, **Vol.20**, **No.6**, 577.

3. **Crystal and molecular structure of the product from solvolysis of DHEA tosylate in benzyl alcohol.**
   P.J.Cox, N.S.Stewart, A.B.Turner and R.A.Howie (1990) **Poster presentation at the 1990 British Crystallographic Association spring conference, Exeter University, England.**

4. **Structure and disorder in schultenite, lead hydrogen arsenate.**
   C.C.Wilson, P.J.Cox and N.S.Stewart (1991) *J.Cryst.Spect.Res.*, **Vol.21**, **No.5**, 589.

5. **Crystal structure and coordination chemistry of (2-carbomethoxyethyl)iodoiphenylstannane, $IPh_2SnCH_2CH_2CO_2Me$.**
   P.Harston, R.A.Howie, G.P.McQuillan, J.L.Wardell, E.Zanetti, S.M.S.V.Doidge-Harrison, N.S.Stewart and P.J.Cox (1991) *Polyhedron*, **Vol.10**, **No.10**, 1085.

6. **Hydrogen atom positions in 3-deazauracil.**
   C.C.Wilson, D.A.Keen and N.S.Stewart (1992) *Chem.Comm.* (submitted)